

Dissertation

submitted to the

Combined Faculties of Natural Sciences and Mathematics

of the Ruperto Carola University of Heidelberg, Germany

for the degree of

Doctor of Natural Sciences

**Put forward by**

Ling Lin

born in Sichuan, China

July 13, 2016



# Gauge Fluxes in F-theory Compactifications

*Referees:*

Prof. Dr. Timo Weigand

Prof. Dr. Jörg Jäckel



## Gauge Fluxes in F-theory Compactifications

In this thesis, we study the geometry and physics of gauge fluxes in F-theory compactifications to four dimensions. Motivated by the phenomenological requirement of chiral matter in realistic model building scenarios, we develop methods for a systematic analysis of primary vertical  $G_4$ -fluxes on torus-fibred Calabi–Yau fourfolds.

In particular, we extend the well-known description of fluxes on elliptic fibrations with sections to the more general set-up of genus-one fibrations with multi-sections. The latter are known to give rise to discrete abelian symmetries in F-theory. We test our proposal for constructing fluxes in such geometries on an explicit model with  $SU(5) \times \mathbb{Z}_2$  symmetry, which is connected to an ordinary elliptically fibration with  $SU(5) \times U(1)$  symmetry by a conifold transition. With our methods we systematically verify anomaly cancellation and tadpole matching in both models. Along the way, we find a novel way of understanding anomaly cancellation in 4D F-theory in purely geometric terms. This observation is further strengthened by a similar analysis of an  $SU(3) \times SU(2) \times U(1)^2$  model.

The obvious connection of this particular model with the Standard Model is then investigated in a more phenomenologically motivated survey. There, we will first provide possible matchings of the geometric spectrum with the Standard Model states, which highlights the role of the additional  $U(1)$  factor as a selection rule. In a second step, we then utilise our novel methods on flux computations to set up a search algorithm for semi-realistic chiral spectra in our Standard-Model-like fibrations over specific base manifolds  $\mathcal{B}$ . As a demonstration, we scan over three choices  $\mathbb{P}^3$ ,  $\text{Bl}_1\mathbb{P}^3$  and  $\text{Bl}_2\mathbb{P}^3$  for the base. As a result we find a consistent flux that gives the chiral Standard Model spectrum with a vector-like triplet exotic, which may be lifted by a Higgs mechanism.

## Eichflüsse in F-Theorie Kompaktifizierungen

In dieser Arbeit beschäftigen wir uns mit der Geometrie und Physik von Eichflüssen in F-Theorie Kompaktifizierungen nach vier Dimensionen. Um phänomenologisch realistische Modelle mit chiraler Materie zu konstruieren, entwickeln wir Methoden für eine systematische Analyse von vertikalen  $G_4$ -Flüssen auf Torus-gefaserten Calabi–Yau Vierfalten.

Insbesondere erweitern wir die vertraute Beschreibung von Flüssen in elliptischen Faserungen mit Schnitten auf allgemeinere Torus-Faserungen mit Multi-Schnitten, welche bekanntermaßen zu diskreten abelschen Symmetrien in F-Theorie führen. Darauf basierend konstruieren wir Flüsse in einem expliziten Multi-Schnitt-Beispiel mit einer  $SU(5) \times \mathbb{Z}_2$  Symmetrie, welche über eine sog. Conifold-Transition in Verbindung zu einer elliptischen Faserung mit  $SU(5) \times U(1)$  Symmetrie steht. Mit unseren Berechnungsmethoden verifizieren wir systematisch Tadpole-Bedingungen und die Kürzung von Anomalien in beiden Modellen. In dieser Analyse finden wir einen neuartigen, rein geometrischen Zugang zur Anomalie-Kürzung in 4D F-Theorie, die wir auf ähnliche Weise auch in der Analyse von einem Modell mit  $SU(3) \times SU(2) \times U(1)^2$  beobachten.

Die offensichtliche Verbindung von diesem Modell zum Standardmodell der Teilchenphysik ist dann der Startpunkt für eine phänomenologische Analyse. Darin untersuchen wir zunächst, wie das geometrische Spektrum mit den Standardmodell-Teilchen identifiziert werden kann und wie die zusätzliche  $U(1)$  die Rolle einer Auswahlregel übernimmt. Im zweiten Schritt benutzen wir dann die zuvor entwickelten Methoden für Fluss-Berechnungen, um einen Such-Algorithmus aufzustellen, der semi-realistische chirale Spektren in unseren Standardmodell-ähnlichen Faserungen über konkrete Basen  $\mathcal{B}$  identifiziert. Als eine Demonstration führen wir eine Suche für drei verschiedene Basen,  $\mathbb{P}^3$ ,  $\text{Bl}_1\mathbb{P}^3$  and  $\text{Bl}_2\mathbb{P}^3$ , durch. Damit finden wir unter anderem eine konsistente Fluss-Konfiguration, die das chirale Standardmodell Spektrum mit einem exotischen vektorartigen Triplet realisiert, welcher prinzipiell mit einem Higgs Mechanismus geliftet werden kann.



# Contents

<b>I</b>	<b>Motivation</b>	<b>1</b>
<b>II</b>	<b>Basics of F-theory</b>	<b>7</b>
1	String Theory in a Nutshell . . . . .	7
1.1	Dynamics of quantum strings . . . . .	7
1.2	Compactifications . . . . .	10
1.3	M-theory and string dualities . . . . .	13
1.4	Type IIB string theory . . . . .	14
2	Introduction to F-theory Compactifications . . . . .	16
2.1	Geometrising the $SL(2, \mathbb{Z})$ invariance of type IIB . . . . .	16
2.2	Torus fibrations . . . . .	19
2.3	Defining F-theory via M-theory . . . . .	22
2.4	F-theory on singular torus fibrations . . . . .	24
2.5	Abelian symmetries in F-theory . . . . .	33
2.6	Constructions with toric geometry . . . . .	39
2.7	Summary — an F-theory dictionary . . . . .	41
<b>III</b>	<b>Gauge Fluxes in F-theory</b>	<b>43</b>
1	$G_4$ -Fluxes in F-theory . . . . .	43
1.1	Mathematical description of $G_4$ -flux . . . . .	44
1.2	Physical implications of $G_4$ -fluxes . . . . .	47
2	Vertical Fluxes . . . . .	49
2.1	Vertical cohomology as intersection theory of divisors . . . . .	49
2.2	Vertical cohomology forms on toric hypersurfaces . . . . .	51
3	Tools from Commutative Algebra . . . . .	53
3.1	Why do we need this? . . . . .	54
3.2	On polynomials and varieties . . . . .	54
3.3	Application to F-theory: matter surfaces and singlet curves . . . . .	61
4	Summary of Chapter III . . . . .	64
<b>IV</b>	<b>Anomalies in 4D Compactifications</b>	<b>65</b>
1	Gauge and Gravitational Anomalies in 4D . . . . .	65
1.1	Field theoretic description of anomalies . . . . .	65
1.2	Gauge and gravitational anomalies in F-theory . . . . .	66
2	F-theory with $SU(5) \times U(1)$ and $SU(5) \times \mathbb{Z}_2$ Gauge Group . . . . .	67
2.1	Elliptic fibrations with $SU(5) \times U(1)$ gauge group . . . . .	68
2.2	Fluxes and anomalies in the $SU(5) \times U(1)$ model . . . . .	71
2.3	Anomalies in the $SU(5) \times \mathbb{Z}_2$ model . . . . .	79
2.4	Comparing fluxes in the conifold transition . . . . .	91
3	Models with $SU(3) \times SU(2) \times U(1)^2$ Symmetry . . . . .	94

3.1	Geometries realising an (extended) Standard Model . . . . .	95
3.2	Cancellation of gauge and gravitational anomalies . . . . .	99
3.3	Flux quantisation and the Witten anomaly . . . . .	105
4	Summary of Chapter IV . . . . .	107
<b>V</b>	<b>Towards the Standard Model in F-theory</b>	<b>109</b>
1	Yukawa Couplings in the $SU(3) \times SU(2) \times U(1)^2$ Geometry . . . . .	109
1.1	F-theory with $U(1) \times U(1)$ gauge group . . . . .	110
1.2	Toric fibrations with additional $SU(2)$ symmetry . . . . .	113
1.3	Toric fibrations with additional $SU(3)$ symmetry . . . . .	120
1.4	Toric $SU(3) \times SU(2) \times U(1)_1 \times U(1)_2$ realisations . . . . .	123
2	Standard Model Embeddings . . . . .	129
2.1	Criteria for Standard Model Embeddings . . . . .	129
2.2	Search for models with realistic chiral spectrum . . . . .	133
3	Summary of Chapter V . . . . .	140
<b>VI</b>	<b>Conclusion and Outlook</b>	<b>143</b>
<b>A</b>	<b>Intersection Theory of algebraic Cycles</b>	<b>149</b>
<b>B</b>	<b>Details on the Construction of the <math>SU(3) \times SU(2) \times U(1)^2</math> Gauge Group</b>	<b>151</b>
1	Details on the Toric Diagrams . . . . .	151
2	Details on $SU(2)$ -II and -III Tops . . . . .	153
2.1	$SU(2)$ -II Top . . . . .	153
2.2	$SU(2)$ -III Top . . . . .	155
3	Details on $SU(3)$ -B and -C Tops . . . . .	158
3.1	$SU(3)$ -B Top . . . . .	158
3.2	$SU(3)$ -C Top . . . . .	159
<b>C</b>	<b>Matching the MSSM-Spectrum</b>	<b>161</b>
<b>D</b>	<b>All realistic chiral Models</b>	<b>177</b>



# Chapter I

## Motivation

The theoretical foundation of contemporary physics can be roughly divided into two realms. On large scales, the gravitational dynamics of satellites and planets, all the way to galaxy clusters and the universe, can be effectively described by the theory of general relativity (GR). At the microscopic level, the framework of quantum field theories (QFTs) covers phenomena ranging from superconducting materials to particle scattering at the LHC. While both theories have proven to be tremendously successful on their own, they are mutually incompatible at the most fundamental level: When applying the techniques of QFT to GR, physical quantities turn out to be divergent in an uncontrollable manner [1]. While many physical systems can be well-approximated by either of the two theories alone, phenomena like black holes or the big bang bear intrinsically quantum and gravitational characteristics. For a complete understanding – at least at the conceptual level – of our physical reality, we therefore require a fully consistent quantum theory of gravity.

One of the arguably most promising candidates is string theory. In the most basic approach to it, string theory can be seen as a quantum theory of one-dimensional objects (a.k.a. strings) which replace the traditional idea of point-like elementary particles. In such a description, our ignorance of the extended nature of strings is a consequence of their extremely small size, which need energies beyond our reach to be resolved. Accordingly, we perceive different excitation states of strings as different point-like particles.

Originally proposed as an ill-fated attempt to describe the strong force, string theory was nearly forgotten with the rise of QCD. Luckily, it was brought back to life when in the 1970s people stumbled across two striking features of string theory. The first observation was the appearance of massless physical excitations with spin 2 – the characteristics of the graviton [2]. The second was that scattering amplitudes of string states exhibit a UV-finite behaviour [3], as opposed to divergent amplitudes that are omnipresent in QFTs with point-like particle states. Thus, with the natural appearance of gravity in a UV-finite quantum description, string theory possesses two pivotal elements of quantum gravity.

Despite these remarkable properties, string theory in its early days was plagued by many conceptual and phenomenological issues. It took the combined work of numerous brilliant minds to resolve problems, which in turn would often lead to further new insights and provide novel links between previously unrelated aspects. E.g. the necessity of fermionic excitations of the string led to the utilisation and subsequent rise to prominence of supersymmetry in string-related and -unrelated theories. Likewise, it was realised that a consistent theory of strings must necessarily include higher-dimensional objects, so-called  $p$ -branes. Being of non-perturbative nature, branes have not only extended our conceptual understanding of string theory, but also vastly increased its phenomenological capabilities, with numerous applications to particle physics or cosmological model building.

One of the most puzzling revelations in the first two decades of string theory was the existence

of five possible supersymmetric formulations of string theory, which seemed to be independent of each other. It was not until the mid 1990s when it was realised that these five string theories are perturbative limits of one big underlying M(ysterious)-theory, and related to each other by so-called dualities (cf. figure I.1). While we do not have a fundamental description, the dualities provide a powerful way to study many aspects of M-theory through the better understood string theories.

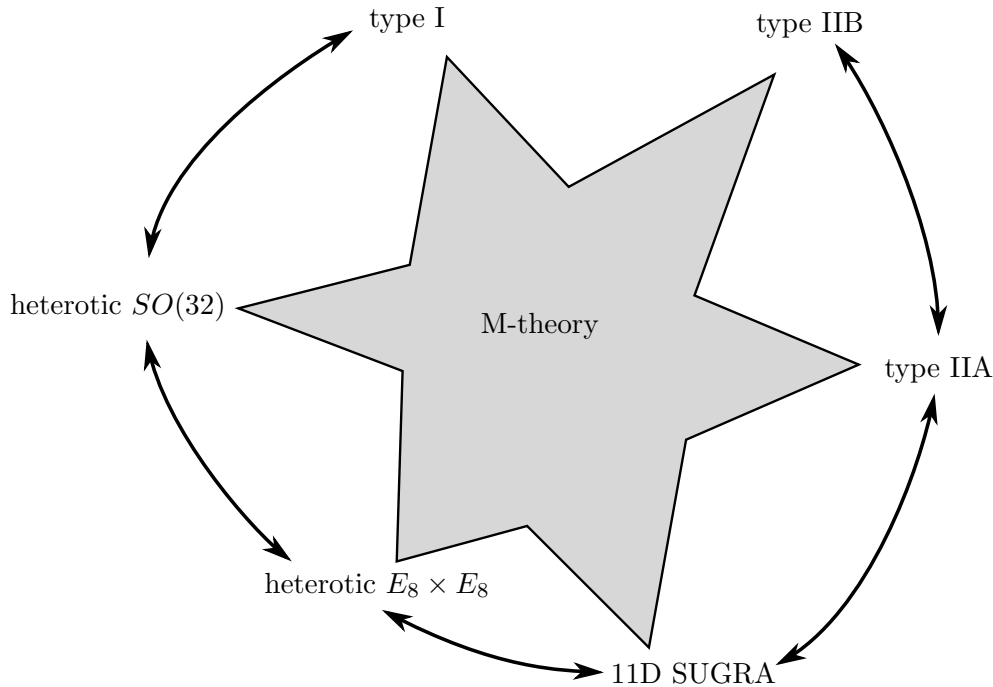


**Figure I.1:** The ‘M-theory star’: A schematic visualisation of the relationship amongst M-theory and its perturbative limits. The grey area represents possible physical configurations of M-theory (also known as its ‘moduli space’). In certain corners, the description is equivalent to one of the five perturbative string theories, or to 11D supergravity (SUGRA). These limits are connected to each other via duality relations indicated by the arrows.

One critical consistency condition of string and M-theory is that they all require spacetime to have extra dimensions going beyond the four we observe in our everyday life (all string theories live in ten dimensions, while M-theory and its low energy limit, 11D SUGRA are eleven-dimensional). One might think that this criterion alone already discards string theory as a viable description of our physical reality. However, salvation comes in form of an idea by Kaluza and Klein dating back to the times of Einstein, which nowadays goes by the name of compactification.

Historically, the theory of Kaluza–Klein was an extension of GR, by generalising Einstein’s formulation of gravity to a five-dimensional spacetime with a periodic spatial dimension, i.e. a (compact) circle. It turns out that the field equations of 5D can be re-interpreted in terms of physics in the four non-compact dimensions as ‘ordinary’ GR coupled to an electromagnetic gauge field. Furthermore, the coupling strength can be related to the size of the circle (i.e. the geometry of the extra dimension). It is therefore not exaggerated to say that (parts of the) physics in 4D is dictated by the geometry of the compact dimensions. Even though the original Kaluza–Klein theory is physically flawed (e.g. it predicts an unrealistic electron mass), this idea prevails throughout string theory.

Unlike the original Kaluza–Klein theory, compactification of string or M-theory employs higher dimensional spaces in order to make contact to 4D physics. These spaces necessarily have much more structure than a simple circle. Consequently, the variety of possible physical theories in the

non-compact dimensions is enormous. In the literature, this huge set of possible physical models is usually called the ‘string landscape’. In particular, it is an outstanding problem to identify amongst all models in the landscape of 4D (four non-compact dimensions) models those which could approximate or even exactly describe our real world. Indeed, most of today’s research in string phenomenology is concerned with this problem.

The difficulties of this program can be summarised very concisely as follows: Geometry of higher dimensional compact manifolds is complicated. As a consequence, many computations yielding physically important quantities can only be carried out in very restrictive set-ups.<sup>1</sup> Somewhat paradoxically, this issue turns out to be one of the main reasons string theory became so popular: Mathematicians became interested in string compactifications. Unlike many physical theories before, where physicists could usually fall back onto known mathematics, the mathematics required to describe string and M-theory compactifications has largely to be invented yet.<sup>2</sup> On the other hand, physical intuition can often serve as a guideline in case rigorous mathematics are lacking, and in turn explain mathematics. For example, the mathematical theory of knots can be understood from studying physics of certain conformal field theories obtained from compactifications to 6D. This principle of ‘physicalisation’ sparked many novel developments in pure mathematics based on research in string compactifications. Mirror symmetry, topological quantum field theories, geometric Langlands correspondence, and moonshine theory are only a few of the salient topics inspired by string theory. At the same time, physicists have also profited extensively from the involvement of mathematicians. Especially the utilisation of algebraic geometry and topology has vastly increased the model building power of string compactifications. Over the last two decades, these novel mathematical methods have helped considerably in the advances through the string landscape.

In particular, people began to push beyond the perturbative limits of M-theory and explore more and more the interior of the M-theory star. Consistent compactifications constructed in this part of the moduli space inherently take certain non-perturbative corrections into account, thus extending the classes of perturbative string models. One of the most prominent non-perturbative frameworks of constructing string compactifications is F-theory.

### **Enter F-theory**

Introduced by Vafa in 1996 [4], F-theory naturally extends the model building powers of the popular type IIB strings by geometrising parts of the physical data. Concretely, Vafa realised that the physical quantity governing the coupling strength between strings<sup>3</sup> exhibit the same characteristics as the modulus  $\tau$  of a torus, which in algebraic geometry is also referred to as an elliptic curve. To formalise this, F-theory introduces an auxiliary elliptic curve attached to every point of the ten-dimensional spacetime of type IIB string theory, whose modulus  $\tau$  encodes the value of the string coupling. By allowing  $\tau$  to vary over spacetime non-trivially, i.e. fibring elliptic curves over spacetime, one can describe type IIB string theory with non-perturbative values of the string coupling. If the total space (fibre plus spacetime) of these so-called elliptic fibrations is globally consistent, then the mathematical formulation automatically takes care of all corrections stemming from non-perturbative back-reactions.

However, this is not the only way to understand F-theory. In fact, as we will see in chapter II, the most accurate definition of F-theory originates from M-theory directly. In this definition,

---

<sup>1</sup>E.g. the scattering amplitude of strings, even at tree level, requires the knowledge of the compact space’s metric, which can be explicitly written down only for a very limited subset of all possibilities.

<sup>2</sup>The only comparable situations was when Newton invented calculus for mechanics and when von Neumann set the foundations of functional analysis in order to understand quantum mechanics. None of the two however compare to the complexity and far-reaching range of the geometric innovations that arose from the study of string theory.

<sup>3</sup>To be precise: It is the complexified string coupling, also called the axio-dilaton. We will discuss the mathematical details in chapter II.

the auxiliary torus becomes part of the eleven-dimensional spacetime of M-theory, and a certain limit process recovers non-perturbative type IIB string theory. Likewise, through an alternative limit, one can actually relate F-theory with heterotic  $E_8 \times E_8$  string theory. Even though this duality will not be of relevance to the content of this thesis, it should be said that much of our understanding of F-theory is derived from the heterotic/F-theory duality [4–9].

Through these dualities, F-theory combines features of heterotic and type IIB strings. One of the most fruitful outcomes is the appearance of exceptional gauge symmetry localised on 7-branes, which proved to be invaluable for model building of Grand Unified Theories (GUTs). Especially, the appearance of  $E_6$  immensely raised the phenomenological interest in F-theory, as the realisation of the top-quark Yukawa coupling in  $SU(5)$  GUTs are tied to  $E_6$ . Indeed, with the development of systematic tools to geometrically engineer gauge symmetries in F-theory [10–12], GUT model building were predominant in the most recent era of F-theory particle phenomenology.

While GUTs certainly have phenomenologically appealing features, their existence and necessity are still open for debate. In particular, one of the main motivations for postulating a unifying gauge group was the apparent unification of the Standard Model couplings at high energies. This unification however is only convincing if one considers the minimal supersymmetric extension of the Standard Model (MSSM), and even then is achieved numerically only if the scale of SUSY breaking is in the TeV range. As the LHC has yet to find any significant signs of SUSY after its first 14TeV run, the scenario of low scale SUSY, and consequently the idea of unification, is under severe tension. Thus, it seems well-motivated to study parts of the string landscape – especially within the F-theory framework – which realise the Standard Model directly, without an underlying GUT structure.

This route has only been accessible recently with a complete understanding of abelian symmetries in F-theory. While  $U(1)$ s are omni-present in type IIB brane-models, their geometric description in F-theory were much harder to identify. However, the pay off for these technical analyses are the phenomenological possibilities that comes with abelian symmetries. Not only can we now construct the hypercharge  $U(1)_Y$  in non-GUT realisations of the Standard Model, but we can also include abelian factors as additional selection rules in various GUT and non-GUT models. Despite the phenomenological advances, abelian symmetries remain an active field of formal investigation, and we will encounter both aspects throughout this thesis.

One key ingredient in F-theory model building is the inclusion of so-called gauge or  $G_4$ -fluxes. These are physical data specifying the low energy, i.e. vacuum configurations of certain background fields in the M-theory description, similar to the Higgs vacuum expectation value (vev) in the Standard Model. From the duality to type IIB, we know that  $G_4$ -fluxes in F-theory have immense impact on phenomenology. They are required by various consistency conditions, e.g. cancelling certain non-perturbative anomalies or stabilising the compactification configuration. For particle phenomenology in 4D,  $G_4$ -fluxes are in particular needed to construct a chiral spectrum. Since the Standard Model is a chiral theory, any realistic F-theory model building must necessarily include gauge fluxes. For the phenomenological investigations in this work, fluxes will thus play a central role.

However, in order for these models to be fully consistent, the flux configurations have to pass the test of anomaly cancellation. Like any chiral QFT, also the 4D field theories obtained from F-theory compactifications have potential chiral anomalies. While these anomalies are shown to be cancelled in very explicit examples, there is until now no argument from first principles, why these cancellations are expected for more generic models. In this thesis, we will attempt to establish such a general argument. As we will see in chapter IV, this will be based on a purely geometric analysis, that in principle can be formalised for generic compactification spaces in F-theory.

## Outline of the thesis

As F-theory is part of the string and M-theory family, we will first give a short review of string

theory in section 1 of chapter II, focusing on compactifications and string dualities. In particular, as F-theory is naturally tied to type IIB strings, we will have a closer look at this theory. In section 2, we will then discuss in detail the mathematical description together with the most important physical aspects of F-theory compactifications.

As gauge fluxes are the central object of interest, we will devote chapter III to them. Most importantly, we will present two sets of mathematical tools that was developed for a systematic treatment of fluxes in F-theory. These tools are heavily utilised in chapter IV, where we focus on chiral anomalies and their cancellation in F-theory. In particular, we will look at three classes of F-theory models with  $SU(5) \times U(1)$ ,  $SU(5) \times \mathbb{Z}_2$ , and  $SU(3) \times SU(2) \times U(1)^2$  gauge symmetry, on which we test our hypothesis of F-theory anomaly cancellation. Along the lines, we will also investigate the role of fluxes in the conifold or Higgsing-transition, which relates the  $SU(5)$  models.

Finally, we will attempt a direct construction of the Standard Model in F-theory based on the  $SU(3) \times SU(2) \times U(1)^2$  models. In chapter V, we will carefully examine the Yukawa coupling structure of matter in these models and discuss how the extra  $U(1)$  factor may be utilised as a phenomenologically interesting selection rule. Utilising the results from chapter IV, we will then proceed to search for explicit models in our landscape of F-theory Standard Models, that have a realistic chiral spectrum.

The results of chapters IV and V have been presented in the publications [13–15].



# Chapter II

## Basics of F-theory

In this chapter we will review the physical and mathematical foundations of F-theory. Starting with a brief introduction to string and M-theory, we will focus on the emergence of F-theory as a non-perturbative extension of type IIB string theory and as a decompactification limit of M-theory compactifications. We will explain how these two pictures are related by dualities. With these ingredients we will then thoroughly discuss the appearance of gauge symmetries, matter states and Yukawa couplings in 4D F-theory compactifications.

### 1 String Theory in a Nutshell

In this section, we will give a short overview of aspects of string theory that is tied to the discussions of this thesis. By now this content is standard textbook material. For detailed string theory introductions, we refer to [3, 16–19].

#### 1.1 Dynamics of quantum strings

String theory replaces our naive picture of point-like elementary particles with one-dimensional strings as the fundamental objects of nature. Classically, a string propagating in a  $d$ -dimensional spacetime  $M_d$  sweeps out a two-dimensional timelike surface  $\Sigma \subset M_d$  called the string-worldsheet. Denoting the local coordinates of this surface by  $\sigma^a = (\sigma^0, \sigma^1) \equiv (\tau, \sigma)$ , the evolution of the string is fully specified by an embedding  $X^\mu(\sigma^a)$  of the worldsheet into spacetime  $M_d$ , which is also called the target space, with coordinates  $X^\mu$ . With this embedding, the metric of the worldsheet induced by the metric  $G_{\mu\nu}$  of  $M_d$  is given by

$$\gamma_{ab} = \frac{\partial X^\mu}{\partial \sigma^a} \frac{\partial X^\nu}{\partial \sigma^b} G_{\mu\nu}.$$

The dynamics of the string, i.e. the dependence of the target space coordinates  $X^\mu$  on  $\sigma^a$ , can be then determined via the so-called Nambu–Goto action

$$S_{\text{NG}} = -T \int_{\Sigma} d\tau d\sigma \sqrt{-\det \gamma}, \quad (\text{II.1})$$

which is nothing but the area of the string worldsheet in  $M_d$ .<sup>1</sup> The pre-factor  $T$  has mass-dimension 2 and can be interpreted as the tension of the string. It is common to re-write  $T = 2\pi/\alpha'$ , where  $2\pi\sqrt{\alpha'} = \ell_s$  is the typical length of strings, also known as the string scale. Since there is until now no direct evidence of strings in nature, the string scale must be far beyond our

---

<sup>1</sup>This is an obvious generalisation of the action for a relativistic point-like particle. In that case the trajectory of the particle is a worldline in  $M_d$ , whose length as a functional of the trajectory is the relativistic action.

current energy scales, most likely only a few orders of magnitude below the Planck scale. Note that in principle, this is the only fundamental scale of string theory.

In the formulation (II.1), string theory can be regarded as a field theory on the worldsheet with fields  $X^\mu$ .<sup>2</sup> These fields are bosonic fields, and consequently, one usually refers to (II.1) as the bosonic string. However, in order to have fermionic string excitations in the target space, one needs to introduce supersymmetric partners  $\psi^\mu$  to the fields  $X^\mu$ . In contrast to the bosonic string, these ‘super-strings’ have a further advantage of being free of unstable (tachyonic) ground states.

One important feature of the (super-)string worldsheet is its invariance under conformal transformations. While this symmetry is hidden in the Nambu–Goto description of the action, there exists an alternative version, called the Polyakov action, which makes this symmetry manifest. Both actions are equivalent at the level of equations of motions, however, the Polyakov action is much better suited for the quantisation of strings. The conformal symmetry of the worldsheet is the single reason we can fully solve the quantum string (at least for flat target space). Irrespective of the quantisation procedure – either using operators or the path integral – one has to make sure that the conformal symmetry persists at the quantum level. Remarkably, this condition restricts the dimension of the target space  $M_d$ . For the bosonic string,  $d$  must be 26, while in the case of super-strings we have  $d = 10$ . As we are ultimately interested in spacetime theories with fermions, we will restrict ourselves to super-string theories in the following. For convenience, we will also drop the prefix ‘super’.

The result of the quantisation process is an infinite spectrum of excitation states of the string, which from the target space perspective may be perceived as different elementary particles with different quantum numbers (e.g. mass and spin in flat target space). Interactions, i.e. scatterings between different states, can be literally pictured as the joining and splitting of strings. The likelihood of this process – in other words the coupling between strings – is measured by the string coupling constant  $g_s$ . In contrast to the scattering of point-like particles, the interaction of strings cannot be localised at one point of spacetime (cf. figure II.1). Indeed, one may attribute the UV-finiteness of string scatterings to this ‘smearing’ [3].

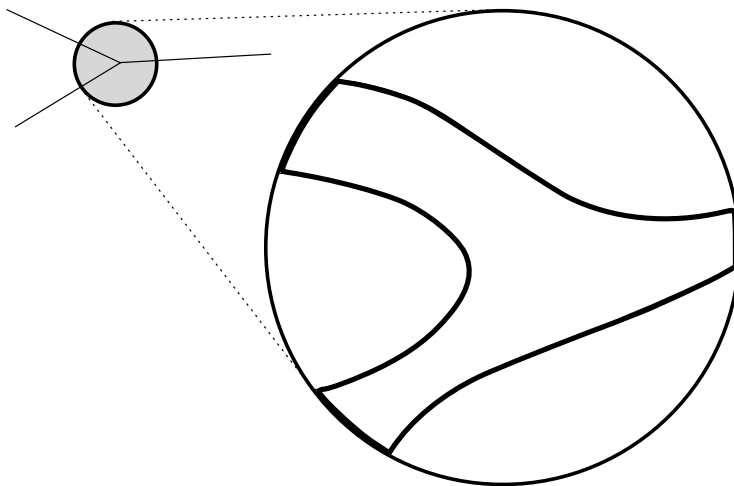


**Figure II.1:** A schematic visualisation of a string scattering. By replacing point-particles with strings, the extended nature of the latter ‘smears’ out the point of interaction; the resulting worldsheet has no singularity, as opposed to the vertex of the ‘Feynman-diagram’.

<sup>2</sup>The metric  $G_{\mu\nu}$  is a priori a fixed background field in the worldsheet formulation. However, it is possible to constrain the metric using consistency conditions of the worldsheet theory. In particular, field theory computations (to first order in perturbation theory) on the worldsheet actually impose  $G_{\mu\nu}$  to be Ricci-flat, i.e. vacuum solutions of Einstein’s equations. For details see e.g. [20].



In addition to the massless excitations, which contain a spin 2 state, there is an infinite tower of massive states. However, the masses of these excitations are proportional to the string scale  $M_s = \ell_s^{-1}$ , and hence are way too massive to be observed in our current experiments. Consequently, if we are interested in the low energy (compared to the string scale) physics, the contributions of these massive states will be highly suppressed and can thus be neglected safely. Meanwhile, the massless excitations and their interactions can be consistently described by a field theory with an effective Lagrangian description. The resulting effective field theories with only massless excitations take the form of a supergravity (SUGRA) theory. The ‘super’ refers to the fact that these theories exhibit a certain amount of spacetime supersymmetry in their massless spectrum, while the ‘gravity’ part comes from the spin-2 excitations which can be interpreted metric perturbations, i.e. gravitons.

The spectrum of string theories is subject to severe consistency conditions arising from the worldsheet formulation of strings. It turns out that there are five inequivalent super-string theories in flat Minkowski spacetime, which fulfil these conditions. They are referred to as type I, type IIA or IIB, and heterotic  $E_8 \times E_8$  or  $SO(32)$  string theories. Each of the five string theories has a corresponding consistent description as an effective supergravity theory at the massless level. These effective field theories in turn can be treated with standard field theory techniques to simplify the more complicated stringy computations for at least the massless excitations.

## Branes

Strings can come in two configurations: either they have two ends, in which case they are called ‘open strings’, or they form a closed loop, i.e. a ‘closed string’. While closed strings can move around freely in spacetime, the equations of motion forces the ends of open strings to lie on certain  $(p + 1)$ -dimensional (i.e.  $p$  spatial and one time dimension) submanifolds of  $M_{10}$ . These submanifolds are the world-volume of so-called  $Dp$ -branes.<sup>3</sup> In particular, as we will see in section 1.4, there are other type of strings arising as D1-branes, which differ from the fundamental strings, which are referred to as F1-strings.

In type II string theories, an important aspect of branes is that they realise gauge symmetry on their world-volume. In a semi-classical picture, the gauge fields can be understood as the perturbations of the brane longitudinal to its world-volume. These perturbations may also be pictured as open strings, with ending on the brane, ‘pulling and pushing’ the brane parallel to its world-volume. The quantised version of these perturbations give rise to gauge bosons propagating along the brane. In this naive picture it is hard to explain the appearance of massless matter charged under the gauge symmetry. However, it can be shown rigorously (see e.g. [19]) that these states arise at the intersection of branes and can be visualised as excitations of open strings stretched between the intersecting branes.

The intuitive picture of brane perturbations suggests that branes are themselves dynamical objects. Indeed, it is possible to generalise the Nambu–Goto action (II.1) to higher dimensional objects, leading to the so-called Dirac–Born–Infeld (DBI) action. From this action, one can, at least classically, derive the existence of a Yang–Mills theory, i.e. gauge fields, on the brane. However, a similar quantisation as that of strings is not possible, because for branes there is no comparable symmetry like conformal symmetry on the string worldsheet. The lack of a clear description of branes can be seen as a result of their non-perturbative nature. To be precise, their dynamics decouples in the limit of vanishing string coupling,  $g_s \rightarrow 0$ . Indeed, one can heuristically argue that the tension of  $Dp$ -branes behaves like  $\ell_s^{-(p+1)} g_s^{-1}$ , implying that their typical mass scale is  $\ell_s^{-1} g_s^{-1/(p+1)}$ . For small values of the string coupling  $g_s$ , the lowest mass scale is set by branes with the lowest  $p$ . Conversely, away from the perturbative limit, we expect

---

<sup>3</sup>The ‘D’ denotes the fact these branes arise from Dirichlet-boundary conditions imposed on the ends of open strings. In the context of F-theory, we will see that other types of branes.

all branes to appear on equal footing.

In the supergravity limit of string theories, branes appear as so-called BPS objects, i.e. massive states whose stability is guaranteed by supersymmetry. Importantly, this stability statement is not tied to any perturbative results, i.e. they hold also in non-perturbative regimes. Indeed, branes appeared prior to their rediscovery in string theory as extremal black hole (or rather black brane), which are known to be stable solutions of supergravity. For example, in type II and heterotic string theories, the fundamental string as a 1-brane are BPS states in the supergravity description, whereas type I string theory contains no BPS strings. Heuristically, this can be understood as the fact that all theories except type I only have closed fundamental strings which are stable. Type I on the other hand has also open fundamental strings, into which closed and open strings can break up into; thus they are not stable and hence not BPS.

## 1.2 Compactifications

Because all string theories and also M-theory are only well-defined in higher dimensions, it takes some further modifications to relate them to the four-dimensional world we see. One of the simplest approaches is called the brane-world scenario, in which one basically assumes that our world is the world-volume of a 3-brane, to which all forces but gravity are constrained. However, the prospect of six large extra dimensions is phenomenologically unfavoured, because this would imply that gravity falls off at large distances much stronger than the behaviour we observe. Thus, it is physically motivated to further employ the mechanism of compactification.

The principle of compactification is fairly simple: One factors the  $d$ -dimensional spacetime into a compact  $M^c$  and a non compact  $M^{\text{nc}}$  part:

$$M_d = M_n^{\text{nc}} \times M_{d-n}^c. \quad (\text{II.2})$$

The physical theory in  $d$  dimensions then descends to a theory in the  $n$ -dimensional non-compact spacetime  $M_n^{\text{nc}}$ , whose precise properties depend heavily on the geometry of  $M_{d-n}^c$ .

### 1.2.1 Five-dimensional examples

To gain some intuition about the process, let us consider a lower dimensional simple example. Concretely, suppose we have a free massless scalar field  $\phi$  in a five-dimensional spacetime  $M_5$  with the standard action

$$S \sim \int_{M_5} d^5x \left( -\frac{1}{2} \partial_A \phi \partial^A \phi \right). \quad (\text{II.3})$$

Now we would like to compactify this theory on a circle, i.e.  $M_5 = M_4 \times S^1$ , where  $M_4$  is flat Minkowski spacetime with coordinates  $x^\mu$  and  $S^1$  the compactification circle with coordinate  $y$ . To obtain an effective description in 4D, we can perform a Fourier-expansion, i.e. an expansion into eigenfunctions of the Laplace operator, along the circle:

$$\phi(x^\mu, y) = \sum_{k \in \mathbb{Z}} \phi_k(x^\mu) e^{i k y / R}, \quad (\text{II.4})$$

with  $R$  denoting the radius of the circle. This allows us to perform the  $y$ -coordinate integration in (II.3) explicitly, yielding

$$S_{4d} \sim \int_{M_4} d^4x \left[ -\frac{1}{2} \partial_\mu \phi_0 \partial^\mu \phi_0 - \sum_{k=1}^{\infty} \left( \partial_\mu \phi_k \partial^\mu \phi_k^* + \frac{k^2}{R^2} \phi_k \phi_k^* \right) \right],$$

with  $\phi_k^* = \phi_{-k}$ . Thus, we see that the compactification of a 5D scalar field on a circle leads to a 4D theory with a massless scalar  $\phi_0$  and an infinite tower of massive scalars  $\phi_k$  with masses

$m_k^2 = k^2/R^2$ . In particular, observers at energies much below the so-called Kaluza–Klein (KK) scale  $1/R$  will only be able to see an effective field theory in 4D with a massless scalar and be completely ignorant about the fifth dimension.

However, the structure of compactified models can be far richer than just the appearance of an infinite tower of massive fields. Indeed, the original Kaluza–Klein theory shows that through compactification one can also enrich the types of fields in the effective theory. To this end, we again consider a five-dimensional spacetime, but we replace the simple scalar field theory by Einstein’s general relativity. The fundamental field is the metric  $G_{AB}$ , whose dynamics is governed by the Einstein–Hilbert action  $\int d^5x \sqrt{-\det G} R_{5d}$ , where  $R_{5d}$  is the five-dimensional Ricci-scalar. Omitting the details, we can readily anticipate the result of the compactification on a circle by a so-called dimensional reduction of the 5D metric, where we express the components into 4D quantities:

$$g_{\mu\nu} := G_{\mu\nu}, \quad A_\mu := G_{\mu 4} = G_{4\mu}, \quad \phi := G_{44}, \quad \text{for } \mu, \nu = 0, \dots, 3.$$

Thus we see that the five-dimensional metric  $G$  contains the same degrees of freedom as a four-dimensional metric  $g$ , a vector field  $A$  and a scalar  $\phi$ . By going through the computations, one indeed finds – in addition to the massive KK modes – that the massless fields in 4D describe Einstein gravity coupled to a  $U(1)$  gauge field  $A_\mu$  and an additional scalar. The gauge symmetry is a remnant of the diffeomorphism invariance of the full 5D theory. The scalar field is a prototypical example of a (geometric) modulus field, whose vev parametrises the radius of the compactification circle.

### 1.2.2 Compactification of string theory

One immediate question arises, when we try to realise our real world as the result of a compactification of string theory: which compact space does the job? An ideal scenario would be if there is a first principle, which predicts the compact space, and it could be due to our still very limited understanding of string theory that we are ignorant about such a principle. However, there is a popular and controversial idea that perhaps there is no such principle at all. Instead, all mathematically consistent compactifications are also physically possible. Our observed universe would then just be one out of many (predictions range between  $10^{500}$  and  $10^{2700}$ ) within the so-called string landscape. Whether our world is the result of a random (or anthropic) selection, or is part of a bigger ‘multi-verse’ containing all possibilities is more of a philosophical debate, which we will not entertain here. In any case, a better understanding of either side requires to study individual (classes of) compactification models in detail and try to single out those which give rise to viable physics in 4D.

But even so, we are still confronted with the difficulties of translating the geometry of a general compactification space into physics of the effective theory. E.g. to perform the analogue of a Fourier-expansion for a higher dimensional space, one needs to know the Laplacian which in turn depends on the metric of the space. Even if we restrict ourselves to Ricci-flat metrics (in order to solve Einstein’s equations in vacuum), we know the explicit form only in a handful of cases. This difficulty in some sense reflects the equally hard problem of explicitly solving all physical models in 4D. However, physical intuition tells us that symmetry principles can often simply life significantly. Given the fact that all string theories have a certain amount of supersymmetry, it is therefore tempting to restrict ourselves to compactifications preserving (part of the) SUSY. After all, despite the growing tension of finding SUSY at the LHC, there are still phenomenological reasons (dark matter, unification) and formal interests (only extension of spacetime symmetry, new types of QFTs) for spacetime supersymmetry, which might be broken at scales higher than we are currently probing.

Demanding SUSY in the non-compact dimensions turns out to be restrictive enough to give us sufficient computational power over the compact space. Mathematically, the condition forces

the compact space to have special holonomy.<sup>4</sup> In particular, a specific class of spaces preserving at least  $\mathcal{N} = 1$  SUSY in 4D has become one of the central objects of interest in string compactifications. These are the so-called Calabi–Yau manifolds.

### Calabi–Yau manifolds

In order to preserve minimal supersymmetry after compactification on a (real)  $2N$ -dimensional compact manifold  $X$ , the holonomy of  $X$  must be  $SU(N) \subset SO(2N)$ . It can be shown mathematically that this statement is equivalent to  $X$  being a compact Kähler manifold of complex dimension  $N$  with vanishing first Chern class. Originally conjectured by Calabi, it was not proved until 1978 – around the same time string theory was first developed – by Yau that such a manifold always admits a Ricci-flat metric. Therefore, these Calabi–Yau manifolds naturally solve Einstein’s vacuum equations. However, one should point out that there are until now only numerical results for the explicit form of such a metric (see e.g. [22, 23]).

Similar to compactifications on a circle, there will also be massive towers of modes coming from the generalisation of a Fourier-expansion when compactifying on a Calabi–Yau manifold. Analogously, they are also referred to as KK-modes, and their ‘typical’ mass  $m_{\text{KK}}$  is the KK-scale.<sup>5</sup> Furthermore, we will also encounter massless modulus fields (or simply moduli), which parametrise different geometric and topological properties of the Calabi–Yau. Typically, their number is in the hundreds. If we want to make contact with our physical reality, where we only expect a handful of light scalar fields (e.g. Higgs, QCD axion, inflaton), then there must be a dynamical mechanism that gives these fields a high enough mass. Such mechanisms for ‘moduli stabilisation’ have been studied extensively in the literature, see e.g. [21, 24–26] for an overview.

The success of Calabi–Yau manifolds and complex geometry in general come with the computational power of algebraic geometry. Essentially, a large portion of the geometry of complex manifolds is encoded in polynomials, which are far simpler than the whole set of differentiable or holomorphic functions. For example, a theorem by Chow states that in any complex projective manifold, complex submanifolds can be generally described by vanishing loci of polynomials. Moreover, there are very simple methods – basically combinatorics – to explicitly construct a subclass of complex projective manifolds and Calabi–Yau spaces as subspaces thereof. These so-called toric geometry methods allows us furthermore to calculate many physically relevant quantities (e.g. charges, chiral indices) by hand or with computer algebra systems. In this thesis, we will exploit both toric geometry methods and polynomial algebra to construct and study compactifications with Calabi–Yau manifolds.

### Branes in compactifications

As branes are extended objects singling out certain directions, their presence would break the isometry of spacetime. Therefore, in order to maintain e.g. Poincaré invariance when we compactify to Minkowski space, the branes must either extend fully into the non-compact directions or not at all. The latter are known as instantons, whose effects we will largely ignore throughout this thesis. The first scenario however will be of great interest to us, as we can realise gauge theories in spacetime (i.e. non-compact dimensions) with branes. In particular, while all branes coincide in spacetime, they will in general have different positions in the compact dimensions. In string theory jargon, we say that the branes wrap certain submanifolds within the compact space. It is no surprise that the geometry of these submanifolds will play a crucial role in determining the physics of the gauge theory on their world-volume.

<sup>4</sup>Strictly speaking, this is only valid for string compactifications without background fluxes. Including these leads to manifolds with G-structures, see e.g. [21] for a review.

<sup>5</sup>For compactifications of the supergravity limit of string theories, we expect the KK-scale to be much lower than the string scale. In addition, if we want to make contact to our physical reality, then we also have to break SUSY at a scale lower than  $m_{\text{KK}}$ .

If we are interested in supersymmetric compactifications, then branes cannot be located arbitrarily in the compact space. In type IIA, branes must wrap so-called co-isotropic submanifolds, where as in IIB they must wrap holomorphic submanifolds. Because we have more mathematical tools for controlling and constructing holomorphic than for co-isotropic submanifolds, model building in type IIB has been more successful in the recent years. In particular, this advantage is enlarged further with the development of F-theory as an extension of type IIB. Note that in general, including the back-reaction of branes will lead to non-Calabi–Yau spaces as compact manifolds. E.g in type II models, where Calabi–Yau compactification actually leads to  $\mathcal{N} = 2$  SUSY in 4D, the inclusion of so-called orientifold-planes (O-planes) reduce spacetime SUSY to  $\mathcal{N} = 1$ . Consequently, the compact space will no longer be Calabi–Yau (but it must still be a Kähler manifold).

### 1.3 M-theory and string dualities

In their 10D formulation, the five string theories appear to be independent. However, with the tools of compactification, we can relate them by dualities. In fact, they can be seen as different limits of a putative 11D theory. Its existence is conjectured by the observation that in eleven dimensions, there is a unique supergravity theory.<sup>6</sup> When compactifying this effective theory in various ways, one can relate it to the supergravity limits of the five string theories. Similarly to these, it is therefore believed that there must be a UV-completion of 11D SUGRA, which is M-theory.

However, because there is no microscopic description of M-theory to date, we have to rely on the SUGRA description. In 11D, the field content fills out complete multiplets of  $\mathcal{N} = 1$  SUSY. The bosonic part consists of the metric  $G$  and an anti-symmetric 3-tensor, i.e. 3-form  $C_3$ , which is also referred to as the M-theory 3-form. Their dynamics is described by the action

$$S_{11D} = \frac{M_{11D}^9}{2} \int_{M_{11}} \left( d^{11}x \sqrt{-\det G} R - \frac{1}{2} G_4 \wedge *G_4 - \frac{1}{6} C_3 \wedge G_4 \wedge G_4 \right),$$

where  $G_4 = dC_3$ , and  $*$  is the Hodge star operator in 11D and  $M_{11D}$  the eleven dimensional Planck mass. Further more,  $G$  is the determinant of the metric  $G_{\mu\nu}$  and  $R$  the Ricci-scalar constructed out of it. Note that this action is invariant under  $C_3 \rightarrow C_3 + d\Lambda_2$ , i.e.  $C_3$  can be interpreted as a gauge potential, with  $G_4$  its field strength. The BPS states of this supergravity theory are (2+1)- and (5+1)-dimensional objects, dubbed M2- and M5-branes, respectively. They are in fact the objects that are charged electrically and magnetically, respectively, under the gauge field  $C_3$ .<sup>7</sup>

The relation to the five string theories comes by studying compactifications of M-theory. In fact, it is straightforward to show that type IIA supergravity can be recovered simply from compactifying 11D SUGRA on an  $S^1$ . Moreover, we can also recover the BPS spectrum of type IIA, e.g. the strings in 10D are M2-branes wrapping the circle, whereas D2-branes of type IIA originate from M2-branes not wrapping the circle. Importantly, the radius  $R$  of the compactification circle is related to the type IIA string coupling as  $g_s \sim R/\ell_s$ . This has a nice interpretation: The decompactification limit  $R \rightarrow \infty$  is equivalent to the strong coupling regime of type IIA string theory. Similar, a compactification of M-theory on an interval  $I \cong S^1/\mathbb{Z}_2$  can be shown to be equivalent to heterotic  $E_8 \times E_8$ , where again the perturbative limit is achieved for vanishing length of the interval. The relationship to the remaining three string theories (type I, IIB and het.  $SO(32)$ ) cannot established by simply considering compactifications of M-theory alone. In-

---

<sup>6</sup>To be precise, the uniqueness is only given with the assumption that there are no fields with spin higher than 2. Without this assumption, one would have to include massless fields of arbitrarily high spins for the theory to be consistent.

<sup>7</sup>Explicitly, an object with world-volume  $W$  is charged electrically under a form-field  $\omega$  if  $\int_W \omega \neq 0$ , and magnetically if  $\int_W *\omega \neq 0$ , where  $*$  is the Hodge-star operator.

stead we also need further properties of the string theories themselves. These are summarised in the so-called S- and T-dualities.

The concept of S-duality can be understood purely field-theoretically as an equivalence of a strongly and a weakly coupled theory. A famous example is the so-called Seiberg-duality between two non-identical 4D  $\mathcal{N} = 1$  supersymmetric gauge theories; there the physics of one theory at weak coupling turn out to be the same as the strong coupling physics of the dual theory. In string theory, we find that type I string theory at coupling  $g_s^I$  is S-dual to heterotic  $SO(32)$  theory at coupling  $g_s^{(32)} = 1/g_s^I$ . Furthermore, type IIB turns out to be self-dual under S-duality.

The other duality relation, called T-duality, is an inherently stringy relation that could not arise for theories with simple point-like degrees of freedom. Concretely, it arises when we consider closed strings in a compactification involving an  $S^1$  as part of the compact space (e.g. if the compact space is a torus). To give a heuristic explanation of T-duality, imagine closed strings wrapped non-trivially  $w$ -times around this circle with radius  $R$ . Since the string has tension  $T \sim 1/\alpha'$ , the ‘ground state energy’ of the wrapped string will be shifted by  $w R/\alpha'$ . At the same time, the string can also carry momentum in the circle direction, which due to the finite size of the circle is quantised as  $k/R$ . Their combined contribution  $w R/\alpha' + k/R$  is clearly invariant under

$$R \longleftrightarrow \frac{\alpha'}{R}, \quad k \longleftrightarrow w. \quad (\text{II.5})$$

In other words, closed strings on a large/small circle are identical, if one replaces the circle by a small/large one and simultaneously exchange winding modes and momentum modes.

As it turns out, type IIA and IIB string theories are T-dual to each other, i.e. a IIA compactification on a circle of radius  $R$  is equivalent to a IIB compactification on a circle of radius  $\alpha'/R$ , and this equivalence proceeds via identifying states arising from excited strings wrapping the circle with excited strings carrying momentum along the circle and vice versa. Similarly, the two heterotic theories compactified to on a circle are T-dual to each. These relations complete our duality web of string and M-theory, which we summarise in figure II.2.

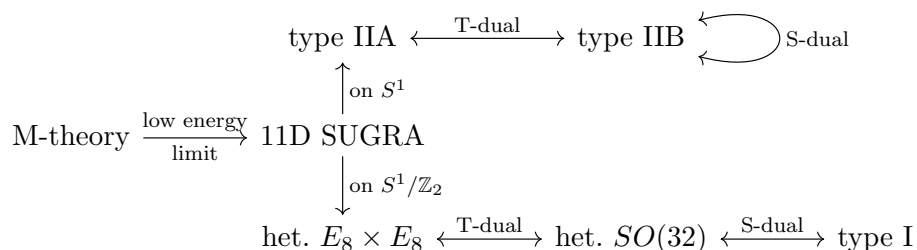


**Figure II.2:** String dualities relating the five string theories and M-theory/11D SUGRA.

## 1.4 Type IIB string theory

In this section, we will have a closer look at type IIB string theory. Its low energy description in flat 10D space, type IIB supergravity, has  $\mathcal{N} = (2, 0)$  supersymmetry. Its bosonic field content is summarised in table II.1. These are of course supplemented by their supersymmetric partners. Amongst these fields, the dilaton  $\phi$  plays a special role in the perturbative description of type IIB strings, as its vev  $\langle \phi \rangle$  encodes the string coupling,  $g_s = e^{\langle \phi \rangle}$ . The BPS objects of type IIB are charged electrically and magnetically under the form fields. Note in particular that the fundamental (F1-) and the D1-string differ by their charges.

In anticipation of the discussions below, we introduce the axio-dilaton  $\tau := C_0 + i e^{-\phi}$ . Further it is customary to define the field strength tensors  $F_{n+1} := dC_n$  for the form fields  $C_n$  and

field	(name)	type	electric BPS state	magnetic BPS state
$\phi$	(dilaton)	scalar	–	–
$G_{\mu\nu}$	(metric)	symmetric 2-tensor	–	–
$B_2$	( $B$ -field)	2-form	F1-string	NS5-brane
$C_0$	(RR 0-form)	0-form	D(–1) instanton	D7-brane
$C_2$	(RR 2-form)	2-form	D1-string	D5-brane
$C_4$	(RR 4-form)	4-form	D3-brane	D3-brane

**Table II.1:** Bosonic field content of 10D type IIB SUGRA.

$H_3 := dB_2$ . Finally, the abbreviations  $G_3 := F_3 - \tau H_3$  and  $\tilde{F}_5 := F_5 - \frac{1}{2}C_2 \wedge H_3 + \frac{1}{2}B_2 \wedge F_3$  allow us to write the bosonic part of the type IIB SUGRA action compactly as [3]

$$\frac{2\pi}{\ell_s^8} \int \left( d^{10}x \sqrt{-G} R - \frac{1}{2(\text{Im } \tau)^2} d\tau \wedge *d\bar{\tau} + \frac{1}{\text{Im } \tau} dG_3 \wedge *d\bar{G}_3 + \frac{1}{2} \tilde{F}_5 \wedge \tilde{F}_5 + C_4 \wedge H_3 \wedge F_3 \right),$$

where  $G$  is the determinant of the metric  $G_{\mu\nu}$  and  $R$  the Ricci-scalar constructed out of it.

One crucial property of this action is an  $SL(2, \mathbb{R})$  symmetry. Concretely, this symmetry acts on the fields in table II.1 as

$$\begin{pmatrix} C_4 \\ G \end{pmatrix} \mapsto \begin{pmatrix} C_4 \\ G \end{pmatrix}, \quad \tau \mapsto \frac{a\tau + b}{c\tau + d}, \quad \begin{pmatrix} C_2 \\ B_2 \end{pmatrix} \mapsto \begin{pmatrix} a & b \\ c & d \end{pmatrix} \begin{pmatrix} C_2 \\ B_2 \end{pmatrix}, \quad \text{with } \begin{pmatrix} a & b \\ c & d \end{pmatrix} \in SL(2, \mathbb{R}). \quad (\text{II.6})$$

While only the discrete subgroup  $SL(2, \mathbb{Z})$  survives as a symmetry upon quantisation<sup>8</sup>, it is believed that this remnant group persists as a symmetry of the full type IIB string theory. Note that the special transformation  $\tau \mapsto -1/\tau$  exchanges strong and weak coupling,  $g_s \mapsto 1/g_s$ , in case  $C_0 = 0$ . Therefore the  $SL(2, \mathbb{Z})$  symmetry contains the invariance of type IIB under S-duality.

Another curious consequence of the  $SL(2, \mathbb{Z})$  invariance is the notion of strings. Since the fields  $B_2$  and  $C_2$  are mixed up by a transformation, the charges of strings are not invariant under  $SL(2, \mathbb{Z})$  transformations. In particular, strings that appear to be fundamental in one  $SL(2, \mathbb{Z})$  frame can be a D1-string in another frame. Consequently, in the full type IIB theory, D1-string should appear on equal footing with the ‘fundamental’ string. In general, strings will carry (quantised) charges under both  $B_2$  and  $C_2$  and are labelled by their charges as  $(p, q)$ -strings. They are stable, i.e. BPS if  $p$  and  $q$  are coprime [27]. In this language, fundamental strings are  $(1, 0)$ -strings, and  $(0, 1)$ -strings represent D1-strings.

### 1.4.1 7-Branes in type IIB

Since branes carry electric and magnetic charges and the form fields, their presence will induce a non-trivial profile for these fields in a similar way an electric or magnetic charge backreacts onto the electromagnetic field. Heuristically, the effects are described by Poisson-like equations. Likewise, the supergravity description of branes also predicts gravitational back-reaction. One can show that for  $p$ -branes with  $p < 7$ , these effects all fall off with  $r^{7-p}$ , where  $r$  is the distance from the brane in the normal directions, and can thus be neglected sufficiently far from the branes. For 7-branes however, when there are only two normal spatial directions, the solution of the Poisson equation is proportional to  $\log(r)$  and hence do not fall off asymptotically. Consequently, we cannot simply ignore their back-reaction.

In particular, since 7-branes carry magnetic charges under  $C_0$ , the back-reaction is also reflected in the behaviour of the axio-dilaton under  $SL(2, \mathbb{Z})$  transformations. Concretely, the

<sup>8</sup>The breaking is induced by D(–1) instantons, which contribute a factor of  $\exp(2\pi i\tau)$  to the partition function; this factor is only invariant under  $SL(2, \mathbb{Z})$  transformations of  $\tau$ .

equations of motion for  $\tau$  force it to have a profile

$$\tau(z) = \frac{1}{2\pi i} \log \frac{z - z_0}{\lambda} + \dots$$

in the vicinity of a D7-brane, where  $z \in \mathbb{C}$  parametrises the plane orthogonal to the brane at  $z_0$ , and  $\lambda$  is some constant. Note that at  $z = z_0$ , the value of  $\tau$  diverges. The apparent issue arising from the monodromy of the logarithm, i.e.  $\tau \mapsto \tau + 1$  when we move around  $z_0$  in a circle, is remedied by realising that this is just an  $SL(2, \mathbb{Z})$  transformation (II.6) given by the matrix  $\begin{pmatrix} 1 & 1 \\ 0 & 1 \end{pmatrix}$ , i.e. a symmetry of the theory. This suggests that one can identify D7-branes by their monodromy effect on the axio-dilaton profile  $\tau$ .

Note that we can use this effect for an alternative description of gauge symmetries along 7-branes in type IIB. Recall from section 1.1 that the spectrum of open strings ending on branes gives rise to gauge theories on their world-volume. In perturbative type IIB, there are in addition to D7-branes also another type of 7-branes called O7-planes.<sup>9</sup> Depending on the brane-configuration, different gauge groups can be realised.  $SU(n)$  gauge theories, for example, live on a so-called stack of  $n$  coincident D7-branes (i.e.  $n$  D7-branes sharing the same world-volume), whereas  $SO(2(n+4))$  theories are realised on  $n + 4$  D7-branes on top of an O7<sub>-</sub>-plane. Studying the back-reacted  $\tau$  profile in the presence of these configurations, we find the following monodromy effects induced by each of them:

$$SU(n) \longleftrightarrow \begin{pmatrix} 1 & n \\ 0 & 1 \end{pmatrix}, \quad SO(2(n+4)) \longleftrightarrow - \begin{pmatrix} 1 & n \\ 0 & 1 \end{pmatrix}. \quad (\text{II.7})$$

Conversely, this means that we can identify loci, around which  $\tau$  exhibits some non-trivial monodromy, with brane configurations and the gauge symmetries associated with them. As in the example above with a single D7-brane,  $\tau$  will diverge at the brane loci. Note that in order to cancel the local brane tadpoles, the  $SO(2n)$  configuration is only stable with at least 4 D7-branes. This is an other consistency condition from the back-reactions of 7-branes.

Moreover, we can generalise the perturbative definition of a D7-brane being the ending locus of open fundamental strings in an obvious way: A  $(p, q)$ -brane is the locus where  $(p, q)$ -strings can end on. A D7-brane is thus a  $(1, 0)$ -brane. For the O7-plane, the situation is slightly more tricky. It was shown in [28] that it is actually a bound state of a  $(3, -1)$ - and a  $(1, -1)$ -brane.

One way of describing non-perturbative type IIB is to study general  $(p, q)$ -strings and -branes utilising so-called string junctions [29–31]. However, the methods of this approach are technical and less geometric. Instead, the above results suggests an alternative, unified description of 7-branes and  $(p, q)$ -strings ending on them by exploiting the  $SL(2, \mathbb{Z})$  transformations of the axio-dilaton and its monodromies. This description is provided by F-theory.

## 2 Introduction to F-theory Compactifications

In this section, we will collect some of the foundations of F-theory. For this, we will necessarily have to introduce some technical definitions and assume some working knowledge of complex geometry, line bundles and divisors. Most of the material are covered in reviews as [26, 32].

### 2.1 Geometrising the $SL(2, \mathbb{Z})$ invariance of type IIB

The success of F-theory as a unified description of type IIB comes from the geometrisation of the  $SL(2, \mathbb{Z})$  invariance. The crucial observation is that by identifying the axio-dilaton  $\tau$  with

<sup>9</sup>Recall that O-planes have been introduced to further the spacetime SUSY in Calabi–Yau compactifications from  $\mathcal{N} = 2$  to  $\mathcal{N} = 1$ . In these constructions they arise as fix loci of a geometric involution on the Calabi–Yau.



the modular parameter of an auxiliary torus, the  $SL(2, \mathbb{Z})$  invariance can be seen as simply the symmetry transformation of that torus.

Recall that a (two-dimensional) torus can be defined as the quotient  $\mathbb{C}/\Lambda$ , where  $\Lambda$  is a lattice in  $\mathbb{C}$ . The lattice  $\Lambda$  can be defined by two vectors  $\vec{a}, \vec{b} \in \mathbb{C} = \mathbb{R}^2$ , such that the torus is given by identifying  $\vec{x} \sim \vec{x} + \vec{a} \sim \vec{x} + \vec{b}$ . The area of the torus is given by the area of the parallelogram spanned by  $\vec{a}$  and  $\vec{b}$ , while the ‘shape’ is determined by the angle and the relative length between the two vectors. In complex geometry, the area is known as the Kähler parameter of the torus, and the shape is the complex structure. These are formally two independent parameters, meaning we can separately encode the area of the torus by the Kähler parameter and the complex structure by the angle and relative length of the two vectors  $\vec{a}$  and  $\vec{b}$ .

It is useful to use these freedoms to fix one of the vectors defining  $\Lambda$  to be  $1 \in \mathbb{C}$ . Then, the complex structure of the torus is completely determined by the other vector, which we call  $\tau$ . In this form, it can be easily shown that the transformations  $\tau \mapsto \tau + 1$  and  $\tau \mapsto -1/\tau$  leave the lattice  $\Lambda$  invariant. In fact, these transformations generate the full group of  $SL(2, \mathbb{Z})$ , which is thus the symmetry group of the torus. In other words, any two complex structure parameters  $\tau, \tau'$  related by a transformation  $\tau' = \frac{a\tau + b}{c\tau + d}$  with  $\begin{pmatrix} a & b \\ c & d \end{pmatrix} \in SL(2, \mathbb{Z})$  define the same torus. By applying  $SL(2, \mathbb{Z})$  transformations, one can map any  $\tau$  into the so-called fundamental region

$$\mathcal{F} = \left\{ \tau \in \mathbb{C} \mid |\tau| \geq 1, -\frac{1}{2} \leq \text{Re}(\tau) \leq \frac{1}{2} \right\}, \tag{II.8}$$

which is the set of complex structures of inequivalent tori.

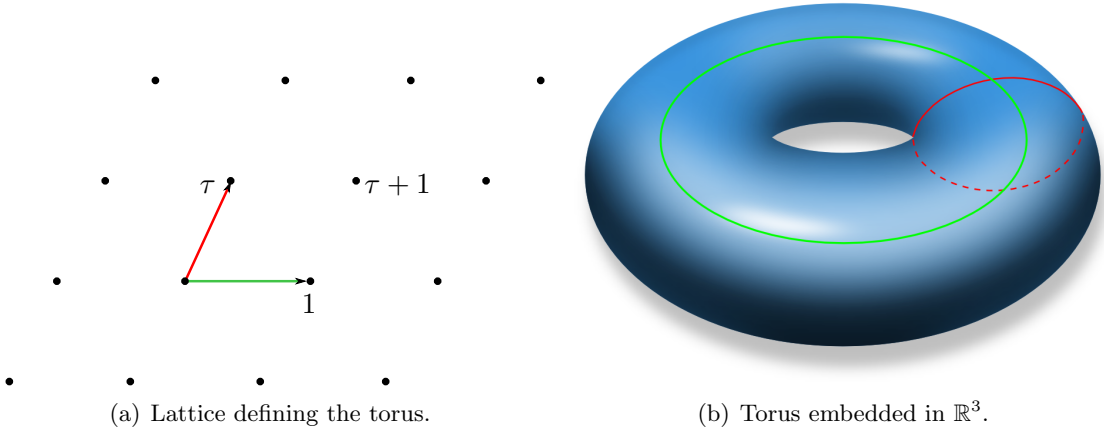


**Figure II.3:** A lattice (a) defining a torus (b). The lattice vectors define corresponding cycles on the torus, indicated as coloured circles in (b).

Furthermore, by representing the torus in the usual way as in figure II.3(b), the lattice vectors spanning  $\Lambda$  can be related to the two non-trivial cycles on the torus, as the colour-coding in figure II.3 suggests. In particular, the ratio of the length of the two cycles can be related to the value of  $\tau$ . With this relationship, an infinite value for  $\tau$  has a very geometric interpretation, namely one of the cycles shrinking to zero size, i.e. the torus becomes singular.

In algebraic geometry, tori are also known as elliptic curves. These have been studied systematically first by Weierstrass. Some of his beautiful results are the foundations of F-theory. In the following, we will briefly review these.

### Tori as elliptic curves

An elliptic curve can be defined as the loci  $\{[x : y : z]\}$  inside the weighted projective space  $\mathbb{P}_{231}$ <sup>10</sup> satisfying the so-called Weierstrass equation

$$y^2 = x^3 + f x z^4 + g z^6 \quad \Leftrightarrow \quad P_T := y^2 - x^3 - f x z^4 - g z^6 = 0. \quad (\text{II.9})$$

Weierstrass showed that any such curve can be identified with a torus defined by a lattice  $\Lambda$ , as discussed above. In his studies of elliptic curves, Weierstrass introduced the famous P-function (also known as the Weierstrass elliptic function), which has been honoured with its own designated symbol in  $\mathbb{A}^1_{\mathbb{C}} \times \mathbb{C}$ . Concretely, for a lattice  $\Lambda \subset \mathbb{C}$  generated by 1 and  $\tau$ , we define

$$\wp(\zeta; \tau) := \frac{1}{\zeta^2} + \sum_{\substack{n, m \in \mathbb{Z}, \\ (n, m) \neq (0, 0)}} \left( \frac{1}{(\zeta + m + n\tau)^2} - \frac{1}{(m + n\tau)^2} \right). \quad (\text{II.10})$$

This function has a double pole at every lattice point, and is doubly periodic,  $\wp(\zeta; \tau) = \wp(\zeta + 1; \tau) = \wp(\zeta + \tau; \tau)$ . Therefore, this is a well-defined meromorphic function on the torus  $\mathbb{C}/\Lambda$ . Furthermore, the P-function satisfies the functional equation

$$\left( \frac{d}{d\zeta} \wp(\zeta; \tau) \right)^2 \equiv (\wp'(\zeta; \tau))^2 = 4\wp^3(\zeta; \tau) - g_2(\tau) \wp(\zeta; \tau) - g_3(\tau),$$

where  $g_{2,3}$  are the so-called Eisenstein series:

$$g_2(\tau) = 60 \sum_{\substack{n, m \in \mathbb{Z}, \\ (n, m) \neq (0, 0)}} (m + n\tau)^{-4}, \quad g_3(\tau) = 140 \sum_{\substack{n, m \in \mathbb{Z}, \\ (n, m) \neq (0, 0)}} (m + n\tau)^{-6}.$$

With this functional equation, it is now obvious that the map

$$\mathbb{C} \rightarrow \mathbb{P}_{231}, \quad \zeta \mapsto \begin{cases} [4^{2/3} \wp(\zeta; \tau) : 2 \wp'(\zeta; \tau) : 1], & \text{if } \zeta \notin \Lambda \\ [1 : 1 : 0], & \text{if } \zeta \in \Lambda \end{cases} \quad (\text{II.11})$$

identifies every point on the torus defined by  $\tau$  with a point of an elliptic curve in the form (II.9), with the coefficients given as  $f(\tau) = -4^{1/3} g_2(\tau)$ ,  $g(\tau) = -4 g_3(\tau)$ .

Conversely, given an elliptic curve defined by  $f$  and  $g$ , it is possible to extract the complex structure  $\tau$  defining the lattice  $\Lambda$ . The connection requires the so-called Klein's  $j$ -invariant or simply  $j$ -function,

$$j(\tau) = \frac{4 \cdot 24^3 f^3(\tau)}{4f^3(\tau) + 27g^2(\tau)}, \quad (\text{II.12})$$

which is an isomorphic  $SL(2, \mathbb{Z})$ -invariant mapping of the fundamental region (II.8) onto  $\mathbb{C} \cup \{\infty\}$ . The expansion of the  $j$ -function,  $j(\tau) = \exp(-2\pi i \tau) + 744 + 196884 \exp(2\pi i \tau) + \dots$ , signals that for  $\tau \rightarrow i\infty$ , the  $j$ -function diverges. Indeed, the vanishing of the numerator,

$$\Delta := 4f^3 + 27g^2, \quad (\text{II.13})$$

is tied to the degeneration of the elliptic curve (II.9), which is precisely the case when the derivatives  $\partial_{x,y,z} P_T$  vanishes together with  $P_T$ . Therefore, by describing a torus through the Weierstrass equation (II.9), the degeneration of the torus, i.e. the divergence of  $\tau$ , is equivalent to the vanishing of the discriminant  $\Delta$  (II.13).

A way to visualise an elliptic curve defined by a Weierstrass equation is by going to inhomogeneous coordinates  $[x : y : 1]$  in  $\mathbb{P}_{231}$ , such that the point  $[1 : 1 : 0]$  lies at infinity. Then one can plot the real parts of the solution. Compared to visualisations of the torus, this depiction can easily differentiate between different types of singularities, cf. figure II.4.

<sup>10</sup>The usual definition of this weighted projective space is as a quotient  $(\mathbb{C}^3 - \{0\}) / \simeq$ , where the equivalence relation is the scaling  $(x, y, z) \simeq (\lambda^2 x, \lambda^3 y, \lambda z)$  with any  $\lambda \in \mathbb{C} - \{0\}$ .

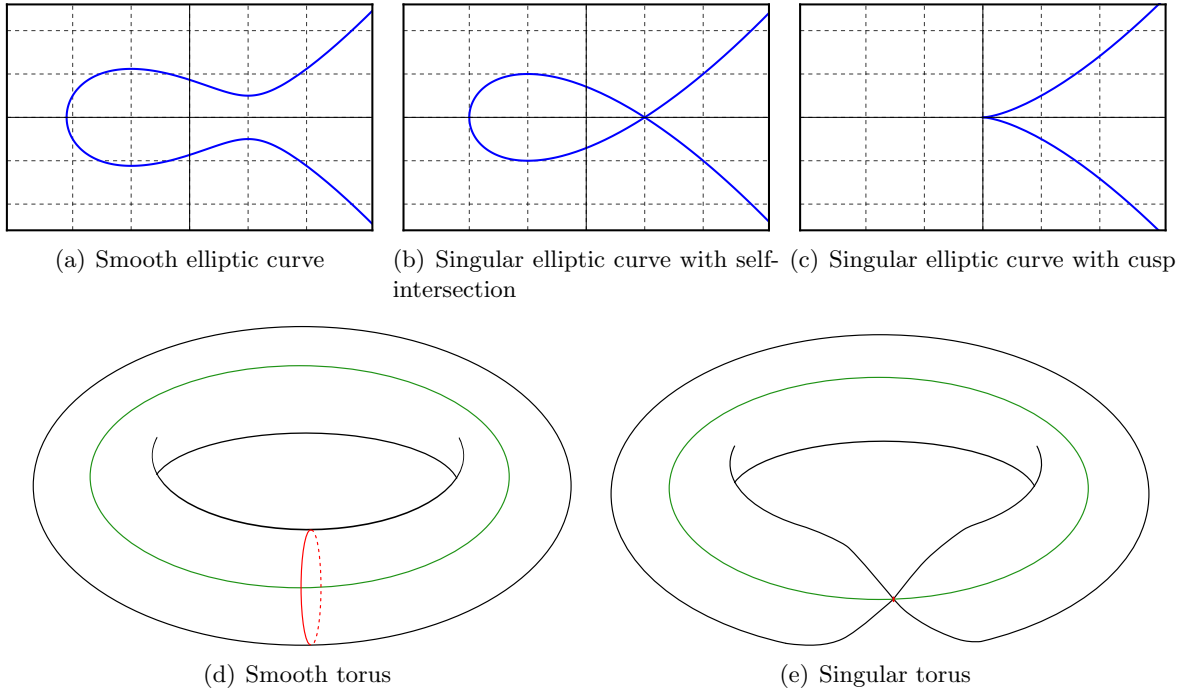


**Figure II.4:** A smooth elliptic curve (a) corresponding to a smooth torus (d). Different singularity types of elliptic curves (b) and (c) correspond to singular tori (e) with different severity of ‘pinching’ (i.e. the shrinking of a cycle).

## 2.2 Torus fibrations

Given the above analysis, it seems tantalising to identify the axio-dilaton in type IIB compactifications with the complex structure of a torus that varies over the compact space, which we shall call  $\mathcal{B}$  here.<sup>11</sup> In mathematics, such a structure is known as a fibration. Concretely, a fibration is a collection of spaces  $(Y, \mathcal{B}, \mathfrak{f})$  with a projection map  $\pi : Y \rightarrow \mathcal{B}$ , such that for any point  $b$  of the base  $\mathcal{B}$ , the pre-image  $\pi^{-1}(b)$  is ‘equivalent’<sup>12</sup> to  $\mathfrak{f}$ , the *fibres*. To each base point  $b$  we can assign the complex structure  $\tau(b)$  of the torus fibre  $\pi^{-1}(b)$ . Clearly  $\tau(b)$  is a function on  $\mathcal{B}$ , called the  $\tau$ -function. Such a structure can be summarised in a diagram as

$$\begin{array}{ccc} \mathfrak{f} & \longrightarrow & Y \\ & & \downarrow \pi \\ & & \mathcal{B} \end{array} \tag{II.14}$$

For our type IIB set-up, where the fibre  $\mathfrak{f}$  is a torus, the *total space*  $Y$  is called a torus fibration (or said to be torus-fibred). While the generic fibre is a smooth torus, the fibres can be singular in special loci on  $\mathcal{B}$ . For these loci, we necessarily have  $\Delta = 0$ . In some extreme cases, we can even have that the fibre  $\pi^{-1}(b_0)$  over certain points  $b_0 \in \mathcal{B}$  no longer a curve (complex dimension one), but a higher dimensional objects. A fibration with such fibres are called non-flat. Since many mathematical results rely on a flat fibration structure, F-theory has been studied so far almost exclusively on flat fibrations only, while disregarding any non-flat fibration encountered in

<sup>11</sup>Recall that  $\tau$  is constant (in fact divergent) in the non-compact spacetime directions, as these are filled with 7-branes in compactification models.

<sup>12</sup>The equivalence is essentially given by homotopy equivalence. For some intuition, simply replace ‘equivalent’ with ‘isomorphic’, in which case one obtains a fibre bundle. As we will see soon, we have to allow for some degeneracy of certain fibres, which requires the generalised notion of fibration.

explicit constructions. We will also follow this route throughout the thesis and implicitly assume all fibrations to be flat. However, there is some work in progress that attempts to understand the physics of non-flat fibres in F-theory [33].

### 2.2.1 The Weierstrass model

With the results from the previous section, a prototype – in fact *the* prototype – of a torus fibration is given by promoting the coefficients of the Weierstrass equation (II.9) to be functions of  $\mathcal{B}$ . While heuristically, it is obvious that this prescription describes a torus embedded into  $\mathbb{P}_{231}$  with varying shape, we would like to set up the mathematically correct description here.

To this end, we first consider a fibration  $X$  of the ambient space  $\mathbb{P}_{231}$  over  $\mathcal{B}$ . This amounts to identify the coordinates with suitable functions of the base. To be precise, they have to transform as sections of certain line bundles defined over  $\mathcal{B}$  under projective rescalings of the base.<sup>13</sup> In anticipation of the Weierstrass equation, we fix a line bundle  $\mathcal{L}$  and pick  $x$  to be a section of  $\mathcal{L}^2$  and  $y$  to be a section of  $\mathcal{L}^3$ ;  $z$  will be section of the trivial bundle  $\mathcal{O}$ . In order for the Weierstrass polynomial  $P_T = y^2 - x^3 - f x z^4 - g z^6$  to have the correct scaling,  $f$  therefore must be a section of  $\mathcal{L}^4$  and  $g$  a section of  $\mathcal{L}^6$ . For every point  $b \in \mathcal{B}$ , the vanishing of the Weierstrass polynomial  $P_T$  defines a torus  $T^2$  as a fibre, which is embedded into the fibre ambient space  $\mathbb{P}_{231}$ :

$$\begin{array}{ccccc}
 T^2 & \hookrightarrow & \mathbb{P}_{231} & \longrightarrow & X \\
 & \searrow & & \nearrow & \downarrow \pi_X \\
 & & Y & \xrightarrow{\pi_Y} & \mathcal{B}
 \end{array} \tag{II.15}$$

In this representation, the torus fibration  $Y$  can also be seen as a hypersurface defined by the vanishing of the Weierstrass polynomial inside  $X$ :

$$Y = \{y^2 - x^3 - f x z^4 - g z^6 = 0\} \subset X. \tag{II.16}$$

Such a torus fibration is known as a Weierstrass model. A key property of the Weierstrass model is the existence of a special point on every fibre given by the intersection  $Y \cap \{z = 0\} = \{y^2 - x^3 = z = 0\}$ . Note first that on this intersection, neither  $x$  nor  $y$  can vanish, because then all three fibre coordinates would be zero, which is forbidden for the homogeneous coordinates of  $\mathbb{P}_{231}$  (see footnote 10). Thus, we can use the scaling relation of  $\mathbb{P}_{231}$  to set  $y$  to 1, implying that also  $x$  must be 1. Therefore, we can associate to base point  $b \in \mathcal{B}$  the  $[1 : 1 : 0]$  in the fibre over  $b$ :

$$\text{Sec}_0(b) := [1 : 1 : 0] \in \pi_Y^{-1}(b) \cong T^2 \subset \mathbb{P}_{231}. \tag{II.17}$$

Such a map  $\text{Sec} : \mathcal{B} \rightarrow Y$  is known as a section of the fibration: It satisfies the condition  $\pi_Y \circ \text{Sec} = \text{id}_{\mathcal{B}}$ . Torus fibrations with sections are known as elliptic fibrations. Historically, F-theory was studied first on elliptic fibrations, as for these, there are much more rigorous mathematical results than for general torus fibrations without sections. For a Weierstrass model, we can use the discriminant formula (II.13) to find the locus  $\{\Delta = 0\} \equiv \{\Delta\} \subset \mathcal{B}$  over which the torus fibre degenerates. For more general types of torus fibrations, there is an analogous locus  $\{\Delta\}$  of singular fibres. In all examples, where the fibration is given as the vanishing locus of a polynomial  $P$ , similar to (II.16), one can determine an expression for  $\Delta$  in terms of the coefficients of  $P$  by finding the loci where all partial derivatives of  $P$  vanishes.

<sup>13</sup>Recall that for SUSY preservation,  $\mathcal{B}$  has to be a Kähler manifold. In simple terms, all our Kähler manifolds can be embedded into a projective space; the sections must therefore transform appropriately under the scaling relations of the embedding space.

### 2.2.2 Torus fibrations as hypersurfaces

The classes of fibrations we consider follow the structure of the Weierstrass model: We embed the torus fibre as an elliptic curve  $\mathbb{E}$  in some complex two-dimensional projective fibre ambient space  $\mathbb{A}$  with homogeneous coordinates  $x_i$ , which itself is a fibration  $X$  over  $\mathcal{B}$ :

$$\begin{array}{ccccc}
 \mathbb{E} & \hookrightarrow & \mathbb{A} & \longrightarrow & X \\
 & \searrow & & \nearrow & \downarrow \pi_X \\
 & & Y & \xrightarrow{\pi_Y} & \mathcal{B}
 \end{array} \tag{II.18}$$

Again, the torus fibration  $Y$  is given as a hypersurface in  $X$ , i.e. the vanishing of a homogeneous polynomial  $P$  with variables  $x_i$ . The coefficients of  $P$  are sections of line bundles over  $\mathcal{B}$ , such that for any point  $q \in \mathcal{B}$ , the solutions of  $P|_q = 0$  give rise to an elliptic curve in  $\mathbb{A}$ . Given an ambient space  $\mathbb{A}$ , the generic polynomial that cuts out an elliptic curve is easily determined: Since the torus is a compact Ricci-flat Kähler manifold, it is actually a Calabi–Yau space of complex dimension one. In fact, tori are the only dimension one Calabi–Yau manifolds. Since Calabi–Yau manifolds must have vanishing first Chern class, this gives an algebraic criterion on the polynomial  $P$ . Concretely, via the adjunction formula one can explicitly compute the first Chern class of the curve  $\mathbb{E}$  cut out by  $P$  inside  $\mathbb{A}$ . The Calabi–Yau condition then restricts only the presence of certain monomials in  $P$ .

For a weighted projective space, this condition is very simple: The sum of the weights of any monomial must be equal to the combined weight of all homogeneous coordinates of  $\mathbb{A}$ . For example, in the fibre ambient space of the Weierstrass model (II.15), the coordinates  $x, y$  and  $z$  have weights 2, 3, and 1, respectively, under the scaling  $(x, y, z) \simeq (\lambda^2 x, \lambda^3 y, \lambda z)$ . The sum is therefore 6, which is the same weight the Weierstrass polynomial  $P_W$  (II.9) has. Thus, the curve defined by  $\{P_W = 0\} \subset \mathbb{P}_{231}$  is a torus/elliptic curve. In this thesis, we will encounter fibrations defined by tori embedded into three other fibre ambient spaces:  $\mathbb{P}_{112}$ ,  $\text{Bl}_1\mathbb{P}_{112}$  and  $\text{Bl}_2\mathbb{P}^2$ . Note that out of these, the fibration with  $\mathbb{A} = \mathbb{P}_{112}$  does not have a section, i.e. is not an elliptic fibration. Nevertheless, since it is given by a polynomial, we can determine the discriminant locus as explained above.

### 2.2.3 Connection to type IIB

Before we continue with technical details, let us pause briefly to fully appreciate the consequences for our understanding of type IIB compactifications. The advantage of the mathematical description using torus fibrations is that a globally consistent fibration automatically takes care of all back-reactions originating from 7-branes. Physically it means that conditions like local (7-brane) tadpole cancellation, which in previous type IIB models had to be ensured ‘by hand’, are now naturally satisfied thanks to the geometric description. In turn, the back-reaction effects – which can be seen as non-perturbative effects stemming from the finite value of  $g_s$  – will in general lead to the splitting of perturbative D7-branes and O7-planes into  $(p, q)$ -branes, which localise along complicated loci in the compact space  $\mathcal{B}$ . Thanks to the mathematical tools, we can nevertheless determine their position by examining the discriminant  $\Delta$ . As we will discuss in section 2.4.2, the types of branes and the gauge symmetries on their world-volume can be inferred from the monodromy behaviour of  $\tau$  around the components of  $\{\Delta = 0\}$ .

While these connections between type IIB compactifications and torus fibrations are quite intuitive, the description so far lacks rigorous tools for extracting physical data from the geometry. These tools are provided by the duality between type IIB and M-theory. In fact, a proper way of *defining* F-theory is through its M-theory description.

### 2.3 Defining F-theory via M-theory

Recall from figure II.2 that M-theory is connected to type IIB string theory via duality relations to type IIA. To understand the connection to F-theory, we need to briefly outline this duality chain. We will work on the level of supergravity theories, where the dualities are explicitly given in terms of the field content and the effective actions. All statements are believed to hold beyond the low energy limit.

First, we consider 11D SUGRA compactified on a torus  $T^2 = S_A^1 \times S_B^1$ . Suppose the remaining nine dimension are flat Minkowski space  $\mathbb{R}^{1,8}$ , then the duality relations implies that in the low energy limit we have type IIA SUGRA on  $\mathbb{R}^{1,8} \times S_B^1$ . By performing a T-duality (II.5), i.e. replacing  $S_B^1$ , which has radius  $R_B$ , with an other circle  $\tilde{S}_B^1$  of radius  $\tilde{R}_B = \alpha'/R_B$ , we obtain a T-dual type IIB SUGRA on  $\mathbb{R}^{1,8} \times \tilde{S}_B^1$ . In particular, in the decompactification limit  $\tilde{R}_B \rightarrow \infty$ , or equivalently  $R_B \rightarrow 0$ , the circle  $\tilde{S}_B^1$  becomes a flat line of infinite length, thus we recover type IIB in  $\mathbb{R}^{1,9}$ . From the 11D perspective, we can perform this limit by keeping the complex structure  $\tau \sim R_A/R_B$  of the torus fixed and shrink its area (i.e. Kähler parameter) which is proportional to  $R_A R_B \sim R_B^2$ .

By carefully reducing the 11D SUGRA fields along the compactification torus à la Kaluza–Klein and tracing the result through the duality chain, it turns out that the axio-dilaton of type IIB is precisely given by the complex structure parameter  $\tau$  of the compactification torus. Meanwhile, the area or Kähler parameter of the torus controls the KK mass scale in the compactification of type IIB to  $\mathbb{R}^{1,8} \times \tilde{S}_B^1$ . By taking this scale to 0, all KK modes become light again and re-arrange themselves into the massless modes of the 10D theory, thus effectively describing the decompactification limit in terms of the matter spectrum. Therefore, we end up with the equivalent description of type IIB string theory in  $\mathbb{R}^{1,9}$  as M-theory on  $\mathbb{R}^{1,8} \times T^2$ , where we take the limit of vanishing torus area while keeping its complex structure fixed.

This duality extends directly to compactifications  $\mathbb{R}^{1,9-d} \times \mathcal{B}$  of type IIB on a compact manifold  $\mathcal{B}$  of (real) dimension  $d$  with varying axio-dilaton  $\tau$ . In this case, the dual M-theory description is a compactification on  $\mathbb{R}^{1,8-d} \times Y$ , where  $Y$  is a torus fibration over  $\mathcal{B}$ . The above limit of shrinking the torus area (also referred to as torus volume) to 0 has now to be performed fibre-wise. By doing so, one direction of  $Y$  ‘grows’ into a non-compact spatial dimension, which combines with the other non-compact dimension into the type IIB spacetime  $\mathbb{R}^{1,9-d}$ . This can be now seen as the **definition** of F-theory:

*F-theory on a torus fibration  $\pi : Y \rightarrow \mathcal{B}$  is defined to be the type IIB compactification on  $\mathcal{B}$  dual to M-theory compactified on  $Y$  in the limit of zero fibre volume.* (II.19)

In contrast to the type IIB description, in which it was merely a book-keeping device, the torus has become a part of the physical space in the M-theory definition of F-theory. Via M-theory, we now have much more rigorous methods to extract physical data from the torus fibration  $Y$  than in the type IIB picture. In particular, there is an additional element in the duality chain that turns out to be extremely helpful in our understanding of F-theory compactifications to  $\mathbb{R}^{1,n}$ . If we compactify M-theory on  $Y$  without taking the limit of zero fibre volume, then we obtain a theory in one dimension lower. This theory on  $\mathbb{R}^{1,n-1}$  is connected to the F-theory model on  $\mathbb{R}^{1,n}$  via a further compactification on a circle. With this element, we can study many aspects of F-theory by analysing the theory in  $\mathbb{R}^{1,n-1}$ . Taking the limit of zero fibre volume is often also referred to as the F-theory limit (of M-theory compactified on  $Y$ ).

One particularly important question that can be answered by this approach is how much spacetime supersymmetry is preserved in F-theory compactifications. For example, it is known that 4D  $\mathcal{N} = 1$  SUSY is equivalent to  $\mathcal{N} = 2$  in 3D. Therefore, if we want to obtain an  $\mathcal{N} = 1$  in 4D from F-theory compactification on  $Y$ , the corresponding M-theory compactification on  $Y$  must preserve at least  $\mathcal{N} = 2$  SUSY in 3D. This constrains the geometry of  $Y$  to be a Calabi–Yau

manifold of complex dimension four. Similarly, by studying theories in 5D, we know that F-theory compactified on an Calabi–Yau threefold gives rise to an  $\mathcal{N} = 1$  theory in 6D. Generically, the base  $\mathcal{B}$  needs not to be Calabi–Yau, but has to still be Kähler. Note that this is not in contradiction to type IIB, since also there, the presence of 7-branes on  $\mathcal{B}$  will render the space non-Calabi–Yau.

In terms of torus fibrations defined as hypersurfaces in an ambient space (II.18), the Calabi–Yau condition can be translated into the choice of line bundles for the coefficients of the hypersurface. E.g. in the Weierstrass model with hypersurface (II.16), we have seen that the coefficients  $f, g$  are sections of powers of an a priori arbitrary line bundle  $\mathcal{L}$ . In order for the resulting fibration  $Y$  to be Calabi–Yau, the line bundle must be the anti-canonical bundle  $c_1(\mathcal{B}) \equiv \bar{\mathcal{K}}$ .

Equipped with the M-theory description, we can now give a (physically) rigorous description of F-theory compactifications with gauge symmetries and matter states.

### Massless states in M-theory

Massless states in  $\mathbb{R}^{1,n}$  will in general reduce upon circle reduction to massless states in  $\mathbb{R}^{1,n-1}$  accompanied by a tower of massive KK modes. Therefore, we should find to each massless state of F-theory compactified on  $Y$  a corresponding massless state in M-theory compactified on  $Y$ .

In M-theory compactifications on  $\mathbb{R}^{1,10-2d} \times Y_d \equiv M \times Y_d$ , with  $d = \dim_{\mathbb{C}} Y_d$ , one source for such massless states is the dimensional reduction of the 3-form  $C_3$ . Concretely, for a basis of 2-forms  $\omega_i$  and a basis  $\eta_j$  of 3-forms,  $C_3$  can be expanded as

$$C_3 = \sum_i A_i \wedge \omega_i + \sum_j \alpha_j \eta_j, \quad (\text{II.20})$$

where the  $A_i$  are 1-forms, i.e. vector fields on  $M$ , and  $\alpha_j$  are scalars. The vectors and scalars will only be massless if they are zero eigenfunctions of the Laplace operator  $\square$ . With the compactification ansatz  $M \times Y_d$ , the Laplacian simply splits into the sum  $\square_M + \square_Y$  of the Laplacian for each factor. For  $\square(A_i \wedge \omega_i + \alpha_j \eta_j) = \square_M(A_i + \alpha_j) + \square_Y(\omega_i + \eta_j) = 0$ ,  $\omega_i$  and  $\alpha_j$  must therefore be harmonic forms, i.e.  $\square_Y \omega_i = 0 = \square_Y \eta_j$ .<sup>14</sup> These harmonic forms are of course precisely counted by the de Rham cohomology. In the following, when we speak of ( $p$ -)forms on  $Y_d$ , we will always mean the cohomology class represented by this form, unless otherwise stated.

The scalars  $\alpha_j$  fall into two categories. Those that arise from 3-forms  $\eta_j$  which are pull-backs of 3-forms  $\eta_j^{(\mathcal{B})}$  from the base of the fibration correspond to so-called bulk  $U(1)$ s, which in the type IIB picture arise from the reduction of the 4-form  $C_4$  (see table II.1) along  $\eta_j^{(\mathcal{B})}$  [34]. The other 3-forms that are not pull-backs of the base give rise to axionic chiral multiplets in the effective theory on  $M$  [35]. As neither of them give rise to non-abelian gauge symmetries and matter charged under those, we will focus our attention on the vectors  $A_i$  coming from 2-forms  $\omega_i$ .

On a Calabi–Yau manifold, the geometry only allows for non-trivial 2-forms of Hodge type  $(1, 1)$ . These in turn are Poincaré-dual to divisors. Therefore, for any independent divisor class, we have an associated massless vector field in the M-theory compactification on  $Y_d$ . However, not all of them lift to vector fields in the F-theory limit. In fact, in the for us most relevant case of F-theory on a fourfold  $Y_4$ , it can be shown [34] that for so-called vertical divisors  $D^{(\mathcal{B})}$  of  $Y_4$ , which are the pre-image of divisors of the base  $\mathcal{B}^{15}$ , the associated vectors  $A_i$  are Hodge dual

<sup>14</sup>Note that we have assumed that none of the fields in the non-compact directions is tachyonic, i.e. have negative eigenvalue under the Laplace operator  $\square_M$ . For a compact Riemannian manifold, as  $Y_d$  is, all eigenvalues of the Laplacian are non-negative.

<sup>15</sup>A vertical divisor is of the form  $\pi^{-1}(D^{(\mathcal{B})})$  with  $D^{(\mathcal{B})}$  a divisor of the base  $\mathcal{B}$ ; it is common to use to abusive notation  $D^{(\mathcal{B})} \equiv \pi^{-1}(D^{(\mathcal{B})})$ . From the perspective of  $Y_d$ , one can also define vertical divisors  $D^{(\mathcal{B})}$  as a divisor of  $Y_d$  satisfying  $\pi^{-1}(\pi(D^{(\mathcal{B})})) = D^{(\mathcal{B})}$ .

(in  $\mathbb{R}^{1,2}$ ) to scalars, which lift to Kähler moduli fields in  $\mathbb{R}^{1,3}$ , i.e. fields whose value parametrise the Kähler structure (e.g. the volume) of  $D^{(\mathcal{B})}$ . We are interested in genuinely 4D vectors that belong to a vector multiplet and therefore can be associated with a gauge field. These can only arise from divisors of  $Y_4$ , which do not originate from the base. Since such divisors are necessarily associated with the fibration structure, they are usually referred to as fibral divisors.

In addition to the  $C_3$  field, M-theory also has BPS states in form of M2- and M5-branes. These can be wrapped on submanifolds  $Z$  of  $Y_d$  of various dimensions. In particular, wrapping M2-branes on holomorphic curves, i.e. complex submanifolds  $Z$  of (complex) dimension one, give rise to states in the effective theory in  $\mathbb{R}^{1,10-2d}$  preserving spacetime SUSY. Note that in particular, the reduction of the two spatial dimensions of the M2-brane along the internal manifold leaves only a time-like direction of the M2-brane's world-volume in  $\mathbb{R}^{1,10-2d}$ , so these states are point-like in the classical limit. In particular, they are charged under 1-form fields, i.e. gauge symmetries, in  $\mathbb{R}^{1,10-2d}$ . Since M2-branes have a finite tension, these states will only be massless if the curve  $Z$  they wrap have zero volume. As we will see now, such shrunken curves appear naturally in singular torus fibrations.

## 2.4 F-theory on singular torus fibrations

In the type IIB description, we have seen that the axio-dilaton  $\tau$  diverges at the position of 7-branes. If we interpret  $\tau$  as the fibre's complex structure in a torus fibration, then the torus fibre must necessarily degenerate over 7-brane loci. As we have argued earlier, the position of these loci is given by the vanishing of the discriminant (II.13). This condition determines a (real) four-dimensional – or (complex) codimension one – submanifold of  $\mathcal{B}$  (in particular these are divisors of  $\mathcal{B}$ ). Away from this locus, the generic fibre over  $\mathcal{B}$  must be a smooth torus.<sup>16</sup> The singular fibres over  $\{\Delta = 0\} \equiv \{\Delta\}$  will in general lead to a singular total space  $Y_4$ . Typically, while singularities are crucial for certain physical aspects, we have to perform geometric modifications in order to study them, which in the process resolve the singularities. In the F-theory context, there are two approaches studied in the literature, the deformation and the blow-up picture. In this thesis we will work exclusively in the blow-up picture. For F-theory with deformation resolution, we refer to [36, 37]. As we will see in the following, the resolution of codimension one singularities, i.e. singularities of  $Y_4$  stemming from the generic (singular) fibre over the codimension one locus  $\{\Delta\}$ , allows for a direct description of non-abelian symmetries in F-theory.

### 2.4.1 Resolution by blow-ups

For simplicity, let us assume that the discriminant locus  $\{\Delta = 0\}$  is irreducible, i.e. it is divisor  $\Theta = \{\theta\}$  given by vanishing of a meromorphic function  $\theta$  of the base  $\mathcal{B}$ . If  $\{\Delta\}$  is reducible, i.e. a collection of divisors  $\Theta_i$ , then one has to perform the resolution process for each component individually.

The idea of a blow-up resolution is to introduce a set of so-called exceptional divisors  $\text{Ex}_i$  in a new total space  $\hat{Y}_4$ , which under the projection  $\pi : \hat{Y}_4 \rightarrow \mathcal{B}$  map to the divisor  $\Theta$  of the base. In other words, these divisors are themselves fibrations  $\tilde{\pi}_i : \text{Ex}_i \rightarrow \Theta$ , where the fibre over a generic point of  $\Theta$  is isomorphic to a  $\mathbb{P}^1$ , possibly with a non-trivial multiplicity  $m_i$ . Over a generic  $t \in \Theta$ , the fibre  $\mathbb{P}^1$ s are ‘inserted’ at the singular point of the torus fibre of  $Y_4$  over  $t$ . In the schematic figure II.4(e), the singular point is marked red. Note that in particular, the singular torus has the topology of a 2-sphere, i.e. a  $\mathbb{P}^1$ , if we disregard the singular point. Thus, after the introduction of the exceptional divisors, the full fibre is now a collection of  $\mathbb{P}^1$ s pasted together in points (cf. picture II.5; the original torus is marked in red). Depending on the severity of  $Y_4$ 's singularity over  $\Theta$ , the (finite) number of divisors  $\text{Ex}_i$  and how their fibre  $\mathbb{P}^1$ s are pasted

<sup>16</sup>In the context of spaces carrying a natural measure (e.g. induced by the metric on a Riemannian manifold and its submanifolds), ‘non-generic’ points can be understood as subsets with zero measure.



together will vary. After the process, the resulting total space  $\hat{Y}_4$  is now smooth. Note that does not mean that the fibres over  $\Theta$  are now smooth! In general they are still singular. After all, they are a collection of  $\mathbb{P}^1$ s which intersect amongst themselves. For these fibres, the individual  $\mathbb{P}^1$ s are referred to as the (irreducible) components of the fibre. The full (reducible) fibre is usually referred to as a singular fibre. Despite the fibres having these so-called normal crossing singularities, they are mild enough such that the total space is smooth. Crucially, the exceptional divisors are not vertical divisors of  $\hat{Y}_4 \xrightarrow{\pi} \mathcal{B}$ , because  $\pi(\text{Ex}_j) = \Theta$ , but  $\pi^{-1}(\Theta)$  contains all  $\mathbb{P}^1$ s from the other  $\text{Ex}_j$ .

The  $\mathbb{P}^1$ s introduced in the resolution process can be regarded as being present already in the singular geometry  $Y_4$ , however with zero size. The resolution process then amounts for ‘blowing up’ these  $\mathbb{P}^1$ s like balloons, explaining the name of this resolution method. In mathematical terms, the singular fibration  $Y_4$  is obtained as a limit of the smooth  $\hat{Y}_4$  by taking the Kähler parameters that control the sizes of the exceptional  $\mathbb{P}^1$ s to zero. Being the inverse to the blow-up process, this limit is usually called the blow-down. In general, there are multiple resolutions  $\hat{Y}_4$  which blow-down to the same singular limit  $Y_4$ . Consequently, the physics of F-theory on the singular fibration  $Y_4$  is independent of the chosen resolution  $\hat{Y}_4$ .

Note that not all resolutions  $\hat{Y}_4$  are physically allowed. In order for the compactification on  $\hat{Y}_4$  to still give an supersymmetric theory, we must maintain the Calabi–Yau condition. This condition constraints the types of singularities one can have. In particular, while through the above resolution process we have generally taken care of codimension one singularities, the total space might still be singular as a result from unresolved singularities in higher codimension. In general, resolution of all higher codimension singularities is a difficult task on a purely mathematical level. In addition, these might violate the Calabi–Yau condition or render the fibration non-flat – two undesired outcomes. Luckily, there is a subclass of singular  $Y_4$  which can be fully resolved by blowing up all codimension one singularities. The resolutions  $\hat{Y}_4$  are determined with so-called tops in the framework of toric geometry (see section 2.6 for a short overview). This framework gives a simple combinatorial description of the geometry after the resolution process. In particular, it can be algorithmised with computer algebra programs like `Sage`. Since all our examples will be constructed in this framework, we will for the sake of simplicity assume in the following that the resolution of all codimension one singularities with exceptional divisors will lead to a fully smooth, flat torus-fibred Calabi–Yau  $\hat{Y}_4$ . A resolution that preserves the Calabi–Yau condition, or more general preserves the first Chern-class is called a crepant resolution. Finally, note that in all situations relevant to us, the resolved fourfold  $\hat{Y}_4$  is still a fibration over  $\mathcal{B}$ , i.e. the resolution process leaves the base unchanged. However, it should be stressed that in certain situations, where the full resolution of the total space requires modifications of the base  $\mathcal{B}$ . In fact, these types resolutions have been studied and understood mainly for F-theory compactifications to 6D [38–41].

### 2.4.2 Kodaira’s classification of codimension one singularities

The systematics behind codimension one singular fibres of elliptic fibrations have a beautiful mathematical description. Although usually referred to as Kodaira’s classification [42, 43], it should be noted that Néron independently obtained the same results [44]. The original works classified the singular fibres of elliptic surfaces, i.e. elliptic fibrations over a (complex) one-dimensional base  $\mathcal{B}$ . We will first present the results for this case, before explaining how it generalises to higher dimensional bases and in particular for torus fibrations that are not elliptic fibrations.

For an elliptic surface  $Y_2$ , the discriminant locus  $\{\Delta\}$  just consists of isolated points, so all singularities are of codimension one. The exceptional divisors resolving the singularities are simply  $\mathbb{P}^1$ s in the fibre over the points of  $\{\Delta\}$  with certain multiplicities. Kodaira and Néron showed that in the resolved surface  $\hat{Y}_2$ , the fibres over  $b \in \{\Delta\}$  are now chains of  $\mathbb{P}^1$ s intersecting each other in the form of the affine ADE Dynkin diagrams – the same diagrams used to classify semi-simple Lie

groups (see figure II.5).<sup>17</sup> In particular, the number of the exceptional  $\mathbb{P}^1$ s correspond to the rank of the corresponding Lie group  $G$ , and the multiplicities of each of the  $\mathbb{P}^1$  components match the Dynkin label of the corresponding node in the Dynkin diagram. Furthermore, the intersection number  $\mathbb{P}_i^1 \cdot \mathbb{P}_j^1$  form the Cartan matrix of  $G$ . The original analysis of Kodaira also includes an explicit criterion of determining the explicit Dynkin diagram in terms of the vanishing orders of the Weierstrass coefficients  $f, g$  and the discriminant  $\{\Delta\}$  at  $b$ .

For a physicist, this is a remarkable result! By geometrising the axio-dilaton of type IIB through torus fibrations, we are led purely by mathematics to the core objects of gauge symmetries, which we expected to find on 7-branes. Indeed, the identification goes further. For each singular fibre over a base point  $b$  with a particular Dynkin diagram, there is an associated gauge group. Kodaira's classification results tell us that the  $SL(2, \mathbb{Z})$  monodromy of  $\tau$  around  $b$  precisely matches the monodromy behaviour of the axio-dilaton around 7-brane configurations realising the same gauge group. While from a type IIB perspective, this seems to be enough evidence to 'believe' Kodaira's classification, we want to explicitly see how these non-abelian gauge groups arise from the definition (II.19) of F-theory through M-theory. Before presenting this analysis in the following section, let us briefly comment on the situation for higher dimensional elliptic and general torus fibrations

The original Kodaira classification shows that for elliptic surfaces, the associated gauge groups are only of ADE type, i.e.  $SU(n+1)$  ( $A_n$ -type),  $SO(2n)$  ( $D_n$ -type for  $n \geq 4$ ) and  $E_{6,7,8}$  (E-type). However, for higher dimensions, i.e. when  $\dim_{\mathbb{C}} \mathcal{B} \geq 2$ , we recover all other semi-simple Lie groups from codimension one singularities:

- the  $B_n$ -types corresponding to  $SO(2n+1)$  with  $n \geq 2$ ,
- the  $C_n$ -types corresponding to  $Sp(n)$  with  $n \geq 3$  (group of unitary  $2n \times 2n$  matrices preserving a symplectic bilinear form),
- the exceptional groups  $F_4$  and  $G_2$ .

The reason that these are only present in higher dimensions can be traced back to certain monodromy effects on the fibre components over the discriminant locus  $\{\Delta\}$ <sup>18</sup>, which is now of at least complex dimension one [46]. These monodromies map one  $\mathbb{P}^1$  component of a generic fibre at  $t \in \{\Delta\}$  onto an other component by transporting them along a non-trivial path within  $\{\Delta\}$ , thus effectively identifying them as the fibres of the same exceptional divisor. In a way, the identification of fibre components via monodromy is analogous to the folding of Dynkin diagrams of ADE type to obtain the diagrams for the above types [47]. The algebraic conditions in explicit fibrations to determine whether such monodromies exist are concisely presented in [41] within the F-theory literature.

In summary, by blowing up the singularities over an irreducible codimension one component  $\Theta$  of the discriminant locus  $\{\Delta\}$ , we introduce a set of exceptional divisors  $\text{Ex}_i \subset \hat{Y}_4$ . These are themselves fibrations over  $\Theta$ , whose generic fibre is a  $\mathbb{P}^1$  with multiplicity  $m_i$ . Over a generic point of  $\Theta$ , the intersection structure of these  $\mathbb{P}^1$ s is encoded by the Dynkin diagram and the Cartan matrix of a semi-simple Lie group, such that the number of exceptional divisors  $\text{Ex}_i$  equals the rank of the gauge group and the multiplicities  $m_i$  match the Dynkin labels of the corresponding diagram. The explicit Lie group is determined by the vanishing orders of  $(f, g, \Delta)$  along  $\Theta$  and certain monodromy conditions. Furthermore, the  $SL(2, \mathbb{Z})$  monodromy of  $\tau$  around  $\Theta$  matches the monodromy behaviour of the axio-dilaton around 7-branes realising the same symmetry group

<sup>17</sup>For simplicity, we will not differentiate between the gauge algebra, which can be read off from the singular fibres, and the actual gauge group. There can in general be several possibilities of the latter for a given gauge algebra, which differ in their global structure. The description of the global structure of gauge groups in F-theory have been thoroughly investigated in [45].

<sup>18</sup>Note that these are not the  $SL(2, \mathbb{Z})$  monodromies of  $\tau$ !

in non-perturbative type IIB. In table II.2, we have collected all possible cases of codimension one singular fibres and their corresponding Lie group.

While these results are only proven for elliptic fibred complex manifolds of dimension less than four, it is believed that they also hold in higher dimensions. In practise, the countless number of explicit fourfold constructions have only reproduced, but never exceeded the possibilities in table II.2. Similar observations were made in explicit models of non-elliptic torus fibrations, though in the literature there are much fewer such examples than for elliptic fibrations. In the following, we will therefore assume that Kodaira's classification extends to a general torus-fibred fourfold  $Y_4$ .

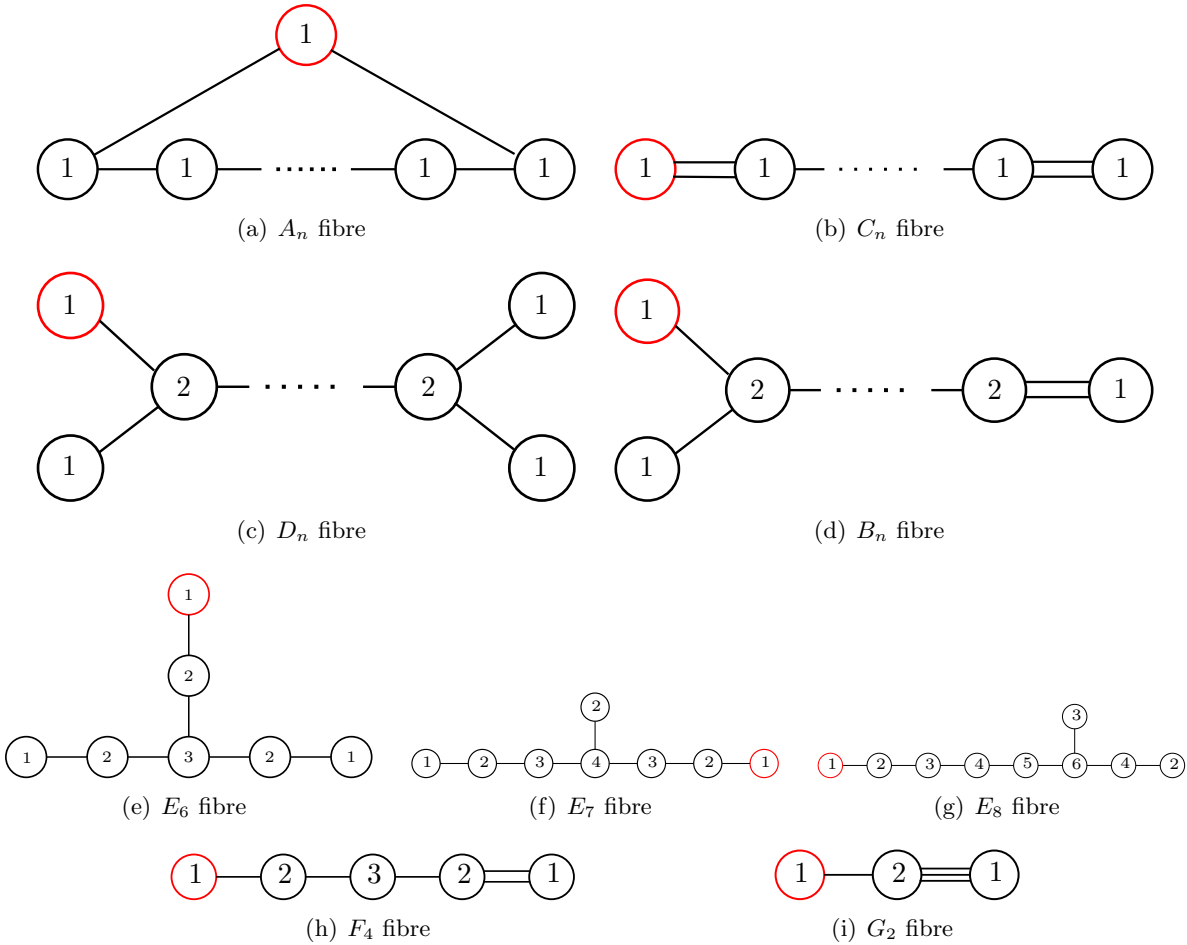


**Figure II.5:** The affine Dynkin diagrams corresponding to the codimension one singular fibres in torus fibrations. Each node represents a  $\mathbb{P}^1$  component, with the multiplicity indicated by the number. Each line is a intersection point between the attached  $\mathbb{P}^1$ s; multiple lines correspond to higher intersection numbers. The node in red marks the so-called affine node. This component of the fibre is the original pinched torus in the singular limit. Note that for the diagrams (a) – (d), the number  $n$  corresponds to the number of non-affine nodes. This is also the rank of the gauge group.

### 2.4.3 Non-abelian gauge symmetries in F-theory

To understand the origin of non-abelian gauge symmetries in F-theory, we consider M-theory compactified on a resolved fourfold  $\hat{Y}_4$ , which has the singular limit  $Y_4$ . Let us assume that resolution process has introduced exceptional divisors  $\text{Ex}_i \subset \hat{Y}_4$ ,  $i = 1, \dots, r$ , over an irreducible

name	Dynkin type	Lie group	ord( $f$ )	ord( $g$ )	ord( $\Delta$ )	comments
$I_0$	–	–	$\geq 0$	$\geq 0$	0	smooth fibre
$I_1$	–	–	0	0	1	‘mild’ sing. no ex. div’s
$I_2$	$A_1$	$SU(2)$	0	0	2	
$I_n, n \geq 3$	$A_{n-1}$ or $C_{\lfloor n/2 \rfloor}$	$SU(n)$ or $Sp(\lfloor n/2 \rfloor)$	0	0	$n$	possible monodromy
$II$	–	–	$\geq 1$	1	2	‘mild’ sing.
$III$	$A_1$	$SU(2)$	1	$\geq 2$	3	
$IV$	$A_2$	$SU(3)$	$\geq 2$	2	4	
$I_0^*$	$D_4, B_3$ or $G_2$	$SO(8), SO(7)$ or $G_2$	$\geq 2$	$\geq 3$	6	possible monodromies
$I_{2n-5}^*, n \geq 3$	$D_{2n-1}$ or $B_{2n-2}$	$SO(4n-2)$ or $SO(4n-3)$	2	3	$2n+1$	possible monodromy
$I_{2n-4}^*, n \geq 3$	$D_{2n}$ or $B_{2n-1}$	$SO(4n)$ or $SO(4n-1)$	2	3	$2n+2$	possible monodromy
$IV^*$	$E_6$ or $F_4$		$\geq 3$	4	8	possible monodromy
$III^*$	$E_7$		3	$\geq 5$	9	
$II^*$	$E_8$		$\geq 4$	5	10	
non-min.	–	–	$\geq 4$	$\geq 6$	$\geq 12$	

**Table II.2:** Kodaira’s classification of codimension one singularities of elliptic fibrations  $Y$ , supplemented with monodromy reduced cases for  $\dim_{\mathbb{C}} Y \geq 3$ . In case there are multiple possibilities due to monodromies, the **bold** entry indicates the original Kodaira result for elliptic surfaces. The explicit conditions determining which of the entries is realised geometrically can be found in [41]. Note that the last entry are so-called non-minimal singularities, which can not be resolved crepantly and in a flat manner.

component  $\Theta$  of the discriminant locus. Let  $G$  denote the Lie group with rank  $G = r$  that the classification result of table II.2 associates with the singular fibres over  $\Theta$ . We would like to argue in the following that in the singular limit, we obtain massless states filling the full adjoint representation of  $G$ , in which all gauge bosons of a  $G$ -gauge theory must sit.

By reducing the M-theory 3-form as in (II.20), with  $\omega_i$  the  $(1, 1)$ -form Poincaré-dual to  $\text{Ex}_i$ , we obtain a set of vector fields  $A_i$  in  $\mathbb{R}^{1,2}$ . These vector fields enjoy a symmetry  $A_i \rightarrow A_i + d\lambda$ , which originates from the analogous symmetry of  $C_3$  in M-theory (cf. section 1.3). Thus the  $A_i$  constitute rank  $G$  massless  $U(1)$  gauge fields. These  $U(1)$ s can be identified with the Cartan (maximal connected abelian) subgroup of  $G$ . The other degrees of freedom for a gauge field with gauge group  $G$  do not arise from  $C_3$  in the M-theory description. Instead, they originate from M2-branes, which upon compactification of M-theory on  $\hat{Y}_4$  can be wrapped on the  $\mathbb{P}^1$  components of the singular fibres over  $\Theta$ . The excitations of these wrapped M2-branes look like point-particle excitations of the effective theory in the non-compact dimensions. Recall from section 1.3 that M2-branes are charged electrically under  $C_3$  by simply integrating  $C_3$  over the M2-world-volume. In particular, if  $C_3 = \sum_i A_i \wedge \omega_i$ , then the coupling between  $C_3$  and M2-branes wrapped on a fibre  $\mathbb{P}_j^1$  of  $\text{Ex}_j$  leads to a charge of the M2-states under the  $U(1)$  field  $A_i$  in the effective theory. The charge is explicitly given as  $q_{j;i} = \int_{\mathbb{P}_j^1} \omega_i$ .

To compute this integral, we use Poincaré-duality between cohomology forms and homology cycles and re-interpret the charge as an intersection number (cf. appendix A). Concretely, since  $\omega_i$  is Poincaré-dual to the exceptional divisor  $\text{Ex}_i$ , the charge is simply the intersection number of the fibre  $\mathbb{P}_j^1$  and this divisor. Now  $\mathbb{P}_j^1$  is just a fibral curve of  $\text{Ex}_j$  over a generic point  $b \in \Theta \subset \mathcal{B}$ . Therefore, the intersection with  $\text{Ex}_i$  must be also localised in the fibre over  $b$ , and is given as the intersection of  $\mathbb{P}_j^1$  with the fibral curve  $\mathbb{P}_i^1$  of  $\text{Ex}_i$ . But by Kodaira's classification, their intersection numbers corresponds to the Cartan matrix  $C_{ij}$  of  $G$ :

$$\int_{\mathbb{P}_j^1} \omega_i = \mathbb{P}_i^1 \cdot \mathbb{P}_j^1 = \mathbb{P}_j^1 \cdot \mathbb{P}_i^1 = -C_{ij}.$$

From basic representation theory it is known that the columns/rows of the Cartan matrix represent the Cartan charges of the simple roots of  $G$ , which are in particular weights of the adjoint representation of  $G$ . Thus, states from M2-branes wrapped on  $\mathbb{P}_j^1$  correspond to a weight vector  $\mathbf{w}_i = -C_{ij}$  of the adjoint rep. In field theory terms, these states are the W-bosons of  $G$ . Since the simple roots generate the full adjoint rep, we therefore obtain all states of the adjoint representation of  $G$  by wrapping M2-branes on  $\mathbb{P}_j^1$ s and suitable chains  $\Gamma$  of  $\mathbb{P}_j^1$ s with both orientations (M2-branes wrapping with the opposite orientation differ by a minus-sign in their weight vectors).<sup>19</sup> Clearly, not arbitrary combinations of  $\mathbb{P}_i^1$ s can be allowed to be wrapped by M2-branes, as this would give rise to infinitely many weight states. Somewhat surprisingly, there is no proposal for a first principle argument on how to restrict the possible linear combinations of fibral  $\mathbb{P}^1$ s to those chains  $\Gamma$  that can be wrapped by M2-branes to give the desired states. Until now, there are only some ad hoc conditions [40]. However, there is some work in progress [48] trying to understand these conditions from a more fundamental point of view.

In any case, let us assume that M2-branes are allowed to wrap precisely those fibre  $\mathbb{P}^1$  combinations that give rise to the full adjoint representation. In the resolved geometry  $\hat{Y}_4$ , the  $\mathbb{P}^1$ s have finite size, thus states from M2-branes wrapped on these will have finite mass due to the non-zero tension of M2s. However, taking the singular limit precisely amounts to sending the size of those  $\mathbb{P}^1$ s to 0, i.e. all the adjoint states become massless. Thus, in the singular limit of M-theory on  $\hat{Y}_4$ , i.e. M-theory on  $Y_4$ , the massless spectrum contains a full adjoint representation of  $G$ . Finally, we have to perform the F-theory limit and lift everything to 4D. In this process,

<sup>19</sup>Strictly speaking, we only obtain all weights with non-zero entries. However, the adjoint of  $G$  generally has rank  $G$  weights that have only zeroes as entries. These weights of course correspond to the Cartan subgroup, which, as we have seen, arise in the M-theory compactification from reduction of  $C_3$ .

we have to make sure that these adjoint states lift to a vector multiplet representation of 4D  $\mathcal{N} = 1$  SUSY. Such an analysis is highly non-trivial and involves the study of so-called twisted super Yang–Mills theories defined along the locus  $\Theta$ . The results [10,11,49] however show that we indeed end up with massless vector multiplets filling out the adjoint representation of  $G$ , i.e. there is a  $G$  gauge theory in the 4D F-theory compactification on  $Y_4$  associated with the divisor  $\Theta$ .

Note that so far we have only considered gauge symmetries arising from a single component  $\Theta$  of the discriminant locus. As a result, we find that we always end up with a single semi-simple Lie group. In order to realise a gauge theory with a product group, e.g. the Standard Model, we have to consider singular fibrations that have two independent components of the discriminant locus with the appropriate singularity structure. As we will see in chapter V, the resolution process can be performed independently for each component in certain classes of models that we will use for our F-theory realisations of the Standard Model.

Before continuing with the origin of matter in F-theory, let us briefly compare the above results to perturbative type IIB compactifications. There, the gauge groups that can be constructed with D7-branes and O7-planes are only  $SU(n)$ ,  $SO(2n)$  and  $Sp(n)$ . All other groups are truly of non-perturbative nature. While it is possible to also construct these groups via string junctions [29,31], they somehow arise much more natural (from a mathematician’s perspective) in the F-theory description of non-perturbative type IIB.

#### 2.4.4 Matter in F-theory

From the type IIB intuition, we expect matter states to arise along intersections of two (stacks of) 7-branes, which wrap divisors  $\Theta_{1,2}$  on  $\mathcal{B}$ . In the F-theory description on the singular torus fibration  $Y$ , the discriminant  $\Delta$  vanishes to certain orders  $n_{1,2} \geq 1$  along  $\Theta_{1,2}$ , therefore the vanishing order of  $\Delta$  increases at the intersection  $C = \Theta_1 \cap \Theta_2$  to  $n_1 + n_2$ . Typically, this indicates that the singularity type of the fibre over the intersection ‘enhances’ compared to the generic fibres over  $\Theta_{1,2}$ . The description ‘enhancement’ can be taken quite literally if we look at the resolved fibration  $\hat{Y}$ . Comparing the generic singular fibre  $\mathfrak{f}_b$  over  $b \in \Theta_i$  with a fibre  $\mathfrak{f}^*$  over the intersection  $C$ , we find that  $\mathfrak{f}^*$  has more fibre components than  $\mathfrak{f}_b$ . These new components can be seen as the splitting of some  $\mathbb{P}_s^1$  in  $\mathfrak{f}_b$  as we move  $b$  to the intersection.

Specifically, if we have a non-abelian gauge symmetry with group  $G$  associated with  $\Theta_1$ , then  $\mathbb{P}_s^1$  corresponds to a weight  $\mathbf{w}_s^{\text{ad}}$  of the adjoint rep of  $G$ . The splitting of  $\mathbb{P}_s^1 \rightarrow \bigcup_k \mathbb{P}_k^1 \subset \mathfrak{f}^*$  corresponds to a decomposition of the adjoint weight  $\mathbf{w}_s^{\text{ad}} \rightarrow \sum_k \mathbf{w}_k$ , where  $\mathbf{w}_k$  is the charge vector of  $\mathbb{P}_k^1$  under the Cartan  $U(1)$ s. In general, these weights lie in a representation  $\mathcal{R}_k$  of  $G$  other than the adjoint rep. By the same logic as for the W-bosons, M2-branes wrapped on  $\mathbb{P}_k^1$  therefore gives rise to a state in  $\mathcal{R}_k$  which becomes massless in the singular limit. Furthermore, [10,11] showed that states from M2-branes wrapping fibral curves, which are only present over codimension two loci on  $\mathcal{B}$ , lift to a chiral and anti-chiral multiplet in the F-theory limit to 4D.<sup>20</sup> In the 4D field theory language, this means that the appearance of the new  $\mathbb{P}_k^1$  as components of codimension two singular fibres  $\mathfrak{f}^*$  gives rise to matter states.

In order for the gauge symmetry to be unbroken by these matter states, it is crucial that we obtain from the splitting process of fibre components *full* representations  $\mathcal{R}_k$ , i.e. we need enough fibral curves to generate all weights in  $\mathcal{R}_k$ . This has been systematically shown to be true in [50,51]. Essentially, it is because we can also associate a Kodaira fibre type listed in table II.2 to singular fibres along a codimension two locus  $C \subset \mathcal{B}$ . For a fibration  $Y$  with an equivalent Weierstrass model, this association is simply given by the vanishing orders of  $(f, g, \Delta)$ . In any case, the explicit inspection of the fibre structure of  $\mathfrak{f}^*$  reveals that in almost all cases, we recover

<sup>20</sup>The number of chiral and anti-chiral multiplets will be modified in the presence of flux, as discussed in the chapter III.

the affine Dynkin diagram of an higher rank group  $H$  containing  $G$  as a subgroup.<sup>21</sup> If these fibres were localised over a codimension one locus, then the result from the previous chapter would imply that M2-branes wrapped on linear combinations of fibre components give rise to the full adjoint  $\mathbf{ad}_H$  of  $H$ . By restricting them to codimension two, the 4D nature of the states change, but their representation theory does not, i.e. we still expect M2-brane states filling all of  $\mathbf{ad}_H$ . However, these states now rearrange themselves into full representations  $\mathcal{R}_k$  of  $G$  determined by the branching rule  $\mathbf{ad}_H \rightarrow \sum_k \mathcal{R}_k$ .

In general, such a branching will be of the form

$$\mathbf{ad}_H \rightarrow \mathbf{ad}_G + \sum_i \mathbf{1}_i + \sum_k (\mathcal{R}_k + \overline{\mathcal{R}}_k) .$$

The adjoint  $\mathbf{ad}_G$  of  $G$  is obviously given by those fibral curves in  $\mathfrak{f}^*$  which are fibral curves of a generic fibre  $\mathfrak{f}_b$  over  $b \in \Theta_1$  in the limit  $b \rightarrow C$ . The singlets  $\mathbf{1}_i$  are actually the group theoretic remnants of the Cartans of  $H$  that are not Cartans of  $G$ . These would arise from exceptional divisors if  $H$  as associated to a codimension one singularity (see footnote 19), hence they are not present in the actual spectrum. Other non-trivial representations  $\mathcal{R}_k$  always come with their conjugate  $\overline{\mathcal{R}}_k$ . In most explicit examples, the rank of  $H$  exceeds that of  $G$  by only one; in these cases, there will be generically only one pair  $(\mathcal{R}_k + \overline{\mathcal{R}}_k)$  of non-trivial representation. In some extreme scenarios, one might be able to tune the singularities such that the rank difference between  $H$  and  $G$  is higher, and consequently, there might be different representations present.

Either way, the states of these representations are associated to the singular fibres over the codimension two locus  $C$ . In the literature, the locus  $C$  is often referred to as a  $H$ -locus or locus of  $H$ -enhancement. However, as  $H$  is not actually realised physically, a perhaps more precise nomenclature would be to label  $C$  by the representation(s)  $\mathcal{R}_k$  that are associated to it. Moreover, on a three dimensional base,  $C$  is a complex curve. Consequently, such curves are usually called matter curves in F-theory compactifications to 4D.

For example, we will examine models with  $SU(5)$  symmetries in chapter IV. There, we encounter codimension two enhancements to  $SU(6)$  and  $SO(10)$ . Their adjoints decompose as  $\mathbf{35} \rightarrow \mathbf{24} + \mathbf{1} + \mathbf{5} + \overline{\mathbf{5}}$  for  $SU(6)$  and  $\mathbf{45} \rightarrow \mathbf{24} + \mathbf{1} + \mathbf{10} + \overline{\mathbf{10}}$  for  $SO(10)$ . Consequently, the  $SU(6)$  enhancement loci are  $\mathbf{5}$ -curves, whereas the  $SO(10)$  loci correspond to  $\mathbf{10}$  curves.

Finally note that if there is a non-trivial gauge group  $\tilde{G}$  on  $\Theta_2$ , then the putative group  $H$  on  $C = \Theta_1 \cap \Theta_2$  will contain the product  $G \times \tilde{G}$ . Accordingly, the matter representations on  $C$  will be given by the branching of  $\mathbf{ad}_H$  into irreducible representations of  $G \times \tilde{G}$ . In our realisations of the Standard Model, studied extensively in chapter V, we realise  $SU(3)$  and  $SU(2)$  along divisors  $W_3$  and  $W_2$ , respectively. At their intersection, we find an  $SU(5)$  enhancement, corresponding to the branching  $\mathbf{24} \rightarrow (\mathbf{8}, \mathbf{1}) + (\mathbf{1}, \mathbf{3}) + (\mathbf{1}, \mathbf{1}) + (\mathbf{3}, \mathbf{2}) + (\overline{\mathbf{3}}, \mathbf{2})$  well-known in GUTs. Consistently, we find bifundamental states  $SU(3) \times SU(2)$  at the intersection curve  $W_3 \cap W_2$ , which for our phenomenological discussions will be identified with left-handed quarks.

### Matter surfaces

As a somewhat trivial observation, we note the collection of all fibral curves  $\Gamma_{\mathbf{w}}$  over  $C$  giving rise to one weight state  $\mathbf{w}$  of a representation  $\mathcal{R}$  defines a fibration  $\gamma_{\mathbf{w}}$  over  $C$ :

$$\begin{array}{ccc} \Gamma_{\mathbf{w}} & \longrightarrow & \gamma_{\mathbf{w}} \\ & & \downarrow \\ & & C \end{array}$$

---

<sup>21</sup>The exceptions are situations where some nodes of the diagram of  $H$  are missing. Such models have been studied in [40].

On a fourfold  $\hat{Y}_4$ , these fibrations have a (complex) two-dimensional total space, as the base  $C$  and the fibres are both curves. It is also customary to count their real dimensions, in which case  $\gamma_{\mathbf{w}}$  is a 4-cycle. These 4-cycles are referred to as matter surfaces. As it turns out, their physical impact are anything but trivial. Indeed, their structure affects the chiral index of the matter states  $\mathbf{w}$ , as we will discuss in the next chapter. In particular, the results of chapter IV will show that the geometry of matter surfaces actually gives a new approach to chiral anomaly cancellation in 4D F-theory.

### 2.4.5 Yukawa couplings

While codimension one singular fibres give rise to gauge bosons, codimension two singular fibres are associated with matter states. For a torus-fibred fourfold  $Y_4 \rightarrow \mathcal{B}$ , we can have further singularity enhancement over codimension three loci, i.e. points, on the base  $\mathcal{B}$ . One might wonder if there are again new states arising from these singularities. However, as shown in [10, 11], this is not the case. Instead, codimension three singularities are related to the presence of (perturbative) Yukawa couplings. Here, we will sketch how this comes about.

In general, codimension three singularities lie on top of common points  $p$  of several matter curves  $C_i$ . Over  $p$ , the fibre structure enhances compared to the generic fibres on  $C_i$ . However, in contrast to the situation in codimension two, no  $\mathbb{P}^1$ s with novel Cartan charges arise. Instead, the  $\mathbb{P}^1$ s that are ‘new’ compare to the fibres on  $C_a$  have already been present on one of the other curves  $C_b$ . Thus, we do not expect any new states to arise from these singularity enhancements. The unusual phenomenon now is that over  $p$ , there are non-trivial chains  $\Gamma$  (i.e. neither empty nor the full fibre) of fibral  $\mathbb{P}^1$ s that have zero charge under any Cartan  $U(1)$ . In particular, such a chain  $\Gamma$  can be decomposed into precisely three subchains  $\Gamma_{1,2,3}$  in a way that each of them correspond to a weight  $\mathbf{w}_{1,2,3}$  of a representation that was already present on one of the  $C_i$ ’s. In other words, there is a gauge invariant combination of three weights:

$$\mathbf{w}_1 + \mathbf{w}_2 + \mathbf{w}_3 = 0 \Leftrightarrow \mathbf{w}_1 + \mathbf{w}_2 = -\mathbf{w}_3.$$

Heuristically, the second equation can be regarded as a ‘Feynman diagram’, which describes how a state  $\mathbf{w}_1$  and a state  $\mathbf{w}_2$  can interact to form a state  $-\mathbf{w}_3$ .

Indeed, this heuristic picture underlies the analysis of [10, 11], which showed that a coupling arises between the three states  $\mathbf{w}_{1,2,3}$  as a result of the chains  $\Gamma_{1,2,3}$  meeting over a point in  $\mathcal{B}$ . Crucially, the analysis shows that it is a coupling between one scalar and two fermions that each sits in one of the chiral multiplets coming from M2-branes wrapped on  $\Gamma_{1,2,3}$ . Thus it is really a Yukawa type coupling.

Note that such a Yukawa coupling can only arise, if amongst the representations  $\mathcal{R}_i$  on  $C_i$ , there is gauge invariant triple product, i.e. a product  $\mathcal{R}_{i_1} \otimes \mathcal{R}_{i_2} \otimes \mathcal{R}_{i_3}$  that in its decomposition of irreducible representations contains a singlet. This is of course the equivalent statement as the existence of chains  $\Gamma$  with the decomposition property mentioned above. In general, we find that only matter curves  $C_i$  with this property will meet at all in a common point  $p$ . Such a point is often referred to as a Yukawa point.

Finally note that in principle there can be fibral chains  $\Gamma_{1,2,3}$  over different matter curves, whose associated weights add to 0, but the curves do not come together at a Yukawa point. In this case, there is now a (real) three-dimensional submanifold  $\tilde{\Gamma}$  of  $Y_4$  having  $\Gamma_{1,2,3}$  as boundaries. As argued in [52], M2-branes wrapped on  $\tilde{\Gamma}$  now corresponds to an instanton in the effective field theory, which still generates a Yukawa coupling between the states. However, these (non-perturbative) couplings will be exponentially suppressed by the (non-zero) volume of  $\tilde{\Gamma}$  compared to the couplings localised over points.

### Fibre structure over Yukawa points

Similar to codimension two singularities, we also find that in general, the fibres over Yukawa



points  $p$  also fall into Kodaira's classification. However, unlike in codimension two, we now find much more frequently that, compared to the full Dynkin diagrams, some nodes are missing in the fibre structure [40]. Nevertheless, there is an unambiguous assignment of a Lie group  $H'$  to  $p$ , even if the fibre structure is incomplete. Therefore, it is consistent to also refer to a Yukawa point as a locus of  $H'$  enhancement.

While in perturbative type IIB, Yukawa couplings appear in a similar manner when three D7-branes meet in one point, the possible couplings are restricted. In particular, one major drawback of those constructions were that in  $SU(5)$ -GUTs, it is not possible to realise a coupling of the type  $\mathbf{10} \mathbf{10} \bar{\mathbf{5}}$ , which however is needed phenomenologically to realise the Yukawa coupling between up-type quarks and the Higgs. From the F-theory perspective, a  $\mathbf{10} \mathbf{10} \mathbf{5}$  coupling originates from a Yukawa point of  $E_6$  enhancement. Since the exceptional group  $E_6$  is not realisable perturbatively in type IIB, this shows that F-theory is a genuine extension of perturbative type IIB of phenomenological interest.

To give some further example, we note that in F-theory models with  $SU(5)$ , we also have the (perturbatively realised)  $\mathbf{10} \bar{\mathbf{5}} \bar{\mathbf{5}}$  coupling at an  $SU(7)$  enhancement point. Note that by tuning the fibration (see e.g. [53]), we can actually 'bring together' points of  $E_6$  and  $SU(7)$  enhancements, resulting in an  $E_7$  enhancement. In the fibre structure, both couplings are now realised. In chapter V, where we examine Standard Model like F-theory models, we will study in detail how the matter curves meet in order to give rise to a Yukawa coupling. It turns out that often, if a coupling of type  $\mathcal{R}_1 \mathcal{R}_1 \mathcal{R}_2$  occurs, the Yukawa point actually lies on the self-intersection of the  $\mathcal{R}_1$ -matter curve, consistent with the  $\mathcal{R}_1$ -states appearing twice in the coupling structure.

## 2.5 Abelian symmetries in F-theory

We now turn our attention to abelian symmetries in F-theory. Unlike non-abelian symmetries which arise from singularities localised in codimension one loci of  $\mathcal{B}$ , abelian symmetries are tied to global structures (i.e. not localised to special subsets of  $\mathcal{B}$ ). One such global structure are given by section sections, which we have already encountered in section 2.2.1 in the context of Weierstrass models. These assign to each point of the base a point in the fibre over it. A related concept is a so-called multi-section, which in contrast to a section assigns multiple points in the fibre to each base point. As we will see in this section, their presence will give rise to  $U(1)$  and  $\mathbb{Z}_n$  symmetries, respectively, in F-theory.

### 2.5.1 Sections and the Mordell–Weil group

Recall from section 2.2.1 that a (holomorphic) section  $\text{Sec}$  of a fibration  $\pi_Y : Y \rightarrow \mathcal{B}$  is simply a (holomorphic) map  $\text{Sec} : \mathcal{B} \rightarrow Y$  satisfying the condition  $\pi_Y \circ \text{Sec} = \text{id}_{\mathcal{B}}$ . The intuitive picture is that a section marks a single point in the fibre over each point of the base, cf. figure II.6. A section therefore can also be seen as defining an embedding of the base  $\mathcal{B}$  into the total space  $Y$ . By doing so, it also defines a divisor, i.e. a complex codimension one submanifold, of  $Y$  with homology class  $[\text{Sec}]$ . In the class of torus fibrations (II.18), where the fibre of  $Y$  is given as the vanishing of a polynomial  $P$  in a fibre ambient space  $\mathbb{A}$  with coordinates  $x_i$ , there is a particular easy way of realising sections. Namely, a section may arise by fibring the intersection point  $\{x_j\} \cap \{P\} \in \mathbb{A}$  over  $\mathcal{B}$ . In such a case it is customary to identify the section with the divisor defined by  $\{x_i = 0\} \equiv \{x_i\}$ , and often also their classes  $[\text{Sec}] = [\{x_i\}]$ . In the generic Weierstrass model the only section is given by II.17 as the intersection of the Weierstrass polynomial (II.9) with  $\{z\} \subset \mathbb{P}_{231}$ . However, there are examples of fibrations which exhibit more sections.

In anticipation of the models in chapter IV, we take a closer look at the  $\text{Bl}_1 \mathbb{P}_{112}$  model. There the fibre ambient space  $\mathbb{A} = \text{Bl}_1 \mathbb{P}_{112}$  is a quotient of  $\mathbb{C}^4 \setminus (\{u = w = 0\} \cup \{v = s = 0\})$ , where  $(u, v, w, s)$  denote the coordinates of  $\mathbb{C}^4$ . The equivalence relation we quotient by are the two independent scaling relations  $(u, v, w, s) \simeq (\lambda u, \lambda v, \lambda^2 w, s) \simeq (u, \mu v, \mu w, \mu s)$ , thus reducing the

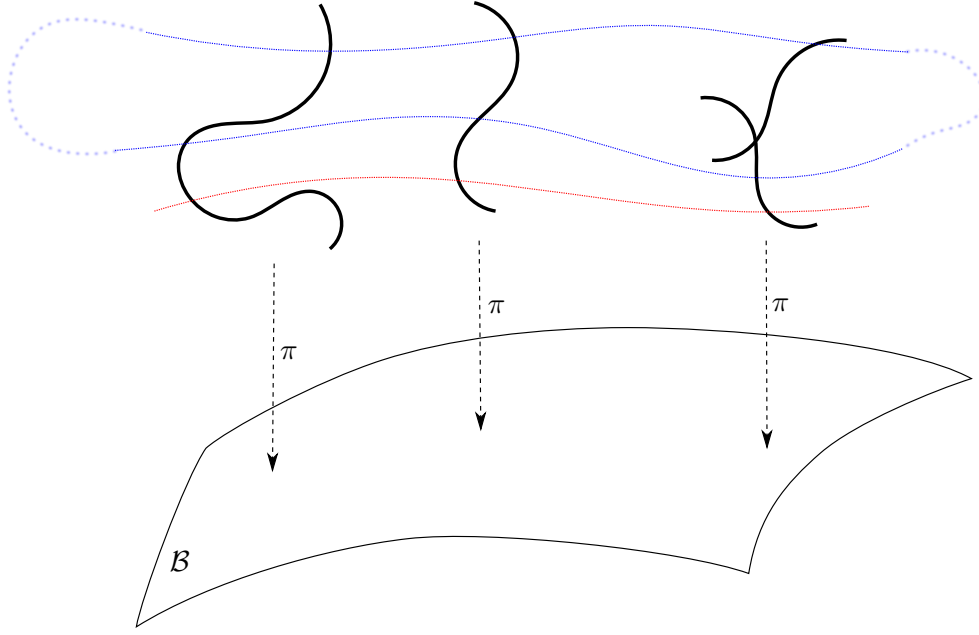


**Figure II.6:** A section (marked in red) of a torus fibration intersects the fibre (here represented as a curve) in one point. In contrast, a bi-section (blue), that will be introduced in section 2.5.4, marks two points in the fibre. Globally, these two points are exchanged by a monodromy.

four independent variables of  $\mathbb{C}^4$  to only two degrees of freedom, i.e.  $\dim_{\mathbb{C}} \text{Bl}_1\mathbb{P}_{112} = 2$ . Note that the total weight of all coordinates under the scaling with  $\lambda$  is 4, and 3 under scaling with  $\mu$ . Therefore, a polynomial describing a Calabi–Yau curve, i.e. a torus, in  $\mathbb{A}$  must have the same weights under the corresponding scalings. A general such polynomial<sup>22</sup> describing a torus fibration is

$$P' = s w^2 + b_0 s^2 u^2 w + b_1 s u v w + b_2 v^2 w + c_0 s^3 u^4 + c_1 s^2 u^3 v + c_2 s u^2 v^2 + c_3 u v^3. \quad (\text{II.21})$$

This fibration has two independent sections. One is given by the intersection

$$\{u = 0\} \cap \{P' = 0\} = \{u = 0\} \cap \underbrace{\{s w^2 + b_2 v^2 w = 0\}}_{\equiv Q'}. \quad (\text{II.22})$$

Note that because  $u$  and  $w$  cannot vanish simultaneously in  $\text{Bl}_1\mathbb{P}_{112}$ , we can exploit the scaling relation  $(u, v, w, s) \simeq (\lambda u, \lambda v, \lambda^2 w, s)$  to rescale  $w \rightarrow 1$  in  $Q'$ :  $Q' \simeq s + b_2 v^2$ . Furthermore, because  $s$  and  $v$  cannot vanish together, neither of them can vanish for  $Q' = 0$ , hence we can also use the second scaling  $(u, v, w, s) \simeq (u, \mu v, \mu w, \mu s)$  to rescale  $v \rightarrow 1$ , so  $Q' \simeq s + b_2$ . Thus, for any value of  $b_2$ , i.e. over any point  $q$  in the base  $\mathcal{B}$ , the intersection  $\{u = 0\} \cap \{P' = 0\}$  corresponds precisely to one point of the torus fibre  $\pi_Y^{-1}(q) \equiv \mathbb{E}_q$ :

$$\forall q \in \mathcal{B} : \text{Sec}_0(q) := [0 : 1 : 1 : -b_2(q)] \in \mathbb{E}_q \subset \text{Bl}_1\mathbb{P}_{112}. \quad (\text{II.23})$$

In addition to this, there is another section given by  $\{s\} \cap \{P'\}$ :

$$\begin{aligned} \{s\} \cap \{P'\} &= \{s\} \cap \{b_2 v^2 w + c_3 u v^3\} \stackrel{v \rightarrow 1}{\simeq} \{s\} \cap \underbrace{\{b_2 w + c_3 u\}}_{Q'_s} \stackrel{u \rightarrow 1}{\simeq} \{s\} \cap \{b_2 w + c_3\} \\ \Rightarrow \text{Sec}_1(q) &:= \left[ 1 : 1 : -\frac{c_3(q)}{b_2(q)} : 0 \right] \end{aligned} \quad (\text{II.24})$$

<sup>22</sup>Note that we have chosen the coefficient in front of  $s w^2$  to be 1. In the most general set-up, this need not to be the case. The consequences for F-theory have been studied most recently in [54].

Note that this section is strictly speaking only well-defined for  $c_3 \neq 0 \neq b_2$ ; over the locus  $\{b_2\} \cap \{c_3\} \subset \mathcal{B}$ , the polynomial  $Q'_s$  vanishes identically, such that the coordinates  $(u, w)$  together with the remaining scaling relation parametrise a full  $\mathbb{P}^1$ .<sup>23</sup> This type of sections – known as rational sections – is still ‘well-behaved’ enough for us, as they still mark a point on the generic fibre.

The set of all rational sections on an elliptic fibration turns out to form an abelian group, the so-called Mordell–Weil (MW) group. The group structure comes from the addition of points on the elliptic fibre, which is most easily seen when we go back to the description of elliptic curves/tori as quotients  $\mathbb{C}/\Lambda$ . On this quotient, points of the torus are simply represented by complex numbers with the natural addition as an abelian group action. It can be shown that this structure carries over to the elliptic curve via the map (II.11) into a well-defined manner: We can geometrically construct the sum of two points  $p, p'$  on the elliptic curve by constructing the straight line passing through  $p$  and  $p'$ ; this line will intersect the curve at a third point (possibly at infinity) corresponding to  $p + p'$  (see e.g. [55] for more details). The addition of sections in an elliptic fibration can be thus fibre-wise defined as the addition of the points marked by the section on each fibre. Being an abelian group, there is a zero-element, which in our context is also called the zero-section. The zero-section is not a priori specified. In fact, one can make an arbitrary choice of identifying any section  $[\text{Sec}_0]$  with the zero-section. The Mordell–Weil theorem states that the group of sections is a finitely generated abelian group, i.e. its group structure is isomorphic to  $\mathbb{Z}^r \oplus \mathbb{Z}_{k_1} \oplus \dots \oplus \mathbb{Z}_{k_n}$ . For the purpose of our thesis, the so-called torsional part  $\mathbb{Z}_{k_1} \oplus \dots \oplus \mathbb{Z}_{k_n}$  is not relevant. However, their meaning in F-theory have been clarified recently in [45]. The so-called rank  $r$  of the MW group is determined by the free part,  $\mathbb{Z}^r$ . Any elliptic fibration with rank  $r$  MW group has  $r + 1$  independent sections (i.e. they have independent divisor classes), since one of them constitutes the zero-section, which does not contribute to the rank. E.g. the generic Weierstrass model has a rank 0 MW group with only the zero-section  $\{z\}$ , while the  $\text{Bl}_1\mathbb{P}_{112}$  model has Mordell–Weil rank 1. The zero-section is given by (II.23), while the other independent generator is (II.24).

### 2.5.2 $U(1)$ s from sections

Since every section  $\text{Sec}$  gives rise to a divisor  $[\text{Sec}]$  on  $Y$ , the reduction (II.20) of the M-theory 3-form  $C_3$  will readily give rise to a massless  $U(1)$  associated to  $\text{Sec}$  when we compactify M-theory on  $Y$ . As the divisors  $[\text{Sec}]$  are not vertical divisors, one might think that these simply lift to  $U(1)$ s in the F-theory limit. However, there is an important caveat to it.

#### The KK $U(1)$

As we have elaborated in section 2.3, the effective theory in  $\mathbb{R}^{1,n-1}$  of M-theory compactified on  $Y$  is a circle reduction of a theory in  $\mathbb{R}^{1,n}$ , which is F-theory on  $Y$ . In particular, the translation invariance of  $\mathbb{R}^{1,n}$  along the direction which is compactified to a circle manifests itself as a  $U(1)$  symmetry in  $\mathbb{R}^{1,n-1}$ . This  $U(1)$  is referred to as the KK  $U(1)$ , because it distinguishes the KK-modes  $\phi_k$  in the Fourier-expansion (II.4). Put differently, the charge of  $\phi_k$  under this KK  $U(1)$  is precisely  $k$ . In elliptic fibrations, this KK  $U(1)$  can be identified with the vector field from the  $C_3$  expansion with any section  $[\text{Sec}]$ . To see this, note that the modes  $\phi_k$  in the circle compactification from F-theory to M-theory on  $Y$  arise from states which wrap the circle  $k$ -times. In terms of the M-theory compactification on  $Y$ , these states arise from M2-branes that wrap the full torus fibre  $k$ -times. Since a section intersects the generic torus fibre precisely once, it will have intersection number  $k$  with those states. The choice of the KK  $U(1)$  corresponds to the choice of zero-section. In the following we will assume that we have made such a choice.

---

<sup>23</sup>From our discussions about matter curves in section 2.4.4, we can already anticipate that the appearance of this fibral  $\mathbb{P}^1$  over the codimension two locus  $\{b_2\} \cap \{c_3\} \subset \mathcal{B}$  is a signal for matter states.

### Gauge $U(1)$ s from the Shioda map

The remaining independent generators of the MW-group give rise to honest, gauge  $U(1)$ s in the F-theory limit. Concretely, they give rise to  $(1, 1)$ -forms  $\omega_i$  on  $Y$  which are called the ‘generators’ for the  $U(1)$  fields  $A_i$  in the expansion  $C_3 = A_i \wedge \omega_i$ . In order for the gauge field to be massless in the F-theory limit and not mix with the KK  $U(1)$ , the generators  $\omega_i$  must have ‘one leg along the fibre and one leg along the base’. For a fourfold  $Y_4$  with a threefold base  $\mathcal{B}$ , these words mean explicitly that

$$\int_{Y_4} \omega_i \wedge D_a^{(\mathcal{B})} \wedge D_b^{(\mathcal{B})} \wedge D_c^{(\mathcal{B})} = 0 = \int_{Y_4} \omega_i \wedge [\text{Sec}_0] \wedge D_a^{(\mathcal{B})} \wedge D_b^{(\mathcal{B})} \quad (\text{II.25})$$

for any vertical divisor  $D_{(\cdot)}^{(\mathcal{B})}$ . Note that we have introduced a common laziness of not distinguishing divisors and their Poincaré-dual  $(1, 1)$ -forms. In this context, there is no ambiguity, as the integral only makes sense for forms. If there is in addition any non-abelian gauge group  $G$ , the  $U(1)$ s should also not mix with the Cartan  $U(1)$ s of  $G$ . This is captured by the condition

$$\int_{Y_4} \omega_i \wedge \text{Ex} \wedge D_a^{(\mathcal{B})} \wedge D_b^{(\mathcal{B})} = 0, \quad (\text{II.26})$$

where Ex is any exceptional divisor associated with  $G$ .

It was shown in [56] that there is a mathematical result that ensures the existence of such a  $(1, 1)$ -form  $\omega_i$  – which is Poincaré-dual to a divisor, denoted abusively by  $\omega_i$  as well – for every generator  $[\text{Sec}_i]$  of the MW-group. The explicit identification of the divisor class  $\omega_i$  with the section is given by the so-called Shioda map. In practise, one can determine the form of  $\omega_i$  up to an overall numerical factor by explicitly solving the conditions (II.25) and (II.26). The numerical factor simply corresponds to the normalisation of charges, which has no physical meaning.

As a result, we find that for any elliptic fibration  $Y$  with a rank  $r$  MW group and generators  $[\text{Sec}_i]$ ,  $i = 0, \dots, r$ , we have a  $U(1)^r$  gauge symmetry when we compactify F-theory on  $Y$ . Each  $U(1)$  factor has a corresponding divisor class  $\omega_i$  generating the symmetry of the form

$$\omega_i \propto [\text{Sec}_i] - [\text{Sec}_0] + \sum_k \mu_k D_k^{(\mathcal{B})} + \sum_l \lambda_l \text{Ex}_l, \quad (\text{II.27})$$

where  $D_k^{(\mathcal{B})}$  is a basis for the set of all vertical divisors. The coefficients  $\mu$  and  $\lambda$  are uniquely determined by the Shioda map, or equivalently, by the conditions (II.25) and (II.26).

For example, in the  $\text{Bl}_1\mathbb{P}_{112}$  model (II.21) we discussed above, the only  $U(1)$  generator is given by  $\omega \propto [\{s\}] - [\{u\}] - \bar{\mathcal{K}} - [b_2]$ , where  $\bar{\mathcal{K}} = \pi^{-1}(c_1(\mathcal{B}))$  is the anti-canonical bundle of the base and  $[b_2]$  is the line bundle class of which  $b_2$  is a section.

### 2.5.3 $U(1)$ charges and singlets

In general, an F-theory compactification with  $U(1)$  symmetries will also have charged singlets, i.e. matter states that are charged under the  $U(1)$ s, but not under any non-abelian gauge groups. Like non-abelian matter, they must be localised along codimension two loci  $C_{1_i}$  of the base  $\mathcal{B}$ . For charged singlets, the singular fibres  $\mathfrak{f}$  over  $C_{1_i}$  are of Kodaira type  $I_2$ , i.e. they have the fibre structure of an affine  $SU(2)$  Dynkin diagram (cf. table II.2). As first examined in [56] for the  $\text{Bl}_1\mathbb{P}_{112}$  model, one can systematically make an ansatz for the factorisation of the fibre into two components, whose codimension two solution set is precisely the collection of all singlet loci  $C_{1_i}$ . Similar analysis has also been performed in [57, 58] for the  $\text{Bl}_2\mathbb{P}^2$  model. It is in general not easy to extract the individual loci  $C_{1_i}$ . Indeed, as first presented in [57], and which we will review in chapter V, it requires some tools for computations with polynomials to determine the singlet loci in general. Irrespective of these difficulties, the  $U(1)$  charge of the singlet  $\mathbf{1}_i$  over  $C_{1_i}$  is computed

analogously to the Cartan charges of non-abelian states, namely as  $\int_{\mathbb{P}^1} \omega_i$ . Of course, the two  $\mathbb{P}^1$ s in the fibre  $\mathfrak{f}$  correspond just to the singlet state  $\mathbf{1}_i$  and its charge conjugate  $\bar{\mathbf{1}}_i$ .

Similarly, one can associate  $U(1)$  charges to non-abelian matter in an representation  $\mathcal{R}$  over  $C_{\mathcal{R}} = \Theta \cap D_1^{(\mathcal{B})}$ , where  $D_1^{(\mathcal{B})}$  is a divisor on the base. However, one apparent issue arises, namely that for gauge invariance all states in  $\mathcal{R}$  must have the same  $U(1)$  charge. To see how this issue is resolved, recall that the fibres of the exceptional divisors  $\text{Ex}_k$  correspond to the simple roots of the gauge group  $G$  on  $\Theta$ . From basic representation theory, we therefore know that different  $\mathbb{P}^1$  chains in the fibre  $\mathfrak{f}_{\mathcal{R}}$  over  $C_{\mathcal{R}}$ , which give rise to states  $\mathcal{R}$ , must differ by a linear combinations of fibres of  $\text{Ex}_k$  over  $C_{\mathcal{R}}$ . Suppose for definiteness, we are over a threefold base  $\mathcal{B}$ . Then a generic point  $b \in C_{\mathcal{R}}$  can be written as the intersection with another divisor, i.e.  $b = C_{\mathcal{R}} \cap D_2^{(\mathcal{B})} = \Theta \cap D_1^{(\mathcal{B})} \cap D_2^{(\mathcal{B})}$ . Since  $\text{Ex}_k$  is a fibration over  $\Theta$ , its fibres over  $b$  is then given by

$$\Gamma_k = \text{Ex}_k \cap \pi^{-1}(D_1^{(\mathcal{B})}) \cap \pi^{-1}(D_2^{(\mathcal{B})}) \equiv \text{Ex}_k \cap D_1^{(\mathcal{B})} \cap D_2^{(\mathcal{B})} \subset Y_4,$$

where by a common abusive notation we have identified the vertical divisors  $\pi^{-1}(D_i^{(\mathcal{B})})$  with their pre-image  $D_i^{(\mathcal{B})}$  in the base. Note that by the compatibility of Poincaré-duality with intersection and wedge products (cf. appendix A), the curve  $\Gamma_k$  is dual to the  $(3, 3)$ -form  $\text{Ex}_k \wedge D_1^{(\mathcal{B})} \wedge D_2^{(\mathcal{B})}$ . Now the  $U(1)$  charges associated with these fibres are given simply by

$$\int_{\Gamma_k} \omega_i = \int_{Y_4} \omega_i \wedge \text{Ex}_k \wedge D_1^{(\mathcal{B})} \wedge D_2^{(\mathcal{B})}$$

which due to the condition (II.26) on the  $U(1)$  generators must vanish. Therefore, we see that the  $U(1)$  charge differences between weights of the same representation  $\mathcal{R}$  is 0, i.e. all states of  $\mathcal{R}$  have the same  $U(1)$  charge.

Finally, note that charged singlets can participate in Yukawa couplings as well. In the presence of additional  $U(1)$  gauge symmetries, it means that gauge invariant couplings must involve states whose  $U(1)$  charges add up to 0.

In the example fibration (II.21), we have already encountered the appearance of singlet matter. Concretely, we say that over the locus  $b_2 = c_3 = 0$ , the section (II.24) given by  $\{s\}$  wraps a whole  $\mathbb{P}^1$ . This  $\mathbb{P}^1$  is of course nothing other than a fibral curve giving rise to states by wrapping M2-branes on it. These states have charge  $-2$  under the  $U(1)$  generator  $[\{s\}] - [\{u\}] - \bar{\mathcal{K}} - [b_2]$ . Furthermore, there is a locus of charge 1 states in this model. For more details we refer to chapter IV.

#### 2.5.4 Multi-sections and discrete abelian symmetries

The appearance of sections in a torus fibration is quite a special property of the fibration. Given our class of fibrations of the type (II.18), these sections appear as fibring the intersection points of certain hyperplanes with the elliptic fibre  $\{P\}$  in  $\mathbb{A}$  over the base  $\mathcal{B}$ .<sup>24</sup> Due to the special form of the fibration, these hyperplanes will always intersect the generic elliptic fibre in precisely one point when one moves around in  $\mathcal{B}$ . However, in the most general scenario, any hyperplane in  $\mathbb{A}$  will intersect  $\{P\}$  in multiple (say  $n$ ) points, if the polynomial  $P$  is not of degree 1 (cf. figure II.6). By fibring these set of points over  $\mathcal{B}$ , one obtains a so-called multi- or  $n$ -section. In contrast to a section, such an  $n$ -section now defines an  $n$ -fold cover of the base  $\mathcal{B}$  inside the torus fibration  $Y$ . Similar to elliptic fibrations, these  $n$ -fold covers of  $\mathcal{B}$  inside  $Y$  still are a (complex) codimension one submanifold of  $Y$ , hence they have an associated divisor class  $N$  in  $Y$ . In order to distinguish them from elliptic fibrations, torus fibrations with only multi-sections and no sections are referred to as genus-one fibrations in the F-theory literature. In general, there can be several  $n$ -sections in

<sup>24</sup>Note that while this type of sections is the simplest to write down, it is quite restrictive. Other types of section have been constructed in e.g. [59, 60].

a genus-one fibration with possibly different  $n$ 's. However, their divisor classes might be linearly dependent. It has been proposed in [61] that the set of independent multi-sections is encoded in the so-called Tate–Shafarevich group.<sup>25</sup> In principle one can also have both independent sections and  $n$ -sections in a single torus fibration. Technically, this would also be an elliptic fibration according to the usual definition. Such examples will not be considered in this thesis, however, they have appeared in F-theory models [54].

An example of a genus-one fibration which we will study extensively in chapter IV is given by the  $\mathbb{P}_{112}$  model. The weighted projective space  $\mathbb{P}_{112}$  can be described by the quotient of  $\mathbb{C}^3 \setminus \{0\}$  with coordinates  $(u, v, w)$  by the scaling  $(u, v, w) \simeq (\lambda u, \lambda v, \lambda^2 w)$ . A polynomial defining an elliptic curve therefore must be of weight 4. In general, we can write it as

$$P = w^2 + b_0 u^2 w + b_1 u v w + b_2 v^2 w + c_0 u^4 + c_1 u^3 v + c_2 u^2 v^2 + c_3 u v^3 + c_4 v^4, \quad (\text{II.28})$$

where the coefficients  $b_i, c_j$  are promoted to sections of the base  $\mathcal{B}$  in order to describe a fibration  $\mathbb{Y} \rightarrow \mathcal{B}$ . Note that this model is very similar to the  $\text{Bl}_1 \mathbb{P}_{112}$  model (II.21). There, one of the sections (II.23) was given by the intersection of the hypersurface with  $\{u\}$ . If we inspect the corresponding locus in the  $\mathbb{P}_{112}$  model, we find

$$\{u = 0\} \cap \{P = 0\} = \{u = 0\} \cap \underbrace{\{w^2 + b_2 v^2 w + c_4 v^4 = 0\}}_{\equiv Q}. \quad (\text{II.29})$$

Again, because neither  $w$  nor  $v$  cannot vanish for  $u = Q = 0$  (since  $u, v, w$  are not allowed to be 0 simultaneously in  $\mathbb{P}_{112}$ ), we can use the scaling  $(u, v, w) \simeq (\lambda u, \lambda v, \lambda^2 w)$  to scale  $v \rightarrow 1$ . However, with this scaling we see that  $Q' \simeq w^2 + b_2 w + c_4 = 0$  has generically two solutions, meaning that the intersection  $\{u = 0\} \cap \{P' = 0\}$  marks two points on the torus fibre:

$$\forall q \in \mathcal{B} : \text{BiSec}(q) := \left\{ \left[ 0 : 1 : \frac{-b_2 \pm \sqrt{b_2^2 - 4c_4}}{2} \right] \right\} \subset \mathbb{E}_q \subset \mathbb{P}_{112}. \quad (\text{II.30})$$

Note that due to the square root, the two points are actually exchanged by a monodromy<sup>26</sup> around the branching locus  $b_2^2 - 4c_4 = 0$ . One therefore cannot separate the two points globally into two independent objects. Only the collection of both points gives a globally well-defined entity. The map (II.30) is precisely a 2- or bi-section. As we will see momentarily, F-theory compactified on the  $\mathbb{P}_{112}$  model will lead to an  $\mathbb{Z}_2$  symmetry.

### The origin of discrete symmetries in F-theory

Let us for simplicity restrict to the case where we have a single independent  $n$ -section on a genus-one fibration  $Y$ , i.e. there is one independent divisor class  $N$  associated with multi-sections. On this divisor class, we can still expand the M-theory 3-form, yielding a massless  $U(1)_N$  in the M-theory compactification on  $Y$  to  $\mathbb{R}^{1,n-1}$ . Similar to the situation with only a zero-section, this  $U(1)$  has to be identified with the remnant of the translation symmetry of the circle reduction of the theory in  $\mathbb{R}^{1,n}$ , i.e. it is a KK  $U(1)$ .

Recall that in this circle reduction of F-theory compactified on  $Y$ , we expect to find an infinite tower of massive states  $\phi_k$  for any field  $\phi$  in  $\mathbb{R}^{1,n}$ . If the excitations of  $\phi$  originate from M2-branes wrapping certain fibral curves  $\Gamma \subset T^2$  of the full torus fibre, then in the M-theory compactification to  $\mathbb{R}^{1,n-1}$  the states  $\phi_k$  correspond to M2-branes wrapping the curve  $\Gamma + k \cdot T^2$ . However, since the  $n$ -section intersects every fibre in  $n$  points (including multiplicity), the states  $\phi_k$  actually have charge  $n k$  under  $U(1)_N$ . Conversely, from the perspective of  $\mathbb{R}^{1,n-1}$ , it appears that the circle

<sup>25</sup>However, there were claims made recently [62] that this is not correct in the most general case, and that one should rather study objects called elliptic Calabi–Yau torsors.

<sup>26</sup>This is of course not the  $SL(2, \mathbb{Z})$  monodromy of the complex structure  $\tau$  of the torus!

reduction of the theory in  $\mathbb{R}^{1,n}$  led to KK-states with levels separated by multiples of  $n$ . So it seems that there is an effective  $\mathbb{Z}_n$  symmetry in  $\mathbb{R}^{1,n}$  that reduce the KK-tower.

The result of this admittedly quite heuristic argument can be made precise in various ways [54, 61, 63–67]. One important insight of these works were that one can understand any genus-one fibration with an  $n$ -section as a deformation of an elliptic fibration with non-trivial MW-group. More precisely, the theory on the elliptic fibration has at least one  $U(1)$  gauge factor and a singlet  $\mathbf{1}_n$  with charge  $n$  under this  $U(1)$ . The deformation then has the field theoretic interpretation as the Higgsing of the theory by giving  $\mathbf{1}_n$  a vev, which breaks the  $U(1)$  to its  $\mathbb{Z}_n$  subgroup. In this process, all other matter representations still remain present. However, some might have had the same  $U(1)$  charge mod  $n$ . If there was no symmetry differentiating these representations other than their  $U(1)$  charge, then they will be indistinguishable after the Higgsing. In the geometry, we see the manifestation of this as a ‘merging’ of the corresponding matter curves, i.e. matter states with the same  $U(1)$  charges mod  $n$  will be localised over the same curve after the Higgsing. The  $\mathbb{Z}_n$  charges of states  $\mathbf{w}$  can be computed as intersection numbers of the corresponding fibral chains  $\Gamma_{\mathbf{w}}$  with the  $n$ -section class  $N$  (see section 2.3.1 of chapter IV for more details). Furthermore, after the Higgsing, the Yukawa couplings realised in the geometry are such that the remnant  $U(1)$  charges of the participating states add up to 0 mod  $n$ , consistent with the interpretation of a  $\mathbb{Z}_n$  symmetry. Importantly, it was shown that the multi-section still gives rise to a KK  $U(1)$  as illustrated above.

Indeed, our example models in  $\text{Bl}_1\mathbb{P}_{112}$  (II.21) and  $\mathbb{P}_{112}$  (II.28) are precisely related to each other by such a deformation/Higgsing process. This has been studied in detail in [63]. Here we note that the deformation is quite obvious from the hypersurface polynomials. Concretely, by first blowing-down the  $\mathbb{P}^1$ s wrapped by the divisor  $\{s\}$  over  $C_2 = \{b_2\} \cap \{c_3\}$  (in the equation (II.21), this amounts for setting  $s$  to 1), we create singularities along  $C_2$  in the total space of the fibration. Note that these  $\mathbb{P}^1$ s were precisely those giving rise to charge 2 states in the  $\text{Bl}_1\mathbb{P}_{112}$  model. These singularities are deformed away by adding the term  $c_4 v^2$  to the polynomial, which yields the hypersurface equation (II.28) of the  $\mathbb{P}_{112}$  model. The singularity type that are created by the shrinking of the  $\mathbb{P}^1$ s is known as a conifold, hence this deformation process is also called a conifold transition. Note the change of ambient space; indeed, the coordinate  $s$  of  $\text{Bl}_1\mathbb{P}_{112}$  precisely corresponds to a blow-up (hence the ‘Bl’) of  $\mathbb{P}_{112}$  which resolves the singularities of the elliptic fibration with hypersurface equation given by (II.28) *without* the  $c_4$  term. However, the transition does not affect the base, i.e. the physical compactification space  $\mathcal{B}$  from the type IIB perspective remains the same. In chapter IV, we will see how this Higgsing affects the matter spectrum and the Yukawa coupling.

Note that the existence of a model with  $U(1)$  which is Higgsed to a model with  $\mathbb{Z}_n$  is expected from the quantum gravity folklore that any discrete symmetry must ultimately be gauged in the UV. While we only have a handful of explicit examples in F-theory, they are all compatible with this folklore, suggesting further that F-theory, or rather string theory, incorporates properties of a quantum theory of gravity at its core.

## 2.6 Constructions with toric geometry

As all our explicit fibration models are constructed and resolved within the framework of toric geometry, we would like to give a working definition of the tools. The power of toric geometry is that it encodes the data of divisors in terms of simple combinatorics. These data can be handled with a computer algebra program, most notably Sage [68]. In our fibration models (II.18), both the fibre ambient spaces  $\mathbb{A}$  and the full ambient space  $X$  have (partly) toric descriptions. In most of our discussions, we keep the base  $\mathcal{B}$  generic, i.e. it can be non-toric, and study the physical phenomena of F-theory that are independent of the choice of  $\mathcal{B}$ . For explicit examples though, e.g. those in chapter V, we also restrict ourselves to toric bases for simplicity.

Toric spaces  $X$  generalises the notion of weighted projective spaces. They can be written as

$\mathbb{C}^r \setminus \Upsilon$  modulo a set of scaling relations. Both  $\Upsilon$  and the scaling relations are encoded using a so-called toric diagram, which is a collection of  $r$  lattice vectors  $\vec{x}_i$  in  $\mathbb{Z}^n$ , where  $\dim_{\mathbb{C}} X = n$ . Certain conditions on these vectors ensure that the space  $X$  is Kähler, compact etc. The vectors  $\vec{x}_i$  are also known as the vertices of the toric diagram. Importantly, each vertex  $\vec{x}_i$  corresponds to a coordinate  $x_i$  of  $\mathbb{C}^r$ . The scaling relations are easily obtained from linear combinations of the vectors that yield zero. Explicitly, we have the scaling relation  $(x_1, \dots, x_r) \sim (\lambda_1^{a_1} x_1, \dots, \lambda_r^{a_r} x_r)$  if  $\sum_k a_k \vec{x}_k = 0$ . By simple counting of dimensions, there must be  $r - n$  such independent relation  $R$ . The set of independent divisor classes in  $X$  and the set of independent relations are in 1-to-1 correspondence. These data can be summarised in a table of the following form:

$$\begin{array}{c|cccc}
 & x_1 & x_2 & \dots & x_r \\
 \hline
 [R] & \lambda_1 & \lambda_2 & \dots & \lambda_r \\
 [\tilde{R}] & \tilde{\lambda}_1 & \tilde{\lambda}_2 & \dots & \tilde{\lambda}_r \\
 \vdots & \vdots & \vdots & \vdots & \vdots
 \end{array} \tag{II.31}$$

where one fixes a choice of the  $r - n$  independent scalings  $R$  and with them the basis of divisor classes  $[R]$ . From this table, one can read off the divisor classes of the vanishing loci of the coordinates  $x_i$  as  $[\{x_i\}] = \lambda_i [R] + \tilde{\lambda}_i [\tilde{R}] + \dots$ . These divisors are called toric divisors. Since divisor classes are equivalent to line bundle classes, one can also read the columns of such a table as ‘ $x_1$  transforms as a section of the bundle  $[R]^{\lambda_1} \otimes [\tilde{R}]^{\lambda_2} \otimes \dots$ ’ For this reason, we often include in such tables the fibration data, i.e. the assignment of line bundles  $\mathcal{L}$  of  $\mathcal{B}$  to the fibral coordinates. Since these line bundles are equivalently interpreted as divisor classes, they can be also regarded as vertical divisors in the fibration. The columns of the table form the so-called linear equivalence ideal (LIN), because it relates the toric divisors linearly to the divisors defined by the scaling relations.

For example, for the Weierstrass model (II.15), the ambient space  $X$  can be partly described by the following table:

$$\begin{array}{c|ccc}
 & x & y & z \\
 \hline
 Z & 2 & 3 & 1 \\
 \overline{\mathcal{K}} & 2 & 3 & \cdot
 \end{array} \tag{II.32}$$

where  $\cdot$  represents 0. Note that the scaling relation of the fibre ambient space  $\mathbb{P}_{231}$  gives rise to a divisor class  $Z$  which can be identified with the toric divisor  $\{z\}$  – the zero-section. The fact that  $x$  transforms as a section of  $\overline{\mathcal{K}}^2$  is reflected now by the contribution  $2\overline{\mathcal{K}}$  to the divisor class of  $\{x\}$ . This shows that we have a fibration of  $\mathbb{P}_{231}$  over  $\mathcal{B}$  and not just a simple direct product. Note that since we want to keep the base generic, we cannot include any coordinates of the base. All the data of the base we need in this table is how certain bundles – in this case  $\overline{\mathcal{K}}$  – enter the fibration structure.

The information about the set  $\Upsilon$  is harder to explain. For details, we refer to the standard textbooks, e.g. [69]. The technical procedure is known as a triangulation of the toric diagram of  $X$ . From such a triangulation, one obtains a representation of  $\Upsilon$  as the union of mutual vanishing loci of coordinates  $x_i$ . E.g. for our example  $\text{Bl}_1\mathbb{P}_{112}$  the set was given just above (II.21) as  $\{u = w = 0\} \cap \{v = s = 0\}$ . In the context of toric geometry,  $\Upsilon$  is encoded in the so-called Stanley–Reisner (SR) ideal, and is given as the collection of products of those coordinates that mutually vanish on  $\Upsilon$ . In the example, the SR-ideal would be said to be generated by  $uw$  and  $vs$ . Note that for a single toric diagram, there can be in general multiple triangulations (in dimensions higher than 2). Each triangulation strictly speaking gives rise to a different toric space. It turns out that in our constructions of F-theory fibrations, the physical results depend only on the triangulation of possible toric data encoding the base  $\mathcal{B}$ . In simple words, when we consider fibrations over generic bases, we have no data about  $\mathcal{B}$  anyways; in these cases, the



choice of triangulations have no impact on the physics of F-theory. These triangulations can be computed using **Sage**.

Given a choice of triangulation, i.e. a choice of SR-ideal, the toric diagram can compute intersection numbers of toric divisors. First, note that because the dimension of  $X$  is  $r$ , more than  $r$  divisors do not generically meet in one point. In terms of intersection number, this means that the intersection product of more than  $r$  divisors always vanishes on  $X$ . Further, if  $x_{i_1} x_{i_2} \dots x_{i_r}$  is a generator of the SR-ideal, then it means their toric divisors do not intersect, i.e. the intersection number  $[\{x_{i_1}\}] \cdot \dots \cdot [\{x_{i_r}\}] = 0$ . Now if we have toric divisors appearing more than once in a product  $[\{x_{i_1}\}] \cdot \dots \cdot [\{x_{i_r}\}]$ , then we can always use the  $n - r$  linear equivalence relations to rearrange the terms such that we end up with (possibly) several products where each factor appears only once. In this case, the intersection number  $[\{x_{i_1}\}] \cdot \dots \cdot [\{x_{i_r}\}]$  can be simply read off from the toric diagram as  $1/\text{Vol}$ , where  $\text{Vol}$  is the lattice volume spanned by the vectors  $\vec{x}_{i_1}, \dots, \vec{x}_{i_r}$ . Finally, by Poincaré-duality, we can re-interpret these intersection numbers as integrals  $\int_X \omega_{i_1} \wedge \dots \wedge \omega_{i_r}$ , where  $\omega_{i_k}$  is the  $(1, 1)$ -form dual to the divisor class  $[\{x_{i_k}\}]$ .

### Toric resolution via tops

The construction of tops, developed in [70] and systematised in [71] is a particularly handy way of engineering and resolving singularities on a torus fibration  $Y$  that lead to a desired gauge group when compactifying F-theory on  $Y$ . Essentially, the top construction describe the exceptional divisors  $\text{Ex}_i$  as toric divisors of the ambient space  $X$  of  $Y$ . Therefore, one associates to them some coordinates  $\text{ex}_i$  of  $X$ .

In our class of fibrations (II.18), codimension one singularities over a divisor  $\Theta = \{\theta\} \subset \mathcal{B}$  arises if the coefficients  $c_i$  of the polynomial  $P$  – which themselves are sections over the base  $\mathcal{B}$  – vanish to certain orders along  $\Theta$ , i.e.  $c_i = c_{i,j} \theta^j$ . The top construction now gives a new polynomial defined in the ambient space  $X$  with divisors  $\{\text{ex}_i\}$  by replacing  $c_i = c_{i,j} \theta^j$  with  $c_{i,j} \text{ex}_0^{i_0} \text{ex}_1^{i_1} \dots$ . The non-negative exponents  $i_k$  are uniquely determined by the so-called dual top, which ensures that the new, resolved hypersurface is a Calabi–Yau space. By an abusive notation, one often denotes the toric divisors  $\{\text{ex}_i\}$  by  $\text{Ex}_i$  as well.

## 2.7 Summary — an F-theory dictionary

To end this chapter, we briefly summarise the geometry and physics of F-theory compactifications. F-theory is a non-perturbative description of type IIB compactifications on  $\mathcal{B}$ , by geometrising the axio-dilaton  $\tau$  into the complex structure of the torus fibre in a Calabi–Yau fibration  $Y \rightarrow \mathcal{B}$ . In a dual description, we recover the same type IIB physics by compactifying M-theory on  $Y$  with a subsequent T-duality along a circle of the torus fibre which then decompactifies. Via this M-theory *definition* of F-theory, we can translate geometric data into physics as follows:

- $U(1)^r$  gauge symmetries arise from a non-trivial rank  $r$  Mordell–Weil group, whose generators map to divisor classes  $\omega_i$  under the Shioda-map.
- $\mathbb{Z}_n$  symmetries arise from an independent  $n$ -section class  $N$ .
- Non-abelian gauge groups  $G$  arise from singularities over codimension one loci on the base. The resolution of these singularities gives rise to exceptional divisors  $\text{Ex}_i$  which correspond to the Cartan  $U(1)$ s of  $G$ . The fibre over these codimension one loci splits into  $\mathbb{P}^1$ s that give rise to the W-bosons of  $G$ .
- Matter states arise from codimension two singularities. Over curves  $C$  in the base, the fibre splits into  $\mathbb{P}^1$ s, whose intersection numbers with  $\omega_i$ ,  $N$  and  $\text{Ex}_i$  give the charges under the corresponding  $U(1)$ ,  $\mathbb{Z}_n$  and  $G$  gauge symmetry.

- The structure of codimension three singularities encode the perturbative Yukawa interactions among matter states.

For the construction of explicit models, we rely on tools from toric geometry and the concept of tops.

One crucial entry is still missing in this dictionary, namely the geometry of fluxes and their physics. The next chapter will be devoted to set up this entry together with the necessary mathematical and computational tools for a systematic study of fluxes in F-theory.

# Chapter III

## Gauge Fluxes in F-theory

In this chapter we will explain the role of gauge fluxes or, more precisely,  $G_4$ -fluxes in F-theory compactification to 4D. After a short survey of the general properties, we will focus on a particular subclass of  $G_4$ -fluxes, namely those lying in the so-called *primary vertical* cohomology, or vertical cohomology in short. As a main result, we will present a computational set-up that simplifies cohomological calculations and in particular allows for a systematic treatment of the vertical cohomology in a broad class of torus fibrations over a generic base.

### 1 $G_4$ -Fluxes in F-theory

In general, fluxes refer to a non-trivial background of the field strength  $F$  of a gauge potential. In type IIB, fluxes have been studied in great detail. Notably, so-called bulk fluxes originating from the 2-form potentials  $B_2$  and  $C_2$  (see table II.1) are of interest for moduli stabilisations (see e.g. [24, 25] for an overview). Another type of fluxes arise in the presence of 7-branes. These are the background values of the field strength of the non-abelian gauge field on the 7-branes.

The brane fluxes are responsible for chiral matter in type IIB compactifications. Given a non-trivial flux configuration on the brane, the flux is described by a line bundle  $\mathcal{L}$  over the brane with first Chern class  $F$ . Matter states arise at curve  $C$  on the brane (which is the intersection with other branes). In [72] it was shown that the cohomology groups

$$H^i(C, \mathcal{L}|_C \otimes \sqrt{K_C})$$

count the chiral ( $i = 0$ ) and anti-chiral ( $i = 1$ ) multiplets over  $C$  (here  $\sqrt{K_C}$  denotes the spin bundle over  $C$ ). The chiral index is then given by the Hirzebruch–Riemann–Roch theorem as

$$\begin{aligned} \chi &= \#(\text{chiral}) - \#(\text{anti-chiral}) \\ &= \dim H^0(C, \mathcal{L}|_C \otimes \sqrt{K_C}) - \dim H^1(C, \mathcal{L}|_C \otimes \sqrt{K_C}) = \int_C F. \end{aligned} \tag{III.1}$$

In the F-theory description, both type of fluxes unified into one object known as the  $G_4$ -flux. Since it incorporates the bulk fluxes from type IIB,  $G_4$ -fluxes can also be used for moduli stabilisation mechanisms in F-theory compactifications (see [26] for a review).<sup>1</sup> In this thesis, we will be concerned with the other aspect, namely the chirality inducing feature of  $G_4$ -fluxes. To this end, we will first introduce a rigorous description of  $G_4$  in terms of cohomology forms.

In the following, we will work under the assumption that all our fibration spaces are smooth Calabi–Yau spaces, i.e. any possible singularities are resolved in a consistent way. It is then

---

<sup>1</sup>Note that it is in this context that the popularly cited ‘ $10^{500}$ ’ for the number of string vacua arose. To be precise, this is the ‘typical’ number of flux configurations allowed for a given compactification manifold. However, by now there are further analyses which have pushed this number up to  $10^{272,000}$  [73].

implied that all physical properties, unless otherwise stated, are considered in the singular limit. In particular, gauge symmetries and matter states always refer to massless fields. Under this assumption, the notation  $\hat{X}$  for a resolution of  $X$  becomes obsolete.

### 1.1 Mathematical description of $G_4$ -flux

Since F-theory is defined via its duality to M-theory, let us briefly discuss  $G_4$ -fluxes in M-theory. There,  $G_4 = dC_3$  is the field strength associated to the M-theory 3-form  $C_3$ . When compactified on a torus-fibred Calabi–Yau fourfold  $Y_4$ , the resulting 3D theory has  $\mathcal{N} = 2$  supersymmetry (which lifts in F-theory to 4D  $\mathcal{N} = 1$ ). To preserve this supersymmetry in non-trivial gauge background (i.e.  $G_4 \neq 0$ ), the flux must be a  $(2,2)$ -form. For details we refer to numerous reviews, e.g. [26]. Furthermore,  $G_4$ -fluxes are subject to the quantisation condition [74]

$$G_4 + \frac{c_2(Y_4)}{2} \in H^4(Y_4, \mathbb{Z}). \quad (\text{III.2})$$

Because the second Chern class  $c_2(Y_4)$  is an integer class,  $G_4$  must lie in

$$H^4(Y_4, \mathbb{Q}) = \bigoplus_{p+q=4} H^{(p,q)}(Y_4, \mathbb{Q}) \supset H^{(2,2)}(Y_4, \mathbb{Q}).$$

Related to the quantisation condition is the cancellation of brane charges from spacetime filling M2-branes. These lift to spacetime filling 3-branes in F-theory; in analogy to type IIB the cancellation is usually referred to as the cancellation of D3-tadpole. The number of M2/D3-branes depends on the flux via [75]

$$n_3 = \frac{\chi(Y_4)}{24} - \frac{1}{2} \int_{Y_4} G_4 \wedge G_4, \quad (\text{III.3})$$

with  $\chi(Y_4)$  being the Euler number of the Calabi–Yau fourfold. Clearly  $n_3$  needs to be an integer. It is typically assumed that an appropriately quantised flux will also lead to an integer D3-tadpole  $n_3$ . To avoid anti-branes, which would destabilise the compactification, we must require that  $n_3 \geq 0$ .

In the context of F-theory compactifications, which by the M-/F-theory duality (cf. chapter II) is the decompactification limit of an M-theory configuration, there are further consistency conditions, the so-called *transversality conditions*. To understand their origin, let us see how  $G_4$ -fluxes behave in the decompactification limit of M-theory on a torus-fibred fourfold. Recall from section 2.3 of the previous chapter that this F-theory limit amounts to sending the fibre volume to zero. Denoting the radii of the two one-cycles of the torus by  $R_A$  and  $R_B$ , the limit is taken in two steps. First, the  $A$ -cycle is identified with the M-theory circle, and the limit  $R_A \rightarrow 0$  is the weakly coupled type IIA limit of M-theory. The second step is a T-duality transformation along the  $B$ -cycle, which gives type IIB on a circle of radius  $\tilde{R}_B = \frac{\alpha'}{R_B}$ . In the limit  $R_B \rightarrow 0$  the dual circle decompactifies and one ends up with a (generically strongly coupled) type IIB theory in four dimensions. Importantly, one of the four large dimensions has its origin in one of the fibre directions of the fourfold. One immediate consequence is that care must be taken when introducing fluxes [75, 76]: Four-dimensional Lorentz invariance forbids fluxes with non-trivial VEV along the circle along which the T-dualisation is performed [77]. More precisely, the  $G_4$  flux must have *one leg in the fibre* to meet this requirement. Indeed, in [77] it was shown that a flux with zero or two legs along the fibre maps to the self-dual 5-form flux  $F_5$  in type IIB string theory. In this case the vacuum expectation value extends along the non-compact directions and breaks Lorentz invariance. The remaining possibility is a flux with one leg in the fibre. These solutions do not lie completely in the base, nor do they fill the two fibre directions.

### 1.1.1 Transversality conditions in elliptic fibrations

This transversality condition [77] is usually expressed in slightly more formal terms as follows. Let us first consider the standard case of an *elliptically* fibred fourfold

$$\pi : Y_4 \rightarrow \mathcal{B}. \quad (\text{III.4})$$

By definition, an elliptic fibration has a zero section  $\text{Sec}_0 : \mathcal{B} \rightarrow Y_4$  which defines an embedding of the base  $\mathcal{B}$  as a divisor  $\text{Sec}_0(\mathcal{B})$  into  $Y_4$ ,

$$\iota_\sigma : \text{Sec}_0(\mathcal{B}) \hookrightarrow Y_4. \quad (\text{III.5})$$

In the presence of several independent sections, i.e. for an elliptic fibration with a Mordell–Weil group of non-zero rank, the choice of zero-section is not unique [78, 79], but the different choices all asymptote to the same effective theory in the F-theory limit.

Let us therefore assume that we have singled out one particular section as our zero-section and denote by  $[\text{Sec}_0] \equiv S_0$  its homology class. For simplicity we assume the zero-section to be holomorphic, but this is not necessary [78, 80]. From the perspective of the 3-dimensional M-theory effective action,  $S_0$  generates a  $U(1)$  gauge group which is to be identified with the Kaluza–Klein  $U(1)$  obtained by reducing the 4-dimensional F-theory compactification along a circle  $S^1$  (see [34] for a recent discussion in the language of 3-dimensional supergravity). In the effective action, charged matter states arise from M2-branes wrapping suitable fibral curves [39, 81–83]. This includes both the non-Cartan vector bosons and related matter states and extra charged localised matter. More precisely, each component field  $\Psi(x, z)$  of an  $\mathcal{N} = 1$  multiplet of the 4-dimensional F-theory action decomposes, upon circle reduction to three dimensions, to a zero mode plus a full tower of Kaluza–Klein excitations  $\Psi(x, z) = \sum_{n \in \mathbb{Z}} \psi_n(x) e^{inz}$ . Here  $x$  denotes external coordinates in the 3-dimensional M-theory vacuum and  $z$  is the KK-circle coordinate. The higher KK states have KK  $U(1)$  charge  $n = \int_{C_n} S_0$ , where  $C_n$  is the fibral curve wrapped by the M2-brane associated with state  $\psi_n(x)$ . Since  $S_0$  is the class of a section, it has intersection number  $+1$  with a generic non-degenerate fibre. This is still true for split fibres in higher codimension, but not all components of the fibre will intersect  $S_0$ . Thus, the zero mode  $\psi_0$  is due to M2-branes wrapping a fibral curve  $C_0$  with vanishing intersection with the zero-section  $S_0$ . The KK partner of KK charge  $n$  is then created by an M2-brane wrapping in addition the full elliptic fibre  $n$ -times such that its associated fibral curve can be written as  $C_n = C_0 + n f$ .

At the cohomological level, the transversality conditions of [77] on gauge fluxes is that (e.g. [10, 84–87])

$$0 = \int_{Y_4} G_4 \wedge S_0 \wedge \pi^{-1}(D_a^{(\mathcal{B})}), \quad (\text{III.6})$$

$$0 = \int_{Y_4} G_4 \wedge \pi^{-1}(D_a^{(\mathcal{B})}) \wedge \pi^{-1}(D_b^{(\mathcal{B})}) = \int_{\pi^{-1}(D_a^{(\mathcal{B})}) \cap \pi^{-1}(D_b^{(\mathcal{B})})} G_4, \quad (\text{III.7})$$

for any divisor classes  $D_a^{(\mathcal{B})}, D_b^{(\mathcal{B})} \in H^{(1,1)}(\mathcal{B})$  in the base.<sup>2</sup> The first condition guarantees that  $G_4$  does not lie completely in the base because it requires that

$$\int_{Y_4} G_4 \wedge S_0 \wedge \pi^{-1}(D_a^{(\mathcal{B})}) = \int_{\text{Sec}_0(\mathcal{B})} \iota_\sigma^* \left( G_4 \wedge \pi^{-1}(D_a^{(\mathcal{B})}) \right) \stackrel{!}{=} 0, \quad (\text{III.8})$$

i.e. the net flux through any divisor  $D_a^{(\mathcal{B})}$  on the base vanishes. The second condition expresses that the solution cannot have two (real) legs along the fibre. This condition can be rephrased as

<sup>2</sup>Note that here and in the following, our notation will not differentiate between  $(1, 1)$ -forms and their Poincaré-dual divisors.

the constraint that the chiral index of all KK partners equals that of the zero mode. Indeed the intersection  $\pi^{-1}(D_a^{(\mathcal{B})}) \cap \pi^{-1}(D_b^{(\mathcal{B})})$  is a 4-cycle<sup>3</sup> on  $Y_4$  extending along the full fibre over a curve  $D_a^{(\mathcal{B})} \cap D_b^{(\mathcal{B})}$  in the base and  $\int_{\pi^{-1}D_a \cap \pi^{-1}D_b} G_4$  computes the chiral index of states associated with M2-branes wrapping the full fibre over  $D_a \cap D_b$ . If the integral over any four-cycle of this type vanishes, this guarantees in particular that the multiplicities of the fields  $\psi_n$  are the same for all  $n$ . This is the field theoretic way of stating the requirement of Lorentz invariance. A discussion along these lines can also be found e.g. in [57, 88].

In models with non-abelian gauge symmetries the Cartan generators correspond to the exceptional divisor classes  $rmEx_i$  from the resolution of the singularity. In order to leave the non-abelian gauge group unbroken in the F-theory limit, we must in addition demand that

$$\int_{Y_4} G_4 \wedge Ex_i \wedge \pi^{-1}(D_a^{(\mathcal{B})}) = 0 \quad \forall D_a^{(\mathcal{B})} \in H^{(1,1)}(\mathcal{B}). \quad (\text{III.9})$$

Indeed, M2-branes wrapping combinations of the rational fibres  $\mathbb{P}_i^1$  of the resolution divisors  $Ex_i$  give rise to non-abelian massless vector bosons in the F-theory limit [81]. The condition (III.9) guarantees that the flux induces no chiral index for the associated gauginos. If one of these conditions fails, the F-theory gauge group will be broken to the commutant of the associated Cartan generator.

### 1.1.2 Transversality conditions in genus-one fibrations

We are now in a position to generalise these criteria to F-theory compactifications on non-elliptic genus-one fibrations  $\mathbb{Y}_4$ . The main distinction from elliptic fibrations is that no section exists, but only one or several multi-sections. Recall that an  $n$ -section is a multi-valued map assigning to each point in the base locally  $n$ -points in the fibre which are globally exchanged by monodromies. This defines an  $n$ -fold branched cover  $\mu_n(\mathcal{B})$  of the base  $\mathcal{B}$  inside  $\mathbb{Y}_4$  together with an embedding

$$\iota_\mu : \mu_n(\mathcal{B}) \hookrightarrow \mathbb{Y}_4. \quad (\text{III.10})$$

Let us denote the homology class of the  $n$ -section as  $N$ . For the purpose of relating the M-theory reduction to F-theory it is necessary to specify a notion of KK  $U(1)$ . As pointed out several times by now [64–67], it is still true that a multi-section defines such a KK  $U(1)$  similarly to the case of an elliptic fibration because it is possible to expand the M-theory 3-form  $C_3$  as  $C_3 = A_{KK} \wedge N + \dots$ . We therefore need to choose an  $n$ -section as the substitute for the zero-section and define transversality with respect to the associated KK frame.

In terms of this embedding multi-section then

$$\int_{\mathbb{Y}_4} G_4 \wedge N \wedge \pi^{-1}(D_a^{(\mathcal{B})}) = \int_{\mu_n(\mathcal{B})} \iota_n^* \left( G_4 \wedge \pi^{-1}(D_a^{(\mathcal{B})}) \right). \quad (\text{III.11})$$

Therefore the analogue of the first condition (III.6) is

$$\int_{\mathbb{Y}_4} G_4 \wedge N \wedge \pi^{-1}(D_a^{(\mathcal{B})}) \stackrel{!}{=} 0, \quad (\text{III.12})$$

which guarantees that the net flux vanishes through every base 4-cycle. Second, since the multi-section still defines the notion of a KK  $U(1)$ , the condition that all elements of the KK tower should have the same chiral index implies that the analogue of (III.7) must still hold.

In principle, this condition suffices in order for the flux to lift properly in the F-theory limit. However, there is one type of fluxes that does not satisfy this condition, which however are

<sup>3</sup>Following the standard convention,  $n$ -cycles are submanifolds of real dimension  $n$ .

expected from a type IIB perspective. These are the so-called Cartan fluxes of the form  $G_4 = \text{Ex}_i \wedge \pi^{-1}(F)$ , with  $F \in H^{(1,1)}(\mathcal{B})$ . In the type IIB limit, they can be seen as the brane fluxes associated with a background for the gauge field along the branes. In general the  $n$ -section intersects more than one of the  $\mathbb{P}^1$ s of the exceptional divisors  $\text{Ex}_i$ . This implies that the Cartan fluxes do not satisfy (III.12) in general. However, as we will see in chapter IV, one may construct a divisor class

$$\hat{N} = N + \sum_i a_i \text{Ex}_i \quad (\text{III.13})$$

and choose the coefficients  $a_i$  such that the modified condition

$$\int_{\mathbb{Y}_4} G_4 \wedge \hat{N} \wedge \pi^{-1}(D_a^{(\mathcal{B})}) = 0 \quad (\text{III.14})$$

is satisfied for Cartan fluxes. The choice of  $\hat{N}$  amounts to a redefinition of the KK  $U(1)$  symmetry such that it does not mix with the Cartan  $U(1)$  generators  $\text{Ex}_i$ . A similar redefinition has been discussed in a different context in [79]. In chapter IV, we will put this proposed form of the transversality condition on genus-one fibrations to test in an explicit example.

## 1.2 Physical implications of $G_4$ -fluxes

The inclusion of fluxes broadens the variety of F-theory compactifications considerably. As we have mentioned earlier, fluxes are key players in moduli stabilisation scenarios. This is especially important for cosmological model building with F-theory (see [26] for a review). As we are interested in particle physics phenomenology, we will focus on the chirality inducing feature of  $G_4$ -fluxes.

### 1.2.1 Chiral charged matter in 4D F-theory

As  $G_4$ -fluxes incorporate brane fluxes from type IIB, they should give rise to chiral matter in F-theory as well. Let us take as an example the Cartan fluxes  $G_4 = \text{Ex}_i \wedge \pi^{-1}(F)$  with  $F \in H^{(1,1)}(\mathcal{B})$ . They satisfy the transversality conditions, but not in general the gauge symmetry condition (III.9). Therefore, they will in general break the gauge group  $G$  to a subgroup  $H$ . Note that this aspect is very attractive for GUT-models in order to re-create the Standard Model [12, 89]. In any case, the matter states over a curve  $C \subset \mathcal{B}$  will decompose accordingly into representations of  $H$ , such that all states in one representation  $\mathcal{R}$  have the same charge  $q$  under the Cartan  $U(1)$  associated with  $\text{Ex}_i$ . Based on the type IIB intuition, the net chirality of these states is expected to be  $q \int_C F$  (see [90] and references therein).

Recall from section 2.4.4 in chapter II that a charged matter state  $\mathbf{w}$  corresponds to a chain  $\Gamma_{\mathbf{w}}$  of fibral  $\mathbb{P}^1$ s into which the torus-fibre splits over  $C$ . Fibring these chains over  $C$  form 4-cycles  $\gamma_{\mathbf{w}} \subset Y_4$ ,

$$\begin{array}{ccc} \Gamma_{\mathbf{w}} & \longrightarrow & \gamma_{\mathbf{w}} \\ & & \downarrow \\ & & C \end{array}$$

which are the matter surfaces. It has been proposed in [10, 84–86, 91] that the chiral index of  $\mathbf{w}$  is given by integrating the flux over the corresponding matter surface:

$$\chi(\mathbf{w}) = \int_{\gamma_{\mathbf{w}}} G_4 = \int_{Y_4} G_4 \wedge [\gamma_{\mathbf{w}}]. \quad (\text{III.15})$$

Here and in the following, we use the notation  $[\gamma]$  to denote the homology class of the 4-cycle  $\gamma$ . By Poincaré-duality,  $[\gamma]$  can be regarded as 4-form on  $Y_4$  as well. For the Cartan fluxes, this formula

indeed produces the desired chirality: By reinterpreting the flux integral  $\int_{Y_4} \text{Ex}_i \wedge \pi^{-1}(F) \wedge [\gamma_{\mathbf{w}}]$  as the intersection number  $\text{Ex}_i \cdot \pi^{-1}(F) \cdot [\gamma_{\mathbf{w}}]$  on the fourfold, we see that the chirality is given as the intersection of the Cartan divisor  $\text{Ex}_i$  with the fibral curve  $\Gamma_{\mathbf{w}}$  of  $\gamma_{\mathbf{w}}$  over the point  $C \cap F$  in the base. Clearly, this intersection number is just the Cartan charge  $q$  of the weight  $\mathbf{w}$  under  $\text{Ex}_i$ , multiplied by the number of points in which  $C$  and  $F$  meet on the base:  $\chi = q \int_{\mathcal{B}} [C] \wedge F = q \int_C F$ .

It should be stressed that (III.15) is still a proposal, i.e. not proven rigorously. However, it can also be argued from the duality to M-theory. Since F-theory is defined via M-theory, let us briefly present the logic behind this argument [87]. By compactifying M-theory on the *smooth* torus fibration  $Y_4$ , we obtain a 3D field theory with massive states. This is of course because the fibre  $\mathbb{P}^1$ s, which M2-branes wrap to give those states, have finite size in the smooth geometry. In this field theory, there are only massless vector fields  $A_i$  arising from the reduction of  $C_3$  over divisors  $\omega_i \in H^{(1,1)}(Y_4)$ . In a non-trivial  $G_4$ -flux background, there is in addition a Chern–Simons coupling  $\int_{11\text{D}} C_3 \wedge G_4 \wedge G_4$  in 11D, which upon compactification induce 3D Chern–Simons terms  $A_i \wedge F_j$ , where  $F_j$  is the field strength of  $A_j$ . Crucially, it was argued in [87] that the 3D coupling constants of these terms,  $\Theta_{ij} = \int_{Y_4} G_4 \wedge \omega_i \wedge \omega_j$ , can be re-interpreted as a 1-loop quantum corrections generated by the massive states, which originate from the massless states in 4D from F-theory compactified on the *singular limit* of  $Y_4$ . In [87] a precise formula was derived that matches  $\Theta_{ij}$  with the chiralities and charges of the massless 4D states. In explicit models, one knows both  $\Theta_{ij}$  as well as the charges of all massless states. Therefore one can use the results of [87] to ‘test’ any proposal for chirality in 4D F-theory. Indeed, (III.15) satisfies this matching in all explicit examples [57, 87, 88]. This motivates us to also trust (III.15) to be the correct way to compute the chirality.

Note that the notion of chirality only makes sense if all states  $\mathbf{w}$  of the same matter representation have the same chiral index. For singlet matter, this is clear since there is only one matter surface associated with the singlet state. In models with a non-abelian gauge group over a divisor  $W = [\{w\}] \subset \mathcal{B}$ , all states of a non-trivial representation  $\mathcal{R}$  are localised over a curve of the form  $C_{\mathcal{R}} = \{w\} \cap \{p\}$ . Here  $p$  is a polynomial (or section to be more precise) on the base, i.e.  $[p] \in H^{(1,1)}(\mathcal{B})$ . Different weight states  $\mathbf{w} \in \mathcal{R}$  differ by linear combinations of simple roots, which themselves are the fibres of the exceptional divisors  $\text{Ex}_i$  that resolve the singularities over  $W$ . In homology, the difference  $[\gamma_{\mathbf{w}}] - [\gamma_{\mathbf{w}'}]$  for two different weights is therefore a linear combination  $\sum_n \delta_n \text{Ex}_n \wedge [p]$ , where the numerical coefficients  $\delta_n$  are dictated by representation theory. The condition (III.9) then ensures that for a valid flux  $G_4$ , the chirality within one representation is well-defined,

$$\int_{Y_4} G_4 \wedge [\gamma_{\mathbf{w}}] - \int_{Y_4} G_4 \wedge [\gamma_{\mathbf{w}'}] = \sum_n \delta_n \int_{Y_4} G_4 \wedge \text{Ex}_n \wedge [p] = 0,$$

i.e. the flux does not break the non-abelian gauge symmetry in the F-theory limit:

$$\forall \mathbf{w}, \mathbf{w}' \in \mathcal{R} : \int_{\gamma_{\mathbf{w}}} G_4 = \int_{\gamma_{\mathbf{w}'}} G_4 =: \chi(\mathcal{R}) \quad (\text{III.16})$$

To keep things simple, we will therefore – unless otherwise stated – only refer to *the* matter surface  $\gamma_{\mathcal{R}}$  of a representation  $\mathcal{R}$ , by which we mean the one (irreducible) surface whose fibre is the  $\mathbb{P}^1$  into which a root splits over  $C_{\mathcal{R}}$ ; this  $\mathbb{P}^1$  carries the weight charges of a state in  $\mathcal{R}$  (which need not to be the highest weight).

Before we continue, let us briefly remark that the  $G_4$ -flux can only provide us with the net chirality, but not the actual number of chiral and anti-chiral matter multiplets. These data also depend on the flat parts of the gauge potential  $C_3$ , i.e. those for which  $G_4$  vanishes. As argued in [92, 93] and further developed in [94, 95], it requires the study of the so-called Deligne cohomology to describe these data geometrically. The tools for such a analysis are still lacking for explicit models, therefore, we will not pursue this route in this thesis.



### 1.2.2 $G_4$ -flux as a topological quantity

Part of our analysis in chapter IV will be a comparison the fluxes in the  $\text{Bl}_1\mathbb{P}_{112}$  model with a  $U(1)$  symmetry and in the related  $\mathbb{P}_{112}$  with a  $\mathbb{Z}_2$  symmetry. These two models are related by a conifold transition. The role of fluxes in such a transition have been studied [84, 94, 96] in more general settings and in [64] in the context of discrete symmetries. The key observation is that  $G_4$ -flux is a topological quantity in the following sense.

By a conifold transition  $Y_4 \rightarrow \mathbb{Y}_4$ , the topology of the space changes. In particular, the Euler numbers  $\chi(Y_4)$  and  $\chi(\mathbb{Y}_4)$  will differ. In an F-theory compactification however, the number  $n_3$  of spacetime filling D3-branes does not change, simply because these D3-branes are not geometrised in the F-theory description of type IIB. Therefore, for the D3-tadpole (III.3) cancellation to be satisfied for both theories, i.e. compactification on  $Y_4$  and  $\mathbb{Y}_4$ , fluxes must be taken into account. In addition, our physical intuition tells us that the conifold transition, which corresponds to a Higgsing, must preserve the net chiralities of un-Higgsed states. Thus, for a consistent geometric description of the F-theory physics, we expect a matching of flux configurations on  $Y_4$  and  $\mathbb{Y}_4$  such that the D3-tadpole  $n_3$  and the net chiral indices are conserved.

Indeed, as we will show in chapter IV, we can establish such a map for the conifold transition between the  $\text{Bl}_1\mathbb{P}_{112}$  and the  $\mathbb{P}_{112}$  model for a certain class of fluxes. This class of fluxes, so-called primary vertical or simply vertical fluxes, have a particularly easy description in terms of geometry, and can be systematically computed with the tools we will develop in this chapter.

## 2 Vertical Fluxes

It is generally known that the middle cohomology of a fourfold splits into

$$H^{(2,2)}(Y_4) = H_{\text{hor}}^{(2,2)}(Y_4) \oplus H_{\text{vert}}^{(2,2)}(Y_4) \oplus H_{\text{rem}}^{(2,2)}(Y_4). \quad (\text{III.17})$$

The primary horizontal component  $H_{\text{hor}}^{(2,2)}(Y_4)$  has been introduced in [97] as the subspace which can be reached from  $H^{(4,0)}(Y_4)$  by two successive variations of Hodge structure. Its elements are Poincaré-dual to those 4-cycles which are algebraic only on a subset of the complex structure moduli space. The part which is computationally accessible in the most straightforward way is the primary vertical subspace,  $H_{\text{vert}}^{(2,2)}(Y_4)$ , which is generated by products of divisors. The dual 4-cycles are thus algebraic for every choice of complex structure moduli. The horizontal and the vertical subspaces are mapped onto each other by mirror symmetry [97–99] and are orthogonal with respect to the intersection pairing. The remainder  $H_{\text{rem}}^{(2,2)}(Y_4)$  was introduced in [100] as the orthogonal complement of  $H_{\text{hor}}^{(2,2)}(Y_4) \oplus H_{\text{vert}}^{(2,2)}(Y_4)$ . In what follows, we will focus on the class of  $G_4$ -fluxes inside  $H_{\text{vert}}^{(2,2)}(Y_4)$ . The aim of this section is to provide the necessary background, which underlies the algorithmic approach to vertical fluxes. The key feature of the vertical cohomology is that, by Poincaré-duality, we can translate everything into the intersection theory of divisors, which for all our toric models boils down to simple combinatorics.

### 2.1 Vertical cohomology as intersection theory of divisors

In appendix A we give a short overview of intersection theory on a general complex projective manifold  $X$  with  $\dim_{\mathbb{C}} X = N$ . The key result is the isomorphism

$$\bigoplus_{k=0}^N H^{(k,k)}(X, \mathbb{Q}) \cong \bigoplus_{k=0}^N H_{2(N-k)}^{\text{alg}}(X, \mathbb{Q}) \quad (\text{III.18})$$

provided by Poincaré-duality, where on the right hand side the elements of  $H_{2(N-k)}^{\text{alg}}(X, \mathbb{Q})$  are rational linear combinations of homology classes of (real) dimension  $2(N-k)$  sub-manifolds,

which are also called  $2(N - k)$ -cycles. E.g. a  $(2, 2)$ -form is Poincaré-dual to a 4-cycle on a complex fourfold. The superscript ‘alg’ denotes the fact<sup>4</sup> that these cycles are algebraic, i.e. they are describable as vanishing loci of polynomials; by a theorem of Chow, these are in 1-to-1 correspondence with complex sub-manifolds of  $X$ . It is also customary to count the codimension of (algebraic) cycles, which is usually given as complex codimension. E.g. in a fourfold, a complex 6-cycle is also referred to as of codimension one, a 4-cycle is of codimension two etc.

The wedge product of forms is translated into the intersection product  $\cdot$  of homology classes, which roughly speaking is a formalised way of appropriately counting the set-theoretic intersection. In particular, because  $H_0(X) \cong H^{(N,N)}(X) \cong \mathbb{Q}$ , an integral  $\int_X \omega \wedge \eta$  with  $\omega \wedge \eta \in H^{(N,N)}(X)$  can be interpreted as an appropriate counting of intersection points – the intersection number – of the homology classes Poincaré-dual to  $\omega$  and  $\eta$ :

$$\int_X \omega \wedge \eta = \text{PD}(\omega) \cdot \text{PD}(\eta) \equiv \omega \cdot \eta. \tag{III.19}$$

Note again that we use the common abusive notation of not differentiating between (co-)homology classes and their Poincaré-duals. Similarly, an integral of a  $(k, k)$ -form  $\omega$  over a  $2k$ -cycle  $\gamma$  can be evaluated as  $\int_\gamma \omega = \int_X \omega \wedge [\gamma] = \omega \cdot [\gamma]$ .

The vertical cohomology  $H_{\text{vert}}^{(k,k)}$  is the linear span of  $(H^{(1,1)})^k$  in  $H^{(k,k)}$ , i.e. linear combinations of  $k$ -fold products of  $(1, 1)$ -forms. By (III.18),  $(1, 1)$ -forms are Poincaré-dual to codimension one cycles. In complex geometry, these cycles are known as divisors, and can be shown to be a collection of zeroes and poles (with appropriate counting) of a meromorphic function. Hence, vertical  $(k, k)$ -forms can be understood by analysing divisors.

In general, formally different intersection products of  $k$  divisors of a generic space  $X$  can be the same as elements of  $H_{2(N-k)}^{\text{alg}}(Z)$ . The reason is that there are certain relations amongst the divisors and their intersections. One can divide these relations into two types:

1. The first type are linear equivalence relations amongst divisors. For our purposes it suffices to understand these as the homological equivalence. E.g. on  $X = \mathbb{P}^n$  with homogeneous coordinates  $[z_0 : \dots : z_n]$ , all hyperplane divisors  $[\{z_i\}]$  are linearly equivalent. This can be formally phrased as  $[\{z_i\}] - [\{z_j\}] = 0$ .

We will use ‘LIN’ to denote the set of all such expressions which are linearly equivalent to 0, and call it the ‘linear equivalence ideal’. Note that any sum/difference of such expressions will again be linearly equivalent to 0, and also products with any other homology class will also yield an expression which is (rationally) equivalent to 0.

2. The second type involves intersection relations amongst divisors. Under the consideration of the linear relations, the intersection relations are fully specified by identifying all intersection products which are rationally equivalent to 0. The underlying geometric statement is that divisors which intersect to 0 in homology do not generically intersect as sub-manifolds. By the analogy to toric spaces (where these relations come from the Stanley–Reisner ideal), we will call them SR-relations, and the set containing all vanishing product expressions is the ‘SR-ideal’ or ‘SRI’.

For  $X = \mathbb{P}^n$ , such a relation is  $[\{z_0\}]^{n+1} = 0$ . Note that together with the linear relations  $[\{z_i\}] - [\{z_j\}] = 0$ , this also implies that any  $(n + 1)$ -fold  $\prod_{k=1}^{n+1} [\{z_{i_k}\}] = 0$ , reflecting the intuition that in  $n$  dimensions,  $n + 1$  generic hyperplanes will not meet. Again, any sum/difference of SRI elements and product of SRI with any other homology class are equivalent to 0 in homology.

---

<sup>4</sup>It requires the assumption of the Hodge conjecture, which is proven for toric spaces, complex threefolds and for 2-cycles, i.e. divisors in general. Since vertical forms are products of divisors, the Hodge conjecture also holds for them.

A convenient way to encode these informations systematically, such that a computer algebra system like **Sage** or **Singular** can handle it, is to construct a quotient polynomial ring as follows. First, notice that formal linear combinations of (arbitrary products of) divisors  $D_i$  with complex coefficients can be regarded as a polynomial  $P \in \mathbb{Q}[D_i]$  with the divisors as formal variables. Secondly, implementing the linear and SR-relations amounts to forming equivalence classes of polynomials differing by elements of LIN and/or SRI, which in the language of polynomial algebra is given by a quotient ring. Combining these ideas with Poincaré-duality, we arrive at the following identification

$$\bigoplus_{k=0}^N H_{\text{vert}}^{(k,k)}(X) \cong \frac{\mathbb{Q}[D_i]}{\text{LIN} + \text{SRI}}, \quad (\text{III.20})$$

where the analogon of the grading of cohomology on the right hand side simply comes from the grading of polynomials.<sup>5</sup> The wedge product of vertical forms translates under this duality to simply the polynomial multiplication in the quotient ring.

In explicit F-theory models on a torus fibration  $Y$ , where one usually knows all divisors  $D_i$ , one needs to work out the relations LIN and SRI in order to fully describe  $H_{\text{vert}}^{(\cdot,\cdot)}(Y)$ . While this is in principle possible, this can be a non-trivial task. E.g. when divisors are only given in terms of complicated loci of the fibration (as in [54,60]) one would need to infer the linear and intersection relations from computing geometric intersections of *generic* hypersurfaces with the corresponding divisor classes. For cases where the loci are given in terms of vanishing of polynomials, one might hope to use the techniques of section 3. However, as we will now see, the situation simplifies considerably for our class of toric constructions.

## 2.2 Vertical cohomology forms on toric hypersurfaces

Originally proven for threefolds, the Shioda–Tate–Wazir theorem [101] states that on an elliptic fibration  $Y \rightarrow \mathcal{B}$ , all divisors are either pullbacks of divisors  $D_i^{(\mathcal{B})}$  in the base (‘vertical divisors’)<sup>6</sup>, exceptional (blow-up) divisors, or sections of the fibration. It is widely believed, although not explicitly shown, that this also holds for fourfolds. In addition, it was argued in [61] that the theorem should also hold, by replacing sections with multi-sections, if  $Y$  is a genus-one fibrations without sections.

Recall that in the construction via tops,  $Y$  is a hypersurface  $\{P_T = 0\} \equiv \{P_T\}$  in an ambient space  $X \rightarrow \mathcal{B}$  of complex dimension  $d + 1$ , which is the fibration of a toric variety – the fibre ambient space – over the same base  $\mathcal{B}$ . In particular, the hypersurface is itself a divisor, i.e. has an associated element (a homology class) in  $H_{2d}^{\text{alg}}(X)$ , which we will denote by  $[Y] \equiv [\{P_T\}]$ . Specifically in our class of models, (multi-)sections and exceptional divisors of  $Y$  arise as intersections  $\{P_T\} \cap D_i^{(T)}$  of the hypersurface with divisors  $D_i^{(T)} \subset X$  defined by the top. Since  $X$  and  $Y$  also share the same base, they share the same vertical divisors, hence all divisors of  $Y$  come from  $X$  by restriction, i.e.  $D_i^{(Y)} \cong D_i \cap \{P_T\}$  for some divisor  $D_i$  of  $X$ . Note that we use ‘ $\cong$ ’ due the fact that  $D_i^{(Y)}$  is a priori defined on  $Y$ . However, the natural embedding of  $Y \xrightarrow{i} X$  defines a push-forward map  $i_*$  in homology. With that, one can identify a divisor on  $Y$  by  $D_i^{(Y)} \equiv i_*(D_i^{(Y)}) = D_i \cap \{P_T\}$  with a 4-cycle in the ambient space. We will now pass from geometric intersections of divisors to the intersection product (cf. appendix A.), and in doing so abuse the notation by using the

<sup>5</sup>Note that the construction of quotient rings, both formally and as required by computer algebra systems like **Singular**, requires the ‘denominator’ to be an ideal of the ring in the ‘numerator’. While ideals in rings will be discussed within a different context in section 3, we note here that LIN and SRI are in fact ideals of  $\mathbb{Q}[D_i]$ , and the ‘+’ in the denominator is really the sum of two ideals.

<sup>6</sup>By an abuse of notation we will here and in the following use the same variable to denote divisors  $D^{(\mathcal{B})}$  of the base and the corresponding vertical divisors  $\pi^{-1}(D^{(\mathcal{B})})$  in the ambient space.

same variable denoting the divisor as a sub-manifold and as a class. Then the identification can be phrased as  $i_* : H_{2(d-1)}^{\text{alg}}(Y) \xrightarrow{\sim} H_{2d}^{\text{alg}}(X) \cdot [Y] \subset H_{2(d-1)}^{\text{alg}}(X)$ .

Furthermore, any intersection product  $\prod_i D_i^{(Y)} = \omega \in H_{2(d-k)}^{\text{alg}}(Y)$  can be calculated on  $X$  as  $\prod_i D_i \cdot [Y] \equiv \tilde{\omega} \cdot [Y] \in H_{2(d-k)}^{\text{alg}}(X)$ , with  $i_*(D_i^{(Y)}) = D_i$ . For a given  $\omega \in H_{2(d-k)}^{\text{alg}}(Y)$ , there can be in general be several  $\tilde{\omega} \in H_{2(d+1-k)}^{\text{alg}}(X)$  such that  $i_*(\omega) = \tilde{\omega} \cdot [Y]$ . In fact, the ambiguity precisely stems from the linear equivalence relations (LIN) and intersection properties (SRI) among divisors *of the ambient space*. To be more precise, due to these relations, two independent vertical  $(k, k)$ -forms  $\tilde{\omega}_1$  and  $\tilde{\omega}_2$  need not be independent upon intersecting with the hypersurface, i.e. we might have  $\tilde{\omega}_1 \cdot [Y] = \tilde{\omega}_2 \cdot [Y] \in H_{2(d-k)}^{\text{alg}}(X)$ .

Our considerations from the previous section of course apply to the ambient space, i.e.

$$H_{\text{vert}}^{(\cdot, \cdot)}(X, \mathbb{Q}) \cong \frac{\mathbb{Q}[D_i]}{\text{SRI} + \text{LIN}}. \quad (\text{III.21})$$

From the above discussion, it also immediately follows that we can represent the vertical cohomology of the hypersurface as

$$H_{\text{vert}}^{(k, k)}(Y, \mathbb{Q}) \cong \frac{\mathbb{Q}[D_i]^{(k)} \cdot [Y]}{\text{SRI} + \text{LIN}} \subset H_{\text{vert}}^{(k+1, k+1)}(X, \mathbb{Q}). \quad (\text{III.22})$$

To compute the intersection product of  $\omega, \eta \in H_{\text{vert}}^{(\cdot, \cdot)}(Y) \cong H_{(\cdot)}^{\text{alg}}(Y)$ , we first find  $\tilde{\omega}, \tilde{\eta} \in H_{(\cdot)}^{\text{alg}}(X)$  such that  $i_*(\omega) = \tilde{\omega} \cdot [Y]$  and  $i_*(\eta) = \tilde{\eta} \cdot [Y]$ , and then compute  $\tilde{\omega} \cdot \tilde{\eta} \cdot [Y] = i_*(\omega \cdot \eta)$ . The ambiguity in the choice of representatives  $\tilde{\omega}$  and  $\tilde{\eta}$  is taken care of by taking the quotient by LIN + SRI after intersecting with  $[Y]$ .

This now effectively allows us to carry out all relevant computations in  $H_{\text{vert}}^{(k, k)}(Y, \mathbb{Q})$  in the ambient space homology. With this understanding, we will – unless otherwise stated – omit the differentiation between co- and homology, and always use  $\cdot$  to indicate that calculations are based on intersection theory of homology classes. Only in expressions with integrals, e.g. in explicit flux computations, we will use the more consistent notation of the wedge product, indicating the presence of cohomology forms. For explicit computation we implement the quotient ring structure (III.22) into `Singular` [102], which is designed for calculations within polynomial rings. The results of chapter IV are all computed in this set-up, we also refer to there for explicit examples of the above method. Furthermore, `Singular` can also readily compute the minimal generating set of vector spaces. Applied to the space  $\mathbb{Q}[D_i]^{(2)} \cdot [Y]/(\text{SRI} + \text{LIN})$ , this in particular gives vector space basis  $\{t_i = D_{a_i} \cdot D_{b_i}\}$  of  $H_{\text{vert}}^{(2, 2)}(Y, \mathbb{Q})$ , which is the starting point of determining a basis of  $G_4$ -fluxes.

### Fibrations with generic Base

By a fibration over a generic base we mean a set-up in which different vertical divisors are treated as linearly independent, and on which intersection products are always non-zero unless the codimension of the intersection exceeds the dimension of the base. The vertical cohomology of a fibration over such a base can be mimicked with a quotient ring of the form

$$H_{\text{vert}}^{(\cdot, \cdot)}(X_5, \mathbb{Q}) \cong \frac{\mathbb{Q}[D_i^{(T)}, D_j^{(\mathcal{B})}]}{\text{SRI}^{(T)} + \text{SRI}^{(\mathcal{B})} + \text{LIN}^{(T)}}, \quad (\text{III.23})$$

where we split the set of divisors into those that come from the top ( $D_i^{(T)}$ ) and the vertical divisors from the base ( $D_j^{(\mathcal{B})}$ ). Since the tops we use to define the fibration fully specifies the fibre ambient space and parts of the fibration data, it relates fibral divisors amongst themselves and to certain vertical divisors, forming the ideal  $\text{LIN}^{(T)}$ . The genericness of  $\mathcal{B}$  is implemented

by assuming no further linear relations amongst the vertical divisors (i.e. no contributions to the ideal LIN involving only base divisors). The ideal SRI will have a part  $\text{SRI}^{(T)}$  coming from the Stanley–Reisner ideal of the top, as well as a part  $\text{SRI}^{(\mathcal{B})}$  encoding intersection properties of the base. Since any intersection with the allowed codimension is non-zero for a generic base, we only have to ensure that any intersection product with more than ‘three legs on the base’ vanishes, as it should with a threefold base  $\mathcal{B}$ . This is realised if we define the ideal  $\text{SRI}^{(\mathcal{B})}$  to be generated by

$$D_1^{(\mathcal{B})} \cdot D_2^{(\mathcal{B})} \cdot \left\{ \begin{array}{l} D_3^{(\mathcal{B})} \cdot D_4^{(\mathcal{B})} \\ D_3^{(\mathcal{B})} \cdot \text{Ex}_i \\ \text{Ex}_j^{G_1} \cdot \text{Ex}_j^{G_2} \end{array} \right\}$$

for any vertical divisor  $D_k^{(\mathcal{B})}$  and any exceptional divisor  $\text{Ex}_i$ . Note that the last entry is included for situations, where we have two independent gauge groups  $G_{1,2}$  localised over two different divisors in the base, e.g. in our ‘Standard Models’.

Aside from the vertical divisors that have non-trivial linear relations with fibral divisors (these are divisor classes associated to the coefficients of the hypersurface), any other vertical divisor will appear on equal footing for a generic base. These can be mimicked by introducing a further ‘dummy’ vertical divisor  $D$  as the formal variables of the polynomial ring (III.23) which is not related to any of the divisors  $D^{(T)}$  by linear relations. We stress that the resulting quotient ring is not truly a cohomology ring, e.g. it does not satisfy Poincaré-duality,  $\dim H_{\text{vert}}^{k,k} = \dim H_{\text{vert}}^{5-k,5-k}$ . However it captures the essential features that we will need for the study of chiral indices and anomaly cancellation.

It is worth noting that it is generally possible to reduce intersections of five divisors in the ambient space to a sum of intersection numbers of three divisors on the base if the fibre ambient space is fully specified. In our implementation of (III.23) into **Singular**, this is reflected as follows: Any degree five polynomial  $P^{(5)} \in H_{\text{vert}}^{(5,5)}(X_5)$  will be reduced into an expression of the form

$$\left( \sum D_a^{(\mathcal{B})} D_b^{(\mathcal{B})} D_c^{(\mathcal{B})} \right) \cdot \left( \sum D_i^{(T)} D_j^{(T)} \right) \equiv \# \cdot \int_{\mathcal{B}} \left( \sum D_a^{(\mathcal{B})} D_b^{(\mathcal{B})} D_c^{(\mathcal{B})} \right), \quad (\text{III.24})$$

with a specific quadratic term  $(\sum D_i^{(T)} D_j^{(T)})$ , which is the same for any polynomial  $P^{(5)}$ .<sup>7</sup> The numerical prefactor represented by the quadratic term is dictated by the toric geometry of the top, as explained in section 2.6 of chapter II. Usually, it is easier to infer the numerical prefactor by reducing an universally known intersection number of the fibration: E.g. in a fibration  $Y_4$  with a section  $S_0$  one reduces the expression  $S_0 \cdot [Y_4] \cdot (\sum D_a^{(\mathcal{B})} D_b^{(\mathcal{B})} D_c^{(\mathcal{B})})$ , which we know is equal to  $1 \cdot \int_{\mathcal{B}} (\sum D_a^{(\mathcal{B})} D_b^{(\mathcal{B})} D_c^{(\mathcal{B})})$ . Analogously for a model with a bisection  $U$ , we compare to  $U \cdot [Y_4] \cdot (\sum D_a^{(\mathcal{B})} D_b^{(\mathcal{B})} D_c^{(\mathcal{B})}) = 2 \cdot \int_{\mathcal{B}} (\sum D_a^{(\mathcal{B})} D_b^{(\mathcal{B})} D_c^{(\mathcal{B})})$ . For an explicit fibration, where the base is fully specified, these steps become obsolete, as **Sage** can readily reduce the expression  $P^{(5)}$  to the intersection number that  $P^{(5)}$  represents in the full ambient space  $X_5$ .

### 3 Tools from Commutative Algebra

With the construction of F-theory geometries becoming more and more sophisticated, it also became evident that the necessary computational tools needed improvements. One such tool, which has been dubbed ‘prime ideal technique’ in [57], is extremely useful in the analysis of

<sup>7</sup>For this to be the case, the polynomial ring (III.23) has to be defined in **Singular** with the appropriate monomial ordering. We always used ‘degree reverse lexicographical ordering’ (‘dp’), in which case the variables for the divisors have to be put in such a order that the base divisors are listed *after* the top divisors.

subspaces of the compactification space defined by the vanishing of polynomials. While the F-theory community has only recently begun to utilise this technique, it is well-established in the mathematical literature and is in fact at the heart of classic algebraic geometry.

### 3.1 Why do we need this?

Before we dive into technical definitions, let us first illustrate the problem we are facing. Suppose, for simplicity, we have a hypothetical hypersurface given by the vanishing of the polynomial  $F = (a + b)xy + cx^2 + dy^2$ . In analogy to our fibrations, assume that the variables  $x, y$  are coordinates of some fibre ambient space, and  $\{a, b, c, d\}$  are generic sections of some line bundles over a base of the fibrations. For generic values of  $\{a, b, c, d\}$ ,  $F$  will not factor, meaning that the locus  $\{F = 0\}$  in the  $(x, y)$ -plane is one single connected curve. However, for  $C = ab - cd = 0$ , this is no longer the case. One way to see this is to solve  $C = 0$  for  $a$  and insert the result into  $F$ , yielding  $\frac{1}{b}(bx + dy)(cx + by)$ . Therefore, over the special locus  $C = 0$  in the base, the curve  $\{F\}$  in the  $(x, y)$ -plane is actually two straight lines,  $A = \{bx + dy\}$  and  $B = \{cx + by\}$ .

However, because of  $b$  being in the denominator, we cannot extend the above factorisation directly to the situation where in addition to  $C = 0$  we also have  $b = 0$ . In other words, the factorisation is not globally valid. Yet such a globally well-defined expression is necessary e.g. for the computation of homology classes, which in turn we need for the discussion of fluxes. In anticipation of the tools we are about to develop, let us regard the restriction of  $F$  to  $C$  as the intersection  $\{F\} \cap \{C\}$  in the total ambient space. Then the factorisation of the fibre curve over  $C$  can be realised as

$$\{F\} \cap \{C\} = \left\{ \begin{array}{l} bx + dy = 0 \\ cx + ay = 0 \\ ab - cd = 0 \end{array} \right\} \cup \left\{ \begin{array}{l} cx + by = 0 \\ ax + dy = 0 \\ ab - cd = 0 \end{array} \right\} \equiv A \cup B. \quad (\text{III.25})$$

To see that this indeed reduces to the above factorisation in the case of  $b \neq 0$ , simply note that for  $a = cd/b$ , the conditions  $bx + dy = 0$  and  $cx + ay = 0$  in  $A$  are equivalent as equations for  $x$  and  $y$  and are in fact the same as the earlier expression for  $A$  (similarly for  $B$ ). Furthermore we can extend these expressions straightforwardly to  $b = 0$ . It is not hard to see that in this case,  $ab - cd = 0$  has two solutions  $c = 0$  or  $d = 0$ . Correspondingly,  $A$  splits into two sets  $A_{c,d}$ , with  $A_c = \{b = c = y = 0\}$  and  $A_d = \{b = d = cx + ay = 0\}$ ; likewise  $B$  splits into  $B_c = \{b = c = ax + dy = 0\}$  and  $B_d = \{b = d = x = 0\}$ . Note that we could have arrived at these special cases if we had directly evaluated  $F$  at  $b = c = 0$  and  $b = d = 0$ . The advantage of the new approach is that we obtain expressions which cover all these cases, because they contain in some sense the global information.

The above example is a demonstration of a ‘primary decomposition’ (section 3.2.4). In the following we will discuss the necessary background, namely the theory of rings and ideals.

### 3.2 On polynomials and varieties

In the classical theory of varieties the key objects of interest are algebraic sets, which by definition are common zero loci of a collection of polynomials. A famous theorem by Chow states that in fact in a complex projective space – which applies to all of the compactifications spaces we are considering in F-theory (with some suitable generalisation) – any closed analytic subspace is also an algebraic subvariety and vice-versa. By virtue of this theorem, geometric problems in classic algebraic geometry are usually translated into a question regarding polynomials, which have been objects of intense research since the time of Euclid.

In the following, we will present a few core results which we will then apply to F-theory constructions. For more details and rigorous proofs, we refer to the numerous textbooks, e.g. [103–105].

### 3.2.1 Ideals and varieties

Commutative rings are the central objects to the field of commutative algebra. A basic and familiar example is the set of integers  $\mathbb{Z}$ ; even though this is not a polynomial ring, most of the ideas discussed in the following also apply to  $\mathbb{Z}$ , which can be used to gain some intuition about the abstract definitions.

The commutative ring we are ultimately interested in is the polynomial ring  $\mathbb{C}[X_1, \dots, X_N]$  in  $N$  variables with complex coefficients. The defining properties, which is also shared by the example  $\mathbb{Z}$ , is that any commutative ring  $R$  has two associative and commutative operations,  $+$  and  $\cdot$ , which are distributively compatible:

$$\forall r_1, r_2, r_3 \in R : \left. \begin{aligned} (r_1 + r_2) + r_3 &= r_1 + (r_2 + r_3), \\ (r_1 \cdot r_2) \cdot r_3 &\equiv (r_1 r_2) r_3 = r_1 (r_2 r_3) \end{aligned} \right\} \begin{array}{l} \text{associative} \\ \text{commutative} \\ \text{distributive} \end{array} \quad (\text{III.26})$$

$$r_1 + r_2 = r_2 + r_1, \quad r_1 r_2 = r_2 r_1$$

$$r_1 (r_2 + r_3) = r_1 r_2 + r_1 r_3$$

Inspired by the basic examples, these operation are usually called addition and multiplication. Importantly,  $(R, +)$  must be a group, i.e. there is a zero element ‘0’ such that  $0 + r = r$  for any  $r \in R$ , and for any  $r$  there exists a unique inverse  $-r$  with  $r + (-r) \equiv r - r = 0$ . While we also require as a definition that there is a  $1 \in R$  satisfying  $1 \cdot r = r$  for any  $r$ , there need not be a multiplicative inverse for all elements. These definitions are of course very familiar for  $R = \mathbb{Z}$  or  $R = \mathbb{C}[X_i]$ .

#### Ideals

One of the key concepts that will play an important role in our discussion is that of ideals. **An ideal**  $I \subset R$  is a non-empty subset of the ring that is closed under addition amongst itself and under multiplication with arbitrary ring elements:

$$\forall a_1, a_2 \in I, \forall r \in R : \quad a_1 + a_2 \in I \text{ and } r \cdot a_1 \equiv r a_1 \in I. \quad (\text{III.27})$$

A generating set (or set of generators) of an ideal  $I$  is a subset  $X \subset I$ , such that any element  $I$  can be written as a finite linear combination of elements in  $X$ ,

$$I = \{r_1 x_1 + \dots + r_n x_n \mid n \in \mathbb{N}, r_i \in R, x_i \in X\}. \quad (\text{III.28})$$

Given a set  $X = \{x_i\} \subset R$ , we will denote the ideal generated by it with  $\langle X \rangle \equiv \langle x_1, x_2, \dots \rangle$ . Trivial examples for any rings are the zero ideal  $\langle 0 \rangle = \{0\} \subset R$  or  $\langle 1 \rangle = R$ . The latter example shows in particular that any ideal containing 1 must necessarily be the whole ring.

As a first non-trivial example, let us consider the ring of integers  $\mathbb{Z}$ . In this case it turns out that any ideal  $I$  must be of the form  $\langle z \rangle$  for a single integer  $z$ , i.e. all multiples of one number. Other such examples are polynomial rings in one variable with real or complex coefficients: Any ideal of these rings is always generated by one single polynomial. To show that not all rings have this property, consider the polynomial ring in two variables,  $x$  and  $y$ . If the ideal  $\langle x, y \rangle$ , which contains all polynomials with vanishing constant term, was generated by a single polynomial  $f$ , then  $x$  and  $y$  must both be of the form  $r f$  for some polynomial  $r$ . However, by simple degree arguments, if  $r f = x$ , then either  $r \sim x$ , implying  $f$  is a constant, so  $\langle f \rangle = R \neq \langle x, y \rangle$ , or  $f \sim x$ , and so  $\tilde{r} f \neq y$  for any  $\tilde{r}$ .

One can define operations amongst ideals to form new ideals. The sum of ideals,  $I + J := \{i + j \mid i \in I, j \in J\}$ , is in fact equivalent to the ideal generated by the union of the generators of  $I = \langle x_1, \dots, x_m \rangle$  and  $J = \langle y_1, \dots, y_n \rangle$ :  $I + J = \langle x_1, \dots, x_m, y_1, \dots, y_n \rangle$ . In particular, the sum  $I + J$

contains the union  $I \cup J$  as sets (the latter need not to be an ideal). The set theoretic intersection of two ideals  $I \cap J$  turns out to be an ideal itself, which contains the product  $IJ := \{i_1 j_1 + \dots + i_k j_k \mid k \in \mathbb{N}, i_p \in I, j_q \in J\}$ .

### Algebraic varieties

Algebraic varieties are a broad class of complex manifolds. In fact, nearly all compact complex manifolds are algebraic varieties, and certainly all those examples we construct for string compactifications fall into this category, because we have a good handle on them by means of algebraic geometry. To keep things simple, we will stick to the affine set-up, knowing that in the end, all our examples are actually in a projective setting. However, all results can be transferred almost identically to the projective case.

**Affine algebraic varieties** are subsets  $V \subset \mathbb{C}^N$  which can be described as the common vanishing locus of a set of polynomials, by regarding the variables  $X_i$  as coordinates of  $\mathbb{C}^N$ .<sup>8</sup> Given  $S \subset \mathbb{C}[X_1, \dots, X_N] = R$ , we call

$$V(S) = \{z \in \mathbb{C}^N \mid \forall f \in S : f(z) = 0\} \tag{III.29}$$

the (affine) variety defined by  $S$ . The function  $V$  defined in this way is decreasing with respect of inclusion: if  $S \subset S'$ , then  $V(S') \subset V(S)$ . Note that if  $f, g \in S$  and  $h \in R$  is any polynomial, then both  $f + g$  and  $hf$  will vanish on  $V(S)$ . Hence, if we take the ideal  $I = \langle S \rangle$  defined by  $S$ , then  $V(S) = V(I)$ . Therefore, w.l.o.g. we can assume that an affine algebraic variety is always defined by an ideal. We can immediately draw some conclusions regarding the union and intersection of varieties. It is straightforward to prove that we have

$$\begin{aligned} V(I) \cup V(J) &= V(I \cap J), \\ V(I) \cap V(J) &= V(I \cup J) = V(I + J). \end{aligned} \tag{III.30}$$

Chow's theorem states that in a complex projective manifold, any closed complex submanifold is in fact a (projective) algebraic variety. So in some sense, even though varieties are naively very restrictive, being defined by polynomials, they are still the most general subspaces we can have in our compactification manifold.

We now define an in some sense dual operation. Suppose  $V \subset \mathbb{C}^N$  is some subset (not necessarily a variety), then

$$I(V) = \{f \in \mathbb{C}[X_1, \dots, X_N] \mid \forall z \in V : f(z) = 0\} \tag{III.31}$$

is called the ideal of  $V$ . Again it is obvious that it indeed defines an ideal in  $R$ .

Some examples of the above results are appropriate. In general, we always have  $V(R) = \emptyset$  and  $V(\langle 0 \rangle) = \mathbb{C}^N$ . Similarly,  $I(\mathbb{C}^N) = \langle 0 \rangle$  and  $I(\emptyset) = \mathbb{C}^N$ . Suppose  $I = \langle x \rangle$ ,  $J = \langle y \rangle$  are ideals in  $R = \mathbb{C}[x, y]$ , then  $V(I) = \{x = 0\}$  is the  $y$ -axis and  $V(J) = \{y = 0\}$  is the  $x$ -axis in  $\mathbb{C}^2$ . The intersection  $V(I) \cap V(J)$  is clearly just the origin. Correspondingly, the ideal  $I + J = \langle x, y \rangle$  precisely vanishes at the origin. Let us look at another example,  $I = \langle xy, x^2 \rangle$ . Clearly, the vanishing of  $x^2$  requires the points of  $V(I)$  to be on the  $y$ -axis. However,  $xy$  also vanishes (in part) on the whole  $y$ -axis, so  $V(I) = \{x = 0\}$  is the whole axis. However,  $I(\{x = 0\}) = \langle x \rangle \supset I$ . This example shows that in general, we only have an inclusion  $I(V(I)) \supset I$ . To find a one-to-one duality, we need the notion of radical ideals.

<sup>8</sup>In the mathematics literature, these vanishing loci would be referred as algebraic sets. Algebraic varieties are a special type of algebraic sets. In the following, we will not make this differentiation.



### 3.2.2 Radical ideals and Hilbert's Nullstellensatz

Given any ideal  $I$ , the **radical of  $I$**  is defined as

$$\sqrt{I} := \{r \in R \mid \exists n \in \mathbb{N} : r^n \in I\}. \quad (\text{III.32})$$

Clearly,  $I \subset \sqrt{I}$ , and if  $I = \sqrt{I}$ , then  $I$  is said to be a radical ideal. Basically this means that a radical ideal contains all the ‘roots’, and a non-radical ideal can be made radical by including all ‘roots’. For simple examples, consider  $R = \mathbb{Z}$ . Then  $\sqrt{\langle 4 \rangle} = \sqrt{\langle 8 \rangle} = \sqrt{\langle 16 \rangle} = \dots = \langle 2 \rangle$ ,  $\sqrt{\langle 6 \rangle} = \langle 6 \rangle = \sqrt{\langle 12 \rangle}$ ; more generally, if  $m = \pm \prod_i p_i^{n_i}$  is the prime factorisation of  $m$ , then  $\sqrt{\langle m \rangle} = \langle \prod_i p_i \rangle$ .

As a more involved example, we revisit the ideal  $I = \langle xy, x^2 \rangle$  in the ring  $R = \mathbb{C}[x, y]$ . Since  $x^2 \in I$ , we necessarily have  $\langle x \rangle \subset \sqrt{I}$ . Conversely, suppose we have  $f \in \sqrt{I}$ , then there is some  $n > 0$  such that  $f^n = pxy + qx^2 = x(py + qx)$  for some  $p, q \in R$ . It immediately follows that  $f = \sum_{i,j \geq 0} a_{ij} x^i y^j$  cannot have a non-zero constant term  $a_{00}$ , because then  $f^n = a_{00}^n + \text{non-constant terms}$ ; furthermore, it cannot have any terms  $a_{0k} y^k$ , because then  $f^n$  will have terms  $a_{0k}^n y^{kn}$  which do not have a factor of  $x$ . Consequently,  $f$  must be of the form  $x\tilde{f}$ , showing that  $f \in \langle x \rangle$ . Thus we have shown that  $\sqrt{I} = \langle x \rangle$ .

Combined with the earlier geometric observation of  $I(\mathbb{V}(\langle xy, x^2 \rangle)) = \langle x \rangle$ , this example illustrates what is known as **Hilbert's Nullstellensatz**:

$$\text{For any ideal } I \subset \mathbb{C}[X_1, \dots, X_N] : \quad I(\mathbb{V}(I)) = \sqrt{I}. \quad (\text{III.33})$$

This theorem furnishes the desired duality between varieties and ideals. It also shows ideals carry more information than just the point set of the corresponding variety: Different ideals with the same radical define identical point sets as varieties. In some sense, primary ideals describe varieties with multiplicities. We will come back to this issue in a moment. Here we just note that this discrepancy between point sets and polynomials in part was the motivation to define modern algebraic geometry solely based on commutative rings.

### 3.2.3 Prime and primary ideals and irreducible varieties

A prime ideal, as the name suggests, generalises the idea of prime numbers. For an arbitrary commutative ring  $R$ , a **prime ideal**  $P \subset R$  is a proper ideal (i.e. not the whole ring) such that

$$\forall r_1, r_2 \in R : \quad \text{if } r_1 r_2 \in P \Rightarrow r_1 \in P \text{ or } r_2 \in P. \quad (\text{III.34})$$

For  $R = \mathbb{Z}$ , it is not a surprise (and a straightforward proof using the definition of prime numbers) that prime ideals are precisely those ideals  $\langle p \rangle$  where  $p$  is a prime number. In the case of polynomial rings in a single variable, there is already a difference in whether we allow for real or complex coefficients. For example, the polynomial  $f = x^2 + 1$  regarded as an element of  $R = \mathbb{C}[x]$  can be factorised as  $f = (x + i)(x - i)$ , with  $i^2 = -1$ ; therefore  $\langle f \rangle$  is not a prime ideal, because it does not contain  $x \pm i$  (multiples of  $f$  necessarily must be polynomials of at least of degree 2), which multiply to  $f$ . However, over  $\mathbb{R}$ , the factorisation is invalid; in fact basic calculus<sup>9</sup> shows that there cannot be a factorisation  $f = gh$  into polynomials  $g, h \notin \langle f \rangle$ , as these necessarily linear polynomials must have real zeroes which would then be real zeroes of  $f = x^2 + 1$ .

Closely related to prime ideals are so-called primary ideals, which as the name suggests are quite like prime ideals. However, a **primary ideal**  $Q$  is a proper ideal satisfying a slightly weaker factorisation property:

$$\forall r_1, r_2 \in R : \quad \text{if } r_1 r_2 \in Q \Rightarrow r_1 \in Q \text{ or } \exists n \in \mathbb{N} \text{ s.t. } r_2^n \in Q. \quad (\text{III.35})$$

<sup>9</sup>It is somewhat amusing that this fundamental theorem of algebra cannot be proven without the use of analysis, in form e.g. of the intermediate value theorem.

For some intuition we again look at the basic example of  $\mathbb{Z}$ . In this case, primary ideals are of the form  $\langle p^k \rangle$  for a prime  $p$ . The property of being primary can be easily understood in this context: If  $r_1 r_2 \in \langle p^k \rangle$ , i.e. the product  $r_1 r_2$  is divisible by  $p^k$ , then either  $r_1$  was already divisible by  $p^k$ , or  $r_2$  must contain  $p$  as one of its prime factors (i.e.  $r_2$  raised to some power – at most  $k$  – is divisible by  $p^k$ ). The relation between primary and prime ideals is simple. Given a primary ideal  $Q$ , the radical  $P = \sqrt{Q}$  is a prime ideal, the so-called associated prime ideal of  $Q$ . In the ring of integers, it is obvious that the prime ideal associated to  $\langle p^k \rangle$  is  $\langle p \rangle$ . As a matter of nomenclature, a primary ideal  $Q$  with associated prime  $P$  is called  $P$ -primary.

### (Ir-)reducible and (non-)reduced varieties

A variety  $V$  is called **irreducible** if it cannot be written as the disjoint union of two non-empty varieties. More precisely, for any decomposition  $V = W_1 \cup W_2$ , with two varieties  $W_{1,2} \neq V$  and  $W_1 \cap W_2 = \emptyset$ , we must have  $W_1 = V$  or  $W_2 = V$  in order for  $V$  to be irreducible. It is a simple exercise to prove the following characterisation of irreducible varieties:

$$V \text{ is irreducible} \Leftrightarrow I(V) \text{ is a prime ideal.} \tag{III.36}$$

For the above example, the fact that the ideal  $I = \langle x^2 + 1 \rangle \subset \mathbb{C}[x]$  is non-prime is reflected in the geometry as  $V(I) = \{\pm i\} \subset \mathbb{C}$  being composed of two separated points, so  $V(I) = \{i\} \cup \{-i\}$ .

Note that (ir-)reducibility defined as above is a statement about the point set  $V$  alone, in particular, it does not differentiate between different ideals  $I_i$  with  $V(I_i) = V$ . So for a prime ideal  $P$ , any  $P$ -primary ideal  $Q$  also defines an irreducible variety  $V(Q)$ . Nevertheless, we will encounter situations in F-theory, where the additional ‘information’ contained in a primary ideal  $Q$ , as opposed to the prime ideal  $\sqrt{Q}$ , is essential for physical quantities. This additional information sparks the notion of (non-)reduced varieties, which depends on the ideal defining the variety.

Concretely, we say that a variety  $V = V(I)$  defined by the ideal  $I$  is **reduced**, if  $I$  is radical, i.e.  $I = \sqrt{I}$ , and otherwise we call it non-reduced. Clearly, reducedness is really a property of the ideal  $I$ , to which the point set  $V$  is insensitive. So from now on, whenever we talk about a variety  $V$ , what we really have in mind is an ideal  $I$  to which we can associate a point set  $V(I)$ , but in addition may have further non-reduced structures. In terms of its cycle and homology classes, non-reduced structure of a variety is reflected precisely in the multiplicity  $[V(I)] = \mu [V(\sqrt{I})]$  (cf. appendix A). We will later present a method to compute  $\mu$ .

For a basic example, take  $I = \langle x^2 - y, y \rangle = \langle x^2 - y \rangle + \langle y \rangle \subset \mathbb{C}[x, y]$ . Geometrically,  $V(I)$  is the intersection of the parabola  $\{y = x^2\}$  and the  $x$ -axis  $\{y = 0\}$ , which clearly is the origin  $\{x = y = 0\}$ . However, this set notation does not capture the fact that the parabola intersects the  $x$ -axis tangentially; in fact  $I(\{x = y = 0\}) = \langle x, y \rangle = \langle x \rangle + \langle y \rangle$  can also be understood as the transverse intersection of the  $x$ - and  $y$ -axis. Meanwhile, the description through the ideals  $\langle x, y \rangle$  and  $I$  can distinguish between a ‘normal’ and a ‘non-transverse’ intersection point.

In our F-theory compactifications, we will regularly encounter ideals defining reducible varieties, of which we need to compute the irreducible components. For this we require the concept of primary decomposition.

### 3.2.4 Primary decomposition and irreducible components

An important property of the integers, going by the name of the ‘fundamental theorem of arithmetic’, is the unique prime factorisation which we have also briefly mentioned above. There is a generalisation to other types of rings including polynomial rings, and hence has imminent impact on geometry.

The prime factorisation of integers,  $m = \pm \prod_i p_i^{n_i}$ , can be rephrased in terms of ideals. To this end, suppose that  $m = p_1^{n_1} p_2^{n_2}$  has two distinct prime factors raised to some power, then clearly  $m \in \langle p_1^{n_1} \rangle$  and  $m \in \langle p_2^{n_2} \rangle$ , so  $m \in \langle p_1^{n_1} \rangle \cap \langle p_2^{n_2} \rangle$ ; conversely, if  $z \in \langle p_1^{n_1} \rangle \cap \langle p_2^{n_2} \rangle$ , so  $z$  is

a multiple of  $p_1^{n_1}$  and of  $p_2^{n_2}$ , then – because  $p_1$  and  $p_2$  are distinct prime numbers –  $z$  must be multiples of  $p_1^{n_1} p_2^{n_2} = m$ , so  $z \in \langle m \rangle$ . It straightforwardly extends to an arbitrary number of prime factors, so we can reformulate the prime factorisation of integers in terms of ideals as

$$\langle m \rangle = \bigcap_{i=1}^n \langle p_i^{n_i} \rangle. \quad (\text{III.37})$$

In other words, any ideal  $I$  in  $\mathbb{Z}$  has a unique decomposition into primary ideals such that  $I$  lies in the intersection of all these primary ideals. This statement can be made almost identically for ideals in any polynomial ring over  $\mathbb{C}$ , with uniqueness being the only property not directly carrying over.

More specifically, if we restrict ourselves to primary decompositions with a minimal number of components (which is always finite), then there are some components that are uniquely determined and some which are not. The unique components of a primary decomposition  $I = \bigcap_i Q_i$  are the set of primary components  $Q_k$  whose associated primes  $\sqrt{Q_k} \supset I$  are ‘minimal’ over  $I$ , i.e.  $\sqrt{Q_k}$  does not properly contain any other prime ideal which itself properly contains  $I$ . To picture it geometrically, if  $\sqrt{Q}$  is a non-minimal associated prime, then there is a prime ideal  $P$  such that  $\sqrt{Q} \supsetneq P \supsetneq I$ , so  $V(\sqrt{Q})$  is contained, or ‘embedded’, in an irreducible subset  $V(P) \subsetneq V(I)$ . Conversely, if an associated prime  $\sqrt{Q}$  is minimal, then it defines in some sense one of the ‘largest’ irreducible components of  $V(I)$ . This motivates the name ‘**isolated component**’ for those  $Q_k$  with minimal associated primes, and ‘**embedded components**’ for those  $Q_k$  with  $\sqrt{Q_k}$  non-minimal. So in the context of polynomial rings<sup>10</sup>, we have the following theorem:

*Any ideal  $I$  has a decomposition  $I = \bigcap_{i=1}^n Q_i$  into primary ideals  $Q_i$  with a minimal  $n \in \mathbb{N}$ .*

*If the associated primes of  $\{Q_{k_1}, \dots, Q_{k_m}\}$  are minimal over  $I$ , then the components*

*$\{Q_{k_1}, \dots, Q_{k_m}\}$  are uniquely determined by  $I$ .*

(III.38)

So the upshot is that even though some ambiguity exists, the primary decomposition uniquely determines the ‘largest’, i.e. the isolated irreducible components, of a larger variety. The embedded components, while not being unique, are irrelevant to us, because intuitively they are of higher codimension and are thus not the objects we are trying to pin down by the decomposition.

To get some feeling for these abstract statements, let us once again come back to the example  $R = \mathbb{C}[x, y]$  and  $I = \langle xy, x^2 \rangle$ . This ideal has in fact several inequivalent primary decompositions into two components, of which some examples are

$$I = \langle x \rangle \cap \langle x^2, xy, y^2 \rangle = \langle x \rangle \cap \langle x^2, y \rangle = \langle x \rangle \cap \langle x^2, x + y \rangle. \quad (\text{III.39})$$

The first component  $Q_1 = \sqrt{Q_1} = \langle x \rangle$  is already prime and is in fact minimal, so by the statement above it appears in every decomposition, hence is unique. The second part of the decomposition differs amongst the various possibilities. However they have in common that their associated prime,  $\sqrt{\langle x, y \rangle^2} = \sqrt{\langle x^2, y \rangle} = \sqrt{\langle x^2, x + y \rangle} = \langle x, y \rangle$ , is *not* minimal over  $I$ , because  $I \subset \langle x \rangle \subset \langle x, y \rangle$ . There are more sophisticated examples showing that not even the non-minimal associated primes are unique. What does that mean in geometry? The ideal  $I = \langle xy, x^2 \rangle = \langle xy \rangle + \langle x^2 \rangle = (\langle x \rangle \cap \langle y \rangle) + \langle x^2 \rangle$  translates into geometry as  $V(I) = (V(x) \cup V(y)) \cap V(x^2) = (V(x) \cap V(x^2)) \cup (V(y) \cap V(x^2))$ . So it has two irreducible components, of which the first one is set theoretically just the  $y$ -axis (codimension one), and the second one the origin (codimension two). Clearly, the

<sup>10</sup>More general, any so-called Noetherian ring has this property.

origin is also contained – or embedded – in the  $y$ -axis, which reflects the non-minimality of the prime  $\langle x, y \rangle$  associated to the origin. So the highest dimension (‘largest’) component of  $V(I)$  is just the  $y$ -axis (note that we have already obtained this result earlier when we computed  $\sqrt{I}$ ). Moreover, the ideal  $I$  also contains the information about the fact that the  $y$ -axis itself carries some non-reduced structure from the  $x^2$  part. To extract this piece of information, we have to introduce one final technical procedure.

### 3.2.5 Ideal saturation and multiplicities

For ideals  $I, J \subset R$ , we define the ideal quotient of  $I$  with respect to (or by)  $J$  as  $I : J^d := \{g \in R \mid gJ^d \subset I\}$ , which is again an ideal. Here the exponential  $J^d$  is the ideal generated by all  $d$ -fold products of  $J$ ’s generators, e.g.  $(\langle x, y \rangle)^2 = \langle x^2, xy, y^2 \rangle$ . Furthermore, we define the **saturation** of  $I$  by  $J$  as

$$I : J^\infty = \{g \in R \mid \exists d \in \mathbb{N} : gJ^d \subset I\}. \tag{III.40}$$

It can be shown that there is a finite exponent  $m$  such that for any  $n > m$  we have  $I : J^n = I : J^m = I : J^\infty$ . So when computing an ideal saturation, we obtain in addition to the ideal  $I : J^\infty$  also a positive integer  $m$ , which we will, for reasons explained momentarily, call **multiplicity**.

Knowing that there are algorithms to compute ideal saturation, we will not attempt it by hand and instead rely on computer algebra systems such as **Singular**, as we will explain in the next section. For now, we first look at the geometric meaning of ideal quotient and saturation:

$$V(I : J^\infty) = \overline{V(I) \setminus V(J)}. \tag{III.41}$$

On the right hand side, the bar denotes topological closure. E.g.  $\langle xy \rangle : \langle x \rangle^\infty = \langle xy \rangle : \langle x \rangle = \langle y \rangle$  can be understood as removing the  $y$ -axis ( $\langle x \rangle$ ) from the union of  $x$ - and  $y$ -axis ( $\langle xy \rangle$ ); in this process, one would also remove the origin from the  $x$ -axis ( $\langle y \rangle$ ), which is ‘recovered’ by taking the closure. Returning to our example  $I = \langle xy, x^2 \rangle$ , we find that  $V(I : \langle x \rangle^\infty) = V(R) = \emptyset$ , confirming that  $I$  contained a single isolated component  $\langle x \rangle$ . Furthermore, the multiplicity (as computed by the saturation) of this component is 2. This can be understood in terms of the homology class associated to the variety<sup>11</sup>: We would associate the class  $2[\{x\}]$  with  $V(I)$  rather than just simply  $[\{x\}]$ .

Recall from appendix A that for any variety  $V = V(I)$ , we have, corresponding to the primary decomposition of  $I$ , the homology class  $[V] = \sum_i m_i [V_i]$ , where  $V_i$  are the isolated irreducible components of  $V$ . For all our models, we can compute  $m_i$  as the multiplicity of the ideal saturation  $I : P_i$ , where  $P_i$  is the minimal prime ideal associated with  $V_i$ .<sup>12</sup>

### 3.2.6 Computational algebraic geometry – theory of Gröbner bases

While in all of the above examples, the calculations could be performed by hand, this will turn out to be an almost impossible task for the ideals we encounter later on. Hence, we have to rely on computer algebra systems to carry out such calculations. The field of computational algebraic geometry is devoted to algorithmic approaches to ideal computations, and relies on the theory of so-called Gröbner bases.

An explanation of a Gröbner basis (see e.g. [107] for an overview) would exceed the scope of this work, since it does not give any new insight on the geometry, but is rather just a tool to handle polynomials. All we need to mention at this point is that all computer algebra systems for

<sup>11</sup>To be precise, this already applies to the element one associates to the variety in the cycle group, cf. appendix A.

<sup>12</sup>The general definition of  $m_i$  in terms of length of Artinian rings can be found e.g. in [106]. The formula we give does not apply to all cases, however will suffice for the analyses we will perform.

polynomial algebra are based on Gröbner bases. One such program is `Singular` [102], on which all our computations are based.

The theory of Gröbner bases allows for an algorithmic computation of the **dimension** of an ideal  $I \subset R = \mathbb{C}[X_1, \dots, X_N]$ , which is defined as the so-called Krull dimension of the quotient ring  $R/I$ . While we omit the ring theoretic definition hereof, the geometric meaning is as one expects: it is the (complex) dimension of  $V(I)$ . If  $V(I)$  is reducible, then the dimension will be that of the highest-dimensional irreducible component. For example,  $\dim R = N$ , and  $\dim(\langle x y, x^2 \rangle) = 1$  in  $R = \mathbb{C}[x, y]$ . For us, it will often be more advantageous to deal with codimension, which simple is given as  $\text{codim}(V(I)) = \dim R - \dim I$ .

With this last ingredient from polynomial algebra, we now turn to F-theory compactifications and see how these tools can help us extracting physically relevant data.

### 3.3 Application to F-theory: matter surfaces and singlet curves

In most explicit compactification models, the Calabi–Yau manifold is given in terms of vanishing loci of polynomials in an ambient space  $X$ . Specifically in F-theory, the elliptic or genus-one fibration  $Y \rightarrow \mathcal{B}$  is often given as a hypersurface, i.e. the vanishing of one polynomial.

Special subloci of the geometry, in particular matter curves in  $\mathcal{B}$  and matter surfaces in  $Y$ , are determined by the factorisation of the fibre over certain loci of  $\mathcal{B}$ . Frequently, the condition for the occurrence of such a factorisation is expressed in terms of the vanishing of some polynomial expressions, which is therefore perfectly suited to be studied with the tools we presented above.

#### 3.3.1 Fibrations with generic basis

Recall that in the class of fibrations (II.18) we consider, the ambient space  $X$  is a fibration of an fibre ambient space over  $\mathcal{B}$ , e.g. in the Weierstrass model, it is  $\mathbb{P}_{231}$  with homogeneous coordinates  $[x : y : z]$ . The hypersurface equation is a polynomial in the fibre ambient space coordinates, with coefficients  $a_i$  being some sections of line bundles over  $\mathcal{B}$ . For a specific base  $\mathcal{B}$ , all these  $a_i$  are essentially polynomials of the base’s coordinates. On a generic base, we do not have such a representation for the sections. In fact, for a generic fibration, in some sense the sections behave themselves like the coordinates of  $\mathcal{B}$ : For a generic base,  $n$  different sections  $a_i$  will generically vanish on a codimension  $n$  locus  $\{a_1\} \cap \dots \cap \{a_n\}$  of  $\mathcal{B}$ . If  $n$  is larger than  $\dim \mathcal{B}$ , then this locus is generically empty. Oftentimes, the special loci mentioned above are given in terms of polynomial expressions of the  $a_i$ , and their vanishing loci can have non-transversal and higher multiplicity intersections, which all can be determined using the technology presented before. This motivates us to describe the polynomial ring of a generic base  $\mathcal{B}$  as  $\mathbb{C}[a_i]$ , and of the full ambient space as  $\mathbb{C}[a_i, x_i]$ , where  $x_i$  are the fibre ambient coordinates.

#### 3.3.2 Matter surfaces

The main application of the commutative algebra tools for us is to study matter surfaces. As explained before in section 1.2.1 these are a crucial part of the geometrical data that defines the chiral spectrum of a 4D F-theory compactification. While the primary decomposition gives us a way to compute the geometric locus of a matter surface, we also require the homology class for the computation of chiral indices. To determine these in general, we have to develop further methods, as will be presented momentarily. We will focus on non-abelian matter, and add a few remarks at the end of this section about singlet matter.

#### Geometric loci

Suppose we have a non-abelian gauge group  $G$  supported on the divisor  $\{w\}$  in the base. In this case, the matter states are localised over curves of the form  $C = \{w\} \cap \{p\}$  in the base, where

$p$  is a polynomial in the sections  $a_i$  which themselves appear as coefficients in the hypersurface polynomial  $P_T$ . Recall that in the full ambient space  $X_5$  of the resolved fourfold  $Y_4$ , the non-abelian divisor  $\{w\}$  is described by the vanishing of the exceptional coordinates  $e_i$  with  $i = 0, \dots, \text{rank } G = r$ . Over the matter curve  $C = \{w\} \cap \{p\} = \{e_0 \dots e_r\} \cap \{p\}$  some exceptional divisors  $E_i = \{e_i\} \cap \{P_T\}$  will split into multiple irreducible curves which, when fibred over  $C$ , form the matter surfaces. Equivalently, the restriction of the full exceptional divisor  $E_i$  to the curve  $C$  – which is itself a surface – splits into several ‘smaller’ surfaces. In other words, the variety  $\{e_i\} \cap \{p\} \cap \{P_T\} \subset X_5$  is reducible, with the irreducible components being the matter surfaces of interest. These are 4-cycles, i.e. codimension three in  $X_5$ . Therefore a primary decomposition of the ideal  $\langle e_i, p, P_T \rangle \subset \mathbb{C}[a_l, e_m, x_n]$ , where the  $x_n$  are the fibre coordinates other than the  $e_m$ ’s, will contain the matter surfaces as isolated components of codimension three. The results will be a globally valid description of the matter surfaces as vanishing loci of some polynomials.

### Homology classes of matter surfaces

In order to calculate the chiral index (III.15) we further need to determine the homology classes of the matter surfaces. In case the matter surface is a complete intersection, i.e. its ideal has three generators, this task is trivial. E.g. if  $p$ , the polynomial defining the matter curve, is one of the sections  $a_l$ , then  $P_T|_{a_l=e_i=0} = \prod_k Q_k$  necessarily factors into irreducible polynomials  $Q_k$ , thus the resulting irreducible components are complete intersections with prime ideals of the form  $\langle e_i, a_l, Q_k \rangle$ . In this simple case the homology class is just  $E_i \cdot [a_l] \cdot [Q_k]$ , with  $\cdot$  denoting the intersection product.

However, if  $p$  is a more complicated polynomial, then one cannot simply evaluate  $P_T|_{p=e_i=0}$  in the above fashion to factorise  $P_T$ . The usual procedure by solving  $p = 0$  for one of its variables and plugging the result into  $P_T$  will generically introduce fractional or irrational expressions, which is no longer well-defined globally. Correspondingly, the primary decomposition of  $\langle P_T, e_i, p \rangle$  will in general yield non-complete intersections as the matter surfaces. Obviously, the homology class of a non-complete intersection cannot be simply the product of the classes of individual generators, since their number exceeds three, and the class obtained in such a way does clearly not correspond to a codimension three cycle. Instead, we have to manipulate the ideals such that we find an alternative description of the non-complete intersection.

To this end, assume that we have the codimension  $d$  irreducible variety  $\gamma = \mathbb{V}(\langle f_1, \dots, f_k \rangle) \equiv \mathbb{V}(I)$  with  $k > d$ . Now consider the ideal  $J$  generated by  $d$  of the generators, w.l.o.g.  $J = \langle f_1, f_2, \dots, f_d \rangle$ , such that it is a complete intersection, i.e.  $\text{codim}(J) = d$ . In general,  $J$  will not be a prime ideal, and thus we can perform a primary decomposition  $J = \bigcap_m Q^{(m)}$ , with associated primes  $J^{(m)} = \sqrt{Q^{(m)}}$  of multiplicity  $\mu^{(m)}$ . As we are only interested in codimension  $d$  components (only these will affect the cycle class of  $\gamma$ ), we may assume that all  $Q^{(m)}$  are isolated components, i.e. are uniquely determined. Since  $J \subset I$  is also of codimension  $d$ ,  $I$  must be a minimal prime associated to one of the isolated components, say  $Q^{(0)}$ . With a suitable choice of the  $d$  generators, all the other components  $Q^{(m)}$  in the decomposition will be complete intersections of codimension  $d$ , i.e. the associated primes  $J^{(m)}$  with  $m \neq 0$  will have  $d$  generators  $f_1^{(m)}, \dots, f_d^{(m)}$ . Since the class of a complete intersection is just the product of the classes of each generator, we have

$$\prod_{k=1}^d [f_k] = [\mathbb{V}(J)] = \mu^{(0)} [\mathbb{V}(I)] + \sum_{m \neq 0} \mu^{(m)} \left[ \mathbb{V} \left( J^{(m)} \right) \right] = \mu^{(0)} [\gamma] + \sum_{m \neq 0} \mu^{(m)} \prod_{k=1}^d [f_k^{(m)}].$$

Therefore, we can simply solve for the homology class of the variety of interest:

$$\iff [\gamma] = \frac{1}{\mu^{(0)}} \left( \prod_{k=1}^d [f_k] - \sum_{m \neq 0} \mu^{(m)} \prod_{k=1}^d [f_k^{(m)}] \right). \quad (\text{III.42})$$

For a demonstration, let us recall the starting example (III.25) of section 3.1, where we have decomposed the ideal  $\langle (a+b)xy + cx^2 + dy^2, ab - cd \rangle$  into  $A = \langle bx + dy, cx + ay, ab - cd \rangle$  and  $B = \langle cx + by, ax + dy, ab - cd \rangle$ . Both are of codimension two, hence are not complete intersections. To obtain the homology class of  $V(A)$ , we form the ideal  $J = \langle bx + dy, cx + ay \rangle \subset A$ . This ideal decomposes as  $J = A \cap \langle x, y \rangle$ , where  $\langle x, y \rangle$  is clearly a prime ideal defining a complete intersection. Hence,  $[V(A)] = [V(J)] - [V(x, y)] = ([b] + [x]) \cdot ([c] + [x]) - [x] \cdot [y]$ .

In an explicit 4D F-theory model, we proceed in the same fashion: If we have the prime ideal of a non-complete-intersection codimension three matter surface  $\gamma$ , we choose three of the generators and form a new ideal  $J$ , which we decompose into primary ideals. With a suitable choice the associated prime ideals of the decomposition will all – except for  $I(\gamma)$  – have three generators. To get their multiplicity, one has to simply compute the ideal saturation of  $J$  with respect to the primes. We relied on `Singular` to perform the primary decomposition and to compute the ideal saturation. In section 2.2.3 of chapter IV, we will present a practical example in a ‘real’ F-theory model where we carry out the above procedure step by step.

Note that the method applies in theory also to singlet curves  $C_{1_i}$ : If the curve is given by an ideal  $I_C \subset \mathbb{C}[a_l, e_m, x_n]$  of codimension two, the torus fibration over this curve is then given by the ideal  $I_C + \langle P_T \rangle$  of codimension three. By the same logic as for the non-abelian matter, the surface corresponding to this ideal must be reducible with two irreducible components (corresponding to the singlets  $\mathbf{1}_i$  and its charge conjugate). However, for complicated curves, where the ideal  $I_C$  is not a complete intersection, `Singular` is not able to compute the primary decomposition of  $I_C + \langle P_T \rangle$ ,<sup>13</sup> so that we do not have a description of the matter surface in terms of an ideal. This also deprives us of the possibility to determine the homology class by the above procedure. At the moment, there is no known method to circumvent this computational deficit, and thus we are unable to provide the homology classes for this type of singlet matter.

### 3.3.3 Singlet curves and Yukawa points

While we are not able to compute the matter surfaces of all singlet states, we can calculate at least the curves over which they are localised as ideals in the polynomial ring  $\mathbb{C}[a_i]$  of the base  $\mathcal{B}$ . This allows us to analyse in detail how different matter curves intersect each other in  $\mathcal{B}$ . Though not related to the chiral indices of the spectrum, the result of this analysis will affect the phenomenology of the 4D effective field theory, since intersection points of matter curves generically give rise to Yukawa couplings.<sup>14</sup> Considering that most of the results in chapter V is based on the presence of Yukawa couplings, it seems appropriate to briefly highlight the key ideas, even though they follow straightforwardly from the concepts of the previous sections.

As we have mentioned before, the matter curves of non-abelian matter in our models will always be given by a complete intersection  $\{w\} \cap \{p\}$ . Calculating their intersection is therefore usually quite simple and can be done by hand. Singlet curves on the other hand will in general be given by a non-complete intersection. More precisely, the condition for singlet states to arise is always tied to the appearance of a conifold singularity of the fibre in the non-resolved fourfold. By making a general ansatz for the fibre that exhibits such a behaviour, one obtains a set of polynomial equations involving the sections  $a_i$  of the base, which can be regarded as an ideal  $J \subset \mathbb{C}[a_i]$ . Since the conifold ansatz does not always distinguish among singlets with different charges (under  $U(1)$ s or discrete  $\mathbb{Z}_{ns}$ ),  $V(J)$  will in general contain several curves hosting states of different charges.

Equipped with our knowledge of commutative algebra, we are inclined to perform a primary decomposition of  $J$  to obtain the different curves. In most practical examples, this will work out

---

<sup>13</sup>The calculations have been mostly carried out on a MacBook Pro Retina (Late 2013) model with Intel i7 (2.8 GHz) and 8GB RAM.

<sup>14</sup>Recall that the absence of such intersection points only means that these couplings are perturbatively suppressed in the field theory. If the charges allow, the couplings can still be mediated by instantons.

fine. However, as we will see in chapter V, there can be ideals which are beyond the computational power of `Singular`. Luckily, in some of these situations, there are some obvious irreducible components, e.g. the vanishing of two sections  $a_{l_1}$  and  $a_{l_2}$  would imply all the generators of  $J$  to vanish. In such a situation, one can perform an ideal saturation  $J : \langle a_{l_1}, a_{l_2} \rangle^\infty$  to ‘simplify’ the reducible locus. For our model, it turns out that a successive simplification of this kind results in an ideal which `Singular` can decompose. In this way, we are able to determine the associated prime ideals for each individual singlet curve in our models.

Having obtained the ideals in this way, it is now straightforward to check for the presence of Yukawa points, i.e. intersection loci of the curves. If the states (now including non-abelian matter) in representations  $\mathcal{R}_{a,b,c}$  are supposed to form a Yukawa coupling  $\mathcal{R}_a \mathcal{R}_b \mathcal{R}_c$ , then the corresponding matter curves must intersect in a point. Let  $I_{a,b,c}$  denote the ideal defining the respective matter curve, then the point corresponds to a codimension three component in the primary decomposition of  $I_a + I_b + I_c$ . Note that because we are only interested in the loci itself without any multiplicities, we can circumvent the primary decomposition and directly compute the minimal associated primes of  $I_a + I_b + I_c$ , which is conveniently implemented into `Singular`.

As a final praise of the commutative algebra approach, we point out another pleasant result from the Gröbner basis calculations: There is an algorithmic way to compute singular loci of a variety in terms of its ideal, which we will not attempt to explain here. However, `Singular` has such a function incorporated, and with it, we are able to show for a complicated example involving a coupling of the form  $\mathcal{R}_a \mathcal{R}_a \mathcal{R}_b$ , that the intersection locus  $V(I_a + I_b)$  is actually part of the singular locus of  $V(I_a)$ , suggesting that is a self-intersection locus of the curve  $V(I_a)$  – consistent with the coupling structure.

## 4 Summary of Chapter III

Before turning to the application to concrete models, let us briefly summarise the methods we have set up in this chapter. They are crucial for the systematic description of vertical fluxes and chiral matter in F-theory.

The vertical cohomology  $H_{\text{vert}}^{(\cdot, \cdot)}$  is generated by  $(1, 1)$ -forms Poincaré-dual to divisors  $D_i$ . For a special class of torus fibrations  $Y_4$  realised as a hypersurface in a toric ambient space  $X_5$ , the vertical cohomology can be fully described by the vertical cohomology of the ambient space. This has a particularly simple realisation as a quotient ring

$$H_{\text{vert}}^{(\cdot, \cdot)}(X_5, \mathbb{Q}) \cong \frac{\mathbb{Q}[D_i]}{\text{SRI} + \text{LIN}}$$

of polynomial expressions in the divisors  $D_i$  of  $X_5$ . These divisors can, together with the quotient ideals SRI and LIN, be read off easily from the toric description. With computer-aided algorithms, all computations within the vertical cohomology can be readily simplified as polynomial multiplications in that ring.

For the computation of chiral indices in F-theory, we require in addition also the knowledge of matter surfaces and their homology classes. In section 3, we have presented a method based on polynomial algebra that allows us to express matter surfaces as vanishing loci of polynomials. Because these loci are in general not complete intersections, an additional procedure needed to be developed in section 3.3.2 to extract the homology class of these matter surfaces.



# Chapter IV

## Anomalies in 4D Compactifications

Having a non-zero  $G_4$ -flux in 4D F-theory compactifications will in general induce a chiral spectrum in the effective field theory. The purpose of this chapter is to study potential anomalies arising from chiral matter. In particular, we will focus on gauge and gravitational anomalies as well as the Witten anomaly in compactifications with  $SU(5) \times U(1)$ ,  $SU(5) \times \mathbb{Z}_2$  and  $SU(3) \times SU(2) \times U(1)^2$  gauge groups. Based on the methods developed in the previous chapters, we will relate these anomalies to geometric properties, and show that for these models, the anomalies are generically cancelled.

### 1 Gauge and Gravitational Anomalies in 4D

Before moving to the explicit F-theory realisations of the gauge theories mentioned above, let us briefly give a summary of how anomalies are quantified in the general field theory description, and how they cancel in general in F-theory.

#### 1.1 Field theoretic description of anomalies

Quantum field theories with a gauge symmetry and chiral fermions suffer from potential anomalies. These anomalies have been studied and understood from the field theory point of view (see e.g. [108] for a review). In a perturbative description, 4D anomalies are quantified by triangle Feynman diagrams with chiral fermions running in the loop. The external legs that couple to the fermions are gauge bosons of potentially anomalous gauge groups  $G$  or gravitons, which for the sake of argument also constitutes a gauge symmetry. Unless the boson is a  $U(1)$  gauge boson (or a discrete subgroup thereof), the external gauge fields carry Lie-algebra indices, which are traced over in the computation of the triangle diagram. Because all but the  $U(1)$  gauge fields are traceless, all diagrams with one gauge group  $G_i \not\cong U(1)$  appearing only once on the external legs vanish. By this simple group theory argument, the combinatorics only allow for the following non-trivial anomalies:

- $G_i^3$  (all three external legs are from a single simple group  $G_i \not\cong U(1)$ )
- $G_i^2 - U(1)$  (two external gauge bosons from  $G_i$  and a photon)
- $U(1)_a - U(1)_b - U(1)_c$  (all three external photons are from possibly different  $U(1)$ s)
- $U(1)$ -gravitational (two external gravitons and a photon)

Going through the field theory computations, one finds that left-handed and right-handed fermions in a representation  $\mathcal{R}$  of  $G$  contribute with opposite sign, i.e. the anomaly is only sensitive to

the chiral index

$$\chi(\mathcal{R}) = \#(\text{left-handed in } \mathcal{R}) - \#(\text{right-handed in } \mathcal{R}).$$

This is of course assuming that all states of each copy of a representation  $\mathcal{R}$  have the same chirality. If this is not the case, then the gauge symmetry is actually broken. Throughout this thesis, we will assume that this is not case. In particular, in F-theory this is guaranteed by the condition (III.9), as we have seen in section 1.2.1 of chapter III.

The full contributions to the above anomalies are given as

$$\begin{aligned} G_i^3 &: \sum_{\mathcal{R}_i} c_3^{(i)}(\mathcal{R}_i) \chi(\mathcal{R}_i), \\ G_i^2 - U(1) &: \sum_{\mathcal{R}_i} c_2^{(i)}(\mathcal{R}_i) q(\mathcal{R}_i) \chi(\mathcal{R}_i), \\ U(1)_a - U(1)_b - U(1)_c &: \sum_{\mathbf{w}} q_a(\mathbf{w}) q_b(\mathbf{w}) q_c(\mathbf{w}) \chi(\mathbf{w}) = \sum_{\mathcal{R}} \dim(\mathcal{R}) q_a(\mathcal{R}) q_b(\mathcal{R}) q_c(\mathcal{R}) \chi(\mathcal{R}), \\ U(1) - \text{gravitational} &: \sum_{\mathbf{w}} q(\mathbf{w}) \chi(\mathbf{w}) = \sum_{\mathcal{R}} \dim(\mathcal{R}) q(\mathcal{R}) \chi(\mathcal{R}), \end{aligned} \tag{IV.1}$$

where the charges of the individual  $U(1)$  gauge factor are denoted by  $q_{(\cdot)}(\mathcal{R})$ . Furthermore, the coefficients  $c_{2,3}^{(i)}$  are group theoretic constants of  $G_i$ . They are defined as the proportionality factors relating the trace of the field strength  $F_i$  in any irreducible representation:

$$\text{tr}_{\mathcal{R}} F_i^3 = c_3(\mathcal{R}) \text{tr}_{\mathbf{f}} F_i^3, \quad \text{tr}_{\mathcal{R}} F_i^2 = c_2(\mathcal{R}) \text{tr}_{\mathbf{f}} F_i^2. \tag{IV.2}$$

The normalisation is chosen such that for the fundamental representation  $\mathbf{f}$  of any group, these constants are 1.

For a gauge theory to be well-defined, these anomalies have to be cancelled appropriately. In a pure field theory description, this is usually accidental, meaning that the cancellation depends on the chiral spectrum which is an input of the theory. For example, the anomaly cancellation in the Standard Model is generally spoiled by ad hoc extensions of the spectrum.

In string/M-theory compactifications, the cancellation of anomalies is a consequence of the anomaly freedom of the full string theory in 10/11D.<sup>1</sup> In particular, the cancellation in lower dimensions is tied to the geometry of the compact space, most notably in form of Green–Schwarz-like mechanisms which cancel potential anomalies. In the following, we will see how these are described in F-theory.

## 1.2 Gauge and gravitational anomalies in F-theory

There have been numerous works in the literature discussing anomalies in 4D F-theory. Through the duality to M-theory, 4D chiral anomalies can be related to anomalies of 3D Chern–Simons theory in the dual M-theory compactification, as done in the works of [57, 88]. In particular, it was shown that while pure non-abelian anomalies must vanish on their own<sup>2</sup>, those involving  $U(1)$ s will in general require a Green–Schwarz (GS) mechanism to be cancelled. Basically, this is due to the presence of further matter states – axions arising from the geometric Kähler moduli

<sup>1</sup>One may argue that the 10/11D cancellation is also purely accidental. However, the prospect of only one anomaly free 11D theory, from which the only five anomaly free 10D theories arise, may seem aesthetically more pleasing than the vast number of anomaly free theories in 4D.

<sup>2</sup>Geometrically, the vanishing of the pure non-abelian anomalies can be traced back to the possibility of redefining the affine node in an F-theory compactification [79].

fields of the base – which couple to the  $U(1)$  gauge field as well. These couplings contribute to said anomalies and are quantified by the so-called GS-counterterms.

The form of the GS-counterterms in F-theory has been worked out in [88] via M-/F-theory duality. Essentially, they are part of the Chern–Simons terms  $\Theta_{\alpha\beta} \sim \int_{Y_4} G_4 \wedge D_\alpha \wedge D_\beta$  that are flux integrals over combinations of divisors  $D_{\alpha,\beta}$  of the resolved fourfold  $Y_4$ . In the following, we summarise the matching conditions between the anomalies (IV.1) (left hand side) and their potential GS-counterterm (right hand side):

$$\begin{aligned}
 G_i^3 &: \sum_{\mathcal{R}_i} c_3(\mathcal{R}_i) \chi(\mathcal{R}_i) \stackrel{!}{=} 0, \\
 G_i^2 - U(1) &: \sum_{\mathcal{R}_i} c_2(\mathcal{R}_i) q(\mathcal{R}_i) \chi(\mathcal{R}_i) \stackrel{!}{=} -\frac{1}{\lambda_i} \int_{Y_4} G_4 \wedge \omega \wedge W_i, \\
 U(1)_a - U(1)_b - U(1)_c &: \sum_{\mathcal{R}} \dim(\mathcal{R}) q_a(\mathcal{R}) q_b(\mathcal{R}) q_c(\mathcal{R}) \chi(\mathcal{R}) \stackrel{!}{=} 3 \int_{Y_4} G_4 \wedge \pi_*(\omega_{(a} \cdot \omega_b) \wedge \omega_c), \\
 U(1) - \text{gravitational} &: \sum_{\mathcal{R}} \dim(\mathcal{R}) q(\mathcal{R}) \chi(\mathcal{R}) \stackrel{!}{=} -6 \int_{Y_4} G_4 \wedge \bar{\mathcal{K}} \wedge \omega.
 \end{aligned} \tag{IV.3}$$

Some explanation of notation is due: In general,  $\omega_{(\cdot)}$  denotes the geometric generator of the corresponding  $U(1)$  symmetry (i.e. the images of sections under the Shioda map). In the GS-counterterm of the  $G_i^2 - U(1)$  anomalies,  $W_i$  denotes the divisor on the base  $\mathcal{B}$  over which the non-abelian gauge group  $G_i$  is localised; furthermore,  $\lambda_i$  is a group theoretic factor given by the quotient  $2 h_i^*/c_3(\mathbf{adj}_i)$ , with the dual Coxeter number  $h_i^*$  of the group  $G_i$  and  $\mathbf{adj}_i$  being its adjoint representation. For the scope of this thesis, it suffices to note that for  $G_i = SU(n_i)$  we have  $\lambda_i = 1$ . In the counterterm for the  $U(1)^3$  anomalies, the map  $\pi_*$  is the projection of 4-cycles in  $Y_4$  to divisors of  $\mathcal{B}^3$ ; moreover the symmetrisation of the indices  $a, b, c$  comes with a factor of  $1/3! = 1/6$ . Finally, for the  $U(1)$ –gravitational anomaly,  $\bar{\mathcal{K}}$  denotes as usual the anti-canonical class of the base  $\mathcal{B}$ .

Note that whenever the GS-counterterms are non-zero, the axion coupling will induce also a flux-induced Stückelberg mass for the  $U(1)$  gauge field in play. For our analysis in chapter V, where we would like to realise the Standard Model, the phenomenological requirement that the hypercharge  $U(1)_Y$  must remain massless implies a vanishing Stückelberg mass for the hypercharge gauge potential. In particular, this means that all the above anomalies vanish for  $U(1)_Y$  by themselves.

## 2 F-theory with $SU(5) \times U(1)$ and $SU(5) \times \mathbb{Z}_2$ Gauge Group

In the following, we will study how the conditions (IV.3) are fulfilled in two models with an  $SU(5)$  gauge group. They differ from each other in the abelian sector, which in one case is a  $U(1)$  gauge group and in the other a related  $\mathbb{Z}_2$  symmetry. These two models are precisely related to each other by a Higgsing/conifold transition, which we have discussed in the introductory chapter II already. In particular, we will not only investigate the impact of fluxes on the chiral spectrum in both models, but also analyse the role  $G_4$  plays in this transition process. The results of this part have been presented in the publication [14]. For the presentation in this thesis, we have slightly modified some computational details and added some further comments, however without changing the results.

<sup>3</sup>Let  $D_\alpha^{(\mathcal{B})}$  and  $\Sigma^\alpha$  denote a basis of divisors and curves, respectively, on the base  $\mathcal{B}$ , such that they are orthogonal under the intersection product on  $\mathcal{B}$ :  $\int_{\mathcal{B}} D_\alpha^{(\mathcal{B})} \wedge \Sigma^\beta = \delta_\alpha^\beta$ . Then, for any 4-cycle  $\gamma \subset Y_4$ , we define  $\pi_*(\gamma) := (\gamma \cdot \pi^{-1}(\Sigma^\alpha)) D_\alpha^{(\mathcal{B})}$ , which is a divisor in  $\mathcal{B}$ .

## 2.1 Elliptic fibrations with $SU(5) \times U(1)$ gauge group

We start our discussion with the geometric realisation of the  $SU(5) \times U(1)$  gauge group in F-theory. Recall from chapter II that in order to have an abelian gauge factor, the compactification space must be an elliptic fibration with an additional rational section. While there are several toric realisations of these known in the literature, we will study hypersurfaces in an  $\text{Bl}_1\mathbb{P}_{112}$  fibration [56, 109, 110]. The advantage of this class of models is that they allow an easy geometric description corresponding to a Higgsing process, which breaks the  $U(1)$  to a  $\mathbb{Z}_2$ . Such discrete symmetries and their interaction with fluxes will be the topic of the next section. In the following we will present the geometry along the lines of [14, 64].

### 2.1.1 Hypersurfaces in a $\text{Bl}_1\mathbb{P}_{112}$ fibration

As originally shown in [56], a broad class of elliptic fibrations with an additional section is described by embedding the elliptic fibre into the fibre ambient space  $\text{Bl}_1\mathbb{P}_{112}$ . This is a toric space with homogeneous coordinates  $[u : v : w : s]$ , subject to the scaling relations

$$(u, v, w, s) \simeq (\lambda u, \lambda v, \lambda^2 w, s) \simeq (u, \mu v, \mu w, \mu s) \quad (\text{IV.4})$$

for any  $\lambda, \mu \in \mathbb{C} \setminus \{0\}$ , and with the Stanley–Reisner ideal generated by  $\{uw, vs\}$ . The coordinates  $[u : v : w]$  together with the scaling involving  $\lambda$  constitute the original  $\mathbb{P}_{112}$ , whereas the coordinate  $s$  and the associated scaling with  $\mu$  comes from the blow-up of  $\mathbb{P}_{112}$ . The elliptic curve is defined by the zero locus of the following polynomial:

$$P_{U(1)} = s w^2 + b_0 s^2 u^2 w + b_1 s u v w + b_2 v^2 w + c_0 s^3 u^4 + c_1 s^2 u^3 v + c_2 s u^2 v^2 + c_3 u v^3. \quad (\text{IV.5})$$

The toric polygon of  $\text{Bl}_1\mathbb{P}_{112}$  as well as the dual polygon giving  $P$  are also depicted in figure IV.1 as the grey (on the left) resp. the blue polygon (on the right).

	$u$	$v$	$w$	$s$
$\beta$	$\cdot$	$\cdot$	$1$	$\cdot$
$\beta - \bar{\mathcal{K}}$	$\cdot$	$1$	$\cdot$	$\cdot$
$U$	$1$	$1$	$2$	$\cdot$
$S$	$\cdot$	$1$	$1$	$1$

**Table IV.1:** Fibration data of the ambient space  $X_5$ , which is a  $\text{Bl}_1\mathbb{P}_{112}$  fibration over a base  $\mathcal{B}$  with anti-canonical bundle  $\bar{\mathcal{K}}$ . The class  $\beta$  is a free parameter of this class of fibrations.

To construct an elliptically fibred Calabi–Yau over a base  $\mathcal{B}$ , we first fibre  $\text{Bl}_1\mathbb{P}_{112}$  over  $\mathcal{B}$  by promoting  $w$  to be a section of a line bundle with class  $\beta \in H^{(1,1)}(\mathcal{B})$ . The total space of this fibration is a five dimensional Kähler manifold  $X_5$  whose fibration structure is summarised in table IV.1. The elliptic fibration is now the hypersurface defined by the zero locus of the polynomial (IV.5) with the coefficients  $b_i, c_j$  promoted to sections of the base. Their classes are chosen such that the hypersurface is Calabi–Yau:

$$\begin{array}{c|c|c|c|c|c|c}
 b_0 & b_1 & b_2 & c_0 & c_1 & c_2 & c_3 \\
 \hline
 \beta & \bar{\mathcal{K}} & 2\bar{\mathcal{K}} - \beta & 2\beta & \beta + \bar{\mathcal{K}} & 2\bar{\mathcal{K}} & 3\bar{\mathcal{K}} - \beta
 \end{array} \quad (\text{IV.6})$$

The zero section is given by the intersection of the divisor  $U = [\{u\}]$  with the hypersurface, while the additional rational section is given by  $S = [\{s\}]$ . Together they generate a rank one

Mordell–Weil group and consequently a  $U(1)$  gauge group in the F-theory compactification. The corresponding generator is given by the image of  $S$  under the Shioda map, which in the absence of any further non-abelian symmetries takes the form

$$\omega = 5(S - U - \bar{\mathcal{K}} - [b_2]), \quad (\text{IV.7})$$

where the factor 5 is chosen to match the normalisation when including  $SU(5)$  symmetry in the next subsection.

Note that the distinction between holomorphic and rational sections in this case gives rise to matter charged under the  $U(1)$ : While the section  $S$  intersects the generic fibre in one point, it is no longer the case for the fibre over the codimension two locus  $C_1 = \{b_2, c_3\}$ . Here the fibre factorises into two components, as can be seen by inspecting the hypersurface polynomial:

$$P|_{b_2=c_3=0} = s(w^2 + b_0 s u^2 w + b_1 u v w + c_0 s^2 u^4 + c_1 s u^3 v + c_2 u^2 v^2). \quad (\text{IV.8})$$

In particular this shows that the section  $S$  wraps one of the two components. The intersection number  $\pm 10$  with  $\omega$  shows that M2 branes wrapping the curve components over the locus  $C_1$  give rise to  $\mathbf{1}_{\pm 10}$  states.

In [56] it was shown that there is another codimension two locus over which the fibre factors. The locus is obtained by making an ansatz for the factorisation of the hypersurface polynomial, which describe a singularity in the fibre associated with singlet matter. This factorisation of course also applies for the locus  $C_1$ , since it also hosts singlets. Thus, the solution of the ansatz, given by the zero locus of the two polynomials,

$$\begin{aligned} p_1 &= -c_1 b_2^4 + b_1 b_2^3 c_2 + b_0 b_2^3 c_3 - b_1^2 b_2^2 c_3 - 2 b_2^2 c_2 c_3 + 3 b_1 b_2 c_2^2 - 2 c_3^3 \\ p_2 &= -c_3^2 b_0^2 + b_1 b_2 b_0^2 c_3 - b_1 b_2^2 b_0 c_1 + b_2^2 c_1^2 + b_1^2 b_2^2 c_0 - 4 b_1 b_2 c_0 c_3 + 4 c_0 c_3^2, \end{aligned} \quad (\text{IV.9})$$

must also contain  $b_2 = c_3 = 0$  as a solution. To confirm that there is only one further codimension two locus hosting matter states, we employ the primary decomposition techniques explained in section 3.2 from chapter III and regard the polynomials as elements of the base’s function ring  $\mathbb{C}[b_i, c_j]$ , and the locus (IV.9) as the variety defined by the ideal  $\langle p_1, p_2 \rangle$ . Saturating this ideal by  $\langle b_2, c_3 \rangle$  – which defines the locus  $C_1$  – we find that indeed there is only one irreducible component  $C_2$  is left. The ideal defining  $C_2$  has 15 generators, whose exact forms do not lead to any new important insights, and thus are left out here. To verify the matter states over  $C_2$ , one can solve  $p_{1,2} = 0$  for two of the coefficients  $b_i, c_j$ , which will introduce fractional expressions. However, away from the zero loci of the denominators and away from  $b_2 = c_3 = 0$ , these expressions can be plugged into the hypersurface polynomial  $P$ , which indeed does factorise into two factors. This analysis, as performed in [56], confirms that the fibre components give rise to  $\mathbf{1}_{\pm 5}$  states over  $C_2$ .

### 2.1.2 Additional $SU(5)$ symmetry via tops

We use the technology of tops to engineer the  $SU(5)$  gauge group. There are four tops, whose resulting matter spectra have been listed in [58]. In the enumeration established there, we will focus on the model prescribed by top 2 (cf. figure IV.1).

To enhance the fibre structure over a divisor  $\Theta = [\{\theta\}] \in H^{(1,1)}(\mathcal{B})$  to host an  $SU(5)$  singularity, the sections  $g_m \in \{b_i, c_j\}$  are restricted to vanish along  $\theta$  to certain orders:

$$b_0 = b_{0,2} \theta^2, \quad c_0 = c_{0,4} \theta^4, \quad c_1 = c_{1,2} \theta^2, \quad c_2 = c_{2,1} \theta, \quad c_3 = c_{3,1} \theta \quad (\text{IV.10})$$

The divisor classes of the sections change accordingly as  $[g_{m,l}] = [g_m] - l \Theta$ . The singular loci of the hypersurface can be inferred from inspecting the discriminant,

$$\Delta \sim \theta^5 [b_1^4 b_2 (b_1 c_{3,1} - b_2 c_{2,1}) (b_1^2 c_{0,4} - b_{0,2} b_1 c_{1,2} + c_{1,2}^2) + \mathcal{O}(\theta)], \quad (\text{IV.11})$$

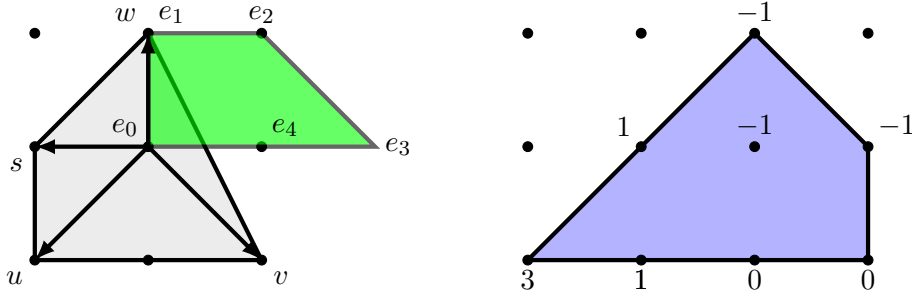


**Figure IV.1:** On the left:  $SU(5)$  top 2 (green) over polygon 6 (grey) from [71] describing the fibre ambient space  $\text{Bl}_1\mathbb{P}_{112}$ . On the right: the dual top with lower bounds on the height of the vertices. This picture is taken from [64].

which indicates that there are four curves hosting matter charged under  $SU(5)$ :

$$\{\theta\} \cap \begin{cases} \{b_1\} \\ \{b_2\} \\ \{b_1 c_{3,1} - b_2 c_{2,1}\} \\ \{(b_1^2 c_{0,4} - b_{0,2} b_1 c_{1,2} + c_{1,2}^2)\} \end{cases} \quad (\text{IV.12})$$

The singlet matter curves  $C_{1,2}$  are still present. Their locus is altered by the presence of the non-abelian divisor; the locus  $V(\langle p_1, p_2 \rangle)$  (IV.9) contains further components along  $\theta = 0$ , which we can eliminate using ideal saturations. The result for the curve  $C_1$  for example is now given by  $C_1 = \{b_2, c_{3,1}\}$ ; the ideal defining the non-complete intersection  $C_2$  can be obtained similarly.

To determine the matter representations over the curves (IV.12), we first need to resolve the singularities. This is achieved by introducing exceptional divisors  $E_i = [\{e_i\}]$  such that  $\Theta \equiv \pi^{-1}(\Theta) = \sum_{i=0}^4 E_i$ , or in terms of the zero loci of the coordinates,  $\pi^{-1}(\{\theta\}) = \{e_0 e_1 \dots e_4\}$ . The resolved hypersurface  $Y_4$  is described by a new polynomial, which can be read off from the top and its dual (cf. figure IV.1):

$$P_{U(1)}^{SU(5)} = e_1 e_2 s w^2 + b_{0,2} s^2 u^2 w e_0^2 e_1^2 e_2 e_4 + b_1 s u v w + b_2 v^2 w e_2 e_3^2 e_4 + c_{0,4} u^4 e_0^4 e_1^3 e_2 e_4^2 + c_{1,2} u^3 v e_0^2 e_1 e_4 + c_{2,1} u^2 v^2 e_0 e_3 e_4 + c_{3,1} u v^3 e_0 e_2 e_3^3 e_4^2 \quad (\text{IV.13})$$

For the chosen triangulation of the top we obtain the Stanley–Reisner ideal generators

$$\{u w, v s, v e_1, v e_2, w e_0, w e_4, u e_1, u e_2, u e_3, u e_4, s e_2, s e_3, s e_4, e_0 e_3, e_1 e_3, e_1 e_4\}. \quad (\text{IV.14})$$

In table IV.2 we summarise the ambient space’s divisor classes and associated scaling relations. In presence of the non-abelian symmetry, the Shioda map is modified to give a  $U(1)$  generator that is orthogonal to the exceptional divisors (II.26). The result is

$$\omega_{U(1)} = 5(S - U - \bar{\mathcal{K}} - [b_2]) + 4E_1 + 3E_2 + 2E_3 + E_4, \quad (\text{IV.15})$$

where the normalisation is chosen such that the charges of all matter states are integer.

While we will analyse in detail the splitting of the fibre components over the curves (IV.12) in the next section, we will collect the matter spectrum including the  $U(1)$  charges in table IV.3. The matter curves intersect at a number of loci, giving rise to six different Yukawa couplings involving  $SU(5)$  charged fields. These are shown in figure IV.2. In addition there is one coupling that is localised outside the GUT divisor. This is the coupling  $\mathbf{1}_{-10}\mathbf{1}_5\mathbf{1}_5$  together with its conjugate, and it exists regardless of the  $SU(5)$  enhancement.

	$u$	$v$	$w$	$s$	$e_0$	$e_1$	$e_2$	$e_3$	$e_4$
$\overline{\mathcal{K}}$	$\cdot$	1	2	$\cdot$	$\cdot$	$\cdot$	$\cdot$	$\cdot$	$\cdot$
$[b_2]$	$\cdot$	-1	-1	$\cdot$	$\cdot$	$\cdot$	$\cdot$	$\cdot$	$\cdot$
$\Theta$	$\cdot$	$\cdot$	$\cdot$	$\cdot$	1	$\cdot$	$\cdot$	$\cdot$	$\cdot$
$U$	1	1	2	$\cdot$	$\cdot$	$\cdot$	$\cdot$	$\cdot$	$\cdot$
$S$	$\cdot$	1	1	1	$\cdot$	$\cdot$	$\cdot$	$\cdot$	$\cdot$
$E_1$	$\cdot$	$\cdot$	-1	$\cdot$	-1	1	$\cdot$	$\cdot$	$\cdot$
$E_2$	$\cdot$	-1	-2	$\cdot$	-1	$\cdot$	1	$\cdot$	$\cdot$
$E_3$	$\cdot$	-2	-2	$\cdot$	-1	$\cdot$	$\cdot$	1	$\cdot$
$E_4$	$\cdot$	-1	-1	$\cdot$	-1	$\cdot$	$\cdot$	$\cdot$	1

**Table IV.2:** Divisor classes (first column) and associated scaling relations for the ambient space of the top-2-model. Note that in comparison to table IV.1 we have secretly exchanged the parameter  $\beta$  by the class  $[b_2] = 2\overline{\mathcal{K}} - \beta$ .

locus in base	irrep $SU(5)_{U(1)}$
$\theta \cap b_1$	$\mathbf{10}_{-2}, \overline{\mathbf{10}}_2$
$\theta \cap b_2$	$\mathbf{5}_{-6}, \overline{\mathbf{5}}_6$
$\theta \cap \{b_1 c_{3,1} - b_2 c_{2,1}\}$	$\mathbf{5}_4, \overline{\mathbf{5}}_{-4}$
$\theta \cap \{b_1^2 c_{0,4} - b_{0,2} b_1 c_{1,2} + c_{1,2}^2\}$	$\mathbf{5}_{-1}, \overline{\mathbf{5}}_1$
$C_1 = b_2 \cap c_{3,1}$	$\mathbf{1}_{\pm 10}$
$C_2$	$\mathbf{1}_{\pm 5}$

**Table IV.3:** Matter curves in the  $SU(5) \times U(1)$  model.

## 2.2 Fluxes and anomalies in the $SU(5) \times U(1)$ model

### 2.2.1 The vertical cohomology ring

In order to investigate the fluxes and their induced chiral spectrum we first need to construct the vertical cohomology  $H_{\text{vert}}^{(\cdot, \cdot)}(Y_4) \subset H_{\text{vert}}^{(\cdot, \cdot)}(X_5)$ . We will use this model to demonstrate how the strategy outlined in section 2 of chapter III is applied in a concrete example.

First we form a polynomial ring  $\mathbb{C}[D^{(T)}, D^{(\mathcal{B})}]$ , where the variables are the ambient spaces divisor classes. For the  $SU(5) \times U(1)$  model, these are

$$\begin{aligned} D^{(T)} &\in \{[u], [v], [w], [s], [e_0], \dots, [e_4]\}, \\ D^{(\mathcal{B})} &\in \{\overline{\mathcal{K}}, [b_2], \Theta, D\}, \end{aligned} \quad (\text{IV.16})$$

where  $D$  collectively denotes any other vertical divisor unrelated to  $\overline{\mathcal{K}}, \Theta$  or  $[b_2]$ . The polynomials are subject to the linear equivalence and intersection relations, which are ideals in  $\mathbb{C}[D^{(T)}, D^{(\mathcal{B})}]$ . The generators of the linear equivalence ideal (LIN) can be read off from the columns in table IV.2:

$$\begin{aligned} \text{LIN} = \langle & -[v] + \overline{\mathcal{K}} - [b_2] + U + S - E_2 - 2E_3 - E_4, \\ & -[w] + 2\overline{\mathcal{K}} - [b_2] + 2U + S - E_1 - 2E_2 - 2E_3 - E_4, \\ & -E_0 + \Theta - E_1 - E_2 - E_3 - E_4 \rangle. \end{aligned} \quad (\text{IV.17})$$

Note that we have omitted those columns with only one ‘1’; these trivially identify the zero loci of the corresponding toric coordinate with its associated divisor class, e.g.  $[u] = [\{u\}] = U$ . The intersection relations (SRI) containing products which are zero in cohomology are in part given

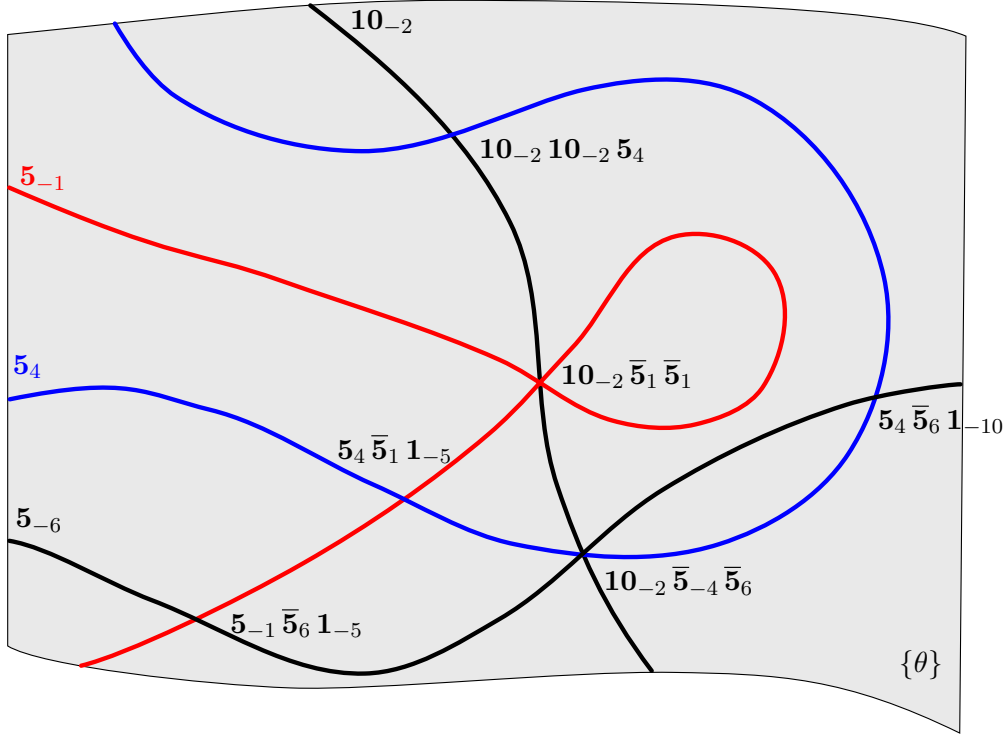


**Figure IV.2:** The matter curves in the  $SU(5)$  divisor  $\{\theta\}$  and the Yukawa couplings involving the  $SU(5)$  charged matter in codimension three. The curves  $C_{1,2}$  hosting the singlets are not displayed, however their intersection with  $\{\theta\}$  mark the Yukawa points of type  $\mathbf{5} \bar{\mathbf{5}} \mathbf{1}$ .

by the SR-ideal (IV.14) with the coordinates being replaced by their associated divisors:

$$\begin{aligned} \text{SRI}^{(T)} = \langle & U [w], [v] S, [v] E_1, [v] E_2, [w] E_0, [w] E_4, \\ & U E_1, U E_2, U E_3, U E_4, S E_2, S E_3, S E_4, E_0 E_3, E_1 E_3, E_1 E_4 \rangle \end{aligned} \quad (\text{IV.18})$$

Furthermore, as the base  $\mathcal{B}$  is a complex threefold, the following generators must be included into SRI:

$$\text{SRI}^{(\mathcal{B})} = \langle E_i D_a^{(\mathcal{B})} D_b^{(\mathcal{B})} D_c^{(\mathcal{B})}, D_a^{(\mathcal{B})} D_b^{(\mathcal{B})} D_c^{(\mathcal{B})} D_d^{(\mathcal{B})} \rangle \quad (\text{IV.19})$$

As explained in section 2 of chapter III, the ambient space's cohomology is then given by (III.23):

$$H_{\text{vert}}^{(\cdot, \cdot)}(X_5) \cong \frac{\mathbb{C}[D^{(T)}, D^{(\mathcal{B})}]}{\text{LIN} + \text{SRI}^{(T)} + \text{SRI}^{(\mathcal{B})}}. \quad (\text{IV.20})$$

### 2.2.2 Vertical $G_4$ -fluxes

To construct all vertical flux solutions, we first have to pick a basis for  $H_{\text{vert}}^{(2,2)}(Y_4)$ . Recall that this is a minimal set  $\{t_i\} \subset H_{\text{vert}}^{(2,2)}(X_5)$  which generates  $H_{\text{vert}}^{(2,2)}(Y_4) \cong H_{\text{vert}}^{(2,2)}(X_5) \cdot [Y_4] \subset H_{\text{vert}}^{(3,3)}(X_5)$ . This set is smaller than a basis of  $H_{\text{vert}}^{(2,2)}(X_5)$ , because of extra redundancies that arise when multiplying with the class of the hypersurface. E.g. the  $(2, 2)$ -forms  $E_2 E_4$  and  $E_4 \bar{K} = E_4 [b_1]$  are linearly independent in  $H_{\text{vert}}^{(2,2)}(X_5)$ , however when restricted to the hypersurface, they actually become the same due to the intersection relations. This can be seen easily in the Poincaré-dual



picture in terms of geometric intersections:

$$\begin{aligned}
 E_2 E_4 [Y_4] &= \left[ \{e_2\} \cap \{e_4\} \cap \left\{ P_{U(1)}^{SU(5)} \right\} \right] = [\{e_2\} \cap \{e_4\} \cap \{b_1 s u v w\}] \\
 &\stackrel{\text{SR-ideal}}{=} [\{e_2\} \cap \{e_4\} \cap \{b_1\}] \stackrel{\text{SR-ideal}}{=} [\{e_1 s w^2 e_2\} \cap \{e_4\} \cap \{b_1\}] \\
 &= \left[ \left\{ P_{U(1)}^{SU(5)} \right\} \cap \{e_4\} \cap \{b_1\} \right] = [Y_4] E_4 [b_1]
 \end{aligned} \tag{IV.21}$$

To eliminate this type of redundancy in the remaining discussion, when we are dealing with (2, 2)-forms on  $Y_4$ , we fix the following basis elements:

$$\{t_i\} = \left\{ D_a^{(\mathcal{B})} D_b^{(\mathcal{B})}, \quad (U, S, E_1, E_2, E_3, E_4) D_c^{(\mathcal{B})}, \quad E_3 E_4, \quad E_1 E_2 \right\}, \tag{IV.22}$$

where  $D_{a,b,c}^{(\mathcal{B})} \in \{\bar{\mathcal{K}}, [b_2], \Theta, D\}$ .

Valid vertical  $G_4$ -fluxes are now subject to the transversality conditions (III.6), (III.7), and the gauge symmetry condition (III.9), i.e. they are linear combinations of  $\{t_i\}$  satisfying

$$\int_{Y_4} \left( \sum_i \lambda_i t_i \right) \wedge D_a^{(\mathcal{B})} \wedge D_b^{(\mathcal{B})} = \int_{Y_4} \left( \sum_i \lambda_i t_i \right) \wedge U \wedge D_c^{(\mathcal{B})} = \int_{Y_4} \left( \sum_i \lambda_i t_i \right) \wedge E_k \wedge D_c^{(\mathcal{B})} = 0 \tag{IV.23}$$

for  $k = 1, \dots, 4$ . With the full knowledge of the fibre ambient space geometry, we can reduce all intersection numbers on  $Y_4$  to intersection numbers on the base. Hence each of the three equations will yield an expression of the form

$$\sum_{\alpha, \beta, \gamma} \varphi_{\alpha\beta\gamma}(\lambda_i) \int_{\mathcal{B}} D_\alpha^{(\mathcal{B})} \wedge D_\beta^{(\mathcal{B})} \wedge D_\gamma^{(\mathcal{B})}, \tag{IV.24}$$

where the coefficients  $\varphi_{\alpha\beta\gamma}(\lambda_i)$  are linear functions in  $\lambda_i$ . For a generic base, the intersection numbers  $\int_{\mathcal{B}} D_\alpha^{(\mathcal{B})} \wedge D_\beta^{(\mathcal{B})} \wedge D_\gamma^{(\mathcal{B})}$  are a priori independent. Therefore, only those solutions where all  $\varphi_{\alpha\beta\gamma}(\lambda_i)$  are independently zero exist for a generic fibration. Previous classifications of vertical gauge fluxes over generic and concrete base spaces have been obtained in [96] and [57, 87, 111, 112], respectively.

As always in the presence of an abelian gauge factor, we find amongst the solutions the  $U(1)$ -flux

$$G_4^0(F) = \omega_{U(1)} \wedge \pi^{-1} F \equiv \omega_{U(1)} \wedge F, \tag{IV.25}$$

which satisfies the transversality conditions for any choice of vertical divisor class  $F \in H^{(1,1)}(\mathcal{B})$ . Other than these fluxes, there are three independent solutions to the transversality conditions, which when expressed in the basis (IV.22) take the form

$$\begin{aligned}
 G_4^{u_1} &= -15 E_1 E_2 + 35 E_3 E_4 - 5 \Theta (4 E_1 + 3 E_2 + 2 E_3 - 6 E_4 + 2 S + 2 U) \\
 &\quad - 5 [b_2] (2 E_1 + E_2 + 3 E_3 - 2 E_4 - 2 \Theta) + \bar{\mathcal{K}} (36 E_1 + 42 E_2 + 28 E_3 - 21 E_4 - 10 \Theta), \\
 G_4^{u_2} &= -2 (5 E_1 E_2 + 5 E_3 E_4 - \bar{\mathcal{K}} (2 E_1 - 6 E_2 - 4 E_3 + 3 E_4)) + 10 [b_2] (E_2 + E_3 - \Theta) \\
 &\quad - 10 \Theta (E_4 - \bar{\mathcal{K}} - S - U), \\
 G_4^{u_3} &= 5 E_1 E_2 + 5 E_3 E_4 + (-2 E_1 + 6 E_2 + 4 E_3 - 3 E_4) \bar{\mathcal{K}} - 5 [b_2] (E_2 + E_3 - 2 \Theta) \\
 &\quad - \Theta (4 E_1 + 3 E_2 + 2 (E_3 - 2 E_4 + 5 S)).
 \end{aligned} \tag{IV.26}$$

Note that for an explicit choice of the fibration data and base  $\mathcal{B}$ , linear equivalences amongst the vertical divisors might render some of the above fluxes linearly dependent. If no such linear

dependences arise, one might wonder if new fluxes can be constructed for a special base  $\mathcal{B}$ : However, it turns out that the only such fluxes are of the form  $G_4^0(F)$  (for new classes of  $F$  in addition to the generic base classes  $[b_2], \Theta, \bar{\mathcal{K}}$ ), but no additional fluxes of the form  $G_4^{u_i}$  not related to a  $U(1)$ -flux can occur. The general vertical flux is thus of the form

$$G_4(F, u_1, u_2, u_3) = G_4^0(F) + u_1 G_4^{u_1} + u_2 G_4^{u_2} + u_3 G_4^{u_3}. \quad (\text{IV.27})$$

In addition to giving rise to chirality, this general form of  $G_4$  will be crucial when we analyse the Higgsing process to the  $SU(5) \times \mathbb{Z}_2$  model.

### 2.2.3 Matter surfaces

Fluxes are only half of the input to the chiral spectrum. The other half are the details on the homology classes  $\gamma$  of matter surfaces. In this part we will present the matter surfaces of the states listed in table IV.3 based on the techniques developed in section 3.2 of chapter III. This section also has the purpose of demonstrating these techniques in an explicit example.

An important observation is that, in the homology of  $X_5$ , we can always find a ‘factorisation’  $[\gamma] = [Y_4] \cdot [\tilde{\gamma}]$ , where the class  $[\tilde{\gamma}]$  is a quadratic expression in the divisors. This means that on the hypersurface  $Y_4$ , the homology of  $\gamma$  is a vertical class (represented by the restriction of the cycle  $\tilde{\gamma}$  to the hypersurface). The chiral index can then be re-expressed as  $\chi = \int_{X_5} G_4 \wedge [P_T] \wedge [\tilde{\gamma}] \equiv \int_{Y_4} G_4 \wedge [\gamma]$ .

#### The $\bar{\mathbf{10}}_2$ surface

Matter in the  $\bar{\mathbf{10}}_2$  representation is localised over  $\{\theta\} \cap \{b_1\}$ . Over this locus, the fibre of the divisor  $E_2$  splits into several components:

$$P_{U(1)}^{SU(5)}|_{b_1=e_2=0} = e_0 (c_{1,2} e_0 e_1 + c_{2,1} e_3) e_4 \quad (\text{IV.28})$$

Let us focus on the component given by  $e_0 = 0 = e_2$  in the fibre. One can verify by computing the intersection numbers of this curve with the exception divisors  $E_i$  (yielding the weight vector  $(1, -1, 0, 1)$ ) and the  $U(1)$ -generator (IV.15) (giving the charge 2) that M2-branes wrapped on it gives rise to a state of  $\bar{\mathbf{10}}_2$ . Therefore, a matter surface of  $\bar{\mathbf{10}}_2$ , given by fibring this  $\mathbb{P}^1$  over the curve in the base, is described by the ideal  $\langle e_2, e_0, b_1 \rangle$ . Further note that setting  $e_0$  and  $e_2$  to zero in the hypersurface polynomial (IV.13) only leaves the term  $b_1 s u v w$ , which due to the SR-ideal (IV.14) only vanishes if  $b_1 = 0$ . This means that the homology class of the matter surface can be written as

$$[\mathcal{C}_{\bar{\mathbf{10}}_2}] \equiv [\bar{\mathbf{10}}_2] = E_2 E_0 [b_1] = [Y_4] \cdot E_2 E_0, \quad (\text{IV.29})$$

which in particular shows that the surface gives rise to the vertical  $(2, 2)$ -form  $E_2 E_0$  on the hypersurface  $Y_4$ .

#### The $\mathbf{5}_{-6}$ surface

To study the second locus  $\{\theta\} \cap \{b_2\}$ , we set  $b_2 = 0$  in the hypersurface polynomial. By doing so, one finds that the affine Dynkin node, i.e. the fibre of the divisor  $E_0$ , splits into two curves. One of these is given by  $e_0 = s = 0$ , carrying a weight of  $\mathbf{5}_{-6}$ . The associated matter surface  $\langle b_2, e_0, s \rangle$  has the homology class

$$[\mathbf{5}_{-6}] = E_0 S [b_2] = E_0 S [Y_4], \quad (\text{IV.30})$$

where we have again used the SR-ideal (IV.14) after realising that the only non-zero term in the hypersurface polynomial is  $b_2 v^2 w e_2 e_3^2 e_4$  when setting  $e_0$  and  $s$  to zero. Again, we find that the matter surface has a vertical class in the hypersurface’s cohomology.

**The  $\bar{\mathbf{5}}_{-4}$  surface**

Over the third locus  $\{\theta\} \cap \{b_1 c_{3,1} - b_2 c_{2,1}\}$  the factorisation of the fibre can be identified by making a local ansatz  $c_{3,1} \neq 0$ , such that the locus can be written as  $b_1 = b_2 c_{2,1}/c_{3,1}$ . Evaluating the hypersurface polynomial with this constraint leads to a factorisation of  $E_1$ :

$$P_{U(1)}^{SU(5)}(e_1 = 0, b_1 = b_2 c_{2,1}/c_{3,1}) = \frac{(c_{3,1} e_2 + c_{2,1} s)(c_{3,1} e_0 + b_2 w)}{c_{3,1}} \quad (\text{IV.31})$$

However this is not a globally well-defined expression. To obtain it, we need to describe the matter surface by an ideal. Since from the local analysis we know that the splitting occurs for the surface to which the divisor  $E_1$  restrict to the matter curve, we compute the primary decomposition of its ideal

$$\langle P_{U(1)}^{SU(5)}, e_1, b_1 c_{3,1} - b_2 c_{2,1} \rangle,$$

which yields three components, which are in fact prime ideal themselves:

$$\begin{aligned} &\langle b_1 c_{3,1} - b_2 c_{2,1}, \quad e_1, \quad c_{3,1} e_2 e_3^2 e_4 v + c_{2,1} u s, \quad b_2 e_2 e_3^2 e_4 v + b_1 u s \rangle =: I, \\ &\langle b_1 c_{3,1} - b_2 c_{2,1}, \quad e_1, \quad c_{3,1} e_0 e_3 e_4 u v + b_2 w, \quad c_{2,1} e_0 e_3 e_4 u v + b_1 w \rangle, \\ &\langle b_1 c_{3,1} - b_2 c_{2,1}, \quad e_1, \quad v \rangle \end{aligned} \quad (\text{IV.32})$$

The third component describes an empty set (or zero in homology), because  $e_1 v$  is one of the generators of the SR-ideal (IV.14). The other two are the components of the  $\mathbf{5}$  and the  $\bar{\mathbf{5}}$  states.

Let us for definiteness focus on the first component  $I$ . It is a globally well-defined description of the matter surface as a non-complete intersection. To obtain its homology class, we need to find a complete intersection  $J$  which is contained in  $I$  it as an isolated component. The easiest such complete intersection is described by the ideal which itself is generated by three of the four generators of  $I$ , say

$$J = \langle b_1 c_{3,1} - b_2 c_{2,1}, \quad e_1, \quad c_{3,1} e_2 e_3^2 e_4 v + c_{2,1} u s \rangle. \quad (\text{IV.33})$$

A primary decomposition of this ideal reveals it is not itself prime, and indeed has  $I$  as one of its primary components (which is already prime); the only other component is another complete intersection,  $J^{(1)} = \langle e_1, c_{2,1}, c_{3,1} \rangle$  with multiplicity 1, as the saturation  $J : (J^{(1)})^\infty$  reveals. This means that as varieties we have  $V(I) = \overline{V(J) \setminus V(J^{(1)})}$ , or in terms of homology:

$$[V(I)] = [V(J)] - [V(J^{(1)})] = ([b_1] + [c_{3,1}]) E_1 ([c_{2,1} + U + S] - E_1 [c_{2,1}] [c_{3,1}]). \quad (\text{IV.34})$$

Calculating the Cartan charges shows that the matter state on this surface is in fact in the  $\bar{\mathbf{5}}_{-4}$  representation. To find a possible vertical  $(2, 2)$ -form on  $Y_4$  representing this class, we expand the expression  $[V(I)] - (\lambda_i t_i) [Y_4]$ , with  $t_i$  the chosen basis (IV.22) of  $H_{\text{vert}}^{(2,2)}(Y_4)$ , in a basis of  $H_{\text{vert}}^{(3,3)}(X_5)$ . If there is a solution of  $\lambda_i$  such that the expression is 0, it means we can identify  $[V(I)]$  as the vertical class  $\lambda_i t_i$  on the hypersurface. In the concrete example, we indeed find a unique solution:

$$\begin{aligned} [V(I)] &\equiv \\ [\bar{\mathbf{5}}_{-4}] &= [Y_4] \cdot (-E_3 E_4 + (E_1 + E_4) \bar{K} + [b_2] (E_1 + E_2 + E_3 - \Theta) + (S - E_4) \Theta) \end{aligned} \quad (\text{IV.35})$$

**The  $\bar{\mathbf{5}}_1$  surface**

By the same methods analyse the fibre structure over the curve  $\{\theta\} \cap \{b_1^2 c_{0,4} - b_{0,2} b_1 c_{1,2} + c_{1,2}^2\}$ . The factorisation process is somewhat more evolved, since the curve is now described by a quadratic equation, and thus the ideals have more generators. To reduce the cluttering, we will not display each step of the calculation.

The local analysis (e.g. by solving  $b_1^2 c_{0,4} - b_{0,2} b_1 c_{1,2} + c_{1,2}^2 = 0$  for  $b_{0,2}$ ) reveals the splitting of  $E_3$ , which can be confirmed by the two non-trivial components resulting from the primary decomposition of  $\langle b_1^2 c_{0,4} - b_{0,2} b_1 c_{1,2} + c_{1,2}^2, e_3, P_{U(1)}^{SU(5)} \rangle$ . One of which – that turns out to be the surface of  $\bar{\mathbf{5}}_1$  states – can be obtained as a prime component of the ideal  $\langle b_1^2 c_{0,4} - b_{0,2} b_1 c_{1,2} + c_{1,2}^2, e_3, c_{1,2} e_0^2 e_1 e_4 u^2 s + b_1 w \rangle$ , which in addition contains the complete intersection  $\langle c_{1,2} b_1 e_3 \rangle$  with multiplicity 2. Thus the matter surface has homology class

$$\begin{aligned} [\bar{\mathbf{5}}_1] &= (2[b_1] + [c_{0,4}]) E_3 ([b_1] + [w]) - 2[c_{1,2}][b_1] E_3 \\ &= [Y_4] \cdot (2 E_3 (E_4 + 2\bar{\mathcal{K}} - \Theta) + [b_2] (\Theta - 2 E_3) + \Theta (E_2 + E_4 - \bar{\mathcal{K}} - S - U)) . \end{aligned}$$

Again we can convince ourselves that the surface has a vertical class.

### The $\mathbf{1}_{-10}$ surface

As we have already discussed section 2.1.1, states of  $\mathbf{1}_{-10}$  arise by M2-branes wrapping the curve  $s = 0$  in the fibre over  $b_2 = c_{3,1} = 0$ . The associated matter surface is therefore given by  $\langle s, b_2, c_{3,1} \rangle$ . The homology class is again vertical on the hypersurface and given by

$$[\mathbf{1}_{-10}] = S [b_2] [c_{3,1}] = [Y_4] \cdot (E_1 (E_2 - \bar{\mathcal{K}}) - S \Theta + [b_2] (E_1 + S - U)) \quad (\text{IV.36})$$

### The $\mathbf{1}_5$ surface

In theory the matter surface of  $\mathbf{1}_5$  states must also be described by a prime ideal, which is a component of the surface with ideal  $\langle \text{generators of } C_2, P_{U(1)}^{SU(5)} \rangle = C_2 + \langle P_{U(1)}^{SU(5)} \rangle$ . However, because of the complexity of  $C_2$ , **Singular** cannot compute the primary decomposition of the above ideal, denying us the possibility of computing the homology class  $[\mathbf{1}_5]$ .

It also means that we cannot study the  $U(1)^3$  and  $U(1)$ -gravitational anomalies directly. However, as we will see in section 2.2.5, both anomalies are *consistent* if we compute the contributions from all the other matter states, of which we know the surfaces.

$\mathcal{R}$	$[\gamma_{\mathcal{R}}] \equiv [\mathcal{R}] \equiv [Y_4] \cdot [\tilde{\mathcal{R}}]$
$\bar{\mathbf{10}}_2$	$[Y_4] \cdot E_2 E_0$
$\mathbf{5}_{-6}$	$[Y_4] \cdot E_0 S$
$\bar{\mathbf{5}}_{-4}$	$[Y_4] \cdot (-E_3 E_4 + (E_1 + E_4) \bar{\mathcal{K}} + [b_2] (E_1 + E_2 + E_3 - \Theta) + (S - E_4) \Theta)$
$\bar{\mathbf{5}}_1$	$[Y_4] \cdot (2 E_3 (E_4 + 2\bar{\mathcal{K}} - \Theta) + [b_2] (\Theta - 2 E_3) + \Theta (E_2 + E_4 - \bar{\mathcal{K}} - S - U))$
$\mathbf{1}_{-10}$	$[Y_4] \cdot (E_1 (E_2 - \bar{\mathcal{K}}) - S \Theta + [b_2] (E_1 + S - U))$

**Table IV.4:** Known homology classes of matter surfaces in the  $SU(5) \times U(1)$  model.

### Fluxes from matter surfaces

As an interlude, we would like to relate the vertical fluxes we computed by systematically implementing the transversality conditions with the matter surfaces. Conceptually we expect such a relation since the  $G_4$  data can be equivalently encoded in rational equivalence classes of 4-cycles [95], which by Poincaré-duality can be viewed as elements of  $H^{(2,2)}(Y_4)$ . Because the matter surfaces naturally give building blocks of algebraic 4-cycles, we would like to see how they can be modified to give rise to fluxes.

In practise the approach is simple: The vertical class representing the matter surface on  $Y_4$  will generally not satisfy the transversality conditions. However we may add vertical correction terms to it such that their contribution to the intersection numbers in the transversality conditions precisely cancel the contribution of the matter surface. By construction this yields a valid vertical  $G_4$ -flux.

For example the matter surface  $[\overline{\mathbf{10}}_2]$  violates the condition  $\int G_4 \wedge E_i \wedge D^{(\mathcal{B})} = 0$ ; explicitly:

$$\int [\overline{\mathbf{10}}_2] \wedge E_i \wedge D^{(\mathcal{B})} = (1, -1, 0, 1)_i \int_{\mathcal{B}} \overline{\mathcal{K}} \wedge \Theta \wedge D^{(\mathcal{B})}.$$

To cancel this contribution, we have to add a suitable linear combination  $\lambda_j E_j \wedge \overline{\mathcal{K}}$ . One can easily convince oneself that such a correction term does not spoil the other two transversality conditions, simply because the exceptional divisors  $E_i$  do not intersect the zero section  $U$  (preserve (III.7)) and are localised in codimension one on the base (preserve (III.6)). It is straightforward to determine the coefficients  $\lambda_j$ : Because we know  $\int_{Y_4} E_j \wedge \overline{\mathcal{K}} \wedge E_i \wedge D^{(\mathcal{B})} = -C_{ji} \int_{\mathcal{B}} \overline{\mathcal{K}} \Theta \wedge D^{(\mathcal{B})}$ , where  $C_{ji} = C_{ij}$  is the Cartan matrix of  $SU(5)$ , the coefficients are simply  $(C^{-1})_{ji}(1, -1, 0, 1)_i = (2/5, -1/5, 1/5, 3/5)_j$ . Hence the flux associated to the matter surface  $[\overline{\mathbf{10}}_2]$  is

$$\begin{aligned} G_4(\overline{\mathbf{10}}_2) &= E_2 E_0 + \frac{1}{5}(2, -1, 1, 3)_j E_j \overline{\mathcal{K}} \\ &= -E_1 E_2 - E_3 E_4 + \frac{1}{5} \overline{\mathcal{K}} (2 E_1 - 6 E_2 - 4 E_3 + 3 E_4) + [b_2] (E_2 + E_3 - \Theta) \\ &\quad - \Theta (E_4 - \overline{\mathcal{K}} - S - U) \end{aligned} \quad (\text{IV.37})$$

Comparing to (IV.26), we see that this flux is precisely  $1/10 G_4^{u_2}$ .

By analogous computations, we can easily find similar relations for the other matter surfaces:

$$\begin{aligned} G_4(\overline{\mathbf{10}}_2) &= \frac{1}{10} G_4^{u_2}, \\ G_4(\mathbf{5}_{-6}) &= \frac{1}{50} (G_4^{u_1} + 6 G_4^{u_2} + 5 G_4^{u_3}), \\ G_4(\overline{\mathbf{5}}_{-4}) &= \frac{1}{50} (-G_4^{u_1} - 6 G_4^{u_2} - 15 G_4^{u_3}) - \frac{1}{5} G_4^0(\Theta), \\ G_4(\overline{\mathbf{5}}_1) &= \frac{1}{50} (2 G_4^{u_1} - 3 G_4^{u_2}), \\ G_4(\mathbf{1}_{-10}) &= \frac{1}{50} (-G_4^{u_1} - G_4^{u_2} + 5 G_4^{u_3}) + \frac{1}{5} G_4^0([b_2]). \end{aligned} \quad (\text{IV.38})$$

This confirms that indeed matter surfaces as algebraic 4-cycles contain the generic vertical fluxes (IV.26) in their geometric data.

## 2.2.4 Chiralities and non-abelian anomalies

We finally turn to the anomalies. After the prelude in the previous sections, we only have to put all the necessary ingredients together. Recall that the chiralities induced by a flux  $G_4$  is computed with the general formula

$$\chi(\mathcal{R}) = \int_{\mathcal{C}_{\mathcal{R}}} G_4 = \int_{X_5} [\mathcal{R}] \wedge G_4, \quad (\text{IV.39})$$

with the matter surface's dual cohomology class  $[\mathcal{R}]$  is given in table IV.4. Note that we can compute the chirality of the conjugate representation  $\overline{\mathcal{R}}$  as  $\chi(\overline{\mathcal{R}}) = -\chi(\mathcal{R})$ , which we will implicitly use in the following.

With the above formula, we obtain the following chiral indices for the non-abelian matter in the presence of the general vertical flux solution  $\sum_i u_i G_4^{u_i} + G_4^0(F)$  (IV.27):

$$\begin{aligned}
 \chi(\overline{\mathbf{10}}_2) &= \left( (-42 u_1 + 12 u_2 - 6 u_3) \overline{\mathcal{K}}^2 + 20 u_1 \overline{\mathcal{K}} [b_2] + (25 u_1 - 20 u_2 + 3 u_3) \overline{\mathcal{K}} \Theta + 2 \overline{\mathcal{K}} F \right) \Theta, \\
 \chi(\overline{\mathbf{5}}_6) &= \left( (-36 u_1 - 4 u_2 + 2 u_3) \overline{\mathcal{K}} [b_2] + 10 u_1 [b_2]^2 + (20 u_1 - 6 u_3) [b_2] \Theta + 6 [b_2] F \right) \Theta, \\
 \chi(\overline{\mathbf{5}}_{-4}) &= \left( (-42 u_1 + 12 u_2 - 6 u_3) \overline{\mathcal{K}}^2 + (-16 u_1 - 4 u_2 + 2 u_3) \overline{\mathcal{K}} [b_2] + 10 u_1 [b_2]^2 \right. \\
 &\quad \left. + (61 u_1 - 12 u_2 + 11 u_3) \overline{\mathcal{K}} \Theta + (10 u_1 + 4 u_3) [b_2] \Theta + (-20 u_1 - 4 u_3) \Theta^2 \right. \\
 &\quad \left. - 8 \overline{\mathcal{K}} F - 4 [b_2] F + 4 \Theta F \right) \Theta, \\
 \chi(\overline{\mathbf{5}}_1) &= \left( (84 u_1 - 24 u_2 + 12 u_3) \overline{\mathcal{K}}^2 + (32 u_1 + 8 u_2 - 4 u_3) \overline{\mathcal{K}} [b_2] - 20 u_1 [b_2]^2 \right. \\
 &\quad \left. + (-86 u_1 + 16 u_2 - 14 u_3) \overline{\mathcal{K}} \Theta + (-30 u_1 + 2 u_3) [b_2] \Theta + (20 u_1 + 4 u_3) \Theta^2 \right. \\
 &\quad \left. + 6 \overline{\mathcal{K}} F - 2 [b_2] F - 4 \Theta F \right) \Theta, \\
 \chi(\mathbf{1}_{-10}) &= 10 u_3 (\overline{\mathcal{K}} [b_2] + [b_2]^2 - [b_2] \Theta) \Theta - 10 (\overline{\mathcal{K}} [b_2] + [b_2]^2 - [b_2] \Theta) F,
 \end{aligned} \tag{IV.40}$$

where every term is understood to be an intersection number of three divisors on the base  $\mathcal{B}$ . With these expressions, one can directly verify that the  $SU(5)$  anomalies are explicitly cancelled, as prescribed in (IV.3). However, we would like to use a different approach by studying the matter surfaces in table IV.4. To this end, we note that in the general anomaly matching formulae (IV.3), both side can be expressed as integrals of  $G_4$  over certain 4-cycles. On the left hand side, this 4-cycle is a linear combination of the matter surfaces; on the right hand side the 4-cycle is given by the geometric contribution to the corresponding GS-counterterm. Therefore, our strategy is to show that these two 4-cycles agree – at least up to irrelevant terms.

### $SU(5)^3$ anomaly

Let us first verify the  $SU(5)^3$  anomaly cancellation

$$\chi(\overline{\mathbf{10}}_2) + \chi(\overline{\mathbf{5}}_1) + \chi(\overline{\mathbf{5}}_{-4}) + \chi(\overline{\mathbf{5}}_6) = 0. \tag{IV.41}$$

Based on the fluxes

In fact, we can directly see the  $SU(5)$  anomaly cancellation in the geometry of the matter surfaces, *without* computing any integration of fluxes explicitly. Instead we only look at the 4-cycle  $[\overline{\mathbf{10}}_2] + [\overline{\mathbf{5}}_1] + [\overline{\mathbf{5}}_{-4}] + [\overline{\mathbf{5}}_6]$  which yields the anomaly (IV.41) if one integrates a flux  $G_4$  over it. With the data in table IV.4, it is easily computed to be

$$\begin{aligned}
 [\overline{\mathbf{10}}_2] + [\overline{\mathbf{5}}_1] + [\overline{\mathbf{5}}_{-4}] + [\overline{\mathbf{5}}_6] &= \\
 [Y_4] \cdot (2[b_2] (E_1 + E_2) + \overline{\mathcal{K}} (-E_2 + 3E_3 + E_4) + \Theta (-[b_2] + E_2 - E_3 - E_4)).
 \end{aligned} \tag{IV.42}$$

Obviously, on the hypersurface this 4-cycle is of the schematic form  $E_i D_a^{(\mathcal{B})} + D_b^{(\mathcal{B})} D_c^{(\mathcal{B})}$ . By the transversality conditions, we can now argue directly that any valid flux (not even necessarily vertical) will integrate to 0 over this 4-cycle, thus giving no  $SU(5)^3$  anomaly.

### $SU(5)^2 - U(1)$ anomaly

The mixed anomaly is in general not zero, but will require a Green–Schwarz mechanism to be cancelled, which in the process will render the  $U(1)$  massive. The cancellation is guaranteed if

$$\begin{aligned}
 q(\overline{\mathbf{10}}_2) c_2(\overline{\mathbf{10}}) \chi(\overline{\mathbf{10}}_2) + \sum_q q \cdot c_2(\overline{\mathbf{5}}) \chi(\overline{\mathbf{5}}_q) &= \\
 2 \cdot 3 \cdot \chi(\overline{\mathbf{10}}_2) + \chi(\overline{\mathbf{5}}_1) - 4 \chi(\overline{\mathbf{5}}_{-4}) + 6 \chi(\overline{\mathbf{5}}_6) &\stackrel{!}{=} - \int_{Y_4} G_4 \wedge \omega_{U(1)} \wedge \Theta,
 \end{aligned} \tag{IV.43}$$

with  $\omega_{U(1)}$  given in (IV.15). Explicit computation shows that the match indeed is given for the generic flux  $G_4 = \sum_i u_i G_4^{u_i} + G_4^0(F)$ .

Again, this anomaly cancellation can be seen directly from the matter surfaces. To show it, we calculate the 4-cycle responsible for the anomaly on the left hand side of (IV.43),

$$\begin{aligned} 6 [\overline{10}_2] + [\overline{5}_1] - 4 [\overline{5}_{-4}] + 6 [\overline{5}_6] &= (-5S + 5U) \Theta \\ + [b_2] (2E_1 + 2E_2) + \overline{\mathcal{K}} (-10E_1 - 6E_2 - 2E_3 - 4E_4 + 5\Theta) &+ \Theta (-[b_2] + E_2 - 2E_3 - E_4). \end{aligned} \quad (\text{IV.44})$$

Note that the only term that gives any non-trivial contribution upon integrating with  $G_4$  is  $-5S\Theta$  in the first line, as the remaining terms are of the schematic form  $U \wedge D^{(\mathcal{B})} + E_i \wedge D_a^{(\mathcal{B})} + D_b^{(\mathcal{B})} \wedge D_c^{(\mathcal{B})}$  and thus irrelevant by the transversality conditions. Similarly, the GS-counterterm on the right hand side of (IV.43) comes from integrating a flux over the 4-cycle  $-\omega_{U(1)} \wedge \Theta = -(5S - 5U - 5\overline{\mathcal{K}} - 5[b_2] + 4E_1 + 3E_2 + 2E_3 + E_4) \wedge \Theta$ , where also only the term  $-5S\Theta$  matters, precisely matching the term from the matter surfaces.

Thus, we can again conclude that the  $SU(5)^2 - U(1)$  anomaly is cancelled by the appropriate GS-counterterm, without having to compute any fluxes explicitly.

### 2.2.5 Abelian and gravitational anomalies

Abelian and mixed abelian-gravitational anomalies receive contributions from all matter states. Since we are lacking the homology class of  $\mathbf{1}_5$ 's matter surface, we cannot verify the cancellation explicitly. However, since we have two distinct anomaly matching equations ( $U(1)^3$  and  $U(1)$ -gravitational), we can at least check if they are consistent with the data we acquired.

To this end, we first use the gravitational anomaly matching (IV.3) to write

$$\begin{aligned} \sum_{\mathcal{R}} \dim(\mathcal{R}) q(\mathcal{R}) \chi(\mathcal{R}) &= -6 \int_{Y_4} G_4 \wedge \overline{\mathcal{K}} \wedge \omega \\ \iff 5 \chi(\mathbf{1}_5) &= - \sum_{\mathcal{R} \neq \mathbf{1}_5} \dim(\mathcal{R}) q(\mathcal{R}) \chi(\mathcal{R}) - 6 \int_{Y_4} G_4 \wedge \overline{\mathcal{K}} \wedge \omega. \end{aligned} \quad (\text{IV.45})$$

Assuming that the  $U(1)$ -gravitational anomaly is cancelled by the GS-counterterm, we can use this expression to compute the chiral index  $\chi(\mathbf{1}_5)$  for any given  $G_4$ . For the fluxes basis (IV.26) we obtain:

$$\begin{aligned} \chi(\mathbf{1}_5) &= 50 u_1 \left( 2[b_2] \overline{\mathcal{K}} - 6 \overline{\mathcal{K}}^2 - [b_2] \Theta + 7 \overline{\mathcal{K}} \Theta - 2, \Theta^2 \right) \Theta \\ &+ 10 (u_3 \Theta - F) \left( 2[b_2]^2 - 4[b_2] \overline{\mathcal{K}} - 6 \overline{\mathcal{K}}^2 + 3[b_2] \Theta + 7 \overline{\mathcal{K}} \Theta - 2 \Theta^2 \right) \end{aligned} \quad (\text{IV.46})$$

As a test of consistency, these chiralities should now lead to a matching of the  $U(1)^3$  anomaly,

$$\begin{aligned} \sum_{\mathcal{R}} \dim(\mathcal{R}) q(\mathcal{R})^3 \chi(\mathcal{R}) &= -6 \int_{Y_4} G_4 \wedge \pi_*(\omega \wedge \omega) \wedge \omega \\ &= -6 \int_{Y_4} G_4 \wedge (-50 \overline{\mathcal{K}} - 50 [b_2] + 20 \Theta) \wedge \omega, \end{aligned} \quad (\text{IV.47})$$

which is indeed satisfied with the chiralities (IV.40) for the other representations.

## 2.3 Anomalies in the $SU(5) \times \mathbb{Z}_2$ model

We now turn to a related fibration that realises a discrete abelian  $\mathbb{Z}_2$  symmetry instead of a continuous  $U(1)$ . As explained in section 2.5.4 of chapter II, the two models are related by a conifold transition that physically corresponds to a Higgsing. Here we will briefly summarise the underlying geometric and physical picture along the lines of [64, 65], before discussing how fluxes enter the whole story.

### 2.3.1 A genus-one fibration with gauge group $SU(5) \times \mathbb{Z}_2$

Let us first establish the connection of the  $\mathbb{Z}_2$ -model with the  $U(1)$ -model in the absence of any non-abelian symmetries. In this situation, the hypersurface is the vanishing locus of the polynomial

$$P_{\mathbb{Z}_2} = w^2 + b_0 u^2 w + b_1 u v w + b_2 v^2 w + c_0 u^4 + c_1 u^3 v + c_2 u^2 v^2 + c_3 u v^3 + c_4 v^4, \quad (\text{IV.48})$$

inside a  $\mathbb{P}_{112}$ -fibration over a base  $\mathcal{B}$ . Note that  $\mathbb{P}_{112}$  is a toric space described by polygon 4 in [71], see also figure IV.3. The link between this model and the  $U(1)$ -model (IV.5) is precisely a conifold transition of first blowing down  $s$  and then deforming the resulting singularity by adding the  $c_4$  term. As explained in section 2.5.4 of chapter II, this hypersurface defines genus-one fibration, because it exhibits no globally well-defined sections.

Instead it has a *bi-section*, given by  $U = \{u\}$ . This bi-section marks two points on the hypersurface give by the zero locus of

$$P_{\mathbb{Z}_2}|_{u=0} = w^2 + b_2 v^2 w + c_4 v^4 = \left( w + \frac{b_2 + \sqrt{b_2^2 - 4c_4}}{2} v^2 \right) \left( w + \frac{b_2 - \sqrt{b_2^2 - 4c_4}}{2} v^2 \right). \quad (\text{IV.49})$$

Away from the branching locus  $b_2^2 = 4c_4$  of the square root, each factor marks a point in the fibre, however one cannot holomorphically extend these points over the branching locus. Monodromy effects will interchange both points, such that only the collection of both is a globally well-defined object – the bi-section  $U$ . Note that in the case  $c_4 = 0$ , the two marked points,  $w = 0$  and  $w + b_2 v^2 = 0$  are well-defined globally and generate the rank 1 Mordell–Weil group in the  $U(1)$ -model.<sup>4</sup>

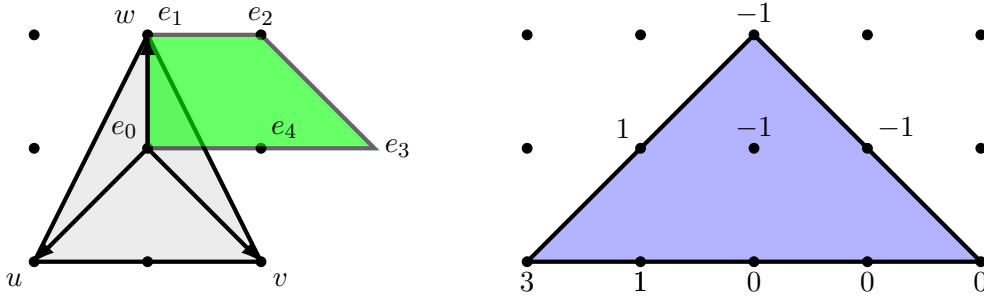


**Figure IV.3:** On the left:  $SU(5)$  top (green) over polygon 4 (grey) from [71] describing the fibre ambient space  $\mathbb{P}_{112}$ . On the right: the dual top with lower bounds on the height of the vertices. This picture is taken from [64].

Analogous to the  $U(1)$ -model, we can construct  $SU(5)$  gauge symmetry via tops. It turns out that there is a top that leads to the same restrictions of the coefficients  $b_i, c_j$  as in the  $U(1)$ -model (except for  $c_4$ , which was absent). This top together with its dual are shown in figure IV.3. This finding is not unexpected, since after all, the physical intuition behind the conifold transition is a Higgsing process by giving the singlet  $\mathbf{1}_{10}$  a vev. While this vev will change the massless spectrum, which we will also discuss in the following, it should not affect the gauge symmetry. In table IV.5 we have collected the fibration data in terms of the divisor classes and associated scaling relations.

<sup>4</sup>Note that after the blow-up by  $s$  in the  $U(1)$ -model, the point with  $w = -b_2 v^2$  is replaced by the intersection of  $s = 0$  with the hypersurface.



	$u$	$v$	$w$	$e_0$	$e_1$	$e_2$	$e_3$	$e_4$
$\bar{\mathcal{K}}$	$\cdot$	1	2	$\cdot$	$\cdot$	$\cdot$	$\cdot$	$\cdot$
$[b_2]$	$\cdot$	-1	-1	$\cdot$	$\cdot$	$\cdot$	$\cdot$	$\cdot$
$\Theta$	$\cdot$	$\cdot$	$\cdot$	1	$\cdot$	$\cdot$	$\cdot$	$\cdot$
$U$	1	1	2	$\cdot$	$\cdot$	$\cdot$	$\cdot$	$\cdot$
$E_1$	$\cdot$	$\cdot$	-1	-1	1	$\cdot$	$\cdot$	$\cdot$
$E_2$	$\cdot$	-1	-2	-1	$\cdot$	1	$\cdot$	$\cdot$
$E_3$	$\cdot$	-2	-2	-1	$\cdot$	$\cdot$	1	$\cdot$
$E_4$	$\cdot$	-1	-1	-1	$\cdot$	$\cdot$	$\cdot$	1

**Table IV.5:** Divisor classes and associated scaling relations for the ambient space  $\mathbb{X}_5$  of the  $\mathbb{Z}_2$ -model.

The hypersurface of the  $SU(5) \times \mathbb{Z}_2$ -model, which we will denote by  $\mathbb{Y}_4$ , is the zero locus of the polynomial

$$P_{\mathbb{Z}_2}^{SU(5)} = e_1 e_2 w^2 + b_{0,2} u^2 w e_0^2 e_1^2 e_2 e_4 + b_1 u v w + b_2 v^2 w e_2 e_3^2 e_4 + c_{0,4} u^4 e_0^4 e_1^3 e_2 e_4^2 + c_{1,2} u^3 v e_0^2 e_1 e_4 + c_{2,1} u^2 v^2 e_0 e_3 e_4 + c_{3,1} u v^3 e_0 e_2 e_3^3 e_4^2 + c_{4,1} v^4 e_0 e_2^2 e_3^5 e_4^3 \quad (\text{IV.50})$$

inside the ambient space  $\mathbb{X}_5$ . As in the  $SU(5) \times U(1)$  model, the fibration is parametrised by the class  $[b_2]$  and the divisor  $\Theta = \sum_{i=0}^4 E_i$  over which the  $SU(5)$  gauge fields live. For  $\mathbb{Y}_4$  to be Calabi–Yau, the coefficients  $b_i$  and  $c_j$  must transform as sections of the bundles displayed in table IV.6. Note that except for  $c_4$ , which is absent in the  $SU(5) \times U(1)$  model, all other classes are the same (cf. table IV.1 and (IV.10)).

$b_{0,2}$	$b_1$	$b_2$	$c_{0,4}$	$c_{1,2}$	$c_{2,1}$	$c_{3,1}$	$c_{4,1}$
$2\bar{\mathcal{K}} - b_2 - 2\Theta$	$\bar{\mathcal{K}}$	$b_2$	$4\bar{\mathcal{K}} - 2b_2 - 4\Theta$	$3\bar{\mathcal{K}} - b_2 - 2\Theta$	$2\bar{\mathcal{K}} - \Theta$	$\bar{\mathcal{K}} + b_2 - \Theta$	$2b_2 - \Theta$

**Table IV.6:** Classes of the coefficients entering (IV.50).

The Stanley–Reisner ideal for our choice of resolution phase is generated by

$$\{v e_0, v e_1, v e_2, w e_0, w e_4, u e_3, e_0 e_3, e_1 e_3, u e_2, e_1 e_4, v w u\}. \quad (\text{IV.51})$$

The linear equivalence ideal, which we require for the flux computations, is given by

$$\begin{aligned} &\langle -[v] + \bar{\mathcal{K}} - [b_2] + U - E_2 - 2e_3 - E_4, \\ &\quad -[w] + 2\bar{\mathcal{K}} - [b_2] + 2U - E_1 - 2E_2 - 2E_3 - E_4, \\ &\quad -E_0 + \Theta - E_1 - E_2 - E_3 - E_4 \rangle. \end{aligned} \quad (\text{IV.52})$$

### $\mathbb{Z}_2$ -generator

The intersection of the ambient divisor  $U = [\{u\}]$  with the hypersurface gives a representative of the homology class of the bisection. From our previous discussion in section 1.1.2 in chapter III, we would like to associate to  $U$  the notion of a KK  $U(1)$  in the 3-dimensional M-theory compactification on  $\mathbb{Y}_4$ . As in the ‘normal’  $U(1)$  case, we would like the non-abelian gauge bosons not to carry any charges under the generator  $\hat{U}$  of this KK  $U(1)$ , i.e.  $\int_{\mathbb{Y}_4} \hat{U} \wedge E_i \wedge D_a^{(\mathcal{B})} \wedge D_b^{(\mathcal{B})} = 0$ . It is here that the shift (III.13) becomes important because the bisection locally intersects both  $E_0$  and  $E_1$  in one point in the fibre. The (up to normalization) unique solution to the constraints (IV.56) is given by

$$\hat{U} = U + \frac{1}{5}(4E_1 + 3E_2 + 2E_3 + E_4). \quad (\text{IV.53})$$

If we fix the (a priori arbitrary) overall normalization to achieve integer intersections with all fibral curves by defining

$$\omega_{\mathbb{Z}_2} = 5 \hat{U}, \quad (\text{IV.54})$$

then the intersection numbers of  $\omega_{\mathbb{Z}_2}$  with the irreducible split fiber components consistently assign  $\mathbb{Z}_2$  charges to the corresponding states modulo 2 in the F-theory limit. Indeed, a  $\mathbb{Z}_2$  subgroup of the KK  $U(1)$ , normalised as in (IV.54), survives in the F-theory limit as an independent discrete gauge group – a full explanation can be found in [64, 65] (see also [54, 63, 66, 67]).<sup>5</sup>

### Matter curves

The discriminant of the singular hypersurface polynomial takes the form

$$\Delta \sim \theta^5 [b_1^4 (b_1^2 c_{0,4} - b_0 b_1 c_{1,2} + c_{1,2}^2) (b_2^2 c_{2,1} - b_1 b_2 c_{3,1} + b_1^4 c_{4,1}) + \mathcal{O}(\theta)], \quad (\text{IV.55})$$

which indicates three matter curves on the  $SU(5)$  divisor  $\Theta$ . Away from  $\Theta$  there is one more matter locus [61], describable as an ideal which defines an irreducible curve on  $\mathcal{B}$  [64]. This complicated codimension-two locus  $C$  over which the fibre splits into two curves hosts singlet states that carry  $\mathbb{Z}_2$  charge. These states originate from the  $\mathbf{1}_5$  states in the  $SU(5) \times U(1)$  model, which in that case were also localised over a non-complete intersection curve  $C_2$ . Consistently, the  $\mathbb{Z}_2$  charges of these singlets are  $1 \equiv 5 \pmod{2}$ , as has been elaborated in [64]. The matter spectrum and the associated  $\mathbb{Z}_2$  charges are summarized in table IV.7.

locus in base	irrep $SU(5)$	$\mathbb{Z}_2$ charge
$\theta \cap b_1$	$\mathbf{10}, \overline{\mathbf{10}}$	[0]
$\theta \cap \{b_1^2 c_{0,4} - b_0 b_1 c_{1,2} + c_{1,2}^2\}$	$\mathbf{5}^A, \overline{\mathbf{5}}^A$	[1]
$\theta \cap \{b_2^2 c_{2,1} - b_1 b_2 c_{3,1} + b_1^4 c_{4,1}\}$	$\mathbf{5}^B, \overline{\mathbf{5}}^B$	[0]
$C$	$\mathbf{1}$	[1]

**Table IV.7:** Matter spectrum in the  $SU(5) \times \mathbb{Z}_2$  model.

The charges of the  $SU(5)$  matter can be computed analogously to the  $U(1)$ -model by studying the fibre enhancement over the matter loci and compute the intersection numbers of the localised fibral curves with the  $\mathbb{Z}_2$ -generator (IV.54). The crucial difference to the  $U(1)$ -charges is that only the intersection numbers modulo 2 will give consistent charges for a full representation  $\mathcal{R}$ . The intersection structure of the matter curves along the  $SU(5)$  divisor  $\Theta$  is shown in figure IV.4. The indicated Yukawa couplings are all consistent with the  $\mathbb{Z}_2$  charges.

### 2.3.2 Vertical fluxes in the $SU(5) \times \mathbb{Z}_2$ model

Recall our proposal for the transversality condition defining  $G_4$ -fluxes in a genus-one fibration, applied to our particular model: The  $\mathbb{Z}_2$ -generator (IV.53) satisfies the orthogonality condition

$$\int_{X_4} E_i \wedge \hat{U} \wedge D_a^{(\mathcal{B})} \wedge D_b^{(\mathcal{B})} = 0 \quad \forall D_a^{(\mathcal{B})}, D_b^{(\mathcal{B})}. \quad (\text{IV.56})$$

Thus  $\hat{U}$  defines the appropriate KK  $U(1)$  for the reduction of the 4-dimensional F-theory vacuum to three dimensions which does not mix with the Cartan generators  $E_i$ . The transversality

<sup>5</sup>Apart from an extra shift in terms of base divisors this agrees with the  $\mathbb{Z}_2$  generator as presented in [54, 64, 66]). This shift does not change the notion of fibral curves and is therefore not of importance for us.

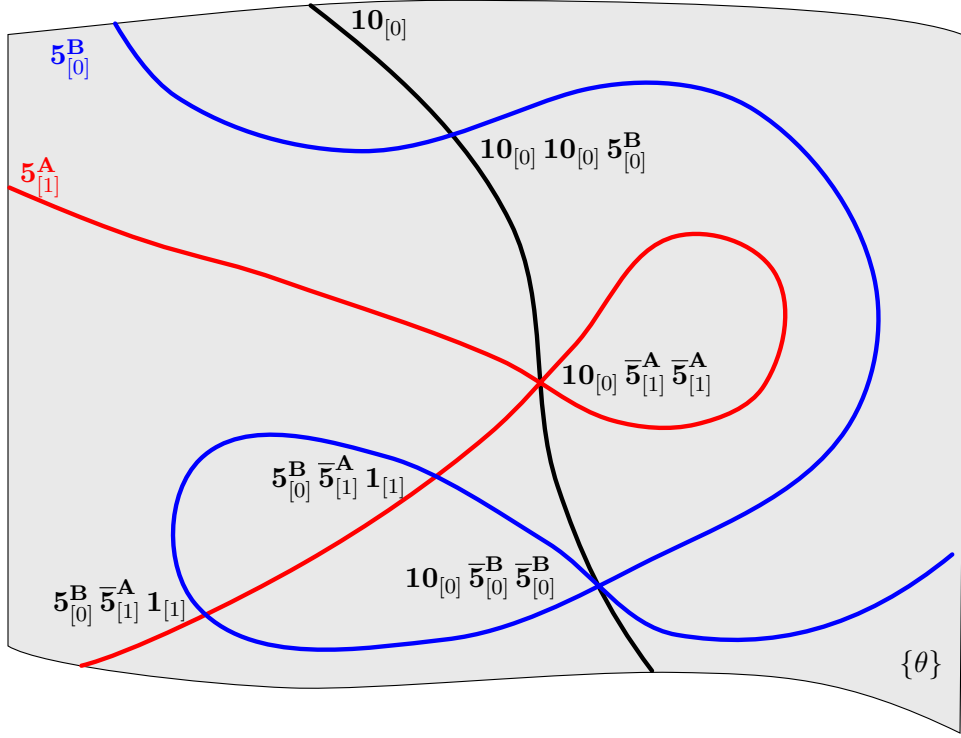


**Figure IV.4:** The matter curves on the  $SU(5)$  divisor  $\{\theta\}$  and the Yukawa couplings involving the  $SU(5)$  charged matter in codimension three. The singlet curve has been omitted, only its intersection points with  $\{\theta\}$  are displayed as the Yukawa points  $5_{[0]}^B 5_{[1]}^A 1_{[1]}$ .

conditions on the fluxes are then

$$\int_{\mathbb{Y}_4} G_4 \wedge \hat{U} \wedge D_a^{(\mathcal{B})} \stackrel{!}{=} 0, \quad (\text{IV.57})$$

$$\int_{\mathbb{Y}_4} G_4 \wedge D_a^{(\mathcal{B})} \wedge D_b^{(\mathcal{B})} \stackrel{!}{=} 0. \quad (\text{IV.58})$$

If the gauge fluxes are not to break any of the non-abelian gauge symmetries, we demand in addition

$$\int_{\mathbb{Y}_4} G_4 \wedge E_i \wedge D_a^{(\mathcal{B})} \stackrel{!}{=} 0. \quad (\text{IV.59})$$

Note in particular that for fluxes satisfying this latter constraint for all  $E_i$ , the transversality condition (IV.57) reduces to the same constraint with  $\hat{U}$  replaced by  $U$ . This simplifies the calculations, but obscures the fact that  $\hat{U}$  is the divisor class identified with the Kaluza-Klein  $U(1)$ .

The scheme to compute all vertical fluxes proceeds analogously as in the  $U(1)$ -model, presented in section 2.2.2. We first implement the cohomology ring of the ambient space as a quotient polynomial ring and compute a basis for  $H_{\text{vert}}^{(2,2)}(\mathbb{Y}_4)$ . In fact, because the geometry of the ambient spaces of the  $U(1)$ - and the  $\mathbb{Z}_2$ -model are so similar, the basis  $(2,2)$ -forms are nearly identical (cf. (IV.22):

$$\{t_i\} = \left\{ D_a^{(\mathcal{B})} D_b^{(\mathcal{B})}, \quad (U, E_1, E_2, E_3, E_4) D_c^{(\mathcal{B})}, \quad E_3 E_4, \quad E_1 E_2 \right\}, \quad (\text{IV.60})$$

with  $D_{a,b,c}^{(\mathcal{B})} \in \{\bar{\mathcal{K}}, [b_2], \Theta, D\}$ , where  $D$  again collectively denotes all other independent vertical divisor classes of the base. With this basis, we can again systematically solve for the transversality

conditions, this time of the form

$$\int_{\mathbb{Y}_4} G_4 \wedge U \wedge D_a^{(\mathcal{B})} = \int_{\mathbb{Y}_4} G_4 \wedge D_a^{(\mathcal{B})} \wedge D_b^{(\mathcal{B})} = \int_{\mathbb{Y}_4} G_4 \wedge E_i \wedge D_a^{(\mathcal{B})} = 0. \quad (\text{IV.61})$$

Going through the algebra, we find two independent fluxes satisfying the modified transversality conditions:

$$\begin{aligned} G_4 &= z_1 G_4^{z_1} + z_2 G_4^{z_2} = \\ & z_1 \left[ 5 (E_1 E_2 + 2 E_3 E_4) + [b_2] (-E_1 - 7 E_2 - 8 E_3 + E_4) + \Theta^2 + 8 [b_2] \Theta \right. \\ & \quad \left. + \bar{\mathcal{K}} (E_1 + 12 E_2 + 8 E_3 - 6 E_4 - 8 \Theta) + \frac{1}{2} \Theta (-4 E_1 - 3 E_2 - 2 E_3 + 19 E_4 - 15 U) \right] \\ & + z_2 \left[ 5 (E_1 E_2 + E_3 E_4) - 5 [b_2] (E_2 + E_3) + \bar{\mathcal{K}} (-2 E_1 + 6 E_2 + 4 E_3 - 3 E_4 - 4 \Theta) \right. \\ & \quad \left. + 5 \Theta ([b_2] + E_4 - U) \right]. \end{aligned} \quad (\text{IV.62})$$

Note that despite the factor  $1/2$  in  $G_4^{z_1}$ , the normalisations for  $G_4^{z_1}$  and  $G_4^{z_2}$  are chosen such that they give manifestly integer chiralities when integrated over matter surfaces (cf. section 2.3.4).

### 2.3.3 An example of horizontal flux

Unlike vertical fluxes, we have no systematic method of determining all horizontal fluxes. Only few explicit examples have been constructed in the literature. In the following we will present one such flux, following [64]. The flux is associated with a special algebraic 4-cycle which appears on the sublocus in complex structure moduli space where  $c_4 = \rho \tau$  factorises. This is modeled after a similar construction in the context of a Tate model [84]. In the presence of an  $SU(5)$  singularity the same type of fluxes exists, *mutatis mutandis*, on the sublocus in moduli space where  $c_{4,1} = \rho \tau$ . In this case the two algebraic 4-cycles described as the complete intersections

$$\sigma_0 = \langle u, w, \rho \rangle, \quad (\text{IV.63})$$

$$\sigma_1 = \langle u, w e_1 + b_2 v^2 e_3^2 e_4, \rho \rangle \quad (\text{IV.64})$$

in the ambient space  $\mathbb{X}_5$  of  $\mathbb{Y}_4$  automatically lie on  $\mathbb{Y}_4$ . Note that the two 4-cycles each define one of the two intersection points of the bisection  $U$  with the fibre, fibred over the divisor  $P = [\{\rho\}] \subset \mathcal{B}$  in the base. This can be easily seen by performing a similar factorisation as in (IV.49) for the  $SU(5)$ -enhanced hypersurface (IV.50) at  $u = 0$  and realising that for a factorised  $c_{4,1} = \rho \tau$ , the locus  $\rho = 0$  implies  $c_{4,1} = 0$ . Over this locus (if present), the two marked points  $w = 0$  and  $w e_1 + b_2 v^2 e_3^2 e_4 = 0$  are not affected by any monodromy actions, and hence the ideals (IV.63) are well-defined.

The dual cohomology classes  $[\sigma_0]$  and  $[\sigma_1]$  clearly are vertical classes in the ambient space, e.g.  $[\sigma_0] = U[w]P$ . We can check that they are indeed not vertical on the hypersurface, because we cannot find a factorisation of the form  $[\sigma_0] = [\mathbb{Y}_4] \cdot (\sum_{i,j} D_i D_j) \in H_{\text{vert}}^{(3,3)}(\mathbb{X}_5)$ . Still, we can compute intersection numbers with other vertical 4-cycles  $D_1 \wedge D_2$  of the hypersurface by

$$\int_{\sigma_i} D_1 \wedge D_2 = \int_{\mathbb{X}_5} [\sigma_i] \wedge D_1 \wedge D_2, \quad (\text{IV.65})$$

because wedging with  $[\sigma_i]$  guarantees that the intersection lies on the hypersurface.

Being algebraic 4-cycles on  $\mathbb{Y}_4$ , the classes  $[\sigma_i]$  are candidates for fluxes. However, they violate the transversality conditions (IV.61):

$$\begin{aligned} \int_{\mathbb{X}_5} [\sigma_0] \wedge D_a^{(\mathcal{B})} \wedge D_b^{(\mathcal{B})} &= \int_{\mathcal{B}} P \wedge D_a^{(\mathcal{B})} \wedge D_b^{(\mathcal{B})}, \\ \int_{\mathbb{X}_5} [\sigma_0] \wedge U \wedge D^{(\mathcal{B})} &= \int_{\mathcal{B}} P \wedge D^{(\mathcal{B})} \wedge ([b_2] - \bar{\mathcal{K}}) \\ \int_{\mathbb{X}_5} [\sigma_0] \wedge E_i \wedge D^{(\mathcal{B})} &= (1, 0, 0, 0)_i \int_{\mathcal{B}} P \wedge D^{(\mathcal{B})} \wedge \Theta \end{aligned} \quad (\text{IV.66})$$

To obtain a well-defined flux we add an ansatz of correction terms  $[\mathbb{Y}_4] \cdot (\sum a_i D_i P)$  where  $D_i$  runs over a basis of divisors and require that they cancel the right hand side of (IV.66). Solving for the coefficients  $a_i$  yields the flux solutions

$$\begin{aligned} G_4^h(P, \sigma_0) &= 5[\sigma_0] + \frac{1}{2}(-5U + (4E_1 + 3E_2 + 2E_3 + E_4) - 2\Theta) P [\mathbb{Y}_4], \\ G_4^h(P, \sigma_1) &= 5[\sigma_1] - \frac{1}{2}(5U + (4E_1 + 3E_2 + 2E_3 + E_4) - 2\Theta) P [\mathbb{Y}_4], \end{aligned} \quad (\text{IV.67})$$

where, for now, the overall normalization is chosen to give manifestly integral chiral indices as will be discussed later. Both flux solutions are not independent, so that we can stick to, say,  $G_4^h(P, \sigma_0) \equiv G_4^h(P)$  for definiteness. Combined with the vertical fluxes (IV.62), we have the following four parameter flux solution,

$$G_4 = a G_4^h(P) + z_1 G_4^{z_1} + z_2 G_4^{z_2}. \quad (\text{IV.68})$$

Note that away from the complex structure moduli, where the 4-cycles  $\sigma_{0,1}$  are algebraic, the horizontal fluxes are no longer describable by (IV.67). However, all quantities computed with that description in the following sections (in particular chiral indices and D3-tadpole) are of topological nature and hence are independent of the complex structure.

### 2.3.4 Matter surfaces

In the following we will collect the data about the matter surfaces of the spectrum in the  $\mathbb{Z}_2$  model, cf. table IV.7. Since the methods of primary decomposition and finding suitable complete intersections are analogous to the situation in the  $U(1)$ -model, we will keep the computational details to a minimum.

#### The $\overline{10}$ surface

A representative of the matter surface  $[\mathcal{C}_{\overline{10}}]$  is given by the complete intersection  $\langle e_0, e_2, b_1 \rangle$  in the ambient space. By employing the SR-ideal we find that restricting the hypersurface to  $\langle e_0, e_2 \rangle$  implies  $b_1 = 0$ , and hence we have  $[\mathcal{C}_{\overline{10}}] = E_0 E_2 [\mathbb{Y}_4]$ .

As in the  $U(1)$  case, we can compare the matter surfaces to the fluxes (IV.62) as algebraic 4-cycles. This amounts in adding correction terms to the matter surface such that the result is a  $(2, 2)$ -form satisfying the transversality conditions. For the surface of  $\overline{10}$ , we find

$$\begin{aligned} G_4(\overline{10}) &= E_0 E_2 - \frac{1}{5} \bar{\mathcal{K}} \Theta - \frac{1}{5} (-2, 1, -1, -3)_i E_i \bar{\mathcal{K}} \\ &= -E_1 E_2 - E_3 + [b_2] (E_2 + E_3) E_4 + \frac{1}{5} \bar{\mathcal{K}} (2E_1 - 6E_2 - 4E_3 + 3E_4) \\ &\quad + \frac{4}{5} \bar{\mathcal{K}} \Theta + \Theta (U - [b_2] - E_4) \end{aligned} \quad (\text{IV.69})$$

where we have rewritten the first line in the chosen vertical basis (IV.60). Up to a factor of  $-5$  the flux agrees exactly with the flux solution with coefficient  $z_2$  in (IV.62).

### The $\bar{\mathfrak{5}}^A$ surface

The matter surface of  $\bar{\mathfrak{5}}^A$  is a non-complete intersection given by the ideal

$$\begin{aligned} \mathcal{C}_{\bar{\mathfrak{5}}^A} = \langle & e_3, \quad b_1^2 c_{0,4} - b_{0,2} b_1 c_{1,2} + c_{1,2}^2, e_0^2 e_1 e_4 u^2 c_{1,2} + w b_1, \\ & e_0^2 e_1 e_4 u^2 b_1 c_{0,4} + w b_{0,2} b_1 - w c_{1,2}, \quad e_0^4 e_1^2 e_4^2 u^4 c_{0,4} + e_0^2 e_1 e_4 u^2 w b_{0,2} + w^2 \rangle. \end{aligned} \quad (\text{IV.70})$$

Applying the same trick as in the  $U(1)$ -model of finding a suitable complete intersection containing this surface, we are able to deduce the following homology class:

$$\begin{aligned} [\bar{\mathfrak{5}}^A] &= 2 E_3 [c_{1,2}] (w + [b_1]) - 2 E_3 [b_1] [c_{1,2}] \\ &= (2 E_3 E_4 - 2 [b_2] E_3 + \bar{\mathcal{K}} (4 E_3 - \Theta) + \Theta ([b_2] + E_2 - 2 E_3 + E_4 - U)) [\mathbb{Y}_4] \end{aligned} \quad (\text{IV.71})$$

From this class we can construct the following vertical flux:

$$\begin{aligned} G_4(\bar{\mathfrak{5}}^A) &= [\bar{\mathfrak{5}}^A] + \{\text{correction terms}\} \\ &= 2 E_3 E_4 - \frac{2}{5} [b_2] (E_1 + 2 E_2 + 3 E_3 - E_4) + \frac{2}{5} \bar{\mathcal{K}} (3 E_1 + 6 E_2 + 4 E_3 - 3 E_4) \\ &\quad + \frac{1}{5} \Theta (-8 \bar{\mathcal{K}} + 2 \Theta + 6 [b_2] - 4 E_1 - 3 E_2 - 2 E_3 + 9 E_4 - 5 U) \\ &= \frac{2}{5} (G_4^{z_1} - G_4^{z_2}). \end{aligned} \quad (\text{IV.72})$$

### The $\bar{\mathfrak{5}}^B$ surface

By the same techniques, we compute the  $\bar{\mathfrak{5}}^B$  surface and its homology class. We find

$$\begin{aligned} [\bar{\mathfrak{5}}^B] &= E_1 (2 [b_2] + [c_{2,1}]) (\bar{\mathcal{K}} + U) - 2 E_1 \bar{\mathcal{K}} [b_2] \\ &= (E_1 E_2 - E_3 E_4 + [b_2] (2 E_1 + E_2 + E_3) + E_4 \bar{\mathcal{K}} - ([b_2] + E_4) \Theta) [\mathbb{Y}_4]. \end{aligned} \quad (\text{IV.73})$$

The associated flux is then

$$\begin{aligned} G_4(\bar{\mathfrak{5}}^B) &= [\bar{\mathfrak{5}}^B] + \{\text{correction terms}\} \\ &= E_1 E_2 - E_3 E_4 + \frac{1}{5} [b_2] (2 E_1 - E_2 + E_3 - 2 E_4) + \frac{1}{5} \bar{\mathcal{K}} (-8 E_1 - 6 E_2 - 4 E_3 + 3 E_4) \\ &\quad + \frac{1}{5} \Theta (4 E_1 + 3 E_2 + 2 E_3 - 4 E_4 - [b_2] + 4 \bar{\mathcal{K}} - 2 \Theta) \\ &= \frac{1}{5} (-2 G_4^{z_1} + 3 G_4^{z_2}). \end{aligned} \quad (\text{IV.74})$$

### The singlet surfaces

Again, we are unable to compute the prime ideal describing the matter surface  $\mathbf{1}$  due to the complexity of the curve  $C$  over which the singlet states are fibred. However, the  $I_2$ -fiber over  $C$  splits into two rational curves  $A$  and  $B$  with  $[A] = [B]$  in homology. Indeed, both curves are exchanged by a global monodromy over  $C$  provided the intersection of the monodromy locus of the bisection with  $C$  is non-empty, as is generically the case [64] (see [52, 113] for a discussion of the implications of the absence of this monodromy point on  $C_2$  in non-generic models). The states associated with an M2-brane wrapping  $A$  and  $B$  have the same quantum numbers. In order to count the number of  $\mathcal{N} = 1$  chiral multiplets of the 4-dimensional F-theory vacuum with  $\mathbb{Z}_2$  charge 1, we must therefore add the zero modes from M2-branes wrapping both fibral curves [65]. One can separately compute the overlap of  $G_4$  with the 4-cycle  $\mathcal{C}_A$  or  $\mathcal{C}_B$  given by fibering  $A$  or  $B$

$\mathcal{R}$	$[\mathcal{R}]$
$\overline{\mathbf{10}}$	$E_0 E_2 [\mathbb{Y}_4]$
$\overline{\mathbf{5}}^{\mathbf{A}}$	$(2 E_3 E_4 - 2 [b_2] E_3 + \overline{\mathcal{K}} (4 E_3 - \Theta) + \Theta ([b_2] + E_2 - 2 E_3 + E_4 - U)) [\mathbb{Y}_4]$
$\overline{\mathbf{5}}^{\mathbf{B}}$	$(E_1 E_2 - E_3 E_4 + [b_2] (2 E_1 + E_2 + E_3) + E_4 \overline{\mathcal{K}} - ([b_2] + E_4) \Theta) [\mathbb{Y}_4]$

**Table IV.8:** Known homology classes of matter surfaces in the  $SU(5) \times \mathbb{Z}_2$  model. While we cannot determine the class  $[\mathbf{1}]$  of the singlet, we can argue on general ground that it must have zero chirality.

over  $C_2$ , and e.g. the flux  $G_4(P, \sigma_0)$  indeed gives a non-zero result for both individual surfaces [65]. However, in total

$$\chi(\mathbf{1}) = \int_{C_A} G_4 + \int_{C_B} G_4 = 0 \quad (\text{IV.75})$$

by the transversality condition (IV.58) because  $A$  and  $B$  sum up to the total fiber class. This is the geometric manifestation of the statement that an  $SU(5)$  singlet carrying only  $\mathbb{Z}_2$  charge does not admit a notion of chirality, of course.

### 2.3.5 Chiralities and the $SU(5)^3$ anomaly

With the the homology classes of the matter surfaces (cf table IV.8) at hand, it is straightforward to compute the induced chiralities for all  $SU(5)$  representations. Using the explicit flux solution (IV.68), we find the following chiralities:

$$\begin{aligned} \chi(\overline{\mathbf{10}}) &= [a P + z_1 (2 [b_2] - 12 \overline{\mathcal{K}} + 9 \Theta) + z_2 (5 \Theta - 6 \overline{\mathcal{K}})] \overline{\mathcal{K}} \Theta, \\ \chi(\overline{\mathbf{5}}^{\mathbf{A}}) &= [-a P + z_1 (-2 [b_2] - 8 \overline{\mathcal{K}} + \Theta) - 4 z_2 \overline{\mathcal{K}}] ([b_2] - 3 \overline{\mathcal{K}} + 2 \Theta) \Theta, \\ \chi(\overline{\mathbf{5}}^{\mathbf{B}}) &= [a P ([b_2] - 4 \overline{\mathcal{K}} + 2 \Theta) + z_1 (2 [b_2]^2 + 3 [b_2] \Theta - 2 (6 \overline{\mathcal{K}}^2 - 5 \overline{\mathcal{K}} \Theta + \Theta^2)) \\ &\quad + z_2 (4 [b_2] - 6 \overline{\mathcal{K}} + 3 \Theta) \overline{\mathcal{K}}] \Theta, \\ \chi(\mathbf{1}) &= 0, \end{aligned} \quad (\text{IV.76})$$

where again the right hand sides are understood as intersection numbers on the base. It is easily checked that the  $SU(5)^3$  anomaly condition

$$\chi(\overline{\mathbf{10}}) + \chi(\overline{\mathbf{5}}^{\mathbf{A}}) + \chi(\overline{\mathbf{5}}^{\mathbf{B}}) = 0 \quad (\text{IV.77})$$

is satisfied without further restrictions on  $a, P, z_1$  and  $z_2$ . In fact, this can be again argued solely based on the geometry of the 4-cycle class  $[\overline{\mathbf{10}}] + [\overline{\mathbf{5}}^{\mathbf{A}}] + [\overline{\mathbf{5}}^{\mathbf{B}}]$ :

$$\begin{aligned} [\overline{\mathbf{10}}] + [\overline{\mathbf{5}}^{\mathbf{A}}] + [\overline{\mathbf{5}}^{\mathbf{B}}] &= \\ [\mathbb{Y}_4] \cdot (2 [b_2] (E_1 + E_2) + \overline{\mathcal{K}} (-E_2 + 3 E_3 + E_4) + \Theta (E_2 - 2 E_3 - E_4) - \Theta [b_2]) . \end{aligned} \quad (\text{IV.78})$$

In this form, it is obvious that *any* valid  $G_4$  yields zero upon integration over this cycle, by virtue of the transversality conditions. Note that the modified condition (IV.57) involving the bi-section does not enter this anomaly cancellation, which only requires the flux not breaking the gauge symmetry and not having two legs along the fibre. The missing condition (IV.57) will become relevant in the context of the discrete  $\mathbb{Z}_2$  anomaly to be discussed momentarily.

### 2.3.6 Flux quantisation and $\mathbb{Z}_2$ anomalies

All results so far have been independent of the overall normalisation of the constructed fluxes and tested only the transversality conditions as such. The proper normalisation becomes crucial for instance when it comes to detecting discrete anomalies such as the ones scrutinised in [74, 114]. In particular, the total number of D3-branes as determined by the tadpole equation (IV.97) must be integer, and this is guaranteed [74] for a flux satisfying the quantisation condition (III.2). Furthermore the chiral indices must be integer in a consistent theory and this should follow from the quantisation condition as well. Indeed, as exemplified in previous sections, we can write the homology classes of all matter surfaces  $\mathcal{C}_{\mathcal{R}}$  in terms of complete intersections on the hypersurface and so the  $[\mathcal{C}_{\mathcal{R}}]$  are integer classes themselves. Hence

$$\int_{\mathcal{C}_{\mathcal{R}}} \left( G_4 + \frac{1}{2} c_2(M_4) \right) = \chi(\mathcal{R}) + \frac{1}{2} \int_{\mathcal{C}_{\mathcal{R}}} c_2(M_4) \in \mathbb{Z} \quad (\text{IV.79})$$

if the flux is appropriately quantised. Thus, as stressed in [96, 115], if  $\frac{1}{2} \int_{\mathcal{C}_{\mathcal{R}}} c_2(M_4)$  is integer by itself for every matter surface, then the quantisation condition ensures integrality of the chiral indices. To the best of our knowledge, it has not been proven from first principles in the literature that  $c_2(M_4)$  automatically satisfies these constraints in any smooth Calabi-Yau elliptic or genus-one fibration  $M_4$ . In the sequel will analyse this constraint for the two fibrations  $M_4 \in \{Y_4, \mathbb{Y}_4\}$ , and relate it to the cancellation of  $\mathbb{Z}_2$  anomalies. Remarkably, this cancellation not only requires the condition (IV.79) in the  $\mathbb{Z}_2$  model, but also in the associated  $U(1)$ -model to which the  $\mathbb{Z}_2$ -model is related by the conifold transition.

#### Arithmetic constraints from the second Chern class

To compute  $c_2(M_4)$  for  $M_4$  either the genus-one fibration  $\mathbb{Y}_4 \subset \mathbb{X}_5$  or the elliptic fibration  $Y_4 \subset X_5$  we use the standard adjunction formula

$$c(M_4) = \frac{c(M_5)}{1 + [P]} = \frac{1 + c_1(M_5) + c_2(M_5) + \dots}{1 + [P]} \quad (\text{IV.80})$$

with  $P$  the respective hypersurface polynomial inside the ambient space  $M_5$ . Because the hypersurface is Calabi-Yau, i.e.  $c_1(M_4) = 0$ , we must have  $[P] = c_1(M_5)$ , and therefore

$$c_2(M_4) = c_2(M_5) - c_1(M_5) [P] + [P]^2 = c_2(M_5). \quad (\text{IV.81})$$

Since our ambient spaces  $M_5$  are fibrations of a toric fibre ambient space over a base  $\mathcal{B}$ , their total Chern-class can be calculated as

$$c(M_5) = c(\mathcal{B}) \frac{\prod_i (1 + D_i^{(T)})}{1 + \Theta}, \quad (\text{IV.82})$$

with  $c(\mathcal{B}) = c_1(\mathcal{B}) + c_2(\mathcal{B}) + \dots = \bar{\mathcal{K}} + c_2(\mathcal{B}) + \dots$ . The  $D_i^{(T)}$  are the toric divisors of the top defining the fibre ambient space. Because these include the exceptional divisors which sum up to  $\Theta$  that is already accounted for in  $c(\mathcal{B})$ , one has to divide out by the denominator.

The result of this analysis for both fibrations is

$$\begin{aligned} c_2(\mathbb{Y}_4) &= 5U^2 - E_1 E_2 + \frac{7}{2} E_2^2 - 6 E_3 E_4 + \frac{1}{2} (-4, 9, 20, 4)_i E_i [b_2] + \frac{1}{2} (0, -19, -34, -3)_i E_i \bar{\mathcal{K}} \\ &\quad + (0, -6, 4, -5)_i E_i \Theta - 5U [b_2] + 11U \bar{\mathcal{K}} + 7U \Theta \\ &\quad - 6 [b_2] \Theta - 5 [b_2] \bar{\mathcal{K}} + 7 \bar{\mathcal{K}} \Theta + [b_2]^2 + 5 \bar{\mathcal{K}}^2 + c_2(\mathcal{B}), \end{aligned} \quad (\text{IV.83})$$

$$\begin{aligned} c_2(Y_4) &= -7U^2 + E_2^2 - E_3 E_4 + (-1, 2, 5, 2)_i E_i [b_2] + (-1, -7, -12, -4)_i E_i \bar{\mathcal{K}} \\ &\quad + (0, -1, 4, 0)_i E_i \Theta + U [b_2] - U \bar{\mathcal{K}} + 2U \Theta - S [b_2] + 6S \bar{\mathcal{K}} + S \Theta \\ &\quad - [b_2] \Theta - 5 [b_2] \bar{\mathcal{K}} + 2 \bar{\mathcal{K}} \Theta + [b_2]^2 + 5 \bar{\mathcal{K}}^2 + c_2(\mathcal{B}). \end{aligned} \quad (\text{IV.84})$$



In principle the quantization condition can now be checked by demanding that the integral of  $G_4 + \frac{1}{2}c_2(M_4)$  over every integer 4-cycle be integer. This requires finding an integral basis of  $H^4(M_4)$ , which we do not attempt here.

However, we make a curious observation: For the elliptic fibration  $Y_4$ , the integral of  $c_2(Y_4)$  over the matter surfaces (cf table IV.4) can be evaluated as

$$\frac{1}{2} \int_{\mathcal{C}_{\overline{10}_2}} c_2(Y_4) = \frac{1}{2} \int_{\mathcal{B}} \Theta^2 \overline{\mathcal{K}}, \quad (\text{IV.85})$$

$$\frac{1}{2} \int_{\mathcal{C}_{\overline{5}_6}} c_2(Y_4) = \frac{1}{2} \int_{\mathcal{B}} (-\overline{\mathcal{K}} [b_2] \Theta + [b_2]^2 \Theta + [b_2] \Theta^2), \quad (\text{IV.86})$$

$$\frac{1}{2} \int_{\mathcal{C}_{\overline{5}_4}} c_2(Y_4) = \frac{1}{2} \int_{\mathcal{B}} (2\overline{\mathcal{K}}^2 \Theta - \Theta^2 \overline{\mathcal{K}} + 3\overline{\mathcal{K}} [b_2] \Theta + [b_2]^2 \Theta - [b_2] \Theta^2), \quad (\text{IV.87})$$

$$\frac{1}{2} \int_{\mathcal{C}_{\overline{1}_{10}}} c_2(Y_4) = \frac{1}{2} \int_{\mathcal{B}} (2\overline{\mathcal{K}} [b_2]^2 + 2[b_2]^3 + \overline{\mathcal{K}} [b_2] \Theta - [b_2]^2 \Theta - [b_2] \Theta^2), \quad (\text{IV.88})$$

$$\frac{1}{2} \int_{\mathcal{C}_{\overline{5}_1}} c_2(Y_4) = \int_{\mathcal{B}} (12\overline{\mathcal{K}}^2 \Theta - 10\overline{\mathcal{K}} [b_2] \Theta + 2[b_2]^2 \Theta - 12\overline{\mathcal{K}} \Theta^2 + 5[b_2] \Theta^2 + 3\Theta^3). \quad (\text{IV.89})$$

Note that the first four expressions are *not* automatically integer. However, in this case also the chiral indices would be non-integer as a result of (IV.79).<sup>6</sup> Physical consistency of the spectrum in the  $U(1)$  model therefore requires the expressions (IV.85) – (IV.88) to be integer, which is equivalent to the following intersection numbers being even:

$$\int_{\mathcal{B}} \Theta^2 \overline{\mathcal{K}} \in 2\mathbb{Z} \quad \text{and} \quad \int_{\mathcal{B}} (\overline{\mathcal{K}} [b_2] \Theta + [b_2]^2 \Theta + [b_2] \Theta^2) \in 2\mathbb{Z}. \quad (\text{IV.90})$$

A similar problem arises in the bisection model  $\mathbb{Y}_4$ , where the potentially non-integer pairings are

$$\begin{aligned} \frac{1}{2} \int_{\mathcal{C}_{\overline{10}}} c_2(\mathbb{Y}_4) &= \frac{1}{2} \int_{\mathcal{B}} \Theta^2 \overline{\mathcal{K}}, \\ \frac{1}{2} \int_{\mathcal{C}_{\overline{5}_A}} c_2(\mathbb{Y}_4) &= \int_{\mathcal{B}} 2[b_2]^2 \Theta + 2\overline{\mathcal{K}} [b_2] \Theta - [b_2] \Theta^2 + \overline{\mathcal{K}}^2 \Theta - \frac{1}{2} \Theta^2 \overline{\mathcal{K}}, \end{aligned} \quad (\text{IV.91})$$

and which would require the intersection number  $\int_{\mathcal{B}} \Theta^2 \overline{\mathcal{K}}$  being even to satisfy (IV.79).

If we assume that the  $SU(5) \times U(1)$  and the  $SU(5) \times \mathbb{Z}_2$  theories are connected by the Higg mechanism corresponding to the conifold transition explained before, then both  $Y_4$  and  $\mathbb{Y}_4$  share the same fibration data  $\mathcal{B}$ ,  $[b_2]$  and  $\Theta$ . In particular it makes sense to compare the intersection numbers in both models. By doing so, we notice that integrality of (IV.85) – (IV.88) of the  $U(1)$ -model implies integrality of the other expressions including (IV.91) on the  $\mathbb{Z}_2$  side, but integrality of (IV.91) alone is not enough to guarantee integrality on the  $U(1)$  side. We will resolve this puzzle momentarily.

In principle, the above observation could hint at an additional physical constraint such as a previously unnoticed anomaly which could require this. A more likely option is that these constraints are automatically satisfied for every smooth Calabi–Yau space  $Y_4$  or  $\mathbb{Y}_4$  described as the respective toric tops. In other words, integrality of the above expressions is most likely a necessary condition for a specific base  $\mathcal{B}$ , together with a consistent choice of  $\Theta$  and  $[b_2]$ , to give rise to a well-defined Calabi–Yau fibration  $Y_4$  or  $\mathbb{Y}_4$ . It would be interesting, but certainly challenging to prove in full generality that in every geometrically consistent fibration  $c_2(M_4)$  automatically satisfies these arithmetic properties.

<sup>6</sup>A related puzzle was also observed in [96] for the integral of  $\frac{1}{2}c_2$  over the  $\mathbf{10}_1$ -matter surface in the vanilla  $SU(5) \times U(1)$  restricted Tate model. Interestingly, existence of a smooth type IIB limit of the latter model implies that this equation is integer, reproducing the known result that the Freed-Witten anomaly cancellation in Type IIB guarantees integer chiralities [115, 116].

### Cancellation of $\mathbb{Z}_2$ anomalies

We finally turn towards the  $\mathbb{Z}_2$  anomalies. Due to the charge assignments and the zero chirality of the singlet, the possible  $\mathbb{Z}_2$  anomalies [117] are solely given by the chiral index of the  $\bar{\mathbf{5}}^{\mathbf{A}}$  states modulo 2,

$$\begin{aligned} \mathcal{A}_{\mathbb{Z}_2^3} &= \sum_{\mathcal{R}} \left( q_{\mathcal{R}}^{\mathbb{Z}_2} \right)^3 \dim(\mathcal{R}) \chi(\mathcal{R}) = \chi(\bar{\mathbf{5}}^{\mathbf{A}}) \pmod{2}, \\ \mathcal{A}_{\mathbb{Z}_2-SU(5)^2} &= \sum_{\mathcal{R}} q_{\mathcal{R}}^{\mathbb{Z}_2} c(\mathcal{R}) \chi(\mathcal{R}) = \chi(\bar{\mathbf{5}}^{\mathbf{A}}) \pmod{2}, \\ \mathcal{A}_{\mathbb{Z}_2\text{-grav.}} &= \sum_{\mathcal{R}} q_{\mathcal{R}}^{\mathbb{Z}_2} \dim(\mathcal{R}) \chi(\mathcal{R}) = \chi(\bar{\mathbf{5}}^{\mathbf{A}}) \pmod{2}, \end{aligned} \quad (\text{IV.92})$$

with  $c(\mathcal{R})$  the index of the representation. In general, discrete field theoretic anomalies need not vanish by themselves provided they are cancelled by a suitable discrete version of the Green-Schwarz mechanism [118]. This happens when an anomalous  $U(1)$  is Higgsed to a discrete subgroup which is also anomalous. In this case, the anomalous discrete subgroup is not preserved at the non-perturbative level because instantons can violate it. In our case, however, the  $\mathbb{Z}_2$  symmetry *is* exact at the non-perturbative level. Potential non-perturbative effects would be M2-brane instantons or fluxed M5-instantons. Their interplay with the discrete symmetry  $\mathbb{Z}_2$  has been studied in detail recently [52, 113], and as expected from the general formalism of [119, 120] the discrete symmetry is indeed non-perturbatively exact. Therefore the mixed  $\mathbb{Z}_2$  anomalies must vanish by themselves. Consistently, we can adapt the analysis of [88] of the Green-Schwarz mechanism for (mixed) abelian anomalies. The potential Green-Schwarz counter-terms would then be proportional to

$$\int_{\mathbb{Y}_4} G_4 \wedge \hat{U} \wedge D^{(\mathcal{B})} \quad (\text{IV.93})$$

As a result of the transversality condition (IV.57) this vanishes identically, confirming once more that the  $\mathbb{Z}_2$  anomalies must vanish by themselves.

We would like to see the manifestation of this field theoretic argument in the geometry. To this end, we revisit the strategy applied earlier when studying the other anomalies and analyse the 4-cycle responsible for the anomaly directly. In this case, it is the matter surface of  $\mathbf{5}^{\mathbf{A}}$ , which we recall here from table IV.8 for convenience:

$$[\bar{\mathbf{5}}^{\mathbf{A}}] = (2 E_3 E_4 - 2 [b_2] E_3 + \bar{\mathcal{K}} (4 E_3 - \Theta) + \Theta ([b_2] + E_2 - 2 E_3 + E_4 - U)) [\mathbb{Y}_4]. \quad (\text{IV.94})$$

We see that if we impose the transversality conditions (IV.57), (IV.58) and the gauge symmetry condition (IV.59) on  $G_4$ , then the only contribution to the chirality is given by

$$\chi(\bar{\mathbf{5}}^{\mathbf{A}}) = \int_{\mathbb{Y}_4} G_4 \wedge (2 E_3 \wedge E_4). \quad (\text{IV.95})$$

The question now is whether  $\int_{\mathbb{Y}_4} G_4 \wedge E_3 \wedge E_4 \in \mathbb{Z}$ , since this would imply that  $\chi(\bar{\mathbf{5}}^{\mathbf{A}})$  is even and therefore the discrete  $\mathbb{Z}_2$  anomalies (IV.92) vanish.

Now we apply the quantisation condition to the 4-cycle  $E_3 \cdot E_4$ : Since this cycle is manifestly integer, an appropriately quantised flux must satisfy  $\int_{\mathbb{Y}_4} (G_4 + \frac{1}{2} c_2(\mathbb{Y}_4)) \wedge E_3 E_4 \in \mathbb{Z}$ . Thus, the integrerness of  $\int_{\mathbb{Y}_4} G_4 \wedge E_3 E_4$  follows from  $1/2 \int_{\mathbb{Y}_4} c_2(\mathbb{Y}_4) \wedge E_3 E_4 \in \mathbb{Z}$ , or  $\int_{\mathbb{Y}_4} c_2(\mathbb{Y}_4) \wedge E_3 E_4 \in 2\mathbb{Z}$ ,

which remains to be shown. A direct calculation reveals that

$$\begin{aligned}
 & \int_{\mathbb{Y}_4} c_2(\mathbb{Y}_4) \wedge E_3 \wedge E_4 \\
 &= \int_{\mathcal{B}} \Theta \wedge \left( (c_2(\mathcal{B}) - \bar{\mathcal{K}}^2) - 2\bar{\mathcal{K}}^2 - 2\Theta^2 \right) - ([b_2]^2 \Theta - 3\bar{\mathcal{K}} [b_2] \Theta + 3 [b_2] \Theta^2 - 5 \Theta^2 \bar{\mathcal{K}}) \quad (\text{IV.96}) \\
 &\equiv \int_{\mathcal{B}} \Theta \wedge (c_2(\mathcal{B}) - \bar{\mathcal{K}}^2) - ([b_2]^2 \Theta + \bar{\mathcal{K}} [b_2] \Theta + [b_2] \Theta^2 + \Theta^2 \bar{\mathcal{K}}) \pmod{2}.
 \end{aligned}$$

While the first term is manifestly even (in [121] it was shown that  $c_2(\mathcal{B}) - \bar{\mathcal{K}}^2$  is an even class for smooth complex threefolds), the latter part is not guaranteed to be without any further input. However, if we assume integrality of all chiral indices in the  $U(1)$  model, which we have argued before to be equivalent to (IV.90), then also (IV.96) is even, and therefore the discrete  $\mathbb{Z}_2$  anomalies (IV.92) vanish by themselves. On the other hand, if we impose integrality of chiral indices (IV.91) as well as the absence of anomalies in the  $\mathbb{Z}_2$  model, the arithmetic constraints on the fibration guarantee a consistent (i.e. integral) chiral spectrum of the  $U(1)$  model.

To summarise, we see that physical consistency conditions on both the  $U(1)$  and the  $\mathbb{Z}_2$  model pose *exactly* the same constraints on the geometry. Since the  $\mathbb{Z}_2$  and the  $U(1)$  model are related by a conifold transition, it is not surprising that cancellation of the  $\mathbb{Z}_2$  anomalies requires not only integrality of (IV.91), but of the corresponding expressions in the  $U(1)$  model. We know that any consistent  $\mathbb{Z}_2$  fibration defined by  $[b_2]$  and  $\Theta$  on the base  $\mathcal{B}$  originates via Higgsing from a  $U(1)$  model over the same base with the same fibration data  $[b_2]$  and  $\Theta$ . Now if the  $U(1)$  model is consistent, the chiralities and therefore also (IV.85) – (IV.88) must be integer. These intersection properties of  $\mathcal{B}$  of course still hold in the  $\mathbb{Z}_2$  model and lead to integrality of (IV.91) as well as the vanishing of the discrete anomaly. From a field theoretic perspective, cancellation of the discrete anomalies is tied to a consistent embedding of the discrete symmetry into a gauged continuous symmetry at high energies. This underlying gauge symmetry is precisely the  $U(1)$  symmetry of the model on  $Y_4$ , and so the relation between consistency of the latter and discrete anomaly cancellation is also expected from this point of view.

Finally, note that the crucial relation (IV.95) depends not only on the conditions (IV.58) and (IV.59), as does the proof for cancellation of the non-abelian cubic anomaly, but also on (IV.57), where the bisection appears explicitly. This serves us as another consistency check of the proposed transversality condition for genus-one fibrations.

## 2.4 Comparing fluxes in the conifold transition

In this section we compare the flux solutions in the bisection fibration  $\mathbb{Y}_4$  (cf. section 2.3.2) and in the related elliptic fibration  $Y_4$  (cf. section 2.2.2) upon performing a topological transition between both sides. Since the construction of fluxes in F-theory models on elliptic fibrations is well established, as is the topology change in the conifold transition, we will interpret this as a final test of our flux construction for the genus-one fibration. In particular, we will construct an explicit map between the flux solutions in both models and show that all fluxes in the bisection model are accounted for by a corresponding flux in the  $U(1)$  model upon performing the conifold transition.<sup>7</sup> In particular, we will see that the horizontal flux contribution in the  $\mathbb{Z}_2$  model is crucial.

### 2.4.1 Topological quantities

In order to find a map between the general flux solutions, we look for quantities that are preserved under the conifold transition, i.e. are of topological nature. The first such quantity is the total D3-brane charge. Recall that the number of D3-branes is related to the flux and curvature induced

<sup>7</sup>Such a map has already been established in [64] in absence of additional non-abelian gauge data.

D3-charge

$$n_3 = \frac{\chi(M_4)}{24} - \frac{1}{2} \int_{M_4} G_4 \wedge G_4, \quad (\text{IV.97})$$

with  $\chi(M_4)$  the Euler number of the Calabi–Yau fourfold  $M_4$ . We are interested in transitions without explicit participation of D3-branes, and for such transitions  $n_3$  must match on both sides of the transition [122]. We therefore demand that

$$\Delta n_3 \equiv n_3|_{\mathbb{Y}_4} - n_3|_{Y_4} \stackrel{!}{=} 0. \quad (\text{IV.98})$$

The topological transition from  $Y_4$  to  $\mathbb{Y}_4$  proceeds by first creating a conifold singularity in the fibre over the curve  $C_1 \subset \mathcal{B}$  given in table IV.3 by blowing down  $s$ , and then deforming by adding the term with  $c_4$  to the hypersurface polynomial [54, 63–67]. The resulting change [84, 94, 96]

$$\Delta \chi = \chi(\mathbb{Y}_4) - \chi(Y_4) = -3\chi(C_1) \quad (\text{IV.99})$$

of the Euler number allows us to rephrase (IV.98) in terms of the flux-induced D3 tadpoles (IV.97) as

$$\frac{1}{2} \int_{\mathbb{Y}_4} G_4 \wedge G_4 \stackrel{!}{=} -\frac{1}{8} \chi(C_1) + \frac{1}{2} \int_{Y_4} \tilde{G}_4 \wedge \tilde{G}_4. \quad (\text{IV.100})$$

Here  $G_4$  and  $\tilde{G}_4$  denote the fluxes on  $\mathbb{Y}_4$  (IV.68) and  $Y_4$  (IV.27), respectively. Note that in particular we need to turn on a flux  $G_4$  on the  $\mathbb{Z}_2$  side even if we start with no flux  $\tilde{G}_4 = 0$  on the  $U(1)$  side. We will see in a moment that this  $G_4$  has to have a contribution from the non-vertical flux  $G_4^h(P)$  (IV.67).

To compute the Euler number  $\chi(C_1)$  of the singlet curve with states  $\mathbf{1}_{\pm 10}$  first recall that  $C_1 = \langle b_2, c_{3,1} \rangle$ . The first Chern class of this curve can be determined with help of the adjunction formula

$$c(C_1) = \frac{c(\mathcal{B})}{1 + [\langle b_2, c_{3,1} \rangle]} \quad (\text{IV.101})$$

$$\Rightarrow c_1(C_1) = c_1(\mathcal{B}) - [b_2] - [c_{3,1}] = \bar{\mathcal{K}} - [b_2] - ([\bar{\mathcal{K}} + [b_2] - \Theta]) = -[c_{4,1}],$$

such that we obtain the Euler number contribution

$$-\frac{1}{8} \chi(C_1) = -\frac{1}{8} \int_{C_1} c_1(C_1) = -\frac{1}{8} \int_{\mathcal{B}} [C_1] \wedge c_1(C_1) = \frac{1}{8} \int_{\mathcal{B}} [b_2] \wedge [c_{3,1}] \wedge [c_{4,1}]. \quad (\text{IV.102})$$

An other set of topological quantities are the chiral indices of the  $U(1)$  spectrum (IV.40) and the  $\mathbb{Z}_2$  spectrum (IV.76), which therefore must also be conserved under the transition. This applies to the notion of chirality with respect to the unbroken gauge subgroups on both sides of the transition. In the case at hand, this is the non-abelian  $SU(5)$  factor. From the field theory perspective this is clear because Higgsing the  $U(1)$  gauge symmetry to a  $\mathbb{Z}_2$  subgroup does not change the  $SU(5)$  chiralities of the states. However, the number of individual matter curves as such is not equal. By comparing the discriminants (IV.55) for  $c_{4,1} \neq 0$  and (IV.11) for  $c_{4,1} = 0$ , we confirm that the matter curves in the base relate as [64, 66]

$$\begin{aligned} \mathbb{Y}_4 & & Y_4 \\ C_{\mathbf{10}} & \leftrightarrow & C_{\mathbf{10}_{-2}} \\ C_{\mathbf{5}^A} & \leftrightarrow & C_{\mathbf{5}_{-1}} \\ C_{\mathbf{5}^B} & \leftrightarrow & C_{\mathbf{5}_4} + C_{\mathbf{5}_{-6}}. \end{aligned} \quad (\text{IV.103})$$

Since the chiral indices are linear in the matter surface classes, we arrive at the following matching condition for the chiral indices:

$$\begin{aligned} \chi(\overline{\mathbf{10}}) & \stackrel{!}{=} \chi(\overline{\mathbf{10}}_2), \\ \chi(\overline{\mathbf{5}}^A) & \stackrel{!}{=} \chi(\overline{\mathbf{5}}_1), \\ \chi(\overline{\mathbf{5}}^B) & \stackrel{!}{=} \chi(\overline{\mathbf{5}}_{-4}) + \chi(\overline{\mathbf{5}}_6). \end{aligned} \quad (\text{IV.104})$$

### 2.4.2 Mapping fluxes across the conifold transition

Going from the  $U(1)$  model to the  $\mathbb{Z}_2$  model via the conifold transition, any existent flux  $\tilde{G}_4$  on  $Y_4$  must be mapped to a flux configuration  $G_4$  on  $\mathbb{Y}_4$  such that (IV.100) and (IV.104) are satisfied.

To gain some intuition for such a map, let us first consider the situation in which we switch on only  $U(1)$ -flux  $G_4^0(F)$  (IV.25) on  $Y_4$  and no further vertical flux solutions. The tadpole contribution on the right hand side of (IV.100) can then be evaluated as

$$\begin{aligned} & -\frac{1}{8}\chi(C_1) + \frac{1}{2} \int_{Y_4} G_4^0(F) \wedge G_4^0(F) = \frac{1}{8} \int_{\mathcal{B}} [b_2] \wedge [c_{3,1}] \wedge [c_{4,1}] - \int_{\mathcal{B}} F^2 \wedge \left( \bar{\mathcal{K}} + [b_2] - \frac{2}{5} \Theta \right) \\ & = \int_{\mathcal{B}} \left[ \frac{1}{8} (2\bar{\mathcal{K}} [b_2]^2 + 2 [b_2]^3 - \bar{\mathcal{K}} [b_2] \Theta - 3 [b_2]^2 \Theta + [b_2] \Theta^2) - F^2 \wedge \left( \bar{\mathcal{K}} + [b_2] - \frac{2}{5} \Theta \right) \right] \end{aligned} \quad (\text{IV.105})$$

From the corresponding transition in [64] without  $SU(5)$  gauge factor, and also from the general considerations in [94], we expect that we must allow, possibly amongst other fluxes, for non-vanishing non-vertical flux  $a G_4^h(P)$  on  $\mathbb{Y}_4$ , with the parameters  $a$  and  $P$  to be determined.

Part of the contribution of such  $a G_4^h(P)$  to the left hand side of (IV.100) is given by the square  $\frac{1}{2} \int (a G_4^h(P))^2$  (in addition to cross-terms with the other fluxes). Recalling that  $G_4^h(P) = 5[\sigma_0] +$  correction terms (IV.67), this expression requires in particular the calculation of the self-intersection of  $[\sigma_0]$ . A practical method for that was demonstrated in [84] and also applied in [64]. For completeness we will briefly explain the procedure here. In general, the self-intersection of a 4-cycle  $\sigma$  inside a fourfold  $M_4$  can be computed as an integral

$$\int_{M_4} [\sigma] \wedge [\sigma] = \int_{\sigma} c_2(N_{\sigma \subset M_4})$$

of the second Chern class of the normal bundle  $N_{\sigma \subset M_4}$  of  $\sigma$  embedded into  $M_4$ . If in addition  $M_4 \subset M_5$  is a hypersurface in an ambient space  $M_5$ , we can use adjunction to write

$$c(N_{\sigma \subset M_4}) = \frac{c(N_{\sigma \subset M_5})}{c(N_{M_4 \subset M_5})},$$

which we can then expand in order to extract the degree 2 terms corresponding to the second Chern class. In our case, the 4-cycle  $\sigma = \sigma_0$  is given as a complete intersection  $\langle u, w, \rho \rangle$  in  $M_5 = \mathbb{X}_5$ , so  $c(N_{\sigma_0 \subset \mathbb{X}_5}) = (1+U)(1+[w])(1+P)$ . Similarly, we have  $c(N_{\mathbb{Y}_4 \subset \mathbb{X}_5}) = 1 + [\mathbb{Y}_4]$ . The expansion and subsequent integration are then straightforward.

Having computed the self-intersection of  $\sigma_0$ , the intersection numbers of  $[\sigma_0]$  with the vertical correction term of the form  $(\sum_i D_i P) [\mathbb{Y}_4]$  in (IV.67) are straightforwardly computed in the ambient space as  $\int_{\mathbb{X}_5} [\sigma_0] (\sum_i D_i P)$ . Likewise, the self-intersection of the vertical correction term is easily computed as  $\int_{\mathbb{X}_5} [\mathbb{Y}_4] (\sum_i D_i P)^2$ . After the dust has settled, we obtain the following tadpole contribution from  $G_4^h(P)$ :

$$\frac{1}{2} \int_{X_4} \left( a G_4^h(P) \right)^2 = \frac{25 a^2}{4} \int_{\mathcal{B}} \left[ -P^2 \wedge \left( \bar{\mathcal{K}} + [b_2] - \frac{2}{5} \Theta \right) + 2\bar{\mathcal{K}} [b_2] P + 2 [b_2]^2 P - 2 [b_2] \Theta P \right] \quad (\text{IV.106})$$

Let us first see if it is sufficient to only invoke  $a G_4^h(P)$  in order to reproduce (IV.105) on the  $\mathbb{Z}_2$  side, i.e. whether we can match (IV.105) and (IV.106). As seen from (IV.105), for a general choice of  $F$  the  $U(1)$ -tadpole has a quadratic term in  $\Theta$  from the singlet curve, and a linear term in  $\Theta$  from the flux contribution. On the other hand, the class  $P$  on the  $\mathbb{Z}_2$  side may a priori be dependent or independent of  $\Theta$ . If it carries no multiple of  $\Theta$ , then the induced tadpole is only linear in the  $SU(5)$  divisor class, which can be excluded. If  $P = \dots + k \Theta$  (which we expect, since

$c_{4,1} = \rho\tau$  contains terms with  $\Theta$ ), then the induced tadpole will have a cubic term in  $\Theta$ , which has to be cancelled in order to match the  $U(1)$ -tadpole and the singlet curve term. We thus conclude that some other flux has to be turned on in order to satisfy the constraint. In order to see what flux contribution is needed we make the general ansatz (IV.68) for the flux on the  $\mathbb{Z}_2$ -side. We furthermore make an ansatz for the class  $P = kF + \alpha[b_2] + \beta\bar{\mathcal{K}} + \gamma\Theta$  as a multiple of  $F$  plus a correction expanded in the base classes which are *generically* available for any choice of base  $\mathcal{B}$ . The resulting matching equations of induced tadpoles (IV.100) and chiral indices (IV.104) are quite lengthy and we do not display them explicitly here. The result is, that in order to match the contributions of the  $U(1)$ -flux  $G_4^0(F)$  on  $Y_4$ , we need a flux  $G_4 = aG_4^h(P) + z_1G_4^{z_1} + z_2G_4^{z_2}$  on  $\mathbb{Y}_4$  with

$$P = 10F + \frac{1}{2}[c_{4,1}], \quad a = \frac{1}{5}, \quad z_1 = -\frac{1}{10}, \quad z_2 = \frac{1}{5}. \quad (\text{IV.107})$$

This confirms that it is not enough to turn on only  $G_4^h(P)$ , but that it is also required to allow for the other vertical fluxes to find a matching configuration. This is in agreement with similar findings in [86, 96] for a transition from an  $SU(5) \times U(1)$  elliptic fibration to an  $SU(5)$  elliptic fibration.

Computing the D3-tadpole contributions for a general linear combination of fluxes on both sides of the conifold transition is tedious, but straightforward. We keep the general flux (IV.68) in the bi-section model and since we are searching for the most general solution, we make the ansatz  $P = kF + \alpha[b_2] + \beta\bar{\mathcal{K}} + \gamma\Theta$ . In the  $U(1)$  model we add the linear combination

$$G_4 = G_4^0(F) + \sum_{i=1}^3 u_i G_4^{u_i} \quad (\text{IV.108})$$

of all vertical flux solutions (IV.26). The reduction of all intersection numbers in (IV.100) and (IV.104) to intersection numbers of base divisors results in a system of equations for the coefficients  $a, z_i, u_i, k, \alpha, \beta$  and  $\gamma$ . The result is that both constraints (IV.100) and (IV.104) can be solved by

$$\begin{aligned} P &= 10F + \frac{1}{2}[c_{4,1}] - 10u_3\Theta, & a &= \frac{1}{5}, \\ z_1 &= \frac{1}{10}(-1 + 100u_1), & z_2 &= \frac{1}{5}(1 - 65u_1 - 10u_2 + 5u_3) \end{aligned} \quad (\text{IV.109})$$

and we further note the  $\Theta$ -term contribution to the class  $P$ .

It is reassuring that the possible range  $0 \leq P \leq c_{4,1}$  of the divisor class  $P = [\rho]$  with  $c_{4,1} = \rho\tau$  is in beautiful agreement with the observation that fluxes on the  $U(1)$  side may obstruct the topological transition provided they induce a purely chiral spectrum of Higgs states [94, 96]. The Higgs fields of this transition are the charged singlets  $\mathbf{1}_{\pm 10}$  localised on the curve  $C_1$ . The formalism of [95] suggests that these are counted by the cohomology groups of a line bundle  $\mathcal{L} \otimes K_{C_1}^{1/2}$  with  $\deg(\mathcal{L}) = \int_{C_1} (10F - 10u_3\Theta) = \int_{\mathcal{B}} [C_1] (10F - 10u_3\Theta)$ . This is in agreement with the direct computation of the chiral index of these states (cf. (IV.40)). A necessary condition for the existence of vector-like pairs of Higgs fields, and thus for the existence of a flat direction for the conifold transition, is that  $\frac{1}{2}c_1(C_1) \leq \deg(\mathcal{L}) \leq -\frac{1}{2}c_1(C_1)$ . With  $c_1(C_1) = -c_{4,1}|_{C_1}$  this is – for the solution  $P = 10F + \frac{1}{2}c_{4,1} - 10u_3\Theta$  – in precise agreement with the inequality  $0 \leq P \leq c_{4,1}$ . For us, this serves as a final consistency check of the whole construction.

### 3 Models with $SU(3) \times SU(2) \times U(1)^2$ Symmetry

In this section, we will discuss anomaly cancellation in toric fibrations with an  $SU(3) \times SU(2) \times U(1)^2$  gauge group. These models were introduced in [13] with the phenomenological motiva-

tion to study direct realisations of the Standard Model gauge group in F-theory without GUT-breaking. Compared to other constructions as in [112, 123–125], our models have in addition to  $U(1)_Y$  one further independent  $U(1)$  factor that can be utilised as a further selection rule.

While we postpone all phenomenological discussions along with the detailed geometric analysis to chapter V, we would like to address the topic of fluxes and anomalies here. On the one hand, it serves as a further demonstration of the techniques we have developed in chapter III for the handling of vertical fluxes. On the other hand, the general results obtained from such an analysis will also be valuable for phenomenological investigations in chapter V, where we will attempt to construct Standard-Model-like fibrations with realistic chiral spectra. The results of this section have been presented in [15].

### 3.1 Geometries realising an (extended) Standard Model

Since we will discuss in full detail the geometries of all possible toric realisations of the gauge group  $SU(3) \times SU(2) \times U(1)^2$  in F-theory in chapter V, we will merely summarise the essential data of the fibrations here that are relevant for the discussion of fluxes and anomalies.

We will focus on one out of the five possible toric realisations, with the understanding that all methods used can be applied straightforwardly for all the other models.

#### 3.1.1 Fibration data and matter spectrum of the $I \times A$ model

The elliptically fibred Calabi–Yau fourfolds  $Y_4 \rightarrow \mathcal{B}$  are constructed as hypersurfaces in a  $\text{Bl}_2\mathbb{P}^2$ -fibration  $X_5 \xrightarrow{\pi} \mathcal{B}$  [57, 58, 80, 126, 127]. The non-abelian gauge symmetry is realised torically using the technique of tops [70, 71]. For the case at hand there are 5 inequivalent tops – labelled as  $I \times A$ ,  $I \times B$ ,  $I \times C$ ,  $\text{III} \times A$  and  $\text{III} \times B$  in [13] – giving rise to the Standard Model gauge algebra with a further  $U(1)$ . The  $U(1)$ s arise from a rank two Mordell–Weil group generated by sections with divisor classes  $S_0$  (zero-section),  $S_1$  and  $U$ . The non-abelian part of the gauge group is localised over two vertical divisors,  $W_2 = [\{w_2\}]$  for  $SU(2)$  and  $W_3 = [\{w_3\}]$  for  $SU(3)$ . The tops define divisors  $E_i$  ( $i = 0, 1$ ) and  $F_j$  ( $j = 0, 1, 2$ ) with associated coordinates  $e_i$  and  $f_j$ , respectively, such that

$$E_0 + E_1 = \pi^{-1}(W_2) \equiv W_2, \quad F_0 + F_1 + F_2 = \pi^{-1}(W_3) \equiv W_3. \quad (\text{IV.110})$$

The intersections of the divisors  $E_i$  and  $F_j$  with the hypersurface  $Y_4$  give rise to the exceptional divisors which resolve the non-abelian singularities; they are given by  $\mathbb{P}^1$ -fibrations over  $W_2$  and  $W_3$ , respectively. The rational fibres are in one-to-one correspondence with the simple roots of  $SU(2)$  and  $SU(3)$  and can split into further  $\mathbb{P}^1$ s over matter curves and Yukawa points.

Given a base  $\mathcal{B}$ , the geometry is specified by a choice of divisor classes  $W_2$  and  $W_3$  as well as of two other base classes  $\alpha, \beta$  which parametrise the  $\text{Bl}_2\mathbb{P}^2$ -fibration. In the following we will focus on one of the five models labelled  $I \times A$ . The fibration data is given by table V.8. The Stanley–Reisner ideal of the fibre ambient space depends on the triangulation of the top.<sup>8</sup> As in [13] we choose a triangulation leading to the SR-ideal generators

$$u \ v, \ u \ w, \ w \ s_0, \ v \ s_1, \ s_0 \ s_1, \ e_0 \ w, \ e_1 \ s_0, \ e_1 \ u, \ f_0 \ w, \ f_0 \ s_1, \ f_1 \ s_0, \ f_1 \ v, \ f_2 \ s_0, \ f_2 \ s_1, \ f_2 \ u, \ f_0 \ e_1. \quad (\text{IV.111})$$

Furthermore one can read off the linear relations amongst the divisors from the non-trivial columns in table V.8, e.g.  $[v] = \beta + U + S_1 + F_1$ . This leads to the following generators of the linear equivalence ideal,

$$\langle \beta + U + S_1 + F_1 - [v], \ \alpha + U + S_0 - E_1 - F_2 - [w], \ W_2 - E_0 - E_1, \ W_3 - F_0 - F_1 - F_2 \rangle. \quad (\text{IV.112})$$

<sup>8</sup>Of course all physical quantities in the F-theory limit are independent of the choice of triangulation.

		coordinates									
		u	v	w	$s_0$	$s_1$	$e_0$	$e_1$	$f_0$	$f_1$	$f_2$
base divisor classes	$W_2$	·	·	·	·	·	1	·	·	·	·
	$W_3$	·	·	·	·	·	·	·	1	·	·
	$\alpha$	·	·	1	·	·	·	·	·	·	·
	$\beta$	·	1	·	·	·	·	·	·	·	·
fibre & excep. divisors	$U$	1	1	1	·	·	·	·	·	·	·
	$S_0$	·	·	1	1	·	·	·	·	·	·
	$S_1$	·	1	·	·	1	·	·	·	·	·
	$E_1$	·	·	-1	·	·	-1	1	·	·	·
	$F_1$	·	1	·	·	·	·	·	-1	1	·
	$F_2$	·	·	-1	·	·	·	·	-1	·	1
top data		-1	0	1	-1	0	0	1	0	0	1
		1	-1	0	0	1	0	0	0	1	0
		$\underline{0}$	$\underline{0}$	$\underline{0}$	$\underline{0}$	$\underline{0}$	$\underline{x}$	$\underline{x}$	$\underline{y}$	$\underline{y}$	$\underline{y}$

**Table IV.9:** Divisor classes and coordinates of the ambient space for model  $I \times A$ . The last row (‘top data’) describes (parts of) the fan of the ambient space  $X_5$ ; for a specific base  $\mathcal{B}$  one has to fix the lattice coordinates  $\underline{x}$  and  $\underline{y}$  as well as further toric data completing the description of  $\mathcal{B}$ .

The polynomial

$$\begin{aligned}
 P_T = & \\
 & v w (c_{1;0,0} e_1 f_2 w s_1 + c_{2;0,1} f_0 f_2 v s_0) + u (b_{0;1,1} e_0 f_0 v^2 s_0^2 + b_1 v w s_0 s_1 + b_{2;0,0} e_1 f_1 f_2 w^2 s_1^2) + \\
 & u^2 (d_{0;1,1} e_0 f_0 f_1 v s_0^2 s_1 + d_{1;0,0} f_1 w s_0 s_1^2 + d_{2;1,1} e_0 f_0 f_1^2 u s_0^2 s_1^2)
 \end{aligned} \tag{IV.113}$$

cuts out the Calabi–Yau hypersurface  $Y_4$  with divisor class  $[Y] \equiv [P_T] = [b_1] + U + [v] + [w] + S_0 + S_1$  in  $X_5$ . The coefficients are sections of specific line bundles, or – equivalently – transform as certain divisor classes,

$$\begin{aligned}
 [b_{0;1,1}] &= \alpha - \beta + \bar{\mathcal{K}} - W_2 - W_3, \quad [b_1] = \bar{\mathcal{K}}, \quad [b_{2;0,0}] = \beta - \alpha + \bar{\mathcal{K}}, \\
 [c_{1;0,0}] &= \bar{\mathcal{K}} - \alpha, \quad [c_{2;0,1}] = \bar{\mathcal{K}} - \beta - W_3, \\
 [d_{0;1,1}] &= \alpha + \bar{\mathcal{K}} - W_2 - W_3, \quad [d_{1;0,0}] = \beta + \bar{\mathcal{K}}, \quad [d_{2;1,1}] = \alpha + \beta + \bar{\mathcal{K}} - W_2 - W_3.
 \end{aligned} \tag{IV.114}$$

Here  $\bar{\mathcal{K}}$  is the anti-canonical class of the base  $\mathcal{B}$ . In this model the  $U(1)$ -generators are

$$\begin{aligned}
 \omega_1^{I \times A} &\equiv \omega_1 = S_1 - S_0 - \bar{\mathcal{K}} + \frac{1}{2} E_1 + \frac{2}{3} F_1 + \frac{1}{3} F_2, \\
 \omega_2^{I \times A} &\equiv \omega_2 = U - S_0 - \bar{\mathcal{K}} - [c_{1;0,0}] + \frac{2}{3} F_1 + \frac{1}{3} F_2.
 \end{aligned} \tag{IV.115}$$

This geometry gives rise to a rich spectrum of matter charged under the  $SU(3) \times SU(2) \times U(1)^2$  gauge symmetry. The various matter representations  $\mathcal{R}$  as well as the curves  $C_{\mathcal{R}}$  on  $\mathcal{B}$  over which this matter is localised are listed in table IV.10.

### 3.1.2 Fluxes over generic Bases

To compute fluxes for a generic base  $\mathcal{B}$ , we proceed analogously as in section 2.2.2: We first determine a basis  $\{t_i\}$  of  $H_{\text{vert}}^{(2,2)}(Y_4)$  and then reduce the transversality and gauge symmetry



$\mathcal{R}$	$U(1)$ -charges	curve $C_{\mathcal{R}}$ in base
$\mathbf{2}_1$	$(\frac{1}{2}, -1)$	$\{w_2\} \cap \{c_{2;0,1}\}$
$\mathbf{2}_2$	$(\frac{1}{2}, 1)$	$\{w_2\} \cap \{c_{1;0,0}^2 d_{1;0,0} - b_1 b_{2;0,0} c_{1;0,0} + b_{2;0,0}^2 c_{2;0,1} w_3\}$
$\mathbf{2}_3$	$(\frac{1}{2}, 0)$	$\{w_2\} \cap \{b_{0;1,1}^2 d_{1;0,0}^2 + b_{0;1,1} (b_1^2 d_{2;1,1} - b_1 d_{0;1,1} d_{1;0,0} - 2 c_{2;0,1} d_{1;0,0} d_{2;1,1} w_3) + c_{2;0,1} w_3 (d_{0;1,1}^2 d_{1;0,0} - b_1 d_{0;1,1} d_{2;1,1} + c_{2;0,1} d_{2;1,1}^2 w_3)\}$
$\mathbf{3}_1$	$(\frac{2}{3}, -\frac{1}{3})$	$\{w_3\} \cap \{b_{0;1,1}\}$
$\mathbf{3}_2$	$(-\frac{1}{3}, -\frac{4}{3})$	$\{w_3\} \cap \{c_{1;0,0}\}$
$\mathbf{3}_3$	$(-\frac{1}{3}, \frac{2}{3})$	$\{w_3\} \cap \{b_{0;1,1} w_2 c_{1;0,0} - b_1 c_{2;0,1}\}$
$\mathbf{3}_4$	$(\frac{2}{3}, \frac{2}{3})$	$\{w_3\} \cap \{b_1 b_{2;0,0} - c_{1;0,0} d_{1;0,0}\}$
$\mathbf{3}_5$	$(-\frac{1}{3}, -\frac{1}{3})$	$\{w_3\} \cap \{b_{0;1,1} d_{1;0,0}^2 - b_1 d_{0;1,1} d_{1;0,0} + b_1^2 d_{2;1,1}\}$
$(\mathbf{3}, \mathbf{2})$	$(\frac{1}{6}, -\frac{1}{3})$	$\{w_2\} \cap \{w_3\}$
$\mathbf{1}^{(1)}$	$(1, -1)$	$\{b_{0;1,1}\} \cap \{c_{2;0,1}\}$
$\mathbf{1}^{(2)}$	$(1, 0)$	$C^{(2)}$
$\mathbf{1}^{(3)}$	$(1, 2)$	$\{b_{2;0,0}\} \cap \{c_{1;0,0}\}$
$\mathbf{1}^{(4)}$	$(1, 1)$	$C^{(4)}$
$\mathbf{1}^{(5)}$	$(0, 2)$	$\{c_{1;0,0}\} \cap \{c_{2;0,1}\}$
$\mathbf{1}^{(6)}$	$(0, 1)$	$C^{(6)}$

**Table IV.10:** Matter representations in the  $I \times A$  model, together with the corresponding codimension two loci in  $\mathcal{B}$  over which they are localised. The singlet curves  $C^{(2)}$ ,  $C^{(4)}$  and  $C^{(6)}$  cannot be written as complete intersections (see [13] for details).

conditions for a general linear combination  $\lambda_i t_i$  to a linear combination of triple intersection numbers on  $\mathcal{B}$ . Imposing that the coefficients for each intersection number vanish individually, we obtain as solutions all fluxes that are present on any base  $\mathcal{B}$ .

For the  $I \times A$  fibration, we obtain the following flux basis satisfying the standard transversality conditions (III.6) and (III.7), and the gauge symmetry condition (III.9):

$$\begin{aligned}
 G_4^{z_1} &= -F_1 (\beta + \bar{\mathcal{K}}) - (F_1 + 3 S_1) W_3 + F_2 (\beta + 3 F_1 - 2 \bar{\mathcal{K}} + W_3), \\
 G_4^{z_2} &= (2 F_1 - 2 F_2) W_2 + E_1 (6 F_2 - 3 W_3), \\
 G_4^{z_3} &= 3 F_2^2 + F_1 (W_2 - \alpha - 2 \bar{\mathcal{K}}) + F_2 (3 E_1 + 3 F_1 - 2 \alpha - \bar{\mathcal{K}} - W_2 - 2 W_3) + (2 F_1 + 3 S_1) W_3, \\
 G_4^{z_4} &= E_1 (3 \beta + 6 F_2 - 3 \bar{\mathcal{K}} + 6 S_1) + 2 (F_1 - F_2 - 3 S_1) W_2, \\
 G_4^{z_5} &= S_1 (E_1 + \bar{\mathcal{K}} + S_1 - W_2), \\
 G_4^{(i)}(\mathcal{D}) &= \omega_i \wedge \mathcal{D} \text{ for } i = 1, 2 \text{ and } \mathcal{D} \in H^{(1,1)}(\mathcal{B}) \text{ (} U(1)_i\text{-fluxes)}.
 \end{aligned} \tag{IV.116}$$

The most general flux on a generic base  $\mathcal{B}$  thus has the form

$$G_4 = \sum_i z_i G_4^{z_i} + G_4^{(1)}(\mathcal{D}) + G_4^{(2)}(\mathcal{D}'). \tag{IV.117}$$

The numerical coefficients  $z_i \in \mathbb{Q}$  and the base divisor classes  $\mathcal{D}$  and  $\mathcal{D}'$  are subject to the quantisation condition (III.2). Note that for an explicit choice of the fibration data and base  $\mathcal{B}$ , linear equivalences amongst the vertical divisors might render some of the above fluxes linearly dependent. If no such linear dependences arise, one might wonder if additional fluxes can be constructed for a special base  $\mathcal{B}$ . However, it turns out that the only such fluxes are of the form  $G_4^{(i)}(\mathcal{D})$  for extra classes of  $\mathcal{D}$  which may exist in addition to the generic base classes  $\alpha, \beta, W_{2,3}, \bar{\mathcal{K}}$ . In contrast, no additional fluxes of the form  $G_4^{z_i}$  not related to a  $U(1)_i$ -flux can occur. This is of course under the assumption that the specific base  $\mathcal{B}$  does not enforce further gauge enhancements, either non-abelian or abelian in the form of non-toric sections, on the full fibration. If this is case, the space of divisors on  $Y_4$  and consequently also  $H_{\text{vert}}^{2,2}(Y_4)$  increases.

For the discussion of the phenomenology of Standard-Model-like vacua, an extra restriction comes from requiring that the hypercharge  $U(1)_Y$  gauge potential does not receive a Stückelberg mass from the D-term induced by the flux:

$$\int_{Y_4} G_4 \wedge \omega_Y \wedge J^{(\mathcal{B})} = 0, \quad (\text{IV.118})$$

with  $J^{(\mathcal{B})} \in H^{(1,1)}(\mathcal{B})$  being the Kähler form of the base. This condition depends on the particular choice of linear combination

$$U(1)_Y = aU(1)_1 + bU(1)_2 \quad \longleftrightarrow \quad \omega_Y = a\omega_1 + b\omega_2, \quad (\text{IV.119})$$

where  $\omega_1$  and  $\omega_2$  are the generators of the two abelian gauge group factors. For completeness, we include here the D-terms induced by the general flux (IV.117) for the individual  $U(1)$  gauge groups,

$$\begin{aligned} \xi_1 &\simeq \int_{Y_4} G_4 \wedge \omega_1 \wedge J^{(\mathcal{B})} = \int_{\mathcal{B}} J^{(\mathcal{B})} \wedge \\ &\left( -2(\mathcal{D} + \mathcal{D}')\bar{\mathcal{K}} + \frac{1}{2}\mathcal{D}W_2 + \frac{1}{3}(2\mathcal{D} - \mathcal{D}')W_3 + 2\bar{\mathcal{K}}W_3z_1 - W_3^2z_1 - W_2W_3z_2 - 5\bar{\mathcal{K}}W_3z_3 \right. \\ &+ W_2W_3z_3 + 2W_3^2z_3 + \alpha(\mathcal{D}' - W_3z_3) + 3\bar{\mathcal{K}}W_2z_4 - 4W_2W_3z_4 - \beta(\mathcal{D}' + W_3z_1 + 3W_2z_4) \\ &\left. + (\alpha - \beta + \bar{\mathcal{K}} - W_2 - W_3)(\beta - \bar{\mathcal{K}} + W_3)z_5 \right), \\ \xi_2 &\simeq \int_{Y_4} G_4 \wedge \omega_2 \wedge J^{(\mathcal{B})} = \int_{\mathcal{B}} J^{(\mathcal{B})} \wedge \\ &\left( \alpha\mathcal{D} - \beta\mathcal{D} + 2\alpha\mathcal{D}' - \mathcal{D}\bar{\mathcal{K}} - 4\mathcal{D}'\bar{\mathcal{K}} - \frac{1}{3}\mathcal{D}W_3 + \frac{2}{3}\mathcal{D}'W_3 + 2\beta W_3z_1 - 4\bar{\mathcal{K}}W_3z_1 + 2W_3^2z_1 \right. \\ &+ 2W_2W_3z_2 - \alpha W_3z_3 - 3\beta W_3z_3 + \bar{\mathcal{K}}W_3z_3 + W_2W_3z_3 - W_3^2z_3 + 6\beta W_2z_4 - 6\bar{\mathcal{K}}W_2z_4 \\ &\left. + 8W_2W_3z_4 + (\beta - \bar{\mathcal{K}} + W_3)(-\alpha + \beta - \bar{\mathcal{K}} + W_2 + W_3)z_5 \right). \end{aligned} \quad (\text{IV.120})$$

Here  $J^{(\mathcal{B})}$  is the Kähler form on the base  $\mathcal{B}$ . For an explicit realisation of the hypercharge generator  $\omega_Y = \lambda_1\omega_1 + \lambda_2\omega_2$ , the corresponding D-term must vanish in a phenomenologically viable model. Likewise, consistency will require the D3-tadpole  $n_3 = \chi(Y_4)/24 - 1/2 \int_{Y_4} G_4^2$  to be integer; the expression for  $1/2 \int_{Y_4} G_4^2$  is quite lengthy and its presentation is relegated to the end of this chapter, cf. formula (IV.146).

### 3.1.3 Homology classes of matter surfaces

As explained in section 3.3.2 of chapter III, and also demonstrated in section 2.2.3 in the  $SU(5) \times U(1)$  model, the matter surfaces of non-abelian matter can be obtained through primary

decomposition. For the  $I \times A$  model, this method determines all homology classes but those of  $\mathbf{1}^{(i)}$  with  $i = 2, 4, 6$  ('missing singlets'). We have collected the results in table IV.11. Note again that all these matter surfaces  $\gamma_{\mathcal{R}}$  are vertical in homology, i.e.  $[\gamma_{\mathcal{R}}] = [Y_4] \cdot [\tilde{\gamma}_{\mathcal{R}}]$ , with  $[\tilde{\gamma}_{\mathcal{R}}] \in H_{\text{vert}}^{(2,2)}(Y_4)$ . With the knowledge of the matter surface classes, we can readily compute the chiral indices induced by the fluxes (IV.117) (cf. table IV.12).

Note that we can again use the abelian anomalies to determine the chiralities of the missing singlets, as presented in table IV.13. Furthermore, as we will demonstrate in section 3.2.2, we can even use anomaly matching to derive homology classes  $[\widetilde{\mathbf{1}}^{(i)}]$  for generic fibrations such that the chiral index  $\chi(\mathbf{1}^{(i)}) := \int_{Y_4} G_4 \wedge [\widetilde{\mathbf{1}}^{(i)}]$  will lead to an anomaly free spectrum for any valid flux  $G_4$ . These classes are also included in table IV.11.

Even though the specific flux basis (IV.116) for the fluxes and the derivation of the matter surfaces made use of the choice of the SR-ideal (IV.111), all physical results are independent of the choice of triangulation of the fibre. In particular the results of tables IV.12 and IV.13 for the chiral indices depend only on intersection numbers on the base. They can be applied straightforwardly to any choice of base  $\mathcal{B}$  provided this choice gives rise to a consistent fibration structure in the sense specified in the paragraph after (IV.115).

### 3.2 Cancellation of gauge and gravitational anomalies

Just like in our previous examples with  $SU(5)$  symmetry, the 4D effective field theory is potentially plagued by gauge anomalies. In the presence of the gauge group  $SU(3) \times SU(2) \times U(1)_1 \times U(1)_2$ , the possible types of non-trivial anomalies are  $SU(3)^3$ ,  $SU(n)^2 - U(1)$ ,  $U(1)_a - U(1)_b - U(1)_c$  and  $U(1)$ -gravitational (note that  $SU(2)^3$  anomalies are trivially 0 because  $SU(2)$  has only real representations). Here the  $U(1)$ s can be any linear combination  $\lambda_1 U(1) + \lambda_2 U(1)_2$ . Adapting the general formulae (IV.3) to this set-up, we obtain the following conditions matching the anomalies with possible GS-counterterms:

$$SU(3)^3 : 2\chi(\mathbf{3}, \mathbf{2}) + \sum_i \chi(\mathbf{3}_i^A) = 0 \quad (\text{IV.121})$$

$$SU(3)^2 - U(1) : 2q(\mathbf{3}, \mathbf{2})\chi(\mathbf{3}, \mathbf{2}) + \sum_i q(\mathbf{3}_i^A)\chi(\mathbf{3}_i^A) = - \int_{Y_4} G_4 \wedge \omega \wedge W_3 \quad (\text{IV.122})$$

$$SU(2)^2 - U(1) : 3q(\mathbf{3}, \mathbf{2})\chi(\mathbf{3}, \mathbf{2}) + \sum_i q(\mathbf{2}_i^I)\chi(\mathbf{2}_i^I) = - \int_{Y_4} G_4 \wedge \omega \wedge W_2 \quad (\text{IV.123})$$

$$U(1)_a - U(1)_b - U(1)_c : \sum_{\mathcal{R}} \dim(\mathcal{R}) q_a(\mathcal{R}) q_b(\mathcal{R}) q_c(\mathcal{R}) \chi(\mathcal{R}) = 3 \int_{Y_4} G_4 \wedge \pi_*(\omega_{(a} \cdot \omega_b) \wedge \omega_c) \quad (\text{IV.124})$$

$$U(1) - \text{gravitational} : \sum_{\mathcal{R}} \dim(\mathcal{R}) q(\mathcal{R}) \chi(\mathcal{R}) = -6 \int_{Y_4} G_4 \wedge \bar{\mathcal{K}} \wedge \omega, \quad (\text{IV.125})$$

where on the left-hand side  $q_{(\cdot)}(\mathcal{R})$  denotes the associated charge of the representation  $\mathcal{R}$  under the  $U(1)_{(\cdot)}$  generator  $\omega_{(\cdot)} = \lambda_1^{(\cdot)} \omega_1 + \lambda_2^{(\cdot)} \omega_2$  (IV.115). The relevant values of the projection  $\pi_*$  of 4-cycles in  $Y_4$  to divisors of the base are

$$\begin{aligned} \pi_*(\omega_1 \cdot \omega_1) &= \frac{1}{2} W_2 + \frac{2}{3} W_3 - 2\bar{\mathcal{K}}, \\ \pi_*(\omega_1 \cdot \omega_2) &= \pi_*(\omega_2 \cdot \omega_1) = -\frac{1}{3} W_3 - \bar{\mathcal{K}} + \alpha - \beta, \\ \pi_*(\omega_2 \cdot \omega_2) &= \frac{2}{3} W_3 - 4\bar{\mathcal{K}} + 2\alpha. \end{aligned} \quad (\text{IV.126})$$

$\mathcal{R}$	homology class $[\gamma_{\mathcal{R}}] = [Y_4] \cdot [\tilde{\gamma}_{\mathcal{R}}]$
$\mathbf{2}_1$	$c_{2;0,1} E_0 (b_1 + S_0 + U + v) = Y_4 \{E_0 (\bar{\mathcal{K}} - S_1 - \beta - W_3)\}$
$\mathbf{2}_2$	$E_0 [(b_1 + b_{2;0,0} + S_0 + v) (b_1 + S_1 + s_0 + U + v) - 2v (d_{1;0,0} + S_0 + U)]$ $= Y_4 \{-\alpha E_0 - W_2 (F_1 - 2\bar{\mathcal{K}} - S_0 + S_1 + U) + E_1 (S_1 - F_2 - 2\bar{\mathcal{K}} + W_3)\}$
$\mathbf{2}_3$	$E_1 [(2b_{0;1,1} + 2d_{1;0,0}) (b_1 + w + v + S_1) + F_1 (b_1 + S_1) + F_0 (b_1 + v)$ $- (b_1 + v + S_1) (d_{0;1,1} + d_{1;0,0} + S_1 + 2F_1) + d_{1;0,0} (b_1 + S_1)]$ $= Y_4 \{E_1 (\alpha - \beta + 2F_2 + 3\bar{\mathcal{K}} - 2S_1 - 2W_2 - 3W_3) + W_2 (\alpha - F_2 + S_0 + U)\}$
$\mathbf{3}_1$	$F_1 w b_{0;1,1} = Y_4 \{F_2 (F_2 + E_1 - \alpha - W_3) + W_3 (\alpha - E_1 + S_0 + U)\}$
$\mathbf{3}_2$	$F_0 U c_{1;0,0} = Y_4 \{(F_1 + F_2) (\alpha - F_2) + W_3 (F_2 - \alpha - S_0)\}$
$\mathbf{3}_3$	$F_1 (b_1 + S_1 + w) (c_{2;0,1} + F_0) = Y_4 \{S_1 W_3 + F_1 (\bar{\mathcal{K}} - F_2)\}$
$\mathbf{3}_4$	$F_0 (b_1 + U + S_0) (d_{1;0,0} + U + S_0)$ $= Y_4 \{F_1 (\alpha - \beta - \bar{\mathcal{K}}) + F_2 (\alpha - \bar{\mathcal{K}} - F_2) + W_3 (F_2 - F_1 - S_1 - U - \alpha + \bar{\mathcal{K}})\}$
$\mathbf{3}_5$	$F_2 [(b_{0;1,1} + d_{1;0,0} + v) (b_{0;1,1} + 2v) - b_{0;1,1} (d_{0;1,1} + v) - d_{2;1,1} v]$ $= Y_4 \{F_2 (E_1 + 2F_1 + F_2 + \beta + \bar{\mathcal{K}} - W_2 - W_3)\}$
$(\mathbf{3}, \mathbf{2})$	$E_0 F_2 (b_1 + v) = Y_4 \{E_0 F_2\}$
$\mathbf{1}^{(1)}$	$b_{0;1,1} c_{2;0,1} (b_1 + S_0 + U + v + w)$ $= P_T \{(\bar{\mathcal{K}} - \beta) (\bar{\mathcal{K}} - \beta + \alpha) - S_1 (S_1 + E_1 + \bar{\mathcal{K}})$ $+ W_2 (\beta - \bar{\mathcal{K}} + S_1 + W_3) + W_3 (W_3 - \alpha + 2\beta - 2\bar{\mathcal{K}})\}$
$\mathbf{1}^{(3)}$	$b_{2;0,0} c_{1;0,0} S_0$ $= Y_4 \{S_0 \bar{\mathcal{K}} + S_1^2 - F_2 (F_1 + F_2) + \beta (S_1 - U)$ $+ \alpha (F_1 + F_2 - S_0 + U) + W_3 (F_2 + U - S_0 + S_1 - \alpha)\}$
$\mathbf{1}^{(5)}$	$c_{1;0,0} c_{2;0,1} (b_1 + S_1 + S_0 + v + w)$ $= Y_4 \{\bar{\mathcal{K}} (\bar{\mathcal{K}} - U) - S_1^2 - \beta (\bar{\mathcal{K}} + S_1 - U) - W_3 (\bar{\mathcal{K}} + S_1 - U) + \alpha (\beta - \bar{\mathcal{K}} + W_3)\}$
$\widetilde{\mathbf{1}}^{(2)}$	$Y_4 \{S_1 \cdot (3S_1 - 2\alpha + 3\beta + 2E_1 - 2\bar{\mathcal{K}} + 4W_3) + U \cdot (\alpha - \beta + 2\bar{\mathcal{K}} - W_2 - 3W_3)$ $- F_2 \cdot (2E_1 + F_1 + 2F_2)\}$
$\widetilde{\mathbf{1}}^{(4)}$	$Y_4 \{S_1 \cdot (2\alpha - 3S_1 - 4\beta - E_1 - 3\bar{\mathcal{K}} + W_2 - 2W_3)$ $+ U \cdot (2\beta - 2\alpha - 2\bar{\mathcal{K}} + W_2 + 4W_3) + F_2 \cdot (E_1 + 2F_1 + 3F_2)\}$
$\widetilde{\mathbf{1}}^{(6)}$	$Y_4 \{2S_1 (S_1 - \alpha + 2\beta + \bar{\mathcal{K}} + W_3) + U (-2\beta - 2\bar{\mathcal{K}} + W_2 - W_3) + (E_1 - F_2) F_2\}$

**Table IV.11:** Homology classes of matter surfaces, given as 4-cycles in the ambient space and on the hypersurface. For formatting reasons the square brackets indicating divisor classes of sections are left out as well as product signs. The classes in the last three entries are not the actual matter surfaces', however they give rise to the correct chiral index when integrated with a valid  $G_4$  flux. See section 3.2.2 for more details.

$\mathcal{R}$	$\chi(\mathcal{R})$
$\mathbf{2}_1$	$W_2 (\bar{\mathcal{K}} - \beta - W_3) [3\beta z_4 + 3\bar{\mathcal{K}} z_4 - 6W_2 z_4 + W_3 (-3z_1 + 3z_2 + 3z_3 + 6z_4 - z_5) + \alpha z_5 - \beta z_5 + \bar{\mathcal{K}} z_5 - W_2 z_5] - (\mathcal{D} - 2\mathcal{D}') W_2 (\beta - \bar{\mathcal{K}} + W_3)/2$
$\mathbf{2}_2$	$-3W_2 (\beta + \bar{\mathcal{K}}) [(\beta - \bar{\mathcal{K}}) z_4 + W_3 (z_2 + 2z_4)] - (\mathcal{D} + 2\mathcal{D}') (2\alpha - \beta - 3\bar{\mathcal{K}}) W_2/2$
$\mathbf{2}_3$	$W_2 \left[ (\alpha - W_2 - W_3) W_3 (3z_3 - z_5) + \bar{\mathcal{K}}^2 (-6z_4 + z_5) + \beta^2 (6z_4 + z_5) + \bar{\mathcal{K}} (W_3 (6z_2 + 9z_3 + 12z_4 - 2z_5) + (\alpha - W_2) z_5) + \beta ((-\alpha - 2\bar{\mathcal{K}} + W_2) z_5 + W_3 (6z_2 + 3z_3 + 12z_4 + 2z_5)) \right] - \mathcal{D} W_2 (-\alpha - 2\bar{\mathcal{K}} + W_2 + W_3)$
$\mathbf{3}_1$	$W_3 (W_2 + W_3 - \alpha + \beta - \bar{\mathcal{K}}) [W_3 z_1 - 2W_2 z_2 + \alpha z_3 - W_2 z_3 - 2W_3 z_3 - 2W_2 z_4 + \bar{\mathcal{K}} (z_1 - z_3 - z_5) + W_3 z_5 + \beta (z_1 + z_5)] + (2\mathcal{D} - \mathcal{D}') (\alpha - \beta + \bar{\mathcal{K}} - W_2 - W_3) W_3/3$
$\mathbf{3}_2$	$W_3 (\alpha - \bar{\mathcal{K}}) [\beta z_1 + W_3 z_1 - 2W_2 z_2 + \alpha z_3 - W_2 z_3 - 2W_3 z_3 + \bar{\mathcal{K}} (z_1 + 2z_3) - 2W_2 z_4] + (\mathcal{D} + 4\mathcal{D}') (\alpha - \bar{\mathcal{K}}) W_3/3$
$\mathbf{3}_3$	$W_3 [\beta W_3 (-z_1 + z_3 - 2z_5) - \beta \bar{\mathcal{K}} (z_1 + z_3 - 2z_5) + \beta^2 (z_1 - z_5) + \alpha \bar{\mathcal{K}} (z_3 - z_5) + W_3^2 (-2z_1 + z_3 - z_5) + \alpha \beta (z_3 + z_5) + \alpha W_3 (z_3 + z_5) - \bar{\mathcal{K}}^2 (2z_1 + z_3 + z_5) + \bar{\mathcal{K}} W_2 (-2z_2 - z_3 + 4z_4 + z_5) - \beta W_2 (2z_2 + z_3 + 8z_4 + z_5) - W_2 W_3 (2z_2 + z_3 + 8z_4 + z_5) + \bar{\mathcal{K}} W_3 (5z_1 - 3z_3 + 2z_5)] + (\mathcal{D} - 2\mathcal{D}') W_3 (\beta - 2\bar{\mathcal{K}} + W_3)/3$
$\mathbf{3}_4$	$W_3 [-\beta^2 z_1 + \alpha \bar{\mathcal{K}} z_1 + \alpha W_3 (z_1 - 2z_3) - \beta W_3 (z_1 - 2z_3) - 2\bar{\mathcal{K}} W_3 (z_1 - 2z_3) + \alpha \beta (z_1 - z_3) + \bar{\mathcal{K}}^2 (z_1 - z_3) + \alpha^2 z_3 + \beta \bar{\mathcal{K}} z_3 - \alpha W_2 (2z_2 + z_3 + 2z_4) + \beta W_2 (2z_2 + z_3 + 2z_4) + 2\bar{\mathcal{K}} W_2 (2z_2 + z_3 + 2z_4)] - 2(\mathcal{D} + \mathcal{D}') (\alpha - \beta - 2\bar{\mathcal{K}}) W_3/3$
$\mathbf{3}_5$	$W_3 \left[ -\beta^2 z_1 - \alpha W_3 z_1 - \alpha^2 z_3 - \beta W_3 z_3 - \alpha \beta (z_1 + z_3) + 3\bar{\mathcal{K}}^2 (z_1 + z_3) + W_3^2 (z_1 + z_3) + \beta \bar{\mathcal{K}} (2z_1 + z_3) - \alpha \bar{\mathcal{K}} (z_1 + 2z_3) - 2\bar{\mathcal{K}} W_3 (z_1 + 2z_3) + 2\alpha W_2 (z_2 + z_3 + z_4) - W_2^2 (2z_2 + z_3 + 2z_4) + \beta W_2 (z_1 + 2z_2 + z_3 + 2z_4) + \bar{\mathcal{K}} W_2 (z_1 + 6z_2 + 2z_3 + 6z_4) + W_2 W_3 (z_1 - 2(z_2 + z_4)) \right] - (\mathcal{D} + \mathcal{D}') (\alpha + \beta + 3\bar{\mathcal{K}} - W_2 - W_3) W_3/3$
$(\mathbf{3}, \mathbf{2})$	$W_2 W_3 [-\alpha z_3 - \beta (z_1 - 3z_4) + W_2 (2z_2 + z_3 + 2z_4) + W_3 (-z_1 + 3z_2 + 2z_3 + 6z_4) - \bar{\mathcal{K}} (z_1 + 6z_2 + 2z_3 + 9z_4)] + (\mathcal{D} - 2\mathcal{D}') W_2 W_3/6$
$\mathbf{1}^{(1)}$	$(-\mathcal{D} + \mathcal{D}') (\alpha - \beta + \bar{\mathcal{K}} - W_2 - W_3) (\beta - \bar{\mathcal{K}} + W_3) + (\bar{\mathcal{K}} - \beta - W_3) (-\alpha + \beta - \bar{\mathcal{K}} + W_2 + W_3) \cdot [W_2 (6z_4 + z_5) - (\alpha - 2\beta + \bar{\mathcal{K}}) z_5 + W_3 (3z_1 - 3z_3 + 2z_5)]$
$\mathbf{1}^{(3)}$	$(\mathcal{D} + 2\mathcal{D}') (\alpha - \bar{\mathcal{K}}) (\alpha - \beta - \bar{\mathcal{K}})$
$\mathbf{1}^{(5)}$	$(\alpha - \bar{\mathcal{K}}) (\beta - \bar{\mathcal{K}} + W_3) (W_3 (3z_1 - 3z_3 + z_5) + W_2 (6z_4 + z_5) - (\alpha - \beta + \bar{\mathcal{K}}) z_5) + 2\mathcal{D}' (\alpha - \bar{\mathcal{K}}) (\beta - \bar{\mathcal{K}} + W_3)$

**Table IV.12:** Chiral indices of states with known matter surfaces in terms of the general flux (IV.117). The terms in the right column are to be understood as intersection numbers on the base.

Finally note that in the chosen normalisation the symmetrisation of the indices  $(a, b, c)$  on the right-hand side of (IV.124) comes with a factor of  $1/3! = 1/6$ .

It is straightforward, though tedious, to directly verify the matching (IV.121) – (IV.123) of non-abelian anomalies with the chiralities in table IV.12. However, to further support the hypothesis that anomaly cancellation in 4D F-theory can be derived solely from the matter surfaces, we will parallel the analysis of sections 2.2.4 and 2.3.5 and present similar results for the  $I \times A$  fibration.

### 3.2.1 Non-abelian Anomalies

We begin with the  $SU(3)^3$  anomaly. According to the general formula (IV.39), the field theory expression (IV.121) is calculated as  $\int_{X_5} G_4 \wedge (2[(\mathbf{3}, \mathbf{2})] + \sum_i [\mathbf{3}_i^A])$  in F-theory, where  $[\mathcal{R}] \equiv [\gamma_{\mathcal{R}}]$  denotes the homology class of the matter surface associated to the state  $\mathcal{R}$ . With the homology classes explicitly given in table IV.11, it is now straightforward using the computational tools from section 2 in chapter III to evaluate

$$\begin{aligned} 2[(\mathbf{3}, \mathbf{2})] + \sum_i [\mathbf{3}_i^A] &= [Y_4] \cdot \{ (2\alpha - \beta - W_3) \cdot F_1 + (\alpha + \beta + W_2) \cdot F_2 - (E_1 + \alpha - \bar{K}) \cdot W_3 \} \\ &\equiv [Y_4] \cdot \eta_4 \\ \implies \int_{X_5} G_4 \wedge \left( 2[(\mathbf{3}, \mathbf{2})] + \sum_i [\mathbf{3}_i^A] \right) &= \int_{Y_4} G_4 \wedge \eta_4. \end{aligned} \tag{IV.127}$$

The 4-form  $\eta_4$  is obviously of the schematic form  $D_1^{(\mathcal{B})} \cdot D_2^{(\mathcal{B})} + \tilde{D}^{(\mathcal{B})} \cdot \text{Ex}_i$ . Thus by construction, any  $G_4$  satisfying (III.6), (III.7) and (III.9) leads to  $\int_{Y_4} G_4 \wedge \eta_4 = 0$ , i.e. the  $SU(3)^3$  anomaly is guaranteed to be cancelled for *any* valid fluxes.

By analogous calculations, one finds for the  $SU(3)^2 - U(1)$  anomaly with  $U(1) = \lambda_1 U(1)_1 + \lambda_2 U(1)_2$  (cf. table IV.10 for the  $U(1)$  charges) that

$$\begin{aligned} 2q(\mathbf{3}, \mathbf{2})[(\mathbf{3}, \mathbf{2})] + \sum_i q(\mathbf{3}_i^A)[\mathbf{3}_i^A] &= 2(\lambda_1 q_1 + \lambda_2 q_2)(\mathbf{3}, \mathbf{2})[(\mathbf{3}, \mathbf{2})] + \sum_i (\lambda_1 q_1 + \lambda_2 q_2)(\mathbf{3}_i^A)[\mathbf{3}_i^A] \\ &= [Y_4] \cdot \frac{1}{3} \left\{ \lambda_1 \left( (\alpha - 2\beta - 3\bar{K} - 2W_3) \cdot F_1 + (2W_2 - \alpha - \beta - 3\bar{K}) \cdot F_2 + (\alpha - 2E_1 + 2\bar{K}) \cdot W_3 \right) \right. \\ &\quad \left. + \lambda_2 \left( -2(\alpha + \beta + W_3) \cdot F_1 - (\alpha + \beta + 3\bar{K} + W_2) \cdot F_2 + (\alpha + E_1 + 2\bar{K}) \cdot W_3 \right) \right. \\ &\quad \left. + (\lambda_1 + \lambda_2) S_0 \cdot W_3 - (\lambda_1 S_1 + \lambda_2 U) \cdot W_3 \right\} \\ &\equiv [Y_4] \cdot \theta_4. \end{aligned} \tag{IV.128}$$

Note that in  $\theta_4$  the term  $-(\lambda_1 S_1 + \lambda_2 U) \cdot W_3$  is the only one giving non-zero contributions when integrated with valid  $G_4$  fluxes. Comparing with (IV.122), we see that this precisely matches the GS-counterterm, which in this case is  $-\int G_4 \wedge \omega \wedge W_3 = -\int G_4 \wedge (\lambda_1 S_1 + \lambda_2 U) \wedge W_3$ .

Concerning the  $SU(2)^2 - U(1)$  anomaly, we have

$$\begin{aligned} 3q(\mathbf{3}, \mathbf{2})[(\mathbf{3}, \mathbf{2})] + \sum_i q(\mathbf{2}_i^I)[\mathbf{2}_i^I] \\ &= [Y_4] \cdot \left\{ \frac{\lambda_1}{2} \left( (2\alpha - W_2 - W_3) \cdot E_1 + (3\bar{K} - \beta - W_2 - F_1 + S_0 - S_1) \cdot W_2 \right) \right. \\ &\quad \left. + \lambda_2 \left( (\alpha - \beta - \bar{K}) \cdot E_1 + (\beta - \alpha - F_1 - F_2 + \bar{K} + W_3 + S_0 - U) \cdot W_2 \right) \right. \\ &\quad \left. + (\lambda_1 + \lambda_2) S_0 \cdot W_2 - (\lambda_1 S_1 + \lambda_2 U) \cdot W_2 \right\} \end{aligned} \tag{IV.129}$$

Again this result agrees with (IV.123) by the same argument.

### 3.2.2 Abelian Anomalies — Determining Chiralities of missing Singlets

The remaining types of chiral anomalies are  $U(1)_a - U(1)_b - U(1)_c$  and  $U(1)$ -gravitational. Unfortunately, it is not possible to analyse these as above since the homology classes of the matter surfaces of the singlets  $\mathbf{1}^{(2)}$ ,  $\mathbf{1}^{(4)}$  and  $\mathbf{1}^{(6)}$ , which contribute to said anomalies, are harder to determine. As a result, we are not able to argue their cancellation directly.

But we can reverse the argumentation and use the anomaly matchings (IV.124) and (IV.125) – which we now assume to hold – to determine the chiralities of those singlets. In fact, with the chiralities all other states at hand (cf. table IV.12), we can explicitly solve (IV.124) and (IV.125) for  $\chi(\mathbf{1}^{(i)})$ ,  $i = 2, 4, 6$ , yielding the chiral indices as in table IV.13. Similar analyses have been also performed e.g. in [57].

$\mathcal{R}$	$\chi(\mathcal{R})$
$\mathbf{1}^{(2)}$	$  \begin{aligned}  & 3\alpha^2 W_3 z_3 + 3W_3 \left[ (\beta^2 + \beta W_3 + \bar{\mathcal{K}}(-3\bar{\mathcal{K}} + 2W_3)) z_1 \right. \\  & \quad \left. + (-2\beta^2 + 5\bar{\mathcal{K}}^2 - \beta(\bar{\mathcal{K}} + W_3) + (W_2 + W_3)^2 - \bar{\mathcal{K}}(3W_2 + 5W_3)) z_3 \right] \\  & + 6(\beta + 2\bar{\mathcal{K}})W_2(\beta - \bar{\mathcal{K}} + W_3)z_4 - \alpha(2\beta + 4\bar{\mathcal{K}} - W_2 - W_3)(\beta - \bar{\mathcal{K}} + W_3)z_5 \\  & \quad + (2\beta + 4\bar{\mathcal{K}} - W_2 - W_3)(\beta - \bar{\mathcal{K}} + W_3)(\beta - \bar{\mathcal{K}} + W_2 + W_3)z_5 \\  & + \alpha \left[ -3W_3(\beta - \bar{\mathcal{K}} + W_3)z_1 + 3(\beta + 2\bar{\mathcal{K}} - 2W_2 - W_3)W_3 z_3 - 6W_2(\beta - \bar{\mathcal{K}} + W_3)z_4 \right] \\  & \quad + \mathcal{D} \left[ \alpha^2 - 2\beta^2 + 5\bar{\mathcal{K}}^2 - 3\bar{\mathcal{K}}W_2 + W_2^2 + \alpha(\beta + 2\bar{\mathcal{K}} - 2W_2 - W_3) \right. \\  & \quad \left. - 5\bar{\mathcal{K}}W_3 + 2W_2W_3 + W_3^2 - \beta(\bar{\mathcal{K}} + W_3) \right]  \end{aligned}  $
$\mathbf{1}^{(4)}$	$  \begin{aligned}  & -3W_3 \left[ \alpha^2 - \beta^2 + \alpha(\bar{\mathcal{K}} - W_2 - W_3) + \beta(-3\bar{\mathcal{K}} + W_2 + W_3) + 2\bar{\mathcal{K}}(-2\bar{\mathcal{K}} + W_2 + W_3) \right] z_3 \\  & \quad + (\bar{\mathcal{K}} - \alpha)(\beta - \bar{\mathcal{K}} + W_3)(-\alpha + \beta - \bar{\mathcal{K}} + W_2 + W_3)z_5 \\  & \quad + (\mathcal{D} + \mathcal{D}') \left[ -2\alpha^2 + \beta^2 + \beta(2\bar{\mathcal{K}} - W_2 - W_3) \right. \\  & \quad \left. + \bar{\mathcal{K}}(5\bar{\mathcal{K}} - 3(W_2 + W_3)) + \alpha(\beta - \bar{\mathcal{K}} + 2(W_2 + W_3)) \right]  \end{aligned}  $
$\mathbf{1}^{(6)}$	$  \begin{aligned}  & 3W_3 \left[ (\alpha^2 + \alpha\beta)z_3 + (-\beta^2 + 5\bar{\mathcal{K}}^2 + \beta W_2 + W_3(W_2 + W_3) - \bar{\mathcal{K}}(W_2 + 4W_3))z_1 \right. \\  & \quad \left. + \bar{\mathcal{K}}(-\beta - 3\bar{\mathcal{K}} + W_2 + W_3)z_3 \right] + 6W_2(\beta - \bar{\mathcal{K}} + W_3)(-\beta - 3\bar{\mathcal{K}} + W_2 + W_3)z_4 \\  & - (2\beta + 4\bar{\mathcal{K}} - W_2 - W_3)(\beta - \bar{\mathcal{K}} + W_3)(\beta - \bar{\mathcal{K}} + W_2 + W_3)z_5 + \alpha \left\{ -3W_3(\beta - \bar{\mathcal{K}} + W_3)z_1 \right. \\  & \quad \left. - 3W_3(-\beta - 2\bar{\mathcal{K}} + W_2 + W_3)z_3 - 6W_2(\beta - \bar{\mathcal{K}} + W_3)z_4 \right. \\  & \quad \left. + (2\beta + 4\bar{\mathcal{K}} - W_2 - W_3)(\beta - \bar{\mathcal{K}} + W_3)z_5 \right\} \\  & + \mathcal{D}'(-2(\alpha^2 + \beta^2 - \alpha W_2 + \bar{\mathcal{K}}(-5\bar{\mathcal{K}} + 2W_2)) + (\alpha - \beta - 7\bar{\mathcal{K}} + W_2)W_3 + W_3^2)  \end{aligned}  $

**Table IV.13:** Chiral indices of the singlets with unknown homology classes induced by the flux (IV.117), computed by imposing anomaly cancellation.

However, we would like to take further advantage of our knowledge of the matter surfaces of the other states. As we will show now, we can actually solve the  $U(1)$ -anomaly matchings (IV.124) and (IV.125) on the level of matter surfaces. The result will be homology classes  $[\mathbf{1}^{(i)}]$ ,  $i = 2, 4, 6$  which are valid for any base  $\mathcal{B}$  and yield anomaly-free chiral indices  $\chi(\mathbf{1}^{(i)}) = \int_{Y_4} G_4 \wedge [\mathbf{1}^{(i)}]$  for any  $G_4$ .

We first consider the  $U(1)_1^2 - U(1)_2$  anomaly. By the charge assignments (IV.10) we see that, out of the missing singlets, only  $\mathbf{1}^{(4)}$  contributes to the left-hand side of the anomaly matching

(IV.124). Assuming the matching to hold, we can therefore deduce that

$$\begin{aligned} \int_{Y_4} G_4 \wedge [\mathbf{1}^{(4)}] &= \dim(\mathbf{1}^{(4)}) q_1^2(\mathbf{1}^{(4)}) q_2(\mathbf{1}^{(4)}) \chi(\mathbf{1}^{(4)}) \\ &= \int_{Y_4} G_4 \wedge \left( \frac{1}{2} (4 \pi_*(\omega_1 \cdot \omega_2) \wedge \omega_1 + 2 \pi_*(\omega_1 \cdot \omega_1) \wedge \omega_2) - \sum_{\mathcal{R} \neq \mathbf{1}^{(4)}} \dim(\mathcal{R}) q_1^2(\mathcal{R}) q_2(\mathcal{R}) [\mathcal{R}] \right). \end{aligned} \quad (\text{IV.130})$$

Since this is now supposed to hold for any  $G_4$  flux satisfying the transversality and gauge symmetry conditions, we conclude that we can compute the chirality of  $\mathbf{1}^{(4)}$  by integrating the flux over the 4-cycle

$$\left( \frac{1}{2} (4 \pi_*(\omega_1 \cdot \omega_2) \wedge \omega_1 + 2 \pi_*(\omega_1 \cdot \omega_1) \wedge \omega_2) - \sum_{\mathcal{R} \neq \mathbf{1}^{(4)}} \dim(\mathcal{R}) q_1^2(\mathcal{R}) q_2(\mathcal{R}) [\mathcal{R}] \right). \quad (\text{IV.131})$$

Inserting all the relevant 4-cycle and divisor classes one finds a lengthy expression which we omit in the interest of readability. However, since terms of the form  $D_1^{(\mathcal{B})} \cdot D_2^{(\mathcal{B})} + D^{(\mathcal{B})} \cdot S_0 + D^{(\mathcal{B})} \cdot \text{Ex}_i$  do not contribute to any  $G_4$  integration, we can drop them for the purpose of computing chirality. The result is now much more compact,

$$\begin{aligned} [\widetilde{\mathbf{1}^{(4)}}] &= S_1 (2 \alpha - 3 S_1 - 4 \beta - E_1 - 3 \bar{\mathcal{K}} + W_2 - 2 W_3) + U (2 \beta - 2 \alpha - 2 \bar{\mathcal{K}} + W_2 + 4 W_3) \\ &\quad + F_2 (E_1 + 2 F_1 + 3 F_2), \end{aligned} \quad (\text{IV.132})$$

while still giving the desired result  $\chi(\mathbf{1}^{(4)}) = \int_{Y_4} G_4 \wedge [\widetilde{\mathbf{1}^{(4)}}]$ . We stress that this is not the homology class of the actual matter surface of  $\mathbf{1}^{(4)}$ .<sup>9</sup>

As a first consistency check, we repeat the analogous computation for the  $U(1)_1 - U(1)_2^2$  anomaly. Again, only  $\mathbf{1}^{(4)}$  out of the missing singlets contributes. Due to the charge assignments, we should now have

$$\begin{aligned} \chi(\mathbf{1}^{(4)}) &= \\ &= \int_{Y_4} G_4 \wedge \left( \frac{1}{2} (4 \pi_*(\omega_1 \cdot \omega_2) \wedge \omega_2 + 2 \pi_*(\omega_2 \cdot \omega_2) \wedge \omega_1) - \sum_{\mathcal{R} \neq \mathbf{1}^{(4)}} \dim(\mathcal{R}) q_1(\mathcal{R}) q_2^2(\mathcal{R}) [\mathcal{R}] \right). \end{aligned}$$

Indeed, we find that while the 4-cycle inside the parentheses does not match the corresponding 4-cycle (IV.131) from the  $U(1)_1^2 - U(1)_2$  anomaly, the difference is of the form  $D_1^{(\mathcal{B})} \cdot D_2^{(\mathcal{B})} + D^{(\mathcal{B})} \cdot S_0 + D^{(\mathcal{B})} \cdot \text{Ex}_i$ , i.e. does not affect the calculation of the chiral index.

Having found a systematic way to compute the chirality for  $\mathbf{1}^{(4)}$ , we can now use the  $U(1)^3$  anomaly to pinpoint the homology class of  $\mathbf{1}^{(2)}$ , since the other still unknown missing singlet  $\mathbf{1}^{(6)}$  does not contribute as it is not charged under  $U(1)_1$ . We proceed as before and isolate the chiral index to be determined from the matching condition (IV.124):

$$\int_{Y_4} G_4 \wedge [\mathbf{1}^{(2)}] = \dim(\mathbf{1}^{(2)}) q_1^3(\mathbf{1}^{(2)}) \chi(\mathbf{1}^{(2)}) = \int_{Y_4} G_4 \wedge \left( \pi_*(\omega_1^2) \wedge \omega_1 - \sum_{\mathcal{R} \neq \mathbf{1}^{(2)}} \dim(\mathcal{R}) q_1^3(\mathcal{R}) [\mathcal{R}] \right). \quad (\text{IV.133})$$

<sup>9</sup> For instance if one computed the Cartan charges of  $\mathbf{1}^{(4)}$  based on this surface, one would find a non-zero result  $\int_{Y_4} \text{Ex}_i \wedge [\widetilde{\mathbf{1}^{(4)}}] \wedge D^{(\mathcal{B})} \neq 0$ .



On the right-hand side the sum now also runs over  $\mathcal{R} = \mathbf{1}^{(4)}$ , for which we use the above result  $[\widetilde{\mathbf{1}^{(4)}}]$  as the matter surface's homology class. By the same arguments as above, we find the expression

$$[\widetilde{\mathbf{1}^{(2)}}] = S_1 (3 S_1 - 2 \alpha + 3 \beta + 2 E_1 - 2 \bar{\mathcal{K}} + 4 W_3) + U (\alpha - \beta + 2 \bar{\mathcal{K}} - W_2 - 3 W_3) - F_2 (2 E_1 + F_1 + 2 F_2) \quad (\text{IV.134})$$

up to terms of the form  $D_1^{(\mathcal{B})} \cdot D_2^{(\mathcal{B})} + D^{(\mathcal{B})} \cdot S_0 + D'^{(\mathcal{B})} \cdot \text{Ex}_i$ .

Similarly, we can use the  $U(1)_2^3$  anomaly to determine the corresponding 4-cycle for  $\mathbf{1}^{(6)}$ . The matching condition in this case reads

$$\int_{Y_4} G_4 \wedge [\mathbf{1}^{(6)}] = \dim(\mathbf{1}^{(6)}) q_2^3(\mathbf{1}^{(6)}) \chi(\mathbf{1}^{(6)}) = \int_{Y_4} G_4 \wedge \left( \pi_*(\omega_2^2) \wedge \omega_2 - \sum_{\mathcal{R} \neq \mathbf{1}^{(6)}} \dim(\mathcal{R}) q_2^3(\mathcal{R}) [\mathcal{R}] \right). \quad (\text{IV.135})$$

Using (IV.132) for  $\mathcal{R} = \mathbf{1}^{(4)}$  ( $\mathbf{1}^{(2)}$  does not contribute) we find

$$[\widetilde{\mathbf{1}^{(6)}}] = 2 S_1 (S_1 - \alpha + 2 \beta + \bar{\mathcal{K}} + W_3) + U (-2 \beta - 2 \bar{\mathcal{K}} + W_2 - W_3) + (E_1 - F_2) F_2. \quad (\text{IV.136})$$

As a further non-trivial consistency check, we consider the  $U(1)$ -gravitational anomalies (IV.125), now using the expressions  $[\widetilde{\mathbf{1}^{(k)}}]$  for  $k = 2, 4, 6$  in the sum on the left-hand side. With these we indeed find that the 4-cycle  $\sum_{\mathcal{R}} \dim(\mathcal{R}) q_l(\mathcal{R}) [\mathcal{R}]$  is, up to terms of the form  $D_1^{(\mathcal{B})} \cdot D_2^{(\mathcal{B})} + D^{(\mathcal{B})} \cdot S_0 + D'^{(\mathcal{B})} \cdot \text{Ex}_k$ , equal to  $-6 S_1 \cdot \bar{\mathcal{K}}$  for  $l = 1$  and  $-6 U \cdot \bar{\mathcal{K}}$  for  $l = 2$ , thus confirming that the matching of  $U(1)$ -gravitational anomalies is consistent with the chiralities for the missing singlets we deduced from the matching of  $U(1)^3$  anomalies. Finally, we can compute the chiralities induced by the fluxes (IV.117), which unsurprisingly are identical to the results in table IV.13.

Note again that the classes  $[\widetilde{\mathbf{1}^{(k)}}]$  for  $k = 2, 4, 6$  are not the actual classes of the matter surfaces (see footnote 9). This implies that we cannot make any statement about whether or not the matter surfaces of these states are vertical in homology, even though this is expected. It would require new techniques to address this issue.

### 3.3 Flux quantisation and the Witten anomaly

In addition to gauge anomalies analysed in the previous section, our model has a further source of perturbative anomaly: the famous Witten anomaly haunting  $SU(2)$  gauge theories. Witten showed in [128] that any theories with an  $SU(2)$  gauge group must have an even number of doublets. In our model the statement can be phrased as

$$3 \chi((\mathbf{3}, \mathbf{2})) + \sum_i \chi(\mathbf{2}_i) \equiv 0 \pmod{2}. \quad (\text{IV.137})$$

Clearly, this is another type of a ‘discrete’ anomaly similar to the  $\mathbb{Z}_2$  anomaly in section 2.3.6, i.e. it depends on the specific integer values of chiral indices. It is not surprising that its cancellation in F-theory again relies on the quantisation condition. In the following we will show that the Witten anomaly is indeed cancelled by virtue of the quantisation condition, *provided* that in a consistent fibration over a smooth base an appropriately quantised flux always induces integer chiralities.

**$c_2(Y_4)$  in the  $I \times A$  Model**

As the quantisation condition involves the second Chern class  $c_2(Y_4)$  of the fourfold, we will briefly present its computation here for completeness. As in the  $SU(5)$  case (cf. section 2.3.6), the computation proceeds via the adjunction formula as

$$c(Y_4) = c(\{P_T\}) = \frac{c(X_5)}{1 + [P_T]} = \frac{1 + c_1(X_5) + c_2(X_5) + \dots}{1 + [P_T]} \quad (\text{IV.138})$$

$$Y_4 \xrightarrow{\text{Calabi-Yau}} c_2(Y_4) = c_2(X_5) - c_1(X_5)[P_T] + [P_T]^2 = c_2(X_5).$$

For a fibration over a generic base  $\mathcal{B}$  with two independent gauge divisors  $W_{2,3}$ , this can be calculated as

$$c(X_5) = c(\mathcal{B}) \frac{\prod_i (1 + D_i^{(T)})}{(1 + W_2)(1 + W_3)}, \quad (\text{IV.139})$$

where the toric divisors  $D_i^{(T)}$  are listed in table IV.9. Collecting all contributions of degree 2, we arrive at

$$\begin{aligned} c_2(Y_4) &= c_2(X_5) \\ &= c_2(\mathcal{B}) + F_2(2E_1 + 2F_1 + 3F_2) - S_1(2E_1 + 5S_1) \\ &\quad - \beta(E_1 - F_1 + F_2 - 2S_0 + 5S_1 - 3U) + \alpha(\beta - E_1 - 3F_1 - 4F_2 + 2S_1 - 2U) \quad (\text{IV.140}) \\ &\quad + \bar{\mathcal{K}}(\alpha + \beta - E_1 + F_1 - F_2 + 2S_0 + 2S_1 + 3U) + (\alpha - F_2 + S_0 + U)W_2 \\ &\quad + (4\alpha - E_1 + F_1 - 3F_2 + 4S_0 - 4S_1 + 4U)W_3. \end{aligned}$$

**Cancellation of Witten anomaly**

First let us, similarly to the previous section, compute the 4-cycle contributing to the anomaly,

$$\begin{aligned} 3[(\mathbf{3}, \mathbf{2})] + \sum_i [\mathbf{2}_i] &= [P_T] \cdot (-2E_1 \cdot F_2 - 2S_1 \cdot W_2 \\ &\quad + \text{terms of the form } D_a^{(\mathcal{B})} \cdot D_b^{(\mathcal{B})} + D^{(\mathcal{B})} \cdot \text{Ex}_i + D^{(\mathcal{B})} \cdot S_0). \end{aligned} \quad (\text{IV.141})$$

For the Witten anomaly to be cancelled, we thus need to show that

$$\begin{aligned} \int_{Y_4} G_4 \wedge (-2E_1 \wedge F_2 - 2S_1 \wedge W_2) &= 2 \int_{Y_4} G_4 \wedge (-E_1 \wedge F_2 - S_1 \wedge W_2) \equiv 0 \pmod{2} \\ \iff \int_{Y_4} G_4 \wedge (-E_1 \wedge F_2 - S_1 \wedge W_2) &\in \mathbb{Z}. \end{aligned} \quad (\text{IV.142})$$

At this point we invoke the quantisation condition: Using the obvious fact that  $E_1 \cdot F_2 + S_1 \cdot W_2$  is a manifestly integer class, (III.2) implies

$$\int_{Y_4} \left( G_4 + \frac{1}{2} c_2(Y_4) \right) \wedge (-E_1 \wedge F_2 - S_1 \wedge W_2) \in \mathbb{Z}, \quad (\text{IV.143})$$

where the second Chern class  $c_2(Y_4)$  can be easily computed by adjunction (for the explicit expression see (IV.140)). Thus (IV.142) follows if we can show that  $\frac{1}{2} \int_{Y_4} c_2(Y_4) \wedge (-E_1 \wedge F_2 - S_1 \wedge W_2) \in \mathbb{Z}$ . By straightforward calculation,

$$\begin{aligned} \frac{1}{2} \int_{Y_4} c_2(Y_4) \wedge (-E_1 \wedge F_2 - S_1 \wedge W_2) &= \\ \int_{\mathcal{B}} \left( \frac{1}{2} (W_2 W_3^2 - W_2^2 W_3 + W_2 W_3 \bar{\mathcal{K}}) + \frac{1}{2} W_2 (\bar{\mathcal{K}}^2 - c_2(\mathcal{B})) + \text{integer terms} \right) &\quad (\text{IV.144}) \end{aligned}$$

is not manifestly integer. However, it was shown in [121] that  $c_2(\mathcal{B}) - \bar{\mathcal{K}}^2$  is an even class for smooth complex threefolds, thus the second summand is integer for a smooth base  $\mathcal{B}$ . To argue that the first term is also integer, we have to make use of our assumption that, for consistent geometries, all chiral indices are integer. If this is true, then, again by the quantisation condition, considering the class  $[(\mathbf{3}, \mathbf{2})]$  (which is manifestly integer as a matter surface) yields the condition

$$\begin{aligned} \chi((\mathbf{3}, \mathbf{2})) + \frac{1}{2} \int_{Y_4} c_2(Y_4) \wedge [(\mathbf{3}, \mathbf{2})] &= \int_{Y_4} \left( G_4 + \frac{1}{2} c_2(Y_4) \right) \wedge [(\mathbf{3}, \mathbf{2})] \in \mathbb{Z} \\ \chi((\mathbf{3}, \mathbf{2})) \in \mathbb{Z} \implies \int_{Y_4} \frac{1}{2} c_2(Y_4) \wedge [(\mathbf{3}, \mathbf{2})] &= \int_{\mathcal{B}} \left( \frac{1}{2} (W_2^2 W_3 + W_2 W_3^2 - W_2 W_3 \bar{\mathcal{K}}) \right) \in \mathbb{Z}, \end{aligned} \quad (\text{IV.145})$$

which then implies the integrality of (IV.144).

To summarise: Based on the assumption that a consistent fibration implies integral chiral indices from a well-quantised flux, we have shown the cancellation of the Witten anomaly (IV.137) for (consistent) fibrations *over any (smooth) base*  $\mathcal{B}$ . Note that the assumption was also crucial to show the cancellation of  $\mathbb{Z}_2$  anomalies in section 2.3.6.

## 4 Summary of Chapter IV

The main topic of this chapter was to study vertical  $G_4$ -fluxes in three explicit F-theory models: a  $\text{Bl}_1\mathbb{P}_{112}$  fibration with  $SU(5) \times U(1)$ , a  $\mathbb{P}_{112}$  fibration with  $SU(5) \times \mathbb{Z}_2$  and a  $\text{Bl}_2\mathbb{P}^2$  fibration with  $SU(3) \times SU(2) \times U(1)^2$  gauge group. These models were constructed torically using the concept of tops. In all discussions, we kept the base of the fibrations generic, i.e. all results we derived are independent of the choice for  $\mathcal{B}$ . With the tools developed in chapter III, we were able to compute all vertical fluxes systematically. In addition, these novel tools also enabled us to determine the matter surfaces and their homology classes of all non-abelian matter states. With these data, we could verify the cancellation of pure and mixed non-abelian gauge anomalies for all models.

However, based on the knowledge of the homology classes of matter surfaces, we provided a different approach to anomalies in F-theory: By identifying appropriate 4-cycles of the fibration that are responsible for the anomaly, we could show in our explicit models that the concrete form of the  $G_4$ -flux is not of importance as long as it satisfies the transversality conditions set up in section 1.1 of chapter III. This geometric approach to anomalies may suggest some unknown mathematical properties common to torus fibred Calabi–Yau fourfolds. These properties, if existent, could be regarded as a geometric proof for the absence of gauge anomalies in 4D F-theory models.

Based on similar techniques, we have also studied discrete anomalies in our models. Concretely, we were concerned with the  $\mathbb{Z}_2$  and the Witten  $SU(2)$  anomalies. Being of discrete nature, it did not come as a surprise that the quantisation of  $G_4$  plays a crucial role. In fact, our analysis also required the physically motivated assumption that chiral indices must be integer in any consistent model. With this, we could prove explicitly that both discrete anomalies are cancelled for fibrations over any (smooth) base  $\mathcal{B}$ . Interestingly, the cancellation of  $\mathbb{Z}_2$  anomalies turned out to be a consequence of having integer chiralities in the  $U(1)$  model. Indeed, the  $\mathbb{Z}_2$  symmetry arises physically from the Higgsing of the  $U(1)$ . Consistency conditions (e.g. having integer chiralities) of the latter are therefore expected to be related to the absence of  $\mathbb{Z}_2$  anomalies.

We have also investigated the role of fluxes in this Higgsing/conifold transition from the  $U(1)$  to the  $\mathbb{Z}_2$  model. Under the transition, the topological quantities of D3-tadpole and chiral indices must be preserved. Thus, the flux background before and after the transition must be correlated. Indeed, we could provide an explicit map that identifies a unique flux background in the  $\mathbb{Z}_2$  fibration for a given configuration of vertical fluxes on the  $U(1)$  side. Crucially, this map requires a non-vertical flux on the  $\mathbb{Z}_2$  side, which was identified as a 4-cycle that becomes algebraic for certain complex structure parameters of the  $\mathbb{P}_{112}$  fibration.

**D3-tadpole of the general flux in Standard Model fibrations**

Here we give, for completeness, the explicit formula for the D3-brane charge  $\frac{1}{2} \int_{Y_4} G_4^2$  induced by the general flux  $G_4 = \sum_i z_i G_4^{z_i} + G_4^{(1)}(\mathcal{D}) + G_4^{(2)}(\mathcal{D}')$  as given in (IV.116). On the right hand side, the threefold products of vertical divisor classes are to be understood as intersection numbers on the base  $\mathcal{B}$ :

$$\begin{aligned}
 \frac{\chi(Y_4)}{24} - n_3 &= \frac{1}{2} \int_{Y_4} G_4 \wedge G_4 = & \text{(IV.146)} \\
 \frac{1}{2} & \left[ (-12 z_2^2 - 12 z_2 z_3 - 24 z_2 z_4 - 3 z_3^2 - 12 z_3 z_4 + 24 z_4^2 + 12 z_4 z_5 + z_5^2) W_2^2 W_3 \right. \\
 & + (12 z_1 z_2 + 6 z_1 z_3 + 48 z_1 z_4 + 6 z_1 z_5 - 18 z_2^2 - 24 z_2 z_3 - 72 z_2 z_4 - 3 z_3^2 - 60 z_3 z_4 - 6 z_3 z_5 - 72 z_4^2 \\
 & + 12 z_4 z_5 + 3 z_5^2) W_2 W_3^2 + (6 z_1^2 - 6 z_1 z_3 + 6 z_1 z_5 + 6 z_3^2 - 6 z_3 z_5 + 2 z_5^2) W_3^3 \\
 & + (-36 z_4^2 - 12 z_4 z_5 - z_5^2) W_2^2 \bar{\mathcal{K}} + (12 z_1 z_2 + 6 z_1 z_3 - 24 z_1 z_4 - 6 z_1 z_5 + 36 z_2^2 + 24 z_2 z_3 + 108 z_2 z_4 \\
 & + 3 z_3^2 + 60 z_3 z_4 + 6 z_3 z_5 + 72 z_4^2 - 24 z_4 z_5 - 5 z_5^2) W_2 W_3 \bar{\mathcal{K}} \\
 & + (-15 z_1^2 + 18 z_1 z_3 - 12 z_1 z_5 - 21 z_3^2 + 12 z_3 z_5 - 5 z_5^2) W_3^2 \bar{\mathcal{K}} + (18 z_4^2 + 12 z_4 z_5 + 2 z_5^2) W_2 \bar{\mathcal{K}}^2 \\
 & + (6 z_1^2 + 6 z_1 z_3 + 6 z_1 z_5 + 6 z_3^2 - 6 z_3 z_5 + 4 z_5^2) W_3 \bar{\mathcal{K}}^2 - z_5^2 \bar{\mathcal{K}}^3 \\
 & + (12 z_2 z_3 + 6 z_3^2 + 12 z_3 z_4 - 12 z_4 z_5 - 2 z_5^2) W_2 W_3 \alpha \\
 & + (-6 z_1 z_3 - 6 z_1 z_5 + 3 z_3^2 + 6 z_3 z_5 - 3 z_5^2) W_3^2 \alpha + (12 z_4 z_5 + 2 z_5^2) W_2 \bar{\mathcal{K}} \alpha \\
 & + (-6 z_1 z_3 + 6 z_1 z_5 - 3 z_3^2 - 6 z_3 z_5 + 5 z_5^2) W_3 \bar{\mathcal{K}} \alpha - 2 z_5^2 \bar{\mathcal{K}}^2 \alpha + (-3 z_3^2 + z_5^2) W_3 \alpha^2 \\
 & - z_5^2 \bar{\mathcal{K}} \alpha^2 + (36 z_4^2 + 12 z_4 z_5 + z_5^2) W_2^2 \beta + (12 z_1 z_2 + 6 z_1 z_3 + 48 z_1 z_4 + 6 z_1 z_5 - 36 z_2 z_4 \\
 & - 36 z_3 z_4 - 6 z_3 z_5 - 72 z_4^2 + 24 z_4 z_5 + 6 z_5^2) W_2 W_3 \beta + (3 z_1^2 - 6 z_1 z_3 + 12 z_1 z_5 - 12 z_3 z_5 \\
 & + 6 z_5^2) W_3^2 \beta + (-24 z_4 z_5 - 5 z_5^2) W_2 \bar{\mathcal{K}} \beta + (3 z_1^2 + 6 z_1 z_3 - 12 z_1 z_5 + 12 z_3 z_5 - 10 z_5^2) W_3 \bar{\mathcal{K}} \beta \\
 & + 4 z_5^2 \bar{\mathcal{K}}^2 \beta + (-12 z_4 z_5 - 2 z_5^2) W_2 \alpha \beta + (-6 z_1 z_3 - 6 z_1 z_5 + 6 z_3 z_5 - 6 z_5^2) W_3 \alpha \beta + 5 z_5^2 \bar{\mathcal{K}} \alpha \beta \\
 & + z_5^2 \alpha^2 \beta + (-18 z_4^2 + 12 z_4 z_5 + 3 z_5^2) W_2 \beta^2 + (-3 z_1^2 + 6 z_1 z_5 - 6 z_3 z_5 + 6 z_5^2) W_3 \beta^2 - 5 z_5^2 \bar{\mathcal{K}} \beta^2 \\
 & - 3 z_5^2 \alpha \beta^2 + 2 z_5^2 \beta^3 + (-2 z_2 + 2 z_3 - 8 z_4 - 2 z_5) W_2 W_3 \mathcal{D} + (-2 z_1 + 4 z_3 - 2 z_5) W_3^2 \mathcal{D} \\
 & + (6 z_4 + 2 z_5) W_2 \bar{\mathcal{K}} \mathcal{D} + (4 z_1 - 10 z_3 + 4 z_5) W_3 \bar{\mathcal{K}} \mathcal{D} - 2 z_5 \bar{\mathcal{K}}^2 \mathcal{D} + (-2 z_3 + 2 z_5) W_3 \alpha \mathcal{D} \\
 & - 2 z_5 \bar{\mathcal{K}} \alpha \mathcal{D} + (-6 z_4 - 2 z_5) W_2 \beta \mathcal{D} + (-2 z_1 - 4 z_5) W_3 \beta \mathcal{D} + 4 z_5 \bar{\mathcal{K}} \beta \mathcal{D} + 2 z_5 \alpha \beta \mathcal{D} \\
 & - 2 z_5 \beta^2 \mathcal{D} + 1/2 W_2 \mathcal{D}^2 + 2/3 W_3 \mathcal{D}^2 - 2 \bar{\mathcal{K}} \mathcal{D}^2 + (4 z_2 + 2 z_3 + 16 z_4 + 2 z_5) W_2 W_3 \mathcal{D}' \\
 & + (4 z_1 - 2 z_3 + 2 z_5) W_3^2 \mathcal{D}' + (-12 z_4 - 2 z_5) W_2 \bar{\mathcal{K}} \mathcal{D}' + (-8 z_1 + 2 z_3 - 4 z_5) W_3 \bar{\mathcal{K}} \mathcal{D}' + 2 z_5 \bar{\mathcal{K}}^2 \mathcal{D}' \\
 & + (-2 z_3 - 2 z_5) W_3 \alpha \mathcal{D}' + 2 z_5 \bar{\mathcal{K}} \alpha \mathcal{D}' + (12 z_4 + 2 z_5) W_2 \beta \mathcal{D}' + (4 z_1 - 6 z_3 + 4 z_5) W_3 \beta \mathcal{D}' \\
 & - 4 z_5 \bar{\mathcal{K}} \beta \mathcal{D}' - 2 z_5 \alpha \beta \mathcal{D}' + 2 z_5 \beta^2 \mathcal{D}' - 2/3 W_3 \mathcal{D} \mathcal{D}' - 2 \bar{\mathcal{K}} \mathcal{D} \mathcal{D}' + 2 \alpha \mathcal{D} \mathcal{D}' - 2 \beta \mathcal{D} \mathcal{D}' \\
 & \left. + 2/3 W_3 \mathcal{D}'^2 - 4 \bar{\mathcal{K}} \mathcal{D}'^2 + 2 \alpha \mathcal{D}'^2 \right].
 \end{aligned}$$

# Chapter V

## Towards the Standard Model in F-theory

After the formal discussions of the previous chapters, we would like to argue in this part that F-theory provides an interesting playground for model building. Specifically, we would like to focus on the compactification with the extended Standard Model gauge group  $SU(3) \times SU(2) \times U(1) \times U(1)$  presented in the previous chapter and compare the phenomenology of the resulting 4D effective field theory to the Standard Model. In a second step, we also include a systematic analysis of fluxes in these compactifications to investigate possible realisations of the correct chiral spectrum. The results of this chapter are taken from [13, 15]

### 1 Yukawa Couplings in the $SU(3) \times SU(2) \times U(1)^2$ Geometry

An important phenomenological aspect of F-theory compactifications are the geometrically realised Yukawa couplings. These will have a leading contribution to the effective coupling in 4D, whereas in comparison other effects like instantons corrections are perturbatively suppressed. In this section we want to explicitly determine all the geometrically realised Yukawa couplings in our extended Standard Models. This requires a more detailed construction of the full geometry than the presentation in the previous chapter, where for compactness we have only focused on the matter surfaces.

The construction of the extended Standard Model gauge group can be split into several steps, along which different sets of Yukawa couplings can be pinpointed:

1. Choose the global fibration structure with the appropriate Mordell–Weil group of rank 2 realising two  $U(1)$  generators. The global structure will determine the spectrum of singlets and their interaction structure.
2. Construct an  $SU(2)$  gauge factor by introducing singularities along divisor  $W_2$  in the base. This introduces matter charged under  $SU(2)$  and both  $U(1)$ s and fixes the interactions among them and the singlets.
3. Analogously construct an  $SU(3)$  gauge factor via singularities along divisor  $W_3$ . The resulting geometry has additional states charged under  $SU(3)$  and the  $U(1)$ s, whose interactions amongst each other and with the singlets can be studied independent of the  $SU(2)$  gauge factor.
4. Combine both singularity structures to obtain the full gauge group. In this step, new matter states charged under all gauge groups arise, along with interactions of these with the  $SU(3)$  and  $SU(2)$  matter. Other couplings involving only  $SU(3)$  or  $SU(2)$  states and/or singlets remain unchanged.

### 1.1 F-theory with $U(1) \times U(1)$ gauge group

F-theory compactifications with two abelian gauge groups are based on elliptic fibrations with Mordell-Weil group of rank two. Such elliptic fibrations allow for a description as the vanishing locus of the hypersurface polynomial [57, 58, 80, 126, 127]

$$P_T = v w (c_1 w s_1 + c_2 v s_0) + u (b_0 v^2 s_0^2 + b_1 v w s_0 s_1 + b_2 w^2 s_1^2) + u^2 (d_0 v s_0^2 s_1 + d_1 w s_0 s_1^2 + d_2 u s_0^2 s_1^2) \quad (\text{V.1})$$

inside a  $\text{Bl}_2\mathbb{P}^2$ -fibration. Such types of fibration had previously been considered also in [129]. The ambient space  $\text{Bl}_2\mathbb{P}^2$  of the elliptic fibre is a toric space which has the toric diagram represented by polygon 5 in the classification [71] (see also figure B.1 in the appendix). Here and in the sequel we will stick to the notation of [58, 126] and denote the coordinates of  $\text{Bl}_2\mathbb{P}^2$  by  $u, v, w, s_0, s_1$ , where  $s_0$  and  $s_1$  correspond to two blow-up  $\mathbb{P}^1$ s inside  $\mathbb{P}^2$  with homogeneous coordinates  $[u : w : v]$ . The Stanley–Reisner ideal is generated by  $\{u v, u w, s_0 w, s_1 v, s_0 s_1\}$  and the divisor classes associated with the fibre ambient space coordinates are given as follows:

	u	v	w	$s_0$	$s_1$	
$\alpha$	·	·	1	·	·	
$\beta$	·	1	·	·	·	
$U$	1	1	1	·	·	
$S_0$	·	·	1	1	·	
$S_1$	·	1	·	·	1	

(V.2)

A fibration of this toric space over a base  $\mathcal{B}$  is parametrised by the choice of two line bundles  $\alpha, \beta \in H^{(1,1)}(\mathcal{B})$ , in which the coordinates  $w$  resp.  $v$  transform as sections. The coefficients  $b_i, c_j, d_k$  transform as sections of certain line bundles over  $\mathcal{B}$ , whose class is determined by the requirement that the hypersurface (V.1) is Calabi–Yau. These classes are collected in table V.1 (taken from [126]; see also [57, 80, 127]). For suitable 3-dimensional base spaces  $\mathcal{B}$  the hypersurface

$b_0$	$b_1$	$b_2$	$c_1$	$c_2$	$d_0$	$d_1$	$d_2$
$\alpha - \beta + \bar{\mathcal{K}}$	$\bar{\mathcal{K}}$	$-\alpha + \beta + \bar{\mathcal{K}}$	$-\alpha + \bar{\mathcal{K}}$	$-\beta + \bar{\mathcal{K}}$	$\alpha + \bar{\mathcal{K}}$	$\beta + \bar{\mathcal{K}}$	$\alpha + \beta + \bar{\mathcal{K}}$

**Table V.1:** Classes of the sections appearing in (V.1), with  $\alpha$  and  $\beta$  pullback of classes of  $\mathcal{B}$  and  $\bar{\mathcal{K}} = \pi^{-1}(c_1(\mathcal{B}))$  the anti-canonical bundle of  $\mathcal{B}$ .

(V.1) then describes a smooth elliptically fibred Calabi–Yau 4-fold

$$\pi : Y_4 \rightarrow \mathcal{B}. \quad (\text{V.3})$$

It exhibits three independent rational sections

$$U = \{u\}, \quad S_0 = \{s_0\}, \quad S_1 = \{s_1\}. \quad (\text{V.4})$$

One of these sections, e.g.  $S_0$ , can be interpreted as the zero-section.<sup>1</sup> The image of the remaining two independent sections under the Shioda map [101, 130, 131] then identifies the generators of two independent  $U(1)$  gauge groups as [57, 58, 80, 126]

$$\begin{aligned} \omega_1 &= S_1 - S_0 - \bar{\mathcal{K}}, \\ \omega_2 &= U - S_0 - \bar{\mathcal{K}} - [c_1], \end{aligned} \quad (\text{V.5})$$

<sup>1</sup>The fact that all three independent sections are rational (as opposed to holomorphic) is an artefact of the representation of the fibration as a hypersurface. Indeed, the fibration is birationally equivalent to a complete intersection which does exhibit a holomorphic zero-section [126]. The pre-image of this section under the birational map can be identified with the zero section [58, 126]. Alternatively, one can define an F-theory compactification with a rational zero-section as in [57, 78, 80].

where  $\overline{\mathcal{K}} = \pi^{-1}\overline{\mathcal{K}}_{\mathcal{B}}$  is the anti-canonical bundle of the base  $\mathcal{B}$ . Here and in the sequel our notation does not distinguish between a divisor (class) and its Poincaré-dual  $(1,1)$ -form. Also, if there is no confusion possible, we denote the divisor and its associated codimension one locus by the same variable.

In our analysis of the matter representations of F-theory compactified on  $Y_4$  we will also need the form of the singular Weierstrass model which is birationally equivalent to the blow-down of the hypersurface (V.1) (i.e. the hypersurface inside the  $\mathbb{P}^2$ -fibration over  $\mathcal{B}$  achieved by setting  $s_0 = s_1 = 1$  in (V.1)). The explicit map of this blow-down to Weierstrass form

$$y^2 = x^3 + f x z^4 + g z^6 \quad (\text{V.6})$$

has been worked out in the physics literature in [57,58,80,126]. In our subsequent analysis we will make use of the expression for the Weierstrass sections  $f$  and  $g$  in terms of the defining sections  $b_i, c_j, d_k$  appearing in (V.1) as given after equation (2.38) and (2.39) in [58], which we recall here for completeness,

$$f = -\frac{1}{3}d^2 + c e \quad \text{and} \quad g = -f \left( \frac{1}{3}d \right) - \left( \frac{1}{3}d \right)^3 + c^2 k, \quad (\text{V.7})$$

where

$$\begin{aligned} d &= b_1^2 + 8 b_0 b_2 - 4 c_1 d_0 - 4 c_2 d_1, \\ c &= -\frac{4}{c_1} (b_0 b_2^2 - b_2 c_1 d_0 + c_1^2 d_2), \\ e &= \frac{2c_1 (b_0 (b_1 c_1 d_1 - b_1^2 b_2 + 2b_2 c_1 d_0 + 2b_2 c_2 d_1 - 2c_1^2 d_2))}{b_0 b_2^2 + c_1 (c_1 d_2 - b_2 d_0)} + \\ &\quad + \frac{2c_1 (-2b_0^2 b_2^2 + c_2 (b_1 b_2 d_0 + b_1 c_1 d_2 - 2b_2 c_2 d_2 - 2c_1 d_0 d_1))}{b_0 b_2^2 + c_1 (c_1 d_2 - b_2 d_0)}, \\ k &= \frac{c_1^2 (b_0 b_1 b_2 - b_0 c_1 d_1 - b_2 c_2 d_0 + c_1 c_2 d_2)^2}{(b_0 b_2^2 + c_1 (c_1 d_2 - b_2 d_0))^2}. \end{aligned} \quad (\text{V.8})$$

### 1.1.1 Charged singlets and their Yukawa couplings

The fibration gives rise to six types of charged singlet states  $\mathbf{1}^{(i)}$  localised on curves on  $\mathcal{B}$ , which have already been analysed in [57,58,80,126,127]. Here we continue with the analysis of [58,126] (alternatively, see [57,80]), which derives the curves as loci in the base over which the fibre of the blown-down version of (V.1) exhibits a conifold singularity. These loci are given as the union of the set of solutions to each of the following three pairs of equations,

$$\begin{aligned} 0 &= d_0 c_2^2 + b_0^2 c_1 - b_0 b_1 c_2, \\ 0 &= d_1 b_0 c_2 - b_0^2 b_2 - c_2^2 d_2, \end{aligned} \quad (\text{V.9})$$

and

$$\begin{aligned} 0 &= d_0 b_2 c_1 - b_0 b_2^2 - c_1^2 d_2, \\ 0 &= d_1 c_1^2 - b_1 b_2 c_1 + b_2^2 c_2, \end{aligned} \quad (\text{V.10})$$

and

$$\begin{aligned} 0 &= d_0 c_1^3 c_2^2 + b_0^2 c_1^4 - b_0 b_1 c_1^3 c_2 - c_2^3 (b_2^2 c_2 - b_1 b_2 c_1 + c_1^2 d_1), \\ 0 &= d_2 c_1^4 c_2^2 + (b_0 c_1^2 + c_2 (-b_1 c_1 + b_2 c_2))(b_0 b_2 c_1^2 + c_2 (-b_1 b_2 c_1 + b_2^2 c_2 + c_1^2 d_1)). \end{aligned} \quad (\text{V.11})$$

In [58, 126] three singlet curves were identified as complete intersections:  $C^{(1)} = \{b_0\} \cap \{c_2\}$  solves both (V.9) and (V.11),  $C^{(3)} = \{b_2\} \cap \{c_1\}$  solves (V.10) and (V.11), and  $C^{(5)} = \{c_1\} \cap \{c_2\}$  solves (V.11). If one inserts these equations into the hypersurface polynomial (V.1) one confirms that the fibre factorises into two  $\mathbb{P}^1$ s and can identify the singlet states as M2-branes wrapping one of the fibre components. The remaining three curves were represented in [58, 126] as (V.9) with  $b_0 \neq 0 \neq c_2$  ( $C^{(2)}$ ), (V.10) with  $b_2 \neq 0 \neq c_1$  ( $C^{(4)}$ ), and (V.11) with  $b_0 \neq 0 \neq b_2$  and  $c_1 \neq 0 \neq c_2$  ( $C^{(6)}$ ). Plugging these more lengthy expressions into the hypersurface equation also leads to a factorisation of the fibre, i.e. the appearance of charged singlets. Their location and charges are summarised in table V.2.

singlet	locus	$(U(1)_1, U(1)_2)$ -charges
$\mathbf{1}^{(1)}/\bar{\mathbf{1}}^{(1)}$	$\{b_0\} \cap \{c_2\}$	$(1, -1)/(-1, 1)$
$\mathbf{1}^{(2)}/\bar{\mathbf{1}}^{(2)}$	$C^{(2)}$	$(1, 0)/(-1, 0)$
$\mathbf{1}^{(3)}/\bar{\mathbf{1}}^{(3)}$	$\{b_2\} \cap \{c_1\}$	$(1, 2)/(-1, -2)$
$\mathbf{1}^{(4)}/\bar{\mathbf{1}}^{(4)}$	$C^{(4)}$	$(1, 1)/(-1, -1)$
$\mathbf{1}^{(5)}/\bar{\mathbf{1}}^{(5)}$	$\{c_1\} \cap \{c_2\}$	$(0, 2)/(0, -2)$
$\mathbf{1}^{(6)}/\bar{\mathbf{1}}^{(6)}$	$C^{(6)}$	$(0, 1)/(0, -1)$

**Table V.2:** Singlet states in the  $\text{Bl}_2\mathbb{P}^2$ -fibration.

From the charge assignment we expect six types of Yukawa couplings. Of these, the couplings  $\mathbf{1}^{(1)}\bar{\mathbf{1}}^{(4)}\mathbf{1}^{(5)}$  over  $b_0 = c_1 = c_2 = 0$ ,  $\mathbf{1}^{(2)}\bar{\mathbf{1}}^{(3)}\mathbf{1}^{(5)}$  over  $b_2 = c_1 = c_2 = 0$ , and  $\mathbf{1}^{(2)}\bar{\mathbf{1}}^{(4)}\mathbf{1}^{(6)}$  over  $C^{(2)} \cap C^{(4)} \cap C^{(6)}$  can in fact be directly seen [58, 80] when plugging in the corresponding equations of the curves into the hypersurface polynomial. However the charges also allow for couplings  $\mathbf{1}^{(1)}\bar{\mathbf{1}}^{(2)}\mathbf{1}^{(6)}$ ,  $\bar{\mathbf{1}}^{(3)}\mathbf{1}^{(4)}\mathbf{1}^{(6)}$  and  $\bar{\mathbf{1}}^{(5)}\mathbf{1}^{(6)}\mathbf{1}^{(6)}$ , which due to the form of the curves  $C^{(2)}$ ,  $C^{(4)}$ ,  $C^{(6)}$  are more complicated to analyse. The difficulty is that the set of solutions to equations (V.9) to (V.11) consists of several irreducible components which intersect each other precisely at the interesting Yukawa points. To find an appropriate form of the singlet curves, we employ the commutative algebra tools described in section 3 of chapter III.

To this end, we regard (V.9) – (V.11) to each define an ideal generated by two polynomials within the polynomial ring  $R = \mathbb{C}[b_i, c_j, d_k]$  of the base  $\mathcal{B}$ , with the sections  $b_i, c_j, d_k$  treated as independent variables. Computing the primary decomposition for each of the three ideals yields several isolated components, of which we are only interested in the curve components, i.e. those of codimension two. Concretely, the decomposition of (V.9) yields a complete intersection  $I^{(1)} = \langle b_0, c_2 \rangle$  and a curve component  $I^{(2)}$  with six generators, corresponding to the loci of  $\mathbf{1}^{(1)}$  and  $\mathbf{1}^{(2)}$ , respectively. Likewise, the decomposition of (V.10) yields  $I^{(3)} = \langle b_2, c_1 \rangle$  and  $I^{(4)}$  with six generators, corresponding to the loci of  $\mathbf{1}^{(3)}$  and  $\mathbf{1}^{(4)}$ . The decomposition of (V.11) is slightly more tricky to compute, because **Singular** cannot compute the associated primes directly. However, as we noted above in the definition of  $C^{(6)}$ , the locus defined by (V.11) also contains the loci  $I^{(1)}$ ,  $I^{(3)}$  and  $I^{(5)} = \langle c_1, c_2 \rangle$ . This means that we can ‘simplify’ the ideal (V.11) by saturating with respect to  $I^{(1)}$ ,  $I^{(3)}$  and  $I^{(5)}$ . Indeed, after this simplification, the resulting ideal has only one irreducible associated prime  $I^{(6)}$  generated by 39 generators, corresponding to the loci of  $\mathbf{1}^{(6)}$ .

With this technique we can now analyse the Yukawa couplings  $\mathbf{1}^{(1)}\bar{\mathbf{1}}^{(2)}\mathbf{1}^{(6)}$ ,  $\bar{\mathbf{1}}^{(3)}\mathbf{1}^{(4)}\mathbf{1}^{(6)}$  and  $\bar{\mathbf{1}}^{(5)}\mathbf{1}^{(6)}\mathbf{1}^{(6)}$ . To this end we first calculate the minimal associated prime ideals of the sum of the ideals corresponding to the curves. In each case we indeed find a prime ideal corresponding to a codimension three locus, confirming the existence of the intersection points of those triplets of



singlet curves. All three codimension three intersection loci are in fact complete intersections,

$$\begin{aligned} & \mathbb{V}(I^{(1)}) \cap \mathbb{V}(I^{(2)}) \cap \mathbb{V}(I^{(6)}) = \\ & \{b_0\} \cap \{c_2\} \cap \{b_2^2 d_0^2 - b_1 b_2 d_0 d_1 + c_1 d_0 d_1^2 + b_1^2 b_2 d_2 - 2 b_2 c_1 d_0 d_2 - b_1 c_1 d_1 d_2 + c_1^2 d_2^2\}, \end{aligned} \quad (\text{V.12})$$

$$\begin{aligned} & \mathbb{V}(I^{(3)}) \cap \mathbb{V}(I^{(4)}) \cap \mathbb{V}(I^{(6)}) = \\ & \{b_2\} \cap \{c_1\} \cap \{b_0^2 d_1^2 - b_0 b_1 d_0 d_1 + c_2 d_1 d_0^2 + b_0 b_1^2 d_2 - b_1 c_2 d_0 d_2 - 2 b_0 c_2 d_1 d_2 + c_2^2 d_2^2\}, \end{aligned} \quad (\text{V.13})$$

$$\begin{aligned} & \mathbb{V}(I^{(5)}) \cap \mathbb{V}(I^{(6)}) \cap \mathbb{V}(I^{(6)}) = \\ & \{c_1\} \cap \{c_2\} \cap \{b_1 d_0 d_1 - b_2 d_0^2 - b_0 d_1^2 - b_1^2 d_2 + 4 b_0 b_2 d_2\}. \end{aligned} \quad (\text{V.14})$$

Interestingly, the last set of Yukawa points (V.14) coincides with a singular locus of  $\mathbb{V}(I^{(6)})$ , which we computed with **Singular**. Due to the complicated form of  $\mathbb{V}(I^{(6)})$ , we are unable to determine the type of the singularity, but the form of the Yukawa coupling involving two  $\mathbf{1}^{(6)}$ -states suggests that it is a point of self-intersection of the  $\mathbf{1}^{(6)}$ -curve where also the  $\mathbf{1}^{(5)}$ -curve passes through.

The final proof for the existence of the Yukawa couplings comes by inspecting the fibre over the intersection points. The couplings  $\mathbf{1}^{(1)} \bar{\mathbf{1}}^{(2)} \mathbf{1}^{(6)}$  and  $\bar{\mathbf{1}}^{(3)} \mathbf{1}^{(4)} \mathbf{1}^{(6)}$  have already been argued to exist geometrically in [57] using the ‘prime ideal technique’, and independently in [126] in an indirect manner by exploiting their formal relation to the chiral index of certain  $G_4$ -fluxes. Here we therefore focus on the remaining  $\bar{\mathbf{1}}^{(5)} \mathbf{1}^{(6)} \mathbf{1}^{(6)}$  coupling. If we solve the last equation in (V.14) for  $b_1 = (d_0 d_1 \pm \sqrt{d_0^2 - 4 b_0 d_2} \sqrt{d_1^2 - 4 b_2 d_2}) / (2 d_2)$ , we see that the complete intersection locus (V.14) really consists of two sets of points defined by each sign. Note that as far as codimension three loci are concerned the appearance of the square root of expressions involving the sections  $b_i, c_j, d_k$ , or of  $d_2$  in the denominator does not pose any problems, as these expressions are just complex numbers and not affected by any monodromy issues. Plugging this together with  $c_1 = c_2 = 0$  into the hypersurface polynomial (V.1) yields, after some tedious algebra, the factorisation

$$\begin{aligned} & P_T|_{c_1=c_2=0, b_1=(d_0 d_1 \pm \sqrt{d_0^2 - 4 b_0 d_2} \sqrt{d_1^2 - 4 b_2 d_2}) / (2 d_2)} = \frac{1}{4 d_2} \mathbf{u} \\ & \times \left[ 2 d_2 s_0 s_1 \mathbf{u} + \left( d_0 - \sqrt{d_0^2 - 4 b_0 d_2} \right) s_0 \mathbf{v} + \left( d_1 \pm \sqrt{d_1^2 - 4 b_2 d_2} \right) s_1 \mathbf{w} \right] \\ & \times \left[ 2 d_2 s_0 s_1 \mathbf{u} + \left( d_0 + \sqrt{d_0^2 - 4 b_0 d_2} \right) s_0 \mathbf{v} + \left( d_1 \mp \sqrt{d_1^2 - 4 b_2 d_2} \right) s_1 \mathbf{w} \right], \end{aligned} \quad (\text{V.15})$$

which is well-defined since no fibre coordinate appears under the square root. The fibre component defined by the factor  $\mathbf{u}$  corresponds to the singlet state  $\bar{\mathbf{1}}^{(5)}$ , as explicit calculation of the intersection numbers with the  $U(1)$  generators (V.5) using the Stanley-Reissner ideal and the divisor table (V.2) quickly shows. The other two components are obviously in the same divisor class of the fibre ambient space and must have the same intersection numbers; indeed their intersection numbers with the  $U(1)$  generators reveal that both correspond to  $\mathbf{1}^{(6)}$ -states. Furthermore, each component intersects the others exactly once, giving rise to an affine  $SU(3)$  diagram. Similar calculations also verify the analogous fibre structure enhancement over the other two Yukawa points (V.12) and (V.13). More details may be found in [132].

Having fully analysed the abelian sector of the models, we now proceed to add non-abelian symmetries, starting with the  $SU(2)$  factor.

## 1.2 Toric fibrations with additional $SU(2)$ symmetry

In this section we analyse in detail toric realisations of gauge group  $SU(2)$  along a base divisor

$$W_2 = [\{w_2 = 0\}] \quad (\text{V.16})$$

in elliptic fibrations of type (V.1). As detailed in appendix 1, the fibres of such toric models are described by the three  $A_1$ -tops over polygon 5 [71].

Recall that the top construction yields resolved fibrations, whose singular limit consists of the restriction of the coefficients  $b_i, c_j, d_k$  to vanish to certain powers along a divisor  $W = \{w\}$ . The resolution of an  $SU(2)$  singularity over a divisor  $W_2$  requires one resolution divisor  $E_1 = \{e_1\}$  corresponding to the single (simple) root  $-\alpha$  of  $SU(2)$ . Over a generic point on  $W_2$ , the fibre splits into two  $\mathbb{P}^1$ -components described by

$$\mathbb{P}_i^1 = \{e_i\} \cap \{P_T\} \cap D_a^{(\mathcal{B})} \cap D_b^{(\mathcal{B})} \quad (\text{V.17})$$

for  $i = 0, 1$ , where  $D_{a,b}^{(\mathcal{B})}$  are two generic divisors in the base. These two  $\mathbb{P}^1$ s intersect in the affine  $SU(2)$  diagram and will split into further  $\mathbb{P}^1$ s over matter curves and Yukawa points.

### 1.2.1 $SU(2)$ -I top

The first  $A_1$ -top, depicted in figure B.2 in appendix 1, corresponds to the following restrictions of the coefficients of the hypersurface polynomial (V.1),

$$b_0 = b_{0,1} e_0, \quad b_2 = b_{2,0} e_1, \quad c_1 = c_{1,0} e_1, \quad d_0 = d_{0,1} e_0, \quad d_2 = d_{2,1} e_0, \quad (\text{V.18})$$

while the other coefficients remain unrestricted. Concretely, the hypersurface describing the resolved elliptic fibration is given by

$$P_T = v(c_{1,0} e_1 w s_1 + c_2 v s_0) + u(b_{0,1} e_0 v^2 s_0^2 + b_1 v w s_0 s_1 + b_{2,0} e_1 w^2 s_1^2) + u^2(d_{0,1} e_0 v s_0^2 s_1 + d_1 w s_0 s_1^2 + d_{2,1} e_0 u s_0^2 s_1^2). \quad (\text{V.19})$$

This is the blow-up of a singular fibration with an  $A_1$ -singular fibre over the base divisor  $W_2 = \{w_2\}$  with  $\pi^{-1}W_2 = E_0 E_1$ . The singular fibration is obtained by setting  $e_1 = 1$  and identifying  $e_0$  with  $w_2$ . One can map this blow-down to Weierstrass form (V.6) and confirm a Kodaira fibre of (split) type  $I_2$  over  $\{w_2\}$  from the vanishing orders  $(0, 0, 2)$  of  $(f, g, \Delta)$ .

The top allows two different triangulations. For definiteness, we choose one of these triangulations, for which the Stanley–Reisner ideal (SRI) is generated by

$$u v, u w, w s_0, v s_1, s_0 s_1, e_0 w, e_1 s_0, e_1 u. \quad (\text{V.20})$$

From the top one can further read off the scaling relations among the coordinates and their corresponding divisor classes in the ambient space, which are summarised in the following table:

	u	v	w	$s_0$	$s_1$	$e_1$	$e_0$
$U$	1	1	1	·	·	·	·
$S_0$	·	·	1	1	·	·	·
$S_1$	·	1	·	·	1	·	·
$E_1$	·	·	-1	·	·	1	-1

(V.21)

In the presence of non-abelian symmetry the  $U(1)$  generators (V.5) need to be corrected such that the  $SU(2)$  root has zero  $U(1)$  charge. The resulting  $U(1)$  generators take the form

$$\begin{aligned} \omega_1^I &= S_1 - S_0 - \bar{\mathcal{K}} + \frac{1}{2} E_1, \\ \omega_2^I &= U - S_0 - \bar{\mathcal{K}} - [c_{1,0}]. \end{aligned} \quad (\text{V.22})$$

Note that the charges (V.2) of the singlets are not affected as these states are not charged under the  $SU(2)$  root.

### 1.2.2 Matter curves in the $SU(2)$ -I model

The Kodaira type of the resolved fibre changes in codimension two, i.e. over curves along the divisor  $W_2$  in the base. These loci can be found by analysing the vanishing order of the discriminant of the singular blow-down of (V.19) along with the Weierstrass sections  $f$  and  $g$  which define the birationally equivalent Weierstrass model (V.6). One finds

$$\Delta \simeq w_2^2 \left( c_2 (c_{1,0}^2 d_1 - b_1 b_{2,0} c_{1,0} + b_{2,0}^2 c_2) \ell_3 (b_1^2 - 4c_2 d_1)^2 + \mathcal{O}(w_2) \right) \quad (\text{V.23})$$

with  $\ell_3$  a complicated expression given in table (V.3). A straightforward analysis of the Weierstrass sections  $f$  and  $g$  reveals that the fibre over the curves  $\{w_2\} \cap \{c_2\}$ ,  $\{w_2\} \cap \{c_{1,0}^2 d_1 - b_1 b_{2,0} c_{1,0} + b_{2,0}^2 c_2\}$  and  $\{w_2\} \cap \{\ell_3\}$  is of split Kodaira type  $I_3$ , corresponding to vanishing orders  $(0, 0, 3)$  for  $(f, g, \Delta)$ . This indicates an enhancement of the singularity type from  $A_1$  to  $A_2$  due to the splitting of one of the fibre components such that the fibre over the curves forms the affine Dynkin diagram of  $SU(3)$ . The curves therefore host massless matter multiplets in  $SU(2)$  representation  $\mathbf{2}_{(q_1, q_2)}$  plus their conjugates, with the subscripts denoting the  $U(1)$  charges.<sup>2</sup> We will explicitly analyse the fibre and compute the  $U(1)$  charges momentarily. By contrast, along  $\{w_2\} \cap \{b_1^2 - 4c_2 d_1\}$  the fibre is of Kodaira type  $III$ , corresponding to vanishing orders  $(1, 2, 3)$  for  $(f, g, \Delta)$ . Since the singularity type remains  $A_1$ , no charged matter representations arise over this curve, consistent in particular with the results of [41]. The matter curves and  $U(1)$  charges are summarised in table V.3.

$\mathcal{R}$	locus = $W_2 \cap \dots$	splitting of fibre components	$U(1)$ -charges	highest weight states
$\mathbf{2}_1^1$	$\{c_2\}$	$\mathbb{P}_0^1 \rightarrow \mathbb{P}_{0s_1}^1 + \mathbb{P}_{0A}^1$	$(\frac{1}{2}, -1)$	$\mathbf{2}: \mathbb{P}_{0A}^1, \bar{\mathbf{2}}: \mathbb{P}_{0s_1}^1$
$\mathbf{2}_2^1$	$\{c_{1,0}^2 d_1 - b_1 b_{2,0} c_{1,0} + b_{2,0}^2 c_2\}$	$\mathbb{P}_0^1 \rightarrow \mathbb{P}_{0B}^1 + \mathbb{P}_{0C}^1$	$(\frac{1}{2}, 1)$	$\mathbf{2}: \mathbb{P}_{0C}^1, \bar{\mathbf{2}}: \mathbb{P}_{0B}^1$
$\mathbf{2}_3^1$	$\{\ell_3\} := \{b_{0,1}^2 d_1^2 + b_{0,1} (b_1^2 d_{2,1} - b_1 d_{0,1} d_1 - 2c_2 d_1 d_{2,1}) + c_2 (d_{0,1}^2 d_1 - b_1 d_{0,1} d_{2,1} + c_2 d_{2,1}^2)\}$	$\mathbb{P}_1^1 \rightarrow \mathbb{P}_{1A}^1 + \mathbb{P}_{1B}^1$	$(\frac{1}{2}, 0)$	$\mathbf{2}: \mathbb{P}_{1B}^1, \bar{\mathbf{2}}: \mathbb{P}_{1A}^1$

**Table V.3:** Matter states and their charges in the  $SU(2)$ -I top. Note that for legibility we have omitted the conjugate  $\bar{\mathbf{2}}$ -states and their charges, which simply come with the opposite sign as the shown charges.

The splitting process in the fibre is due to the factorisation of the hypersurface polynomial over the enhancement loci. For the first curve, the factorisation is straightforward to see after setting  $c_2 = e_0 = 0$  in (V.19),

$$P_T|_{(e_0=0, c_2=0)} = s_1 w (c_{1,0} e_1 v w + b_1 s_0 u v + b_{2,0} e_1 s_1 w u + d_1 s_0 s_1 u^2). \quad (\text{V.24})$$

Since  $e_0 w$  is in the SR-ideal,  $w$  cannot vanish so that the zero locus of (V.24) splits into the zero locus of  $s_1$  and of the expression in brackets, defining the components  $\mathbb{P}_{0s_1}$  and  $\mathbb{P}_{0A}$ . One can further calculate the intersections between these components and  $\mathbb{P}_1^1$  (which does not split and remains the root of  $SU(2)$ ) and easily verify the structure to be an affine  $SU(3)$  diagram. Explicit calculations identify  $\mathbb{P}_{0A}^1$  with the highest weight state of the  $\mathbf{2}$ -representation with  $U(1)$  charges  $(\frac{1}{2}, -1)$ , whose states we denote by  $\mathbf{2}_1^1$ . Correspondingly  $\mathbb{P}_{0s_1}^1$  is the highest weight state of the conjugate representation  $\bar{\mathbf{2}}_1^1$ , whose states have  $U(1)$  charges  $(-\frac{1}{2}, 1)$ .

<sup>2</sup> Note that the anti-fundamental representation of  $SU(2)$  is equivalent to the fundamental, but in the present context it has the opposite  $U(1)$  charges and will therefore be denoted by  $\bar{\mathbf{2}}$ .

For the second curve defined by  $W_2 \cap \{c_{1,0}^2 d_1 - b_1 b_{2,0} c_{1,0} + b_{2,0}^2 c_2\}$ , one could solve the equation for  $b_1$ ,  $c_2$  or  $d_1$  and plug the expressions into (V.19) to detect a factorisation. However any of these expressions will involve division by  $c_{1,0}$  or  $b_{2,0}$ , which for the analysis of Yukawa points below turns out to be disadvantageous. Instead we factorise

$$c_{1,0}^2 d_1 - b_1 b_{2,0} c_{1,0} + b_{2,0}^2 c_2 = \frac{1}{d_1} \mathcal{C}_+ \mathcal{C}_- \quad \text{with} \quad \mathcal{C}_\pm = c_{1,0} d_1 - b_{2,0} \left( \frac{b_1}{2} \pm \sqrt{\frac{b_1^2}{4} - c_2 d_1} \right), \quad (\text{V.25})$$

corresponding to a splitting of the curve into two components  $W_2 \cap \{\mathcal{C}_\pm = 0\}$ . Note that the square root introduces a branch cut in the base along which the two components are interchanged. Therefore the whole locus  $W_2 \cap \{c_{1,0}^2 d_1 - b_1 b_{2,0} c_{1,0} + b_{2,0}^2 c_2\}$  is still one irreducible curve. Furthermore the above factorisation is valid for generic points for which  $d_1 \neq 0$ . Since, as it turns out, at  $d_1 = 0$  no Yukawa points are localised, this is sufficient for our purposes.

The factorisation (V.25) now allows us to solve  $\mathcal{C}_\pm = 0$  for  $c_{1,0}$  and substitute it into the hypersurface polynomial. With this substitution we can see that over each part of the curve,  $\mathbb{P}_0^1$  splits into two components,

$$\begin{aligned} & P_T|_{(e_0=0, c_\pm=0)} \\ &= \frac{1}{d_1} \underbrace{\left[ d_1 s_1 u + v \left( \frac{b_1}{2} \pm \sqrt{\frac{b_1^2}{4} - c_2 d_1} \right) \right]}_{\mathbb{P}_{0B}^1} \underbrace{\left[ b_{2,0} e_1 s_1 + d_1 s_0 s_1 u + s_0 v \left( \frac{b_1}{2} \mp \sqrt{\frac{b_1^2}{4} - c_2 d_1} \right) \right]}_{\mathbb{P}_{0C}^1}, \end{aligned} \quad (\text{V.26})$$

where we have set  $w = 1$  using the SR-ideal. First note that there is no fibre coordinate appearing under the square roots. Therefore the factorisation defines two irreducible fibre components over each part  $W_2 \cap \mathcal{C}_\pm$ . At the branch cut the first/second component over one part of the curve is identified with the first/second component over the other part so there is no monodromy acting on the fibre components, making  $\mathbb{P}_{0B}^1$  and  $\mathbb{P}_{0C}^1$  well-defined on the whole curve. Explicit calculations show that  $\mathbb{P}_{0B}^1$ ,  $\mathbb{P}_{0C}^1$  and  $\mathbb{P}_1^1$  (which again does not split) intersect each other in the affine  $SU(3)$  diagram.  $\mathbb{P}_{0C}^1$  is the highest weight state of  $\mathbf{2}_2^1$  with charges  $(\frac{1}{2}, 1)$ , and  $\mathbb{P}_{0B}^1$  is that of  $\overline{\mathbf{2}}_2^1$  with charges  $(-\frac{1}{2}, -1)$ .

For the third curve, we apply a similar factorisation method; the defining equation can be written as

$$\ell_3 = 1/d_1^2 \mathcal{D}_+ \mathcal{D}_- \quad \text{with} \quad \mathcal{D}_\pm = b_{0,1} d_1^2 - \left[ c_2 d_1 d_{2,1} + (d_{0,1} d_1 - b_1 d_{2,1}) \left( \frac{b_1}{2} \pm \sqrt{\frac{b_1^2}{4} - c_2 d_1} \right) \right]. \quad (\text{V.27})$$

Again, there is a branch cut in the base coming from the square root which identifies the two parts  $W_2 \cap \{\mathcal{D}_\pm = 0\}$  at the branch locus. The fibre enhancement over each part can be deduced (after some calculation) by solving  $\mathcal{D}_\pm = 0$  for  $b_{0,1}$  and inserting the expression into the hypersurface

polynomial (V.19). We find that  $\mathbb{P}_1^1$  splits into two components,

$$\begin{aligned}
 P_T|_{(e_1=0, \mathcal{D}_\pm=0)} = & \\
 & \frac{1}{d_1} \left[ \underbrace{d_1 s_1 + \left( \frac{b_1}{2} \pm \sqrt{\frac{b_1^2}{4} - c_2 d_1} \right) v}_{\mathbb{P}_{1A}^1} \right] \\
 & \times \left[ \underbrace{d_{2,1} e_0 s_1 + \left[ d_{0,1} - \frac{d_{2,1}}{d_1} \left( \frac{b_1}{2} \pm \sqrt{\frac{b_1^2}{4} - c_2 d_1} \right) \right] e_0 v + d_1 w s_1 + \left( \frac{b_1}{2} \mp \sqrt{\frac{b_1^2}{4} - c_2 d_1} \right) v w}_{\mathbb{P}_{1B}^1} \right].
 \end{aligned} \tag{V.28}$$

Analogous to the situation over the second curve, the factors are not interchanged by any monodromy when passing the branch locus in the base, making the splitting  $\mathbb{P}_1^1 \rightarrow \mathbb{P}_{1A}^1 + \mathbb{P}_{1B}^1$  well-defined over the whole curve. The intersection structure together with  $\mathbb{P}_0^1$  (which remains irreducible) turns out to be again the affine  $SU(3)$  diagram.  $\mathbb{P}_{1B}^1$  is the highest weight state of  $\mathbf{2}_3^1$  with charges  $(\frac{1}{2}, 0)$  and  $\mathbb{P}_{1A}^1$  is that of  $\bar{\mathbf{2}}_3^1$  with charges  $(-\frac{1}{2}, 0)$ .

### 1.2.3 Yukawa couplings in the $SU(2)$ -I model

$SU(2)$  matter and singlet curves intersect at codimension three loci in the base to form gauge invariant Yukawa couplings of the form  $\mathbf{2}\bar{\mathbf{2}}(\mathbf{1}/\bar{\mathbf{1}})$  and  $\mathbf{2}\mathbf{2}(\mathbf{1}/\bar{\mathbf{1}})$ . We list all such couplings in table V.4.

coupling	locus = $W_2 \cap \dots$	splitting of fibre components
$\mathbf{2}_1^1 \mathbf{2}_2^1 \bar{\mathbf{1}}^{(2)}$	$\{c_2\} \cap \{c_{1,0} d_1 - b_1 b_{2,0}\}$	$\mathbb{P}_0^1 \rightarrow \mathbb{P}_{0s_1C}^1 + \mathbb{P}_{0AB}^1 + \mathbb{P}_{0AC}^1$
$\mathbf{2}_1^1 \bar{\mathbf{2}}_2^1 \mathbf{1}^{(5)}$	$\{c_2\} \cap \{c_{1,0}\}$	$\mathbb{P}_0^1 \rightarrow \mathbb{P}_{0s_1B}^1 + \mathbb{P}_{0AB'}^1 + \mathbb{P}_{0AC'}^1$
$\mathbf{2}_1^1 \mathbf{2}_3^1 \bar{\mathbf{1}}^{(1)}$	$\{c_2\} \cap \{b_{0,1}\}$	$\mathbb{P}_0^1 \rightarrow \mathbb{P}_{0s_1}^1 + \mathbb{P}_{0A}^1, \mathbb{P}_1^1 \rightarrow \mathbb{P}_{1A}^1 + \mathbb{P}_{1B}^1$
$\mathbf{2}_1^1 \bar{\mathbf{2}}_3^1 \mathbf{1}^{(6)}$	$\{c_2\} \cap \{b_1^2 d_{2,1} - b_1 d_{0,1} d_1 + b_{0,1} d_1^2\}$	$\mathbb{P}_0^1 \rightarrow \mathbb{P}_{0s_1}^1 + \mathbb{P}_{0A}^1, \mathbb{P}_1^1 \rightarrow \mathbb{P}_{1A}^1 + \mathbb{P}_{1B}^1$
$\mathbf{2}_2^1 \mathbf{2}_3^1 \bar{\mathbf{1}}^{(4)}$	$(\{\mathcal{C}_+\} \cap \{\mathcal{D}_+\}) \cup (\{\mathcal{C}_-\} \cap \{\mathcal{D}_-\})$	$\mathbb{P}_0^1 \rightarrow \mathbb{P}_{0B}^1 + \mathbb{P}_{0C}^1, \mathbb{P}_1^1 \rightarrow \mathbb{P}_{1A}^1 + \mathbb{P}_{1B}^1$
$\mathbf{2}_2^1 \bar{\mathbf{2}}_3^1 \bar{\mathbf{1}}^{(6)}$	$(\{\mathcal{C}_+\} \cap \{\mathcal{D}_-\}) \cup (\{\mathcal{C}_-\} \cap \{\mathcal{D}_+\})$	$\mathbb{P}_0^1 \rightarrow \mathbb{P}_{0B}^1 + \mathbb{P}_{0C}^1, \mathbb{P}_1^1 \rightarrow \mathbb{P}_{1A}^1 + \mathbb{P}_{1B}^1$
$\mathbf{2}_2^1 \mathbf{2}_2^1 \bar{\mathbf{1}}^{(3)}$	$\{b_{2,0}\} \cap \{c_{1,0}\}$	$\mathbb{P}_0^1 \rightarrow \mathbb{P}_{0B}^1 + \mathbb{P}_{0Cs_0}^1 + \mathbb{P}_{0C'}^1$
$\mathbf{2}_3^1 \mathbf{2}_3^1 \bar{\mathbf{1}}^{(2)}$	$\{b_{0,1} d_1 - c_2 d_{2,1}\} \cap \{b_1 d_{2,1} - d_{0,1} d_1\}$	$\mathbb{P}_1^1 \rightarrow \mathbb{P}_{1A}^1 + \mathbb{P}_{1B'}^1 + \mathbb{P}_{1B''}^1$

**Table V.4:** Yukawa couplings in the  $SU(2)$ -I top.

To derive these, one first checks explicitly that none of the possible Yukawa couplings lies at  $d_1 = 0$  so that the factorisations (V.25) and (V.27) are applicable. The first two couplings arise over the intersection locus of the  $\mathbf{2}_1^1$ - and  $\mathbf{2}_2^1$ -curves. This locus splits into two sets of points, which can be identified with the intersection of  $\{c_2\}$  with  $\{\mathcal{C}_+\}$  and  $\{d_1 \mathcal{C}_-\}$ , respectively. The intersection with  $\{\mathcal{C}_+\}$  leads to the first set of Yukawa points, over which the fibre of the divisor  $E_0$  splits into three components  $\mathbb{P}_{0s_1C}^1$ ,  $\mathbb{P}_{0AB}^1$  and  $\mathbb{P}_{0AC}^1$ . The intersection structure of these three components and  $\mathbb{P}_1^1$  (which does not split) forms an affine  $SU(4)$  diagram. The splitting of the fibre components (V.3) over the respective  $\mathbf{2}$ -curves arises as follows:

- Approaching the Yukawa points along the  $\mathbf{2}_1^I$ -curve,  $\mathbb{P}_{0s_1}^1 \rightarrow \mathbb{P}_{0s_1C}^1$  remains irreducible while  $\mathbb{P}_{0A}^1$  splits into two components,  $\mathbb{P}_{0AB}^1 + \mathbb{P}_{0AC}^1$ .
- From the perspective of the  $\mathbf{2}_2^I$ -curve the Yukawa points lie on the  $\{\mathcal{C}_+\}$ -part, where the fibre components  $\mathbb{P}_{0B}^1$  and  $\mathbb{P}_{0C}^1$  are defined in (V.26) with ‘+’-sign for  $\mathbb{P}_{0B}^1$  and ‘-’-sign for  $\mathbb{P}_{0C}^1$ . When we approach the Yukawas by setting  $c_2 = 0$ ,  $\mathbb{P}_{0B}^1 \rightarrow \mathbb{P}_{0AB}^1$  remains irreducible while the equation for  $\mathbb{P}_{0C}^1$  splits off a factor  $s_1$ , giving the splitting  $\mathbb{P}_{0C}^1 \rightarrow \mathbb{P}_{0s_1C}^1 + \mathbb{P}_{0AC}^1$ .

The second set of Yukawa points  $W_2 \cap \{c_2\} \cap \{c_{1,0}\}$  can be viewed as the intersection of the  $\{d_1\mathcal{C}_-\}$ -part of  $\mathbf{2}_2^I$  with  $\mathbf{2}_1^I$ . Again  $E_0$  splits into three components,  $\mathbb{P}_{0s_1B}^1$ ,  $\mathbb{P}_{0AB'}^1$  and  $\mathbb{P}_{0AC'}^1$  (the primes denote that these have different charges under the  $SU(2)$  root and the  $U(1)$  generators, corresponding to the conjugate  $\mathbf{2}_2^I$ -state and a different singlet), which together with  $\mathbb{P}_1^1$  form the affine  $SU(4)$  diagram. The splitting processes are as follows:

- Along  $\mathbf{2}_1^I$ , again the component  $\mathbb{P}_{0s_1}^1$  remains irreducible and  $\mathbb{P}_{0A}^1 \rightarrow \mathbb{P}_{0AB'}^1 + \mathbb{P}_{0AC'}^1$  splits. The primes denote that the charge of the components under the  $SU(2)$  root and the  $U(1)$  generators are different than over the first Yukawa point.
- Along  $\mathbf{2}_2^I$ , we have to look at the fibre components  $\mathbb{P}_{0B}^1$  and  $\mathbb{P}_{0C}^1$  over  $\{\mathcal{C}_-\}$ , which are defined through (V.26) with the second sign choice; setting  $c_2 = 0$  now leaves  $\mathbb{P}_{0C}^1$  irreducible, while the equation for  $\mathbb{P}_{0B}^1$  just becomes  $d_1 s_1 u$ , defining the components  $\mathbb{P}_{0s_1B}^1$  (where  $s_1 = 0$ ) and  $\mathbb{P}_{0AB'}^1$  (where  $u = 0$ ).

The third and fourth sets of Yukawa points are the intersection points of the  $\mathbf{2}_1^I$ -curve over  $\{c_2\}$  with  $\mathbf{2}_3^I$  over  $\{d_1\mathcal{D}_-\}$  and  $\{\mathcal{D}_+\}$ , respectively. The splitting is straightforward and gives the same  $\mathbb{P}^1$ s with identical charges over both points. What differs, though, is the intersection *pattern*. Over the third set, the pattern is  $\mathbb{P}_{0s_1}^1 - \mathbb{P}_{0A}^1 - \mathbb{P}_{1A}^1 - \mathbb{P}_{1B}^1(-\mathbb{P}_{0s_1}^1)$ ; M2-branes can wrap the combination  $\mathbb{P}_{0s_1}^1 + \mathbb{P}_{1B}^1$  giving rise to  $\bar{\mathbf{1}}^{(1)}$ -states, but not  $\mathbb{P}_{0s_1}^1 + \mathbb{P}_{1A}^1$ , which is needed for  $\mathbf{1}^{(6)}$ -states. Accordingly, the intersection pattern over the fourth set is  $\mathbb{P}_{0s_1}^1 - \mathbb{P}_{0A}^1 - \mathbb{P}_{1B}^1 - \mathbb{P}_{1A}^1(-\mathbb{P}_{0s_1}^1)$ , allowing  $\mathbf{1}^{(6)}$ - but not  $\bar{\mathbf{1}}^{(1)}$ -states. Of course, both patterns have the same structure as the affine  $SU(4)$  diagram.

The fifth and sixth types of couplings arise over the intersection points between the  $\mathbf{2}_2^I$ - and  $\mathbf{2}_3^I$ -curve. With the factorisations (V.25) and (V.27), these points group into the four intersection loci of  $\{\mathcal{C}_\pm\}$  and  $\{\mathcal{D}_\pm\}$ . Analogously to the situation over the previous two types of Yukawa points, one finds for both the fifth and sixth coupling the same  $\mathbb{P}^1$ s with the same charges, but different intersection patterns, leading to either  $\bar{\mathbf{1}}^{(4)}$ -states over  $\{\mathcal{C}_\pm\} \cap \{\mathcal{D}_\pm\}$  or  $\bar{\mathbf{1}}^{(6)}$ -states over  $\{\mathcal{C}_\pm\} \cap \{\mathcal{D}_\mp\}$ . The intersection structure is an affine  $SU(4)$  diagram in both cases.

The last two Yukawa points are self-intersection points of  $\mathbf{2}_2^I$  resp.  $\mathbf{2}_3^I$ . This can again be checked by using `Singular` to analyse the ideals defining the respective matter curve. However, because we have already split the curves into two parts,  $\mathcal{C}_\pm$  resp.  $\mathcal{D}_\pm$ , the self-intersection structure is evident. For  $\mathbf{2}_2^I$  it is the intersection point  $W_2 \cap \{b_{2,0}\} \cap \{c_{1,0}\}$  of  $\{\mathcal{C}_+\}$  with  $\{\mathcal{C}_-\}$  which also lies on the singlet curve  $\mathbf{1}^{(3)}$ .<sup>3</sup> From the factorisation of the hypersurface polynomial (V.26) one easily sees that, irrespective of along which part we approach the point,  $\mathbb{P}_{0B}^1$  remains irreducible, while the equation of  $\mathbb{P}_{0C}^1$  splits off a factor  $s_0$  as we set  $b_{2,0} = 0$ , thus  $\mathbb{P}_{0C}^1 \rightarrow \mathbb{P}_{0Cs_0}^1 + \mathbb{P}_{0C'}^1$ . The last coupling is over the point of  $\{\mathcal{D}_+\} \cap \{\mathcal{D}_-\}$  which lies on  $\mathbf{1}^{(2)}$ . The splitting process here is not obvious from (V.28), but straightforward calculation reveals that  $\mathbb{P}_{1B}^1$  splits into two components. Again, the intersection structure is an affine  $SU(4)$  diagram over both self-intersection points.

Note that, while for the discussion of the Yukawas above we have only used the loci of the  $\mathbf{2}$ -curves to determine the Yukawa points, we have used `Singular` to verify that indeed all the

<sup>3</sup> $\{\mathcal{C}_+\}$  and  $\{\mathcal{C}_-\}$  also have the codimension three locus  $W_2 \cap \{b_1^2 - 4c_2d_1\} \cap \{c_1d_1 - 1/2b_1b_2\}$  in common, which is just the branch locus of the square root. However this set of points does not lie on any singlet curve; consistently there is no further enhancement in the fibre.

Yukawa points (V.4) also lie on the corresponding singlet curve. This is consistent with the appearance of the associated singlet states in the split fibres as discussed above.

#### 1.2.4 $SU(2)$ -II and -III tops

The analysis of the remaining two  $A_1$ -tops as depicted in figure B.2 is very analogous and is carried out in appendix 2, to which we refer for more details. Here we merely collect the massless spectrum and the associated Yukawa couplings as these will be needed for our construction of Standard-Model-like F-theory compactifications.

##### $SU(2)$ -II top

The second  $A_1$ -top, called  $SU(2)$ -II top in appendix 2.1, leads to an  $SU(2)$ -charged matter spectrum of the following form:

$\mathcal{R}$	$U(1)$ – charges	
$\mathbf{2}_1^{\text{II}}$	$(\frac{1}{2}, \frac{3}{2})$	(V.29)
$\mathbf{2}_2^{\text{II}}$	$(\frac{1}{2}, -\frac{1}{2})$	
$\mathbf{2}_3^{\text{II}}$	$(\frac{1}{2}, \frac{1}{2})$	

All Yukawa couplings allowed by the  $U(1)$  charges are realised geometrically. More precisely the set of Yukawas is given by

$$\begin{aligned}
 & \mathbf{2}_1^{\text{II}} \mathbf{2}_2^{\text{II}} \bar{\mathbf{1}}^{(4)}, & \mathbf{2}_1^{\text{II}} \mathbf{2}_2^{\text{II}} \bar{\mathbf{1}}^{(5)}, & \mathbf{2}_1^{\text{II}} \mathbf{2}_3^{\text{II}} \bar{\mathbf{1}}^{(3)}, & \mathbf{2}_1^{\text{II}} \mathbf{2}_3^{\text{II}} \bar{\mathbf{1}}^{(6)}, \\
 & \mathbf{2}_2^{\text{II}} \mathbf{2}_3^{\text{II}} \bar{\mathbf{1}}^{(2)}, & \mathbf{2}_2^{\text{II}} \mathbf{2}_3^{\text{II}} \mathbf{1}^{(6)}, & \mathbf{2}_2^{\text{II}} \mathbf{2}_2^{\text{II}} \bar{\mathbf{1}}^{(1)}, & \mathbf{2}_3^{\text{II}} \mathbf{2}_3^{\text{II}} \bar{\mathbf{1}}^{(4)}.
 \end{aligned}
 \tag{V.30}$$

In fact the  $SU(2)$ -II top is equivalent to the  $SU(2)$ -I top. One way to see this is to notice that upon identifying the  $U(1)$  charges in the two tops as

$$\begin{aligned}
 U(1)_1^{\text{II}} &= -U(1)_1^{\text{I}}, \\
 U(1)_2^{\text{II}} &= U(1)_2^{\text{I}} - U(1)_1^{\text{I}},
 \end{aligned}
 \tag{V.31}$$

the spectrum and Yukawa structure is exactly the same if one identifies the states  $\mathbf{2}_i^{\text{II}} \leftrightarrow \bar{\mathbf{2}}_i^{\text{I}}, i = 1, 2, 3$  and exchanges the singlets  $\mathbf{1}^{(1)} \leftrightarrow \bar{\mathbf{1}}^{(3)}, \mathbf{1}^{(2)} \leftrightarrow \bar{\mathbf{1}}^{(4)}$ . One can also arrive at this identification from the symmetries of the tops. More details can be found in appendix 1.

Although both models are the same when considering only the gauge group  $SU(2) \times U(1)_1 \times U(1)_2$ , they will give rise to different models when combining them with an  $SU(3)$ -top, as we will discuss below in section 1.4.

##### $SU(2)$ -III top

The last  $A_1$ -top is the  $SU(2)$ -III top with matter content

$\mathcal{R}$	$U(1)$ – charges	
$\mathbf{2}_1^{\text{III}}$	$(1, 0)$	(V.32)
$\mathbf{2}_2^{\text{III}}$	$(1, 1)$	
$\mathbf{2}_3^{\text{III}}$	$(0, 1)$	

In this top, in addition to the three fundamental matter curves and a notorious type *III* enhancement locus with no additional matter, one finds a change of fibre type to *non-split*  $I_3$  type over yet another curve. As explained in appendix 2, the non-split fibre type can either be seen from the Weierstrass data or be explicitly confirmed by analysing the monodromies along the curve in question. As a result of the monodromy, this locus does not carry massless matter.

The geometrically realised Yukawa couplings

$$\begin{aligned}
 \mathbf{2}_1^{\text{III}} \bar{\mathbf{2}}_2^{\text{III}} \mathbf{1}^{(6)}, & \quad \mathbf{2}_1^{\text{III}} \mathbf{2}_3^{\text{III}} \bar{\mathbf{1}}^{(4)}, & \quad \mathbf{2}_1^{\text{III}} \bar{\mathbf{2}}_3^{\text{III}} \bar{\mathbf{1}}^{(1)}, \\
 \mathbf{2}_2^{\text{III}} \mathbf{2}_3^{\text{III}} \bar{\mathbf{1}}^{(3)}, & \quad \mathbf{2}_2^{\text{III}} \bar{\mathbf{2}}_3^{\text{III}} \bar{\mathbf{1}}^{(2)}, & \quad \mathbf{2}_3^{\text{III}} \mathbf{2}_3^{\text{III}} \bar{\mathbf{1}}^{(5)}
 \end{aligned} \tag{V.33}$$

exhaust again all gauge invariant combinations.

This top is inequivalent to the first two tops. Under the transformation  $U(1)'_1 \equiv -U(1)_1$ ,  $U(1)'_2 \equiv U(1)_2 - U(1)_1$  analogous to (V.31) (with the same identification of the singlets), the spectrum and Yukawa structure of the  $SU(2)$ -III top is mapped to itself as  $\mathbf{2}_1^{\text{III}} \leftrightarrow \bar{\mathbf{2}}_2^{\text{III}}$  and  $\mathbf{1}^{(1)} \leftrightarrow \bar{\mathbf{1}}^{(3)}$ ,  $\mathbf{1}^{(2)} \leftrightarrow \bar{\mathbf{1}}^{(4)}$ .

### 1.3 Toric fibrations with additional $SU(3)$ symmetry

The construction of  $SU(3)$  gauge symmetry via tops is analogous to the  $SU(2)$  cases. The resolution of the  $A_2$ -singularity over a divisor  $W_3 : w_3 = 0$  in the base introduces three toric divisors  $F_0, F_1, F_2$  given by the vanishing locus of the coordinates  $f_0, f_1, f_2$ . Each  $F_i$  is a  $\mathbb{P}^1$ -fibration over  $W_3$ , and  $\pi^{-1}W_3 = F_0 F_1 F_2$ . Over a generic point on  $W_3$  the intersection structure of the  $\mathbb{P}^1$ -fibres reproduces the affine  $SU(3)$  diagram. We choose the root assignment  $F_1 \leftrightarrow -\alpha_1$ ,  $F_2 \leftrightarrow -\alpha_2$ ,  $F_0 \leftrightarrow \alpha_1 + \alpha_2$ . There exist three  $SU(3)$  tops, which we will now present in detail.

#### 1.3.1 $SU(3)$ -A top

The first top corresponds to the following restriction of the hypersurface coefficients,

$$\begin{aligned}
 b_0 &= b_{0,1} f_0, & b_2 &= b_{2,0} f_1 f_2, & c_1 &= c_{1,0} f_2, & c_2 &= c_{2,1} f_0 f_2, \\
 d_0 &= d_{0,1} f_0 f_1, & d_1 &= d_{1,0} f_1, & d_2 &= d_{2,1} f_0 f_1^2,
 \end{aligned} \tag{V.34}$$

where only  $b_1$  remains unchanged. Out of the four different triangulations we choose the one whose SR-ideal is generated by

$$\mathbf{u} \mathbf{v}, \mathbf{u} \mathbf{w}, \mathbf{w} \mathbf{s}_0, \mathbf{v} \mathbf{s}_1, \mathbf{s}_0 \mathbf{s}_1, \mathbf{f}_0 \mathbf{w}, \mathbf{f}_0 \mathbf{s}_1, \mathbf{f}_1 \mathbf{s}_0, \mathbf{f}_1 \mathbf{v}, \mathbf{f}_2 \mathbf{s}_0, \mathbf{f}_2 \mathbf{s}_1, \mathbf{f}_2 \mathbf{u}. \tag{V.35}$$

The coordinates and their corresponding divisor classes are summarised in the following table:

	u	v	w	$s_0$	$s_1$	$f_1$	$f_2$	$f_0$
U	1	1	1	·	·	·	·	·
$S_0$	·	·	1	1	·	·	·	·
$S_1$	·	1	·	·	1	·	·	·
$F_1$	·	1	·	·	·	1	·	-1
$F_2$	·	·	-1	·	·	·	1	-1

(V.36)

The  $U(1)$  generators (V.5) need to be corrected such that the roots of  $SU(3)$  have zero  $U(1)$  charge. The generators with this property take the form

$$\begin{aligned}
 \omega_1^A &= S_1 - S_0 - \bar{\mathcal{K}} + \frac{2}{3} F_1 + \frac{1}{3} F_2, \\
 \omega_2^A &= U - S_0 - \bar{\mathcal{K}} - [c_{1,0}] + \frac{2}{3} F_1 + \frac{1}{3} F_2.
 \end{aligned} \tag{V.37}$$

The charges (V.2) of the singlets are not affected as they are not charged under the roots of  $SU(3)$ .



### 1.3.2 Matter curves in the $SU(3)$ -A model

The matter curves are found by analysing the discriminant of the associated Weierstrass model

$$\Delta \simeq w^3 \left( b_{0,1} c_{1,0} (b_{0,1} c_{1,0} - b_1 c_{2,1}) (b_1 b_{2,0} - c_{1,0} d_{1,0}) (b_{0,1} d_{1,0}^2 - b_1 d_{0,1} d_{1,0} + b_1^2 d_{2,1}) b_1^3 + \mathcal{O}(w_3) \right).$$

As can be read off from the Weierstrass sections  $f$  and  $g$ , the fibre along the five curves associated with the first five factors in the bracket is of split Kodaira type  $I_4$ . The fibre components intersect as in the affine  $SU(4)$  diagram, corresponding to  $SU(3)$  matter in the fundamental representation (plus conjugate). Their  $U(1)$  charges together with the geometric data can be found in table V.5.

$\mathcal{R}$	locus = $W_3 \cap \dots$	splitting of fibre components	$U(1)$ -charges	highest weight states of...
$\mathbf{3}_1^A$	$\{b_{0,1}\}$	$\mathbb{P}_1^1 \rightarrow \mathbb{P}_{1w}^1 + \mathbb{P}_{1A}^1$	$(\frac{2}{3}, -\frac{1}{3})$	$\mathbf{3}: \mathbb{P}_{1w}^1 + \mathbb{P}_0^1 + \mathbb{P}_2^1, \bar{\mathbf{3}}: \mathbb{P}_{1A}^1 + \mathbb{P}_0^1$
$\mathbf{3}_2^A$	$\{c_{1,0}\}$	$\mathbb{P}_0^1 \rightarrow \mathbb{P}_{0u}^1 + \mathbb{P}_{0A}^1$	$(-\frac{1}{3}, -\frac{4}{3})$	$\mathbf{3}: \mathbb{P}_{0u}^1, \bar{\mathbf{3}}: \mathbb{P}_{0A}^1$
$\mathbf{3}_3^A$	$\{b_{0,1} c_{1,0} - b_1 c_{2,1}\}$	$\mathbb{P}_1^1 \rightarrow \mathbb{P}_{1B}^1 + \mathbb{P}_{1C}^1$	$(-\frac{1}{3}, \frac{2}{3})$	$\mathbf{3}: \mathbb{P}_{1C}^1 + \mathbb{P}_0^1 + \mathbb{P}_2^1, \bar{\mathbf{3}}: \mathbb{P}_{1B}^1 + \mathbb{P}_0^1$
$\mathbf{3}_4^A$	$\{b_1 b_{2,0} - c_{1,0} d_{1,0}\}$	$\mathbb{P}_0^1 \rightarrow \mathbb{P}_{0B}^1 + \mathbb{P}_{0C}^1$	$(\frac{2}{3}, \frac{2}{3})$	$\mathbf{3}: \mathbb{P}_{0B}^1, \bar{\mathbf{3}}: \mathbb{P}_{0C}^1$
$\mathbf{3}_5^A$	$\{b_{0,1} d_{1,0}^2 - b_1 d_{0,1} d_{1,0} + b_1^2 d_{2,1}\}$	$\mathbb{P}_2^1 \rightarrow \mathbb{P}_{2A}^1 + \mathbb{P}_{2B}^1$	$(-\frac{1}{3}, -\frac{1}{3})$	$\mathbf{3}: \mathbb{P}_{2A}^1 + \mathbb{P}_0^1, \bar{\mathbf{3}}: \mathbb{P}_{2B}^1 + \mathbb{P}_0^1 + \mathbb{P}_1^1$

**Table V.5:** Matter states in the  $SU(3)$ -A top.

The splitting process over the first four curves can be straightforwardly verified. For the fifth curve, we proceed as for the  $SU(2)$  tops and use expressions with square roots to split the curve into two parts; because  $d_{2,1} \neq 0$  for all the Yukawa points below, we factorise the quadratic term such that we can solve for  $b_1$  (analogously to e.g. (V.25), where  $c_{1,0}$  played the role of  $b_1$  here). Inserting the resulting expressions (one for each of the two parts of the curve) for  $b_1$  into the hypersurface polynomial, we find that  $\mathbb{P}_2^1$  splits into two components on both parts of the curve; similarly to the  $SU(2)$ -tops, there is no monodromy interchanging the components when passing from one part of the curve to the other and back.

In addition, over the curve  $\{w_3\} \cap \{b_1\}$  the Weierstrass data  $(f, g, \Delta)$  vanish to orders  $(2, 2, 4)$ . This indicates a Kodaira type  $IV$  fibre in which no extra  $\mathbb{P}^1$  splits off, but rather the three fibre components intersect in a single point, as can be checked explicitly. Over this curve, no extra matter representation arises.

### 1.3.3 Yukawa couplings in the $SU(3)$ -A model

The  $SU(3)$  matter and the singlet curves intersect at certain codimension three loci in the base to form gauge invariant Yukawa couplings  $\mathbf{3}\bar{\mathbf{3}}(\mathbf{1}/\bar{\mathbf{1}})$ . In this case the fibre is enhanced to the affine  $SU(5)$ -diagram, and the realised couplings are in 1-to-1 correspondence with the gauge theoretic selection rules. In addition one can also form gauge invariant couplings of the type  $\mathbf{3}\mathbf{3}\mathbf{3}$ . As it turns out all such gauge invariant couplings are indeed realised geometrically, and the fibre structure is the affine  $SO(8)$ -diagram, cf. table V.6.

There, in the last column, the subscripts should help to visualise  $\mathbb{P}^1$ 's' splitting process. E.g. if we approach the second Yukawa point along the  $\mathbf{3}_1^A$ -curve, then we find that  $\mathbb{P}_{1w}^1$  remains a single component and  $\mathbb{P}_{1A}^1$  splits into two,  $\mathbb{P}_{1AB}^1$  and  $\mathbb{P}_{1AC}^1$ ;  $\mathbb{P}_{1AB}^1$  is the component  $\mathbb{P}_{1B}^1$  from the  $\mathbf{3}_3^A$ -curve that does not split over the Yukawa point, while  $\mathbb{P}_{1C}^1$  splits into two components, of which one is identified with  $\mathbb{P}_{1AC}^1$  and the other one coincides with  $\mathbb{P}_{1w}^1$ , hence the notation  $\mathbb{P}_{1wC}^1$ .

Over the last three Yukawa points with the coupling type  $\mathbf{3}\mathbf{3}\mathbf{3}$ , two of the three divisors  $F_{0,1,2}$  each split off the same  $\mathbb{P}^1$ -component, which therefore is a multiplicity 2 component; this

coupling	locus = $W_3 \cap \dots$	splitting of fibre components
$\mathbf{3}_1^A \overline{\mathbf{3}}_2^A \overline{\mathbf{1}}^{(4)}$	$\{b_{0,1}\} \cap \{c_{1,0}\}$	$\mathbb{P}_0^1 \rightarrow \mathbb{P}_{0u}^1 + \mathbb{P}_{0A}^1, \mathbb{P}_1^1 \rightarrow \mathbb{P}_{1w}^1 + \mathbb{P}_{1A}^1$
$\mathbf{3}_1^A \overline{\mathbf{3}}_3^A \mathbf{1}^{(1)}$	$\{b_{0,1}\} \cap \{c_{2,1}\}$	$\mathbb{P}_1^1 \rightarrow \mathbb{P}_{1wC}^1 + \mathbb{P}_{1AB}^1 + \mathbb{P}_{1AC}^1$
$\mathbf{3}_1^A \overline{\mathbf{3}}_4^A \mathbf{1}^{(6)}$	$\{b_{0,1}\} \cap \{b_1 b_{2,0} - c_{1,0} d_{1,0}\}$	$\mathbb{P}_0^1 \rightarrow \mathbb{P}_{0B}^1 + \mathbb{P}_{0C}^1, \mathbb{P}_1^1 \rightarrow \mathbb{P}_{1w}^1 + \mathbb{P}_{1A}^1$
$\mathbf{3}_1^A \overline{\mathbf{3}}_5^A \overline{\mathbf{1}}^{(2)}$	$\{b_{0,1}\} \cap \{b_1 d_{2,1} - d_{0,1} d_{1,0}\}$	$\mathbb{P}_1^1 \rightarrow \mathbb{P}_{1w}^1 + \mathbb{P}_{1D}^1, \mathbb{P}_2^1 \rightarrow \mathbb{P}_{2A}^1 + \mathbb{P}_{2B}^1$
$\mathbf{3}_2^A \overline{\mathbf{3}}_3^A \mathbf{1}^{(5)}$	$\{c_{1,0}\} \cap \{c_{2,0}\}$	$\mathbb{P}_0^1 \rightarrow \mathbb{P}_{0u}^1 + \mathbb{P}_{0A}^1, \mathbb{P}_1^1 \rightarrow \mathbb{P}_{1B}^1 + \mathbb{P}_{1C}^1$
$\mathbf{3}_2^A \overline{\mathbf{3}}_4^A \mathbf{1}^{(3)}$	$\{c_{1,0}\} \cap \{b_{2,0}\}$	$\mathbb{P}_0^1 \rightarrow \mathbb{P}_{0uA}^1 + \mathbb{P}_{0AB}^1 + \mathbb{P}_{0AC}^1$
$\mathbf{3}_2^A \overline{\mathbf{3}}_5^A \mathbf{1}^{(6)}$	$\{c_{1,0}\} \cap (\mathbf{3}_5^A\text{-locus})$	$\mathbb{P}_0^1 \rightarrow \mathbb{P}_{0u}^1 + \mathbb{P}_{0A}^1, \mathbb{P}_2^1 \rightarrow \mathbb{P}_{2A}^1 + \mathbb{P}_{2B}^1$
$\mathbf{3}_3^A \overline{\mathbf{3}}_4^A \mathbf{1}^{(2)}$	$(\mathbf{3}_3^A) \cap (\mathbf{3}_4^A) \setminus (\{c_{1,0}\} \cap \{b_1\})$	$\mathbb{P}_0^1 \rightarrow \mathbb{P}_{0B}^1 + \mathbb{P}_{0C}^1, \mathbb{P}_1^1 \rightarrow \mathbb{P}_{1B}^1 + \mathbb{P}_{1C}^1$
$\mathbf{3}_3^A \overline{\mathbf{3}}_5^A \overline{\mathbf{1}}^{(6)}$	$(\mathbf{3}_3^A) \cap (\mathbf{3}_5^A) \setminus (\{b_{0,1}\} \cap \{b_1\})$	$\mathbb{P}_1^1 \rightarrow \mathbb{P}_{1B}^1 + \mathbb{P}_{1C}^1, \mathbb{P}_2^1 \rightarrow \mathbb{P}_{2A}^1 + \mathbb{P}_{2B}^1$
$\mathbf{3}_4^A \overline{\mathbf{3}}_5^A \overline{\mathbf{1}}^{(4)}$	$(\mathbf{3}_4^A) \cap (\mathbf{3}_5^A) \setminus (\{d_{1,0}\} \cap \{b_1\})$	$\mathbb{P}_0^1 \rightarrow \mathbb{P}_{0B}^1 + \mathbb{P}_{0C}^1, \mathbb{P}_2^1 \rightarrow \mathbb{P}_{2A}^1 + \mathbb{P}_{2B}^1$
$\mathbf{3}_1^A \mathbf{3}_3^A \mathbf{3}_5^A$	$\{b_{0,1}\} \cap \{b_1\}$	$\mathbb{P}_1^1 \rightarrow \mathbb{P}_{1wB}^1 + \mathbb{P}_{1AB'}^1 + \mathbb{P}_{1AC'}^1, \mathbb{P}_2^1 \rightarrow \mathbb{P}_{2A}^1 + \mathbb{P}_{2B}^1,$ $\mathbb{P}_{AB'}^1 = \mathbb{P}_{2A}^1$
$\mathbf{3}_2^A \mathbf{3}_3^A \mathbf{3}_4^A$	$\{c_{1,0}\} \cap \{b_1\}$	$\mathbb{P}_0^1 \rightarrow \mathbb{P}_{0uC}^1 + \mathbb{P}_{0AB'}^1 + \mathbb{P}_{0AC'}^1, \mathbb{P}_1^1 \rightarrow \mathbb{P}_{1B}^1 + \mathbb{P}_{1C}^1,$ $\mathbb{P}_{0AC}^1 = \mathbb{P}_{1C}^1$
$\mathbf{3}_4^A \mathbf{3}_5^A \mathbf{3}_5^A$	$\{d_{1,0}\} \cap \{b_1\}$	$\mathbb{P}_0^1 \rightarrow \mathbb{P}_{0B}^1 + \mathbb{P}_{0C}^1, \mathbb{P}_2^1 \rightarrow \mathbb{P}_{2A}^1 + \mathbb{P}_{2B0}^1 + \mathbb{P}_{2B'}^1,$ $\mathbb{P}_{0B}^1 = \mathbb{P}_{2B0}^1$

**Table V.6:** Yukawa couplings in the  $SU(3)$ -A top.

corresponds to the central node of the affine  $SO(8)$ -diagram with dual Coxeter label 2. Note that the  $\mathbf{3}_4^A \mathbf{3}_5^A \mathbf{3}_5^A$  coupling is located on the self-intersection locus of the  $\mathbf{3}_5^A$ -curve, which can be verified either by the factorisation of the curve with square root expressions or by using **Singular**.

### 1.3.4 $SU(3)$ -B and -C top

Let us briefly list the main results from the analysis of the remaining two  $SU(3)$  tops, with more details relegated to appendix 3.

#### $SU(3)$ -B top

The  $SU(3)$ -B top gives rise to five  $\mathbf{3}$ -matter curves with the following  $U(1)$  charges:

$\mathcal{R}$	$U(1)$ – charges	matter	$U(1)$ – charges
$\mathbf{3}_1^B$	$(-\frac{2}{3}, -\frac{4}{3})$	$\mathbf{3}_4^B$	$(\frac{1}{3}, \frac{2}{3})$
$\mathbf{3}_2^B$	$(-\frac{2}{3}, \frac{2}{3})$	$\mathbf{3}_5^B$	$(\frac{1}{3}, -\frac{1}{3})$
$\mathbf{3}_3^B$	$(-\frac{2}{3}, -\frac{1}{3})$		

(V.38)

These enjoy a rich spectrum of geometrically realised Yukawa couplings with the singlets,

$$\begin{aligned}
 & \mathbf{3}_1^B \bar{\mathbf{3}}_2^B \mathbf{1}^{(5)}, & \mathbf{3}_1^B \bar{\mathbf{3}}_3^B \mathbf{1}^{(6)}, & \mathbf{3}_1^B \bar{\mathbf{3}}_4^B \mathbf{1}^{(3)}, & \mathbf{3}_1^B \bar{\mathbf{3}}_5^B \mathbf{1}^{(4)}, \\
 & \mathbf{3}_2^B \bar{\mathbf{3}}_3^B \bar{\mathbf{1}}^{(6)}, & \mathbf{3}_2^B \bar{\mathbf{3}}_4^B \mathbf{1}^{(2)}, & \mathbf{3}_2^B \bar{\mathbf{3}}_5^B \mathbf{1}^{(1)}, & \mathbf{3}_3^B \bar{\mathbf{3}}_4^B \mathbf{1}^{(4)}, \\
 & \mathbf{3}_3^B \bar{\mathbf{3}}_5^B \mathbf{1}^{(2)}, & \mathbf{3}_4^B \bar{\mathbf{3}}_5^B \bar{\mathbf{1}}^{(6)} & & 
 \end{aligned} \tag{V.39}$$

and among one another,

$$\mathbf{3}_3^B \mathbf{3}_4^B \mathbf{3}_5^B, \quad \mathbf{3}_1^B \mathbf{3}_4^B \mathbf{3}_4^B, \quad \mathbf{3}_2^B \mathbf{3}_5^B \mathbf{3}_5^B, \tag{V.40}$$

which is in 1-to-1 correspondence with the gauge theoretic selection rules.

Under the transformation  $U(1)'_1 \equiv -U(1)_1$ ,  $U(1)'_2 \equiv U(1)_2 - U(1)_1$ , the spectrum and Yukawa couplings remains invariant with the identification  $\mathbf{3}_1^B \leftrightarrow \bar{\mathbf{3}}_2^B$ ,  $\mathbf{3}_4^B \leftrightarrow \bar{\mathbf{3}}_5^B$  and  $\mathbf{1}^{(1)} \leftrightarrow \bar{\mathbf{1}}^{(3)}$ ,  $\mathbf{1}^{(2)} \leftrightarrow \bar{\mathbf{1}}^{(4)}$ .

### **$SU(3)$ -C top**

The third top  $SU(3)$ -C gives rise to  $SU(3)$ -charged states with the following  $U(1)$  charges:

$\mathcal{R}$	$U(1) - \text{charges}$	matter	$U(1) - \text{charges}$
$\mathbf{3}_1^C$	$(-\frac{2}{3}, -1)$	$\mathbf{3}_4^C$	$(-\frac{2}{3}, 0)$
$\mathbf{3}_2^C$	$(\frac{1}{3}, -1)$	$\mathbf{3}_5^C$	$(\frac{1}{3}, 0)$
$\mathbf{3}_3^C$	$(\frac{1}{3}, 1)$		

(V.41)

The couplings

$$\begin{aligned}
 & \mathbf{3}_1^C \bar{\mathbf{3}}_2^C \mathbf{1}^{(2)}, & \mathbf{3}_1^C \bar{\mathbf{3}}_3^C \mathbf{1}^{(3)}, & \mathbf{3}_1^C \bar{\mathbf{3}}_4^C \mathbf{1}^{(6)}, & \mathbf{3}_1^C \bar{\mathbf{3}}_5^C \mathbf{1}^{(4)}, \\
 & \mathbf{3}_2^C \bar{\mathbf{3}}_3^C \mathbf{1}^{(5)}, & \mathbf{3}_2^C \bar{\mathbf{3}}_4^C \bar{\mathbf{1}}^{(1)}, & \mathbf{3}_2^C \bar{\mathbf{3}}_5^C \mathbf{1}^{(6)}, & \mathbf{3}_3^C \bar{\mathbf{3}}_4^C \bar{\mathbf{1}}^{(4)}, \\
 & \mathbf{3}_3^C \bar{\mathbf{3}}_5^C \bar{\mathbf{1}}^{(6)}, & \mathbf{3}_4^C \bar{\mathbf{3}}_5^C \mathbf{1}^{(2)} & & 
 \end{aligned} \tag{V.42}$$

and

$$\mathbf{3}_1^C \mathbf{3}_3^C \mathbf{3}_5^C, \quad \mathbf{3}_2^C \mathbf{3}_3^C \mathbf{3}_4^C, \quad \mathbf{3}_4^C \mathbf{3}_5^C \mathbf{3}_5^C \tag{V.43}$$

are in agreement with gauge theoretic expectations.

Similar to the situation with the  $SU(2)$  tops, the  $SU(3)$ -C top is in fact equivalent to the  $SU(3)$ -A top (cf. appendix 1). Analogous to the  $U(1)$  charges identification (V.31), we find with

$$\begin{aligned}
 U(1)_1^C &= -U(1)_1^A, \\
 U(1)_2^C &= U(1)_2^A - U(1)_1^A
 \end{aligned} \tag{V.44}$$

that the spectrum agrees by identifying the states  $\mathbf{3}_i^A \leftrightarrow \mathbf{3}_i^C$ ,  $i = 1, \dots, 5$  and  $\mathbf{1}^{(1)} \leftrightarrow \bar{\mathbf{1}}^{(3)}$ ,  $\mathbf{1}^{(2)} \leftrightarrow \bar{\mathbf{1}}^{(4)}$ . Again one needs both the  $SU(3)$ -A and -C top to construct all inequivalent toric  $SU(3) \times SU(2) \times U(1)_1 \times U(1)_2$  models.

### **1.4 Toric $SU(3) \times SU(2) \times U(1)_1 \times U(1)_2$ realisations**

We are now ready to construct F-theory compactifications with gauge group  $SU(3) \times SU(2) \times U(1)_1 \times U(1)_2$ . To this end we start with our elliptic fibration realised as the hypersurface (V.1) within a  $\text{Bl}_2\mathbb{P}^2$ -fibration over  $\mathcal{B}$  and realise an  $SU(2)$  and an  $SU(3)$  singularity over two

independent base divisors  $W_2$  and  $W_3$ , respectively. We focus here on the torically realisable singularities and their resolutions enforced by the tops described in the previous sections. In the singular fourfold the base sections  $g_m \in \{b_i, c_j, d_k\}$  in (V.1) must now be of the form

$$g_m = g_{m;k,l} w_2^k w_3^l \quad (\text{V.45})$$

with  $\{w_n = 0\} = W_n$  and  $g_{m;k,l}$  generic sections in the class  $[g_m] - k[w_2] - l[w_3]$ . The powers  $k$  and  $l$  depend on which of the three  $SU(2)$  and  $SU(3)$  tops are combined. However, as we will discuss shortly, only 5 of the  $3 \times 3 = 9$  possible tops leading to the gauge group  $SU(3) \times SU(2) \times U(1)_1 \times U(1)_2$  are inequivalent.

The discriminant of the fibration takes the form

$$\Delta = w_2^2 w_3^3 (P + \mathcal{O}(w_2) + \mathcal{O}(w_3)) \quad (\text{V.46})$$

with  $P$  a section of the base that does not vanish identically along  $W_2$  and  $W_3$ . For generic choice of  $w_2$  and  $w_3$ , the fibration over  $w_2$  and  $w_3$  then looks like the three individual  $SU(2)$  and  $SU(3)$  fibrations with vanishing orders  $k$  and  $l$  over  $w_2$  and  $w_3$ , respectively, but with an additional enhancement over the intersection curve  $\{w_2\} \cap \{w_3\}$  of the two non-abelian loci. Here, the generic choice of  $w_2$  and  $w_3$  in particular means that this intersection locus is assumed not to coincide with any of the matter curves of the individual tops.

In a toric construction, this means that the polytope for the complete five-dimensional ambient space consists of two tops over the polygon for the fibre ambient space. The two tops extend in two mutually orthogonal directions of a five-dimensional lattice, each introducing resolution divisors  $E_{0/1} = \{e_{0/1} = 0\}$  and  $F_{0/1/2} = \{f_{0/1/2} = 0\}$ . If the polytope is reflexive, then toric geometry guarantees the smoothness of the fourfold  $\hat{Y}_4$  that is cut out by the hypersurface polynomial inside the five-dimensional ambient space. A triangulation of the full polytope will in particular give rise to a triangulation of the  $SU(2)$  and  $SU(3)$  sub-tops, so the corresponding full SR-ideal will – as sub-ideals – contain an SR-ideal of each the  $SU(2)$  and the  $SU(3)$  sub-model; in addition, there will be further generators that involve both  $e_i$  and  $f_j$ . To use the results of sections 1.2 and 1.3, we choose a triangulation of the full polytope that leads to an SR-ideal which as sub-ideals contains the SR-ideals we used when studying the corresponding  $SU(2)$  and  $SU(3)$  tops individually.

Because the  $E_i$  and  $F_j$  are fibred over different divisors of the base, intersections of the form

$$\int_{\hat{Y}_4} E_i \wedge F_j \wedge D_a^{(\mathcal{B})} \wedge D_b^{(\mathcal{B})}, \quad (\text{V.47})$$

with vertical divisors  $D_{a/b}^{(\mathcal{B})}$ , will yield zero. This just means that the roots of  $SU(2)$  are uncharged under  $SU(3)$  and vice versa – as one would expect from a product structure  $SU(3) \times SU(2)$  of the gauge group. Because the enhancement loci over  $W_2$  away from  $W_3$  are of the same form as in a model with only the  $SU(2)$  singularity over  $W_2$  (and similarly for the  $SU(3)$  singularity over  $W_3$  away from  $W_2$ ), one will also find the same spectrum of matter charged only under  $SU(2)$  or  $SU(3)$ . In addition one will find matter charged both under  $SU(2)$  and  $SU(3)$  at the enhancement loci  $W_2 \cap W_3$ . As it turns out, this matter transforms in the bifundamental representation  $(\mathbf{3}, \mathbf{2})$ .

The  $U(1)$  generators are now subject to the condition that the  $SU(2)$  and  $SU(3)$  roots are uncharged under them. However, since the  $SU(2)$  and  $SU(3)$  roots are mutually uncharged, this condition is met by setting

$$\omega_i^{SU(2) \times SU(3)} = \omega_i + \sum_j t_j E_j + \sum_j \tilde{t}_j F_j, \quad (\text{V.48})$$

where  $\omega_i$  are the generators of the form (V.5) and the correction terms  $t_j$  and  $\tilde{t}_j$  are the same as for the individual Shioda maps for the  $SU(2)$  and  $SU(3)$  tops.

Due to the equivalences amongst the  $SU(2)$  and  $SU(3)$  tops described in the previous sections, some of the combined  $SU(3) \times SU(2) \times U(1)_1 \times U(1)_2$  models are also equivalent. In fact those models whose spectrum and Yukawa couplings can be mapped onto each other with the  $U(1)$  transformation  $U(1)'_1 = -U(1)_1$ ,  $U(1)'_2 = U(1)_2 - U(1)_1$  are equivalent. One finds four inequivalent pairs of  $SU(2) \times SU(3)$  top combinations,  $I \times A \simeq II \times C$ ,  $I \times B \simeq II \times B$ ,  $I \times C \simeq II \times A$ ,  $III \times A \simeq III \times C$ , and the invariant model  $III \times B$ . A more detailed explanation based on the tops can be found in appendix 1.

To summarise, in order to construct toric F-theory models with  $SU(3) \times SU(2) \times U(1)_1 \times U(1)_2$  gauge symmetry we take an  $SU(2)$  and an  $SU(3)$  top of the form studied in the sections 1.2 and 1.3 and combine them into one new top. Some of the tops obtained in this way are equivalent. The previous sections readily give us the spectrum of  $\mathbf{2}$ - and  $\mathbf{3}$ -matter including their Yukawa couplings. What we need to compute is the bifundamental matter  $(\mathbf{3}, \mathbf{2})$  as well as all the Yukawa couplings it is involved in.

The result of this analysis is shown in table V.7 for all five mutually inequivalent combinations of tops. In all cases the geometrically realised Yukawa couplings are in 1-to-1 correspondence with the set of gauge theoretically allowed couplings including the  $U(1)_i$  selection rules.

top-combination $SU(2) \times SU(3)$	$(U(1)_1, U(1)_2)$ - charge of $(\mathbf{3}, \mathbf{2})$	additional gauge invariant Yukawas, $(\mathbf{3}, \mathbf{2}) - \dots$
$I \times A$	$(\frac{1}{6}, -\frac{1}{3})$	$\bar{\mathbf{3}}_1^A \mathbf{2}_3^I, \bar{\mathbf{3}}_2^A \mathbf{2}_2^I, \bar{\mathbf{3}}_3^A \mathbf{2}_1^I, \bar{\mathbf{3}}_4^A \mathbf{2}_2^I, \bar{\mathbf{3}}_5^A \mathbf{2}_3^I;$ $(\mathbf{3}, \mathbf{2}) \mathbf{3}_3^A$
$I \times B$	$(-\frac{1}{6}, -\frac{1}{3})$	$\bar{\mathbf{3}}_1^B \mathbf{2}_2^I, \bar{\mathbf{3}}_2^B \mathbf{2}_1^I, \bar{\mathbf{3}}_3^B \mathbf{2}_3^I, \bar{\mathbf{3}}_4^B \mathbf{2}_2^I, \bar{\mathbf{3}}_5^B \mathbf{2}_3^I;$ $(\mathbf{3}, \mathbf{2}) \mathbf{3}_4^B$
$I \times C$	$(-\frac{1}{6}, 0)$	$\bar{\mathbf{3}}_1^C \mathbf{2}_2^I, \bar{\mathbf{3}}_2^C \mathbf{2}_1^I, \bar{\mathbf{3}}_3^C \mathbf{2}_2^I, \bar{\mathbf{3}}_4^C \mathbf{2}_3^I, \bar{\mathbf{3}}_5^C \mathbf{2}_3^I;$ $(\mathbf{3}, \mathbf{2}) \mathbf{3}_5^C$
$III \times A$	$(-\frac{1}{3}, -\frac{1}{3})$	$\bar{\mathbf{3}}_1^A \mathbf{2}_1^{III}, \bar{\mathbf{3}}_2^A \mathbf{2}_3^{III}, \bar{\mathbf{3}}_3^A \mathbf{2}_3^{III}, \bar{\mathbf{3}}_4^A \mathbf{2}_2^{III};$ $(\mathbf{3}, \mathbf{2}) \mathbf{3}_4^A$
$III \times B$	$(-\frac{2}{3}, -\frac{1}{3})$	$\bar{\mathbf{3}}_1^B \mathbf{2}_3^{III}, \bar{\mathbf{3}}_2^B \mathbf{2}_3^{III}, \bar{\mathbf{3}}_4^B \mathbf{2}_2^{III}, \bar{\mathbf{3}}_5^B \mathbf{2}_1^{III};$ $(\mathbf{3}, \mathbf{2}) \mathbf{3}^B$ non-existent

**Table V.7:**  $U(1)$  charges of the bifundamental matter and additional Yukawa couplings involving at least one  $(\mathbf{3}, \mathbf{2})$ , as arising in the five inequivalent combinations of the  $SU(2)$  and  $SU(3)$  tops studied in the previous chapters.

In the following we will focus on the combination  $I \times A$  as an example. Combining the  $SU(2)$ -I and the  $SU(3)$ -A top amounts to restricting the sections appearing in (V.1) as

$$\begin{aligned}
 b_0 &= b_{0;1,1} e_0 f_0, & b_2 &= b_{2;0,0} e_1 f_1 f_2, & c_1 &= c_{1;0,0} e_1 f_2, & c_2 &= c_{2;0,1} f_0 f_2, \\
 d_0 &= d_{0;1,1} e_0 f_0 f_1, & d_1 &= d_{1;0,0} f_1, & d_2 &= d_{2;1,1} e_0 f_0 f_1^2,
 \end{aligned} \tag{V.49}$$

with the following associated divisor classes

$$\begin{aligned}
 [b_{0;1,1}] &= \alpha - \beta + \bar{\mathcal{K}} - W_2 - W_3, & [b_1] &= \bar{\mathcal{K}}, & [b_{2;0,0}] &= \beta - \alpha + \bar{\mathcal{K}}, \\
 [c_{1;0,0}] &= \bar{\mathcal{K}} - \alpha, & [c_{2;0,1}] &= \bar{\mathcal{K}} - \beta - W_3, \\
 [d_{0;1,1}] &= \alpha + \bar{\mathcal{K}} - W_2 - W_3, & [d_{1;0,0}] &= \beta + \bar{\mathcal{K}}, & [d_{2;1,1}] &= \alpha + \beta + \bar{\mathcal{K}} - W_2 - W_3.
 \end{aligned} \tag{V.50}$$

In table V.8 we list the divisor classes and the corresponding scaling relations among the fibre coordinates. The last part shows the lattice vectors of the top that describes the ambient space.

The vectors  $\underline{x}$  and  $\underline{y}$  should be linearly independent, but otherwise unspecified for a generic base  $\mathcal{B}$ . For this top there exist 16 different triangulations. We choose a triangulation for which the SR-ideal is the union of the individual ideals (V.20) and (V.35) together with the element  $\{f_0 e_1\}$ , i.e. it is generated by

$$\mathbf{u} \mathbf{v}, \mathbf{u} \mathbf{w}, \mathbf{w} s_0, \mathbf{v} s_1, s_0 s_1, e_0 \mathbf{w}, e_1 s_0, e_1 \mathbf{u}, f_0 \mathbf{w}, f_0 s_1, f_1 s_0, f_1 \mathbf{v}, f_2 s_0, f_2 s_1, f_2 \mathbf{u}, f_0 e_1. \quad (\text{V.51})$$

	u	v	w	s <sub>0</sub>	s <sub>1</sub>	e <sub>0</sub>	e <sub>1</sub>	f <sub>0</sub>	f <sub>1</sub>	f <sub>2</sub>
[W <sub>2</sub> ]	·	·	·	·	·	1	·	·	·	·
[W <sub>3</sub> ]	·	·	·	·	·	·	·	1	·	·
α	·	·	1	·	·	·	·	·	·	·
β	·	1	·	·	·	·	·	·	·	·
U	1	1	1	·	·	·	·	·	·	·
S <sub>0</sub>	·	·	1	1	·	·	·	·	·	·
S <sub>1</sub>	·	1	·	·	1	·	·	·	·	·
E <sub>1</sub>	·	·	-1	·	·	-1	1	·	·	·
F <sub>1</sub>	·	1	·	·	·	·	·	-1	1	·
F <sub>2</sub>	·	·	-1	·	·	·	·	-1	·	1
toric data	-1	0	1	-1	0	0	1	0	0	1
	1	-1	0	0	1	0	0	0	1	0
	<u>0</u>	<u>0</u>	<u>0</u>	<u>0</u>	<u>0</u>	<u>x</u>	<u>x</u>	<u>y</u>	<u>y</u>	<u>y</u>

**Table V.8:** Divisor classes and coordinates of the ambient space for top-combination  $\mathbf{I} \times \mathbf{A}$ .

Irrespective of the chosen triangulation, one recovers from the discriminant the **2**- and **3**-matter curves of the two individual tops, (V.3) and (V.5), where of course the base sections  $g_{m,k}$  defining the matter curves are modified in agreement with (V.49).<sup>4</sup> E.g. the representation  $\mathbf{2}_1^1$  is located at the intersection  $\{w_2\} \cap \{c_{2;0,1}\}$  (because in the singular model the locus  $\{w_2\} \cap \{c_2\}$  appearing in (V.3) splits into  $\{w_2\} \cap \{c_{2;0,1}\}$  and  $\{w_2\} \cap \{w_3\}$ , but the latter contributes to matter charged under both  $SU(2)$  and  $SU(3)$ ); similarly the curve hosting  $\mathbf{3}_3^A$  is now given by  $\{w_3\} \cap \{b_{0;1,1} w_2 c_{1;0,0} - b_1 c_{2;0,1}\}$ .

What is new is that along the curve  $\{w_2\} \cap \{w_3\}$  the Kodaira type of the fibre enhances to split type  $I_5$ , corresponding to vanishing orders  $(0, 0, 5)$  of  $(f, g, \Delta)$  in the Weierstrass model. Indeed, the fibre components straightforwardly split to form the affine Dynkin diagram of  $SU(5)$ ; more precisely the five fibre components are given by

$$\begin{aligned}
 \mathbb{P}_{00}^1 &\equiv P_T|_{\{e_0\} \cap \{f_0\}} = b_{2;0,0} f_1 f_2 \mathbf{u} + d_{1;0,0} f_1 s_0 \mathbf{u}^2 + c_{1;0,0} f_2 \mathbf{v} + b_1 s_0 \mathbf{u} \mathbf{v}, \\
 \mathbb{P}_{01}^1 &\equiv P_T|_{\{e_0\} \cap \{f_1\}} = c_{2;0,1} f_0 f_2 + c_{1;0,0} e_1 f_2 s_1 + b_1 s_1 \mathbf{u}, \\
 \mathbb{P}_{02}^1 &\equiv P_T|_{\{e_0\} \cap \{f_2\}} = d_{1;0,0} f_1 + b_1 \mathbf{v}, \\
 \mathbb{P}_{11}^1 &\equiv P_T|_{\{e_1\} \cap \{f_1\}} = b_{0;1,1} e_0 + c_{2;0,1} f_2 \mathbf{w} + b_1 s_1 \mathbf{w}, \\
 \mathbb{P}_{12}^1 &\equiv P_T|_{\{e_1\} \cap \{f_2\}} = d_{2;1,1} e_0 f_1^2 + d_{0;1,1} e_0 f_1 \mathbf{v} + b_{0;1,1} e_0 \mathbf{v}^2 + d_{1;0,0} f_1 \mathbf{w} + b_1 \mathbf{v} \mathbf{w},
 \end{aligned} \quad (\text{V.52})$$

where we used the SR-ideal to set as many coordinates to one as possible. Note that  $e_1$  and  $f_0$  do not intersect due to the SR-ideal relations so that the locus  $P_T|_{\{e_1\} \cap \{f_0\}}$  is absent in (V.52).

The fibre component  $\mathbb{P}_{00}^1 + \mathbb{P}_{02}^1$  is identified with the highest weight of the bifundamental representation  $(\mathbf{3}, \mathbf{2})$ ; the  $U(1)_1$  and  $U(1)_2$  charges are found to be  $(\frac{1}{6}, -\frac{1}{3})$  by computing the

<sup>4</sup>In addition, the same type *III* and *IV* enhancement loci arise as before, which do not carry matter representations.

intersection product with the generators

$$\begin{aligned}\omega_1^{I \times A} &= S_1 - S_0 - \bar{\mathcal{K}} + \frac{1}{2}E_1 + \frac{2}{3}F_1 + \frac{1}{3}F_2, \\ \omega_2^{I \times A} &= U - S_0 - \bar{\mathcal{K}} - [c_{1;0,0}] + \frac{2}{3}F_1 + \frac{1}{3}F_2.\end{aligned}\tag{V.53}$$

Finally, we have analysed the intersection of  $\{w_2\} \cap \{w_3\}$  with each of the **3**- and **2**-curves to identify extra fibre enhancements signalling Yukawa couplings involving the new  $(\mathbf{3}, \mathbf{2})$ -state. The fibres over the Yukawa points  $(\mathbf{3}, \mathbf{2}) - \bar{\mathbf{3}} - (\mathbf{2}/\bar{\mathbf{2}})$  are of split Kodaira type  $I_6$ , and the fibre components can be explicitly checked to form the affine Dynkin diagram of  $SU(6)$ . The base points are found by intersecting  $W_3$  and  $W_2$  with the five **3**-curves and noting that the intersection points also lie on top of one of the **2**-curves.

A special role is played by the intersection locus  $\{w_3\} \cap \{w_2\} \cap \{b_{0;1,1} w_2 c_{1;0,0} - b_1 c_{2;0,1}\}$ , where the last term comes from the  $\mathbf{3}_3^A$ -curve. Using `Singular`, or simply by staring at it, one easily convinces oneself that there are two separate sets of points in this intersection locus: Apart from the point  $\{w_3\} \cap \{w_2\} \cap \{c_{2;0,1}\}$ , where the  $(\mathbf{3}, \mathbf{2}) \bar{\mathbf{3}}_3^A \bar{\mathbf{2}}_1^I$  Yukawa coupling is localised, there is also the intersection  $\{w_3\} \cap \{w_2\} \cap \{b_1\}$ , which does not lie on any of the **2**-curves. At the latter point the vanishing orders  $(2, 3, 7)$  of  $(f, g, \Delta)$  in the corresponding Weierstrass model points towards a locus of  $SO(10)$ -enhancement i.e. the fibre being of Kodaira type  $I_1^*$ . Yet the fibre structure does not reproduce the full affine  $SO(10)$  Dynkin diagram, but rather a reduced diagram where one of the multiplicity 2 nodes is deleted, such that the adjacent three nodes intersect at one point. Nevertheless, the remaining fibre components are sufficient to realise the Yukawa coupling  $(\mathbf{3}, \mathbf{2}) (\mathbf{3}, \mathbf{2}) \mathbf{3}_3^A$ .<sup>5</sup>

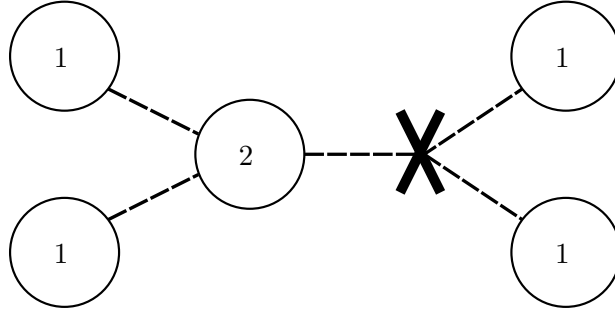


**Figure V.1:** Non-standard fibre structure at the  $(\mathbf{3}, \mathbf{2}) (\mathbf{3}, \mathbf{2}) \mathbf{3}$  Yukawa point. The ‘X’ marks the intersection point of the three adjacent  $\mathbb{P}^1$ s. Inserting an additional  $\mathbb{P}^1$  at this point would recreate the full affine  $SO(10)$  Dynkin diagram.

### Explicit example over $\mathcal{B} = \mathbb{P}^3$

We have checked the above calculations for a specific fibration over the base  $\mathcal{B} = \mathbb{P}^3$  with  $H^{1,1}(\mathbb{P}^3) = \{n \cdot H | n \in \mathbb{Z}\}$ , where  $H$  is the hyperplane class, and  $\bar{\mathcal{K}} = 4H$ . For simplicity we take  $w_2$  and  $w_3$  to be two of the four homogeneous coordinates  $(z_0 : z_1 : z_2 : z_3)$ , e.g.  $w_2 = z_0$  and  $w_3 = z_1$ ; then  $W_2 = W_3 = H$ . Recall that  $b_i, c_j, d_k$  must transform as sections of specific line bundles, see table V.1, where there is freedom left in choosing  $\alpha$  and  $\beta$ . They are subject to further constraints as the restricted sections (V.49) in the presence of the non-abelian symmetry must be effective classes. Over  $\mathcal{B} = \mathbb{P}^3$ , these constraints are met with a particular choice  $\alpha = 2H$ ,

<sup>5</sup>Similar phenomena have been observed in other geometries such as at the  $E_6$ -enhancement point in  $SU(5)$  models realising the **10 10 5** coupling, or at the  $E_8$  point in  $E_6$  models realising the **27 27 27** coupling.

coupling	locus = $W_2 \cap W_3 \cap \dots$	fibre type
$(\mathbf{3}, \mathbf{2}) \bar{\mathbf{3}}_1^A \mathbf{2}_3^I$	$\{b_{0;1,1}\}$	$I_6$
$(\mathbf{3}, \mathbf{2}) \bar{\mathbf{3}}_2^A \mathbf{2}_2^I$	$\{c_{1;0,0}\}$	$I_6$
$(\mathbf{3}, \mathbf{2}) \bar{\mathbf{3}}_3^A \mathbf{2}_1^I$	$\{c_{2;0,1}\}$	$I_6$
$(\mathbf{3}, \mathbf{2}) \bar{\mathbf{3}}_4^A \mathbf{2}_2^I$	$\{b_1 b_{2;0,0} - c_{1;0,0} d_{1;0,0}\}$	$I_6$
$(\mathbf{3}, \mathbf{2}) \bar{\mathbf{3}}_5^A \mathbf{2}_3^I$	$\{b_{0;1,1}, d_{1;0,0}^2 - b_1 d_{0;1,1} d_{1;0,0} + b_1^2 d_{2;1,1}\}$	$I_6$
$(\mathbf{3}, \mathbf{2}) (\mathbf{3}, \mathbf{2}) \mathbf{3}_3^A$	$\{b_1\}$	reduced $I_1^*$

**Table V.9:** Details on the additional Yukawas involving bifundamental matter in the top combination  $I \times A$ .

$\beta = H$ , in which case the classes of the restricted sections must be

$$\begin{aligned}
 [b_{0;1,1}] &= 3H, & [b_1] &= 4H, & [b_{2;0,0}] &= 3H, & [c_{1;0,0}] &= 2H, \\
 [c_{2;0,1}] &= 2H, & [d_{0;1,1}] &= 4H, & [d_{1;0,0}] &= 5H, & [d_{2;1,1}] &= 5H.
 \end{aligned} \tag{V.54}$$

From this choice of  $\alpha$  and  $\beta$  we have to impose the condition  $2\vec{w} + \vec{v} + \vec{e}_0 + \vec{f}_0 + \vec{z}_2 + \vec{z}_3 = 0$ , where  $(\vec{\cdot})$  is the  $(\cdot)$ -coordinate's lattice vector of the toric diagram of the full fibration ('toric data' in table V.8). This condition is met by the toric ambient space  $\hat{X}_5$ , whose toric diagram has the lattice vectors shown in table V.10. The resulting polytope is reflexive, guaranteeing that the fourfold cut out by the hypersurface polynomial inside this toric ambient space is smooth. The Euler characteristic of the fourfold is 1440.

$\vec{u}$	$\vec{v}$	$\vec{w}$	$\vec{s}_0$	$\vec{s}_1$	$\vec{e}_0$	$\vec{f}_0$	$\vec{z}_2$	$\vec{z}_3$	$\vec{e}_1$	$\vec{f}_1$	$\vec{f}_2$
-1	0	1	-1	0	0	0	-2	0	1	0	1
1	-1	0	0	1	0	0	1	0	0	1	0
0	0	0	0	0	1	0	0	-1	1	0	0
0	0	0	0	0	0	1	0	-1	0	1	1
0	0	0	0	0	0	0	1	-1	0	0	0

**Table V.10:** Toric diagram for the ambiente space  $\hat{X}_5$  of the model  $I \times A$  over the base  $\mathcal{B} = \mathbb{P}^3$ .

### Other top combinations

The above analysis can be repeated for the remaining four inequivalent combinations of tops and leads to the couplings listed in (V.7). Note that for the top combinations  $III \times A$  and  $III \times B$  no gauge invariant coupling  $(\mathbf{3}, \mathbf{2}) \bar{\mathbf{3}}_5^A \mathbf{2}$  resp.  $(\mathbf{3}, \mathbf{2}) \bar{\mathbf{3}}_3^B \mathbf{2}$  exists. In both cases, the intersection point of the  $(\mathbf{3}, \mathbf{2})$ - and the corresponding  $\bar{\mathbf{3}}$ -curve lies on the curve of non-split  $I_3$ -enhancement described after (B.18) in appendix 2. Were it not for a monodromy along that curve, an additional  $\mathbf{2}$ -representation would arise, which in fact would have the correct quantum numbers to couple as in  $(\mathbf{3}, \mathbf{2}) \bar{\mathbf{3}}_5^A \mathbf{2}$  (or  $(\mathbf{3}, \mathbf{2}) \bar{\mathbf{3}}_3^B \mathbf{2}$ ). Correspondingly, the fibre over the triple intersection of these curves does enhance to form an  $I_6$  Kodaira fibre, but due to the described monodromy no physical Yukawa couplings result as the  $\mathbf{2}$ -state in question is projected out.



More drastically, the top combination  $\text{III} \times \text{B}$  exhibits a non-Kodaira enhancement in the fibre over  $\{w_3\} \cap \{w_2\} \cap \{b_1\}$ .<sup>6</sup> At this set of points, several matter curves collide and the vanishing orders of  $(f, g, \Delta)$  in the Weierstrass model take the values  $(4, 6, 12)$ . For such high enhancement no flat crepant resolution can be found. To see how this manifest itself, consider the triangulation of the  $\text{III} \times \text{B}$  top leading to an SR-ideal generated by (B.11) (for the  $SU(2)$  part), (B.20) (for the  $SU(3)$  part) and the new elements  $\{s_1 e_0 f_1, e_1 f_0 f_2\}$ : For this SR-ideal the fibration becomes non-flat over  $\{w_3\} \cap \{w_2\} \cap \{b_1\}$  as the hypersurface polynomial  $P_T$  becomes trivial for  $b_1 = e_0 = f_1 = 0$ . Therefore, in order for the top combination  $\text{III} \times \text{B}$  to give rise to a well-defined F-theory compactification, the point set  $\{w_3\} \cap \{w_2\} \cap \{b_1\}$  must be empty. Since  $b_1$  is universally in the class  $\bar{\mathcal{K}}$ , these points cannot be turned off by a suitable choice of classes  $\alpha$  and  $\beta$  appearing in table (V.1). While it is not excluded that  $W_2$  and  $W_3$  can be found such that no intersection points  $\{w_3\} \cap \{w_2\} \cap \{b_1\}$  arise, we do currently not have an example of this type.

## 2 Standard Model Embeddings

The toric fibrations with gauge group  $SU(3) \times SU(2) \times U(1)_1 \times U(1)_2$  constructed in the previous section are the starting point of our search for F-theory vacua with Standard Model gauge group and matter. In this section we want to investigate how the Standard Model spectrum can be embedded into the geometrically realised spectrum. For the moment we will not address chirality and only base our analysis on the possible  $U(1)$  charges.

### 2.1 Criteria for Standard Model Embeddings

Our discussion will be phrased in the framework of the  $\mathcal{N} = 1$  Minimal Supersymmetric Standard Model (MSSM), potentially extended by further singlets, with the understanding that supersymmetry is broken a priori unknown energy below the compactification scale in agreement with current lower collider bounds. To fix our conventions we recall the MSSM spectrum plus right-handed neutrinos  $\nu_R^c$  (taking all fields to be chiral  $\mathcal{N} = 1$  superfields) in table V.11. We also allow for the possibility of the  $\mu$ -term in the Higgs sector being generated via the VEV of an MSSM singlet  $\mathbf{1}_\mu$ , as studied extensively in the literature in the framework of the NMSSM (see e.g [133] and references therein).<sup>7</sup>

At the level of renormalisable couplings, the superpotential of the singlet-extended MSSM takes the form

$$W = W_1 + W_2 + W_{\text{singlet}}, \quad (\text{V.55})$$

$$W_1 = Y_u Q H_u u_R^c + Y_d Q H_d d_R^c + Y_e L H_d e_R^c + Y_\nu L H_u \nu_R^c + \mu H_u H_d, \quad (\text{V.56})$$

$$W_2 = \alpha Q L d_R^c + \beta u_R^c d_R^c d_R^c + \gamma L L e_R^c + \kappa L H_u, \quad (\text{V.57})$$

$$W_{\text{singlet}} = \delta_{3,0} \mathbf{1}_\mu \mathbf{1}_\mu \mathbf{1}_\mu + \delta_{2,1} \mathbf{1}_\mu \mathbf{1}_\mu \nu_R^c + \delta_{1,2} \mathbf{1}_\mu \nu_R^c \nu_R^c + \delta_{0,3} \nu_R^c \nu_R^c \nu_R^c, \quad (\text{V.58})$$

where we are suppressing family indices. Here,  $W_1$  contains the Yukawa couplings that give rise to the masses for the up-quarks, down-quarks and the charged leptons as well as potential Dirac masses for the right-handed neutrinos. We also include here the  $\mu$ -term for the Higgs sector, with the understanding that this term might originate from a Yukawa coupling  $Y_\mu \mathbf{1}_\mu H_u H_d$  if the scalar in the superfield  $\mathbf{1}_\mu$  acquires a non-trivial VEV. For completeness we have furthermore listed possible dimension-four singlet couplings  $W_{\text{singlet}}$ . If  $\langle \mathbf{1}_\mu \rangle \neq 0$  the third term in  $W_{\text{singlet}}$

<sup>6</sup>In the other four top combinations this point corresponds to the  $(\mathbf{3}, \mathbf{2})(\mathbf{3}, \mathbf{2})\mathbf{3}$  coupling. For  $\text{III} \times \text{B}$ , however, there is no suitable  $\mathbf{3}$  state.

<sup>7</sup>A detailed and systematic analysis of such singlet extensions of the MSSM in perturbative Type II intersecting brane quivers has been performed in [134].

matter		representation	hypercharge
left-handed quarks	$Q$	$(\mathbf{3}, \mathbf{2})$	$\frac{1}{6}$
right-handed up-quarks	$u_R^c$	$(\bar{\mathbf{3}}, \mathbf{1}) \equiv \bar{\mathbf{3}}_u$	$-\frac{2}{3}$
right-handed down-quarks	$d_R^c$	$(\bar{\mathbf{3}}, \mathbf{1}) \equiv \bar{\mathbf{3}}_d$	$\frac{1}{3}$
Higgs-up	$H_u$	$(\mathbf{1}, \mathbf{2}) \equiv \mathbf{2}_u$	$\frac{1}{2}$
Higgs-down	$H_d$	$(\mathbf{1}, \mathbf{2}) \equiv \mathbf{2}_d$	$-\frac{1}{2}$
left-handed leptons	$L$	$(\mathbf{1}, \mathbf{2}) \equiv \mathbf{2}_L$	$-\frac{1}{2}$
right-handed electrons	$e_R^c$	$(\mathbf{1}, \mathbf{1}) \equiv \mathbf{1}_e$	1
right-handed neutrinos	$\nu_R^c$	$(\mathbf{1}, \mathbf{1}) \equiv \mathbf{1}_\nu$	0
$\mu$ -singlet		$(\mathbf{1}, \mathbf{1}) \equiv \mathbf{1}_\mu$	0

**Table V.11:** Matter spectrum of the MSSM.

effectively contributes to the Majorana mass term for the right-handed neutrinos, while the first term would induce an F-term in the vacuum and is therefore of interest in the context of supersymmetry breaking. We have not listed potential tadpole and holomorphic mass terms involving the singlets, which are also allowed by the MSSM gauge group.

The couplings in  $W_2$  each violate R-parity  $(-1)^{2S+3(B-L)}$  with  $S$  the spin and  $B, L$  baryon and lepton number. The second term does in addition not conserve baryon number, while the remaining terms are lepton-number violating. In particular, some combinations of terms within  $W_2$  lead to rapid proton decay and are therefore severely constrained [135, 136]. Proton decay due to dimension-four operators requires both baryon and lepton-number violating contributions. The most severe constraints arise from tree-level induced proton decay, which is generated only if both  $\alpha$  and  $\beta$  are non-zero simultaneously. However, the precise bounds on the couplings depend, amongst other things, on the scale of supersymmetry breaking. In models with intermediate or high-scale supersymmetry breaking some of the constraints on  $W_2$  are considerably relaxed compared to TeV-scale supersymmetric scenarios. For more details of the extremely rich phenomenology of R-parity violating couplings we refer in addition to [135–137] and references therein.

At mass dimension five, the MSSM allows for the following baryon or lepton number violating operators [137],

$$W_3 = \lambda_1 Q Q Q L + \lambda_2 u_R^c u_R^c d_R^c e_R^c + \lambda_3 Q Q Q H_d + \lambda_4 Q u_R^c e_R^c H_d + \lambda_5 L L H_u H_u + \lambda_6 L H_d H_u H_u, \quad (\text{V.59})$$

$$K \supset \lambda_7 u_R^c (d_R^c)^* e_R^c + \lambda_8 H_u^* H_d e_R^c + \lambda_9 Q u_R^c L^* + \lambda_{10} Q Q (d_R^c)^*. \quad (\text{V.60})$$

Additional dimension-five terms are possible which involve the singlets  $\nu_R^c$  and  $\mathbf{1}_\mu$ . In particular, any of the dimension-four operators present in (V.55) can in principle be dressed with such a singlet. We do not list these couplings explicitly here.

Our attitude towards lepton and baryon number violating couplings is as follows: In order to fully explore the parameter space of possible Standard Models within our framework we do not insist on TeV scale supersymmetry a priori, but rather allow for the possibility of intermediate scale supersymmetry breaking. While the viability of such a scenario will ultimately be determined experimentally, a higher supersymmetry breaking scale is in fact a natural option in direct Standard Model constructions. After all, the exact unification of the gauge couplings at a scale around  $10^{16}$  GeV, which is one of the predictions of the TeV scale MSSM, is not immediate if

the gauge groups  $SU(3)$ ,  $SU(2)$  and  $U(1)_Y$  are constructed independently. More importantly perhaps, intermediate scale supersymmetry is well-motivated by a 126 GeV Higgs as studied in string theoretic frameworks recently in [138–142] (see also [143–146] and references therein for other recent examples in the literature motivating an intermediate supersymmetry breaking scale). Keeping an open mind towards the supersymmetry breaking scale, we do therefore not require absence of all dimension-four and -five lepton and baryon number violating couplings in our search criterion for Standard Model configurations, but will only list which of these couplings are present. A more detailed study of the associated phenomenology, taking into account the details of supersymmetry breaking, is left for future explorations. Having said that, in many cases the  $U(1)$  selection rules do prevent potentially dangerous such operators as we will see explicitly.

For each of the five combinations of tops with gauge group  $SU(3) \times SU(2) \times U(1)_1 \times U(1)_2$  a plethora of possibilities arises for identifying the massless representations with the MSSM fields. This identification will in particular determine which linear combination of  $U(1)_1$  and  $U(1)_2$  corresponds to hypercharge  $U(1)_Y$ . The orthogonal combination is then massless in absence of gauge fluxes and will remain as a perturbative selection rule after gauge fluxes induce a Stückelberg mass for the associated gauge potential. At the same time it must be ensured that the gauge fluxes do not render hypercharge massive. In the sequel we classify the possible identifications along the following lines:

- Since the fibrations under consideration contain only one type of  $(\mathbf{3}, \mathbf{2})$ -curve, all three generations of left-handed quark fields  $Q$  must reside on this single  $(\mathbf{3}, \mathbf{2})$ -curve. The  $U(1)_1 \times U(1)_2$  charges of  $Q$  for the five possible tops are listed in table V.7.
- In a second step we identify the fields  $(H_u, H_d)$  with two of the  $\mathbf{2}_i$ -representations or their conjugate representations  $\bar{\mathbf{2}}_i$ ,  $i = 1, 2, 3$ . A definite assignment of  $(H_u, H_d)$  together with the  $U(1)$  charges of  $Q$  determines  $U(1)_Y$  as a linear combination

$$U(1)_Y = aU(1)_1 + bU(1)_2, \quad a, b \in \mathbb{R}. \quad (\text{V.61})$$

We then identify the different possible choices of  $\mathbf{2}_i$ - or  $\bar{\mathbf{2}}_i$ -states for the left-handed leptons  $L$  based on their hypercharge. The same value of  $(a, b)$  and identification of  $(H_u, H_d)$  may be compatible with more than one choice for  $L$ . In this case, different generations of leptons  $L$  may reside on different matter curves and will then be distinguished by their charge under the linear combination of  $U(1)_1$  and  $U(1)_2$  orthogonal to  $U(1)_Y$ .

- For the specific values of  $(a, b)$  in (V.61) we next check which of the six singlets  $\mathbf{1}^{(k)}$ ,  $k = 1, \dots, 6$  (and their conjugates) have the correct hypercharge to be identified with the fields  $\nu_R^c$  and  $e_R^c$ , and similarly which of the  $\bar{\mathbf{3}}_j$ -representations for  $j = 1, \dots, 5$  have the correct hypercharge to be identified with  $u_R^c$  and  $d_R^c$ . If there is no possible assignment of  $e_R^c$ ,  $u_R^c$  or  $d_R^c$  we discard this choice of hypercharge. However, to be as general as possible, we do allow for configurations with no right-handed neutrinos  $\nu_R^c$ .
- There are now two types of right-handed leptons and quarks: If the Yukawa couplings  $W_1$  in (V.55) are indeed among the geometrically realised couplings as analysed in the previous sections, the fields acquire a perturbative mass term upon electro-weak symmetry breaking. Those generations of MSSM matter for which this is the case will therefore be called ‘heavy’.<sup>8</sup> Otherwise, the Yukawas, which are now forbidden by the extra  $U(1)$

<sup>8</sup>Note that if two or more families are localised on the same matter curve the rank of the perturbative Yukawa coupling matrix is non-maximal, at least if there exists only one Yukawa coupling point, as studied in the F-theory GUT literature [53, 147–149]. In this case some of the ‘heavy’ fields do not receive a perturbative mass after all. Non-perturbative effects can solve this rank-one problem [150–153].

selection rules, must be generated either by non-perturbative effects [154–158], here by M5-brane instantons<sup>9</sup>, or via higher non-renormalisable couplings involving one or more extra singlet states as these acquire a VEV. In both cases the mass terms will generically be suppressed and the corresponding fields will be called ‘light’. Again it is understood that different generations can be distributed over the various matter curves. In particular, if only one of the generations enjoys a perturbative coupling, this could serve as a realisation of the observed mass hierarchies in the MSSM.<sup>10</sup> Note that while the generation of masses for the ‘light’ generations by M5-instantons depends on the specific geometry of the base  $\mathcal{B}$ , the mechanism involving singlet fields could be analysed already at this general level by checking for the existence of singlets with appropriate  $U(1)_i$ -charges to form a dimension-5 coupling of the required type. We leave such a more advanced analysis for further studies.

- The  $U(1)_Y$  charges together with the spectrum of perturbative couplings also provide candidates for  $\mu$ -singlets  $\mathbf{1}_\mu$  with a Yukawa coupling  $\mathbf{1}_\mu H_u H_d$ , which we list. As anticipated, if  $\langle \mathbf{1}_\mu \rangle \neq 0$  this will induce a  $\mu$ -term in the Higgs sector. In absence of such a VEV the  $\mu$ -term can in principle be generated via M5-instantons. Note that sometimes the same type of singlets can also have several interpretations. We furthermore list which other couplings in  $W_{\text{singlet}}$  are allowed. Since there is only one type of  $\mathbf{1}_\mu$ , the term  $\mathbf{1}_\mu^3$  term is always forbidden perturbatively, but for  $\nu_R^c$  a cubic coupling for the neutrino involving families distributed over different curves can exist. Note that tadpole terms in the superpotential, linear in the singlets, can only be generated non-perturbatively. Holomorphic quadratic terms involving either different families of  $\nu_R^c$  or one  $\nu_R^c$  and  $\mathbf{1}_\mu$  are allowed by gauge invariance for vector-like pairs of such fields, even though we do not list this explicitly. Determining their presence amounts to computing the vector-like spectrum of massless states. Otherwise quadratic singlet terms, especially Majorana mass terms for  $\nu_R^c$ , are only generated non-perturbatively [154, 155] or as effective couplings from the cubic interactions with  $\langle \mathbf{1}_\mu \rangle \neq 0$ .
- Based on the various assignments of fields we list the perturbative  $R$ -parity violating dimension-four couplings  $W_2$  in (V.55) which are allowed in view of the structure of geometrically realised Yukawa couplings. More precisely, we list for which of the possible choice of (‘heavy’ or ‘light’) right-handed quark and lepton fields a coupling of type  $\alpha, \beta, \gamma$  is realised. The coupling  $\kappa$  is allowed by the  $U(1)$  selection rules whenever  $L$  and  $H_u$  reside on the same matter curve and are thus vector-like with respect to all gauge symmetries. Such terms correspond to effective mass couplings and their presence can be read off from the precise vector-like spectrum of the compactification, which can be computed in F-theory once the gauge background is specified [95].
- Finally we check for which matter identifications the potentially dangerous dimension-five couplings (V.59) are perturbatively allowed, based on the  $U(1)_i$  charges of the involved fields. Note that in principle, this does not necessarily imply that the couplings are actually non-zero; to check this one would have to analyse in more detail how precisely the non-renormalisable couplings arise by exchange of heavy intermediate states. Depending on the details of the set-up the resulting couplings can be negligibly small. This is left for a more in-depth analysis, and we take the results based purely on  $U(1)_i$  selection rules merely as a first indication. Let us also note that some of the non-perturbative effects required to induce the Yukawa couplings for the ‘light’ generations may at the same time induce other baryon or lepton-number violating or other undesirable operators [172–175]. We do not check for this possibility here. Furthermore we reiterate that the constraints on

<sup>9</sup>The generation of charged operators via D3/M5-branes in F-theory along the lines of [154–158] has been studied recently in [159, 159–165], and related aspects of such instantons in F-theory appear in [166–171].

<sup>10</sup>The generation of such mass hierarchies in perturbative Type II MSSM quivers has been studied systematically in [172–174].

both dimension-four and -five couplings are relaxed in scenarios with intermediate or even high-scale supersymmetry breaking.

The results of this scan over possible Standard-Model-like embeddings is presented in appendix C. In configurations where the matter states can be localised at different curves, we do not list all possible combinations separately. In particular our analysis so far does not make any statements about whether it is possible to realise precisely the Standard Model context by inclusion of fluxes. Irrespective of our relaxed attitude towards baryon and lepton number violation, a number of configurations exists in which all dangerous dimension-four and in particular the dimensions-five operators  $\lambda_1$  and  $\lambda_2$  in (V.59) are absent as a result of the  $U(1)$  selection rules.

### A Specific Example

As an example consider model number 5 in the top combination  $I \times A$  listed in table C.1 with  $U(1)_Y = U(1)_1$ . In perhaps the simplest scenario, the  $H_u$ ,  $H_d$  and all families of left-handed leptons  $L$  are realised as the states  $\bar{\mathbf{2}}_1^1$ ,  $\bar{\mathbf{2}}_2^1$  and  $\bar{\mathbf{2}}_3^1$  respectively. In particular,  $U(1)_2$  therefore distinguishes these states. Perturbative lepton masses arise if we identify  $\nu_R^c = \bar{\mathbf{1}}^{(6)}$  and  $e_R^c = \mathbf{1}^{(1)}$ . For the choice  $(u_R^c, d_R^c) = (\bar{\mathbf{3}}_4^A, \bar{\mathbf{3}}_3^A)$  the quark masses are also realised perturbatively with the caveat noted in footnote 8. For the described assignment of matter all R-parity violating dimension-four couplings are perturbatively forbidden, as are the potentially problematic dimension-five couplings  $\lambda_1 Q Q Q L$  and  $\lambda_2 u_R^c u_R^c d_R^c e_R^c$ .

However, more complicated assignments are possible. For instance, if one or more families of leptons  $L$  are instead identified with the state  $\bar{\mathbf{2}}_2$ , then in this family the right-handed neutrino, which could be any of the states  $\mathbf{1}^{(5)}$ ,  $\mathbf{1}^{(6)}$  or their conjugates, does not have a perturbative Dirac mass. In this case, the Dirac mass would have to be generated directly by non-perturbative effects as proposed in [176], naturally explaining the smallness of the neutrino masses via the non-perturbative suppression. If both types of matter identifications are combined for different families, a lepton-number violating dimension-four term  $\mathbf{2}_3 \mathbf{2}_3 \mathbf{1}_2$  arises, where  $\mathbf{1}^{(2)}$  is now the ‘massive’  $e_R^c$  which couples perturbatively to the  $L$ -family  $\bar{\mathbf{2}}_2$ . This coupling is innocuous for the proton as no baryon-lepton number violating terms are created.

## 2.2 Search for models with realistic chiral spectrum

Having classified all possible matchings of the geometric spectrum with the (N)MSSM, we want to study now whether, in explicit compactifications,  $G_4$  fluxes can actually induce a realistic chiral spectrum in our F-theory ‘Standard Models’. We will present the full analysis of the model  $I \times A$  here.

With our methods and results from chapters III and IV, we are in a position to systematically scan over all possible vertical fluxes to search for realistic chiral indices. For convenience, we recall from the earlier chapters, that a vertical flux is an element  $G_4 \in H_{\text{vert}}^{(2,2)}(Y_4)$  satisfying the conditions

$$\int_{Y_4} G_4 \wedge S_0 \wedge D_a^{(\mathcal{B})} = \int_{Y_4} G_4 \wedge D_a^{(\mathcal{B})} \wedge D_b^{(\mathcal{B})} = \int_{Y_4} G_4 \wedge E_i \wedge D_a^{(\mathcal{B})} = 0 \quad \forall D_{a,b}^{(\mathcal{B})} \in H^{(1,1)}(\mathcal{B}), \quad (\text{V.62})$$

obeying the quantisation

$$G_4 + \frac{1}{2}c_2(Y_4) \in H^4(Y_4, \mathbb{Z}), \quad (\text{V.63})$$

as well as the D3-tadpole cancellation condition

$$n_{D_3} = \frac{\chi(Y_4)}{24} - \int_{Y_4} G_4 \wedge G_4 \in \mathbb{Z}. \quad (\text{V.64})$$

The chiral index of states in representation  $\mathcal{R}$  localised on a matter surface  $\gamma_{\mathcal{R}}$  is computed as

$$\chi(\mathcal{R}) = \int_{\gamma_{\mathcal{R}}} G_4 = \int_{Y_4} G_4 \wedge [\gamma_{\mathcal{R}}], \quad (\text{V.65})$$

which for a consistent flux must all be integer. The (co-)homology classes  $[\gamma_{\mathcal{R}}]$  of the  $I \times A$  model leading to an anomaly free spectrum are summarised in table IV.11.

An important phenomenological restriction arises from the requirement that the MSSM hypercharge

$$U(1)_Y = aU(1)_1 + bU(1)_2 \quad (\text{V.66})$$

must not receive a Stückelberg mass. This is guaranteed precisely if

$$\int_{Y_4} G_4 \wedge \omega_Y \wedge D_a^{(\mathcal{B})} = 0 \quad \forall D_a \in H^{(1,1)}(\mathcal{B}), \quad \text{where } \omega_Y = a\omega_1 + b\omega_2 \quad (\text{V.67})$$

is the hypercharge generator defined in terms of the generators of the two  $U(1)_i$ , c.f. (V.48). This condition ensures that no  $U(1)_Y$ -D-term is induced by the flux, which is equivalent to stating that the fluxes do not lead to a  $U(1)_Y$ -dependent gauging of the axions as would be the case if the  $U(1)_Y$  boson received a Stückelberg mass. Recalling the Green–Schwarz counterterms for  $U(1)$ -anomalies from chapter IV, this in particular implies that these are 0 for vanishing D-term. Note that for the model  $I \times A$  there are three possibilities for the geometric  $U(1)_{1,2}$  to form the hypercharge  $U(1)_Y = aU(1)_1 + bU(1)_2$ , namely  $(a, b) = (1, 0)$ ,  $(a, b) = (0, -1/2)$  and  $(a, b) = (-1, -1)$ . These three possibilities will lead to different  $G_4$  solutions, as we will require the flux to induce no D-term potential for hypercharge via (V.67).

To obtain explicit chiral indices we have to specify the full fibration data, i.e. a choice for the base  $\mathcal{B}$  and the classes  $\alpha, \beta$  as well as  $W_2, W_3$  entering (V.50). We then determine the space of valid  $G_4$ -fluxes and scan over part of it to search for configurations giving rise to realistic chiralities. In this scan we restrict ourselves to fluxes with induced chiral spectra in the range  $|\chi| < 10$ .

There are two possible routes one can take for such a search. With the results from the previous chapter, the obvious procedure would be to use the fluxes (IV.116) derived for a generic base, specialise to a concrete (consistent) fibration, and make use of the chiralities in tables IV.12 and IV.13 as well as the formulae for the D-terms (IV.120) and the D3-tadpole (IV.146). This route seems very attractive because one can impose the chirality of many states to take a desired value and then solve for the flux parameters  $z_i$  and  $\mathcal{D}, \mathcal{D}'$ . In particular, one could in principle pick one's favourite Standard Model identification from table C.1 and try to construct a suitable flux. However, while the chiralities can often be tweaked into a more or less favourable scenario, we found that with this approach, it is generically very hard to find an appropriately quantised flux, e.g. such that the D3-tadpole is integer. The existence of suitably quantised flux solutions which give rise to a given spectrum depends of course on the concrete choice of base  $\mathcal{B}$ , and for suitable  $\mathcal{B}$  this approach may well lead to satisfactory results.

In the sequel, we will follow an alternative strategy and instead scan over part of the flux landscape to investigate how closely the resulting models resemble the Standard Model. In principle one could use the basis (IV.116) and simply specialise it to a concrete base space  $\mathcal{B}$ . However, the lattice spanned by the fluxes (IV.116) is usually too coarse because the vertical divisors  $\overline{\mathcal{K}}, \alpha$  and  $\beta$  are in general not prime divisors. The effect is that the resulting chiral indices in tables IV.12 and IV.13 are generically very large for order 1 values of the coefficients  $z_i$ , and a suitable scan would require highly fractional coefficients, which in turn obscure the quantisation of the fluxes. It is therefore more convenient to compute a basis of fluxes for each individual fibration. This basis will still be equivalent to the generic fluxes (IV.116) (modulo

redundancies from the specialisation of the fibration) as a  $\mathbb{Q}$ -vector basis. However, we find that in general, these basis elements span a finer lattice in the sense that they induce small chiral indices even if we allow for integer coefficients. This allows in particular for a finer scan over the flux landscape than using the fluxes (IV.116).

### 2.2.1 Search algorithm

We have constructed fibrations over the toric bases  $\mathcal{B} \in \{\mathbb{P}^3, \text{Bl}_1\mathbb{P}^3, \text{Bl}_2\mathbb{P}^3\}$ . For simplicity we identify each of the coordinates  $w_2$  and  $w_3$  describing the  $SU(2)$  and  $SU(3)$  brane divisors with one of the homogeneous coordinates of  $\mathcal{B}$ .<sup>11</sup> Having fixed this choice, we then restrict the classes  $\alpha$  and  $\beta$  such that all the sections (V.50) have effective classes. Each allowed pair  $(\alpha, \beta)$  fixes a polytope for the toric ambient space  $X_5$ . To fully define  $X_5$ , we need to find a suitable triangulation of the polytope that defines a toric fan compatible with the fibration structure, and ultimately also determines the Stanley–Reisner-ideal. We use the Sage package Topcom to find all possible triangulations and then pick one whose SR-ideal contains (V.51) as a subset. This allows us to use the results on the matter surfaces as listed in table IV.11, which crucially depend on the SR-ideal.

Note that while for the bases  $\mathbb{P}^3$  and  $\text{Bl}_1\mathbb{P}^3$  it is always possible to find such a triangulation, this need not generally be the case. In such a situation, one would need to repeat the analysis of matter surfaces in section 3.1.3 of chapter IV with another suitable SR-ideal. In our search we encounter this situation only for fibrations over the base  $\mathcal{B} = \text{Bl}_2\mathbb{P}^3$ . These particular models would not be suitable for phenomenological applications anyway, because they are only compatible with a fibration in which the divisors  $W_2$  and  $W_3$  of our fixed choice do not intersect on  $\mathcal{B}$ . On the resulting fourfold we would have no bifundamental  $(\mathbf{3}, \mathbf{2})$  states.

Having fully defined the toric ambient space  $X_5$  it is straightforward to compute the cohomology ring (III.21) using Sage. Note that for toric spaces the vertical cohomology (III.21) constitutes in fact the full cohomology ring. This is of course not the case for the hypersurface  $Y_4$ . We then proceed to find a basis  $\{t_i\}$  of  $H_{\text{vert}}^{(2,2)}(Y_4)$ . It is not necessarily the same as the basis of  $H^{(2,2)}(X_5)$ , since different  $(2, 2)$ -forms can – and in fact do – become equivalent when restricted to the hypersurface  $P_T$ .<sup>12</sup> As explained in the section 2 of chapter IV, we use Singular to determine the basis  $\{t_i\}$ . The output is of the form  $t_i = D_{a_i} \wedge D_{b_i}$ , where  $D_{a_i, b_i}$  are toric divisors of the ambient space  $X_5$ .

Valid  $G_4$ -fluxes are linear combinations of  $t_i$  that satisfy (V.62) and (V.67).<sup>13</sup> We add one further restriction on the fluxes, namely that the chirality of the bifundamental states  $(\mathbf{3}, \mathbf{2})$  is  $\chi((\mathbf{3}, \mathbf{2})) = 3$ . This has obvious phenomenological motivation as we only have one matter curve hosting this representation, and thus all three generations of left-handed quarks must reside here. We accommodate this constraint in our search by first determining the subspace  $V \subset H_{\text{vert}}^{(2,2)}(Y_4)$  satisfying

$$\int_{Y_4} v \wedge D_a^{(\mathcal{B})} \wedge D_b^{(\mathcal{B})} = \int_{Y_4} v \wedge Z \wedge D_a^{(\mathcal{B})} = \int_{Y_4} v \wedge \omega_Y \wedge D_a^{(\mathcal{B})} = 0 = \int_{Y_4} v \wedge [(\mathbf{3}, \mathbf{2})] \quad (\text{V.68})$$

for any vertical divisor  $D_{a,b}^{(\mathcal{B})}$  and any  $v \in V$ . Then, for any particular flux solution  $p$  satisfying (V.62) and (V.67), with  $\int_{Y_4} p \wedge [(\mathbf{3}, \mathbf{2})] = 3$ , the affine space  $p + V$  clearly contains all fluxes giving rise to a spectrum with three generations of left-handed quarks. For our scan, we determine a basis  $\{b_i\}$  of  $V$ , s.t.  $G_4 = p + \sum_i \lambda_i b_i$ , and then vary the  $\lambda_i$  discretely over a finite range. Due

<sup>11</sup>Any other more complicated identification requires working with complete-intersection fourfolds.

<sup>12</sup>The inverse phenomenon would arise e.g. when an ambient divisor splits into two independent divisors on the hypersurface. In the fibrations under consideration in this paper this does not occur.

<sup>13</sup>Note again there are three different choices for the hypercharge that lead to three inequivalent sets of valid  $G_4$ -fluxes.

to computational limitations, we have to restrict the range to be a subset of  $[-10, 10]$ , with the number of independent  $\lambda_i$  ranging between 3 and 7, depending on the base and fibration data.

Because of the discrete increments, we need the lattice spanned by  $\{b_i\}$  to be not too coarse. Furthermore, the basis vectors should have roughly equal ‘length’, so that, by varying all  $\lambda_i$  over the same range, we cover a ‘sphere’ in  $V$ , i.e. extending equally into all independent directions of the flux configuration space. This is accommodated by the following strategy:

- The conditions (V.68) can be rearranged into a matrix whose  $k$ -th column is defined by the intersection numbers (V.68) with  $v$  replaced by the basis vector  $t_k$  of  $H_{\text{vert}}^{(2,2)}(Y_4)$ . The kernel of this matrix is  $V \subset H_{\text{vert}}^{(2,2)}(Y_4)$ , written in the basis  $\{t_k\}$ .
- Using **Sage**, we compute this kernel over  $\mathbb{Z}$ , i.e. the resulting basis vectors  $\{\tilde{b}_i\}$  are  $\mathbb{Z}$ -linear combinations of  $\{t_k\}$ .
- Finally we apply the Lenstra–Lenstra–Lovász (LLL) algorithm – which is conveniently implemented in **Sage** – to this set, yielding the basis  $\{b_i\}$ . The scan will then vary the coefficients  $\lambda_i$  over the interval  $[-10, 10]$  in increments of 1.

The LLL algorithm computes a ‘short’, ‘nearly’ orthogonal lattice basis of the input lattice generated by  $\{\tilde{b}_i\}$ . Here, ‘orthogonality’ is with respect to the bilinear form  $t_i \cdot t_j := \delta_{ij}$ , which clearly is not the metric on  $H^{(2,2)}$  induced by the intersection product, and therefore is irrelevant to us. However, the attribute ‘short’ – which a priori is also with respect to the wrong metric – is helpful to us, because the resulting flux basis  $\{b_i\}$  is expressed with the smallest possible integer coefficients in terms of the  $t_i$  (in practise mostly 0’s and 1’s). In our models, the intersection numbers  $\int_{Y_4} t_i t_j$  are all of order 1 to 10, so arguably the  $b_i$  are (up to factors of order 1) of the same length with respect to the intersection product.

With this basis, we find that when we vary different  $\lambda_i$  with equal step-sizes, also the values of the chiral indices and D3-tadpole change in roughly equal increments. We found in all our examples that the LLL-reduced basis  $\{b_i\}$  is much more advantageous in this respect than the basis  $\{\tilde{b}_i\}$ , which is obtained by Gauss elimination. We also choose the vector  $p = \sum \mu_k t_k$  to be as ‘short’ as possible, i.e. with smallest possible coefficients  $\mu_k$ . These coefficients are not necessarily integer due to the condition  $\int_{Y_4} p \wedge [(\mathbf{3}, \mathbf{2})] = 3$ . Having established the basis flux vectors, we compute for each set  $\{\lambda_i\}$  the chiral indices by integrating the flux  $p + \sum_i \lambda_i b_i$  over the matter surfaces listed in table IV.11.

We observe here that if we were to perform a similar search with the flux basis (IV.116), then the condition of vanishing D-term for  $\omega_Y$  would already introduce fractional coefficients. Furthermore, if we vary the coefficients in the basis (IV.116) in integer (or even half-integer) increments, the values for  $\chi(\mathcal{R})$  will change by much larger step-sizes compared to the basis  $\{b_i\}$ . This makes the latter more practical for a scan.

### A note on the quantisation condition

Let us comment briefly on the quantisation condition,  $G_4 + c_2(Y_4)/2 \in H^4(Y_4, \mathbb{Z})$ . Traditionally, it is a hard problem to systematically solve this condition for explicit geometries [115, 121]. We make no attempt of doing so within the scope of this work. Instead, we follow the usual method of performing a few sanity checks for explicit fluxes. Specifically we check if

$$\chi(\mathcal{R}) \in \mathbb{Z} \quad \forall \mathcal{R}, \quad \int_{Y_4} \left( G_4 + \frac{c_2(Y_4)}{2} \right) \wedge D_i \wedge D_j \in \mathbb{Z},$$

$$n_3 = \frac{1}{24} \chi(Y_4) - \frac{1}{2} \int_{Y_4} G_4 \wedge G_4 \in \mathbb{Z},$$

where the second condition is evaluated for any two toric divisors  $D_{i,j}$ . Clearly, these are necessary conditions to be satisfied by a suitably quantised  $G_4$ -flux.



As remarked at the beginning of this section, we find that the fluxes  $p = \sum \mu_k t_k$  are much likelier to be well-quantised than a flux expressed as a linear combination of the basis (IV.116), whose fractional coefficients are determined by fixing certain chiral indices.

### 2.2.2 Summary of Search Procedure

Here we give a short summary of the scope of the search and comment on the generic chiral spectrum.

In general, we found that the apart from the actual scan over the parameter space of the  $\lambda_i$ 's, the most computation time consuming procedure is performing the triangulations of the toric polytopes defining  $X_5$ . E.g. for the base choice  $\mathcal{B} = \text{Bl}_2\mathbb{P}^3$ , the triangulation of all 59 polytopes with `Topcom` took roughly 4 months.<sup>14</sup> For this reason, we restricted ourselves to the three simplest toric bases. To perform a broader scan more efficiently, one would certainly need to find a faster algorithm for triangulations of toric polytopes, perhaps similar to the strategy of [177] developed for threefolds.

The simplest base we considered is the standard choice  $\mathcal{B} = \mathbb{P}^3$ , with usual homogeneous coordinates  $[z_0, z_1, z_2, z_3]$ . Up to coordinate re-definition this allows for one single choice  $(w_2, w_3) = (z_0, z_1)$  for the coordinates of the non-abelian divisors. There are then 16 consistent fibrations, i.e. pairs of classes  $(\alpha, \beta)$  entering (V.50). For each of these 16 fibrations the number of basis vectors  $b_i$  is between 3 and 5. Out of the 16 different fibrations, only one produced well-quantised fluxes with 'reasonable' chiral indices (in the range  $|\chi| < 10$ ) within our search process.

Next, the base  $\mathcal{B} = \text{Bl}_1\mathbb{P}^3$  is obtained by blowing-up  $\mathbb{P}^3$  in a point. The blow-up coordinate  $x$  and associated divisor class  $X$  corresponds to the ray  $(0, 0, 0, -1)$  in the toric description. There are several inequivalent choices for the coordinates  $w_{2,3}$ . We have analysed the two possibilities  $(w_2, w_3) = (z_0, x)$  and  $(w_2, w_3) = (x, z_0)$ , or in terms of divisor classes,  $(W_2, W_3) = (H, X)$  and  $(W_2, W_3) = (X, H)$ , with  $H$  the hyperplane class of  $\mathbb{P}^3$ . The first choice gives rise to 36 different fibrations. Out of these we find 8 with fluxes leading to 'reasonable' chiralities (in the range  $|\chi| < 10$ ). The second choice  $(W_2, W_3) = (X, H)$  allows for 40 different fibrations, amongst which there are four with 'reasonable' flux configurations. These fibrations have 5 or 6 independent basis vectors  $b_i$ .

We have also attempted to extend our search algorithm to  $\mathcal{B} = \text{Bl}_2\mathbb{P}^3$  with blowup coordinates  $x$  and  $y$  corresponding to the rays  $(0, 0, 0, -1)$  and  $(0, 0, -1, 0)$ . With the choice  $(w_2, w_3) = (x, y)$ , only one of the two inequivalent triangulations of the polytope for  $\mathcal{B}$  is phenomenologically interesting, namely the one for which  $xy$  is not in the SR-ideal. As we have mentioned earlier, the reason is of course that we insist on the presence of the bifundamental states  $(\mathbf{3}, \mathbf{2})$ , which are localised at the intersection. It turns out, however, that for many choices of  $(\alpha, \beta)$  giving rise to effective classes (V.50), the resulting space  $X_5$  does not exhibit a compatible fibration structure over  $\mathcal{B}$  (with the chosen intersection property of  $\{x\}$  and  $\{y\}$ ). In addition, all these cases lead to dimension-one singularities in  $X_5$ , so they would generically induce point-like singularities on  $Y_4$ . Out of the 59 possible choices for  $(\alpha, \beta)$ , only 30 have compatible fibrations. Of these, none has a properly quantised flux solution leading to chiral indices smaller than 10.

All of the 'reasonable' spectra we found do not reproduce the Standard Model exactly. They all have chiral exotics, which can potentially give rise to interesting Beyond-the-Standard-Model physics. However, in most cases, the excess is still too large to comfortably relate them with the Standard Model. In the following we will discuss one example which is closest to the MSSM. The remaining models are listed in appendix D.

---

<sup>14</sup>The computation was carried out with an Intel E6700 (3.2GHz) dual-core CPU and 4GB RAM.

### 2.2.3 An almost Standard-Model-like Example

The class of fibrations over  $\mathcal{B} = \text{Bl}_1\mathbb{P}^3$  with  $\bar{\mathcal{K}} = 4H + 2X$  is parametrised by the two divisors

$$\alpha = \alpha_H H + \alpha_X X, \quad \beta = \beta_H H + \beta_X X, \quad (\text{V.69})$$

where  $X$  and  $H$  denote the two independent divisors of  $\mathcal{B}$ . With only one possible triangulation of the toric polytope,  $\mathcal{B}$  has the following independent intersection numbers:

$$\int_{\mathcal{B}} X^3 = 1, \quad \int_{\mathcal{B}} X^2 \wedge H = -1, \quad \int_{\mathcal{B}} X \wedge H^2 = 1, \quad \int_{\mathcal{B}} H^3 = 0. \quad (\text{V.70})$$

With the choice  $(w_2, w_3) = (x, z_0)$  corresponding to  $(W_2, W_3) = (X, H)$ , the ambient space  $X_5$  can be described by the following polytope:

u	v	w	$s_0$	$s_1$	$e_1$	$f_1$	$f_2$	$e_0$	$f_0$	$z_1$	$z_2$	$z_3$
-1	0	1	-1	0	1	0	1	0	0	$\alpha_X - \alpha_H$	0	$-\alpha_X$
1	-1	0	0	1	0	1	0	0	0	$\beta_H - \beta_X$	0	$\beta_X$
0	0	0	0	0	0	-1	-1	0	-1	1	0	0
0	0	0	0	0	0	-1	-1	0	-1	0	1	0
0	0	0	0	0	-1	-1	-1	-1	-1	0	0	1

(V.71)

As explained before, the coefficients  $\alpha_{(\cdot)}, \beta_{(\cdot)}$  must be chosen such that the classes (V.50) are effective, i.e. their expansion in  $X$  and  $H$  must have positive coefficients. There are 40 tuples  $(\alpha_H, \alpha_X, \beta_H, \beta_X)$  satisfying this condition.

Within our scan, the flux configuration coming closest to the Standard-Model spectrum is based on the fibration defined by  $\alpha = 3H + X$ ,  $\beta = H + X$ . The Euler number of the elliptic fourfold inside  $X_5$  is  $\chi(Y_4) = 1794$ . The flux configuration of interest is furthermore defined for the hypercharge identification  $U(1)_Y = U(1)_1$ , and takes the form

$$\begin{aligned} G_4 &= \frac{1}{2} (E_1 \wedge (2H - 3F_2 - S_1) + X \wedge (F_2 - F_1 + S_1)) \\ &= -\frac{1}{6} G_4^{z_2} - \frac{1}{12} G_4^{z_4}. \end{aligned} \quad (\text{V.72})$$

In the second line we have identified this flux with the specialisation of general fluxes (IV.116) we derived in the generic setting to this particular fibration. Explicit checks confirm that this flux satisfies all necessary conditions for being appropriately quantised: the intersection numbers  $\int_{Y_4} (G_4 + c_2(Y_4)/2) \wedge D_i \wedge D_j$  are all integer, all the chiral indices are integer (see below), and the number of D3-branes required to cancel the D3-tadpole is

$$n_3 = \frac{1}{24} \chi(Y_4) - \frac{1}{2} \int_{Y_4} G_4^2 = 72. \quad (\text{V.73})$$

It turns out the flux induces a vanishing D-term not only for  $U(1)_Y$ , as required, but in fact for  $U(1)_1$  and  $U(1)_2$  individually,

$$\int_{Y_4} G_4 \wedge \omega_1 \wedge D_a^{\mathcal{B}} = \int_{Y_4} G_4 \wedge \omega_2 \wedge D_a^{\mathcal{B}} = 0 \quad \forall D_a^{\mathcal{B}} \in H^{1,1}(\mathcal{B}). \quad (\text{V.74})$$

In particular, the flux (V.72) is not a  $U(1)_i$  gauge flux. Therefore, neither of the abelian gauge factors acquires a Stückelberg mass and the gauge symmetry is  $SU(3) \times SU(2) \times U(1)_Y \times U(1)_2$ , with an extra massless abelian gauge group factor compared to the Standard Model.

The induced chiral spectrum is summarised in table V.12 and follows directly from the expressions in tables IV.12 and IV.13 with the help of the base intersection numbers (V.70). As one

$\mathcal{R}$	$\mathbf{2}_1$	$\mathbf{2}_2$	$\mathbf{2}_3$	$\mathbf{3}_1$	$\mathbf{3}_2$	$\mathbf{3}_3$	$\mathbf{3}_4$	$\mathbf{3}_5$
$(q_1, q_2)$	$(\frac{1}{2}, -1)$	$(\frac{1}{2}, 1)$	$(\frac{1}{2}, 0)$	$(\frac{2}{3}, -\frac{1}{3})$	$(-\frac{1}{3}, -\frac{4}{3})$	$(-\frac{1}{3}, \frac{2}{3})$	$(\frac{2}{3}, \frac{2}{3})$	$(-\frac{1}{3}, -\frac{1}{3})$
$\chi$	-2	1	-2	-2	0	1	-1	-4
$\mathcal{R}$	$\mathbf{(3, 2)}$	$\mathbf{1}^{(1)}$	$\mathbf{1}^{(2)}$	$\mathbf{1}^{(3)}$	$\mathbf{1}^{(4)}$	$\mathbf{1}^{(5)}$	$\mathbf{1}^{(6)}$	
$(q_1, q_2)$	$(\frac{1}{6}, -\frac{1}{3})$	$(1, -1)$	$(1, 0)$	$(1, 2)$	$(1, 1)$	$(0, 2)$	$(0, 1)$	
$\chi$	3	2	1	0	0	0	-4	

**Table V.12:** The chiral spectrum induced by the flux (V.72). For completeness we have included the  $U(1)_1 \times U(1)_2$  charges  $(q_1, q_2)$  of the states.

can see, the largest (absolute value of) chirality is 4, which is among the smallest values we have been able to find within our search process; in particular this means that there are necessarily chiral exotics beyond the MSSM spectrum.

To actually make contact with particle physics, we invoke our classification of possible Standard Model matchings from appendix C. Specifically, we consider the possibility no. 7 in table C.1. This leads to the identifications listed in table V.13.

$\mathcal{R}$	$\bar{\mathbf{2}}_1$	$\mathbf{2}_2$	$\bar{\mathbf{2}}_3$	$\bar{\mathbf{3}}_1$	$\bar{\mathbf{3}}_2$	$\bar{\mathbf{3}}_3$	$\bar{\mathbf{3}}_4$	$\bar{\mathbf{3}}_5$
$\chi$	2	1	2	2	0	-1	1	4
SM states	$L$	$H_u$	$L + H_d$	light $u_R^c$	light $d_R^c$	light $d_R^c$	heavy $u_R^c$	heavy $d_R^c$
$\mathcal{R}$	$\mathbf{(3, 2)}$	$\mathbf{1}^{(1)}$	$\mathbf{1}^{(2)}$	$\mathbf{1}^{(3)}$	$\mathbf{1}^{(4)}$	$\mathbf{1}^{(5)}$	$\bar{\mathbf{1}}^{(6)}$	
$\chi$	3	2	1	0	0	0	4	
SM states	$Q$	heavy $e_R^c$	heavy $e_R^c$	-	heavy $e_R^c$	-	heavy $\nu_R^c$ , $\mu$ -term	

**Table V.13:** Possible matching of the chiral spectrum obtained from the flux (V.72) with the (N)MSSM spectrum.

The exotics which do not fit into the MSSM are a pair of triplets residing on the curves  $\mathbf{3}_3$  and  $\mathbf{3}_5$ , as well as the singlets on  $\mathbf{1}^{(6)}$ . If indeed the chirality 2 for  $\bar{\mathbf{2}}_3$  is distributed as 1 for  $H_d$  and 1 for the leptons  $L$ , then the Higgs  $(H_u, \bar{H}_d)$  come as a vector-like pair. Likewise, the excess of chiral triplets can be grouped into a vector-like pair  $(\bar{\mathbf{3}}_3)^c + \bar{\mathbf{3}}_5$  charged like the Standard-Model down-quarks. In light of recent events at the LHC, these exotics could possibly be of interest (e.g. in the spirit of [178–180]), but we will not attempt any detailed phenomenological discussion in this direction. Irrespective of the question of exotics, the model must be considered in the context of intermediate or high scale supersymmetry breaking because the charge assignments and resulting Yukawa couplings give rise to dimension-four proton decay operators which would be incompatible with a TeV supersymmetry scale. This happens despite the appearance of the extra  $U(1)_2$  selection rule. The complete list of such operators can be found in table C.1.

Finally, note that we have only computed the chiral spectrum. On top of this, extra vector-like pairs of massless matter localised over a single curve may exist. Their computation, e.g. along the lines of [95], is considerably more involved and beyond the scope of this work.

To arrive at the precise Standard-Model spectrum, and to remove the extra massless  $U(1)_2$  from the spectrum, one can imagine Higgsing the latter with a vector-like pair of massless singlets

$\mathbf{1}^{(6)} + \bar{\mathbf{1}}^{(6)}$  in a D-flat manner,

$$\langle \mathbf{1}^{(6)} \rangle = \langle \bar{\mathbf{1}}^{(6)} \rangle \neq 0. \quad (\text{V.75})$$

This of course assumes that at least one such vector-like pair is available. The recombination singlets couple to the massless matter multiplets as follows [13]:

$$\begin{aligned} \mathcal{L} \supset & \mathbf{1}^{(6)} \mathbf{3}_2 \bar{\mathbf{3}}_5 + \mathbf{1}^{(6)} \mathbf{3}_1 \bar{\mathbf{3}}_4 + \bar{\mathbf{1}}^{(6)} \mathbf{3}_3 \bar{\mathbf{3}}_5 + \mathbf{1}^{(6)} \mathbf{2}_1 \bar{\mathbf{2}}_3 + \bar{\mathbf{1}}^{(6)} \mathbf{2}_2 \bar{\mathbf{2}}_3 + \\ & \mathbf{1}^{(6)} \mathbf{1}^{(2)} \bar{\mathbf{1}}^{(4)} + \mathbf{1}^{(6)} \mathbf{1}^{(1)} \bar{\mathbf{1}}^{(2)} + \mathbf{1}^{(6)} \mathbf{1}^{(4)} \bar{\mathbf{1}}^{(3)} + \mathbf{1}^{(6)} \mathbf{1}^{(6)} \bar{\mathbf{1}}^{(5)} + c.c. \end{aligned} \quad (\text{V.76})$$

Note that the last term would induce an F-term for  $\bar{\mathbf{1}}^{(5)}$  in the background (V.75). It therefore comes as a relief that the chiral index associated with the singlets  $\mathbf{1}^{(5)} + \bar{\mathbf{1}}^{(5)}$  is indeed vanishing, see table V.12. Absence of an F-term obstruction to the recombination then requires that in addition no vector-like pair  $\mathbf{1}^{(5)} + \bar{\mathbf{1}}^{(5)}$  of massless such singlets exist. If this condition is satisfied, the Higgsing (V.75) recombines the curves  $\mathbf{3}_1$  and  $\mathbf{3}_4$ , the curves  $\mathbf{3}_3$  and  $\mathbf{3}_5$ , furthermore all the  $\mathbf{2}_i$  curves as well as the singlet curves  $\mathbf{1}^{(1)}$ ,  $\mathbf{1}^{(2)}$  and  $\mathbf{1}^{(3)}$ , in agreement with the couplings (V.76). This leads to the following spectrum:

state	$(\mathbf{3}, \mathbf{2})$	$\bar{\mathbf{3}}_1 + \bar{\mathbf{3}}_4$	$\bar{\mathbf{3}}_3 + \bar{\mathbf{3}}_5$	$\bar{\mathbf{2}}_1 + \bar{\mathbf{2}}_2 + \bar{\mathbf{2}}_3$
$\chi$	3	3	3	3
SM states	$Q$	$u_R^c$	$d_R^c$	$L + H_u + H_d$
state	$\mathbf{1}^{(1)} + \mathbf{1}^{(2)} + \mathbf{1}^{(4)}$	$\mathbf{1}^{(5)}$	$\mathbf{1}^{(6)}$	$\bar{\mathbf{1}}^{(6)}$
$\chi$	3	0	—	—
SM states	$e_R^c$	—	vev	vev

Note that now the Higgs-doublet is localised on the same curve, similar to the 3-chiral generation MSSM realised in [112]. Phenomenological viability therefore requires one extra massless vectorlike pair of associated states after the recombination.

### 3 Summary of Chapter V

In this chapter we have presented the explicit construction of five F-theory models with a Standard-Model-like gauge group  $SU(3) \times SU(2) \times U(1)_1 \times U(1)_2$ . These models were realised as hypersurfaces in a  $\text{Bl}_2\mathbb{P}^2$  fibration. Non-abelian gauge symmetries were introduced via tops. All these models had in common that their matter spectrum consists of five  $\mathbf{3}$ , three  $\mathbf{2}$ , six  $\mathbf{1}$  and one  $(\mathbf{3}, \mathbf{2})$  representations. We explicitly analysed all the Yukawa couplings realised in these models. For the coupling amongst the singlets, we again relied on the technique of primary decompositions developed in section 3 of chapter III. It turns out that indeed, all couplings that are allowed by gauge invariance are realised geometrically.

For an F-theory realisation of the Standard Model with these models, the left-handed quarks must necessarily be identified with the only available  $(\mathbf{3}, \mathbf{2})$ -states. However, there are many possibilities to match the remaining representations with the Standard Model spectrum. In particular, any matching requires a prior identification of the hypercharge  $U(1)_Y$  in terms of the geometric  $U(1)$ s. The orthogonal  $U(1)$  can then serve as a selection rule for the possible couplings. In section 2.1, we performed a search for all possible matchings that are compatible with the only available  $(\mathbf{3}, \mathbf{2})$ -state being the left-handed quarks. For all matchings, we also analysed what type of dimension four and five couplings in the resulting physical model are allowed. All these data have been collected in appendix C.

In the next step, we included non-trivial backgrounds for  $G_4$ -fluxes in order to generate a chiral spectrum. We have restricted ourselves to the  $I \times A$  fibration, although the methods and algorithms readily apply for any of the remaining four models. For explicit chiral indices, we have to restrict the fibration to specific bases  $\mathcal{B}$ . In our analysis, we have considered the possibilities  $\mathcal{B} \in \{\mathbb{P}^3, \text{Bl}_1\mathbb{P}^3, \text{Bl}_2\mathbb{P}^3\}$ . For each of these bases, we have set up a search algorithm in section 2.2.1 based on the results and tools from chapters III and IV to scan over a part of the vacua of vertical  $G_4$ -fluxes in the full fibration. In the search we were only interested in chiral spectra whose largest (absolute value of) chiral index is less than 10. It turns out that for the multitude of possible fibrations, only a small portion of flux configurations satisfies this requirement. In addition, none of them gives directly the MSSM spectrum. However, we could identify one configuration presented in section 2.2.3 that gives an almost Standard-Model-like spectrum. This contains, in addition to the full MSSM matter, a vector-like pair charged like the down-quarks under Standard Model gauge group, and extra singlets. By Higgsing the latter, one could in principle reproduce the exact chiral spectrum of the MSSM, however an explicit geometric description of this process is beyond the scope of this work.



## Chapter VI

# Conclusion and Outlook

F-theory has tremendously broadened our systematic understanding of the string landscape. By geometrising the axio-dilaton of type IIB string theory, F-theory allows for a systematic description of consistent type IIB compactifications with 7-branes at finite coupling. Through the duality to M-theory, we have a very precise understanding of gauge symmetries, charged matter and their interactions in terms of the geometry of torus-fibred Calabi–Yau spaces. With the development of systematic tools for model building, F-theory has become a very vivid field for particle phenomenology. At the same time, many formal aspects of F-theory are still not fully understood. In fact, both formal and phenomenological aspects are closely intertwined, and either side can benefit greatly from the study of the other. The purpose of this thesis was to investigate these two facets for the subject of  $G_4$ -fluxes in F-theory. In particular, our main interest lied in the chirality inducing feature of  $G_4$ -fluxes. From a phenomenological perspective, fluxes are of course a crucial input in order to re-create the chiral spectrum of the Standard Model in F-theory. On the other hand, a geometric understanding of the cancellation of chiral anomalies would also be desirable. Given the close connection between these two challenges, it seems appropriate to set up a more systematic analysis of fluxes that can tackle both issues.

To this end, we have first developed computational tools that are required for the systematic treatment of fluxes. In particular, as we have seen in section 2 of chapter III, the subclass of vertical fluxes can be modelled by a quotient polynomial ring. On torus fibrations realised as toric hypersurfaces, this quotient ring can be described easily in terms of the intersection theory on the ambient toric space. The description we give can be readily implemented into a computer algebra system (we used **Sage** and **Singular**) to algorithmically simplify cohomological computations that arise naturally in the analysis of fluxes. While similar techniques have been proposed before, a particular upshot of our formulation is that it is independent of the fibration’s base  $\mathcal{B}$ , and thus can be straightforwardly applied to any (consistent) choice of  $\mathcal{B}$ . In addition, the base-independent formulation also allows us to study properties that are inherent to the fibration structure, which hold irrespective of the precise structure of  $\mathcal{B}$ . Furthermore, we have also presented a novel method to determine the homology classes of matter surfaces in section 3 of chapter III. This method is based on the algebraic description of complex submanifolds by ideals of polynomials. Again we can rely on computer algebra systems like **Singular** and the underlying theory of Gröbner basis to systematise this method. Originally introduced in F-theory to examine Yukawa coupling structures, we adapted the ideas for the computation of matter surfaces. By integrating the flux over these surfaces, we obtain the chiral indices of the corresponding matter states. However, in these calculations, we need the homology classes of these surfaces, which can only be extracted with a further ‘trick’, as described in section 3.3.2. The method has one caveat however, as it fails to determine the homology classes of certain singlet matter surfaces. It should be stressed though that this failure is due to the limitations of the computer algorithms. Mathematically, the method is still applicable to those cases.

Equipped with these tools, we then proceeded with the detailed analyses of fluxes and anomalies in three different fibrations. These fibrations give rise to an  $SU(5) \times U(1)$  and an  $SU(5) \times \mathbb{Z}_2$  model, which are related by a Higgsing/conifold transition. The third fibration realises the gauge group  $SU(3) \times SU(2) \times U(1)^2$ . As elucidated at the beginning of chapter IV, the anomalies are cancelled in F-theory by a generalised Green–Schwarz (GS) mechanism. The corresponding GS-counterterms have been identified in previous works explicitly as the integral of  $G_4$  over certain 4-cycles. With the explicit expressions for vertical fluxes and matter surfaces computed from the methods of chapter III, we were able to show that in all our F-theory models, the non-abelian anomalies induced by vertical fluxes cancel for any base  $\mathcal{B}$ . Due to our computational limitations with singlet matter surfaces, we cannot verify the anomaly cancellation explicitly for pure  $U(1)$  and mixed  $U(1)$ -gravitational anomalies. However, we could reverse the argument and use anomaly cancellation to consistently determine the chiralities of those singlets, such that the resulting spectrum is free of any gauge anomalies. Note that while for elliptic fibrations, fluxes have been included in explicit models for a long time, the role of fluxes in genus-one fibrations has been much less studied. In particular, an analogue of the transversality conditions has not been derived and tested for fibrations with no sections. These conditions are to ensure that the flux configuration in the dual M-theory compactification lifts properly in the F-theory limit. Guided by the intuition of a KK  $U(1)$  that ought to arise in the circle reduction from F-theory to M-theory, we proposed a multi-section version of the transversality conditions. It is reassuring to see that indeed, this proposal survived the first consistency test of anomaly cancellation.

Moreover, while all the above investigations relied on having explicit  $G_4$  solutions to the transversality conditions, we have found a different approach to anomaly cancellation in 4D F-theory compactifications. This is based on the observation that both the anomaly and its potential GS-counterterm are given as an integral of  $G_4$  over some 4-cycle; for the first it is a linear combination of the matter surfaces, whereas for the second it is a specific 4-cycle determined from a related Chern–Simons theory in the dual M-theory compactification. Indeed, we could show for the anomalies not involving singlets that these 4-cycles agree in homology up to terms that are guaranteed by the transversality conditions to vanish upon  $G_4$ -integration. Therefore, we could provide a geometric argument in terms of certain 4-cycle classes – without reference to any explicit  $G_4$ -flux – for the cancellation of chiral anomalies in 4D F-theory models. Note that this base independent argument also extends to non-vertical fluxes.

Motivated by this observation, we also studied two types of discrete anomalies – the  $\mathbb{Z}_2$  and the Witten  $SU(2)$  anomaly – based solely on the analysis of matter surface classes. Unlike the gauge anomalies, these discrete anomalies are cancelled only for appropriately quantised  $G_4$ -fluxes. In particular, this analysis also revealed a new link between the  $\mathbb{Z}_2$  and the  $U(1)$  model related by Higgsing. It turned out that the  $\mathbb{Z}_2$  anomaly is cancelled if and only if in the corresponding  $U(1)$  model, all chiral indices are integer. While somewhat surprising from the geometric point of view, this is in full agreement with our physical intuition, since the  $\mathbb{Z}_2$  symmetry must be anomaly free if it arises as the discrete remnant of a continuous  $U(1)$  symmetry after a Higgsing process. Note that in order to establish this link, we also had to understand how the flux background changes in the Higgsing process. Indeed, we found an explicit map that identifies the flux configurations on both sides of the transition. This serves as another consistency check for the proposed transversality conditions in genus-one fibrations.

In chapter V, we turned our attention to more phenomenological applications. The goal here was to find possible realisations of the Standard Model in F-theory. To this end, we constructed all toric models with an  $SU(3) \times SU(2) \times U(1)_1 \times U(1)_2$  symmetry. These models have an abundant matter spectrum with a rich Yukawa coupling structure. Our explicit analysis in section 1 showed that all the couplings allowed by gauge invariance are in fact realised geometrically at intersections of the corresponding matter curves. In order to compare these F-theory models with the Standard Model, we first had to appropriately identify the geometric spectrum with the Standard Model



spectrum. In particular, this amounts to an identification  $U(1)_Y = aU(1)_1 + bU(1)_2$  of the hypercharge with the geometric  $U(1)$ s. To be as general as possible, we only insisted on this identification to be compatible with the left-handed quarks arising from the only bifundamental states geometrically available. As a result, there is a plurality of possible matches, which mostly differ by the dimension four and five operators in the effective field theory. This difference can be attributed to the remaining  $U(1)$  orthogonal to  $U(1)_Y$ , which serves as a selection rule for these operators.

Based on those matchings, we have then investigated possible flux configurations that give rise to chirality. We restricted ourselves to one model out of the five possible toric realisations of the extended Standard Model group. For this model we have already studied the vertical fluxes and matter surfaces before in chapter IV. Thus the results, especially those on chiralities of singlet matter derived from the anomaly conditions, carried over straightforwardly. Unlike the analyses in chapter IV however, we now had to specialise the fibrations to explicit bases in order to obtain actual numbers for the chiral indices. For the scope of this thesis, we studied three possible base manifolds:  $\mathbb{P}^3$ ,  $\text{Bl}_1\mathbb{P}^3$  and  $\text{Bl}_2\mathbb{P}^3$ . For each base, there are multiple choices of fibrations allowed. For each fibration, we computed a basis  $\{b_i\}$  of vertical fluxes and scanned over the flux configurations  $G_4 = \sum_i \lambda_i b_i$  by varying  $\lambda_i$  discretely over a finite range. During this scan, we searched for fluxes that give rise to a chiral spectrum with chiralities lower than 10. It turned out that there are only a few configurations that give semi-realistic spectra. In particular, we did not find ‘just’ the Standard Model. In general, there are many exotic states that go beyond the Standard Model spectrum. Amongst these semi-realistic models, we presented a particular one in section 2.2.3 of chapter V that resembles the Standard Model the most within our search. This model has one exotic vector-like pair of **3**-states and extra singlet states. We argued that in principle, one recovers the exact Standard Model spectrum by Higgsing these singlets.

However, this argument requires certain assumptions about the exact massless spectrum that goes beyond the chiral index. These data are not contained in the  $G_4$ -flux, but are encoded in the gauge potential  $C_3$ . To access these, one needs a better handle of the so-called Deligne cohomology, as proposed in [95]. Despite the rather formal character of such an analysis, the result would have great benefits for phenomenology. After all, any F-theory realisation of particle physics must in the end be able to realise the exact number of left- and right-handed fermions and not just the net chirality. Unfortunately, such an analysis is far beyond the scope of this work.

Nevertheless, the results of chapter IV are evidence that fluxes are worthwhile to study. In particular, the novel approach to anomalies in 4D F-theory can be put into a mathematical statement: On any torus-fibred Calabi–Yau fourfold, the 4-cycles prescribed by F-theory anomaly cancellation must be zero in homology modulo terms that are trivial under the transversality conditions. Note that while anomaly cancellation might be expected from a physical point of view, there is (so far) no apparent mathematical reason why these 4-cycles should behave as such. Since topologists and geometers are generally interested in any universal properties of manifolds, this F-theory ‘prediction’ could lead to a new ‘classification’ method for certain subclasses of fourfolds. Note that similar predictions have been made in F-theory compactifications to 6D [41, 181]. Also there, anomaly cancellation was used as a physical input to derive purely mathematical conditions on Calabi–Yau threefolds. In fact, these works derived an explicit relationship between the geometric description of matter in 6D F-theory and their associated anomaly contribution in a general setting. In the four-dimensional setting, the best we can do at the moment is to verify the statement for a given fibration with a specific fibre structure. It would be interesting to see if and how one can formalise the four-dimensional statement in a similarly general way as in 6D.

In addition to these efforts, one should also extend the systematic approach presented in this thesis to non-vertical fluxes. If nothing else, then such methods would be of great interest in other phenomenological quests. For example, a better handle on horizontal fluxes can open up

new possibilities for moduli stabilisation in F-theory [97–99]. Such mechanisms must ultimately be considered in any realistic compactification model to ensure vacuum stability and absence of light scalars. Furthermore, the remaining fluxes that are neither horizontal nor vertical are of great importance to GUT phenomenology. Indeed, it was shown in [100] that the hypercharge flux that breaks an  $SU(5)$  GUT to the MSSM must be of this type. An extension of the works [182,183] might be able to give a more efficient way of describing hypercharge flux breaking, and possibly revive the phenomenological interest in F-theory GUTs.

Finally, a more thorough search for realistic chiral spectra might shed some light on the likelihood of obtaining directly the Standard Model in F-theory without the detour via GUTs. In fact, our search results seem to suggest that it is extremely rare to find a realisation with only few chiral exotics. However, one should not be too hasty with such a conclusion. Indeed, our search algorithm was rather simple and only covered three different bases. It is conceivable that for more sophisticated bases, there might be a plethora of flux configurations with realistic chiralities. As our search algorithm is limited in several respects, an improved version will be needed to perform a more efficient and far reaching scan for other fibrations. It would be interesting to also extend the search to other types of F-theory models that lead to Standard-Model-like gauge groups. In particular, a comparison with the flux vacua of three generation F-theory GUTs might reveal whether a direct realisation of Standard Model in F-theory is preferred or not. In the end, we will need to answer all these questions in order to unfold the full model building power of F-theory. It is certain though that our understanding of the string landscape will benefit tremendously from these endeavours.

## Acknowledgements

Even though it goes without saying, I would like to express my deepest gratitude for my supervisor Timo Weigand. For his constant support and motivation that guided me through the last three years, for the countless invaluable discussions from which my understanding of physics and math benefited enormously, and – last but not least – for introducing me to F-theory, I will always be grateful.

I would also like to thank Prof. Jörg Jäckel, who graciously agreed to be the second referee for this dissertation despite his busy calendar.

Furthermore, much of the research in this thesis would not have been possible without the help of Christoph Mayrhofer, from whom I learned a lot about **Sage**, toric geometry, and F-theory in general. Likewise, many ideas in this thesis were developed in formal and informal discussions with my collaborator and office mate Oskar Till. It was also a great pleasure to talk with Eran Palti about several questions in F-theory which hopefully will be answered soon in upcoming publications.

In addition I would like to thank Florent Baume and Fengjun Xu for stimulating conversations as well as for the numerous enjoyable moments we had in our office. Moreover, I would like to also thank Arthur Hebecker, Lukas Witkowski, Patrick Mangat and Fabrizio Rompineve for many interesting conversations.

Finally, I am grateful to my parents and ♡ for their unwavering support during the time of my PhD studies.



# Appendix A

## Intersection Theory of algebraic Cycles

Throughout this thesis, we make heavy use of the duality between cohomology forms and homology classes of certain submanifolds of our fibration geometry, which we can write down explicitly as vanishing loci of polynomials. Thus it seems appropriate to present the mathematical foundation of this duality. This foundation is provided by intersection theory. Intersection theory on a smooth, projective, complex manifold  $X$  is a rich topic by itself, as the amount of textbooks on it shows (e.g. [106, 184, 185]). Here, we will not attempt any thorough discussion and merely give a brief overview.

Poincaré-duality provides an isomorphism between homology and cohomology. On a smooth, projective, complex manifold  $X$ , the translation of cohomology into homology is particularly useful. The reason is that  $(k, k)$ -forms are mapped under Poincaré-duality to homology classes of complex submanifolds and vice versa. For projective manifolds  $X$ , it is known that any complex submanifold is an algebraic cycle, i.e. can be described by the vanishing of polynomials.

In section 3 of chapter III, we have introduced algebraic cycles as subvarieties.<sup>1</sup> There we have seen that any subvariety  $V \subset X$  can be (up to embedded components) uniquely decomposed via primary decomposition into irreducible components  $V_i$  with associated multiplicity  $m_i$ . We then define the cycle class of  $V$  to be the formal linear combination  $\sum_i m_i V_i$ . Clearly, the set of all cycles can be seen as being formally generated by the irreducible subvarieties  $V_i$  of  $X$ . One can easily define sums of two cycles  $C_1 = \sum_i m_i^{(1)} V_i$  and  $C_2 = \sum_i m_i^{(2)} V_i$  as the formal linear combination  $C_1 + C_2 := \sum_i (m_i^{(1)} + m_i^{(2)}) V_i$ . One can imagine this to be the analogue of the geometric union  $C_1 \cup C_2$  including the multiplicities. Note that in this definition, the embedded components are neglected. With the empty set representing the neutral element under the putative addition, it is easy to see that the cycles form an abelian group called the group of algebraic cycles of  $X$ . This additive structure of course carries over to homology, i.e. when we consider homological equivalence classes of algebraic cycles.

Let us denote the set of all homology class of algebraic cycles on  $X$  by  $A(X)$ . Then  $A(X)$  carries a multiplication induced by the intersection of submanifolds: Suppose  $Z, Z' \subset X$  are of (complex) codimension  $k$  resp.  $k'$ , then they intersect ‘transversely’ or ‘properly’, if all connected components of  $Z \cap Z'$  have pure codimension  $k + k'$ . The so-called Moving Lemma then asserts that for any two equivalence classes  $C, C' \in A(X)$  of pure codimension  $k$  resp.  $k'$ , there are always representatives  $Z$  resp.  $Z'$  which intersect properly in a cycle  $Z \cap Z'$  of codimension  $k + k'$ . One can show that this gives a well-behaved intersection product  $\cdot$  by defining  $C \cdot C' := [Z] \cdot [Z'] = [Z \cap Z']$ . Note that this multiplication induces a natural grading  $A(X) = \bigoplus_{k=0}^n A^k(X)$ , such that  $A^i \times A^j \rightarrow A^{i+j}$ , where  $A^k$  are the cycle classes of codimension  $i$ . With this multiplication,  $A(X)$

---

<sup>1</sup>‘Cycles’ is a term common to intersection theory.

becomes a ring.

Note that the famous Hodge conjecture asserts that  $A(X)$  is actually isomorphic to the cohomology groups of type  $(k, k)$ :

$$\bigoplus_{k=0}^n H^{(k,k)}(X, \mathbb{Q}) \cong A(X) \otimes \mathbb{Q} = \bigoplus_{k=0}^n A^k(X) \otimes \mathbb{Q}, \quad (\text{A.1})$$

where on the right hand side, the tensor product  $A^k(X) \otimes \mathbb{C}$  is just fancy way to say that we allow for linear combinations of cycles classes with rational coefficients. The Hodge conjecture is yet to be proven in full generality. However there are instances, where the conjecture is known to hold. In particular, it is known to hold for any threefold, for all toric spaces, and for  $H^{(1,1)}$ . Note that in section 2.1 of chapter III, we have used a different notation for  $A^k(X) \otimes \mathbb{Q}$ . There, for consistency, we denoted this group by  $H_{2(N-k)}^{\text{alg}}(X, \mathbb{Q})$ , where  $N = \dim_{\mathbb{C}} X$ .

Given (A.1), we now have a geometric way to compute wedge products of  $(k, k)$ -forms as the intersection product of their Poincaré-dual (PD) algebraic cycle classes:

$$\text{PD}(\omega_1 \wedge \dots \wedge \omega_k) = \text{PD}(\omega_1) \cdot \dots \cdot \text{PD}(\omega_k). \quad (\text{A.2})$$

In particular, an integral  $\int_Z \omega$  of a  $(k, k)$ -form over a  $2k$  algebraic cycle  $Z$  can now also be computed as the intersection number  $[Z] \cdot \text{PD}(\omega) \equiv [Z] \cdot [W]$ . Geometrically, this is just the number of points (counted with multiplicity and orientation) in the intersection of two *transverse* intersecting representatives  $Z' \in [Z]$  and  $W' \in [W]$ . This is for example very handy when computing the Cartan charges of matter  $\mathbb{P}^1$ s in F-theory. As an integral, the charge under the Cartan  $U(1)$  associated with the exceptional divisor  $\text{Ex}_i$  is given as  $\int_{\mathbb{P}^1} \text{PD}(\text{Ex}_i)$ . This may now be interpreted as the intersection  $\text{Ex}_i \cdot \mathbb{P}^1$ , which can be read off from the fibre structure in F-theory.

This identification is extremely helpful for our computation of fluxes. Note that for divisors, the Hodge conjecture is proven. Therefore, the identification (A.1) for the vertical cohomology on the left hand side and the ring generated by divisor classes on the right is actually a fact.

## Appendix B

# Details on the Construction of the $SU(3) \times SU(2) \times U(1)^2$ Gauge Group

### 1 Details on the Toric Diagrams

In this appendix we present the toric diagrams of the  $SU(2)$  and  $SU(3)$  tops. Special emphasis will be put on the symmetries which identify some of the models as equivalent pairs. The relationship between toric geometry and the geometry of Calabi-Yau hypersurfaces is described in e.g. [71].

The ambient space  $\text{Bl}_2\mathbb{P}^2$  has the toric diagram depicted on the left in figure B.1. The lattice points of the dual diagram on the right correspond to the terms of the hypersurface equation (V.1). Clearly the diagrams share a common reflection symmetry along the dotted diagonal axis.



**Figure B.1:** Polygon 5 (in the classification of [71]) describing the fibre ambient space  $\text{Bl}_2\mathbb{P}^2$ ; every lattice point of the dual polygon (right) gives an individual term of the hypersurface equation. The reflection symmetry along the dotted diagonal is manifest.

The symmetry exchanges fibre coordinates  $s_0 \leftrightarrow s_1$ ,  $v \leftrightarrow w$  and coefficients  $b_0 \leftrightarrow b_2$ ,  $c_1 \leftrightarrow c_2$ ,  $d_0 \leftrightarrow d_1$  of the hypersurface equation. Consequently, the  $U(1)$  generators (V.5) are also transformed, namely as

$$\begin{aligned} \omega_1 &= S_1 - S_0 - \bar{\mathcal{K}} \longrightarrow S_0 - S_1 - \bar{\mathcal{K}} = -\omega_1 + 2\bar{\mathcal{K}}, \\ \omega_2 &= U - S_0 - \bar{\mathcal{K}} - [c_1] \longrightarrow U - S_1 - \bar{\mathcal{K}} - [c_2] = \omega_2 - \omega_1 - \bar{\mathcal{K}} + [c_1] - [c_2]. \end{aligned} \tag{B.1}$$

These forms do not satisfy the verticality condition, i.e. they are not in the image of the Shioda map. However they only differ from such by the pullback of divisors of the base. Since such pullbacks never contribute to the  $U(1)$  charges of any states, the  $U(1)$  charges indeed transform

as

$$\begin{aligned} U(1)'_1 &= -U(1)_1, \\ U(1)'_2 &= U(1)_2 - U(1)_1. \end{aligned} \tag{B.2}$$

The symmetry also exchanges the singlets (as the coefficients  $b_i, c_j, d_k$  are exchanged), namely  $\mathbf{1}^{(1)} \leftrightarrow \bar{\mathbf{1}}^{(3)}, \mathbf{1}^{(2)} \leftrightarrow \bar{\mathbf{1}}^{(4)}$ , while  $\mathbf{1}^{(5)}$  and  $\mathbf{1}^{(6)}$  are invariant.

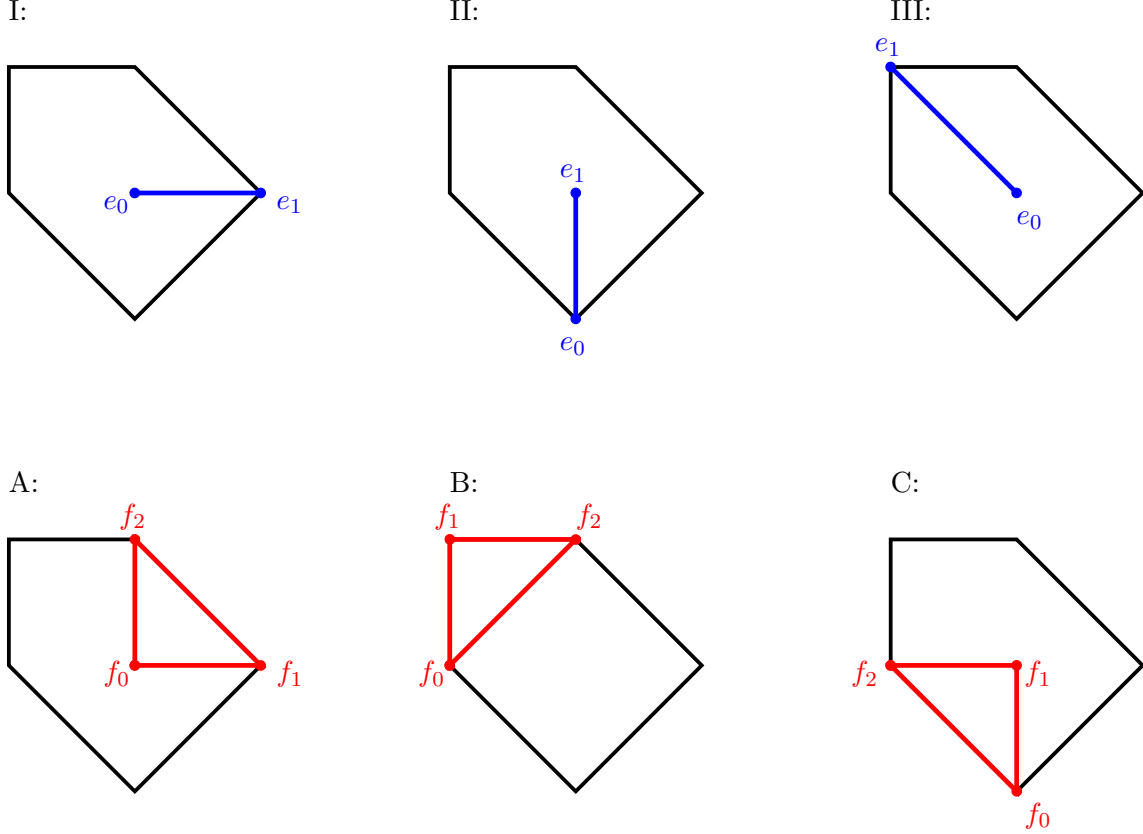


**Figure B.2:** Possible  $SU(2)$  (upper) and  $SU(3)$  (lower) tops. The coloured lines and vertices are the ‘top layer’ of the three-dimensional toric diagram, projected down onto the layer containing the base polygon representing the fibre ambient space.

The same symmetry relates the  $SU(2)$  and  $SU(3)$  tops as well as combinations of those. As shown in figure B.2, the  $SU(2)$ -I and -II tops are precisely matched onto each other, however only if one also exchanges the resolution coordinates  $e_0 \leftrightarrow e_1$ . The  $U(1)$  generators on both sides can be similarly matched. The first generator transforms as  $\omega_1^I \rightarrow S_0^{\text{II}} - S_1^{\text{II}} - \bar{\mathcal{K}} + \frac{1}{2}E_0^{\text{II}} = -(S_1^{\text{II}} - S_0^{\text{II}} - \bar{\mathcal{K}} + \frac{1}{2}E_1^{\text{II}}) + 2\bar{\mathcal{K}} + \frac{1}{2}\pi^*W_2 = -\omega_1^{\text{II}} + 2\bar{\mathcal{K}} + \frac{1}{2}\pi^*W_2$ , where the first equality exploits the relation  $E_0 + E_1 = \pi^*W_2$  for the resolution divisors of an  $SU(2)$  singularity. For the second generator one now needs to take into account that  $c_1^I = c_{1,0}^I e_1^I$  is mapped onto  $c_2^{\text{II}} = c_{2,1}^{\text{II}} e_0^{\text{II}}$ , from which one can easily verify the transformation  $\omega_2^I \rightarrow \omega_2^{\text{II}} - \omega_1^{\text{II}} + [c_1^{\text{II}}] - [c_{2,1}^{\text{II}}] - \bar{\mathcal{K}}$ . As mentioned after (V.31), the spectrum of  $SU(2)$ -charged states is also exchanged as  $\mathbf{2}_i^I \leftrightarrow \bar{\mathbf{2}}_i^{\text{II}}, i = 1, 2, 3$ . Obviously the  $SU(2)$ -III top is invariant under the reflection symmetry. The spectrum and  $U(1)$  charges transform as stated in subsection 1.2.4. Similarly one can see that the  $SU(3)$ -A and -C tops are equivalent to each other, while the -B top is invariant under reflection. Analogous calculations as above show that the  $U(1)$  generators transform accordingly.



When we combine the  $SU(2)$  and  $SU(3)$  tops, we see that among the nine possibilities there are in fact five inequivalent models with  $SU(2) \times SU(3)$  gauge group. The redundancy comes again from reflecting along the symmetry axis of the base polygon, which identifies four pairs of models to be equivalent (cf. figure B.3). The combination  $\text{III} \times \text{B}$  is invariant under the reflection transformation. The equivalence of the pairs of models can also be checked in a similar fashion as above, by inspecting the transformation of the  $U(1)$  generators and the matter states.

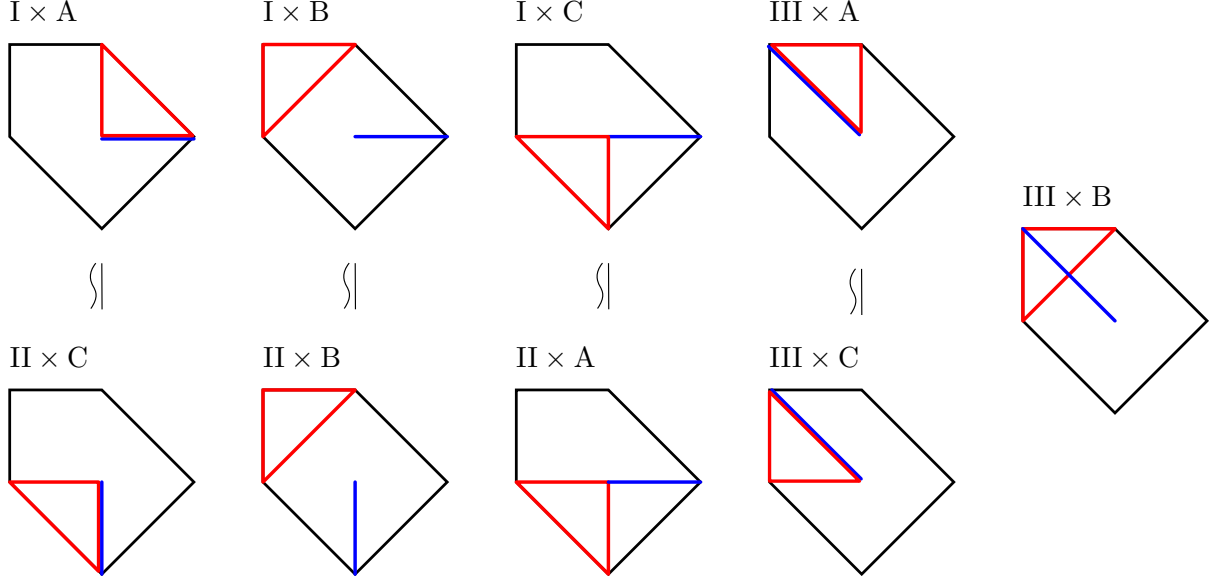


**Figure B.3:** The combination of  $SU(2)$  and  $SU(3)$  tops gives rise to five inequivalent models. Their toric diagram lies in a four-dimensional lattice, where the ‘top layers’ corresponding to  $SU(2)$  and  $SU(3)$  resolution divisors extend into two linearly independent directions that do not lie in the plane spanned by the base polygon. For this figure we have projected the tops down into said plane. The four pairs of tops that are equivalent are related to each other by reflection along the diagonal in the plane of the base polygon.

## 2 Details on $SU(2)$ -II and -III Tops

In this part we provide more details on the matter and Yukawa couplings of the  $SU(2)$ -II and -III top which have not been discussed at length in the corpus of this paper.

### 2.1 $SU(2)$ -II Top

The top corresponds to restricting the hypersurface coefficients as

$$b_0 = b_{0,1} e_0, \quad b_2 = b_{2,0} e_1, \quad c_2 = c_{2,1} e_0, \quad d_1 = d_{1,0} e_1, \quad d_2 = d_{2,0} e_1. \quad (\text{B.3})$$

There are two possible SR-ideals, of which we choose

$$u v, u w, w s_0, v s_1, s_0 s_1, e_0 s_1, e_0 u, e_1 v. \quad (\text{B.4})$$

The scaling relations and divisor classes for this top are as follows:

$$\begin{array}{c|cccccc|c}
 & \mathbf{u} & \mathbf{v} & \mathbf{w} & s_0 & s_1 & e_1 & e_0 \\
 \hline
 U & 1 & 1 & 1 & \cdot & \cdot & \cdot & \cdot \\
 S_0 & \cdot & \cdot & 1 & 1 & \cdot & \cdot & \cdot \\
 S_1 & \cdot & 1 & \cdot & \cdot & 1 & \cdot & \cdot \\
 E_1 & \cdot & 1 & \cdot & \cdot & \cdot & 1 & -1
 \end{array} \tag{B.5}$$

The  $U(1)$  generators, normalised such that the  $SU(2)$  root remains uncharged, are given by

$$\begin{aligned}
 \omega_1^{\text{II}} &= S_1 - S_0 - \bar{\mathcal{K}} + \frac{1}{2}E_1, \\
 \omega_2^{\text{II}} &= U - S_0 - \bar{\mathcal{K}} - [c_1] + \frac{1}{2}E_1.
 \end{aligned} \tag{B.6}$$

The discriminant locus now takes the form

$$\Delta \simeq w_2^2 \left( c_1 (c_{2,1}^2 d_0 - b_{0,1} b_1 c_{2,1} + b_{0,1}^2 c_1) \ell_3 (b_1^2 - 4c_1 d_0)^2 + \mathcal{O}(w_2) \right). \tag{B.7}$$

The fibres over the intersection of the first three factors inside the big bracket in (B.7) with  $\{w_2\}$  are indeed of split Kodaira type  $I_3$ . A similar analysis as for the  $SU(2)$ -I top confirms matter in the  $\mathbf{2}$  representation (together with their charge conjugates  $\bar{\mathbf{2}}$ ) on the matter curves displayed in table B.1.

$\mathcal{R}$	locus = $W_2 \cap \dots$	splitting of fibre components	$U(1)$ – charges
$\mathbf{2}_1^{\text{II}}$	$\{c_1\}$	$\mathbb{P}_1^1 \rightarrow \mathbb{P}_{1s_0}^1 + \mathbb{P}_{1A}^1$	$(\frac{1}{2}, \frac{3}{2})$
$\mathbf{2}_2^{\text{II}}$	$\{c_{2,1}^2 d_0 - b_{0,1} b_1 c_{2,1} + b_{0,1}^2 c_1\}$	$\mathbb{P}_1^1 \rightarrow \mathbb{P}_{1B}^1 + \mathbb{P}_{1C}^1$	$(\frac{1}{2}, -\frac{1}{2})$
$\mathbf{2}_3^{\text{II}}$	$\{\ell_3\} := \{b_{2,0}^2 d_0^2 + b_{2,0} (b_1^2 d_{2,0} - 2c_1 d_0 d_{2,0} - b_1 d_0 d_{1,0}) + c_1 (d_0 d_{1,0}^2 + d_{2,0} (c_1 d_{2,0} - b_1 d_{1,0}))\}$	$\mathbb{P}_0^1 \rightarrow \mathbb{P}_{0A}^1 + \mathbb{P}_{0B}^1$	$(\frac{1}{2}, \frac{1}{2})$

**Table B.1:** Matter states in the  $SU(2)$ -II top.

The splitting of the fibre components over the first curve and the resulting enhancement of the intersection structure to that of an affine  $SU(3)$  diagram is straightforward to see. For the second curve, we factorise

$$c_{2,1}^2 d_0 - b_{0,1} b_1 c_{2,1} + b_{0,1}^2 c_1 = \frac{1}{d_0} \mathcal{C}_+ \mathcal{C}_- \quad \text{with} \quad \mathcal{C}_{\pm} = c_{2,1} d_0 - b_{0,1} \left( \frac{b_1}{2} \pm \sqrt{\frac{b_1^2}{4} - c_1 d_0} \right), \tag{B.8}$$

which splits the curve into two parts  $W_2 \cap \{C_{\pm} = 0\}$  that are connected at a branch cut. Similar to the results (V.26) of the first  $SU(2)$  top, we find that over these two parts the fibre of the divisor  $E_1$  splits into two components,  $\mathbb{P}_{1B}^1$  and  $\mathbb{P}_{1C}^1$ , that can be extended over the whole curve without being interchanged by any monodromy. The intersection structure is again that of the affine  $SU(3)$  diagram. Analogously, the third curve can be written as  $W_2 \cap \ell_3$  with

$$\ell_3 = 1/d_0^2 \mathcal{D}_+ \mathcal{D}_-, \quad \mathcal{D}_{\pm} = b_{2,0} d_0^2 - \left[ c_1 d_0 d_{2,0} + (d_0 d_{1,0} - b_1 d_{2,0}) \left( \frac{b_1}{2} \pm \sqrt{\frac{b_1^2}{4} - c_1 d_0} \right) \right]. \tag{B.9}$$

A similar calculation as (V.28) shows that the divisor  $E_0$  splits into  $\mathbb{P}_{0A}^1 + \mathbb{P}_{0B}^1$ , with both components well-defined over the whole curve. As expected one finds the intersection structure to be an affine  $SU(3)$  diagram.

Note that apart from the three matter curves discussed above, the vanishing order of the discriminant increases from 2 to 3 also along the curve  $\{w_2\} \cap \{b_1^2 - 4c_1 d_0\}$ ; however, the fibre is of Kodaira type *III* since the Weierstrass sections  $f$  and  $g$  vanish to order 1 and 2 respectively. Thus no extra charged matter representations arise here, in agreement with the formalism of [41].

The Yukawa couplings involving  $SU(2)$  matter are summarised in table B.2. The fibre structure enhancement for each Yukawa point can be read off from the last column in an analogous fashion as with the first  $SU(2)$  top (cf. table V.4). We find the affine  $SU(4)$  diagram as the intersection structure over all Yukawa points. Note that for the second and third pair of Yukawa points, the same split products of each pair arrange themselves into different intersection *patterns*, realising either  $\mathbf{2}_i - \mathbf{2}_j - \mathbf{1}/\bar{\mathbf{1}}$  or  $\mathbf{2}_i - \bar{\mathbf{2}}_j - \mathbf{1}/\bar{\mathbf{1}}$  couplings.

coupling	locus = $W_2 \cap \dots$	splitting of fibre components
$\mathbf{2}_1^{\text{II}} \mathbf{2}_2^{\text{II}} \bar{\mathbf{1}}^{(4)}$	$\{c_1\} \cap \{c_{2,1} d_0 - b_{0,1} b_1\}$	$\mathbb{P}_1^1 \rightarrow \mathbb{P}_{1s_0C}^1 + \mathbb{P}_{1AB}^1 + \mathbb{P}_{1AC}^1$
$\mathbf{2}_1^{\text{II}} \bar{\mathbf{2}}_2^{\text{II}} \bar{\mathbf{1}}^{(5)}$	$\{c_1\} \cap \{c_{2,1}\}$	$\mathbb{P}_1^1 \rightarrow \mathbb{P}_{1s_0B}^1 + \mathbb{P}_{1AB'}^1 + \mathbb{P}_{1AC'}^1$
$\mathbf{2}_1^{\text{II}} \mathbf{2}_3^{\text{II}} \bar{\mathbf{1}}^{(3)}$	$\{c_1\} \cap \{b_{2,0}\}$	$\mathbb{P}_0^1 \rightarrow \mathbb{P}_{0A}^1 + \mathbb{P}_{0B}^1, \mathbb{P}_1^1 \rightarrow \mathbb{P}_{1s_0}^1 + \mathbb{P}_{1A}^1$
$\mathbf{2}_1^{\text{II}} \bar{\mathbf{2}}_3^{\text{II}} \bar{\mathbf{1}}^{(6)}$	$\{c_1\} \cap \{b_{2,0} d_0^2 + b_1 (d_0 d_{1,0} - b_1 d_{2,0})\}$	$\mathbb{P}_0^1 \rightarrow \mathbb{P}_{0A}^1 + \mathbb{P}_{0B}^1, \mathbb{P}_1^1 \rightarrow \mathbb{P}_{1s_0}^1 + \mathbb{P}_{1A}^1$
$\mathbf{2}_2^{\text{II}} \mathbf{2}_3^{\text{II}} \bar{\mathbf{1}}^{(2)}$	$(\{\mathcal{C}_+\} \cap \{\mathcal{D}_+\}) \cup (\{\mathcal{C}_-\} \cap \{\mathcal{D}_-\})$	$\mathbb{P}_0^1 \rightarrow \mathbb{P}_{0A}^1 + \mathbb{P}_{0B}^1, \mathbb{P}_1^1 \rightarrow \mathbb{P}_{1B}^1 + \mathbb{P}_{1C}^1$
$\mathbf{2}_2^{\text{II}} \bar{\mathbf{2}}_3^{\text{II}} \mathbf{1}^{(6)}$	$(\{\mathcal{C}_+\} \cap \{\mathcal{D}_-\}) \cup (\{\mathcal{C}_-\} \cap \{\mathcal{D}_+\})$	$\mathbb{P}_0^1 \rightarrow \mathbb{P}_{0A}^1 + \mathbb{P}_{0B}^1, \mathbb{P}_1^1 \rightarrow \mathbb{P}_{1B}^1 + \mathbb{P}_{1C}^1$
$\mathbf{2}_2^{\text{II}} \mathbf{2}_2^{\text{II}} \bar{\mathbf{1}}^{(1)}$	$\{b_{0,1}\} \cap \{c_{2,1}\}$	$\mathbb{P}_1^1 \rightarrow \mathbb{P}_{1B}^1 + \mathbb{P}_{1s_1C}^1 + \mathbb{P}_{1C'}^1$
$\mathbf{2}_3^{\text{II}} \bar{\mathbf{2}}_3^{\text{II}} \bar{\mathbf{1}}^{(4)}$	$\{b_1 d_{2,0} - d_0 d_{1,0}\} \cap \{c_1 d_{2,0} - b_{2,0} d_0\}$	$\mathbb{P}_0^1 \rightarrow \mathbb{P}_{0A}^1 + \mathbb{P}_{0B'}^1 + \mathbb{P}_{0B''}^1$

**Table B.2:** Yukawa couplings in the  $SU(2)$ -II top.

## 2.2 $SU(2)$ -III Top

This top restricts the hypersurface coefficients as

$$c_1 = c_{1,1} e_0, \quad c_2 = c_{2,1} e_0, \quad d_0 = d_{0,0} e_1, \quad d_1 = d_{1,0} e_1, \quad d_2 = d_{2,0} e_1^2. \quad (\text{B.10})$$

For this top there are four possible SR-ideals, of which we choose

$$\mathbf{u} \mathbf{v}, \mathbf{u} \mathbf{w}, \mathbf{w} \mathbf{s}_0, \mathbf{v} \mathbf{s}_1, \mathbf{s}_0 \mathbf{s}_1, \mathbf{e}_0 \mathbf{u}, \mathbf{e}_0 \mathbf{s}_0, \mathbf{e}_1 \mathbf{w}. \quad (\text{B.11})$$

The scaling relations and divisor classes for this top are

	u	v	w	$s_0$	$s_1$	$e_1$	$e_0$
U	1	1	1	·	·	·	·
$S_0$	·	·	1	1	·	·	·
$S_1$	·	1	·	·	1	·	·
$E_1$	·	1	1	·	·	1	-1

(B.12)

The  $SU(2)$  root in this top is uncharged under the generators (V.5) so that no correction term is needed,

$$\begin{aligned}\omega_1^{\text{III}} &= S_1 - S_0 - \bar{\mathcal{K}}, \\ \omega_2^{\text{III}} &= U - S_0 - \bar{\mathcal{K}} - [c_{1,1}].\end{aligned}\tag{B.13}$$

This time the discriminant of the singular blow-down takes the form

$$\begin{aligned}\Delta &= w_2^2 \left( b_0 b_2 (b_0 c_{1,1}^2 - b_1 c_{1,1} c_{2,1} + b_2 c_{2,1}^2) (b_1^2 - 4b_0 b_2)^2 \right. \\ &\quad \left. (-b_2 d_0^2 + b_1 d_{0,0} d_{1,0} - b_0 d_{1,0}^2 - b_1^2 d_{2,0} + 4b_0 b_2 d_{2,0}) + \mathcal{O}(w_2) \right).\end{aligned}\tag{B.14}$$

Over the intersection of  $\{w_2\}$  with the first three factors in the bracket in (B.14), the fibre type enhances to split Kodaira type  $I_3$ . This gives rise to matter states in the  $\mathbf{2}$  representation (together with their charge conjugate  $\bar{\mathbf{2}}$  states) summarised in tabe B.3.

By setting  $b_0/b_2 = 0$  in the hypersurface equation, it is again straightforward to see the splitting process and the enhancement of the intersection structure to an affine  $SU(3)$  diagram over the first/second  $\mathbf{2}$ -curve. The quadratic equation defining the third curve can be again factorised analogously to (V.25). However, because of the Yukawa points that are present in this top (see below), we need two different factorisations,

$$b_0 c_{1,1}^2 - b_1 c_{1,1} c_{2,1} + b_2 c_{2,1}^2 = \frac{1}{b_0} \mathcal{C}_+ \mathcal{C}_- = \frac{1}{b_2} \mathcal{D}_+ \mathcal{D}_-\tag{B.15}$$

with

$$\mathcal{C}_\pm = c_{1,1} b_0 - c_{2,1} \left( \frac{b_1}{2} \pm \sqrt{\frac{b_1^2}{4} - b_0 b_2} \right), \quad \mathcal{D}_\pm = c_{2,1} b_2 - c_{1,1} \left( \frac{b_1}{2} \mp \sqrt{\frac{b_1^2}{4} - b_0 b_2} \right).\tag{B.16}$$

The two factorisations describe the same splittings of the curve into two parts which are connected at the branch cut of the square root. With these two factorisations, one can analyse the splitting of the fibre when either  $b_0$  or  $b_2$  is non-zero.<sup>1</sup> When  $b_0 \neq 0$ , we can solve  $\mathcal{C}_\pm$  for  $c_{1,1}$  and plug the result into the hypersurface equation; if  $b_2 \neq 0$ , we solve  $\mathcal{D}_\pm$  for  $c_{2,1}$ . Doing so, we find no splitting for  $\mathbb{P}_0^1$ , but  $\mathbb{P}_1^1$  splits as follows:

$$\begin{aligned}P_T(e_1 = 0, \mathcal{C}_\pm/\mathcal{D}_\pm = 0) \\ \stackrel{b_0 \neq 0}{=} \frac{1}{b_0} \left[ \underbrace{\left[ \left( \frac{b_1}{2} \pm \sqrt{\frac{b_1^2}{4} - b_0 b_2} \right) s_1 + b_0 s_0 v \right]}_{\mathbb{P}_{1B}^1} \right] \left[ \underbrace{\left[ \left( \frac{b_1}{2} \mp \sqrt{\frac{b_1^2}{4} - b_0 b_2} \right) s_1 u + c_{2,1} e_0 v + b_0 s_0 u v \right]}_{\mathbb{P}_{1C}^1} \right]\end{aligned}\tag{B.17}$$

$$\stackrel{b_2 \neq 0}{=} \frac{1}{b_2} \left[ \underbrace{\left[ b_2 s_1 + \left( \frac{b_1}{2} \mp \sqrt{\frac{b_1^2}{4} - b_0 b_2} \right) s_0 v \right]}_{\mathbb{P}_{1B}^1} \right] \left[ \underbrace{\left[ b_2 s_1 u + c_{1,1} e_0 v + \left( \frac{b_1}{2} \pm \sqrt{\frac{b_1^2}{4} - b_0 b_2} \right) s_0 u v \right]}_{\mathbb{P}_{1C}^1} \right]\tag{B.18}$$

The fibre over  $\{w_2\} \cap \{b_1^2 - 4b_0 b_2\}$  is of Kodaira type  $III$  and thus no massless matter arises. Interestingly, over the remaining locus  $\{w_2\} \cap \{-b_2 d_0^2 + b_1 d_{0,0} d_{1,0} - b_0 d_{1,0}^2 - b_1^2 d_{2,0} + 4b_0 b_2 d_{2,0}\}$ ,  $(f, g, \Delta)$  vanish to order  $(0, 0, 3)$ , but the fibre is of *non-split* Kodaira type  $I_3$ . This can be read off from the specifics of the Weierstrass sections  $f$  and  $g$  following Tate's algorithm. Moreover, an explicit analysis of the resolved fibre confirms that it locally factors into three  $\mathbb{P}^1$ s, two of which

<sup>1</sup>On a generic base of complex dimension 3,  $b_0$  and  $b_2$  cannot both vanish on the codimension 2 curve.

$\mathcal{R}$	locus = $W_2 \cap \dots$	splitting of fibre components	$U(1)$ – charges
$\mathbf{2}_1^{\text{III}}$	$\{b_0\}$	$\mathbb{P}_0^1 \rightarrow \mathbb{P}_{0s_1}^1 + \mathbb{P}_{0A}^1$	(1, 0)
$\mathbf{2}_2^{\text{III}}$	$\{b_2\}$	$\mathbb{P}_1^1 \rightarrow \mathbb{P}_{1v}^1 + \mathbb{P}_{1A}^1$	(1, 1)
$\mathbf{2}_3^{\text{III}}$	$\{b_0 c_{1,1}^2 - b_1 c_{1,1} c_{2,1} + b_2 c_{2,1}^2\}$	$\mathbb{P}_1^1 \rightarrow \mathbb{P}_{1B}^1 + \mathbb{P}_{1C}^1$	(0, 1)

**Table B.3:** Matter states in the  $SU(2)$ -III top.

are however exchanged by a monodromy along the curve in the base. Since the corresponding singularity type is merely  $\text{Sp}(1)$  (as opposed to  $SU(3)$ ) no massless matter arises here. Note that this conclusion is not in contradiction with the results of [41], especially table 9, which would naively indicate fundamental matter along this curve. However, the analysis of [41] holds on Calabi-Yau 3-folds and therefore does not account for potential monodromies along the matter loci.

The possible Yukawa couplings are summarised in table B.4. The splitting process over the first type of Yukawa points is straightforward to see when one evaluates the hypersurface equation on the locus.

coupling	locus = $W_2 \cap \dots$	splitting of fibre components
$\mathbf{2}_1^{\text{III}} \mathbf{2}_2^{\text{III}} \mathbf{1}^{(6)}$	$\{b_0\} \cap \{b_2\}$	$\mathbb{P}_0^1 \rightarrow \mathbb{P}_{0s_1}^1 + \mathbb{P}_{0A}^1, \mathbb{P}_1^1 \rightarrow \mathbb{P}_{1v}^1 + \mathbb{P}_{1A}^1$
$\mathbf{2}_1^{\text{III}} \mathbf{2}_3^{\text{III}} \mathbf{1}^{(4)}$	$\{b_0\} \cap \{c_{2,1} b_2 - c_{1,1} b_1\}$	$\mathbb{P}_0^1 \rightarrow \mathbb{P}_{0s_1}^1 + \mathbb{P}_{0A}^1, \mathbb{P}_1^1 \rightarrow \mathbb{P}_{1B}^1 + \mathbb{P}_{1C}^1$
$\mathbf{2}_1^{\text{III}} \mathbf{2}_3^{\text{III}} \mathbf{1}^{(1)}$	$\{b_0\} \cap \{c_{2,1}\}$	$\mathbb{P}_0^1 \rightarrow \mathbb{P}_{0s_1}^1 + \mathbb{P}_{0A}^1, \mathbb{P}_1^1 \rightarrow \mathbb{P}_{1B'}^1 + \mathbb{P}_{1C}^1$
$\mathbf{2}_2^{\text{III}} \mathbf{2}_3^{\text{III}} \mathbf{1}^{(3)}$	$\{b_2\} \cap \{c_{1,1}\}$	$\mathbb{P}_1^1 \rightarrow \mathbb{P}_{1vB}^1 + \mathbb{P}_{1AB}^1 + \mathbb{P}_{1AC}^1$
$\mathbf{2}_2^{\text{III}} \mathbf{2}_3^{\text{III}} \mathbf{1}^{(2)}$	$\{b_2\} \cap \{c_{1,1} b_0 - c_{2,1} b_1\}$	$\mathbb{P}_1^1 \rightarrow \mathbb{P}_{1vC}^1 + \mathbb{P}_{1AB'}^1 + \mathbb{P}_{1AC'}^1$
$\mathbf{2}_3^{\text{III}} \mathbf{2}_3^{\text{III}} \mathbf{1}^{(5)}$	$\{c_{1,1}\} \cap \{c_{2,1}\}$	$\mathbb{P}_1^1 \rightarrow \mathbb{P}_{1B}^1 + \mathbb{P}_{1uC}^1 + \mathbb{P}_{1C'}^1$

**Table B.4:** Yukawa couplings in the  $SU(2)$ -III top.

The second and third groups of couplings arise over the intersection of the  $\mathbf{2}_3^{\text{III}}$ -curve with  $b_0 = 0$  and hence require the factorisation (B.18). The second Yukawa point lies over  $\mathcal{D}_- = 0$ , corresponding to the downstairs signs in (B.18); the third point lies over  $\mathcal{D}_+ = 0$ , corresponding to upstairs signs. In both cases, we see that there is no further splitting of  $\mathbb{P}_{1B}^1$  and  $\mathbb{P}_{1C}^1$  when we set  $b_0 = 0$ . Rather,  $\mathbb{P}_0^1$  splits, coming from the already present enhancement over the  $\mathbf{2}_1^{\text{III}}$  curve.

The fourth and fifth Yukawa point are the intersection points of  $\mathbf{2}_3^{\text{III}}$  and  $b_2 = 0$ , hence we make use of the factorisation (B.17). The fourth/fifth point lies on  $\mathcal{C}_-/\mathcal{C}_+ = 0$ , correspondingly we take the downstairs/upstairs signs in (B.17). Setting  $b_2 = 0$ , we see that for the fourth coupling,  $\mathbb{P}_{1B}^1$  splits off a factor  $v$ , while  $\mathbb{P}_{1C}^1$  remains irreducible; for the fifth coupling, it is  $\mathbb{P}_{1C}^1$  that splits.

Finally, over the last Yukawa point, which is a self-intersection point, neither  $b_0$  nor  $b_2$  are 0, and so both factorisations (B.17) and (B.18) should give the same splitting process in the fibre. Indeed, setting  $c_{2,1} = 0$  in (B.17) and  $c_{1,1} = 0$  in (B.18) shows that  $\mathbb{P}_{1B}^1$  remains irreducible while  $\mathbb{P}_{1C}^1$  splits off a factor  $u$ .

Over all Yukawa points we find that the intersection structure of the  $\mathbb{P}^1$  components is the affine  $SU(4)$  diagram.

### 3 Details on $SU(3)$ -B and -C Tops

Here we go through the remaining  $SU(3)$  tops in more detail.

#### 3.1 $SU(3)$ -B Top

The  $SU(3)$ -B top leads to the restrictions of the following coefficients

$$\begin{aligned} b_0 &= b_{0,2} f_0^2 f_1, & b_2 &= b_{2,0} f_1 f_2^2, & c_1 &= c_{1,0} f_2, & c_2 &= c_{2,1} f_0, \\ d_0 &= d_{0,1} f_0 f_1, & d_1 &= d_{1,0} f_1 f_2, & d_2 &= d_{2,0} f_1, \end{aligned} \quad (\text{B.19})$$

while  $b_1$  remain unrestricted. There are eight different triangulations. For definiteness, we choose the one leading to the following SR-ideal:

$$u v, u w, w s_0, v s_1, s_0 s_1, f_0 u, f_0 s_1, f_1 v, f_1 w, f_2 u, f_2 s_0, f_2 v. \quad (\text{B.20})$$

The coordinates and their corresponding divisor classes are summarised in the following table:

	u	v	w	$s_0$	$s_1$	$f_1$	$f_2$	$f_0$
U	1	1	1	·	·	·	·	·
$S_0$	·	·	1	1	·	·	·	·
$S_1$	·	1	·	·	1	·	·	·
$F_1$	·	1	·	·	·	1	·	-1
$F_2$	·	1	-1	·	·	·	1	-1

(B.21)

For  $SU(3)$  roots to have zero  $U(1)$  charge, the generators (V.5) receive the following correction:

$$\begin{aligned} \omega_1^{\text{B}} &= S_1 - S_0 - \bar{\mathcal{K}} + \frac{1}{3}F_1 + \frac{2}{3}F_2, \\ \omega_2^{\text{B}} &= U - S_0 - \bar{\mathcal{K}} - [c_{1,0}] + \frac{2}{3}F_1 + \frac{1}{3}F_2. \end{aligned} \quad (\text{B.22})$$

We find codimension 2 enhancement with  $\mathbf{3}$  and  $\bar{\mathbf{3}}$  matter over loci and with charges as presented in table B.5. Over the curve  $\{w_3\} \cap \{b_1\}$  the fibre type changes to Kodaira type  $IV$ , but such fibres do not give rise to additional charged matter.

The gauge invariant Yukawa coupling appearing are listed in table B.6.

$\mathcal{R}$	locus = $W_3 \cap \dots$	splitting of fibre components	$U(1)$ – charges
$\mathbf{3}_1^{\text{B}}$	$\{c_{1,0}\}$	$\mathbb{P}_1^1 \rightarrow \mathbb{P}_{1s_0}^1 + \mathbb{P}_{1A}^1$	$(-\frac{2}{3}, -\frac{4}{3})$
$\mathbf{3}_2^{\text{B}}$	$\{c_{2,1}\}$	$\mathbb{P}_1^1 \rightarrow \mathbb{P}_{1s_1}^1 + \mathbb{P}_{1B}^1$	$(-\frac{2}{3}, \frac{2}{3})$
$\mathbf{3}_3^{\text{B}}$	$\{d_{2,0}\}$	$\mathbb{P}_0^1 \rightarrow \mathbb{P}_{0w}^1 + \mathbb{P}_{0A}^1$	$(-\frac{2}{3}, -\frac{1}{3})$
$\mathbf{3}_4^{\text{B}}$	$\{b_1^2 b_{2,0} - b_1 c_{1,0} d_{1,0} + c_{1,0}^2 d_{2,0}\}$	$\mathbb{P}_0^1 \rightarrow \mathbb{P}_{0B}^1 + \mathbb{P}_{0C}^1$	$(\frac{1}{3}, \frac{2}{3})$
$\mathbf{3}_5^{\text{B}}$	$\{b_{0,2} b_1^2 + c_{2,1}^2 d_{2,0} - b_1 c_{2,1} d_{0,1}\}$	$\mathbb{P}_2^1 \rightarrow \mathbb{P}_{2A}^1 + \mathbb{P}_{2B}^1$	$(\frac{1}{3}, -\frac{1}{3})$

**Table B.5:** Matter states in the  $SU(3)$ -B top.

coupling	locus = $W_3 \cap \dots$	splitting of fibre components
$\mathbf{3}_1^B \overline{\mathbf{3}}_2^B \mathbf{1}^{(5)}$	$\{c_{1,0}\} \cap \{c_{2,1}\}$	$\mathbb{P}_1^1 \rightarrow \mathbb{P}_{1s_0B}^1 + \mathbb{P}_{1s_1A}^1 + \mathbb{P}_{1AB}^1$
$\mathbf{3}_1^B \overline{\mathbf{3}}_3^B \mathbf{1}^{(6)}$	$\{c_{1,0}\} \cap \{d_{2,0}\}$	$\mathbb{P}_0^1 \rightarrow \mathbb{P}_{0w}^1 + \mathbb{P}_{0A}^1, \mathbb{P}_1^1 \rightarrow \mathbb{P}_{1s_0}^1 + \mathbb{P}_{1A}^1$
$\mathbf{3}_1^B \overline{\mathbf{3}}_4^B \mathbf{1}^{(3)}$	$\{c_{1,0}\} \cap \{b_{2,0}\}$	$\mathbb{P}_0^1 \rightarrow \mathbb{P}_{0B}^1 + \mathbb{P}_{0C}^1, \mathbb{P}_1^1 \rightarrow \mathbb{P}_{1s_0}^1 + \mathbb{P}_{1A}^1$
$\mathbf{3}_1^B \overline{\mathbf{3}}_5^B \mathbf{1}^{(4)}$	$\{c_{1,0}\} \cap (\mathbf{3}_5^B)$	$\mathbb{P}_1^1 \rightarrow \mathbb{P}_{1s_0}^1 + \mathbb{P}_{1A}^1, \mathbb{P}_2^1 \rightarrow \mathbb{P}_{2A}^1 + \mathbb{P}_{2B}^1$
$\mathbf{3}_2^B \overline{\mathbf{3}}_3^B \overline{\mathbf{1}}^{(6)}$	$\{c_{2,1}\} \cap \{d_{2,0}\}$	$\mathbb{P}_0^1 + \mathbb{P}_{0w}^1 + \mathbb{P}_{0A}^1, \mathbb{P}_1^1 \rightarrow \mathbb{P}_{1s_1}^1 + \mathbb{P}_{1B}^1$
$\mathbf{3}_2^B \overline{\mathbf{3}}_4^B \mathbf{1}^{(2)}$	$\{c_{2,1}\} \cap (\mathbf{3}_4^B)$	$\mathbb{P}_0^1 \rightarrow \mathbb{P}_{0B}^1 + \mathbb{P}_{0C}^1, \mathbb{P}_1^1 \rightarrow \mathbb{P}_{1s_1}^1 + \mathbb{P}_{1B}^1$
$\mathbf{3}_2^B \overline{\mathbf{3}}_5^B \mathbf{1}^{(1)}$	$\{b_{0,2}\} \cap \{c_{2,1}\}$	$\mathbb{P}_1^1 \rightarrow \mathbb{P}_{1s_1}^1 + \mathbb{P}_{1B}^1, \mathbb{P}_2^1 \rightarrow \mathbb{P}_{2A}^1 + \mathbb{P}_{2B}^1$
$\mathbf{3}_3^B \overline{\mathbf{3}}_4^B \mathbf{1}^{(4)}$	$\{d_{2,0}\} \cap \{b_1 b_{2,0} - c_{1,0} d_{1,0}\}$	$\mathbb{P}_0^1 \rightarrow \mathbb{P}_{0wC}^1 + \mathbb{P}_{0AC}^1 + \mathbb{P}_{0AB}^1$
$\mathbf{3}_3^B \overline{\mathbf{3}}_5^B \mathbf{1}^{(2)}$	$\{d_{2,0}\} \cap \{b_{0,2} b_1 - c_{2,1} d_{0,1}\}$	$\mathbb{P}_0^1 + \mathbb{P}_{0w}^1 + \mathbb{P}_{0A}^1, \mathbb{P}_2^1 \rightarrow \mathbb{P}_{2A}^1 + \mathbb{P}_{2B}^1$
$\mathbf{3}_4^B \overline{\mathbf{3}}_5^B \overline{\mathbf{1}}^{(6)}$	$(\mathbf{3}_4^B) \cap (\mathbf{3}_5^B) \setminus (\{d_{2,0}\} \cap \{b_1\})$	$\mathbb{P}_0^1 \rightarrow \mathbb{P}_{0B}^1 + \mathbb{P}_{0C}^1, \mathbb{P}_2^1 \rightarrow \mathbb{P}_{2A}^1 + \mathbb{P}_{2B}^1$
$\mathbf{3}_3^B \mathbf{3}_4^B \mathbf{3}_5^B$	$\{d_{2,0}\} \cap \{b_1\}$	$\mathbb{P}_0^1 \rightarrow \mathbb{P}_{0wB}^1 + \mathbb{P}_{0AB'}^1 + \mathbb{P}_{0AC'}^1, \mathbb{P}_2^1 \rightarrow \mathbb{P}_{2A}^1 + \mathbb{P}_{2B}^1$ $\mathbb{P}_{0AB'}^1 = \mathbb{P}_{2A}^1$
$\mathbf{3}_1^B \mathbf{3}_4^B \mathbf{3}_4^B$	$\{c_{1,0}\} \cap \{b_1\}$	$\mathbb{P}_0^1 \rightarrow \mathbb{P}_{0B}^1 + \mathbb{P}_{0C'}^1 + \mathbb{P}_{0C1}^1, \mathbb{P}_1^1 \rightarrow \mathbb{P}_{1s_0}^1 + \mathbb{P}_{1A}^1$ $\mathbb{P}_{0C1}^1 = \mathbb{P}_{1A}^1$
$\mathbf{3}_2^B \mathbf{3}_5^B \mathbf{3}_5^B$	$\{c_{2,1}\} \cap \{b_1\}$	$\mathbb{P}_1^1 \rightarrow \mathbb{P}_{1s_1}^1 + \mathbb{P}_{1B'}^1, \mathbb{P}_2^1 \rightarrow \mathbb{P}_{2A}^1 + \mathbb{P}_{2B'}^1 + \mathbb{P}_{2B1}^1$ $\mathbb{P}_{1B}^1 = \mathbb{P}_{2B1}^1$

**Table B.6:** Yukawa couplings in the  $SU(3)$ -B top.

### 3.2 $SU(3)$ -C Top

The third top leads to the restrictions of the following coefficients

$$\begin{aligned}
 b_0 &= b_{0,1} f_0 f_2, & b_2 &= b_{2,0} f_1, & c_1 &= c_{1,1} f_0 f_1, & c_2 &= c_{2,1} f_0, \\
 d_0 &= d_{0,0} f_2, & d_1 &= d_{1,0} f_1 f_2, & d_2 &= d_{2,0} f_1 f_2^2,
 \end{aligned}
 \tag{B.23}$$

while  $b_1$  remain unrestricted. The top allows 4 different triangulations. For definiteness, we choose the one leading to the following SR-ideal:

$$u v, u w, w s_0, v s_1, s_0 s_1, f_0 u, f_0 s_0, f_0 s_1, f_1 s_0, f_1 v, f_2 w, f_2 s_1.
 \tag{B.24}$$

The coordinates and their corresponding divisor classes are summarised in the following table:

	u	v	w	$s_0$	$s_1$	$f_1$	$f_2$	$f_0$
U	1	1	1	.	.	.	.	.
$S_0$	.	.	1	1	.	.	.	.
$S_1$	.	1	.	.	1	.	.	.
$F_1$	.	1	.	.	.	1	.	-1
$F_2$	.	1	1	.	.	.	1	-1

(B.25)

For  $SU(3)$  roots to have zero  $U(1)$  charge, the generators (V.5) receive the following correction:

$$\begin{aligned}
 \omega_1^C &= S_1 - S_0 - \overline{\mathcal{K}} + \frac{1}{3}F_1 - \frac{1}{3}F_2, \\
 \omega_2^C &= U - S_0 - \overline{\mathcal{K}} - [c_{1,1}].
 \end{aligned}
 \tag{B.26}$$

The Kodaira type of the fibre enhances from  $I_3$  to  $I_4$  (split) over the codimension-2 loci displayed in table B.7, which therefore give rise to  $\mathbf{3}$  and  $\overline{\mathbf{3}}$  matter. In addition, over the curve  $\{w_3\} \cap \{b_1\}$  the fibre type changes to Kodaira type  $IV$ , but no matter representation arises over this locus.

The gauge invariant Yukawa coupling appearing are summarised in table B.8.

$\mathcal{R}$	locus = $W_3 \cap \dots$	splitting of fibre components	$U(1) - \text{charges}$
$\mathbf{3}_1^C$	$\{b_{2,0}\}$	$\mathbb{P}_2^1 \rightarrow \mathbb{P}_{2v}^1 + \mathbb{P}_{2A}^1$	$(-\frac{2}{3}, -1)$
$\mathbf{3}_2^C$	$\{c_{2,1}\}$	$\mathbb{P}_1^1 \rightarrow \mathbb{P}_{1u}^1 + \mathbb{P}_{1A}^1$	$(\frac{1}{3}, -1)$
$\mathbf{3}_3^C$	$\{b_1 c_{1,1} - b_{2,0} c_{2,1}\}$	$\mathbb{P}_2^1 \rightarrow \mathbb{P}_{2B}^1 + \mathbb{P}_{2C}^1$	$(\frac{1}{3}, 1)$
$\mathbf{3}_4^C$	$\{b_{0,1} b_1 - c_{2,1} d_{0,0}\}$	$\mathbb{P}_1^1 \rightarrow \mathbb{P}_{1B}^1 + \mathbb{P}_{1C}^1$	$(-\frac{2}{3}, 0)$
$\mathbf{3}_5^C$	$\{b_{2,0} d_{0,0}^2 + b_1^2 d_{2,0} - b_1 d_{0,0} d_{1,0}\}$	$\mathbb{P}_0^1 \rightarrow \mathbb{P}_{0A}^1 + \mathbb{P}_{0B}^1$	$(\frac{1}{3}, 0)$

**Table B.7:** Matter states in the  $SU(3)$ -C top.

coupling	locus = $W_3 \cap \dots$	splitting of fibre components
$\mathbf{3}_1^C \overline{\mathbf{3}}_2^C \mathbf{1}^{(2)}$	$\{b_{2,0}\} \cap \{c_{2,1}\}$	$\mathbb{P}_1^1 \rightarrow \mathbb{P}_{1u}^1 + \mathbb{P}_{1A}^1, \mathbb{P}_2^1 \rightarrow \mathbb{P}_{2v}^1 + \mathbb{P}_{2A}^1$
$\mathbf{3}_1^C \overline{\mathbf{3}}_3^C \mathbf{1}^{(3)}$	$\{b_{2,0}\} \cap \{c_{1,1}\}$	$\mathbb{P}_2^1 \rightarrow \mathbb{P}_{2vC}^1 + \mathbb{P}_{2AB}^1 + \mathbb{P}_{2C'}^1$
$\mathbf{3}_1^C \overline{\mathbf{3}}_4^C \mathbf{1}^{(6)}$	$\{b_{2,0}\} \cap \{b_{0,1} b_1 - c_{2,1} d_{0,0}\}$	$\mathbb{P}_1^1 \rightarrow \mathbb{P}_{1B}^1 + \mathbb{P}_{1C}^1, \mathbb{P}_2^1 \rightarrow \mathbb{P}_{2v}^1 + \mathbb{P}_{2A}^1$
$\mathbf{3}_1^C \overline{\mathbf{3}}_5^C \mathbf{1}^{(4)}$	$\{b_{2,0}\} \cap \{b_1 d_{2,0} - d_{0,0} d_{1,0}\}$	$\mathbb{P}_0^1 \rightarrow \mathbb{P}_{0A}^1 + \mathbb{P}_{0B}^1, \mathbb{P}_2^1 \rightarrow \mathbb{P}_{2v}^1 + \mathbb{P}_{2A}^1$
$\mathbf{3}_2^C \overline{\mathbf{3}}_3^C \mathbf{1}^{(5)}$	$\{c_{2,1}\} \cap \{c_{1,1}\}$	$\mathbb{P}_1^1 \rightarrow \mathbb{P}_{1u}^1 + \mathbb{P}_{1A}^1, \mathbb{P}_2^1 \rightarrow \mathbb{P}_{2B}^1 + \mathbb{P}_{2C}^1$
$\mathbf{3}_2^C \overline{\mathbf{3}}_4^C \overline{\mathbf{1}}^{(1)}$	$\{c_{2,1}\} \cap \{b_{0,1}\}$	$\mathbb{P}_1^1 \rightarrow \mathbb{P}_{1uB}^1 + \mathbb{P}_{1B'}^1 + \mathbb{P}_{1AC}^1$
$\mathbf{3}_2^C \overline{\mathbf{3}}_5^C \mathbf{1}^{(6)}$	$\{c_{2,1}\} \cap (\mathbf{3}_5^C)$	$\mathbb{P}_0^1 \rightarrow \mathbb{P}_{0A}^1 + \mathbb{P}_{0B}^1, \mathbb{P}_1^1 \rightarrow \mathbb{P}_{1u}^1 + \mathbb{P}_{1A}^1$
$\mathbf{3}_3^C \overline{\mathbf{3}}_4^C \overline{\mathbf{1}}^{(4)}$	$(\mathbf{3}_3^C) \cap (\mathbf{3}_4^C) \setminus (\{c_{2,1}\} \cap \{b_1\})$	$\mathbb{P}_1^1 \rightarrow \mathbb{P}_{1B}^1 + \mathbb{P}_{1C}^1, \mathbb{P}_2^1 \rightarrow \mathbb{P}_{2B}^1 + \mathbb{P}_{2C}^1$
$\mathbf{3}_3^C \overline{\mathbf{3}}_5^C \overline{\mathbf{1}}^{(6)}$	$(\mathbf{3}_3^C) \cap (\mathbf{3}_5^C) \setminus (\{b_{2,0}\} \cap \{b_1\})$	$\mathbb{P}_0^1 \rightarrow \mathbb{P}_{0A}^1 + \mathbb{P}_{0B}^1, \mathbb{P}_2^1 \rightarrow \mathbb{P}_{2B}^1 + \mathbb{P}_{2C}^1$
$\mathbf{3}_4^C \overline{\mathbf{3}}_5^C \mathbf{1}^{(2)}$	$(\mathbf{3}_4^C) \cap (\mathbf{3}_5^C) \setminus (\{d_{0,0}\} \cap \{b_1\})$	$\mathbb{P}_0^1 \rightarrow \mathbb{P}_{0A}^1 + \mathbb{P}_{0B}^1, \mathbb{P}_1^1 \rightarrow \mathbb{P}_{1B}^1 + \mathbb{P}_{1C}^1$
$\mathbf{3}_1^C \mathbf{3}_3^C \mathbf{3}_5^C$	$\{b_{2,0}\} \cap \{b_1\}$	$\mathbb{P}_0^1 \rightarrow \mathbb{P}_{0A}^1 + \mathbb{P}_{0B}^1, \mathbb{P}_2^1 \rightarrow \mathbb{P}_{2vB}^1 + \mathbb{P}_{2B'}^1 + \mathbb{P}_{2AC}^1$ $\mathbb{P}_{0A}^1 = \mathbb{P}_{2B'}^1$
$\mathbf{3}_2^C \mathbf{3}_3^C \mathbf{3}_4^C$	$\{c_{2,1}\} \cap \{b_1\}$	$\mathbb{P}_1^1 \rightarrow \mathbb{P}_{1uC}^1 + \mathbb{P}_{1C'}^1 + \mathbb{P}_{1AB}^1, \mathbb{P}_2^1 \rightarrow \mathbb{P}_{2B}^1 + \mathbb{P}_{2C}^1$ $\mathbb{P}_{1C'}^1 = \mathbb{P}_{2C}^1$
$\mathbf{3}_4^C \mathbf{3}_5^C \mathbf{3}_5^C$	$\{d_{0,0}\} \cap \{b_1\}$	$\mathbb{P}_0^1 \rightarrow \mathbb{P}_{0B}^1 + \mathbb{P}_{0C'}^1 + \mathbb{P}_{0C1}^1, \mathbb{P}_1^1 \rightarrow \mathbb{P}_{1B}^1 + \mathbb{P}_{1C}^1$ $\mathbb{P}_{0C'}^1 = \mathbb{P}_{1C}^1$

**Table B.8:** Yukawa couplings in the  $SU(3)$ -C top.



# Appendix C

## Matching the MSSM-Spectrum

With the search criteria and algorithm presented in section 2.1, we find, for each of the toric  $SU(3) \times SU(2) \times U(1)_1 \times U(1)_2$  models described in section 1.4, a significant number of possibilities to match the geometric spectrum with matter states of the MSSM including right-handed neutrinos and  $\mu$ -singlets. The results are listed in the left column of the tables below, in the notation introduced in section 2.1. In the right column, we have listed which of the baryon and lepton number violating couplings (cf. (V.57) to (V.60)) are allowed by the  $U(1)$  selection rules, although – for space-saving reasons – in a slightly altered order. Furthermore we do not explicitly write down the states associated with  $H_u$ ,  $H_d$  and  $Q$  in each coupling that appears, as these states are fixed for each possible match. For example the  $\alpha$ -term comes from a coupling  $Q L d_R^c$ , where there can be, depending on the matching, several different states for  $L$  and  $d_R^c$ , while  $Q$  is given by the unique  $(\mathbf{3}, \mathbf{2})$ -state. In our table we list such an existing coupling as  $(\mathbf{2}, \mathbf{3})$ , where the  $\mathbf{2}$ -state is the lepton  $L$  and  $\mathbf{3}$  the down-quark, i.e. the states appear in the same order as in the corresponding term in equations (V.57) – (V.60). When there is no  $Q$  and  $H$  involved in a coupling we give all the states involved, again in the order as they appear in the corresponding term; e.g. for the  $\beta$ -term  $u_R^c u_R^c d_R^c$  the corresponding entry in the table looks like  $\mathbf{3}_i \mathbf{3}_j \mathbf{3}_k$ , with the first up-quark involved being the state  $\mathbf{3}_i$ , the second one being  $\mathbf{3}_j$ , and the down-quark being  $\mathbf{3}_k$ . Note that we have summarised all possible terms of  $W_{\text{singlet}}$  (V.58) in the entry  $\delta$ . Another special entry is the  $\lambda_3$ -term in (V.59) of the form  $Q Q Q H_d$ ; since there is no ambiguity in this term from the matching of the states, we simply list whether the coupling is allowed by the selection rules ( $\checkmark$ ) or not ( $-$ ).

We need to point out one case where the search algorithm does not completely fix the identification of the states with the MSSM fields. This happens when the choice of the Higgs states  $H_{u/d}$  together with the charges of  $Q = (\mathbf{3}, \mathbf{2})$  does not completely fix the coefficients  $a$  and  $b$  of the hypercharge in terms of  $U(1)_{1/2}$ . In fact this is the case whenever there is a linear combination of  $U(1)_{1/2}$  under which  $Q$  and  $H_{u/d}$  are all uncharged, which is the orthogonal linear combination to  $U(1)_Y$ . In such a case there might be some other states that are also uncharged under this particular  $U(1)$  charge combination and can be identified with some Standard Model states. As these states are uncharged under the orthogonal  $U(1)$ , they are not subject to any selection rules, so that the dimension-four and -five operators in (V.57) – (V.60) will be present if all states involved are present. In this case there may be more possibilities to match the spectrum, which we do not work out explicitly here. For every top combination (except for III  $\times$  B, where there is no such case) we have listed the corresponding case at the end of the tables below. In the I  $\times$  A-model for example, this happens when  $H_u = \mathbf{2}_1^I$ ,  $H_d = \overline{\mathbf{2}}_1^I$ , and any assignment  $U(1)_Y = (2b + 1)U(1)_1 + bU(1)_2$  for arbitrary  $b$  gives the correct hypercharge for the Higgs and the left-handed quarks, because they are uncharged under the linear combination  $2U(1)_1 + U(1)_2$ . To match states charged under this  $U(1)$  one needs to specify the value of  $b$ . It would be interesting to see if, after Higgsing the particular linear combination of  $U(1)_{1/2}$  under which  $H_{u/d}$

and  $Q$  are uncharged, the geometric spectrum can be embedded into the most general F-theory compactification with only one abelian factor [56].

Finally, recall from section 1.4 that the top-combination  $\text{III} \times \text{B}$  generically suffers from a non-Kodaira point, which, at least as far as our current understanding of F-theory is concerned, must be absent in order for the fibration to describe a well-defined vacuum.

**Table C.1:** Possible matches for  $\text{I} \times \text{A}$

<i>Matter spectrum</i>	<i>Baryon- and Lepton number violation</i>
<p><i>possibility no. 1</i></p> <p><math>a = 0, b = -\frac{1}{2}; (H_u, H_d) = (\mathbf{2}_1^{\text{I}}, \mathbf{2}_2^{\text{I}})</math></p> <p>heavy <math>(u_R^c, d_R^c): (-, \overline{\mathbf{3}}_4^{\text{A}})</math></p> <p>light <math>u_R^c: \overline{\mathbf{3}}_2^{\text{A}}; \text{light } d_R^c: \overline{\mathbf{3}}_3^{\text{A}}</math></p> <p>heavy generations of <math>(L, \nu_R^c, e_R^c):</math>  <math>(\overline{\mathbf{2}}_1^{\text{I}}, -, \overline{\mathbf{1}}^{(5)}), (\mathbf{2}_2^{\text{I}}, \overline{\mathbf{1}}^{(2)}, \overline{\mathbf{1}}^{(3)})</math></p> <p>light <math>\nu_R^c: \mathbf{1}^{(2)}; \text{light } e_R^c: -</math></p> <p><math>\mathbf{1}_\mu: \overline{\mathbf{1}}^{(2)}</math></p>	<p><math>\alpha: (\overline{\mathbf{2}}_1^{\text{I}}, \overline{\mathbf{3}}_3^{\text{A}}), (\mathbf{2}_2^{\text{I}}, \overline{\mathbf{3}}_4^{\text{A}}); \beta: \overline{\mathbf{3}}_2^{\text{A}} \overline{\mathbf{3}}_4^{\text{A}} \overline{\mathbf{3}}_3^{\text{A}}; \delta: -;</math></p> <p><math>\gamma: \overline{\mathbf{2}}_1^{\text{I}} \mathbf{2}_2^{\text{I}} \overline{\mathbf{1}}^{(5)}, \mathbf{2}_2^{\text{I}} \mathbf{2}_2^{\text{I}} \overline{\mathbf{1}}^{(3)};</math></p> <p><math>\lambda_1: \mathbf{2}_1^{\text{I}}; \lambda_3: -; \lambda_6: -; \lambda_8: \overline{\mathbf{1}}^{(5)}; \lambda_{10}: (\overline{\mathbf{3}}_3^{\text{A}})^*;</math></p> <p><math>\lambda_4: (\overline{\mathbf{3}}_2^{\text{A}}, \overline{\mathbf{1}}^{(3)}); \lambda_5: (\overline{\mathbf{2}}_1^{\text{I}}, \overline{\mathbf{2}}_1^{\text{I}});</math></p> <p><math>\lambda_9: (\overline{\mathbf{3}}_2^{\text{A}}, (\mathbf{2}_2^{\text{I}})^*);</math></p> <p><math>\lambda_7: \overline{\mathbf{3}}_2^{\text{A}} (\overline{\mathbf{3}}_4^{\text{A}})^* \overline{\mathbf{1}}^{(3)}, \overline{\mathbf{3}}_2^{\text{A}} (\overline{\mathbf{3}}_3^{\text{A}})^* \overline{\mathbf{1}}^{(5)};</math></p> <p><math>\lambda_2: \overline{\mathbf{3}}_2^{\text{A}} \overline{\mathbf{3}}_2^{\text{A}} \overline{\mathbf{3}}_4^{\text{A}} \overline{\mathbf{1}}^{(5)}, \overline{\mathbf{3}}_2^{\text{A}} \overline{\mathbf{3}}_2^{\text{A}} \overline{\mathbf{3}}_3^{\text{A}} \overline{\mathbf{1}}^{(3)}</math></p>
<p><i>possibility no. 2</i></p> <p><math>a = 1, b = 0; (H_u, H_d) = (\mathbf{2}_1^{\text{I}}, \overline{\mathbf{2}}_2^{\text{I}})</math></p> <p>heavy <math>(u_R^c, d_R^c): (-, \overline{\mathbf{3}}_2^{\text{A}})</math></p> <p>light <math>u_R^c: \overline{\mathbf{3}}_1^{\text{A}}, \overline{\mathbf{3}}_4^{\text{A}}; \text{light } d_R^c: \overline{\mathbf{3}}_3^{\text{A}}, \overline{\mathbf{3}}_5^{\text{A}}</math></p> <p>heavy generations of <math>(L, \nu_R^c, e_R^c):</math>  <math>(\overline{\mathbf{2}}_1^{\text{I}}, -, \mathbf{1}^{(2)}), (\overline{\mathbf{2}}_2^{\text{I}}, \mathbf{1}^{(5)}, \mathbf{1}^{(3)}), (\overline{\mathbf{2}}_3^{\text{I}}, \mathbf{1}^{(6)}, \mathbf{1}^{(4)})</math></p> <p>light <math>\nu_R^c: \overline{\mathbf{1}}^{(5)}, \overline{\mathbf{1}}^{(6)}; \text{light } e_R^c: \mathbf{1}^{(1)}</math></p> <p><math>\mathbf{1}_\mu: \mathbf{1}^{(5)}</math></p>	<p><math>\alpha: (\overline{\mathbf{2}}_1^{\text{I}}, \overline{\mathbf{3}}_3^{\text{A}}), (\mathbf{2}_2^{\text{I}}, \overline{\mathbf{3}}_2^{\text{A}}), (\overline{\mathbf{2}}_3^{\text{I}}, \overline{\mathbf{3}}_5^{\text{A}}); \beta: \overline{\mathbf{3}}_1^{\text{A}} \overline{\mathbf{3}}_3^{\text{A}} \overline{\mathbf{3}}_5^{\text{A}},</math>  <math>\overline{\mathbf{3}}_4^{\text{A}} \overline{\mathbf{3}}_2^{\text{A}} \overline{\mathbf{3}}_3^{\text{A}}, \overline{\mathbf{3}}_4^{\text{A}} \overline{\mathbf{3}}_5^{\text{A}} \overline{\mathbf{3}}_5^{\text{A}}; \delta: \overline{\mathbf{1}}^{(5)} \mathbf{1}^{(6)} \mathbf{1}^{(6)}, \mathbf{1}^{(5)} \overline{\mathbf{1}}^{(6)} \overline{\mathbf{1}}^{(6)};</math></p> <p><math>\gamma: \overline{\mathbf{2}}_1^{\text{I}} \overline{\mathbf{2}}_2^{\text{I}} \mathbf{1}^{(2)}, \overline{\mathbf{2}}_1^{\text{I}} \overline{\mathbf{2}}_3^{\text{I}} \mathbf{1}^{(1)}, \overline{\mathbf{2}}_2^{\text{I}} \overline{\mathbf{2}}_2^{\text{I}} \mathbf{1}^{(3)}, \overline{\mathbf{2}}_2^{\text{I}} \overline{\mathbf{2}}_3^{\text{I}} \mathbf{1}^{(4)}, \overline{\mathbf{2}}_3^{\text{I}} \overline{\mathbf{2}}_3^{\text{I}} \mathbf{1}^{(2)};</math></p> <p><math>\lambda_1: \mathbf{2}_1^{\text{I}}; \lambda_3: -; \lambda_6: -; \lambda_8: \mathbf{1}^{(2)}; \lambda_{10}: (\overline{\mathbf{3}}_3^{\text{A}})^*;</math></p> <p><math>\lambda_4: (\overline{\mathbf{3}}_1^{\text{A}}, \mathbf{1}^{(4)}), (\overline{\mathbf{3}}_4^{\text{A}}, \mathbf{1}^{(3)}); \lambda_5: (\overline{\mathbf{2}}_1^{\text{I}}, \overline{\mathbf{2}}_1^{\text{I}});</math></p> <p><math>\lambda_9: (\overline{\mathbf{3}}_4^{\text{A}}, (\overline{\mathbf{2}}_2^{\text{I}})^*), (\overline{\mathbf{3}}_1^{\text{A}}, (\overline{\mathbf{2}}_3^{\text{I}})^*);</math></p> <p><math>\lambda_7: \overline{\mathbf{3}}_1^{\text{A}} (\overline{\mathbf{3}}_2^{\text{A}})^* \mathbf{1}^{(4)}, \overline{\mathbf{3}}_1^{\text{A}} (\overline{\mathbf{3}}_3^{\text{A}})^* \mathbf{1}^{(1)}, \overline{\mathbf{3}}_1^{\text{A}} (\overline{\mathbf{3}}_5^{\text{A}})^* \mathbf{1}^{(2)},</math>  <math>\overline{\mathbf{3}}_4^{\text{A}} (\overline{\mathbf{3}}_2^{\text{A}})^* \mathbf{1}^{(3)}, \overline{\mathbf{3}}_4^{\text{A}} (\overline{\mathbf{3}}_3^{\text{A}})^* \mathbf{1}^{(2)}, \overline{\mathbf{3}}_4^{\text{A}} (\overline{\mathbf{3}}_5^{\text{A}})^* \mathbf{1}^{(4)};</math></p> <p><math>\lambda_2: \overline{\mathbf{3}}_1^{\text{A}} \overline{\mathbf{3}}_1^{\text{A}} \overline{\mathbf{3}}_3^{\text{A}} \mathbf{1}^{(2)}, \overline{\mathbf{3}}_1^{\text{A}} \overline{\mathbf{3}}_1^{\text{A}} \overline{\mathbf{3}}_5^{\text{A}} \mathbf{1}^{(1)}, \overline{\mathbf{3}}_1^{\text{A}} \overline{\mathbf{3}}_4^{\text{A}} \overline{\mathbf{3}}_2^{\text{A}} \mathbf{1}^{(1)},</math>  <math>\overline{\mathbf{3}}_1^{\text{A}} \overline{\mathbf{3}}_4^{\text{A}} \overline{\mathbf{3}}_3^{\text{A}} \mathbf{1}^{(4)}, \overline{\mathbf{3}}_1^{\text{A}} \overline{\mathbf{3}}_4^{\text{A}} \overline{\mathbf{3}}_5^{\text{A}} \mathbf{1}^{(2)}, \overline{\mathbf{3}}_4^{\text{A}} \overline{\mathbf{3}}_4^{\text{A}} \overline{\mathbf{3}}_2^{\text{A}} \mathbf{1}^{(2)},</math>  <math>\overline{\mathbf{3}}_4^{\text{A}} \overline{\mathbf{3}}_4^{\text{A}} \overline{\mathbf{3}}_3^{\text{A}} \mathbf{1}^{(3)}, \overline{\mathbf{3}}_4^{\text{A}} \overline{\mathbf{3}}_4^{\text{A}} \overline{\mathbf{3}}_5^{\text{A}} \mathbf{1}^{(4)}</math></p>
<p><i>possibility no. 3</i></p> <p><math>a = -1, b = -1; (H_u, H_d) = (\mathbf{2}_1^{\text{I}}, \mathbf{2}_3^{\text{I}})</math></p> <p>heavy <math>(u_R^c, d_R^c): (-, \overline{\mathbf{3}}_1^{\text{A}})</math></p> <p>light <math>u_R^c: \overline{\mathbf{3}}_5^{\text{A}}; \text{light } d_R^c: \overline{\mathbf{3}}_3^{\text{A}}</math></p> <p>heavy generations of <math>(L, \nu_R^c, e_R^c):</math>  <math>(\overline{\mathbf{2}}_1^{\text{I}}, -, \overline{\mathbf{1}}^{(6)}), (\mathbf{2}_3^{\text{I}}, \overline{\mathbf{1}}^{(1)}, \overline{\mathbf{1}}^{(2)})</math></p> <p>light <math>\nu_R^c: \mathbf{1}^{(1)}; \text{light } e_R^c: -</math></p> <p><math>\mathbf{1}_\mu: \overline{\mathbf{1}}^{(1)}</math></p>	<p><math>\alpha: (\overline{\mathbf{2}}_1^{\text{I}}, \overline{\mathbf{3}}_3^{\text{A}}), (\mathbf{2}_3^{\text{I}}, \overline{\mathbf{3}}_1^{\text{A}}); \beta: \overline{\mathbf{3}}_5^{\text{A}} \overline{\mathbf{3}}_1^{\text{A}} \overline{\mathbf{3}}_3^{\text{A}}; \delta: -;</math></p> <p><math>\gamma: \overline{\mathbf{2}}_1^{\text{I}} \mathbf{2}_3^{\text{I}} \overline{\mathbf{1}}^{(6)}, \mathbf{2}_3^{\text{I}} \mathbf{2}_3^{\text{I}} \overline{\mathbf{1}}^{(2)};</math></p> <p><math>\lambda_1: \mathbf{2}_1^{\text{I}}; \lambda_3: -; \lambda_6: -; \lambda_8: \overline{\mathbf{1}}^{(6)}; \lambda_{10}: (\overline{\mathbf{3}}_3^{\text{A}})^*;</math></p> <p><math>\lambda_4: (\overline{\mathbf{3}}_5^{\text{A}}, \overline{\mathbf{1}}^{(2)}); \lambda_5: (\overline{\mathbf{2}}_1^{\text{I}}, \overline{\mathbf{2}}_1^{\text{I}});</math></p> <p><math>\lambda_9: (\overline{\mathbf{3}}_5^{\text{A}}, (\mathbf{2}_3^{\text{I}})^*);</math></p> <p><math>\lambda_7: \overline{\mathbf{3}}_5^{\text{A}} (\overline{\mathbf{3}}_1^{\text{A}})^* \overline{\mathbf{1}}^{(2)}, \overline{\mathbf{3}}_5^{\text{A}} (\overline{\mathbf{3}}_3^{\text{A}})^* \overline{\mathbf{1}}^{(6)};</math></p> <p><math>\lambda_2: \overline{\mathbf{3}}_5^{\text{A}} \overline{\mathbf{3}}_5^{\text{A}} \overline{\mathbf{3}}_1^{\text{A}} \overline{\mathbf{1}}^{(6)}, \overline{\mathbf{3}}_5^{\text{A}} \overline{\mathbf{3}}_5^{\text{A}} \overline{\mathbf{3}}_3^{\text{A}} \overline{\mathbf{1}}^{(2)}</math></p>
<p><i>possibility no. 4</i></p> <p><math>a = 1, b = 0; (H_u, H_d) = (\mathbf{2}_1^{\text{I}}, \overline{\mathbf{2}}_3^{\text{I}})</math></p> <p>heavy <math>(u_R^c, d_R^c): (-, \overline{\mathbf{3}}_5^{\text{A}})</math></p> <p>light <math>u_R^c: \overline{\mathbf{3}}_1^{\text{A}}, \overline{\mathbf{3}}_4^{\text{A}}; \text{light } d_R^c: \overline{\mathbf{3}}_2^{\text{A}}, \overline{\mathbf{3}}_3^{\text{A}}</math></p> <p>heavy generations of <math>(L, \nu_R^c, e_R^c):</math>  <math>(\overline{\mathbf{2}}_1^{\text{I}}, -, \mathbf{1}^{(1)}), (\overline{\mathbf{2}}_2^{\text{I}}, \mathbf{1}^{(5)}, \mathbf{1}^{(4)}), (\overline{\mathbf{2}}_3^{\text{I}}, \mathbf{1}^{(6)}, \mathbf{1}^{(2)})</math></p> <p>light <math>\nu_R^c: \overline{\mathbf{1}}^{(5)}, \overline{\mathbf{1}}^{(6)}; \text{light } e_R^c: \mathbf{1}^{(3)}</math></p> <p><math>\mathbf{1}_\mu: \mathbf{1}^{(6)}</math></p>	<p><math>\alpha: (\overline{\mathbf{2}}_1^{\text{I}}, \overline{\mathbf{3}}_3^{\text{A}}), (\mathbf{2}_2^{\text{I}}, \overline{\mathbf{3}}_2^{\text{A}}), (\overline{\mathbf{2}}_3^{\text{I}}, \overline{\mathbf{3}}_5^{\text{A}}); \beta: \overline{\mathbf{3}}_1^{\text{A}} \overline{\mathbf{3}}_5^{\text{A}} \overline{\mathbf{3}}_3^{\text{A}},</math>  <math>\overline{\mathbf{3}}_4^{\text{A}} \overline{\mathbf{3}}_5^{\text{A}} \overline{\mathbf{3}}_5^{\text{A}}, \overline{\mathbf{3}}_4^{\text{A}} \overline{\mathbf{3}}_2^{\text{A}} \overline{\mathbf{3}}_3^{\text{A}}; \delta: \overline{\mathbf{1}}^{(5)} \mathbf{1}^{(6)} \mathbf{1}^{(6)}, \mathbf{1}^{(5)} \overline{\mathbf{1}}^{(6)} \overline{\mathbf{1}}^{(6)};</math></p> <p><math>\gamma: \overline{\mathbf{2}}_1^{\text{I}} \overline{\mathbf{2}}_2^{\text{I}} \mathbf{1}^{(2)}, \overline{\mathbf{2}}_1^{\text{I}} \overline{\mathbf{2}}_3^{\text{I}} \mathbf{1}^{(1)}, \overline{\mathbf{2}}_2^{\text{I}} \overline{\mathbf{2}}_2^{\text{I}} \mathbf{1}^{(3)}, \overline{\mathbf{2}}_2^{\text{I}} \overline{\mathbf{2}}_3^{\text{I}} \mathbf{1}^{(4)}, \overline{\mathbf{2}}_3^{\text{I}} \overline{\mathbf{2}}_3^{\text{I}} \mathbf{1}^{(2)};</math></p> <p><math>\lambda_1: \mathbf{2}_1^{\text{I}}; \lambda_3: -; \lambda_6: -; \lambda_8: \mathbf{1}^{(1)}; \lambda_{10}: (\overline{\mathbf{3}}_3^{\text{A}})^*;</math></p> <p><math>\lambda_4: (\overline{\mathbf{3}}_1^{\text{A}}, \mathbf{1}^{(2)}), (\overline{\mathbf{3}}_4^{\text{A}}, \mathbf{1}^{(4)}); \lambda_5: (\overline{\mathbf{2}}_1^{\text{I}}, \overline{\mathbf{2}}_1^{\text{I}});</math></p> <p><math>\lambda_9: (\overline{\mathbf{3}}_4^{\text{A}}, (\overline{\mathbf{2}}_2^{\text{I}})^*), (\overline{\mathbf{3}}_1^{\text{A}}, (\overline{\mathbf{2}}_3^{\text{I}})^*);</math></p> <p><math>\lambda_7: \overline{\mathbf{3}}_1^{\text{A}} (\overline{\mathbf{3}}_5^{\text{A}})^* \mathbf{1}^{(2)}, \overline{\mathbf{3}}_1^{\text{A}} (\overline{\mathbf{3}}_2^{\text{A}})^* \mathbf{1}^{(4)}, \overline{\mathbf{3}}_1^{\text{A}} (\overline{\mathbf{3}}_3^{\text{A}})^* \mathbf{1}^{(1)},</math>  <math>\overline{\mathbf{3}}_4^{\text{A}} (\overline{\mathbf{3}}_5^{\text{A}})^* \mathbf{1}^{(4)}, \overline{\mathbf{3}}_4^{\text{A}} (\overline{\mathbf{3}}_2^{\text{A}})^* \mathbf{1}^{(3)}, \overline{\mathbf{3}}_4^{\text{A}} (\overline{\mathbf{3}}_3^{\text{A}})^* \mathbf{1}^{(2)};</math></p> <p><math>\lambda_2: \overline{\mathbf{3}}_1^{\text{A}} \overline{\mathbf{3}}_1^{\text{A}} \overline{\mathbf{3}}_5^{\text{A}} \mathbf{1}^{(1)}, \overline{\mathbf{3}}_1^{\text{A}} \overline{\mathbf{3}}_1^{\text{A}} \overline{\mathbf{3}}_3^{\text{A}} \mathbf{1}^{(2)}, \overline{\mathbf{3}}_1^{\text{A}} \overline{\mathbf{3}}_4^{\text{A}} \overline{\mathbf{3}}_5^{\text{A}} \mathbf{1}^{(2)},</math>  <math>\overline{\mathbf{3}}_1^{\text{A}} \overline{\mathbf{3}}_4^{\text{A}} \overline{\mathbf{3}}_2^{\text{A}} \mathbf{1}^{(1)}, \overline{\mathbf{3}}_1^{\text{A}} \overline{\mathbf{3}}_4^{\text{A}} \overline{\mathbf{3}}_3^{\text{A}} \mathbf{1}^{(4)}, \overline{\mathbf{3}}_4^{\text{A}} \overline{\mathbf{3}}_4^{\text{A}} \overline{\mathbf{3}}_5^{\text{A}} \mathbf{1}^{(4)},</math>  <math>\overline{\mathbf{3}}_4^{\text{A}} \overline{\mathbf{3}}_4^{\text{A}} \overline{\mathbf{3}}_2^{\text{A}} \mathbf{1}^{(2)}, \overline{\mathbf{3}}_4^{\text{A}} \overline{\mathbf{3}}_4^{\text{A}} \overline{\mathbf{3}}_3^{\text{A}} \mathbf{1}^{(3)}</math></p>

Continued on next page

Table C.1, Possible matches for  $\mathbf{I} \times \mathbf{A}$  – continued from previous page

Matter spectrum	Baryon- and Lepton number violation
<p>possibility no. 5</p> <p><math>a = 1, b = 0; (H_u, H_d) = (\mathbf{2}_1^I, \mathbf{2}_1^I)</math></p> <p>heavy <math>(u_R^c, d_R^c): (\mathbf{3}_4^A, \mathbf{3}_3^A)</math></p> <p>light <math>u_R^c: \mathbf{3}_1^A</math>; light <math>d_R^c: \mathbf{3}_2^A, \mathbf{3}_5^A</math></p> <p>heavy generations of <math>(L, \nu_R^c, e_R^c):</math>  <math>(\mathbf{2}_1^I, \mathbf{1}^{(5)}, -), (\mathbf{2}_2^I, -, \mathbf{1}^{(2)}), (\mathbf{2}_3^I, \mathbf{1}^{(6)}, \mathbf{1}^{(1)})</math></p> <p>light <math>\nu_R^c: \mathbf{1}^{(5)}, \mathbf{1}^{(6)}</math>; light <math>e_R^c: \mathbf{1}^{(3)}, \mathbf{1}^{(4)}</math></p> <p><math>\mathbf{1}_\mu: \mathbf{1}^{(5)}</math></p>	<p><math>\alpha: (\mathbf{2}_1^I, \mathbf{3}_3^A), (\mathbf{2}_2^I, \mathbf{3}_2^A), (\mathbf{2}_3^I, \mathbf{3}_5^A); \beta: \mathbf{3}_4^A \mathbf{3}_3^A \mathbf{3}_2^A,</math>  <math>\mathbf{3}_4^A \mathbf{3}_5^A \mathbf{3}_5^A, \mathbf{3}_1^A \mathbf{3}_3^A \mathbf{3}_5^A; \delta: \mathbf{1}^{(5)} \mathbf{1}^{(6)} \mathbf{1}^{(6)}, \mathbf{1}^{(5)} \mathbf{1}^{(6)} \mathbf{1}^{(6)};</math></p> <p><math>\gamma: \mathbf{2}_1^I \mathbf{2}_2^I \mathbf{1}^{(2)}, \mathbf{2}_1^I \mathbf{2}_3^I \mathbf{1}^{(1)}, \mathbf{2}_2^I \mathbf{2}_2^I \mathbf{1}^{(3)}, \mathbf{2}_2^I \mathbf{2}_3^I \mathbf{1}^{(4)}, \mathbf{2}_3^I \mathbf{2}_3^I \mathbf{1}^{(2)};</math></p> <p><math>\lambda_1: \mathbf{2}_1^I; \lambda_3: \checkmark; \lambda_6: -; \lambda_8: \mathbf{1}^{(2)}; \lambda_{10}: (\mathbf{3}_3^A)^*;</math></p> <p><math>\lambda_4: (\mathbf{3}_4^A, \mathbf{1}^{(2)}), (\mathbf{3}_1^A, \mathbf{1}^{(1)}); \lambda_5: (\mathbf{2}_2^I, \mathbf{2}_2^I);</math></p> <p><math>\lambda_9: (\mathbf{3}_4^A, (\mathbf{2}_2^I)^*), (\mathbf{3}_1^A, (\mathbf{2}_3^I)^*);</math></p> <p><math>\lambda_7: \mathbf{3}_4^A (\mathbf{3}_3^A)^* \mathbf{1}^{(2)}, \mathbf{3}_4^A (\mathbf{3}_2^A)^* \mathbf{1}^{(3)}, \mathbf{3}_4^A (\mathbf{3}_5^A)^* \mathbf{1}^{(4)},</math>  <math>\mathbf{3}_1^A (\mathbf{3}_3^A)^* \mathbf{1}^{(1)}, \mathbf{3}_1^A (\mathbf{3}_2^A)^* \mathbf{1}^{(4)}, \mathbf{3}_1^A (\mathbf{3}_5^A)^* \mathbf{1}^{(2)};</math></p> <p><math>\lambda_2: \mathbf{3}_4^A \mathbf{3}_4^A \mathbf{3}_3^A \mathbf{1}^{(3)}, \mathbf{3}_4^A \mathbf{3}_4^A \mathbf{3}_2^A \mathbf{1}^{(2)}, \mathbf{3}_4^A \mathbf{3}_4^A \mathbf{3}_5^A \mathbf{1}^{(4)},</math>  <math>\mathbf{3}_4^A \mathbf{3}_1^A \mathbf{3}_3^A \mathbf{1}^{(4)}, \mathbf{3}_4^A \mathbf{3}_1^A \mathbf{3}_2^A \mathbf{1}^{(1)}, \mathbf{3}_4^A \mathbf{3}_1^A \mathbf{3}_5^A \mathbf{1}^{(2)},</math>  <math>\mathbf{3}_1^A \mathbf{3}_1^A \mathbf{3}_3^A \mathbf{1}^{(2)}, \mathbf{3}_1^A \mathbf{3}_1^A \mathbf{3}_5^A \mathbf{1}^{(1)}</math></p>
<p>possibility no. 6</p> <p><math>a = 1, b = 0; (H_u, H_d) = (\mathbf{2}_1^I, \mathbf{2}_2^I)</math></p> <p>heavy <math>(u_R^c, d_R^c): (\mathbf{3}_4^A, \mathbf{3}_2^A)</math></p> <p>light <math>u_R^c: \mathbf{3}_1^A</math>; light <math>d_R^c: \mathbf{3}_3^A, \mathbf{3}_5^A</math></p> <p>heavy generations of <math>(L, \nu_R^c, e_R^c):</math>  <math>(\mathbf{2}_1^I, \mathbf{1}^{(5)}, \mathbf{1}^{(2)}), (\mathbf{2}_2^I, -, \mathbf{1}^{(3)}), (\mathbf{2}_3^I, \mathbf{1}^{(6)}, \mathbf{1}^{(4)})</math></p> <p>light <math>\nu_R^c: \mathbf{1}^{(5)}, \mathbf{1}^{(6)}</math>; light <math>e_R^c: \mathbf{1}^{(1)}</math></p> <p><math>\mathbf{1}_\mu: -</math></p>	<p><math>\alpha: (\mathbf{2}_1^I, \mathbf{3}_3^A), (\mathbf{2}_2^I, \mathbf{3}_2^A), (\mathbf{2}_3^I, \mathbf{3}_5^A); \beta: \mathbf{3}_4^A \mathbf{3}_2^A \mathbf{3}_3^A,</math>  <math>\mathbf{3}_4^A \mathbf{3}_5^A \mathbf{3}_5^A, \mathbf{3}_1^A \mathbf{3}_3^A \mathbf{3}_5^A; \delta: \mathbf{1}^{(5)} \mathbf{1}^{(6)} \mathbf{1}^{(6)}, \mathbf{1}^{(5)} \mathbf{1}^{(6)} \mathbf{1}^{(6)};</math></p> <p><math>\gamma: \mathbf{2}_1^I \mathbf{2}_2^I \mathbf{1}^{(2)}, \mathbf{2}_1^I \mathbf{2}_3^I \mathbf{1}^{(1)}, \mathbf{2}_2^I \mathbf{2}_2^I \mathbf{1}^{(3)}, \mathbf{2}_2^I \mathbf{2}_3^I \mathbf{1}^{(4)}, \mathbf{2}_3^I \mathbf{2}_3^I \mathbf{1}^{(2)};</math></p> <p><math>\lambda_1: \mathbf{2}_1^I; \lambda_3: -; \lambda_6: \mathbf{2}_1^I; \lambda_8: \mathbf{1}^{(3)}; \lambda_{10}: (\mathbf{3}_3^A)^*;</math></p> <p><math>\lambda_4: (\mathbf{3}_4^A, \mathbf{1}^{(3)}), (\mathbf{3}_1^A, \mathbf{1}^{(4)}); \lambda_5: (\mathbf{2}_2^I, \mathbf{2}_2^I);</math></p> <p><math>\lambda_9: (\mathbf{3}_4^A, (\mathbf{2}_2^I)^*), (\mathbf{3}_1^A, (\mathbf{2}_3^I)^*);</math></p> <p><math>\lambda_7: \mathbf{3}_4^A (\mathbf{3}_2^A)^* \mathbf{1}^{(3)}, \mathbf{3}_4^A (\mathbf{3}_3^A)^* \mathbf{1}^{(2)}, \mathbf{3}_4^A (\mathbf{3}_5^A)^* \mathbf{1}^{(4)},</math>  <math>\mathbf{3}_1^A (\mathbf{3}_2^A)^* \mathbf{1}^{(4)}, \mathbf{3}_1^A (\mathbf{3}_3^A)^* \mathbf{1}^{(1)}, \mathbf{3}_1^A (\mathbf{3}_5^A)^* \mathbf{1}^{(2)};</math></p> <p><math>\lambda_2: \mathbf{3}_4^A \mathbf{3}_4^A \mathbf{3}_2^A \mathbf{1}^{(2)}, \mathbf{3}_4^A \mathbf{3}_4^A \mathbf{3}_3^A \mathbf{1}^{(3)}, \mathbf{3}_4^A \mathbf{3}_4^A \mathbf{3}_5^A \mathbf{1}^{(4)},</math>  <math>\mathbf{3}_4^A \mathbf{3}_1^A \mathbf{3}_2^A \mathbf{1}^{(1)}, \mathbf{3}_4^A \mathbf{3}_1^A \mathbf{3}_3^A \mathbf{1}^{(4)}, \mathbf{3}_4^A \mathbf{3}_1^A \mathbf{3}_5^A \mathbf{1}^{(2)},</math>  <math>\mathbf{3}_1^A \mathbf{3}_1^A \mathbf{3}_3^A \mathbf{1}^{(2)}, \mathbf{3}_1^A \mathbf{3}_1^A \mathbf{3}_5^A \mathbf{1}^{(1)}</math></p>
<p>possibility no. 7</p> <p><math>a = 1, b = 0; (H_u, H_d) = (\mathbf{2}_1^I, \mathbf{2}_3^I)</math></p> <p>heavy <math>(u_R^c, d_R^c): (\mathbf{3}_4^A, \mathbf{3}_5^A)</math></p> <p>light <math>u_R^c: \mathbf{3}_1^A</math>; light <math>d_R^c: \mathbf{3}_2^A, \mathbf{3}_3^A</math></p> <p>heavy generations of <math>(L, \nu_R^c, e_R^c):</math>  <math>(\mathbf{2}_1^I, \mathbf{1}^{(5)}, \mathbf{1}^{(1)}), (\mathbf{2}_2^I, -, \mathbf{1}^{(4)}), (\mathbf{2}_3^I, \mathbf{1}^{(6)}, \mathbf{1}^{(2)})</math></p> <p>light <math>\nu_R^c: \mathbf{1}^{(5)}, \mathbf{1}^{(6)}</math>; light <math>e_R^c: \mathbf{1}^{(3)}</math></p> <p><math>\mathbf{1}_\mu: \mathbf{1}^{(6)}</math></p>	<p><math>\alpha: (\mathbf{2}_1^I, \mathbf{3}_3^A), (\mathbf{2}_2^I, \mathbf{3}_2^A), (\mathbf{2}_3^I, \mathbf{3}_5^A); \beta: \mathbf{3}_4^A \mathbf{3}_5^A \mathbf{3}_3^A,</math>  <math>\mathbf{3}_4^A \mathbf{3}_2^A \mathbf{3}_3^A, \mathbf{3}_1^A \mathbf{3}_5^A \mathbf{3}_3^A; \delta: \mathbf{1}^{(5)} \mathbf{1}^{(6)} \mathbf{1}^{(6)}, \mathbf{1}^{(5)} \mathbf{1}^{(6)} \mathbf{1}^{(6)};</math></p> <p><math>\gamma: \mathbf{2}_1^I \mathbf{2}_2^I \mathbf{1}^{(2)}, \mathbf{2}_1^I \mathbf{2}_3^I \mathbf{1}^{(1)}, \mathbf{2}_2^I \mathbf{2}_2^I \mathbf{1}^{(3)}, \mathbf{2}_2^I \mathbf{2}_3^I \mathbf{1}^{(4)}, \mathbf{2}_3^I \mathbf{2}_3^I \mathbf{1}^{(2)};</math></p> <p><math>\lambda_1: \mathbf{2}_1^I; \lambda_3: -; \lambda_6: -; \lambda_8: \mathbf{1}^{(4)}; \lambda_{10}: (\mathbf{3}_3^A)^*;</math></p> <p><math>\lambda_4: (\mathbf{3}_4^A, \mathbf{1}^{(4)}), (\mathbf{3}_1^A, \mathbf{1}^{(2)}); \lambda_5: (\mathbf{2}_2^I, \mathbf{2}_2^I);</math></p> <p><math>\lambda_9: (\mathbf{3}_4^A, (\mathbf{2}_2^I)^*), (\mathbf{3}_1^A, (\mathbf{2}_3^I)^*);</math></p> <p><math>\lambda_7: \mathbf{3}_4^A (\mathbf{3}_5^A)^* \mathbf{1}^{(4)}, \mathbf{3}_4^A (\mathbf{3}_2^A)^* \mathbf{1}^{(3)}, \mathbf{3}_4^A (\mathbf{3}_3^A)^* \mathbf{1}^{(2)},</math>  <math>\mathbf{3}_1^A (\mathbf{3}_5^A)^* \mathbf{1}^{(2)}, \mathbf{3}_1^A (\mathbf{3}_2^A)^* \mathbf{1}^{(4)}, \mathbf{3}_1^A (\mathbf{3}_3^A)^* \mathbf{1}^{(1)};</math></p> <p><math>\lambda_2: \mathbf{3}_4^A \mathbf{3}_4^A \mathbf{3}_5^A \mathbf{1}^{(4)}, \mathbf{3}_4^A \mathbf{3}_4^A \mathbf{3}_2^A \mathbf{1}^{(2)}, \mathbf{3}_4^A \mathbf{3}_4^A \mathbf{3}_3^A \mathbf{1}^{(3)},</math>  <math>\mathbf{3}_4^A \mathbf{3}_1^A \mathbf{3}_5^A \mathbf{1}^{(2)}, \mathbf{3}_4^A \mathbf{3}_1^A \mathbf{3}_2^A \mathbf{1}^{(1)}, \mathbf{3}_4^A \mathbf{3}_1^A \mathbf{3}_3^A \mathbf{1}^{(4)},</math>  <math>\mathbf{3}_1^A \mathbf{3}_1^A \mathbf{3}_5^A \mathbf{1}^{(1)}, \mathbf{3}_1^A \mathbf{3}_1^A \mathbf{3}_3^A \mathbf{1}^{(2)}</math></p>
<p>possibility no. 8</p> <p><math>a = 0, b = -\frac{1}{2}; (H_u, H_d) = (\mathbf{2}_2^I, \mathbf{2}_1^I)</math></p> <p>heavy <math>(u_R^c, d_R^c): (\mathbf{3}_2^A, \mathbf{3}_3^A)</math></p> <p>light <math>u_R^c: -</math>; light <math>d_R^c: \mathbf{3}_4^A</math></p> <p>heavy generations of <math>(L, \nu_R^c, e_R^c):</math>  <math>(\mathbf{2}_1^I, \mathbf{1}^{(2)}, -), (\mathbf{2}_2^I, -, \mathbf{1}^{(5)})</math></p> <p>light <math>\nu_R^c: \mathbf{1}^{(2)}</math>; light <math>e_R^c: \mathbf{1}^{(3)}</math></p> <p><math>\mathbf{1}_\mu: \mathbf{1}^{(2)}</math></p>	<p><math>\alpha: (\mathbf{2}_1^I, \mathbf{3}_3^A), (\mathbf{2}_2^I, \mathbf{3}_4^A); \beta: \mathbf{3}_2^A \mathbf{3}_3^A \mathbf{3}_4^A; \delta: -;</math></p> <p><math>\gamma: \mathbf{2}_1^I \mathbf{2}_2^I \mathbf{1}^{(5)}, \mathbf{2}_2^I \mathbf{2}_2^I \mathbf{1}^{(3)};</math></p> <p><math>\lambda_1: \mathbf{2}_1^I; \lambda_3: \checkmark; \lambda_6: -; \lambda_8: \mathbf{1}^{(5)}; \lambda_{10}: (\mathbf{3}_3^A)^*;</math></p> <p><math>\lambda_4: (\mathbf{3}_2^A, \mathbf{1}^{(5)}); \lambda_5: (\mathbf{2}_2^I, \mathbf{2}_2^I);</math></p> <p><math>\lambda_9: (\mathbf{3}_2^A, (\mathbf{2}_2^I)^*);</math></p> <p><math>\lambda_7: \mathbf{3}_2^A (\mathbf{3}_3^A)^* \mathbf{1}^{(5)}, \mathbf{3}_2^A (\mathbf{3}_4^A)^* \mathbf{1}^{(3)};</math></p> <p><math>\lambda_2: \mathbf{3}_2^A \mathbf{3}_2^A \mathbf{3}_3^A \mathbf{1}^{(3)}, \mathbf{3}_2^A \mathbf{3}_2^A \mathbf{3}_4^A \mathbf{1}^{(5)}</math></p>

Continued on next page



**Table C.1, Possible matches for  $I \times A$  – continued from previous page**

<i>Matter spectrum</i>	<i>Baryon- and Lepton number violation</i>
<p><i>possibility no. 13</i></p> <p><math>a = -1, b = -1; (H_u, H_d) = (\bar{\mathbf{2}}_3^I, \bar{\mathbf{2}}_1^I)</math></p> <p>heavy <math>(u_R^c, d_R^c): (\bar{\mathbf{3}}_5^A, \bar{\mathbf{3}}_3^A)</math></p> <p>light <math>u_R^c: -</math>; light <math>d_R^c: \bar{\mathbf{3}}_1^A</math></p> <p>heavy generations of <math>(L, \nu_R^c, e_R^c):</math>  <math>(\bar{\mathbf{2}}_1^I, \mathbf{1}^{(1)}, -), (\mathbf{2}_3^I, -, \bar{\mathbf{1}}^{(6)})</math></p> <p>light <math>\nu_R^c: \bar{\mathbf{1}}^{(1)}</math>; light <math>e_R^c: \bar{\mathbf{1}}^{(2)}</math></p> <p><math>\mathbf{1}_\mu: \mathbf{1}^{(1)}</math></p>	<p><math>\alpha: (\bar{\mathbf{2}}_1^I, \bar{\mathbf{3}}_3^A), (\mathbf{2}_3^I, \bar{\mathbf{3}}_1^A); \beta: \bar{\mathbf{3}}_5^A \bar{\mathbf{3}}_3^A \bar{\mathbf{3}}_1^A; \delta: -;</math></p> <p><math>\gamma: \bar{\mathbf{2}}_1^I \mathbf{2}_3^I \bar{\mathbf{1}}^{(6)}, \mathbf{2}_3^I \mathbf{2}_3^I \bar{\mathbf{1}}^{(2)};</math></p> <p><math>\lambda_1: \mathbf{2}_1^I; \lambda_3: \checkmark; \lambda_6: -; \lambda_8: \bar{\mathbf{1}}^{(6)}; \lambda_{10}: (\bar{\mathbf{3}}_3^A)^*;</math></p> <p><math>\lambda_4: (\bar{\mathbf{3}}_5^A, \bar{\mathbf{1}}^{(6)}); \lambda_5: (\mathbf{2}_3^I, \mathbf{2}_3^I);</math></p> <p><math>\lambda_9: (\bar{\mathbf{3}}_5^A, (\mathbf{2}_3^I)^*);</math></p> <p><math>\lambda_7: \bar{\mathbf{3}}_5^A (\bar{\mathbf{3}}_3^A)^* \bar{\mathbf{1}}^{(6)}, \bar{\mathbf{3}}_5^A (\bar{\mathbf{3}}_1^A)^* \bar{\mathbf{1}}^{(2)};</math></p> <p><math>\lambda_2: \bar{\mathbf{3}}_5^A \bar{\mathbf{3}}_5^A \bar{\mathbf{3}}_3^A \bar{\mathbf{1}}^{(2)}, \bar{\mathbf{3}}_5^A \bar{\mathbf{3}}_5^A \bar{\mathbf{3}}_1^A \bar{\mathbf{1}}^{(6)}</math></p>
<p><i>possibility no. 14</i></p> <p><math>a = -1, b = -1; (H_u, H_d) = (\bar{\mathbf{2}}_3^I, \mathbf{2}_3^I)</math></p> <p>heavy <math>(u_R^c, d_R^c): (\bar{\mathbf{3}}_5^A, \bar{\mathbf{3}}_1^A)</math></p> <p>light <math>u_R^c: -</math>; light <math>d_R^c: \bar{\mathbf{3}}_3^A</math></p> <p>heavy generations of <math>(L, \nu_R^c, e_R^c):</math>  <math>(\bar{\mathbf{2}}_1^I, \mathbf{1}^{(1)}, \bar{\mathbf{1}}^{(6)}), (\mathbf{2}_3^I, -, \bar{\mathbf{1}}^{(2)})</math></p> <p>light <math>\nu_R^c: \bar{\mathbf{1}}^{(1)}</math>; light <math>e_R^c: -</math></p> <p><math>\mathbf{1}_\mu: -</math></p>	<p><math>\alpha: (\bar{\mathbf{2}}_1^I, \bar{\mathbf{3}}_3^A), (\mathbf{2}_3^I, \bar{\mathbf{3}}_1^A); \beta: \bar{\mathbf{3}}_5^A \bar{\mathbf{3}}_1^A \bar{\mathbf{3}}_3^A; \delta: -;</math></p> <p><math>\gamma: \bar{\mathbf{2}}_1^I \mathbf{2}_3^I \bar{\mathbf{1}}^{(6)}, \mathbf{2}_3^I \mathbf{2}_3^I \bar{\mathbf{1}}^{(2)};</math></p> <p><math>\lambda_1: \mathbf{2}_1^I; \lambda_3: -; \lambda_6: \bar{\mathbf{2}}_1^I; \lambda_8: \bar{\mathbf{1}}^{(2)}; \lambda_{10}: (\bar{\mathbf{3}}_3^A)^*;</math></p> <p><math>\lambda_4: (\bar{\mathbf{3}}_5^A, \bar{\mathbf{1}}^{(2)}); \lambda_5: (\mathbf{2}_3^I, \mathbf{2}_3^I);</math></p> <p><math>\lambda_9: (\bar{\mathbf{3}}_5^A, (\mathbf{2}_3^I)^*);</math></p> <p><math>\lambda_7: \bar{\mathbf{3}}_5^A (\bar{\mathbf{3}}_1^A)^* \bar{\mathbf{1}}^{(2)}, \bar{\mathbf{3}}_5^A (\bar{\mathbf{3}}_3^A)^* \bar{\mathbf{1}}^{(6)};</math></p> <p><math>\lambda_2: \bar{\mathbf{3}}_5^A \bar{\mathbf{3}}_5^A \bar{\mathbf{3}}_1^A \bar{\mathbf{1}}^{(6)}, \bar{\mathbf{3}}_5^A \bar{\mathbf{3}}_5^A \bar{\mathbf{3}}_3^A \bar{\mathbf{1}}^{(2)}</math></p>
<p><i>Incomplete match</i></p> <p><math>a = 2b + 1; (H_u, H_d) = (\mathbf{2}_1^I, \bar{\mathbf{2}}_1^I)</math></p> <p>heavy <math>d_R^c: \bar{\mathbf{3}}_3^A</math></p> <p><math>\mathbf{1}_\mu: -</math></p> <p>other states depend on value of <math>b</math></p>	<p><math>\lambda_3: \checkmark, \lambda_{10}: \checkmark</math></p> <p>other couplings depend on value of <math>b</math></p>

**Table C.2: Possible matches for  $I \times B$** 

<i>Matter spectrum</i>	<i>Baryon- and Lepton number violation</i>
<p><i>possibility no. 1</i></p> <p><math>a = 0, b = -\frac{1}{2}; (H_u, H_d) = (\mathbf{2}_1^I, \bar{\mathbf{2}}_1^I)</math></p> <p>heavy <math>(u_R^c, d_R^c): (-, \bar{\mathbf{3}}_2^B)</math></p> <p>light <math>u_R^c: \bar{\mathbf{3}}_1^B</math>; light <math>d_R^c: \bar{\mathbf{3}}_4^B</math></p> <p>heavy generations of <math>(L, \nu_R^c, e_R^c):</math>  <math>(\bar{\mathbf{2}}_1^I, -, -), (\mathbf{2}_2^I, \bar{\mathbf{1}}^{(2)}, \bar{\mathbf{1}}^{(5)})</math></p> <p>light <math>\nu_R^c: \mathbf{1}^{(2)}</math>; light <math>e_R^c: \bar{\mathbf{1}}^{(3)}</math></p> <p><math>\mathbf{1}_\mu: -</math></p>	<p><math>\alpha: (\bar{\mathbf{2}}_1^I, \bar{\mathbf{3}}_2^B), (\mathbf{2}_2^I, \bar{\mathbf{3}}_4^B); \beta: \bar{\mathbf{3}}_1^B \bar{\mathbf{3}}_4^B \bar{\mathbf{3}}_2^B; \delta: -;</math></p> <p><math>\gamma: \bar{\mathbf{2}}_1^I \mathbf{2}_2^I \bar{\mathbf{1}}^{(5)}, \mathbf{2}_2^I \mathbf{2}_2^I \bar{\mathbf{1}}^{(3)};</math></p> <p><math>\lambda_1: \bar{\mathbf{2}}_1^I; \lambda_3: -; \lambda_6: \mathbf{2}_1^I; \lambda_8: -; \lambda_{10}: (\bar{\mathbf{3}}_4^B)^*;</math></p> <p><math>\lambda_4: (\bar{\mathbf{3}}_1^B, \bar{\mathbf{1}}^{(5)}); \lambda_5: (\bar{\mathbf{2}}_1^I, \bar{\mathbf{2}}_1^I);</math></p> <p><math>\lambda_9: (\bar{\mathbf{3}}_1^B, (\mathbf{2}_2^I)^*);</math></p> <p><math>\lambda_7: \bar{\mathbf{3}}_1^B (\bar{\mathbf{3}}_2^B)^* \bar{\mathbf{1}}^{(5)}, \bar{\mathbf{3}}_1^B (\bar{\mathbf{3}}_4^B)^* \bar{\mathbf{1}}^{(3)};</math></p> <p><math>\lambda_2: \bar{\mathbf{3}}_1^B \bar{\mathbf{3}}_1^B \bar{\mathbf{3}}_4^B \bar{\mathbf{1}}^{(3)}</math></p>
<p><i>possibility no. 2</i></p> <p><math>a = 0, b = -\frac{1}{2}; (H_u, H_d) = (\mathbf{2}_1^I, \mathbf{2}_2^I)</math></p> <p>heavy <math>(u_R^c, d_R^c): (-, \bar{\mathbf{3}}_4^B)</math></p> <p>light <math>u_R^c: \bar{\mathbf{3}}_1^B</math>; light <math>d_R^c: \bar{\mathbf{3}}_2^B</math></p> <p>heavy generations of <math>(L, \nu_R^c, e_R^c):</math>  <math>(\bar{\mathbf{2}}_1^I, -, \bar{\mathbf{1}}^{(5)}), (\mathbf{2}_2^I, \bar{\mathbf{1}}^{(2)}, \bar{\mathbf{1}}^{(3)})</math></p> <p>light <math>\nu_R^c: \mathbf{1}^{(2)}</math>; light <math>e_R^c: -</math></p> <p><math>\mathbf{1}_\mu: \bar{\mathbf{1}}^{(2)}</math></p>	<p><math>\alpha: (\bar{\mathbf{2}}_1^I, \bar{\mathbf{3}}_2^B), (\mathbf{2}_2^I, \bar{\mathbf{3}}_4^B); \beta: \bar{\mathbf{3}}_1^B \bar{\mathbf{3}}_4^B \bar{\mathbf{3}}_2^B; \delta: -;</math></p> <p><math>\gamma: \bar{\mathbf{2}}_1^I \mathbf{2}_2^I \bar{\mathbf{1}}^{(5)}, \mathbf{2}_2^I \mathbf{2}_2^I \bar{\mathbf{1}}^{(3)};</math></p> <p><math>\lambda_1: \bar{\mathbf{2}}_1^I; \lambda_3: \checkmark; \lambda_6: -; \lambda_8: \bar{\mathbf{1}}^{(5)}; \lambda_{10}: (\bar{\mathbf{3}}_4^B)^*;</math></p> <p><math>\lambda_4: (\bar{\mathbf{3}}_1^B, \bar{\mathbf{1}}^{(3)}); \lambda_5: (\bar{\mathbf{2}}_1^I, \bar{\mathbf{2}}_1^I);</math></p> <p><math>\lambda_9: (\bar{\mathbf{3}}_1^B, (\mathbf{2}_2^I)^*);</math></p> <p><math>\lambda_7: \bar{\mathbf{3}}_1^B (\bar{\mathbf{3}}_4^B)^* \bar{\mathbf{1}}^{(3)}, \bar{\mathbf{3}}_1^B (\bar{\mathbf{3}}_2^B)^* \bar{\mathbf{1}}^{(5)};</math></p> <p><math>\lambda_2: \bar{\mathbf{3}}_1^B \bar{\mathbf{3}}_1^B \bar{\mathbf{3}}_4^B \bar{\mathbf{1}}^{(3)}</math></p>

Continued on next page









Table C.2, Possible matches for  $I \times B$  – continued from previous page

Matter spectrum	Baryon- and Lepton number violation
<p><i>possibility no. 14</i></p> <p><math>a = -1, b = 0; (H_u, H_d) = (\bar{\mathbf{2}}_3^I, \mathbf{2}_3^I)</math></p> <p>heavy <math>(u_R^c, d_R^c): (\bar{\mathbf{3}}_3^B, \bar{\mathbf{3}}_5^B)</math></p> <p>light <math>u_R^c: \bar{\mathbf{3}}_1^B, \bar{\mathbf{3}}_2^B</math>; light <math>d_R^c: \bar{\mathbf{3}}_4^B</math></p> <p>heavy generations of <math>(L, \nu_R^c, e_R^c): (\mathbf{2}_1^I, \mathbf{1}^{(6)}, \bar{\mathbf{1}}^{(1)}), (\mathbf{2}_2^I, \bar{\mathbf{1}}^{(6)}, \bar{\mathbf{1}}^{(4)}), (\mathbf{2}_3^I, -, \bar{\mathbf{1}}^{(2)})</math></p> <p>light <math>\nu_R^c: \mathbf{1}^{(5)}, \bar{\mathbf{1}}^{(5)}</math>; light <math>e_R^c: \bar{\mathbf{1}}^{(3)}</math></p> <p><math>\mathbf{1}_\mu: -</math></p>	<p><math>\alpha: (\mathbf{2}_2^I, \bar{\mathbf{3}}_4^B), (\mathbf{2}_3^I, \bar{\mathbf{3}}_5^B); \beta: \bar{\mathbf{3}}_3^B \bar{\mathbf{3}}_5^B \bar{\mathbf{3}}_4^B, \bar{\mathbf{3}}_1^B \bar{\mathbf{3}}_4^B \bar{\mathbf{3}}_4^B, \bar{\mathbf{3}}_2^B \bar{\mathbf{3}}_5^B \bar{\mathbf{3}}_5^B; \delta: \bar{\mathbf{1}}^{(5)} \mathbf{1}^{(6)} \mathbf{1}^{(6)}, \mathbf{1}^{(5)} \bar{\mathbf{1}}^{(6)} \bar{\mathbf{1}}^{(6)}</math>;</p> <p><math>\gamma: \mathbf{2}_1^I \mathbf{2}_2^I \bar{\mathbf{1}}^{(2)}, \mathbf{2}_1^I \mathbf{2}_3^I \bar{\mathbf{1}}^{(1)}, \mathbf{2}_2^I \mathbf{2}_2^I \bar{\mathbf{1}}^{(3)}, \mathbf{2}_2^I \mathbf{2}_3^I \bar{\mathbf{1}}^{(4)}, \mathbf{2}_3^I \mathbf{2}_3^I \bar{\mathbf{1}}^{(2)}</math>;</p> <p><math>\lambda_1: \bar{\mathbf{2}}_1^I; \lambda_3: -; \lambda_6: \mathbf{2}_2^I; \lambda_8: \bar{\mathbf{1}}^{(2)}; \lambda_{10}: (\bar{\mathbf{3}}_4^B)^*</math>;</p> <p><math>\lambda_4: (\bar{\mathbf{3}}_3^B, \bar{\mathbf{1}}^{(2)}), (\bar{\mathbf{3}}_1^B, \bar{\mathbf{1}}^{(4)}), (\bar{\mathbf{3}}_2^B, \bar{\mathbf{1}}^{(1)}); \lambda_5: (\mathbf{2}_1^I, \mathbf{2}_2^I), (\mathbf{2}_3^I, \mathbf{2}_3^I)</math>;</p> <p><math>\lambda_9: (\bar{\mathbf{3}}_2^B, (\mathbf{2}_1^I)^*), (\bar{\mathbf{3}}_1^B, (\mathbf{2}_2^I)^*), (\bar{\mathbf{3}}_3^B, (\mathbf{2}_3^I)^*)</math>;</p> <p><math>\lambda_7: \bar{\mathbf{3}}_3^B (\bar{\mathbf{3}}_5^B)^* \bar{\mathbf{1}}^{(2)}, \bar{\mathbf{3}}_3^B (\bar{\mathbf{3}}_4^B)^* \bar{\mathbf{1}}^{(4)}, \bar{\mathbf{3}}_1^B (\bar{\mathbf{3}}_5^B)^* \bar{\mathbf{1}}^{(4)}, \bar{\mathbf{3}}_1^B (\bar{\mathbf{3}}_4^B)^* \bar{\mathbf{1}}^{(3)}, \bar{\mathbf{3}}_2^B (\bar{\mathbf{3}}_5^B)^* \bar{\mathbf{1}}^{(1)}, \bar{\mathbf{3}}_2^B (\bar{\mathbf{3}}_4^B)^* \bar{\mathbf{1}}^{(2)}</math>;</p> <p><math>\lambda_2: \bar{\mathbf{3}}_3^B \bar{\mathbf{3}}_3^B \bar{\mathbf{3}}_5^B \bar{\mathbf{1}}^{(4)}, \bar{\mathbf{3}}_3^B \bar{\mathbf{3}}_3^B \bar{\mathbf{3}}_4^B \bar{\mathbf{1}}^{(2)}, \bar{\mathbf{3}}_3^B \bar{\mathbf{3}}_1^B \bar{\mathbf{3}}_5^B \bar{\mathbf{1}}^{(3)}, \bar{\mathbf{3}}_3^B \bar{\mathbf{3}}_1^B \bar{\mathbf{3}}_4^B \bar{\mathbf{1}}^{(4)}, \bar{\mathbf{3}}_3^B \bar{\mathbf{3}}_2^B \bar{\mathbf{3}}_5^B \bar{\mathbf{1}}^{(2)}, \bar{\mathbf{3}}_3^B \bar{\mathbf{3}}_2^B \bar{\mathbf{3}}_4^B \bar{\mathbf{1}}^{(1)}, \bar{\mathbf{3}}_1^B \bar{\mathbf{3}}_1^B \bar{\mathbf{3}}_4^B \bar{\mathbf{1}}^{(3)}, \bar{\mathbf{3}}_1^B \bar{\mathbf{3}}_2^B \bar{\mathbf{3}}_5^B \bar{\mathbf{1}}^{(4)}, \bar{\mathbf{3}}_1^B \bar{\mathbf{3}}_2^B \bar{\mathbf{3}}_4^B \bar{\mathbf{1}}^{(2)}, \bar{\mathbf{3}}_2^B \bar{\mathbf{3}}_2^B \bar{\mathbf{3}}_5^B \bar{\mathbf{1}}^{(1)}</math></p>
<p><i>Incomplete match</i></p> <p><math>a = -2b - 1; (H_u, H_d) = (\bar{\mathbf{2}}_2^I, \mathbf{2}_2^I)</math></p> <p>heavy <math>(u_R^c, d_R^c): (\bar{\mathbf{3}}_1^B, \bar{\mathbf{3}}_4^B)</math></p> <p><math>e_R^c: \bar{\mathbf{1}}^{(3)}</math></p> <p><math>\mathbf{1}_\mu: -</math></p> <p>other states depend on value of <math>b</math></p>	<p><math>\beta: \checkmark, \lambda_2: \checkmark, \lambda_3: \checkmark, \lambda_4: \checkmark, \lambda_7: \checkmark, \lambda_8: \checkmark, \lambda_{10}: \checkmark</math></p> <p>other couplings depend on value of <math>b</math></p>

 Table C.3: Possible matches for  $I \times C$ 

Matter spectrum	Baryon- and Lepton number violation
<p><i>possibility no. 1</i></p> <p><math>a = -1, b = -1; (H_u, H_d) = (\mathbf{2}_1^I, \bar{\mathbf{2}}_1^I)</math></p> <p>heavy <math>(u_R^c, d_R^c): (\bar{\mathbf{3}}_2^C, -)</math></p> <p>light <math>u_R^c: \bar{\mathbf{3}}_4^C</math>; light <math>d_R^c: \bar{\mathbf{3}}_5^C</math></p> <p>heavy generations of <math>(L, \nu_R^c, e_R^c): (\bar{\mathbf{2}}_1^I, -, -), (\mathbf{2}_3^I, \bar{\mathbf{1}}^{(1)}, \bar{\mathbf{1}}^{(6)})</math></p> <p>light <math>\nu_R^c: \mathbf{1}^{(1)}</math>; light <math>e_R^c: \bar{\mathbf{1}}^{(2)}</math></p> <p><math>\mathbf{1}_\mu: -</math></p>	<p><math>\alpha: (\mathbf{2}_3^I, \bar{\mathbf{3}}_5^C); \beta: \bar{\mathbf{3}}_4^C \bar{\mathbf{3}}_5^C \bar{\mathbf{3}}_5^C; \delta: -;</math></p> <p><math>\gamma: \bar{\mathbf{2}}_1^I \mathbf{2}_3^I \bar{\mathbf{1}}^{(6)}, \mathbf{2}_3^I \mathbf{2}_3^I \bar{\mathbf{1}}^{(2)}</math>;</p> <p><math>\lambda_1: \bar{\mathbf{2}}_1^I; \lambda_3: -; \lambda_6: \mathbf{2}_1^I; \lambda_8: -; \lambda_{10}: (\bar{\mathbf{3}}_5^C)^*</math>;</p> <p><math>\lambda_4: (\bar{\mathbf{3}}_4^C, \bar{\mathbf{1}}^{(6)}); \lambda_5: (\bar{\mathbf{2}}_1^I, \bar{\mathbf{2}}_1^I)</math>;</p> <p><math>\lambda_9: (\bar{\mathbf{3}}_2^C, (\bar{\mathbf{2}}_1^I)^*), (\bar{\mathbf{3}}_4^C, (\mathbf{2}_3^I)^*)</math>;</p> <p><math>\lambda_7: \bar{\mathbf{3}}_2^C (\bar{\mathbf{3}}_5^C)^* \bar{\mathbf{1}}^{(6)}, \bar{\mathbf{3}}_4^C (\bar{\mathbf{3}}_5^C)^* \bar{\mathbf{1}}^{(2)}</math>;</p> <p><math>\lambda_2: \bar{\mathbf{3}}_2^C \bar{\mathbf{3}}_4^C \bar{\mathbf{3}}_5^C \bar{\mathbf{1}}^{(6)}, \bar{\mathbf{3}}_4^C \bar{\mathbf{3}}_4^C \bar{\mathbf{3}}_5^C \bar{\mathbf{1}}^{(2)}</math></p>
<p><i>possibility no. 2</i></p> <p><math>a = -1, b = -1; (H_u, H_d) = (\mathbf{2}_1^I, \mathbf{2}_3^I)</math></p> <p>heavy <math>(u_R^c, d_R^c): (\bar{\mathbf{3}}_2^C, \bar{\mathbf{3}}_5^C)</math></p> <p>light <math>u_R^c: \bar{\mathbf{3}}_4^C</math>; light <math>d_R^c: -</math></p> <p>heavy generations of <math>(L, \nu_R^c, e_R^c): (\bar{\mathbf{2}}_1^I, -, \bar{\mathbf{1}}^{(6)}), (\mathbf{2}_3^I, \bar{\mathbf{1}}^{(1)}, \bar{\mathbf{1}}^{(2)})</math></p> <p>light <math>\nu_R^c: \mathbf{1}^{(1)}</math>; light <math>e_R^c: -</math></p> <p><math>\mathbf{1}_\mu: \bar{\mathbf{1}}^{(1)}</math></p>	<p><math>\alpha: (\mathbf{2}_3^I, \bar{\mathbf{3}}_5^C); \beta: \bar{\mathbf{3}}_4^C \bar{\mathbf{3}}_5^C \bar{\mathbf{3}}_5^C; \delta: -;</math></p> <p><math>\gamma: \bar{\mathbf{2}}_1^I \mathbf{2}_3^I \bar{\mathbf{1}}^{(6)}, \mathbf{2}_3^I \mathbf{2}_3^I \bar{\mathbf{1}}^{(2)}</math>;</p> <p><math>\lambda_1: \bar{\mathbf{2}}_1^I; \lambda_3: \checkmark; \lambda_6: -; \lambda_8: \bar{\mathbf{1}}^{(6)}; \lambda_{10}: (\bar{\mathbf{3}}_5^C)^*</math>;</p> <p><math>\lambda_4: (\bar{\mathbf{3}}_2^C, \bar{\mathbf{1}}^{(6)}), (\bar{\mathbf{3}}_4^C, \bar{\mathbf{1}}^{(2)}); \lambda_5: (\bar{\mathbf{2}}_1^I, \bar{\mathbf{2}}_1^I)</math>;</p> <p><math>\lambda_9: (\bar{\mathbf{3}}_2^C, (\bar{\mathbf{2}}_1^I)^*), (\bar{\mathbf{3}}_4^C, (\mathbf{2}_3^I)^*)</math>;</p> <p><math>\lambda_7: \bar{\mathbf{3}}_2^C (\bar{\mathbf{3}}_5^C)^* \bar{\mathbf{1}}^{(6)}, \bar{\mathbf{3}}_4^C (\bar{\mathbf{3}}_5^C)^* \bar{\mathbf{1}}^{(2)}</math>;</p> <p><math>\lambda_2: \bar{\mathbf{3}}_2^C \bar{\mathbf{3}}_4^C \bar{\mathbf{3}}_5^C \bar{\mathbf{1}}^{(6)}, \bar{\mathbf{3}}_4^C \bar{\mathbf{3}}_4^C \bar{\mathbf{3}}_5^C \bar{\mathbf{1}}^{(2)}</math></p>

Continued on next page







Table C.4: Possible matches for III  $\times$  A

<i>Matter spectrum</i>	<i>Baryon- and Lepton number violation</i>
<p><i>possibility no. 1</i></p> <p><math>a = \frac{1}{2}, b = -1; (H_u, H_d) = (\mathbf{2}_1^{\text{III}}, \bar{\mathbf{2}}_1^{\text{III}})</math></p> <p>heavy <math>(u_R^c, d_R^c): (\bar{\mathbf{3}}_1^A, -)</math></p> <p>light <math>u_R^c: -</math>; light <math>d_R^c: \bar{\mathbf{3}}_4^A</math></p> <p>heavy generations of <math>(L, \nu_R^c, e_R^c)</math>:  <math>(\bar{\mathbf{2}}_1^{\text{III}}, -, -), (\mathbf{2}_2^{\text{III}}, -, \bar{\mathbf{1}}^{(6)})</math></p> <p>light <math>\nu_R^c: -</math>; light <math>e_R^c: -</math></p> <p><math>\mathbf{1}_\mu: -</math></p>	<p><math>\alpha: (\mathbf{2}_2^{\text{III}}, \bar{\mathbf{3}}_4^A); \beta: -; \delta: -;</math></p> <p><math>\gamma: \bar{\mathbf{2}}_1^{\text{III}} \mathbf{2}_2^{\text{III}} \bar{\mathbf{1}}^{(6)};</math></p> <p><math>\lambda_1: \bar{\mathbf{2}}_1^{\text{III}}; \lambda_3: -; \lambda_6: \mathbf{2}_1^{\text{III}}; \lambda_8: -; \lambda_{10}: (\bar{\mathbf{3}}_4^A)^*;</math></p> <p><math>\lambda_4: -; \lambda_5: (\bar{\mathbf{2}}_1^{\text{III}}, \bar{\mathbf{2}}_1^{\text{III}});</math></p> <p><math>\lambda_9: (\bar{\mathbf{3}}_1^A, (\bar{\mathbf{2}}_1^{\text{III}})^*);</math></p> <p><math>\lambda_7: \bar{\mathbf{3}}_1^A (\bar{\mathbf{3}}_4^A)^* \bar{\mathbf{1}}^{(6)};</math></p> <p><math>\lambda_2: -</math></p>
<p><i>possibility no. 2</i></p> <p><math>a = \frac{1}{2}, b = -1; (H_u, H_d) = (\mathbf{2}_1^{\text{III}}, \mathbf{2}_2^{\text{III}})</math></p> <p>heavy <math>(u_R^c, d_R^c): (\bar{\mathbf{3}}_1^A, \bar{\mathbf{3}}_4^A)</math></p> <p>light <math>u_R^c: -</math>; light <math>d_R^c: -</math></p> <p>heavy generations of <math>(L, \nu_R^c, e_R^c)</math>:  <math>(\bar{\mathbf{2}}_1^{\text{III}}, -, \bar{\mathbf{1}}^{(6)}), (\mathbf{2}_2^{\text{III}}, -, -)</math></p> <p>light <math>\nu_R^c: -</math>; light <math>e_R^c: -</math></p> <p><math>\mathbf{1}_\mu: -</math></p>	<p><math>\alpha: (\mathbf{2}_2^{\text{III}}, \bar{\mathbf{3}}_4^A); \beta: -; \delta: -;</math></p> <p><math>\gamma: \bar{\mathbf{2}}_1^{\text{III}} \mathbf{2}_2^{\text{III}} \bar{\mathbf{1}}^{(6)};</math></p> <p><math>\lambda_1: \bar{\mathbf{2}}_1^{\text{III}}; \lambda_3: \checkmark; \lambda_6: -; \lambda_8: \bar{\mathbf{1}}^{(6)}; \lambda_{10}: (\bar{\mathbf{3}}_4^A)^*;</math></p> <p><math>\lambda_4: (\bar{\mathbf{3}}_1^A, \bar{\mathbf{1}}^{(6)}); \lambda_5: (\bar{\mathbf{2}}_1^{\text{III}}, \bar{\mathbf{2}}_1^{\text{III}});</math></p> <p><math>\lambda_9: (\bar{\mathbf{3}}_1^A, (\bar{\mathbf{2}}_1^{\text{III}})^*);</math></p> <p><math>\lambda_7: \bar{\mathbf{3}}_1^A (\bar{\mathbf{3}}_4^A)^* \bar{\mathbf{1}}^{(6)};</math></p> <p><math>\lambda_2: -</math></p>
<p><i>possibility no. 3</i></p> <p><math>a = \frac{1}{2}, b = -1; (H_u, H_d) = (\bar{\mathbf{2}}_2^{\text{III}}, \bar{\mathbf{2}}_1^{\text{III}})</math></p> <p>heavy <math>(u_R^c, d_R^c): (-, -)</math></p> <p>light <math>u_R^c: \bar{\mathbf{3}}_1^A</math>; light <math>d_R^c: \bar{\mathbf{3}}_4^A</math></p> <p>heavy generations of <math>(L, \nu_R^c, e_R^c)</math>:  <math>(\bar{\mathbf{2}}_1^{\text{III}}, -, -), (\mathbf{2}_2^{\text{III}}, -, \bar{\mathbf{1}}^{(6)})</math></p> <p>light <math>\nu_R^c: -</math>; light <math>e_R^c: -</math></p> <p><math>\mathbf{1}_\mu: -</math></p>	<p><math>\alpha: (\mathbf{2}_2^{\text{III}}, \bar{\mathbf{3}}_4^A); \beta: -; \delta: -;</math></p> <p><math>\gamma: \bar{\mathbf{2}}_1^{\text{III}} \mathbf{2}_2^{\text{III}} \bar{\mathbf{1}}^{(6)};</math></p> <p><math>\lambda_1: \bar{\mathbf{2}}_1^{\text{III}}; \lambda_3: -; \lambda_6: -; \lambda_8: \bar{\mathbf{1}}^{(6)}; \lambda_{10}: (\bar{\mathbf{3}}_4^A)^*;</math></p> <p><math>\lambda_4: -; \lambda_5: (\mathbf{2}_2^{\text{III}}, \mathbf{2}_2^{\text{III}});</math></p> <p><math>\lambda_9: (\bar{\mathbf{3}}_1^A, (\bar{\mathbf{2}}_1^{\text{III}})^*);</math></p> <p><math>\lambda_7: \bar{\mathbf{3}}_1^A (\bar{\mathbf{3}}_4^A)^* \bar{\mathbf{1}}^{(6)};</math></p> <p><math>\lambda_2: -</math></p>
<p><i>possibility no. 4</i></p> <p><math>a = 0, b = -\frac{1}{2}; (H_u, H_d) = (\bar{\mathbf{2}}_2^{\text{III}}, \mathbf{2}_3^{\text{III}})</math></p> <p>heavy <math>(u_R^c, d_R^c): (-, \bar{\mathbf{3}}_3^A)</math></p> <p>light <math>u_R^c: \bar{\mathbf{3}}_2^A</math>; light <math>d_R^c: \bar{\mathbf{3}}_4^A</math></p> <p>heavy generations of <math>(L, \nu_R^c, e_R^c)</math>:  <math>(\mathbf{2}_2^{\text{III}}, -, \bar{\mathbf{1}}^{(3)}), (\mathbf{2}_3^{\text{III}}, \mathbf{1}^{(2)}, \bar{\mathbf{1}}^{(5)})</math></p> <p>light <math>\nu_R^c: \bar{\mathbf{1}}^{(2)}</math>; light <math>e_R^c: -</math></p> <p><math>\mathbf{1}_\mu: \mathbf{1}^{(2)}</math></p>	<p><math>\alpha: (\mathbf{2}_2^{\text{III}}, \bar{\mathbf{3}}_4^A), (\mathbf{2}_3^{\text{III}}, \bar{\mathbf{3}}_3^A); \beta: \bar{\mathbf{3}}_2^A \bar{\mathbf{3}}_3^A \bar{\mathbf{3}}_4^A; \delta: -;</math></p> <p><math>\gamma: \mathbf{2}_2^{\text{III}} \mathbf{2}_3^{\text{III}} \bar{\mathbf{1}}^{(3)}, \mathbf{2}_3^{\text{III}} \mathbf{2}_3^{\text{III}} \bar{\mathbf{1}}^{(5)};</math></p> <p><math>\lambda_1: \mathbf{2}_1^{\text{III}}; \lambda_3: -; \lambda_6: -; \lambda_8: \bar{\mathbf{1}}^{(3)}; \lambda_{10}: (\bar{\mathbf{3}}_4^A)^*;</math></p> <p><math>\lambda_4: (\bar{\mathbf{3}}_2^A, \bar{\mathbf{1}}^{(5)}); \lambda_5: (\mathbf{2}_2^{\text{III}}, \mathbf{2}_2^{\text{III}});</math></p> <p><math>\lambda_9: (\bar{\mathbf{3}}_2^A, (\mathbf{2}_3^{\text{III}})^*);</math></p> <p><math>\lambda_7: \bar{\mathbf{3}}_2^A (\bar{\mathbf{3}}_3^A)^* \bar{\mathbf{1}}^{(5)}, \bar{\mathbf{3}}_2^A (\bar{\mathbf{3}}_4^A)^* \bar{\mathbf{1}}^{(3)};</math></p> <p><math>\lambda_2: \bar{\mathbf{3}}_2^A \bar{\mathbf{3}}_2^A \bar{\mathbf{3}}_3^A \bar{\mathbf{1}}^{(3)}, \bar{\mathbf{3}}_2^A \bar{\mathbf{3}}_2^A \bar{\mathbf{3}}_4^A \bar{\mathbf{1}}^{(5)}</math></p>
<p><i>possibility no. 5</i></p> <p><math>a = -1, b = \frac{1}{2}; (H_u, H_d) = (\bar{\mathbf{2}}_2^{\text{III}}, \bar{\mathbf{2}}_3^{\text{III}})</math></p> <p>heavy <math>(u_R^c, d_R^c): (-, \bar{\mathbf{3}}_2^A)</math></p> <p>light <math>u_R^c: \bar{\mathbf{3}}_3^A</math>; light <math>d_R^c: \bar{\mathbf{3}}_4^A</math></p> <p>heavy generations of <math>(L, \nu_R^c, e_R^c)</math>:  <math>(\mathbf{2}_2^{\text{III}}, -, \bar{\mathbf{1}}^{(2)}), (\bar{\mathbf{2}}_3^{\text{III}}, \mathbf{1}^{(3)}, \mathbf{1}^{(5)})</math></p> <p>light <math>\nu_R^c: \bar{\mathbf{1}}^{(3)}</math>; light <math>e_R^c: -</math></p> <p><math>\mathbf{1}_\mu: \mathbf{1}^{(3)}</math></p>	<p><math>\alpha: (\mathbf{2}_2^{\text{III}}, \bar{\mathbf{3}}_4^A), (\bar{\mathbf{2}}_3^{\text{III}}, \bar{\mathbf{3}}_2^A); \beta: \bar{\mathbf{3}}_3^A \bar{\mathbf{3}}_2^A \bar{\mathbf{3}}_4^A; \delta: -;</math></p> <p><math>\gamma: \mathbf{2}_2^{\text{III}} \bar{\mathbf{2}}_3^{\text{III}} \bar{\mathbf{1}}^{(2)}, \bar{\mathbf{2}}_3^{\text{III}} \bar{\mathbf{2}}_3^{\text{III}} \mathbf{1}^{(5)};</math></p> <p><math>\lambda_1: \mathbf{2}_1^{\text{III}}; \lambda_3: -; \lambda_6: -; \lambda_8: \bar{\mathbf{1}}^{(2)}; \lambda_{10}: (\bar{\mathbf{3}}_4^A)^*;</math></p> <p><math>\lambda_4: (\bar{\mathbf{3}}_3^A, \mathbf{1}^{(5)}); \lambda_5: (\mathbf{2}_2^{\text{III}}, \mathbf{2}_2^{\text{III}});</math></p> <p><math>\lambda_9: (\bar{\mathbf{3}}_3^A, (\bar{\mathbf{2}}_3^{\text{III}})^*);</math></p> <p><math>\lambda_7: \bar{\mathbf{3}}_3^A (\bar{\mathbf{3}}_2^A)^* \mathbf{1}^{(5)}, \bar{\mathbf{3}}_3^A (\bar{\mathbf{3}}_4^A)^* \bar{\mathbf{1}}^{(2)};</math></p> <p><math>\lambda_2: \bar{\mathbf{3}}_3^A \bar{\mathbf{3}}_3^A \bar{\mathbf{3}}_2^A \bar{\mathbf{1}}^{(2)}, \bar{\mathbf{3}}_3^A \bar{\mathbf{3}}_3^A \bar{\mathbf{3}}_4^A \mathbf{1}^{(5)}</math></p>

Continued on next page

Table C.4, Possible matches for III  $\times$  A – continued from previous page

Matter spectrum	Baryon- and Lepton number violation
<p>possibility no. 6</p> <p><math>a = -1, b = \frac{1}{2}; (H_u, H_d) = (\mathbf{2}_3^{\text{III}}, \mathbf{2}_2^{\text{III}})</math></p> <p>heavy <math>(u_R^c, d_R^c): (\overline{\mathbf{3}}_3^A, \overline{\mathbf{3}}_4^A)</math></p> <p>light <math>u_R^c: -</math>; light <math>d_R^c: \overline{\mathbf{3}}_2^A</math></p> <p>heavy generations of <math>(L, \nu_R^c, e_R^c): (\mathbf{2}_2^{\text{III}}, \overline{\mathbf{1}}^{(3)}, -), (\overline{\mathbf{2}}_3^{\text{III}}, -, \overline{\mathbf{1}}^{(2)})</math></p> <p>light <math>\nu_R^c: \mathbf{1}^{(3)}</math>; light <math>e_R^c: \mathbf{1}^{(5)}</math></p> <p><math>\mathbf{1}_\mu: \overline{\mathbf{1}}^{(3)}</math></p>	<p><math>\alpha: (\mathbf{2}_2^{\text{III}}, \overline{\mathbf{3}}_4^A), (\overline{\mathbf{2}}_3^{\text{III}}, \overline{\mathbf{3}}_2^A); \beta: \overline{\mathbf{3}}_3^A \overline{\mathbf{3}}_4^A \overline{\mathbf{3}}_2^A; \delta: -;</math></p> <p><math>\gamma: \mathbf{2}_2^{\text{III}} \overline{\mathbf{2}}_3^{\text{III}} \overline{\mathbf{1}}^{(2)}, \overline{\mathbf{2}}_3^{\text{III}} \overline{\mathbf{2}}_3^{\text{III}} \mathbf{1}^{(5)};</math></p> <p><math>\lambda_1: \mathbf{2}_1^{\text{III}}; \lambda_3: \checkmark; \lambda_6: -; \lambda_8: \overline{\mathbf{1}}^{(2)}; \lambda_{10}: (\overline{\mathbf{3}}_4^A)^*;</math></p> <p><math>\lambda_4: (\overline{\mathbf{3}}_3^A, \overline{\mathbf{1}}^{(2)}); \lambda_5: (\overline{\mathbf{2}}_3^{\text{III}}, \overline{\mathbf{2}}_3^{\text{III}});</math></p> <p><math>\lambda_9: (\overline{\mathbf{3}}_3^A, (\mathbf{2}_3^{\text{III}})^*);</math></p> <p><math>\lambda_7: \overline{\mathbf{3}}_3^A (\overline{\mathbf{3}}_4^A)^* \overline{\mathbf{1}}^{(2)}, \overline{\mathbf{3}}_3^A (\overline{\mathbf{3}}_2^A)^* \mathbf{1}^{(5)};</math></p> <p><math>\lambda_2: \overline{\mathbf{3}}_3^A \overline{\mathbf{3}}_3^A \overline{\mathbf{3}}_4^A \mathbf{1}^{(5)}, \overline{\mathbf{3}}_3^A \overline{\mathbf{3}}_3^A \overline{\mathbf{3}}_2^A \overline{\mathbf{1}}^{(2)}</math></p>
<p>possibility no. 7</p> <p><math>a = -1, b = \frac{1}{2}; (H_u, H_d) = (\mathbf{2}_3^{\text{III}}, \overline{\mathbf{2}}_3^{\text{III}})</math></p> <p>heavy <math>(u_R^c, d_R^c): (\overline{\mathbf{3}}_3^A, \overline{\mathbf{3}}_2^A)</math></p> <p>light <math>u_R^c: -</math>; light <math>d_R^c: \overline{\mathbf{3}}_4^A</math></p> <p>heavy generations of <math>(L, \nu_R^c, e_R^c): (\mathbf{2}_2^{\text{III}}, \overline{\mathbf{1}}^{(3)}, \overline{\mathbf{1}}^{(2)}), (\overline{\mathbf{2}}_3^{\text{III}}, -, \mathbf{1}^{(5)})</math></p> <p>light <math>\nu_R^c: \mathbf{1}^{(3)}</math>; light <math>e_R^c: -</math></p> <p><math>\mathbf{1}_\mu: -</math></p>	<p><math>\alpha: (\mathbf{2}_2^{\text{III}}, \overline{\mathbf{3}}_4^A), (\overline{\mathbf{2}}_3^{\text{III}}, \overline{\mathbf{3}}_2^A); \beta: \overline{\mathbf{3}}_3^A \overline{\mathbf{3}}_2^A \overline{\mathbf{3}}_4^A; \delta: -;</math></p> <p><math>\gamma: \mathbf{2}_2^{\text{III}} \overline{\mathbf{2}}_3^{\text{III}} \overline{\mathbf{1}}^{(2)}, \overline{\mathbf{2}}_3^{\text{III}} \overline{\mathbf{2}}_3^{\text{III}} \mathbf{1}^{(5)};</math></p> <p><math>\lambda_1: \mathbf{2}_1^{\text{III}}; \lambda_3: -; \lambda_6: \overline{\mathbf{2}}_1^{\text{III}}; \lambda_8: \mathbf{1}^{(5)}; \lambda_{10}: (\overline{\mathbf{3}}_4^A)^*;</math></p> <p><math>\lambda_4: (\overline{\mathbf{3}}_3^A, \mathbf{1}^{(5)}); \lambda_5: (\overline{\mathbf{2}}_3^{\text{III}}, \overline{\mathbf{2}}_3^{\text{III}});</math></p> <p><math>\lambda_9: (\overline{\mathbf{3}}_3^A, (\mathbf{2}_3^{\text{III}})^*);</math></p> <p><math>\lambda_7: \overline{\mathbf{3}}_3^A (\overline{\mathbf{3}}_2^A)^* \mathbf{1}^{(5)}, \overline{\mathbf{3}}_3^A (\overline{\mathbf{3}}_4^A)^* \overline{\mathbf{1}}^{(2)};</math></p> <p><math>\lambda_2: \overline{\mathbf{3}}_3^A \overline{\mathbf{3}}_3^A \overline{\mathbf{3}}_2^A \overline{\mathbf{1}}^{(2)}, \overline{\mathbf{3}}_3^A \overline{\mathbf{3}}_3^A \overline{\mathbf{3}}_4^A \mathbf{1}^{(5)}</math></p>
<p>possibility no. 8</p> <p><math>a = 0, b = -\frac{1}{2}; (H_u, H_d) = (\overline{\mathbf{2}}_3^{\text{III}}, \mathbf{2}_2^{\text{III}})</math></p> <p>heavy <math>(u_R^c, d_R^c): (\overline{\mathbf{3}}_2^A, \overline{\mathbf{3}}_4^A)</math></p> <p>light <math>u_R^c: -</math>; light <math>d_R^c: \overline{\mathbf{3}}_3^A</math></p> <p>heavy generations of <math>(L, \nu_R^c, e_R^c): (\mathbf{2}_2^{\text{III}}, \overline{\mathbf{1}}^{(2)}, -), (\mathbf{2}_3^{\text{III}}, -, \overline{\mathbf{1}}^{(3)})</math></p> <p>light <math>\nu_R^c: \mathbf{1}^{(2)}</math>; light <math>e_R^c: \overline{\mathbf{1}}^{(5)}</math></p> <p><math>\mathbf{1}_\mu: \overline{\mathbf{1}}^{(2)}</math></p>	<p><math>\alpha: (\mathbf{2}_2^{\text{III}}, \overline{\mathbf{3}}_4^A), (\mathbf{2}_3^{\text{III}}, \overline{\mathbf{3}}_3^A); \beta: \overline{\mathbf{3}}_2^A \overline{\mathbf{3}}_4^A \overline{\mathbf{3}}_3^A; \delta: -;</math></p> <p><math>\gamma: \mathbf{2}_2^{\text{III}} \mathbf{2}_3^{\text{III}} \overline{\mathbf{1}}^{(3)}, \mathbf{2}_3^{\text{III}} \mathbf{2}_3^{\text{III}} \overline{\mathbf{1}}^{(5)};</math></p> <p><math>\lambda_1: \mathbf{2}_1^{\text{III}}; \lambda_3: \checkmark; \lambda_6: -; \lambda_8: \overline{\mathbf{1}}^{(3)}; \lambda_{10}: (\overline{\mathbf{3}}_4^A)^*;</math></p> <p><math>\lambda_4: (\overline{\mathbf{3}}_2^A, \overline{\mathbf{1}}^{(3)}); \lambda_5: (\mathbf{2}_3^{\text{III}}, \mathbf{2}_3^{\text{III}});</math></p> <p><math>\lambda_9: (\overline{\mathbf{3}}_2^A, (\mathbf{2}_3^{\text{III}})^*);</math></p> <p><math>\lambda_7: \overline{\mathbf{3}}_2^A (\overline{\mathbf{3}}_4^A)^* \overline{\mathbf{1}}^{(3)}, \overline{\mathbf{3}}_2^A (\overline{\mathbf{3}}_3^A)^* \overline{\mathbf{1}}^{(5)};</math></p> <p><math>\lambda_2: \overline{\mathbf{3}}_2^A \overline{\mathbf{3}}_2^A \overline{\mathbf{3}}_4^A \overline{\mathbf{1}}^{(5)}, \overline{\mathbf{3}}_2^A \overline{\mathbf{3}}_2^A \overline{\mathbf{3}}_3^A \overline{\mathbf{1}}^{(3)}</math></p>
<p>possibility no. 9</p> <p><math>a = 0, b = -\frac{1}{2}; (H_u, H_d) = (\overline{\mathbf{2}}_3^{\text{III}}, \mathbf{2}_3^{\text{III}})</math></p> <p>heavy <math>(u_R^c, d_R^c): (\overline{\mathbf{3}}_2^A, \overline{\mathbf{3}}_3^A)</math></p> <p>light <math>u_R^c: -</math>; light <math>d_R^c: \overline{\mathbf{3}}_4^A</math></p> <p>heavy generations of <math>(L, \nu_R^c, e_R^c): (\mathbf{2}_2^{\text{III}}, \overline{\mathbf{1}}^{(2)}, \overline{\mathbf{1}}^{(3)}), (\mathbf{2}_3^{\text{III}}, -, \overline{\mathbf{1}}^{(5)})</math></p> <p>light <math>\nu_R^c: \mathbf{1}^{(2)}</math>; light <math>e_R^c: -</math></p> <p><math>\mathbf{1}_\mu: -</math></p>	<p><math>\alpha: (\mathbf{2}_2^{\text{III}}, \overline{\mathbf{3}}_4^A), (\mathbf{2}_3^{\text{III}}, \overline{\mathbf{3}}_3^A); \beta: \overline{\mathbf{3}}_2^A \overline{\mathbf{3}}_3^A \overline{\mathbf{3}}_4^A; \delta: -;</math></p> <p><math>\gamma: \mathbf{2}_2^{\text{III}} \mathbf{2}_3^{\text{III}} \overline{\mathbf{1}}^{(3)}, \mathbf{2}_3^{\text{III}} \mathbf{2}_3^{\text{III}} \overline{\mathbf{1}}^{(5)};</math></p> <p><math>\lambda_1: \mathbf{2}_1^{\text{III}}; \lambda_3: -; \lambda_6: \overline{\mathbf{2}}_1^{\text{III}}; \lambda_8: \overline{\mathbf{1}}^{(5)}; \lambda_{10}: (\overline{\mathbf{3}}_4^A)^*;</math></p> <p><math>\lambda_4: (\overline{\mathbf{3}}_2^A, \overline{\mathbf{1}}^{(5)}); \lambda_5: (\mathbf{2}_3^{\text{III}}, \mathbf{2}_3^{\text{III}});</math></p> <p><math>\lambda_9: (\overline{\mathbf{3}}_2^A, (\mathbf{2}_3^{\text{III}})^*);</math></p> <p><math>\lambda_7: \overline{\mathbf{3}}_2^A (\overline{\mathbf{3}}_3^A)^* \overline{\mathbf{1}}^{(5)}, \overline{\mathbf{3}}_2^A (\overline{\mathbf{3}}_4^A)^* \overline{\mathbf{1}}^{(3)};</math></p> <p><math>\lambda_2: \overline{\mathbf{3}}_2^A \overline{\mathbf{3}}_2^A \overline{\mathbf{3}}_3^A \overline{\mathbf{1}}^{(3)}, \overline{\mathbf{3}}_2^A \overline{\mathbf{3}}_2^A \overline{\mathbf{3}}_4^A \overline{\mathbf{1}}^{(5)}</math></p>
<p>Incomplete match</p> <p><math>a = -\frac{1}{2} - b; (H_u, H_d) = (\overline{\mathbf{2}}_2^{\text{III}}, \mathbf{2}_2^{\text{III}})</math></p> <p>heavy <math>d_R^c: \overline{\mathbf{3}}_4^A</math></p> <p><math>\mathbf{1}_\mu: -</math></p> <p>other states depend on value of <math>b</math></p>	<p><math>\lambda_3: \checkmark, \lambda_{10}: \checkmark</math></p> <p>other couplings depend on value of <math>b</math></p>

Table C.5: Possible matches for III  $\times$  B

Matter spectrum	Baryon- and Lepton number violation
<p><i>possibility no. 1</i></p> <p><math>a = -\frac{1}{2}, b = \frac{1}{2}; (H_u, H_d) = (\bar{\mathbf{2}}_1^{\text{III}}, \mathbf{2}_1^{\text{III}})</math></p> <p>heavy <math>(u_R^c, d_R^c): (-, \bar{\mathbf{3}}_5^{\text{B}})</math></p> <p>light <math>u_R^c: \bar{\mathbf{3}}_2^{\text{B}}; \text{light } d_R^c: \bar{\mathbf{3}}_1^{\text{B}}</math></p> <p>heavy generations of <math>(L, \nu_R^c, e_R^c):</math>  <math>(\mathbf{2}_1^{\text{III}}, -, -), (\bar{\mathbf{2}}_3^{\text{III}}, \mathbf{1}^{(4)}, \bar{\mathbf{1}}^{(1)})</math></p> <p>light <math>\nu_R^c: \bar{\mathbf{1}}^{(4)}; \text{light } e_R^c: \mathbf{1}^{(5)}</math></p> <p><math>\mathbf{1}_\mu: -</math></p>	<p><math>\alpha: (\mathbf{2}_1^{\text{III}}, \bar{\mathbf{3}}_5^{\text{B}}), (\bar{\mathbf{2}}_3^{\text{III}}, \bar{\mathbf{3}}_1^{\text{B}}); \beta: \bar{\mathbf{3}}_2^{\text{B}} \bar{\mathbf{3}}_5^{\text{B}} \bar{\mathbf{3}}_5^{\text{B}}; \delta: -;</math></p> <p><math>\gamma: \mathbf{2}_1^{\text{III}} \bar{\mathbf{2}}_3^{\text{III}} \bar{\mathbf{1}}^{(1)}, \bar{\mathbf{2}}_3^{\text{III}} \mathbf{2}_3^{\text{III}} \mathbf{1}^{(5)};</math></p> <p><math>\lambda_1: -; \lambda_3: -; \lambda_6: \mathbf{2}_1^{\text{III}}; \lambda_8: -; \lambda_{10}: -;</math></p> <p><math>\lambda_4: (\bar{\mathbf{3}}_2^{\text{B}}, \bar{\mathbf{1}}^{(1)}); \lambda_5: (\mathbf{2}_1^{\text{III}}, \mathbf{2}_1^{\text{III}});</math></p> <p><math>\lambda_9: (\bar{\mathbf{3}}_2^{\text{B}}, (\bar{\mathbf{2}}_3^{\text{III}})^*);</math></p> <p><math>\lambda_7: \bar{\mathbf{3}}_2^{\text{B}} (\bar{\mathbf{3}}_5^{\text{B}})^* \bar{\mathbf{1}}^{(1)}, \bar{\mathbf{3}}_2^{\text{B}} (\bar{\mathbf{3}}_1^{\text{B}})^* \mathbf{1}^{(5)};</math></p> <p><math>\lambda_2: \bar{\mathbf{3}}_2^{\text{B}} \bar{\mathbf{3}}_2^{\text{B}} \bar{\mathbf{3}}_5^{\text{B}} \bar{\mathbf{1}}^{(1)}</math></p>
<p><i>possibility no. 2</i></p> <p><math>a = -\frac{1}{2}, b = \frac{1}{2}; (H_u, H_d) = (\bar{\mathbf{2}}_1^{\text{III}}, \bar{\mathbf{2}}_3^{\text{III}})</math></p> <p>heavy <math>(u_R^c, d_R^c): (-, \bar{\mathbf{3}}_1^{\text{B}})</math></p> <p>light <math>u_R^c: \bar{\mathbf{3}}_2^{\text{B}}; \text{light } d_R^c: \bar{\mathbf{3}}_5^{\text{B}}</math></p> <p>heavy generations of <math>(L, \nu_R^c, e_R^c):</math>  <math>(\mathbf{2}_1^{\text{III}}, -, \bar{\mathbf{1}}^{(1)}), (\bar{\mathbf{2}}_3^{\text{III}}, \mathbf{1}^{(4)}, \mathbf{1}^{(5)})</math></p> <p>light <math>\nu_R^c: \bar{\mathbf{1}}^{(4)}; \text{light } e_R^c: -</math></p> <p><math>\mathbf{1}_\mu: \mathbf{1}^{(4)}</math></p>	<p><math>\alpha: (\mathbf{2}_1^{\text{III}}, \bar{\mathbf{3}}_5^{\text{B}}), (\bar{\mathbf{2}}_3^{\text{III}}, \bar{\mathbf{3}}_1^{\text{B}}); \beta: \bar{\mathbf{3}}_2^{\text{B}} \bar{\mathbf{3}}_5^{\text{B}} \bar{\mathbf{3}}_5^{\text{B}}; \delta: -;</math></p> <p><math>\gamma: \mathbf{2}_1^{\text{III}} \bar{\mathbf{2}}_3^{\text{III}} \bar{\mathbf{1}}^{(1)}, \bar{\mathbf{2}}_3^{\text{III}} \bar{\mathbf{2}}_3^{\text{III}} \mathbf{1}^{(5)};</math></p> <p><math>\lambda_1: -; \lambda_3: -; \lambda_6: -; \lambda_8: \bar{\mathbf{1}}^{(1)}; \lambda_{10}: -;</math></p> <p><math>\lambda_4: (\bar{\mathbf{3}}_2^{\text{B}}, \mathbf{1}^{(5)}); \lambda_5: (\mathbf{2}_1^{\text{III}}, \mathbf{2}_1^{\text{III}});</math></p> <p><math>\lambda_9: (\bar{\mathbf{3}}_2^{\text{B}}, (\bar{\mathbf{2}}_3^{\text{III}})^*);</math></p> <p><math>\lambda_7: \bar{\mathbf{3}}_2^{\text{B}} (\bar{\mathbf{3}}_1^{\text{B}})^* \mathbf{1}^{(5)}, \bar{\mathbf{3}}_2^{\text{B}} (\bar{\mathbf{3}}_5^{\text{B}})^* \bar{\mathbf{1}}^{(1)};</math></p> <p><math>\lambda_2: \bar{\mathbf{3}}_2^{\text{B}} \bar{\mathbf{3}}_2^{\text{B}} \bar{\mathbf{3}}_5^{\text{B}} \bar{\mathbf{1}}^{(1)}</math></p>
<p><i>possibility no. 3</i></p> <p><math>a = 0, b = -\frac{1}{2}; (H_u, H_d) = (\bar{\mathbf{2}}_2^{\text{III}}, \mathbf{2}_2^{\text{III}})</math></p> <p>heavy <math>(u_R^c, d_R^c): (-, \bar{\mathbf{3}}_4^{\text{B}})</math></p> <p>light <math>u_R^c: \bar{\mathbf{3}}_1^{\text{B}}; \text{light } d_R^c: \bar{\mathbf{3}}_2^{\text{B}}</math></p> <p>heavy generations of <math>(L, \nu_R^c, e_R^c):</math>  <math>(\mathbf{2}_2^{\text{III}}, -, -), (\mathbf{2}_3^{\text{III}}, \mathbf{1}^{(2)}, \bar{\mathbf{1}}^{(3)})</math></p> <p>light <math>\nu_R^c: \bar{\mathbf{1}}^{(2)}; \text{light } e_R^c: \bar{\mathbf{1}}^{(5)}</math></p> <p><math>\mathbf{1}_\mu: -</math></p>	<p><math>\alpha: (\mathbf{2}_2^{\text{III}}, \bar{\mathbf{3}}_4^{\text{B}}), (\mathbf{2}_3^{\text{III}}, \bar{\mathbf{3}}_2^{\text{B}}); \beta: \bar{\mathbf{3}}_1^{\text{B}} \bar{\mathbf{3}}_4^{\text{B}} \bar{\mathbf{3}}_4^{\text{B}}; \delta: -;</math></p> <p><math>\gamma: \mathbf{2}_2^{\text{III}} \mathbf{2}_3^{\text{III}} \bar{\mathbf{1}}^{(3)}, \mathbf{2}_3^{\text{III}} \mathbf{2}_3^{\text{III}} \bar{\mathbf{1}}^{(5)};</math></p> <p><math>\lambda_1: -; \lambda_3: -; \lambda_6: \mathbf{2}_1^{\text{III}}; \lambda_8: -; \lambda_{10}: -;</math></p> <p><math>\lambda_4: (\bar{\mathbf{3}}_1^{\text{B}}, \bar{\mathbf{1}}^{(3)}); \lambda_5: (\mathbf{2}_2^{\text{III}}, \mathbf{2}_2^{\text{III}});</math></p> <p><math>\lambda_9: (\bar{\mathbf{3}}_1^{\text{B}}, (\mathbf{2}_3^{\text{III}})^*);</math></p> <p><math>\lambda_7: \bar{\mathbf{3}}_1^{\text{B}} (\bar{\mathbf{3}}_4^{\text{B}})^* \bar{\mathbf{1}}^{(3)}, \bar{\mathbf{3}}_1^{\text{B}} (\bar{\mathbf{3}}_2^{\text{B}})^* \bar{\mathbf{1}}^{(5)};</math></p> <p><math>\lambda_2: \bar{\mathbf{3}}_1^{\text{B}} \bar{\mathbf{3}}_1^{\text{B}} \bar{\mathbf{3}}_4^{\text{B}} \bar{\mathbf{1}}^{(3)}</math></p>
<p><i>possibility no. 4</i></p> <p><math>a = 0, b = -\frac{1}{2}; (H_u, H_d) = (\bar{\mathbf{2}}_2^{\text{III}}, \mathbf{2}_3^{\text{III}})</math></p> <p>heavy <math>(u_R^c, d_R^c): (-, \bar{\mathbf{3}}_2^{\text{B}})</math></p> <p>light <math>u_R^c: \bar{\mathbf{3}}_1^{\text{B}}; \text{light } d_R^c: \bar{\mathbf{3}}_4^{\text{B}}</math></p> <p>heavy generations of <math>(L, \nu_R^c, e_R^c):</math>  <math>(\mathbf{2}_2^{\text{III}}, -, \bar{\mathbf{1}}^{(3)}), (\mathbf{2}_3^{\text{III}}, \mathbf{1}^{(2)}, \bar{\mathbf{1}}^{(5)})</math></p> <p>light <math>\nu_R^c: \bar{\mathbf{1}}^{(2)}; \text{light } e_R^c: -</math></p> <p><math>\mathbf{1}_\mu: \mathbf{1}^{(2)}</math></p>	<p><math>\alpha: (\mathbf{2}_2^{\text{III}}, \bar{\mathbf{3}}_4^{\text{B}}), (\mathbf{2}_3^{\text{III}}, \bar{\mathbf{3}}_2^{\text{B}}); \beta: \bar{\mathbf{3}}_1^{\text{B}} \bar{\mathbf{3}}_4^{\text{B}} \bar{\mathbf{3}}_4^{\text{B}}; \delta: -;</math></p> <p><math>\gamma: \mathbf{2}_2^{\text{III}} \mathbf{2}_3^{\text{III}} \bar{\mathbf{1}}^{(3)}, \mathbf{2}_3^{\text{III}} \mathbf{2}_3^{\text{III}} \bar{\mathbf{1}}^{(5)};</math></p> <p><math>\lambda_1: -; \lambda_3: -; \lambda_6: -; \lambda_8: \bar{\mathbf{1}}^{(3)}; \lambda_{10}: -;</math></p> <p><math>\lambda_4: (\bar{\mathbf{3}}_1^{\text{B}}, \bar{\mathbf{1}}^{(5)}); \lambda_5: (\mathbf{2}_2^{\text{III}}, \mathbf{2}_2^{\text{III}});</math></p> <p><math>\lambda_9: (\bar{\mathbf{3}}_1^{\text{B}}, (\mathbf{2}_3^{\text{III}})^*);</math></p> <p><math>\lambda_7: \bar{\mathbf{3}}_1^{\text{B}} (\bar{\mathbf{3}}_2^{\text{B}})^* \bar{\mathbf{1}}^{(5)}, \bar{\mathbf{3}}_1^{\text{B}} (\bar{\mathbf{3}}_4^{\text{B}})^* \bar{\mathbf{1}}^{(3)};</math></p> <p><math>\lambda_2: \bar{\mathbf{3}}_1^{\text{B}} \bar{\mathbf{3}}_1^{\text{B}} \bar{\mathbf{3}}_4^{\text{B}} \bar{\mathbf{1}}^{(3)}</math></p>
<p><i>possibility no. 5</i></p> <p><math>a = -\frac{1}{2}, b = \frac{1}{2}; (H_u, H_d) = (\mathbf{2}_3^{\text{III}}, \mathbf{2}_1^{\text{III}})</math></p> <p>heavy <math>(u_R^c, d_R^c): (\bar{\mathbf{3}}_2^{\text{B}}, \bar{\mathbf{3}}_5^{\text{B}})</math></p> <p>light <math>u_R^c: -; \text{light } d_R^c: \bar{\mathbf{3}}_1^{\text{B}}</math></p> <p>heavy generations of <math>(L, \nu_R^c, e_R^c):</math>  <math>(\mathbf{2}_1^{\text{III}}, \bar{\mathbf{1}}^{(4)}, -), (\bar{\mathbf{2}}_3^{\text{III}}, -, \bar{\mathbf{1}}^{(1)})</math></p> <p>light <math>\nu_R^c: \mathbf{1}^{(4)}; \text{light } e_R^c: \mathbf{1}^{(5)}</math></p> <p><math>\mathbf{1}_\mu: \bar{\mathbf{1}}^{(4)}</math></p>	<p><math>\alpha: (\mathbf{2}_1^{\text{III}}, \bar{\mathbf{3}}_5^{\text{B}}), (\bar{\mathbf{2}}_3^{\text{III}}, \bar{\mathbf{3}}_1^{\text{B}}); \beta: \bar{\mathbf{3}}_2^{\text{B}} \bar{\mathbf{3}}_5^{\text{B}} \bar{\mathbf{3}}_5^{\text{B}}; \delta: -;</math></p> <p><math>\gamma: \mathbf{2}_1^{\text{III}} \bar{\mathbf{2}}_3^{\text{III}} \bar{\mathbf{1}}^{(1)}, \bar{\mathbf{2}}_3^{\text{III}} \mathbf{2}_3^{\text{III}} \mathbf{1}^{(5)};</math></p> <p><math>\lambda_1: -; \lambda_3: -; \lambda_6: -; \lambda_8: \bar{\mathbf{1}}^{(1)}; \lambda_{10}: -;</math></p> <p><math>\lambda_4: (\bar{\mathbf{3}}_2^{\text{B}}, \bar{\mathbf{1}}^{(1)}); \lambda_5: (\bar{\mathbf{2}}_3^{\text{III}}, \bar{\mathbf{2}}_3^{\text{III}});</math></p> <p><math>\lambda_9: (\bar{\mathbf{3}}_2^{\text{B}}, (\bar{\mathbf{2}}_3^{\text{III}})^*);</math></p> <p><math>\lambda_7: \bar{\mathbf{3}}_2^{\text{B}} (\bar{\mathbf{3}}_5^{\text{B}})^* \bar{\mathbf{1}}^{(1)}, \bar{\mathbf{3}}_2^{\text{B}} (\bar{\mathbf{3}}_1^{\text{B}})^* \mathbf{1}^{(5)};</math></p> <p><math>\lambda_2: \bar{\mathbf{3}}_2^{\text{B}} \bar{\mathbf{3}}_2^{\text{B}} \bar{\mathbf{3}}_5^{\text{B}} \bar{\mathbf{1}}^{(1)}</math></p>

Continued on next page

Table C.5, Possible matches for III  $\times$  B – continued from previous page

Matter spectrum	Baryon- and Lepton number violation
<p>possibility no. 6</p> <p><math>a = -\frac{1}{2}, b = \frac{1}{2}; (H_u, H_d) = (\mathbf{2}_3^{\text{III}}, \bar{\mathbf{2}}_3^{\text{III}})</math></p> <p>heavy <math>(u_R^c, d_R^c): (\bar{\mathbf{3}}_2^{\text{B}}, \bar{\mathbf{3}}_1^{\text{B}})</math></p> <p>light <math>u_R^c: -</math>; light <math>d_R^c: \bar{\mathbf{3}}_5^{\text{B}}</math></p> <p>heavy generations of <math>(L, \nu_R^c, e_R^c):</math>  <math>(\mathbf{2}_1^{\text{III}}, \bar{\mathbf{1}}^{(4)}, \bar{\mathbf{1}}^{(1)}), (\bar{\mathbf{2}}_3^{\text{III}}, -, \mathbf{1}^{(5)})</math></p> <p>light <math>\nu_R^c: \mathbf{1}^{(4)}</math>; light <math>e_R^c: -</math></p> <p><math>\mathbf{1}_\mu: -</math></p>	<p><math>\alpha: (\mathbf{2}_1^{\text{III}}, \bar{\mathbf{3}}_5^{\text{B}}), (\bar{\mathbf{2}}_3^{\text{III}}, \bar{\mathbf{3}}_1^{\text{B}}); \beta: \bar{\mathbf{3}}_2^{\text{B}} \bar{\mathbf{3}}_5^{\text{B}} \bar{\mathbf{3}}_5^{\text{B}}; \delta: -;</math></p> <p><math>\gamma: \mathbf{2}_1^{\text{III}} \bar{\mathbf{2}}_3^{\text{III}} \bar{\mathbf{1}}^{(1)}, \bar{\mathbf{2}}_3^{\text{III}} \bar{\mathbf{2}}_3^{\text{III}} \mathbf{1}^{(5)};</math></p> <p><math>\lambda_1: -; \lambda_3: -; \lambda_6: \bar{\mathbf{2}}_1^{\text{III}}; \lambda_8: \mathbf{1}^{(5)}; \lambda_{10}: -;</math></p> <p><math>\lambda_4: (\bar{\mathbf{3}}_2^{\text{B}}, \mathbf{1}^{(5)}); \lambda_5: (\bar{\mathbf{2}}_3^{\text{III}}, \bar{\mathbf{2}}_3^{\text{III}});</math></p> <p><math>\lambda_9: (\bar{\mathbf{3}}_2^{\text{B}}, (\mathbf{2}_3^{\text{III}})^*);</math></p> <p><math>\lambda_7: \bar{\mathbf{3}}_2^{\text{B}} (\bar{\mathbf{3}}_1^{\text{B}})^* \mathbf{1}^{(5)}, \bar{\mathbf{3}}_2^{\text{B}} (\bar{\mathbf{3}}_5^{\text{B}})^* \bar{\mathbf{1}}^{(1)};</math></p> <p><math>\lambda_2: \bar{\mathbf{3}}_2^{\text{B}} \bar{\mathbf{3}}_2^{\text{B}} \bar{\mathbf{3}}_5^{\text{B}} \bar{\mathbf{1}}^{(1)}</math></p>
<p>possibility no. 7</p> <p><math>a = 0, b = -\frac{1}{2}; (H_u, H_d) = (\bar{\mathbf{2}}_3^{\text{III}}, \mathbf{2}_2^{\text{III}})</math></p> <p>heavy <math>(u_R^c, d_R^c): (\bar{\mathbf{3}}_1^{\text{B}}, \bar{\mathbf{3}}_4^{\text{B}})</math></p> <p>light <math>u_R^c: -</math>; light <math>d_R^c: \bar{\mathbf{3}}_2^{\text{B}}</math></p> <p>heavy generations of <math>(L, \nu_R^c, e_R^c):</math>  <math>(\mathbf{2}_2^{\text{III}}, \bar{\mathbf{1}}^{(2)}, -), (\mathbf{2}_3^{\text{III}}, -, \bar{\mathbf{1}}^{(3)})</math></p> <p>light <math>\nu_R^c: \mathbf{1}^{(2)}</math>; light <math>e_R^c: \bar{\mathbf{1}}^{(5)}</math></p> <p><math>\mathbf{1}_\mu: \bar{\mathbf{1}}^{(2)}</math></p>	<p><math>\alpha: (\mathbf{2}_2^{\text{III}}, \bar{\mathbf{3}}_4^{\text{B}}), (\mathbf{2}_3^{\text{III}}, \bar{\mathbf{3}}_2^{\text{B}}); \beta: \bar{\mathbf{3}}_1^{\text{B}} \bar{\mathbf{3}}_4^{\text{B}} \bar{\mathbf{3}}_4^{\text{B}}; \delta: -;</math></p> <p><math>\gamma: \mathbf{2}_2^{\text{III}} \mathbf{2}_3^{\text{III}} \bar{\mathbf{1}}^{(3)}, \mathbf{2}_3^{\text{III}} \mathbf{2}_3^{\text{III}} \bar{\mathbf{1}}^{(5)};</math></p> <p><math>\lambda_1: -; \lambda_3: -; \lambda_6: -; \lambda_8: \bar{\mathbf{1}}^{(3)}; \lambda_{10}: -;</math></p> <p><math>\lambda_4: (\bar{\mathbf{3}}_1^{\text{B}}, \bar{\mathbf{1}}^{(3)}); \lambda_5: (\mathbf{2}_3^{\text{III}}, \mathbf{2}_3^{\text{III}});</math></p> <p><math>\lambda_9: (\bar{\mathbf{3}}_1^{\text{B}}, (\mathbf{2}_3^{\text{III}})^*);</math></p> <p><math>\lambda_7: \bar{\mathbf{3}}_1^{\text{B}} (\bar{\mathbf{3}}_4^{\text{B}})^* \bar{\mathbf{1}}^{(3)}, \bar{\mathbf{3}}_1^{\text{B}} (\bar{\mathbf{3}}_2^{\text{B}})^* \bar{\mathbf{1}}^{(5)};</math></p> <p><math>\lambda_2: \bar{\mathbf{3}}_1^{\text{B}} \bar{\mathbf{3}}_1^{\text{B}} \bar{\mathbf{3}}_4^{\text{B}} \bar{\mathbf{1}}^{(3)}</math></p>
<p>possibility no. 8</p> <p><math>a = 0, b = -\frac{1}{2}; (H_u, H_d) = (\bar{\mathbf{2}}_3^{\text{III}}, \mathbf{2}_3^{\text{III}})</math></p> <p>heavy <math>(u_R^c, d_R^c): (\bar{\mathbf{3}}_1^{\text{B}}, \bar{\mathbf{3}}_2^{\text{B}})</math></p> <p>light <math>u_R^c: -</math>; light <math>d_R^c: \bar{\mathbf{3}}_4^{\text{B}}</math></p> <p>heavy generations of <math>(L, \nu_R^c, e_R^c):</math>  <math>(\mathbf{2}_2^{\text{III}}, \bar{\mathbf{1}}^{(2)}, \bar{\mathbf{1}}^{(3)}), (\mathbf{2}_3^{\text{III}}, -, \bar{\mathbf{1}}^{(5)})</math></p> <p>light <math>\nu_R^c: \mathbf{1}^{(2)}</math>; light <math>e_R^c: -</math></p> <p><math>\mathbf{1}_\mu: -</math></p>	<p><math>\alpha: (\mathbf{2}_2^{\text{III}}, \bar{\mathbf{3}}_4^{\text{B}}), (\mathbf{2}_3^{\text{III}}, \bar{\mathbf{3}}_2^{\text{B}}); \beta: \bar{\mathbf{3}}_1^{\text{B}} \bar{\mathbf{3}}_4^{\text{B}} \bar{\mathbf{3}}_4^{\text{B}}; \delta: -;</math></p> <p><math>\gamma: \mathbf{2}_2^{\text{III}} \mathbf{2}_3^{\text{III}} \bar{\mathbf{1}}^{(3)}, \mathbf{2}_3^{\text{III}} \mathbf{2}_3^{\text{III}} \bar{\mathbf{1}}^{(5)};</math></p> <p><math>\lambda_1: -; \lambda_3: -; \lambda_6: \bar{\mathbf{2}}_1^{\text{III}}; \lambda_8: \bar{\mathbf{1}}^{(5)}; \lambda_{10}: -;</math></p> <p><math>\lambda_4: (\bar{\mathbf{3}}_1^{\text{B}}, \bar{\mathbf{1}}^{(5)}); \lambda_5: (\mathbf{2}_3^{\text{III}}, \mathbf{2}_3^{\text{III}});</math></p> <p><math>\lambda_9: (\bar{\mathbf{3}}_1^{\text{B}}, (\mathbf{2}_3^{\text{III}})^*);</math></p> <p><math>\lambda_7: \bar{\mathbf{3}}_1^{\text{B}} (\bar{\mathbf{3}}_2^{\text{B}})^* \bar{\mathbf{1}}^{(5)}, \bar{\mathbf{3}}_1^{\text{B}} (\bar{\mathbf{3}}_4^{\text{B}})^* \bar{\mathbf{1}}^{(3)};</math></p> <p><math>\lambda_2: \bar{\mathbf{3}}_1^{\text{B}} \bar{\mathbf{3}}_1^{\text{B}} \bar{\mathbf{3}}_4^{\text{B}} \bar{\mathbf{1}}^{(3)}</math></p>



## Appendix D

# All realistic chiral Models

Here, we give for completeness the other ‘reasonable’ flux configurations we found with our search presented in section 2.2 of chapter V. Recall that our search was performed over the bases  $\mathbb{P}^3$ ,  $\text{Bl}_1\mathbb{P}^3$  and  $\text{Bl}_2\mathbb{P}^3$ . Only for the first two did we find any reasonable fluxes, i.e. those that give chiral indices with absolute values smaller than 10.

$\mathcal{B} = \mathbb{P}^3$

This base has only one independent divisor class  $H$ . The divisors of the non-abelian groups are therefore identified with this divisor:  $W_2 = W_3 = H$ . The only fibration with a reasonable flux is for  $\alpha = H, \beta = 2H$ . The flux is for the identification  $U(1)_Y = -1/2U(1)_2$  and is given by

$$-S_1 E_1 - S_1 F_1 - 3H F_1 - E_1 F_1 - 2F_1^2 + H F_2 - 2F_1 F_2.$$

The D3-tadpole of this flux is 60. The induced spectrum is:

$\mathcal{R}$	$\mathbf{2}_1$	$\mathbf{2}_2$	$\mathbf{2}_3$	$\mathbf{3}_1$	$\mathbf{3}_2$	$\mathbf{3}_3$	$\mathbf{3}_4$	$\mathbf{3}_5$	$(\mathbf{3}, \mathbf{2})$	$\mathbf{1}^{(1)}$	$\mathbf{1}^{(2)}$	$\mathbf{1}^{(3)}$	$\mathbf{1}^{(4)}$	$\mathbf{1}^{(5)}$	$\mathbf{1}^{(6)}$
$\chi$	-3	0	-2	5	-3	6	-9	-5	3	-1	-9	0	-6	-3	5

$\mathcal{B} = \text{Bl}_1\mathbb{P}^3$

This base has two independent divisor classes  $H$  and  $X$ . We identified the non-abelian divisors as  $W_2 = X$  and  $W_3 = H$ . There are three fibrations with reasonable fluxes.

$\alpha = \mathbf{0}, \beta = -2H$

For this fibration, there are two reasonable fluxes. The first flux is for the identification  $U(1)_Y = U(1)_1$  and is given by

$$\frac{1}{2}(-9 E_1 F_2 - 3 E_1 H + 6 E_1 S_1 - 3 F_1 X + 12 H X + 3 S_0 X - 3 S_1 X - 3 [w] X + 6 X^2)$$

with the D3-tadpole being 40. The chiral spectrum is:

$\mathcal{R}$	$\mathbf{2}_1$	$\mathbf{2}_2$	$\mathbf{2}_3$	$\mathbf{3}_1$	$\mathbf{3}_2$	$\mathbf{3}_3$	$\mathbf{3}_4$	$\mathbf{3}_5$	$(\mathbf{3}, \mathbf{2})$	$\mathbf{1}^{(1)}$	$\mathbf{1}^{(2)}$	$\mathbf{1}^{(3)}$	$\mathbf{1}^{(4)}$	$\mathbf{1}^{(5)}$	$\mathbf{1}^{(6)}$
$\chi$	0	3	-6	0	0	3	-3	-6	3	0	3	0	0	0	-6

The second flux is for  $U(1)_Y = -1/2U(1)_2$  and is given by

$$\frac{1}{2}(-7 E_1 F_2 - E_1 H + 4 E_1 S_1 - 3 F_1 X + 12 H X + 3 S_0 X - 3 S_1 X - 2 [w] X + 6 X^2)$$

with D3-tadpole 42. The chiral spectrum is:

$\mathcal{R}$	$\mathbf{2}_1$	$\mathbf{2}_2$	$\mathbf{2}_3$	$\mathbf{3}_1$	$\mathbf{3}_2$	$\mathbf{3}_3$	$\mathbf{3}_4$	$\mathbf{3}_5$	$(\mathbf{3}, \mathbf{2})$	$\mathbf{1}^{(1)}$	$\mathbf{1}^{(2)}$	$\mathbf{1}^{(3)}$	$\mathbf{1}^{(4)}$	$\mathbf{1}^{(5)}$	$\mathbf{1}^{(6)}$
$\chi$	0	3	-2	-2	0	3	-3	-4	3	-6	-5	0	-8	0	-4

$$\alpha = \mathbf{H} + \mathbf{X}, \beta = -\mathbf{H} + \mathbf{X}$$

For this fibration, there are two reasonable fluxes. The first flux is for the identification  $U(1)_Y = U(1)_1$  and is given by

$$\frac{1}{2}(-9 E_1 F_2 - 3 E_1 H + 6 E_1 S_1 - 3 F_1 X + 12 H X + 3 S_0 X - 3 S_1 X - 3 [w] X + 6 X^2)$$

with D3-tadpole 41. The chiral spectrum is:

$\mathcal{R}$	$\mathbf{2}_1$	$\mathbf{2}_2$	$\mathbf{2}_3$	$\mathbf{3}_1$	$\mathbf{3}_2$	$\mathbf{3}_3$	$\mathbf{3}_4$	$\mathbf{3}_5$	$(\mathbf{3}, \mathbf{2})$	$\mathbf{1}^{(1)}$	$\mathbf{1}^{(2)}$	$\mathbf{1}^{(3)}$	$\mathbf{1}^{(4)}$	$\mathbf{1}^{(5)}$	$\mathbf{1}^{(6)}$
$\chi$	0	3	-6	0	0	3	-3	-6	3	0	3	0	0	0	-6

The second flux is for  $U(1)_Y = -1/2 U(1)_2$  and is given by

$$\frac{1}{2}(-7 E_1 F_2 - E_1 H + 4 E_1 S_1 - 3 F_1 X + 12 H X + 3 S_0 X - 3 S_1 X - 2 [w] X + 6 X^2)$$

with D3-tadpole 43. The chiral spectrum is:

$\mathcal{R}$	$\mathbf{2}_1$	$\mathbf{2}_2$	$\mathbf{2}_3$	$\mathbf{3}_1$	$\mathbf{3}_2$	$\mathbf{3}_3$	$\mathbf{3}_4$	$\mathbf{3}_5$	$(\mathbf{3}, \mathbf{2})$	$\mathbf{1}^{(1)}$	$\mathbf{1}^{(2)}$	$\mathbf{1}^{(3)}$	$\mathbf{1}^{(4)}$	$\mathbf{1}^{(5)}$	$\mathbf{1}^{(6)}$
$\chi$	0	3	-2	-2	0	3	-3	-4	3	-6	-5	0	-8	0	-4

Compared to the previous fibration, the two pairs of flux configurations are formally the same, yielding the same chiral spectrum. The only quantity they differ in are the D3-tadpoles.

$$\alpha = \mathbf{H} + \mathbf{X}, \beta = \mathbf{0}$$

For this fibration, there is one reasonable flux. It is determined for the identification  $U(1)_Y = U(1)_1$  and given as

$$\frac{1}{2}(-3 E_1 F_2 + 2 E_1 H - E_1 S_1 - F_1 X + F_2 X + S_1 X)$$

with D3-tadpole 49. The chiral spectrum is:

$\mathcal{R}$	$\mathbf{2}_1$	$\mathbf{2}_2$	$\mathbf{2}_3$	$\mathbf{3}_1$	$\mathbf{3}_2$	$\mathbf{3}_3$	$\mathbf{3}_4$	$\mathbf{3}_5$	$(\mathbf{3}, \mathbf{2})$	$\mathbf{1}^{(1)}$	$\mathbf{1}^{(2)}$	$\mathbf{1}^{(3)}$	$\mathbf{1}^{(4)}$	$\mathbf{1}^{(5)}$	$\mathbf{1}^{(6)}$
$\chi$	-2	1	-2	-1	-1	1	-2	-3	3	1	2	0	0	-1	-3

# Bibliography

- [1] M. H. Goroff and A. Sagnotti, “QUANTUM GRAVITY AT TWO LOOPS,” *Phys. Lett.* **B160** (1985) 81–86. (p. 1)
- [2] S. Weinberg, *The quantum theory of fields. Vol. 2: Modern applications*. Cambridge University Press, 2013. (p. 1)
- [3] J. Polchinski, *String theory. Vol. 1: An introduction to the bosonic string*. Cambridge University Press, 2007. (pp. 1, 7, 8, and 15)
- [4] C. Vafa, “Evidence for F-Theory,” *Nucl. Phys.* **B469** (1996) 403–418, [arXiv:hep-th/9602022](#). (pp. 3 and 4)
- [5] D. R. Morrison and C. Vafa, “Compactifications of F theory on Calabi-Yau threefolds. 1,” *Nucl.Phys.* **B473** (1996) 74–92, [arXiv:hep-th/9602114](#) [[hep-th](#)]. (p. 4)
- [6] D. R. Morrison and C. Vafa, “Compactifications of F theory on Calabi-Yau threefolds. 2.,” *Nucl.Phys.* **B476** (1996) 437–469, [arXiv:hep-th/9603161](#) [[hep-th](#)]. (p. 4)
- [7] R. Friedman, J. Morgan, and E. Witten, “Vector bundles and F theory,” *Commun.Math.Phys.* **187** (1997) 679–743, [arXiv:hep-th/9701162](#) [[hep-th](#)]. (p. 4)
- [8] J. J. Heckman, H. Lin, and S.-T. Yau, “Building Blocks for Generalized Heterotic/F-theory Duality,” *Adv. Theor. Math. Phys.* **18** no. 6, (2014) 1463–1503, [arXiv:1311.6477](#) [[hep-th](#)]. (p. 4)
- [9] L. B. Anderson and W. Taylor, “Geometric constraints in dual F-theory and heterotic string compactifications,” *JHEP* **08** (2014) 025, [arXiv:1405.2074](#) [[hep-th](#)]. (p. 4)
- [10] R. Donagi and M. Wijnholt, “Model Building with F-Theory,” *Adv.Theor.Math.Phys.* **15** (2011) 1237–1318, [arXiv:0802.2969](#) [[hep-th](#)]. (pp. 4, 30, 32, 45, and 47)
- [11] C. Beasley, J. J. Heckman, and C. Vafa, “GUTs and Exceptional Branes in F-theory - I,” *JHEP* **0901** (2009) 058, [arXiv:0802.3391](#) [[hep-th](#)]. (pp. 4, 30, and 32)
- [12] C. Beasley, J. J. Heckman, and C. Vafa, “GUTs and Exceptional Branes in F-theory - II: Experimental Predictions,” *JHEP* **01** (2009) 059, [arXiv:0806.0102](#) [[hep-th](#)]. (pp. 4 and 47)
- [13] L. Lin and T. Weigand, “Towards the Standard Model in F-theory,” *Fortsch.Phys.* **63** no. 2, (2015) 55–104, [arXiv:1406.6071](#) [[hep-th](#)]. (pp. 5, 94, 95, 97, 109, and 140)
- [14] L. Lin, C. Mayrhofer, O. Till, and T. Weigand, “Fluxes in F-theory Compactifications on Genus-One Fibrations,” *JHEP* **01** (2016) 098, [arXiv:1508.00162](#) [[hep-th](#)]. (pp. 5, 67, and 68)

- [15] L. Lin and T. Weigand, “G4-Flux and Standard Model Vacua in F-theory,” [arXiv:1604.04292](https://arxiv.org/abs/1604.04292) [hep-th]. (pp. 5, 95, and 109)
- [16] M. B. Green, J. H. Schwarz, and E. Witten, *SUPERSTRING THEORY. VOL. 1: INTRODUCTION*. 1988.  
<http://www.cambridge.org/us/academic/subjects/physics/theoretical-physics-and-mathematical-physics/superstring-theory-volume-1>. (p. 7)
- [17] M. B. Green, J. H. Schwarz, and E. Witten, *SUPERSTRING THEORY. VOL. 2: LOOP AMPLITUDES, ANOMALIES AND PHENOMENOLOGY*. 1988.  
<http://www.cambridge.org/us/academic/subjects/physics/theoretical-physics-and-mathematical-physics/superstring-theory-volume-2>. (p. 7)
- [18] J. Polchinski, *String theory. Vol. 2: Superstring theory and beyond*. Cambridge University Press, 2007. (p. 7)
- [19] L. E. Ibanez and A. M. Uranga, *String theory and particle physics: an introduction to string phenomenology*. Cambridge Univ. Press, Cambridge, 2012.  
<https://cds.cern.ch/record/1428137>. (pp. 7 and 9)
- [20] D. Tong, “String Theory,” [arXiv:0908.0333](https://arxiv.org/abs/0908.0333) [hep-th]. (p. 8)
- [21] M. Grana, “Flux compactifications in string theory: A Comprehensive review,” *Phys. Rept.* **423** (2006) 91–158, [arXiv:hep-th/0509003](https://arxiv.org/abs/hep-th/0509003) [hep-th]. (p. 12)
- [22] M. R. Douglas, R. L. Karp, S. Lukic, and R. Reinbacher, “Numerical Calabi-Yau metrics,” *J. Math. Phys.* **49** (2008) 032302, [arXiv:hep-th/0612075](https://arxiv.org/abs/hep-th/0612075) [hep-th]. (p. 12)
- [23] V. Braun, T. Brelidze, M. R. Douglas, and B. A. Ovrut, “Calabi-Yau Metrics for Quotients and Complete Intersections,” *JHEP* **05** (2008) 080, [arXiv:0712.3563](https://arxiv.org/abs/0712.3563) [hep-th]. (p. 12)
- [24] M. R. Douglas and S. Kachru, “Flux compactification,” *Rev. Mod. Phys.* **79** (2007) 733–796, [arXiv:hep-th/0610102](https://arxiv.org/abs/hep-th/0610102) [hep-th]. (pp. 12 and 43)
- [25] F. Denef, M. R. Douglas, and S. Kachru, “Physics of String Flux Compactifications,” *Ann. Rev. Nucl. Part. Sci.* **57** (2007) 119–144, [arXiv:hep-th/0701050](https://arxiv.org/abs/hep-th/0701050) [hep-th]. (pp. 12 and 43)
- [26] F. Denef, “Les Houches Lectures on Constructing String Vacua,” in *String theory and the real world: From particle physics to astrophysics. Proceedings, Summer School in Theoretical Physics, 87th Session, Les Houches, France, July 2-27, 2007*, pp. 483–610. 2008. [arXiv:0803.1194](https://arxiv.org/abs/0803.1194) [hep-th].  
<https://inspirehep.net/record/780946/files/arXiv:0803.1194.pdf>. (pp. 12, 16, 43, 44, and 47)
- [27] E. Witten, “Bound states of strings and p-branes,” *Nucl. Phys.* **B460** (1996) 335–350, [arXiv:hep-th/9510135](https://arxiv.org/abs/hep-th/9510135) [hep-th]. (p. 15)
- [28] A. Sen, “F theory and orientifolds,” *Nucl. Phys.* **B475** (1996) 562–578, [arXiv:hep-th/9605150](https://arxiv.org/abs/hep-th/9605150) [hep-th]. (p. 16)
- [29] M. R. Gaberdiel and B. Zwiebach, “Exceptional groups from open strings,” *Nucl. Phys.* **B518** (1998) 151–172, [arXiv:hep-th/9709013](https://arxiv.org/abs/hep-th/9709013) [hep-th]. (pp. 16 and 30)

- [30] M. R. Gaberdiel, T. Hauer, and B. Zwiebach, “Open string-string junction transitions,” *Nucl. Phys.* **B525** (1998) 117–145, [arXiv:hep-th/9801205 \[hep-th\]](#). (p. 16)
- [31] O. DeWolfe and B. Zwiebach, “String junctions for arbitrary Lie algebra representations,” *Nucl. Phys.* **B541** (1999) 509–565, [arXiv:hep-th/9804210 \[hep-th\]](#). (pp. 16 and 30)
- [32] T. Weigand, “Lectures on F-theory compactifications and model building,” *Class. Quant. Grav.* **27** (2010) 214004, [arXiv:1009.3497 \[hep-th\]](#). (p. 16)
- [33] L. Lin, C. Mayrhofer, E. Palti, and T. Weigand, “Tba.” To appear. (p. 20)
- [34] T. W. Grimm, “The N=1 effective action of F-theory compactifications,” *Nucl. Phys.* **B845** (2011) 48–92, [arXiv:1008.4133 \[hep-th\]](#). (pp. 23 and 45)
- [35] T. W. Grimm, M. Kerstan, E. Palti, and T. Weigand, “Massive Abelian Gauge Symmetries and Fluxes in F-theory,” *JHEP* **1112** (2011) 004, [arXiv:1107.3842 \[hep-th\]](#). (p. 23)
- [36] A. Grassi, J. Halverson, and J. L. Shaneson, “Matter From Geometry Without Resolution,” *JHEP* **10** (2013) 205, [arXiv:1306.1832 \[hep-th\]](#). (p. 24)
- [37] A. Grassi, J. Halverson, and J. L. Shaneson, “Non-Abelian Gauge Symmetry and the Higgs Mechanism in F-theory,” *Commun. Math. Phys.* **336** no. 3, (2015) 1231–1257, [arXiv:1402.5962 \[hep-th\]](#). (p. 24)
- [38] M. Bershadsky and A. Johansen, “Colliding singularities in F theory and phase transitions,” *Nucl. Phys.* **B489** (1997) 122–138, [arXiv:hep-th/9610111 \[hep-th\]](#). (p. 25)
- [39] K. A. Intriligator, D. R. Morrison, and N. Seiberg, “Five-dimensional supersymmetric gauge theories and degenerations of Calabi-Yau spaces,” *Nucl. Phys.* **B497** (1997) 56–100, [arXiv:hep-th/9702198 \[hep-th\]](#). (pp. 25 and 45)
- [40] D. R. Morrison and W. Taylor, “Matter and singularities,” *JHEP* **1201** (2012) 022, [arXiv:1106.3563 \[hep-th\]](#). (pp. 25, 29, 31, and 33)
- [41] A. Grassi and D. R. Morrison, “Anomalies and the Euler characteristic of elliptic Calabi-Yau threefolds,” *Commun. Num. Theor. Phys.* **6** (2012) 51–127, [arXiv:1109.0042 \[hep-th\]](#). (pp. 25, 26, 28, 115, 145, 155, and 157)
- [42] K. Kodaira, “On the structure of compact complex analytic surfaces, i,” *American Journal of Mathematics* **86** no. 4, (1964) 751–798. <http://www.jstor.org/stable/2373157>. (p. 25)
- [43] K. Kodaira, “On the structure of compact complex analytic surfaces, ii,” *American Journal of Mathematics* **88** no. 3, (1966) 682–721. <http://www.jstor.org/stable/2373150>. (p. 25)
- [44] A. Néron, “Modèles minimaux des variétés abéliennes sur les corps locaux et globaux,” *Publications Mathématiques de l’Institut des Hautes Études Scientifiques* **21** no. 1, 5–125. <http://dx.doi.org/10.1007/BF02684271>. (p. 25)
- [45] C. Mayrhofer, D. R. Morrison, O. Till, and T. Weigand, “Mordell-Weil Torsion and the Global Structure of Gauge Groups in F-theory,” *JHEP* **10** (2014) 16, [arXiv:1405.3656 \[hep-th\]](#). (pp. 26 and 35)

- [46] J. Tate, *Modular Functions of One Variable IV: Proceedings of the International Summer School, University of Antwerp, RUCA, July 17 – August 3, 1972*, ch. Algorithm for determining the type of a singular fiber in an elliptic pencil, pp. 33–52. Springer Berlin Heidelberg, Berlin, Heidelberg, 1975. <http://dx.doi.org/10.1007/BFb0097582>. (p. 26)
- [47] R. Stekolshchik, *Notes on Coxeter Transformations and the McKay Correspondence*. Springer Monographs in Mathematics. Springer Berlin Heidelberg, 2008. <https://books.google.de/books?id=gtwR-rd4--UC>. (p. 26)
- [48] L. Lin, C. Mayrhofer, E. Palti, and T. Weigand, “Tba’.” to appear. (p. 29)
- [49] M. Bershadsky, A. Johansen, T. Pantev, and V. Sadov, “On four-dimensional compactifications of F theory,” *Nucl. Phys.* **B505** (1997) 165–201, [arXiv:hep-th/9701165](https://arxiv.org/abs/hep-th/9701165) [hep-th]. (p. 30)
- [50] H. Hayashi, C. Lawrie, D. R. Morrison, and S. Schafer-Nameki, “Box Graphs and Singular Fibers,” *JHEP* **05** (2014) 048, [arXiv:1402.2653](https://arxiv.org/abs/1402.2653) [hep-th]. (p. 30)
- [51] A. P. Braun and S. Schafer-Nameki, “Box Graphs and Resolutions I,” *Nucl. Phys.* **B905** (2016) 447–479, [arXiv:1407.3520](https://arxiv.org/abs/1407.3520) [hep-th]. (p. 30)
- [52] L. Martucci and T. Weigand, “Non-perturbative selection rules in F-theory,” *JHEP* **09** (2015) 198, [arXiv:1506.06764](https://arxiv.org/abs/1506.06764) [hep-th]. (pp. 32, 86, and 90)
- [53] J. J. Heckman and C. Vafa, “Flavor Hierarchy From F-theory,” *Nucl.Phys.* **B837** (2010) 137–151, [arXiv:0811.2417](https://arxiv.org/abs/0811.2417) [hep-th]. (pp. 33 and 131)
- [54] D. Klevers, D. K. Mayorga Pena, P.-K. Oehlmann, H. Piragua, and J. Reuter, “F-Theory on all Toric Hypersurface Fibrations and its Higgs Branches,” *JHEP* **01** (2015) 142, [arXiv:1408.4808](https://arxiv.org/abs/1408.4808) [hep-th]. (pp. 34, 38, 39, 51, 82, and 92)
- [55] J. H. Silverman, *The arithmetic of elliptic curves*, vol. 106 of *Graduate Texts in Mathematics*. Springer, Dordrecht, second ed., 2009. <http://dx.doi.org/10.1007/978-0-387-09494-6>. (p. 35)
- [56] D. R. Morrison and D. S. Park, “F-Theory and the Mordell-Weil Group of Elliptically-Fibered Calabi-Yau Threefolds,” *JHEP* **1210** (2012) 128, [arXiv:1208.2695](https://arxiv.org/abs/1208.2695) [hep-th]. (pp. 36, 68, 69, and 162)
- [57] M. Cveti, A. Grassi, D. Klevers, and H. Piragua, “Chiral Four-Dimensional F-Theory Compactifications With SU(5) and Multiple U(1)-Factors,” *JHEP* **04** (2014) 010, [arXiv:1306.3987](https://arxiv.org/abs/1306.3987) [hep-th]. (pp. 36, 46, 48, 53, 66, 73, 95, 103, 110, 111, and 113)
- [58] J. Borchmann, C. Mayrhofer, E. Palti, and T. Weigand, “Elliptic fibrations for  $SU(5) \times U(1) \times U(1)$  F-theory vacua,” *Phys.Rev.* **D88** no. 4, (2013) 046005, [arXiv:1303.5054](https://arxiv.org/abs/1303.5054) [hep-th]. (pp. 36, 69, 95, 110, 111, and 112)
- [59] M. Cvetic, D. Klevers, H. Piragua, and P. Song, “Elliptic fibrations with rank three Mordell-Weil group: F-theory with  $U(1) \times U(1) \times U(1)$  gauge symmetry,” *JHEP* **03** (2014) 021, [arXiv:1310.0463](https://arxiv.org/abs/1310.0463) [hep-th]. (p. 37)
- [60] M. Cvetic, D. Klevers, H. Piragua, and W. Taylor, “General U(1)U(1) F-theory compactifications and beyond: geometry of unHiggsings and novel matter structure,” *JHEP* **11** (2015) 204, [arXiv:1507.05954](https://arxiv.org/abs/1507.05954) [hep-th]. (pp. 37 and 51)

- [61] V. Braun and D. R. Morrison, “F-theory on Genus-One Fibrations,” *JHEP* **08** (2014) 132, [arXiv:1401.7844 \[hep-th\]](#). (pp. 38, 39, 51, and 82)
- [62] D. R. Morrison, “Mathematical aspects of f-theory.” Talk given at conference ‘*F-theory at 20*’, Caltech, February, 2016. (p. 38)
- [63] D. R. Morrison and W. Taylor, “Sections, multisections, and U(1) fields in F-theory,” [arXiv:1404.1527 \[hep-th\]](#). (pp. 39, 82, and 92)
- [64] C. Mayrhofer, E. Palti, O. Till, and T. Weigand, “Discrete Gauge Symmetries by Higgsing in four-dimensional F-Theory Compactifications,” *JHEP* **12** (2014) 068, [arXiv:1408.6831 \[hep-th\]](#). (pp. 39, 46, 49, 68, 70, 79, 80, 82, 84, 86, 91, 92, and 93)
- [65] C. Mayrhofer, E. Palti, O. Till, and T. Weigand, “On Discrete Symmetries and Torsion Homology in F-Theory,” *JHEP* **06** (2015) 029, [arXiv:1410.7814 \[hep-th\]](#). (pp. 39, 46, 79, 82, 86, 87, and 92)
- [66] I. Garca-Etxebarria, T. W. Grimm, and J. Keitel, “Yukawas and discrete symmetries in F-theory compactifications without section,” *JHEP* **11** (2014) 125, [arXiv:1408.6448 \[hep-th\]](#). (pp. 39, 46, 82, and 92)
- [67] L. B. Anderson, I. Garca-Etxebarria, T. W. Grimm, and J. Keitel, “Physics of F-theory compactifications without section,” *JHEP* **12** (2014) 156, [arXiv:1406.5180 \[hep-th\]](#). (pp. 39, 46, 82, and 92)
- [68] T. S. Developers, *SageMath, the Sage Mathematics Software System (Version x.y.z)*, 2014. <http://www.sagemath.org>. (p. 39)
- [69] D. Cox, J. Little, and H. Schenck, *Toric Varieties*. Graduate studies in mathematics. American Mathematical Society, 2011. <http://books.google.de/books?id=eXLGwYD4pmAC>. (p. 40)
- [70] P. Candelas and A. Font, “Duality between the webs of heterotic and type II vacua,” *Nucl.Phys.* **B511** (1998) 295–325, [arXiv:hep-th/9603170 \[hep-th\]](#). (pp. 41 and 95)
- [71] V. Bouchard and H. Skarke, “Affine Kac-Moody algebras, CHL strings and the classification of tops,” *Adv.Theor.Math.Phys.* **7** (2003) 205–232, [arXiv:hep-th/0303218 \[hep-th\]](#). (pp. 41, 70, 80, 95, 110, 114, and 151)
- [72] S. H. Katz and E. Sharpe, “D-branes, open string vertex operators, and Ext groups,” *Adv.Theor.Math.Phys.* **6** (2003) 979–1030, [arXiv:hep-th/0208104 \[hep-th\]](#). (p. 43)
- [73] W. Taylor and Y.-N. Wang, “The F-theory geometry with most flux vacua,” *JHEP* **12** (2015) 164, [arXiv:1511.03209 \[hep-th\]](#). (p. 43)
- [74] E. Witten, “On flux quantization in M theory and the effective action,” *J.Geom.Phys.* **22** (1997) 1–13, [arXiv:hep-th/9609122 \[hep-th\]](#). (pp. 44 and 88)
- [75] S. Sethi, C. Vafa, and E. Witten, “Constraints on low dimensional string compactifications,” *Nucl.Phys.* **B480** (1996) 213–224, [arXiv:hep-th/9606122 \[hep-th\]](#). (p. 44)
- [76] K. Becker and M. Becker, “M theory on eight manifolds,” *Nucl.Phys.* **B477** (1996) 155–167, [arXiv:hep-th/9605053 \[hep-th\]](#). (p. 44)
- [77] K. Dasgupta, G. Rajesh, and S. Sethi, “M theory, orientifolds and G - flux,” *JHEP* **9908** (1999) 023, [arXiv:hep-th/9908088 \[hep-th\]](#). (pp. 44 and 45)

- [78] T. W. Grimm, A. Kapfer, and J. Keitel, “Effective action of 6D F-Theory with U(1) factors: Rational sections make Chern-Simons terms jump,” *JHEP* **1307** (2013) 115, [arXiv:1305.1929 \[hep-th\]](#). (pp. 45 and 110)
- [79] T. W. Grimm and A. Kapfer, “Anomaly Cancellation in Field Theory and F-theory on a Circle,” [arXiv:1502.05398 \[hep-th\]](#). (pp. 45, 47, and 66)
- [80] M. Cvetič, D. Klevers, and H. Piragua, “F-Theory Compactifications with Multiple U(1)-Factors: Constructing Elliptic Fibrations with Rational Sections,” *JHEP* **1306** (2013) 067, [arXiv:1303.6970 \[hep-th\]](#). (pp. 45, 95, 110, 111, and 112)
- [81] E. Witten, “Phase transitions in M theory and F theory,” *Nucl. Phys.* **B471** (1996) 195–216, [arXiv:hep-th/9603150 \[hep-th\]](#). (pp. 45 and 46)
- [82] S. H. Katz and C. Vafa, “Matter from geometry,” *Nucl.Phys.* **B497** (1997) 146–154, [arXiv:hep-th/9606086 \[hep-th\]](#). (p. 45)
- [83] P. S. Aspinwall, S. Katz, and D. R. Morrison, “Lie groups, Calabi–Yau threefolds, and F-theory,” *Adv. Theor. Math. Phys.* **4** (2000) 95–126, [hep-th/0002012](#). (p. 45)
- [84] A. P. Braun, A. Collinucci, and R. Valandro, “G-flux in F-theory and algebraic cycles,” *Nucl.Phys.* **B856** (2012) 129–179, [arXiv:1107.5337 \[hep-th\]](#). (pp. 45, 47, 49, 84, 92, and 93)
- [85] J. Marsano and S. Schafer-Nameki, “Yukawas, G-flux, and Spectral Covers from Resolved Calabi- Yau’s,” *JHEP* **11** (2011) 098, [arXiv:1108.1794 \[hep-th\]](#). (pp. 45 and 47)
- [86] S. Krause, C. Mayrhofer, and T. Weigand, “ $G_4$  flux, chiral matter and singularity resolution in F-theory compactifications,” *Nucl.Phys.* **B858** (2012) 1–47, [arXiv:1109.3454 \[hep-th\]](#). (pp. 45, 47, and 94)
- [87] T. W. Grimm and H. Hayashi, “F-theory fluxes, Chirality and Chern-Simons theories,” *JHEP* **1203** (2012) 027, [arXiv:1111.1232 \[hep-th\]](#). (pp. 45, 48, and 73)
- [88] M. Cvetič, T. W. Grimm, and D. Klevers, “Anomaly Cancellation And Abelian Gauge Symmetries In F-theory,” *JHEP* **02** (2013) 101, [arXiv:1210.6034 \[hep-th\]](#). (pp. 46, 48, 66, 67, and 90)
- [89] R. Donagi and M. Wijnholt, “Breaking GUT Groups in F-Theory,” *Adv.Theor.Math.Phys.* **15** (2011) 1523–1604, [arXiv:0808.2223 \[hep-th\]](#). (p. 47)
- [90] R. Blumenhagen, V. Braun, T. W. Grimm, and T. Weigand, “GUTs in Type IIB Orientifold Compactifications,” *Nucl. Phys.* **B815** (2009) 1–94, [arXiv:0811.2936 \[hep-th\]](#). (p. 47)
- [91] H. Hayashi, R. Tatar, Y. Toda, T. Watari, and M. Yamazaki, “New Aspects of Heterotic–F Theory Duality,” *Nucl. Phys.* **B806** (2009) 224–299, [arXiv:0805.1057 \[hep-th\]](#). (p. 47)
- [92] R. Donagi, “Heterotic / F theory duality: ICMP lecture,” in *Mathematical physics. Proceedings, 12th International Congress, ICMP’97, Brisbane, Australia, July 13-19, 1997*. 1998. [arXiv:hep-th/9802093 \[hep-th\]](#). <http://alice.cern.ch/format/showfull?sysnb=0270001>. (p. 48)
- [93] G. Curio and R. Y. Donagi, “Moduli in N=1 heterotic / F theory duality,” *Nucl.Phys.* **B518** (1998) 603–631, [arXiv:hep-th/9801057 \[hep-th\]](#). (p. 48)



- [94] K. Intriligator, H. Jockers, P. Mayr, D. R. Morrison, and M. R. Plesser, “Conifold Transitions in M-theory on Calabi-Yau Fourfolds with Background Fluxes,” *Adv.Theor.Math.Phys.* **17** (2013) 601–699, [arXiv:1203.6662 \[hep-th\]](#). (pp. 48, 49, 92, 93, and 94)
- [95] M. Bies, C. Mayrhofer, C. Pehle, and T. Weigand, “Chow groups, Deligne cohomology and massless matter in F-theory,” [arXiv:1402.5144 \[hep-th\]](#). (pp. 48, 76, 94, 132, 139, and 145)
- [96] S. Krause, C. Mayrhofer, and T. Weigand, “Gauge Fluxes in F-theory and Type IIB Orientifolds,” *JHEP* **1208** (2012) 119, [arXiv:1202.3138 \[hep-th\]](#). (pp. 49, 73, 88, 89, 92, and 94)
- [97] B. R. Greene, D. R. Morrison, and M. Plesser, “Mirror manifolds in higher dimension,” *Commun.Math.Phys.* **173** (1995) 559–598, [arXiv:hep-th/9402119 \[hep-th\]](#). (pp. 49 and 146)
- [98] T. W. Grimm, T.-W. Ha, A. Klemm, and D. Klevers, “Computing Brane and Flux Superpotentials in F-theory Compactifications,” *JHEP* **1004** (2010) 015, [arXiv:0909.2025 \[hep-th\]](#). (pp. 49 and 146)
- [99] N. C. Bizet, A. Klemm, and D. V. Lopes, “Landscaping with fluxes and the E8 Yukawa Point in F-theory,” [arXiv:1404.7645 \[hep-th\]](#). (pp. 49 and 146)
- [100] A. P. Braun and T. Watari, “The Vertical, the Horizontal and the Rest: anatomy of the middle cohomology of Calabi-Yau fourfolds and F-theory applications,” *JHEP* **01** (2015) 047, [arXiv:1408.6167 \[hep-th\]](#). (pp. 49 and 146)
- [101] R. Wazir, “Arithmetic on elliptic threefolds,” *Compos.Math.* **140** (2001) 567–580, [arXiv:math.NT/0112259](#). (pp. 51 and 110)
- [102] W. Decker, G.-M. Greuel, G. Pfister, and H. Schönemann, “SINGULAR 3-1-6 — A computer algebra system for polynomial computations.” <http://www.singular.uni-kl.de>, 2012. (pp. 52 and 61)
- [103] D. A. Cox, J. N. Little, and D. O’Shea, *Ideals, Varieties, and Algorithms*. Undergraduate Texts in Mathematics. Springer New York, New York, NY, 3., rd ed. 2007. corr. 2nd printing. softcover version of original hardcover edition 2007 ed., 2010. (p. 54)
- [104] W. Fulton, “Algebraic curves,” *An Introduction to Algebraic Geom* (2008) . (p. 54)
- [105] D. Perrin, *Algebraic geometry: an introduction*. Springer Science & Business Media, 2007. (p. 54)
- [106] W. Fulton, *Introduction to Intersection Theory in Algebraic Geometry*. No. 54 in Cbms Regional Conference Series in Mathematics. American Mathematical Society, 1984. (pp. 60 and 149)
- [107] D. A. Cox, J. Little, and D. O’Shea, *Using algebraic geometry*. No. 185 in Graduate texts in mathematics ; 185 ; Graduate texts in mathematics. Springer, New York, NY, 2. ed. ed., 2005. Includes bibliographical references and index. (p. 60)
- [108] A. Bilal, “Lectures on Anomalies,” [arXiv:0802.0634 \[hep-th\]](#). (p. 65)
- [109] C. Mayrhofer, E. Palti, and T. Weigand, “U(1) symmetries in F-theory GUTs with multiple sections,” *JHEP* **1303** (2013) 098, [arXiv:1211.6742 \[hep-th\]](#). (p. 68)

- 
- [110] V. Braun, T. W. Grimm, and J. Keitel, “Geometric Engineering in Toric F-Theory and GUTs with U(1) Gauge Factors,” *JHEP* **1312** (2013) 069, [arXiv:1306.0577 \[hep-th\]](#). (p. 68)
- [111] V. Braun, T. W. Grimm, and J. Keitel, “New Global F-theory GUTs with U(1) symmetries,” *JHEP* **1309** (2013) 154, [arXiv:1302.1854 \[hep-th\]](#). (p. 73)
- [112] M. Cvetič, D. Klevers, D. K. M. Pena, P.-K. Oehlmann, and J. Reuter, “Three-Family Particle Physics Models from Global F-theory Compactifications,” *JHEP* **08** (2015) 087, [arXiv:1503.02068 \[hep-th\]](#). (pp. 73, 95, and 140)
- [113] L. Martucci and T. Weigand, “Hidden Selection Rules, M5-instantons and Fluxes in F-theory,” *JHEP* **10** (2015) 131, [arXiv:1507.06999 \[hep-th\]](#). (pp. 86 and 90)
- [114] D. S. Freed and E. Witten, “Anomalies in string theory with D-branes,” *Asian J. Math.* **3** (1999) 819, [arXiv:hep-th/9907189 \[hep-th\]](#). (p. 88)
- [115] A. Collinucci and R. Savelli, “On Flux Quantization in F-Theory II: Unitary and Symplectic Gauge Groups,” *JHEP* **1208** (2012) 094, [arXiv:1203.4542 \[hep-th\]](#). (pp. 88, 89, and 136)
- [116] R. Minasian and G. W. Moore, “K theory and Ramond-Ramond charge,” *JHEP* **11** (1997) 002, [arXiv:hep-th/9710230 \[hep-th\]](#). (p. 89)
- [117] L. E. Ibanez and G. G. Ross, “Discrete gauge symmetry anomalies,” *Phys. Lett.* **B260** (1991) 291–295. (p. 90)
- [118] L. E. Ibanez, “More about discrete gauge anomalies,” *Nucl. Phys.* **B398** (1993) 301–318, [arXiv:hep-ph/9210211 \[hep-ph\]](#). (p. 90)
- [119] M. Berasaluce-Gonzalez, L. E. Ibanez, P. Soler, and A. M. Uranga, “Discrete gauge symmetries in D-brane models,” *JHEP* **1112** (2011) 113, [arXiv:1106.4169 \[hep-th\]](#). (p. 90)
- [120] P. G. Camara, L. E. Ibanez, and F. Marchesano, “RR photons,” *JHEP* **1109** (2011) 110, [arXiv:1106.0060 \[hep-th\]](#). (p. 90)
- [121] A. Collinucci and R. Savelli, “On Flux Quantization in F-Theory,” *JHEP* **1202** (2012) 015, [arXiv:1011.6388 \[hep-th\]](#). (pp. 91, 107, and 136)
- [122] D. Gaiotto, M. Guica, L. Huang, A. Simons, A. Strominger, *et al.*, “D4-D0 branes on the quintic,” *JHEP* **0603** (2006) 019, [arXiv:hep-th/0509168 \[hep-th\]](#). (p. 92)
- [123] K.-S. Choi and T. Kobayashi, “Towards the MSSM from F-theory,” *Phys.Lett.* **B693** (2010) 330–333, [arXiv:1003.2126 \[hep-th\]](#). (p. 95)
- [124] K.-S. Choi, “SU(3) x SU(2) x U(1) Vacua in F-Theory,” *Nucl.Phys.* **B842** (2011) 1–32, [arXiv:1007.3843 \[hep-th\]](#). (p. 95)
- [125] K.-S. Choi, “On the Standard Model Group in F-theory,” *Eur. Phys. J.* **C74** (2014) 2939, [arXiv:1309.7297 \[hep-th\]](#). (p. 95)
- [126] J. Borchmann, C. Mayrhofer, E. Palti, and T. Weigand, “SU(5) Tops with Multiple U(1)s in F-theory,” *Nucl.Phys.* **B882** (2014) 1–69, [arXiv:1307.2902 \[hep-th\]](#). (pp. 95, 110, 111, 112, and 113)

- [127] M. Cvetič, D. Klevers, and H. Piragua, “F-Theory Compactifications with Multiple U(1)-Factors: Addendum,” *JHEP* **1312** (2013) 056, [arXiv:1307.6425 \[hep-th\]](#). (pp. 95, 110, and 111)
- [128] E. Witten, “An SU(2) Anomaly,” *Phys. Lett.* **B117** (1982) 324–328. (p. 105)
- [129] A. Klemm, P. Mayr, and C. Vafa, “BPS states of exceptional noncritical strings,” [*Nucl. Phys. Proc. Suppl.*58,177(1997)] (1996) , [arXiv:hep-th/9607139 \[hep-th\]](#). (p. 110)
- [130] T. Shioda, “Mordell-Weil Lattices and Galois Representation. I,” *Proc. Japan Acad.* **A65** (1989) 268–271. (p. 110)
- [131] D. S. Park, “Anomaly Equations and Intersection Theory,” *JHEP* **01** (2012) 093, [arXiv:1111.2351 \[hep-th\]](#). (p. 110)
- [132] P. Arras, “Using Computational Algebraic Geometry in F-theory,” Bachelor thesis, University of Heidelberg, 2014. (p. 113)
- [133] U. Ellwanger, C. Hugonie, and A. M. Teixeira, “The Next-to-Minimal Supersymmetric Standard Model,” *Phys.Rept.* **496** (2010) 1–77, [arXiv:0910.1785 \[hep-ph\]](#). (p. 129)
- [134] M. Cvetič, J. Halverson, and P. Langacker, “Singlet Extensions of the MSSM in the Quiver Landscape,” *JHEP* **1009** (2010) 076, [arXiv:1006.3341 \[hep-th\]](#). (p. 129)
- [135] B. Allanach, A. Dedes, and H. K. Dreiner, “Bounds on R-parity violating couplings at the weak scale and at the GUT scale,” *Phys.Rev.* **D60** (1999) 075014, [arXiv:hep-ph/9906209 \[hep-ph\]](#). (p. 130)
- [136] P. Nath and P. Fileviez Perez, “Proton stability in grand unified theories, in strings and in branes,” *Phys.Rept.* **441** (2007) 191–317, [arXiv:hep-ph/0601023 \[hep-ph\]](#). (p. 130)
- [137] B. Allanach, A. Dedes, and H. Dreiner, “R parity violating minimal supergravity model,” *Phys.Rev.* **D69** (2004) 115002, [arXiv:hep-ph/0309196 \[hep-ph\]](#). (p. 130)
- [138] A. Hebecker, A. K. Knochel, and T. Weigand, “A Shift Symmetry in the Higgs Sector: Experimental Hints and Stringy Realizations,” *JHEP* **1206** (2012) 093, [arXiv:1204.2551 \[hep-th\]](#). (p. 131)
- [139] L. E. Ibanez, F. Marchesano, D. Regalado, and I. Valenzuela, “The Intermediate Scale MSSM, the Higgs Mass and F-theory Unification,” *JHEP* **1207** (2012) 195, [arXiv:1206.2655 \[hep-ph\]](#). (p. 131)
- [140] A. Hebecker, A. K. Knochel, and T. Weigand, “The Higgs mass from a String-Theoretic Perspective,” *Nucl.Phys.* **B874** (2013) 1–35, [arXiv:1304.2767 \[hep-th\]](#). (p. 131)
- [141] L. E. Ibanez and I. Valenzuela, “The Higgs Mass as a Signature of Heavy SUSY,” *JHEP* **1305** (2013) 064, [arXiv:1301.5167 \[hep-ph\]](#). (p. 131)
- [142] A. Hebecker and J. Unwin, “Precision Unification and Proton Decay in F-Theory GUTs with High Scale Supersymmetry,” *JHEP* **09** (2014) 125, [arXiv:1405.2930 \[hep-th\]](#). (p. 131)
- [143] A. Chatzistavrakidis, E. Erfani, H. P. Nilles, and I. Zavala, “Axiology,” *JCAP* **1209** (2012) 006, [arXiv:1207.1128 \[hep-ph\]](#). (p. 131)
- [144] L. J. Hall and Y. Nomura, “Grand Unification and Intermediate Scale Supersymmetry,” *JHEP* **1402** (2014) 129, [arXiv:1312.6695 \[hep-ph\]](#). (p. 131)

- 
- [145] L. E. Ibanez and I. Valenzuela, “BICEP2, the Higgs Mass and the SUSY-breaking Scale,” *Phys. Lett.* **B734** (2014) 354–357, [arXiv:1403.6081 \[hep-ph\]](#). (p. 131)
- [146] L. J. Hall, Y. Nomura, and S. Shirai, “Grand Unification, Axion, and Inflation in Intermediate Scale Supersymmetry,” *JHEP* **06** (2014) 137, [arXiv:1403.8138 \[hep-ph\]](#). (p. 131)
- [147] A. Font and L. Ibanez, “Matter wave functions and Yukawa couplings in F-theory Grand Unification,” *JHEP* **0909** (2009) 036, [arXiv:0907.4895 \[hep-th\]](#). (p. 131)
- [148] S. Cecotti, M. C. N. Cheng, J. J. Heckman, and C. Vafa, “Yukawa Couplings in F-theory and Non-Commutative Geometry,” [arXiv:0910.0477 \[hep-th\]](#). (p. 131)
- [149] J. P. Conlon and E. Palti, “Aspects of Flavour and Supersymmetry in F-theory GUTs,” *JHEP* **1001** (2010) 029, [arXiv:0910.2413 \[hep-th\]](#). (p. 131)
- [150] F. Marchesano and L. Martucci, “Non-perturbative effects on seven-brane Yukawa couplings,” *Phys.Rev.Lett.* **104** (2010) 231601, [arXiv:0910.5496 \[hep-th\]](#). (p. 131)
- [151] L. Aparicio, A. Font, L. E. Ibanez, and F. Marchesano, “Flux and Instanton Effects in Local F-theory Models and Hierarchical Fermion Masses,” *JHEP* **1108** (2011) 152, [arXiv:1104.2609 \[hep-th\]](#). (p. 131)
- [152] A. Font, L. E. Ibanez, F. Marchesano, and D. Regalado, “Non-perturbative effects and Yukawa hierarchies in F-theory SU(5) Unification,” *JHEP* **1303** (2013) 140, [arXiv:1211.6529 \[hep-th\]](#). (p. 131)
- [153] A. Font, F. Marchesano, D. Regalado, and G. Zoccarato, “Up-type quark masses in SU(5) F-theory models,” *JHEP* **1311** (2013) 125, [arXiv:1307.8089 \[hep-th\]](#). (p. 131)
- [154] R. Blumenhagen, M. Cvetič, and T. Weigand, “Spacetime instanton corrections in 4D string vacua: The Seesaw mechanism for D-Brane models,” *Nucl.Phys.* **B771** (2007) 113–142, [arXiv:hep-th/0609191 \[hep-th\]](#). (p. 132)
- [155] L. Ibanez and A. Uranga, “Neutrino Majorana Masses from String Theory Instanton Effects,” *JHEP* **0703** (2007) 052, [arXiv:hep-th/0609213 \[hep-th\]](#). (p. 132)
- [156] M. Haack, D. Krefl, D. Lust, A. Van Proeyen, and M. Zagermann, “Gaugino Condensates and D-terms from D7-branes,” *JHEP* **0701** (2007) 078, [arXiv:hep-th/0609211 \[hep-th\]](#). (p. 132)
- [157] B. Florea, S. Kachru, J. McGreevy, and N. Saulina, “Stringy Instantons and Quiver Gauge Theories,” *JHEP* **0705** (2007) 024, [arXiv:hep-th/0610003 \[hep-th\]](#). (p. 132)
- [158] R. Blumenhagen, M. Cvetič, S. Kachru, and T. Weigand, “D-Brane Instantons in Type II Orientifolds,” *Ann.Rev.Nucl.Part.Sci.* **59** (2009) 269–296, [arXiv:0902.3251 \[hep-th\]](#). (p. 132)
- [159] J. Marsano, N. Saulina, and S. Schafer-Nameki, “An Instanton Toolbox for F-Theory Model Building,” *JHEP* **1001** (2010) 128, [arXiv:0808.2450 \[hep-th\]](#). (p. 132)
- [160] R. Blumenhagen, A. Collinucci, and B. Jurke, “On Instanton Effects in F-theory,” *JHEP* **1008** (2010) 079, [arXiv:1002.1894 \[hep-th\]](#). (p. 132)
- [161] R. Donagi and M. Wijnholt, “MSW Instantons,” *JHEP* **06** (2013) 050, [arXiv:1005.5391 \[hep-th\]](#). (p. 132)

- [162] M. Cvetič, I. García Etxebarria, and J. Halverson, “Three Looks at Instantons in F-theory – New Insights from Anomaly Inflow, String Junctions and Heterotic Duality,” *JHEP* **1111** (2011) 101, [arXiv:1107.2388 \[hep-th\]](#). (p. 132)
- [163] J. Marsano, N. Saulina, and S. Schfer-Nameki, “G-flux, M5 instantons, and U(1) symmetries in F-theory,” *Phys. Rev.* **D87** (2013) 066007, [arXiv:1107.1718 \[hep-th\]](#). (p. 132)
- [164] T. W. Grimm, M. Kerstan, E. Palti, and T. Weigand, “On Fluxed Instantons and Moduli Stabilisation in IIB Orientifolds and F-theory,” *Phys.Rev.* **D84** (2011) 066001, [arXiv:1105.3193 \[hep-th\]](#). (p. 132)
- [165] M. Kerstan and T. Weigand, “Fluxed M5-instantons in F-theory,” *Nucl.Phys.* **B864** (2012) 597–639, [arXiv:1205.4720 \[hep-th\]](#). (p. 132)
- [166] M. Cvetič, I. García-Etxebarria, and R. Richter, “Branes and instantons at angles and the F-theory lift of O(1) instantons,” *AIP Conf.Proc.* **1200** (2010) 246–260, [arXiv:0911.0012 \[hep-th\]](#). (p. 132)
- [167] M. Cvetič, I. García-Etxebarria, and J. Halverson, “Global F-theory Models: Instantons and Gauge Dynamics,” *JHEP* **1101** (2011) 073, [arXiv:1003.5337 \[hep-th\]](#). (p. 132)
- [168] M. Bianchi, A. Collinucci, and L. Martucci, “Magnetized E3-brane instantons in F-theory,” *JHEP* **1112** (2011) 045, [arXiv:1107.3732 \[hep-th\]](#). (p. 132)
- [169] M. Bianchi, G. Inverso, and L. Martucci, “Brane instantons and fluxes in F-theory,” *JHEP* **1307** (2013) 037, [arXiv:1212.0024 \[hep-th\]](#). (p. 132)
- [170] M. Cvetič, R. Donagi, J. Halverson, and J. Marsano, “On Seven-Brane Dependent Instanton Prefactors in F-theory,” *JHEP* **1211** (2012) 004, [arXiv:1209.4906 \[hep-th\]](#). (p. 132)
- [171] L. Martucci, “Topological duality twist and brane instantons in F-theory,” *JHEP* **06** (2014) 180, [arXiv:1403.2530 \[hep-th\]](#). (p. 132)
- [172] L. Ibanez and R. Richter, “Stringy Instantons and Yukawa Couplings in MSSM-like Orientifold Models,” *JHEP* **0903** (2009) 090, [arXiv:0811.1583 \[hep-th\]](#). (p. 132)
- [173] M. Cvetič, J. Halverson, and R. Richter, “Realistic Yukawa structures from orientifold compactifications,” *JHEP* **0912** (2009) 063, [arXiv:0905.3379 \[hep-th\]](#). (p. 132)
- [174] M. Cvetič, J. Halverson, and R. Richter, “Mass Hierarchies from MSSM Orientifold Compactifications,” *JHEP* **1007** (2010) 005, [arXiv:0909.4292 \[hep-th\]](#). (p. 132)
- [175] E. Kiritsis, M. Lennek, and B. Schellekens, “SU(5) orientifolds, Yukawa couplings, Stringy Instantons and Proton Decay,” *Nucl.Phys.* **B829** (2010) 298–324, [arXiv:0909.0271 \[hep-th\]](#). (p. 132)
- [176] M. Cvetič and P. Langacker, “D-Instanton Generated Dirac Neutrino Masses,” *Phys.Rev.* **D78** (2008) 066012, [arXiv:0803.2876 \[hep-th\]](#). (p. 133)
- [177] C. Long, L. McAllister, and P. McGuirk, “Heavy Tails in Calabi-Yau Moduli Spaces,” *JHEP* **10** (2014) 187, [arXiv:1407.0709 \[hep-th\]](#). (p. 137)
- [178] M. Cvetič, J. Halverson, and P. Langacker, “String Consistency, Heavy Exotics, and the 750 GeV Diphoton Excess at the LHC,” [arXiv:1512.07622 \[hep-ph\]](#). (p. 139)

- [179] M. Cvetič, J. Halverson, and P. Langacker, “String Consistency, Heavy Exotics, and the 750 GeV Diphoton Excess at the LHC: Addendum,” [arXiv:1602.06257](#) [[hep-ph](#)]. (p. 139)
- [180] E. Palti, “Vector-Like Exotics in F-Theory and 750 GeV Diphotons,” [arXiv:1601.00285](#) [[hep-ph](#)]. (p. 139)
- [181] A. Grassi and D. R. Morrison, “Group representations and the Euler characteristic of elliptically fibered Calabi-Yau threefolds,” [arXiv:math/0005196](#) [[math-ag](#)]. (p. 145)
- [182] C. Mayrhofer, E. Palti, and T. Weigand, “Hypercharge Flux in IIB and F-theory: Anomalies and Gauge Coupling Unification,” *JHEP* **09** (2013) 082, [arXiv:1303.3589](#) [[hep-th](#)]. (p. 146)
- [183] A. P. Braun, A. Collinucci, and R. Valandro, “Hypercharge flux in F-theory and the stable Sen limit,” *JHEP* **07** (2014) 121, [arXiv:1402.4096](#) [[hep-th](#)]. (p. 146)
- [184] W. Fulton, *Intersection Theory*. Springer, 1998. (p. 149)
- [185] D. Eisenbud and J. Harris, *3264 & All that*. Cambridge University Press, 2016. (p. 149)